

Ki-Taek Lim

Kamel A. Abd-Elsalam *Editors*

Nanorobotics and Nanodiagnosics in Integrative Biology and Biomedicine



Springer

Nanorobotics and Nanodiagnostics in Integrative Biology and Biomedicine

Ki-Taek Lim • Kamel A. Abd-Elsalam
Editors

Nanorobotics and Nanodiagnostics in Integrative Biology and Biomedicine

 Springer

Editors

Ki-Taek Lim
Department of Biosystems Engineering
Kangwon National University
Chuncheon, (Republic of Korea)

Kamel A. Abd-Elsalam 
Agricultural Research Center
Plant Pathology Research Institute
Giza, Egypt

ISBN 978-3-031-16083-7 ISBN 978-3-031-16084-4 (eBook)
<https://doi.org/10.1007/978-3-031-16084-4>

© The Editor(s) (if applicable) and The Author(s), under exclusive license to Springer Nature Switzerland AG 2023

This work is subject to copyright. All rights are solely and exclusively licensed by the Publisher, whether the whole or part of the material is concerned, specifically the rights of translation, reprinting, reuse of illustrations, recitation, broadcasting, reproduction on microfilms or in any other physical way, and transmission or information storage and retrieval, electronic adaptation, computer software, or by similar or dissimilar methodology now known or hereafter developed.

The use of general descriptive names, registered names, trademarks, service marks, etc. in this publication does not imply, even in the absence of a specific statement, that such names are exempt from the relevant protective laws and regulations and therefore free for general use.

The publisher, the authors, and the editors are safe to assume that the advice and information in this book are believed to be true and accurate at the date of publication. Neither the publisher nor the authors or the editors give a warranty, expressed or implied, with respect to the material contained herein or for any errors or omissions that may have been made. The publisher remains neutral with regard to jurisdictional claims in published maps and institutional affiliations.

This Springer imprint is published by the registered company Springer Nature Switzerland AG
The registered company address is: Gewerbestrasse 11, 6330 Cham, Switzerland

Preface

Nanorobotics and nanodiagnostics are the emerging tools in the history of nanotechnology to combat several animal and plant diseases. Nanorobots or nanobots of approximately 50–100 nm wide can perform various works, such as targeted drug delivery, biosensing, tumor clearance, and surgery. Nanodiagnostics uses various nano-biosensors acting as biological recognition elements for detecting various analytes (glucose, antibiotics, toxins, etc.). Robotically coupled nano-micromotors inserted into the blood may be able to sense, detect, and eliminate potential microorganisms, tumor cells, or toxic substances. The nanorobotics and nanodiagnostics are integrated parts of human health and the agroecosystem. Nanorobotic agriculture tools include nonporous platforms, wearable devices, micro-nanoneedle patches, nanoparticle-based sensors, quantum dots, and CRISPR/Cas9-based tools that can precisely sense and eliminate plant pathogens for sustainable agriculture and the food industry. This book, *Nanorobotics and Nanodiagnostics in Integrated Biology and Biomedicine*, is the first volume of the original book series approved by Springer Publishing Ltd. More specifically, this book focuses on the recent developments and significant breakthroughs in nanorobotics and nanodiagnostics based on various nano- or biopolymer materials, Lab-on-a-chip devices, printed nanobots, biomolecule sensors, and advanced stimuli-responsive nanodevices, beneficial for human health and agriculture. The present volume comprises 18 chapters prepared by magnificent authors from Brazil, China, Pakistan, Egypt, India, South Africa, South Korea, Saudi Arabia, and the United States. We hope that a combination of 18 outstanding chapters written by professionals and experts represents an extensive knowledge of nanorobotics and nanodiagnostics techniques. We express our sincere gratitude to all the contributing authors who helped us and made their comments about editing the entire book. Without their excellent skills, extensive efforts, and support, writing this book might not have been possible. We hope that the present volume not only encourages the people working in this field but also inspires young scientists and researchers to enlighten the future nanorobotics and nanodiagnostics skills. Last but not least, we would like to thank Springer Publishers for supporting and helping us throughout the journey. We express our sincere gratitude to the Springer staff, editorial directors

(Paul Ross and Guido Zosimo-Landolfo), senior editor (Eric Stannard), and managing staff for their tremendous efforts and assistance. We also want to thank all the reviewers for spending their precious time during the review of chapters. We would also like to thank our family members and colleagues for their continuous support and assistance.

Chuncheon, (Republic of Korea)
Giza, Egypt

Ki-Taek Lim
Kamel A. Abd-Elsalam

Contents

| | | |
|----------|---|-----------|
| 1 | Nanorobotics and Nanodiagnostics in Integrative Biology and Biomedicine: A Note from the Editors | 1 |
| | Ki-Taek Lim and Kamel A. Abd-El salam | |
| 1.1 | Introduction | 1 |
| 1.2 | Historical Background | 5 |
| 1.3 | Overview of the Book | 8 |
| 1.4 | Conclusion | 10 |
| | References. | 10 |
| 2 | Nanorobots for Drug Delivery, Surgery, and Biosensing | 15 |
| | Qing Ye and Jianfei Sun | |
| 2.1 | Introduction | 15 |
| 2.2 | Design of Nanorobots | 17 |
| 2.3 | Application. | 21 |
| | 2.3.1 Drug Delivery | 21 |
| | 2.3.2 Surgery | 23 |
| | 2.3.3 Biosensing. | 25 |
| 2.4 | Conclusion | 27 |
| | References. | 28 |
| 3 | Biomolecule-Based Nanorobot for Targeted Delivery of Therapeutics | 35 |
| | Keya Ganguly, Sayan Deb Dutta, Dinesh K. Patel, Tejal V. Patil, Rachmi Luthfikasari, and Ki-Taek Lim | |
| 3.1 | Introduction | 35 |
| 3.2 | DNA and Proteins | 36 |
| 3.3 | CAD Systems for Bio-nanorobotics Simulation | 38 |
| 3.4 | Biomolecule-Loaded Therapeutic Delivery. | 39 |
| | 3.4.1 Pharmaceuticals | 39 |
| | 3.4.2 Biologics and Genes | 41 |
| | 3.4.3 Living Cell-Based Therapies | 42 |
| 3.5 | Selected Diseases. | 45 |

| | | |
|----------|--|-----------|
| 3.5.1 | Cancer | 45 |
| 3.6 | Challenges and Prospects. | 48 |
| | References. | 48 |
| 4 | Printable Nanorobots and Microswimmers for Therapeutic Advancement: Present Status and Future Opportunities | 53 |
| | Sayan Deb Dutta, Keya Ganguly, Dinesh K. Patel, Tejal V. Patil, Rachmi Luthfikasari, and Ki-Taek Lim | |
| 4.1 | Introduction | 53 |
| 4.2 | Overview of 3D Printing Techniques for Nanorobot Fabrication | 54 |
| 4.2.1 | Powder-Bed Fusion. | 55 |
| 4.2.2 | Vat Polymerization | 56 |
| 4.2.3 | Inkjet Printing | 57 |
| 4.2.4 | Extrusion and Direct-Ink-Writing Printing. | 57 |
| 4.2.5 | Direct Laser Writing Printing | 58 |
| 4.3 | Materials for 3D Printing of Micro-/Nanomotors | 60 |
| 4.4 | Shape Reconfiguration for Tunable Multifunctionality | 61 |
| 4.5 | Types of Nanomotors and Their Function | 63 |
| 4.5.1 | Helical Micro-/Nanoswimmers. | 63 |
| 4.5.2 | Tubular Micro-/Nanoswimmers | 64 |
| 4.5.3 | Micro-/Nanomotors with Mixed Functions | 66 |
| 4.6 | Propulsion Mechanism of Nanomotors | 66 |
| 4.6.1 | Chemical and Biological Propulsion | 66 |
| 4.6.2 | Magnetic Propulsion. | 67 |
| 4.6.3 | Ultrasonic Propulsion | 69 |
| 4.7 | Therapeutic Applications | 69 |
| 4.8 | Key Challenges and Future Outlook | 70 |
| 4.9 | Concluding Remarks | 73 |
| | References. | 74 |
| 5 | Fundamental in Polymer-/Nanohybrid-Based Nanorobotics for Theranostics. | 79 |
| | Tejal V. Patil and Ki-Taek Lim | |
| 5.1 | Introduction | 79 |
| 5.2 | Polymers | 82 |
| 5.2.1 | Natural Polymers | 83 |
| 5.2.2 | Synthetic Biopolymer | 87 |
| 5.3 | Fabrication of Theranostic Nanorobots | 90 |
| 5.3.1 | Magnetic Nanoparticle-Based Theranostics. | 90 |
| 5.3.2 | Micelles. | 91 |
| 5.3.3 | Dendrimers | 92 |
| 5.3.4 | Nanogels | 94 |
| 5.3.5 | Hybrid Conjugates | 96 |
| 5.4 | Bioconjugation Process | 97 |
| 5.5 | Application in Theranostics. | 98 |
| 5.5.1 | Cancer Diagnosis and Therapy | 98 |

| | | |
|----------|---|------------|
| 5.5.2 | Bacterial Infections and Wound Healing | 100 |
| 5.6 | Conclusion | 101 |
| | References | 101 |
| 6 | Magneto-Responsive Nanohybrids for Bioimaging | 109 |
| | S. T. Mhaske, D. A. Patil, and S. U. Mestry | |
| 6.1 | Introduction | 109 |
| 6.2 | Nanohybrids | 111 |
| 6.2.1 | Carbon-Carbon NHs | 112 |
| 6.2.2 | Carbon-Metal NHs | 113 |
| 6.2.3 | Metal-Metal NHs | 114 |
| 6.2.4 | Organic Molecule-Coated NHs | 114 |
| 6.2.5 | Virus Nanoparticles (VNPs) | 121 |
| 6.3 | Characterizations of Nanohybrids | 124 |
| 6.3.1 | ICP-MS and ICP-OES | 124 |
| 6.3.2 | EDS | 128 |
| 6.3.3 | SEM and TEM | 129 |
| 6.3.4 | XRD | 131 |
| 6.3.5 | Magnetic Properties of Nanohybrids | 131 |
| 6.4 | Conclusion | 134 |
| | References | 135 |
| 7 | Photothermal Nanomaterials for Wound Monitoring and Cancer Biomedicine | 139 |
| | Ashwini Shinde, Kavitha Illath, Sayan Deb Dutta, Ki-Taek Lim, and Tuhin Subhra Santra | |
| 7.1 | Introduction | 139 |
| 7.2 | Photothermal Nanomaterials: Application for Wound Healing and Monitoring | 142 |
| 7.2.1 | Photothermal and Photodynamic Therapy for Wound Healing | 143 |
| 7.2.2 | Photothermal Nanomaterials for Skin Wound Healing | 144 |
| 7.2.3 | Photothermal Nanomaterials for Bone and Cartilage Defects | 149 |
| 7.3 | Photothermal Nanomaterials: Applications for Cancer Biomedicine | 154 |
| 7.3.1 | Photothermal Therapy Using Metal Nanomaterials | 154 |
| 7.3.2 | Photothermal Therapy Using Semiconductor Nanomaterials | 156 |
| 7.3.3 | Photothermal Therapy Using Carbon-Based Nanomaterials | 158 |
| 7.3.4 | Photothermal Therapy Using Conducting Polymers | 159 |
| 7.4 | Limitations and Future Prospect | 161 |
| 7.5 | Conclusion | 163 |
| | References | 163 |

| | | |
|-----------|--|-----|
| 8 | Polymer Nanohybrid-Based Smart Platforms for Controlled Delivery and Wound Management | 171 |
| | Dinesh K. Patel, Tejal V. Patil, Keya Ganguly, Sayan Deb Dutta, Rachmi Luthfikasari, and Ki-Taek Lim | |
| 8.1 | Introduction | 171 |
| 8.2 | Classification of the Polymers | 173 |
| | 8.2.1 Natural Polymers | 173 |
| | 8.2.2 Synthetic Polymers | 174 |
| 8.3 | Kinds of Nanomaterials | 174 |
| | 8.3.1 0D and 1D Nanomaterials | 174 |
| | 8.3.2 2D and 3D Nanomaterials | 178 |
| 8.4 | Application of Polymer Nanohybrid-Based Smart Platforms | 179 |
| | 8.4.1 Delivery of Active Molecules | 179 |
| | 8.4.2 Wound Management | 185 |
| 8.5 | Conclusion | 192 |
| | References | 194 |
| 9 | Development of Efficient Strategies for Physical Stimuli-Responsive Programmable Nanotherapeutics | 201 |
| | Pravin P. Upare, Hyung Sub Shin, Jun Hak Lee, and Byung Gyu Park | |
| 9.1 | Introduction | 201 |
| 9.2 | Stimuli-Responsive Nanomaterials | 203 |
| | 9.2.1 Temperature-Responsive Nanomaterial | 203 |
| | 9.2.2 Ultrasound-Responsive Materials | 212 |
| | 9.2.3 Magnetic Field-Responsive Nanomaterials | 216 |
| 9.3 | Concluding Remarks and Future Perspectives | 221 |
| | References | 222 |
| 10 | The Flexible and Wearable Pressure Sensing Microsystems for Medical Diagnostics | 229 |
| | Hui Li, Ronghua Lan, Jing Chen, and Lin Li | |
| 10.1 | Introduction | 229 |
| 10.2 | Materials | 230 |
| | 10.2.1 Substrate Materials | 232 |
| | 10.2.2 Active Materials | 233 |
| 10.3 | Fundamentals of Pressure Sensors | 235 |
| | 10.3.1 Sensing Mechanisms | 235 |
| | 10.3.2 Key Parameters of Pressure Sensor | 238 |
| 10.4 | Applications for Flexible Pressure Sensors | 241 |
| | 10.4.1 Detecting Heart Rate or Pulse | 243 |
| | 10.4.2 Detecting Pressure In Vivo | 245 |
| | 10.4.3 Gait Monitoring | 246 |
| | 10.4.4 Recognition of Sound Signal | 248 |
| | 10.4.5 Breath Detection | 250 |

| | | |
|-----------|--|------------|
| 10.4.6 | Tactile Perception | 252 |
| 10.5 | Conclusions and Perspectives | 253 |
| | References | 255 |
| 11 | Microfluidics and Lab-on-a-Chip for Biomedical Applications | 263 |
| | Dinesh K. Patel, Maria Mercedes Espinal, Tejal V. Patil, Keya Ganguly, Sayan Deb Dutta, Rachmi Luthfikasari, and Ki-Taek Lim | |
| 11.1 | Introduction | 263 |
| 11.2 | Fabrication of Microfluidic System | 267 |
| 11.3 | Significance of Nonlinear Process in Microfluidics | 268 |
| 11.4 | Significance of Microfluidic Systems | 271 |
| 11.5 | Biomedical Applications | 273 |
| 11.5.1 | Organs-on-Chips (OoCs) | 273 |
| 11.5.2 | Lung-on-a-Chip (LuoC) | 274 |
| 11.5.3 | Brain-on-a-Chip (BoC) | 276 |
| 11.5.4 | Joint/Muscle-on-a-Chip (JoC) and Human-on-a-Chip (HoC) | 277 |
| 11.6 | Conclusion and Future Perspectives | 279 |
| | References | 279 |
| 12 | Lab-on-a-Chip Devices for Medical Diagnosis II: Strategies for Pathogen Detection | 285 |
| | Rachmi Luthfikasari, Tejal V. Patil, Dinesh K. Patel, Keya Ganguly, Sayan Deb Dutta, and Ki-Taek Lim | |
| 12.1 | Introduction | 285 |
| 12.2 | LoC Fabrication for Medical Diagnosis | 286 |
| 12.3 | Pathogen Diagnosis | 291 |
| 12.4 | Conclusion and Future Perspective | 295 |
| | References | 296 |
| 13 | Nanodiagnosics: New Tools for Detection of Animal Pathogens | 299 |
| | Atef A. Hassan, Rasha M. H. Sayed-ElAhl, Ahmed M. El Hamaky, Mogda K. Mansour, Noha H. Oraby, and Mahmoud H. Barakat | |
| 13.1 | Introduction | 299 |
| 13.2 | Traditional Methods for Detection of Animal Diseases | 300 |
| 13.3 | Recent Approaches of Nanomaterial Applications in Detection of Animal Diseases | 301 |
| 13.3.1 | Types of Nanodiagnosics | 301 |
| 13.3.2 | Biomedical Applications of Nanodiagnosics | 302 |
| 13.4 | Methods of Nanoparticle Functionalization for Disease Diagnosis | 306 |
| 13.4.1 | Immuno-Based Methods | 307 |
| 13.4.2 | Molecular-Based Methods | 310 |
| 13.5 | Nano Biosensors Using Biomarkers | 311 |
| 13.5.1 | Types of Biosensors | 311 |
| 13.5.2 | Optical Biosensor | 313 |

| | | |
|-----------|--|------------|
| 13.5.3 | Mass-Based Biosensor | 313 |
| 13.5.4 | Calorimetric Biosensor | 314 |
| 13.5.5 | Detection of Antibody Markers | 314 |
| 13.5.6 | DNA Sensors | 314 |
| 13.5.7 | Aptasensors | 315 |
| 13.5.8 | Immunosensors | 315 |
| 13.5.9 | Miscellaneous | 316 |
| 13.6 | Conclusions and Future Prospective | 316 |
| | References | 317 |
| 14 | Nano-Based Robotic Technologies for Plant Disease Diagnosis | 327 |
| | Farah K. Ahmed, Mousa A. Alghuthaymi, Kamel A. Abd-Elsalam, Mythili Ravichandran, and Anu Kalia | |
| 14.1 | Introduction | 327 |
| 14.2 | Pathogen Detection Methods | 329 |
| 14.2.1 | Morphological Tools | 330 |
| 14.2.2 | Molecular Tools | 330 |
| 14.2.3 | Omics Tools | 330 |
| 14.2.4 | Nano-Based Diagnostics Tools | 331 |
| 14.2.5 | Nanobiosensors | 336 |
| 14.2.6 | Nanochips | 339 |
| 14.2.7 | Nanopore-Based Detection | 339 |
| 14.3 | Robotics Techniques for Plant Pathogens Detection | 340 |
| 14.4 | Nanotools for Detection of Plant Pathogens | 342 |
| 14.4.1 | Detection of Bacterial Pathogens | 343 |
| 14.4.2 | Fungal Pathogens Detection | 344 |
| 14.4.3 | Viral Pathogen Detection | 345 |
| 14.5 | Diagnosis of the Plant Varieties and Other Forms | 346 |
| 14.6 | Challenges | 349 |
| 14.7 | Future Trends | 351 |
| 14.8 | Conclusions | 351 |
| | References | 352 |
| 15 | Nanodiagnostic Tools for Mycotoxins Detection | 361 |
| | Velaphi C. Thipe, Giovanna de Oliveira Asenjo Mendes, Victoria M. Alves, Thayna Souza, Rachel Fanelwa Ajayi, Ademar B. Lugao, and Kattesh V. Katti | |
| 15.1 | Introduction | 362 |
| 15.2 | Conventional Diagnostics for Mycotoxins in Agriculture | 363 |
| 15.3 | Nanosurveillance to Mitigate Mycotoxins | 365 |
| 15.4 | Nanodiagnosics for Mycotoxins | 366 |
| 15.4.1 | Sensors Based on Nanomaterials for Mycotoxin Surveillance | 366 |
| 15.4.2 | Metallic Nanoparticles | 367 |

| | | |
|-----------|--|------------|
| 15.5 | Smart Nanosensors. | 367 |
| 15.5.1 | Nanoparticles with Conductivity-Based Sensors. | 367 |
| 15.5.2 | Antibody-Coupled Nanomaterials. | 370 |
| 15.6 | Smart and Antifungal Packaging Nanosurveillance. | 376 |
| 15.7 | Concluding Remarks | 377 |
| | References. | 378 |
| 16 | CRISPR/Cas Systems: A New Biomedical and Agricultural Diagnostic Devices for Viral Diseases | 383 |
| | Aftab Ahmad, Sabin Aslam, Ahmad Munir, Farah K. Ahmed, and Kamel A. Abd-Elsalam | |
| 16.1 | Introduction | 383 |
| 16.2 | CRISPR/Cas-Based Diagnostic Tools | 385 |
| 16.2.1 | CRISPR: An Introduction | 385 |
| 16.2.2 | Applications of CRISPR | 385 |
| 16.2.3 | CRISPR/Cas. | 386 |
| 16.2.4 | CRISPR/Cas Mechanism. | 386 |
| 16.2.5 | CRISPR/Cas System | 388 |
| 16.2.6 | CRISPR Methods and Techniques. | 390 |
| 16.2.7 | CRISPR/Cas Diagnostic Tools. | 392 |
| 16.2.8 | Challenges | 405 |
| 16.2.9 | Conclusion and Future Outlook | 407 |
| | References. | 407 |
| 17 | DNA-Nanosensors for Environmental Monitoring of Heavy Metal Ions | 411 |
| | Heba Elbasiouny, Nahed S. Amer, Sherifa F. M. Dawoud, Amina M. G. Zedan, and Fathy Elbehiry | |
| 17.1 | Introduction | 411 |
| 17.2 | Heavy Metals Pollution and Detection | 413 |
| 17.3 | Nanobiosensors and Pollution Detection. | 414 |
| 17.4 | DNA Biosensor and DNA Nanobiosensors. | 418 |
| 17.5 | Nanosensors and DNA Nanosensors for Heavy Metals Detection | 421 |
| 17.6 | Challenges | 426 |
| 17.7 | Conclusion and Future Prospective | 427 |
| | References. | 428 |
| 18 | Smart Nanosensors for Pesticides and Heavy Metals Detection. | 433 |
| | Nilesh Satpute, Kamlesh Shrivastava, and Khemchand Dewangan | |
| 18.1 | Introduction | 433 |
| 18.2 | Overview of Sensing Techniques. | 435 |
| 18.2.1 | The Need for Smart and Intelligent Nanosensors | 435 |
| 18.2.2 | Smart Nanosensors and Nanobiosensors | 436 |
| 18.2.3 | Operation Modes of Nanosensors | 436 |

| | | |
|--------------|---|------------|
| 18.3 | Nanomaterials and their Types..... | 437 |
| 18.3.1 | General Aspect of Nanomaterials..... | 437 |
| 18.3.2 | Type of Nanomaterials..... | 438 |
| 18.4 | Nanomaterial-Based Nanosensors/Nanobiosensors and Their Applications..... | 439 |
| 18.4.1 | Nanosensors for Pesticides and Heavy Metal Detection..... | 440 |
| 18.4.2 | Nanobiosensors for Pesticides and Heavy Metal Detection..... | 443 |
| 18.5 | Conclusion and Future Prospective..... | 447 |
| | References..... | 448 |
| Index | | 453 |

Chapter 1

Nanorobotics and Nanodiagnostics in Integrative Biology and Biomedicine: A Note from the Editors



Ki-Taek Lim and Kamel A. Abd-Elsalam 

1.1 Introduction

Nanorobotics and nanodiagnostics are the emerging fields of biomedical nanotechnology that have revolutionized biomedical research and biomedicine (Wang et al. 2021a; Moniz and Krings 2022; Guo et al. 2022; Lastra et al. 2021). While nanorobotics includes robots performing at a nanometer scale inside the dynamic human body system, nanodiagnostics implies the application of nanotechnology in molecular diagnosis-based health monitoring and treatment (Moffatt 2016; Wang 2021). Nanorobotics and nanodiagnostics are thus the current techniques developed for nanotechnology-based healthcare (Kala et al. 2022; Salamanca-Buentello and Daar 2021).

The word “robot” evokes a plethora of images, either as the humanoid machine created to serve humanity or as a dangerous technological invention that might have an adverse effect. Robotic inventions have expanded since the twentieth century despite robo-ethical skepticism. With their massive impression on the industrial front, the confluence of diverse technologies has enabled a robotic revolution in biomedical and biotechnological applications. Tremendous advancements have been achieved in medical and agricultural robotics with macroscale robotic designs. For example, a few currently developed robots used in hospitals and medical centers include the *da Vinci*[®] surgical robot, the Xenex germ-zapping robot, the PARO

K.-T. Lim (✉)

Department of Biosystems Engineering, Kangwon National University,
Chuncheon, Republic of Korea
e-mail: ktlim@kangwon.ac.kr

K. A. Abd-Elsalam

Agricultural Research Center, Plant Pathology Research Institute, Giza, Egypt

therapeutic robot, the CyberKnife radiation therapy robot, and the TUG material handling robot (Ginoya et al. 2021).

Similarly, the rise of artificial intelligence has caused the world of agricultural robotics to explode with innovation. These include Ecorobotix, the weed removal drone, Naïo Technologies perfect farm hand robot, Energid citrus picking system, Agrobot E-series, Blue River LettuceBot2, Agribotix, Vision Robotics, RoBoPlant, and PrecisionHawk (Gil et al. 2023). Despite these innovations, we are yet to create robots that can delve deep into living organisms to work at the cellular or subcellular levels. Therefore, designing miniaturized and versatile robots at a nanometer scale would allow precise access at the cellular level for biomedical and agro-economic breakthrough achievements. Small-scale nanorobots have extensively been investigated for targeted drug delivery, biosensing, single-cell manipulation strategies, surgery, tumor therapy, and many more (Fig. 1.1) (Li and Pumera 2021). Most nanorobots synthesized for such biomedical applications are nature-inspired and involve various thermodynamic parameters such as motion, momentum, solvation, and heat dissipation, among others. For instance, mimicking the molecular structure and function of cellular structures like actin-myosin and transporting cargo has been attempted with great zeal. Despite the effort, the synthetically designed nanomotors are still distant from resembling their natural counterparts (Mavroidis and Ferreira 2013). One of the reasons for the difference is their challenging fabrication process which is crucial in determining the success of the nanobots. Most fabrication techniques involve the bottom-up or top-down approaches. The top-down approach comprises physical vapor deposition, roll-up techniques for the fabrication of nanotubes and helical nanobots, and the 3D printing techniques including direct ink writing. The bottom-up strategy includes wet chemical synthesis, self-assembly techniques, and electrochemical deposition methods.

Several notable examples, including the construction of molecular shuttles, molecular cars, and molecular pumps, have gained worldwide recognition for transporting molecules and desired cellular functions (Stoddart 2017). The design of nanorobots for biomedical applications requires refined structural design (rigid or soft) and component design (micro/nano, rigid/flexible, tubes/helical) to suit the demands of the human-machine interface. The elements highly favored in the fabrication of nanobots for biomedical applications are shown in Fig. 1.2. It includes ~20 elements, including metals, non-metals, and transitional elements. The compositional design of the nanorobots determines the functionality, biocompatibility, and biodegradability of the nanobots. Many biodegradable micro-/nano-machines have been developed for in vivo use like Mg, Zn, and CaCO₃ (Wang et al. 2021a).

Similarly, modern diagnostics aims to be precise, rapid, and inexpensive at the early detection of diseases. In this regard, nanodiagnosics uses advances in nanotechnology to diagnose, investigate, and treat diseases at the molecular level (Woodman et al. 2021; Sabir et al. 2021; Zhang et al. 2018). Ideally, but not limited to, the advanced nanodiagnosics tools are designed to address the urgency of early detection followed by effective treatment cost-effectively. Unquestionably, the choice of nanomaterial is a crucial determining factor that governs the success of nanodiagnosics (Li et al. 2020a). Remarkably, the functionalization of

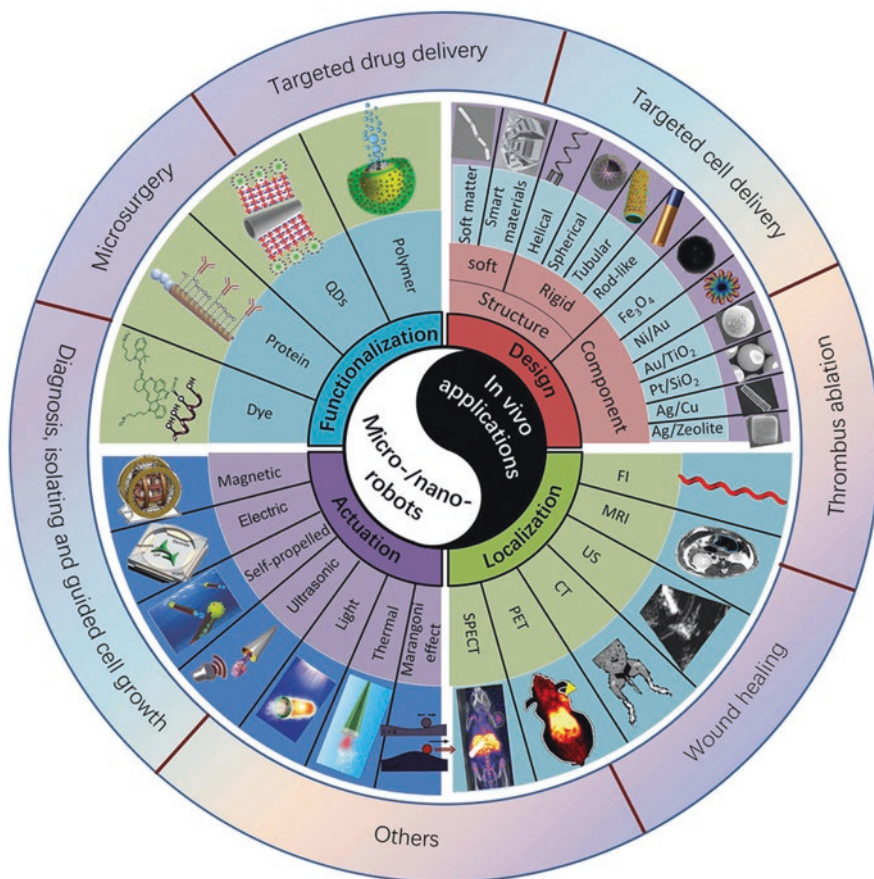


Fig. 1.1 The design, functionalization, actuation, and localization of micro–/nanobots for bio-medical applications, including microsurgery, targeted drug delivery, targeted cell delivery, thrombus ablation, wound healing, diagnosis, and other applications. (Wang et al. 2021a)

Elements for m-bots design

| IIA | | Elements for m-bots design | | | | | | | | | | | | | | | | IIIA | IVA | VA | VIA | |
|------------------|----|----------------------------|----|------------------|------------------|------------------|------------------|------------------|------------------|------------------|------------------|------------------|------------------|----|--|--|--|------|------------------|------------------|-----------------|-----------------|
| Be | | | | | | | | | | | | | | | | | | B | C | N | O | |
| ¹² Mg | | | | | | | | | | | | | | | | | | | ¹³ Al | ¹⁴ Si | ¹⁵ P | ¹⁶ S |
| ²⁰ Ca | Sc | ²² Ti | V | ²⁴ Cr | ²⁵ Mn | ²⁶ Fe | ²⁷ Co | ²⁸ Ni | Cu | ³⁰ Zn | ³¹ Ga | Ge | As | Se | | | | | | | | |
| Sr | Y | Zr | Nb | Mo | Tc | ⁴⁴ Ru | Rh | ⁴⁶ Pd | ⁴⁷ Ag | Cd | ⁴⁹ In | ⁵⁰ Sn | Sb | Te | | | | | | | | |
| Ba | Lu | Hf | Ta | W | Re | Os | ⁷⁷ Ir | ⁷⁸ Pt | ⁷⁹ Au | Hg | Tl | Pb | ⁸³ Bi | Po | | | | | | | | |

Fig. 1.2 Periodic table showing the elements (orange boxes) useful in fabricating nanorobots for biomedical applications. (Wang et al. 2021a)

nanomaterials and their biocompatibility, retention effect in the body, responsiveness to stimuli, and biosensing properties are among the vital qualities that connect diagnosis and therapy, commonly referred to as theranostic (Zhong et al. 2022). Moreover, the choice of polymer can synergistically affect the overall property of the developed nanodiagnosics platforms (Jaymand 2019). The modulus and stiffness of the component polymer greatly determine the physicochemical and physiological properties of the soft nanorobots, like changing shapes during navigation (Liu et al. 2019; Gan et al. 2019).

For instance, polymer-nanomaterial-based innovative materials are heavily used for targeted drug delivery (Singh et al. 2021; Jana et al. 2021), photothermal therapy (Chen et al. 2021; Zhen et al. 2021; Wang et al. 2021b), flexible sensors (Zhou et al. 2021a; Tao et al. 2021; Xu et al. 2021), and microfluidic devices (Han et al. 2022; Shakeri et al. 2021) for numerous applications in biomedicine. Researchers have fabricated a myriad of *in vitro* biomolecular assessment nanodevices. The targeted analytes generally include DNA (Zhou et al. 2021b; Li et al. 2021), RNA (Basiri et al. 2021; Verma et al. 2022), peptides (Amarasekara et al. 2022; Sitkov et al. 2021; Gachpazan et al. 2021), antibodies (Silva 2021; Liu et al. 2021), antigen (Cate et al. 2015; Barbosa et al. 2015), secretomes (Marrazzo et al. 2021; Hu et al. 2018; Kshitiz et al. 2019), and other small analytes (Beauchamp et al. 2019). However, the use of nanomaterials and polymer-nanohybrids for *in vivo* disease diagnosis and treatment is in its infancy, mainly owing to unpreventable toxicity, clearance machinery, and limited device sensitivity. Nevertheless, such limitations are expected to be overcome steadily but certainly (Park et al. 2017). Similarly, developments have been made toward enhancing the diagnostic potential of clinically translatable *in vivo* nanodiagnosics platforms.

Besides the structural designs and composition, the operation of nanorobots is greatly determined by the responsiveness of the component materials to external stimuli. Stimuli (pH, redox, chemical, photo, photothermal) have been an obvious scenario implemented to carry out the desired functioning of the nanobots in many cases (Li et al. 2017). Artificial molecular machines such as “rotaxane” and “catenanes” have been promising in developing nanobots for medicine (Harada et al. 2009). Rotaxane comprises “dumbbell-shaped molecular structures interlocked through macrocycle chemical moieties”. This structural feature has enabled the synthesis of many biomimicked structures like ion transports (Chen et al. 2018) and DNA rotaxane actuators (Yu et al. 2021; Ackermann et al. 2010). On the other hand, molecular nanocars are being intensively researched for the fabrication of nanovehicles equipped with chemical chassis, wheels, and chemical motor groups to power the displacement of the nanovehicles (Joachim and Rapenne 2013). Interestingly, researchers have even successfully synthesized peptides in milligram quantities by developing an artificial rotaxane assembly line resembling the arrangement of ribosomes. The molecular assembly line could travel along a molecular strand, picking up amino acids on its way and synthesizing peptides in a sequence-specific manner (Lewandowski et al. 2013). These inventions have undoubtedly paved the bright future for developing more sophisticated nanobots for biomedical applications and agroecosystem management (Buriak et al. 2022). Nanodiagnosics technology and

artificial intelligence have revolutionized the early detection of plant diseases caused by viruses, fungi, and other pathogens. Moreover, the CRISPR-Cas system has ramped up the disease diagnosis in crops. Innovative nanosensors are teeming in detecting pesticides and heavy metals (Li et al. 2020b).

The first edition of *Nanorobotics and Nanodiagnostics in Integrative Biology and Biomedicine* is an initiative to bring insight into some recent signs of progress with robots at the nanoscale in the biomedical/agricultural realm propelled murky scientific fantasy to apparent reality. In our attempt to dive deeper into the progress of nanobots in biomedicine, we have primarily focused on discussing the goals associated with nanobots in drug delivery, surgery, and biosensing through the perspective of tissue engineering and regenerative medicine. We then go on to describe the latest technologies used in the fabrication of these nanobots. Besides, we focus on using external stimuli to achieve the desired function using the nanobots. Furthermore, we discuss nanotechnology in diagnostics emphasizing the latest advances in some selected areas of medical applications, including photothermal nanomaterials, polymer-nanohybrid-based intelligent platforms, and physical stimuli responsive programmable nanotherapeutics, pressure sensing microsystems in medical diagnostics, and microfluidic and lab-on-a-chip devices in biomedicine. We briefly discussed the current status of nanodiagnostics in the agroecosystem.

1.2 Historical Background

The idea of injecting robots inside the human body was introduced as early as 1986 by K. Eric Drexler. An analogy that used protein molecules as molecular motors and bearings was envisioned to perform complex tasks like rotating and moving molecules in living cells (Drexler 1986). The idea found its expression through the marvelous design of Robert A. Freitas, who simulated a few of the earliest nanomedical devices that could function as artificial erythrocytes (respirocytes), and artificial platelets (clottocytes), and hypothetical nanobots that could destroy microbes (microbivores). These artificial nanodevices termed respirocytes are expected to deliver 236 times more oxygen to the tissue pre-unit volume w.r.t. the natural red blood cells (Fig. 1.3a). The respirocyte is built of tough diamondoid material, equipped with various chemical, thermal, and pressure sensors. Additionally, the nanodevices will operate through an onboard nano-computer and are remotely reprogrammable via external acoustic signals. The nanobot is designed to draw power from natural serum glucose. The respirocyte would harbor water ballast chambers responsible for controlling neutral buoyancy. Strikingly, the respirocyte is quick-witted and can be stored virtually incessantly (Fig. 1.3b). With the advancement in nanotechnology regarding power supply, nanoscale computation, atomic-scale manipulation, biocompatibility, and specific communication, we can hope to bring the respirocyte to reality. In modern medical practices, respirocytes are perceived as an alternative to red blood cell transfusion without needing blood grouping. These nanobots can overcome the transmission of disease vectors like HIV,

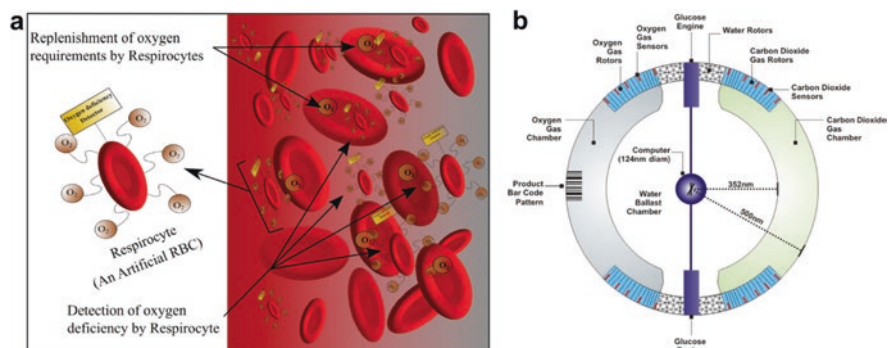


Fig. 1.3 Erythrocyte mimicking respirocyte. (a) Respirocyte nanobot carrying oxygen like an artificial erythrocyte (Suhail et al. 2022). (b) The transverse sectional view of the hypothetical respirocyte indicating the designed attributes. (Manjunath and Kishore 2014)

hepatitis, and venereal diseases. They can serve the treatment of anemia since they can increase the oxygen-carrying capacity. Similarly, clottocytes have been theoretically designed to attain hemostasis in about a second, making them 100–1000 times faster than the natural hemostatic system. The instant hemostasis could provide a unique super-biological capability in biomedicine.

The clottocytes (or artificial mechanical platelets) nanobots are hypothetically designed to mimic spherical blood platelets (~2 microns) powered by serum-oxyglucose entrapped in a fiber mesh compactly folded onboard. Upon command from its control computer, the device promptly unfurls its mesh packet near an injured blood vessel. Similarly, numerous other nanobots used in medicine include vasculoids, pharmacocytes, chromalloocytes, dentifrobots, and microbivores.

As we look forward to establishing the hypothetical nanobots in medical applications, the multitude of research works representing the present status in nanorobotics and nanodiagnostics bears a somewhat different picture. Researchers throughout the globe are developing nanorobots using nanomaterials, metal oxides, polymers, and biomolecules, in conjugation with nanoelectronic facilities to target drug delivery, surgery, biosensing of analytes, or pathogens, theranostic, and wound management, to name a few. While significant attention is drawn to treating cancer, diabetes, cardiovascular diseases, arthritis, anemia, and infectious diseases are at par in nanobot-mediated therapies' surveillances. One of the critical aspects in determining the efficiency of the nanobots is the functionalization of the bots with desirable chemical moieties, equipping them for donor-recipient interactions. Remarkable research outcomes have been demonstrated in recent inventions. Self-propelled microtubular engines composed of gold, nickel, polyaniline, and platinum are designed for the rapid, real-time isolation of *Escherichia coli* (*E. coli*) bacteria from clinical samples when functionalized with concanavalin A (ConA) bioreceptor. Moreover, the microengine was capable of on-demand drug delivery (Campuzano

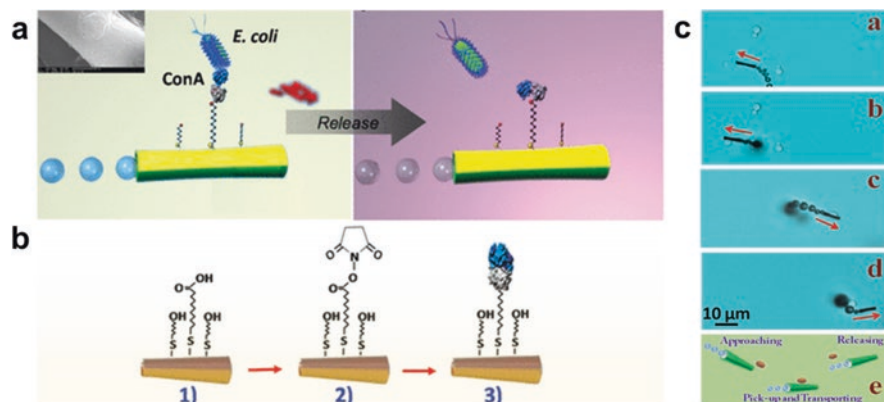


Fig. 1.4 Micro-/nano-engines for (a) bacterial isolation showing the selective capturing, transport, and release of bacteria by the ConA-modified microbot (Campuzano et al. 2012). (b) The functionalization of the microbot surface with lectin receptor (Campuzano et al. 2012). (c) PAPBA/Ni/Pt microbot-mediated capture, transport, and release of yeast cells. (Kuralay et al. 2012)

et al. 2012). Not only bacteria but researchers have also developed robotic systems that can transport yeast cells in media. Such a microtube device was made up of poly(3-aminophenylboronic acid) (PAPBA)/Ni/Pt functionalized with boronic acid that could selectively recognize and bond with the monosaccharide of the yeast cells (Fig. 1.4) (Kuralay et al. 2012). Ultrasound-actuated nanobots designed for the detoxification in bio-systems have shown excellent motility inside blood vessels, and the functional proteins of the hybrid system endowed the bots the potentiality to capture *Staphylococcus* bacteria and neutralize their α -toxins (Fig. 1.5) (Xu et al. 2015). A list of the in vivo applications of micro-/nanobots is summarized in Table 1.1.

Broadly, nanodiagnostics has already made a profound impact in biomedical applications. The constant giant strides in the fields of nanodiagnostics give high hope for more possibilities owing to the physicochemical properties of the components, the sensitivity of the nanodiagnostics platforms, cost-effective production, and point-of-care diagnostic tools, which are expected to attain high success based on global coordination. Most nanomaterials that have played crucial roles in the success of nanodiagnostics include nanotubes of carbon, silicon, and nanocrystals; nanobots, nanowires, quantum dots, and several nanotechnology-based biochips; and microfluidic arrays. Based on the terms mentioned above, we have included some selected areas in nanorobotics and nanodiagnostics in healthcare and agricultural applications in our following chapters.

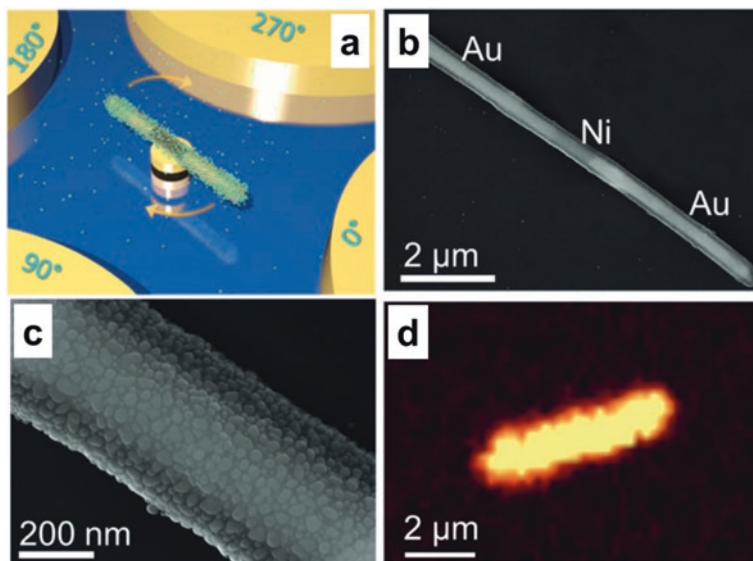


Fig. 1.5 (a) Illustration of a rotary nanomotors sensor releasing molecules. (b) Scanning electron microscopy (SEM) images of the three-layered plasmonic nanorod of Au-Ni-Au nanowire core, a silica coating, and (c) a dense layer of Ag nanoparticles on the outer surface of silica. (d) Raman mapping of 1 μM R6G dispersed on a plasmonic rotor showing essentially uniform SERS intensity on the surface. (Xu et al. 2015)

1.3 Overview of the Book

The Springer book of *Nanorobotics and Nanodiagnostics in Integrative Biology and Biomedicine* presents selected topics in nanorobotics and nanodiagnostics from the perspective of tissue engineering and regenerative medicine. Accordingly, we have arranged the chapters in three sections, including nanorobotics in biomedicine, nanodiagnostics in biomedicine, and nanodiagnostics in the agroecosystem. “Nanorobotics in biomedicine” comprises five chapters presenting some general concepts of nanobots for drug delivery, surgery, and biosensing application; the latest printing technology used in the fabrication of the nanobots in biomedicine; polymer-nanohybrid-based nanobots for theranostic; and stimuli-responsive nanohybrid for bioimaging. “Nanodiagnostics in biomedicine” comprises seven chapters focusing on photothermal nanomaterials for wound monitoring, polymer-nanohybrid-based smart platforms in tissue engineering, and stimuli-responsive programmable nanotherapeutics, flexible sensors in medical diagnostics, and lab-on-a-chip devices in nanodiagnostics. “Nanodiagnostics in agroecosystem” includes five chapters describing nano-based robotic technologies for plant pathogen and disease diagnosis, CRISPR-Cas system in diagnostic devices, smart nanosensors for pesticide, mycotoxin, and heavy metal detection.

Table 1.1 Selected list of notable in vivo applications of micro-/nanobots (Wang et al. 2021a)

| In vivo application | Material | Geometry | Propulsion mode | Method | Animal model | Targeting site | Delivery method |
|---------------------|----------------------------------|-----------------------|-------------------|--------------------------|---------------|--|------------------------------------|
| Microsurgery | Cu, Ni, Cr, Si, polymer | Starfish-like gripper | Magnetic | Photolithography | Pig | Bile duct | Catheter from the mouth |
| Thrombus ablation | PS, Ni | Rod-like | Magnetic | Oblique angle deposition | Mouse | Femoral vessel | Retro-orbital IV injection |
| Delivery | Photoresist, Ni, Ti, NIR-797 dye | Helical flagella | Magnetic | DLW and surface grafting | Mouse | Intraperitoneal cavity | Injected to intraperitoneal cavity |
| Wound healing | CaCO ₃ , organic acid | Sphere | Bubble propulsion | Wet chemical method | Mouse and pig | Mouse liver and tail, pig femoral artery | Topical application |
| Drug delivery | Mg, Au, PEDOT | Tubular | Bubble propulsion | Template method | Mouse | Gastrointestinal tract | Oral administration |

The book is interdisciplinary and expected to serve students, teachers, researchers, and scientists in nanotechnology, material science, biology, chemistry, biophysics, biomedical engineering, agricultural sciences, and biotechnology. The content of the chapters has been designed keeping in mind the broad research audience. Each chapter is preceded by a summary, introductory section, and the current trend in the research topic, followed by the conclusion.

1.4 Conclusion

The advancements in nanorobotics and nanodiagnostics are expected to revolutionize the healthcare system. Modern diagnostics aims to be precise, rapid, and inexpensive at the early detection of diseases. In this regard, nanodiagnostics uses advances in nanotechnology to diagnose, investigate, and treat diseases at the molecular level. The constant giant strides in the fields of nanodiagnostics give high hope for more possibilities owing to the physicochemical properties of the components, the sensitivity of the nanodiagnostics platforms, cost-effective production, and point-of-care diagnostic tools, which are expected to attain high success based on global coordination.

Acknowledgments This work was supported by the “Basic Science Research Program” through the “National Research Foundation of Korea” funded by the Ministry of Education (NRF-2018R1A16A1A03025582, NRF- 2019R1D1A3A03103828, and NRF- 2022R1I1A3063302).

References

- Ackermann D, Schmidt TL, Hannam JS, Purohit CS, Heckel A, Famulok M. A double-stranded DNA rotaxane. *Nat Nanotechnol.* 2010;5:436–42.
- Amarasekara H, Oshaben KM, Jeans KB, Rezvan Sangsari P, Morgan NY, O’Farrell B, et al. Cyclopentane peptide nucleic acid: gold nanoparticle conjugates for the detection of nucleic acids in a microfluidic format. *Biopolymers.* 2022;113:e23481.
- Barbosa AI, Gehlot P, Sidapra K, Edwards AD, Reis NM. Portable smartphone quantitation of prostate specific antigen (PSA) in a fluoropolymer microfluidic device. *Biosens Bioelectron.* 2015;70:5–14.
- Basiri A, Heidari A, Nadi MF, Fallahy MTP, Nezamabadi SS, Sedighi M, et al. Microfluidic devices for detection of RNA viruses. *Rev Med Virol.* 2021;31:1–11.
- Beauchamp MJ, Nielsen AV, Gong H, Nordin GP, Woolley AT. 3D printed microfluidic devices for microchip electrophoresis of preterm birth biomarkers. *Anal Chem.* 2019;91:7418–25.
- Buriak JM, Liz-Marzán LM, Parak WJ, Chen X. *Nano and plants.* ACS Publications; 2022. p. 1681–4.
- Campuzano S, Orozco J, Kagan D, Guix M, Gao W, Sattayasamitsathit S, et al. Bacterial isolation by lectin-modified microengines. *Nano Lett.* 2012;12:396–401.
- Cate DM, Adkins JA, Mettakoonpitak J, Henry CS. Recent developments in paper-based microfluidic devices. *Anal Chem.* 2015;87:19–41.

- Chen S, Wang Y, Nie T, Bao C, Wang C, Xu T, et al. An artificial molecular shuttle operates in lipid bilayers for ion transport. *J Am Chem Soc.* 2018;140:17992–8.
- Chen Y, Sun B, Jiang X, Yuan Z, Chen S, Sun P, et al. Double-acceptor conjugated polymers for NIR-II fluorescence imaging and NIR-II photothermal therapy applications. *J Mater Chem B.* 2021;9:1002–8.
- Drexler KE. *Engines of creation.* Anchor Books; 1986.
- Gachpazan M, Mohammadinejad A, Saeidinia A, Rahimi HR, Ghayour-Mobarhan M, Vakilian F, et al. A review of biosensors for the detection of B-type natriuretic peptide as an important cardiovascular biomarker. *Anal Bioanal Chem.* 2021;413:5949–67.
- Gan T, Shang W, Handschuh-Wang S, Zhou X. Light-induced shape morphing of liquid metal nanodroplets enabled by polydopamine coating. *Small.* 2019;15:1804838.
- Gil G, Casagrande D, Cortés LP, Verschae R. Why the low adoption of robotics in the farms? Challenges for the establishment of commercial agricultural robots. *Smart Agric Technol.* 2023;3:100069.
- Ginoya T, Maddahi Y, Zareinia K. A historical review of medical robotic platforms. *J Robot.* 2021;2021:6640031.
- Guo Y, Chen W, Zhao J, Yang G-Z. Medical robotics: opportunities in China. *Annu Rev Control Robot Auton Syst.* 2022;5:361–83.
- Han X, Zhang Y, Tian J, Wu T, Li Z, Xing F, et al. Polymer-based microfluidic devices: a comprehensive review on preparation and applications. *Polym Eng Sci.* 2022;62:3–24.
- Harada A, Hashidzume A, Yamaguchi H, Takashima Y. Polymeric rotaxanes. *Chem Rev.* 2009;109:5974–6023.
- Hu Q, Luni C, Elvassore N. Microfluidics for secretome analysis under enhanced endogenous signaling. *Biochem Biophys Res Commun.* 2018;497:480–4.
- Jana P, Shyam M, Singh S, Jayaprakash V, Dev A. Biodegradable polymers in drug delivery and oral vaccination. *Eur Polym J.* 2021;142:110155.
- Jaymand M. Chemically modified natural polymer-based theranostic nanomedicines: are they the golden gate toward a de novo clinical approach against cancer? *ACS Biomater Sci Eng.* 2019;6:134–66.
- Joachim C, Rapenne G. Molecule concept nanocars: chassis, wheels, and motors? *ACS Nano.* 2013;7:11–4.
- Kala D, Gupta S, Kaushal A. Nanotechnology in healthcare. In: *Synthesis and applications of nanoparticles.* Springer; 2022. p. 405–16.
- Kshitiz, Ellison DD, Suhail Y, Afzal J, Woo L, Kilic O, et al. Dynamic secretome of bone marrow-derived stromal cells reveals a cardioprotective biochemical cocktail. *Proc Natl Acad Sci.* 2019;116:14374–83.
- Kuralay F, Sattayasamitsathit S, Gao W, Uygun A, Katzenberg A, Wang J. Self-propelled carbohydrate-sensitive microtransporters with built-in boronic acid recognition for isolating sugars and cells. *J Am Chem Soc.* 2012;134:15217–20.
- Lastra LS, Sharma V, Farajpour N, Nguyen M, Freedman KJ. Nanodiagnosics: a review of the medical capabilities of nanopores. *Nanomedicine.* 2021;37:102425.
- Lewandowski B, De Bo G, Ward JW, Papmeyer M, Kuschel S, Aldegunde MJ, et al. Sequence-specific peptide synthesis by an artificial small-molecule machine. *Science.* 2013;339:189–93.
- Li J, Pumera M. 3D printing of functional microrobots. *Chem Soc Rev.* 2021;50:2794–838.
- Li T, Li J, Morozov KI, Wu Z, Xu T, Rozen I, et al. Highly efficient freestyle magnetic nanoswimmer. *Nano Lett.* 2017;17:5092–8.
- Li B, Tan Q, Fan Z, Xiao K, Liao Y. Next-generation theranostics: functionalized nanomaterials enable efficient diagnosis and therapy of tuberculosis. *Adv Ther.* 2020a;3:1900189.
- Li Z, Yu T, Paul R, Fan J, Yang Y, Wei Q. Agricultural nanodiagnosics for plant diseases: recent advances and challenges. *Nanoscale Adv.* 2020b;2:3083–94.
- Li Z, Bai Y, You M, Hu J, Yao C, Cao L, et al. Fully integrated microfluidic devices for qualitative, quantitative and digital nucleic acids testing at point of care. *Biosens Bioelectron.* 2021;177:112952.

- Liu M, Wang Y, Kuai Y, Cong J, Xu Y, Piao HG, et al. Magnetically powered shape-transformable liquid metal micromotors. *Small*. 2019;15:1905446.
- Liu SC, Yoo PB, Garg N, Lee AP, Rasheed S. A microfluidic device for blood plasma separation and fluorescence detection of biomarkers using acoustic microstreaming. *Sensors Actuators A Phys*. 2021;317:112482.
- Manjunath A, Kishore V. The promising future in medicine: nanorobots. *Biomed Sci Eng*. 2014;2:42–7.
- Marrazzo P, Pizzuti V, Zia S, Sargenti A, Gazzola D, Roda B, et al. Microfluidic tools for enhanced characterization of therapeutic stem cells and prediction of their potential antimicrobial secretome. *Antibiotics*. 2021;10:750.
- Mavroidis C, Ferreira A. Nanorobotics: past, present, and future. In: *Nanorobotics*. Springer; 2013. p. 3–27.
- Moffatt S. Nanodiagnosics: a revolution in biomedical nanotechnology. *MOJ Proteom Bioinform*. 2016;3:00080.
- Moniz AB, Krings B-J. “Manufacturing life” in real work processes? New manufacturing environments with micro-and nanorobotics. *NanoEthics*. 2022;16:115–31.
- Park S-m, Aalipour A, Vermesh O, Yu JH, Gambhir SS. Towards clinically translatable in vivo nanodiagnosics. *Nat Rev Mater*. 2017;2:1–20.
- Sabir F, Barani M, Mukhtar M, Rahdar A, Cucchiari M, Zafar MN, et al. Nanodiagnosis and nanotreatment of cardiovascular diseases: an overview. *Chemosensors*. 2021;9:67.
- Salamanca-Buentello F, Daar AS. Nanotechnology, equity and global health. *Nat Nanotechnol*. 2021;16:358–61.
- Shakeri A, Khan S, Didar TF. Conventional and emerging strategies for the fabrication and functionalization of PDMS-based microfluidic devices. *Lab Chip*. 2021;21:3053–75.
- Silva MLS. Microfluidic devices for glyco-biomarker detection in cancer. *Clin Chim Acta*. 2021;521:229–43.
- Singh N, Son S, An J, Kim I, Choi M, Kong N, et al. Nanoscale porous organic polymers for drug delivery and advanced cancer theranostics. *Chem Soc Rev*. 2021;50:12883–96.
- Sitkov N, Zimina T, Kolobov A, Karasev V, Romanov A, Luchinin V, et al. Toward development of a label-free detection technique for microfluidic fluorometric peptide-based biosensor systems. *Micromachines*. 2021;12:691.
- Stoddart JF. Mechanically interlocked molecules (MIMs) – molecular shuttles, switches, and machines (Nobel Lecture). *Angew Chem Int Ed*. 2017;56:11094–125.
- Suhail M, Khan A, Rahim MA, Naeem A, Fahad M, Badshah SF, et al. Micro and nanorobot-based drug delivery: an overview. *J Drug Target*. 2022;30:349–58.
- Tao X, Liao S, Wang Y. Polymer-assisted fully recyclable flexible sensors. *EcoMat*. 2021;3:e12083.
- Verma N, Walia S, Pandya A. Micro/nanofluidic devices for DNA/RNA detection and separation. In: *Micro/nanofluidics and lab-on-chip based emerging technologies for biomedical and translational research applications-Part A*; 2022. p. 85.
- Wang J. Will future microbots be task-specific customized machines or multi-purpose “all in one” vehicles? *Nat Commun*. 2021;12:1–3.
- Wang B, Kostarelos K, Nelson BJ, Zhang L. Trends in micro-/nanorobotics: materials development, actuation, localization, and system integration for biomedical applications. *Adv Mater*. 2021a;33:2002047.
- Wang S, Zhang L, Zhao J, He M, Huang Y, Zhao S. A tumor microenvironment-induced absorption red-shifted polymer nanoparticle for simultaneously activated photoacoustic imaging and photothermal therapy. *Sci Adv*. 2021b;7:eabe3588.
- Woodman C, Vundu G, George A, Wilson CM. Applications and strategies in nanodiagnosis and nanotherapy in lung cancer. In: *Seminars in cancer biology*. Elsevier; 2021. p. 349–64.
- Xu X, Kim K, Fan D. Tunable release of multiplex biochemicals by plasmonically active rotary nanomotors. *Angew Chem*. 2015;127:2555–9.
- Xu S, Fan Z, Yang S, Zhao Y, Pan L. Flexible, self-powered and multi-functional strain sensors comprising a hybrid of carbon nanocoils and conducting polymers. *Chem Eng J*. 2021;404:126064.

- Yu Z, Centola M, Valero J, Matthies M, Sulc P, Famulok M. A self-regulating DNA rotaxane linear actuator driven by chemical energy. *J Am Chem Soc.* 2021;143:13292–8.
- Zhang W, Wang W, Yu DX, Xiao Z, He Z. Application of nanodiagnostics and nanotherapy to CNS diseases. *Nanomedicine.* 2018;13:2341–71.
- Zhen X, Pu K, Jiang X. Photoacoustic imaging and photothermal therapy of semiconducting polymer nanoparticles: signal amplification and second near-infrared construction. *Small.* 2021;17:2004723.
- Zhong X, Dai X, Wang Y, Wang H, Qian H, Wang X. Copper-based nanomaterials for cancer theranostics. *Wiley Interdiscip Rev Nanomed Nanobiotechnol.* 2022;14(4):e1797.
- Zhou H, Wang Z, Zhao W, Tong X, Jin X, Zhang X, et al. Robust and sensitive pressure/strain sensors from solution processable composite hydrogels enhanced by hollow-structured conducting polymers. *Chem Eng J.* 2021a;403:126307.
- Zhou W, Dou M, Timilsina SS, Xu F, Li X. Recent innovations in cost-effective polymer and paper hybrid microfluidic devices. *Lab Chip.* 2021b;21:2658–83.

Chapter 2

Nanorobots for Drug Delivery, Surgery, and Biosensing



Qing Ye and Jianfei Sun

2.1 Introduction

“Nanorobots” is an emerging technology in engineering. The development of nanorobots belongs to the category of “molecular nanotechnology (referred to as MNT),” which is based on the biological principles of the molecular level as a design prototype and design and manufacture of “functional molecular devices” that can operate on nanospace (Wan et al. 2020). A nanorobot is a multifunctional, controllable machine made from inorganic or polymeric nanomaterials and then modified with biomimetic materials (Zhou et al. 2021). At present, there is no strict definition of the size of nanorobots in the world; size between 100 nanometer and 1000 nanometer is used to be called as nanorobots (Patel et al. 2006). The structures of nanorobots have aroused enormous interest among researchers and engineers in nanobiology (Garcia-Gradilla et al. 2013; Li et al. 2014). The first generation of nanorobots is an organic combination of biological systems and mechanical systems, which can be injected into blood vessels for health examination and disease treatment, while it can also be used to repair human organs, perform cosmetic surgery, and install normal DNA from genes instead of harmful DNA in genes in order to make the body function properly. The second generation of nanorobots is a nanoscale molecular device assembled directly from atoms or molecules with specific functions, while the third generation will contain nanocomputers, which are devices that can perform human-machine dialogue (Sobczak et al. 2012; van den Heuvel and Dekker 2007; Seeman 2003). Recently, the Indian Institute of

Q. Ye · J. Sun (✉)

State Key Laboratory of Bioelectronics, Jiangsu Key Laboratory for Biomaterials and Devices, School of Biological Science and Medical Engineering, Southeast University, Nanjing, China

e-mail: sunzaghi@seu.edu.cn

Technology in Guwahati has creatively developed a third-generation (3G) self-propelled robot consisting of chemically modified multi-walled carbon nanotubes (CNTs) that can achieve multi-mode self-driving in response to acidic, alkaline, magnetic, and light stimulation. Meanwhile, dye degradation can also be effectively realized by inducing dye degradation through advanced oxidation (Mitra et al. 2020) (Fig. 2.1). Compared to conventional robots, nanorobots provide advantages over their suitability and great biocompatibility for applications in drug delivery, surgery, and biosensing, which improve the safety and efficacy of drugs for targeted hard-to-reach cells and tissues (Orive et al. 2003; Hu et al. 2020; Mertz 2018; Chen et al. 2019a). Owing to small size, nanorobots are able to move and perform operations in microscopic environments that are not accessible to traditional devices. For example, nanorobots can enter microfluidic chips to micro-manipulate and assemble microstructures, enter the natural passages or blood vessels of organisms for detection and drug delivery, and even enter the interior of a single cell to measure the nucleus (Zhou et al. 2021; Solovev et al. 2012; Sitti et al. 2015). Nanorobots allow scientists to control their populations to change configurations through narrow pipes and reach targeted locations to release drugs (Mitragotri et al. 2014). Nanorobots hold considerable application in various fields, especially for advancing diagnosis and treatment of disease, which are able to precisely kill cancer cells, unclog blood clots, remove fat deposits within the arteries, and clean general surgical procedures (Bucolo et al. 2022; Lee et al. 2022; Lueg and Jungo 2021). The

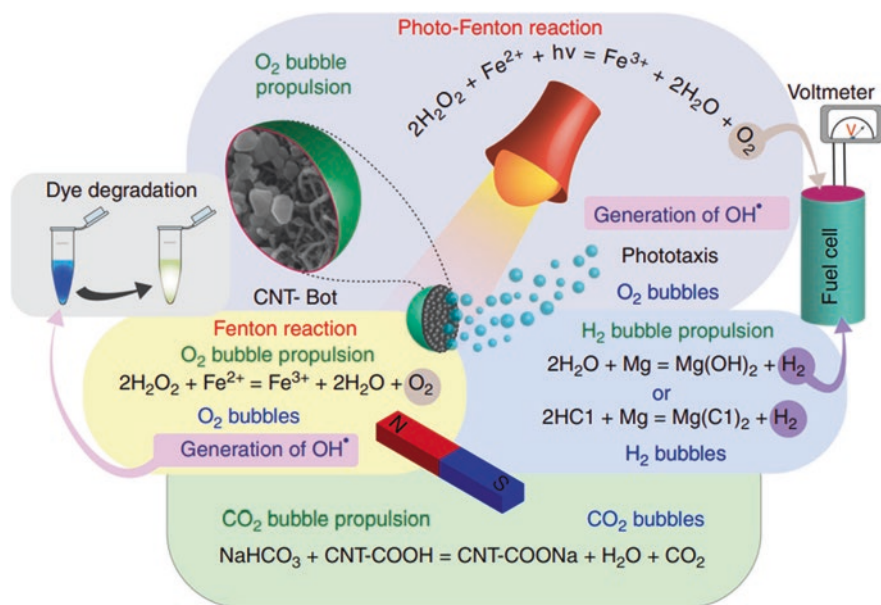


Fig. 2.1 Schematic of a CNT-bot composed of a $-\text{COOH}$ -functionalized MWCNT cluster doped with a ferrous (Fe^{2+}) salt and magnetite nanoparticles (FeONPs) before being coated with a Mg film. (Figure was reproduced with permission from Mitra et al. 2020)

concept of treatment with the tool of nanorobots has been proposed for decades (Jager et al. 2000; Morgado et al. 2019). Richard Feynman (Olsman and Goentoro 2018) pioneered the concept of using nanorobots to treat diseases in the field of medicine; with the continuous advancement of industrial manufacturing technology, nanotechnology provides a novel approach, as it can be applied in targeted drug delivery and disease treatment, making significant progress in the treatment of some complex diseases (Mak et al. 2014; Ewart et al. 2018). Meanwhile, 3D printing provides the benefit in the field of nanorobots, which performs a series of operations on atomic and cellular structures at the molecular level that humans are unable to manipulate (Wei et al. 2020; Kim et al. 2020; Li et al. 2020; Khan et al. 2018). Nanorobots are used to pass through the vitreous body, a colorless, transparent colloidal substance that fills the eyeball between the retina and the crystal, which delivery drugs into the retina to treat aging-related diseases, such as macular degeneration (Kim et al. 2013). A golden nanorobot covered by a mixed coating constructed of platelets and blood cell membranes was developed creatively by scientists at the University of California, which was 25 times thinner than a human hair and travelled at a speed of 35 microns per second in ultrasonically powered blood. When they crossed the bloodstream by ultrasound, the platelet membranes trap bacteria, and the blood cell membranes trap toxins. Platelet and blood cell membrane coatings, on the other hand, can also prevent proteins from attaching to nanorobots, preventing them from being attacked by other cells (Wu et al. 2019). From a medical point of view, nanorobots are a potential therapeutic approach to enter specifically target in the human body. Once reaching the target, they can carry out executive function, such as delivering drugs or getting real-time insights into how the drugs are working. After completing these goals, the nanorobot can be degraded without leaving a trace rapidly (Mostaghaci et al. 2017; Hosseinidoust et al. 2016; Li et al. 2018). Overall, nanorobots provide unlimited possibilities for intelligent sensing detection, controllable drug delivery, precision collaborative medicine, and other large health fields. However, their practical applications face a variety of problems. For example, considering that only a few tenths of a human hair and locating in human body is difficult them the controlled autonomous movement of nanorobots in the human body has always been a problem; if they entered the blood vessels, they are wrapped and impacted by blood, etc. and faced with the challenge in uncontrolled movement (Schuerle et al. 2019).

2.2 Design of Nanorobots

For nearly two decades, researchers have been trying to perform biomedical tasks such as drug-targeted delivery, cancer treatment, and microsurgery by designing nanorobots that can convert energy such as chemical energy, magnetic energy, electrical energy, light energy, and ultrasound energy in the environment into mechanical motion. However, how to improve the biocompatibility, anti-blood fouling ability, and drug-carrying capacity of nanorobots and the therapeutic effect of

cancer cells are the challenges faced by nanorobots for future biomedical applications. In recent years, the research of self-driven synthetic nanomachines has aroused widespread interest from scientists around the world, because they are expected to enter the human body to travel freely in the blood and perform micro-scale tasks, such as active drug delivery and precision treatment of tumors. However, how to achieve self-driven nanomotors to quickly open cell membranes or carry drugs into the inside of cells still faces huge challenges. Considering the following four aspects is required special considerations in order to obtain a micro-scale robot: (Wan et al. 2020) the composition and structure of nanorobots, biocompatibility and biodegradability; (Zhou et al. 2021) the function, such as we can load the robot with certain drugs, proteins, fluorescent dyes to achieve certain applications or positioning functions; (Patel et al. 2006) driving control, such as magnetism, light, ultrasound and other different energy forms; (Garcia-Gradilla et al. 2013) in vivo tracking methods: such as in shallow tissues, fluorescence imaging tracking, and in deep tissues or organs, ultrasound imaging or magnetic resonance imaging and other techniques can reach. After fully considering the above factors, we can use micro-/nanorobotics to handle with many complex problems in the field of biomedicine. Compared with passively diffused colloidal particles or nanocarriers, nanorobots induce distinctive initiative, which is conducive to optimizing and enhancing the directional enrichment of carriers at the culprit lesion site (Fournier-Bidoz et al. 2005; Mei et al. 2011; Karshalev et al. 2018; Teo et al. 2016).

Challenges in the development process mainly of nanorobots are energy, drive, and control. Traditional chemotherapy was more limited in clinical implementation, and chemotherapy drugs spread widely in the patient's body, making it difficult for the targeted tissue to reach the optimal therapeutic concentration of the drug, and the causal distribution of the drug may cause greater toxic side effects (Kumar 2011; Deshpande et al. 2015). Therefore, nanorobots with drive-response systems have great application prospects in the process of drug delivery. Drive-response system is the "engine" in the nanoscale, which can convert other forms of energy into the energy that drives nanorobots to work (Mathesh et al. 2022; Ortiz-Rivera et al. 2018). Unlike macroscopic robots, nanorobots cannot connect external wires or carry batteries to power, nor can they load motors to generate motion. In addition, in the microscopic environment, how to observe and wirelessly control nanorobots according to instructions to move and operate is also a difficult problem to overcome. In response to these problems, recent progress on nanorobots that scientists have carried out mainly (Li et al. 2016; Chatzipirpiridis et al. 2015; Yang et al. 2020; Fan et al. 2021) includes light-driven (Nature 2022; Kirui et al. 2014; Peng et al. 2022), thermal-driven (Pinan Basualdo et al. 2021; Barbot et al. 2019; Ongaro et al. 2017), chemically driven (Mitra et al. 2020; Xuan et al. 2014; Sanchez et al. 2015), and microbial robots' in vivo tracking and localization. In 2013, a research team at the University of Georgia in the United States developed a magnetically driven nanorobot that accelerates thrombolysis by facilitating the delivery of tissue plasminogen activators; in the same year, Pumera's team first studied the toxic effects of a self-propelled nanorobot on human cells, making the nanorobot a solid step toward clinical application (Cheng et al. 2014; Chng et al. 2014). Cai Lintao's team selected

ocean-derived magnetotropic bacteria (AMB-1) as a template, used Michael's addition reaction to load nano-photosensitizers onto the surface of bacteria, and built an intelligent micro-/nanorobot (AI microrobot), which realized magnetron navigation, tumor penetration, and photothermal ablation in mice through magnetic/light sequence manipulation (Deng et al. 2020; Chen et al. 2019b). An AI micro-/nanorobot driven by sequential magnetism and light triggered, and used to achieve active targeting of cancer treatment, was designed by Cai Lintao's team at the Shenzhen Institute of Advanced Technology of the Chinese Academy of Sciences for the treatment of tumors. By implanting an AI micro-/nano-biological robot in a tumor patient, it can automatically swim to the tumor foci site and eliminate the tumor, and then the robot itself can be absorbed by the human body without causing any damage to health. Using the magnetic and hypoxia integrated targeting of micro-/nano-biological robots, after breaking through the complex physiological barrier with photosensitizer into the tumor interior, the remote near-infrared laser trigger is used to generate local high temperature, and the visualized and precise treatment of tumors is realized in the experiment (Xing et al. 2021).

Recently, using liquid metal gallium as the material, the research team realized the mass fabrication of the white blood cell membrane surface camouflage liquid metal gallium needle-like swimming nanorobot by combining nanoporous template plastic forming and cell membrane coating technology. This liquid metal swimming nanorobot that combines driving motion, deformation-fusion, drug loading, photothermal absorption, and anti-blood fouling capabilities is expected to provide new research ideas for the design of a new generation of swimming nanorobots (Wang et al. 2020). A new type of thrombolytic drug delivery strategy has been designed, which developed an open space C-shaped magnetic drive system with functions such as laser positioning and ultrasound imaging navigation to achieve in vivo applications (Wang et al. 2021a). Nanorobots with chemical response as driving forces have received great attention and are currently a common driving method (Lyu et al. 2021). Hydrogen peroxide was used as a fuel, which decomposed to release oxygen bubbles, creating a thrust that drove nanorobots to swim in the liquid. However, current designs are primarily based on complex three-dimensional (3D) structures with limited accessible surface area at catalytic reaction sites, requiring higher fuel concentrations to drive. The team at Deakin University in Australia recently designed an enzyme-based nanorobot that can be actively driven at ultra-low fuel concentration (0.003% H_2O_2) by studying the weak interaction of the two-dimensional nanostructure-enzyme interface and designing, constructing, and regulating the catalytic reaction dynamics of biological enzymes at the single-molecule level (Mathesh et al. 2022). The controlled surface chemistry of the two-dimensional enzyme nanostructure, the high specific surface area, and the scalable synthesis method make it ideal for the development of efficient nanorobots. Ultrasonic response serves an important role during driving nanorobots work in vivo. The development of a needle-type acoustic-electrical composite electrode realized the generalized cluster control of tubular and spherical nanorobots and the controllable switching of motion modes. Through the electrolyzed water bubble generation technology, a micron-sized bubble vibration core was formed at the

electrode tip, which resonated with ultrasonic field excitation, and then formed a locally enhanced sound flow field, driving the neighboring nanorobot to quickly disperse to other areas. However, after removing the bubbles, the acoustic-electrical composite electrode could be used as an acoustic isolator, providing a fixed boundary to block the propagation of acoustic energy in the fluid and then forming an energy potential trap around the electrode, driving a wide range of dispersed nanorobots to enrich below the electrode. Surprisingly, these two functional modes of the acoustic-electrical composite electrode did not have coupling interference under different ultrasonic frequency excitation. Although the current limitation of this study was that it cannot effectively drive large nanorobots with a diameter of more than 30 μm to carry out cluster movements, the clustered control platform achieved a high degree of integration with existing electrochemical detection platforms, providing a possibility for the realization of active ultrasensitivity detection technology based on nanorobots (Lu et al. 2021). In the intricate body, only the nanorobots that drive the system cannot discern the direction and complete the task of targeting tumors (Yuan et al. 2017). Therefore, it is necessary to carry a navigation system at the same time. At present, scientists mainly use magnetic fields, infrared rays, ultrasonic, and other signals with strong penetration and directionality to guide the direction of movement of nanorobots. Combined with the emerging in vivo imaging technology, it is expected to realize the remote and precise control of nanorobots (Soto et al. 2022). Meanwhile, a “tracker” for tumor cells for the nanorobot has been installed, tumor cells often have specific protein receptors that are overexpressed on the surface, and ligands that specifically recognize these receptors can be accurately identified and bound to tumor cells by connecting them on the surface of the nanorobot (Zhang et al. 2021a). The team of Fudan University in China cleverly used the simultaneous (alkenyl) radical polymerization reaction and (trimethoxysilane) hydrolyzed polymerization reaction in the precursor to achieve selective island growth of silicon on the surface of polystyrene nanoparticles and then obtained a nanorobot with a selective hollow structure after wrapping polydopamine and calcination at high temperature. In addition, parameters such as the size and quantity of island silicones can be precisely adjusted, and then multifunctional nanorobots with adjustable topologies can be synthesized according to different needs, and the super-assembly strategy can achieve rapid movement, intelligent drug delivery, and collaborative precision treatment of cancer (Xie et al. 2022).

The response system of nanorobots is also an urgent consideration for their application. For example, nanorobots containing various response elements gushed out in tumor-specific microenvironments. Responding element remains stable in blood circulation and normal tissues, while a selective response occurs in the tumor microenvironment and releases the drug. It not only ensures the fixed-point delivery of drugs but also realizes the specific treatment of tumors. A piece of DNA sequence capable of binding highly selectively to the target tumor is used as a “drug release switch” for the nanorobot, enabling it to release the drug at the tumor site at a fixed point (Li et al. 2018). The Shanghai Institute of Materia Medica of the Chinese Academy of Sciences has designed and prepared a drug-carrying nanorobot based

on Boolean operation, which will dissociate different drugs for acidic, reducing, and special enzymes to achieve drug release response (Hou et al. 2020).

It is worth mentioning that nano-manipulation and intelligence need to be considered in the application of nanorobots. Nano-manipulation technology is the precise manipulation of a tiny object at the micro- or nanoscale (Drinkwater 2016; Nelson et al. 2010). Intelligence is an important step in the practical application of nanorobots, which aims to use simple machines to explore and make decisions in complex environments (Ceylan et al. 2017). Tang et al. prepared a nanorobot of TiO_2 nanotree, which will react with photocells under light, generate anions and cations at the opposite ends of the nanotree, form an electric field, and then promote the forward movement of the nanotree under the action of the electric field. By adjusting the electric potential and the direction of light, an asymmetrical concentration field/photoelectric field can be generated, and the nanotree is deflected, thus achieving different dimensions of freedom (Dai et al. 2016).

The unique advantages of nanorobots in self-driving, in vivo navigation, and intelligent response give it a promising future in drug delivery, surgery, and sensing.

2.3 Application

2.3.1 Drug Delivery

The traditional treatment of diseases is mainly based on drugs, but due to the lack of precious targeting, the concentration of lesions in the body is insufficient, causing poor treatment effect, and even the drug is diffuse, resulting in damage to healthy tissues and causing side effects in patients (Orive et al. 2003; Zelikin et al. 2016). Some scholars have made statistics on drug delivery in the past 30 years and found that after about 12 hours of traditional delivery, less than 1% of the drugs reached the target location. This means that the vast majority of medications have been lost on the road (Yao et al. 2012). Therefore, the construction of a new type of drug active transportation channel has become a research hotspot in the industry (Suri et al. 2016; Wang et al. 2016). As mentioned, nanorobots are subject to controlled driving forces and navigation and response systems, which attract the attention of the research field (Nelson et al. 2010; Torne et al. 2013). A variety of micro- and nanodrug carrier robots rely on self-propulsion movements to cross the barrier of multiple biological barriers to send drugs to the bottom of the eyeball or deep in the brain tissue, so that the thorny medical problems such as glaucoma, epilepsy, glioblastoma, stroke hemiplegia, and so on can be solved (Lee et al. 2012; Fu et al. 2021). Since 2004, a variety of chemical and external physics (such as photoelectromagnetic heat)-driven swimming micro-/nanorobots have emerged in the industry, which can swim efficiently in water. These micro- and nanorobots can not only swim efficiently in water or other biological fluids but also control their movement behavior with the help of chemistry, light, magnetism, etc., so that they can reach

the specified location according to people's wishes (Douglas et al. 2012). However, the human internal environment is very complex, especially in the body; there are also a variety of biological barriers such as blood-brain barriers and blood-eye barriers, which protect the human body from the invasion of foreign bacteria and viruses at the same time, but also prevent these robots from accurately delivering drugs to the patient area (Gallego and Cena 2020; Pourgholi et al. 2016).

The early swimming micro-/nanorobots were basically composed of components such as microelectromechanical systems, and their own materials were mainly metals, metal oxides, and artificial polymers. After micro-/nanorobots enter the body, they cannot be degraded at first, so they have great danger; secondly, these metals and metal polymers are human exogenous substances and have poor biocompatibility; once they enter the body, they will trigger the "alarm" of the immune system and then be surrounded by immune cells; and before they reach the lesion, they may have been strangled by the human immune system (Zhang et al. 2004). As early as 2010, the first swimming nanorobot research and development team in China, applying chemical methods, for the first time to assemble atoms into micro-/nanostructures, successfully performed controlled swimming under the chemical field or external light and magnetic field and even directly guided to the target cell (Bayrac et al. 2017). Scientists innovatively proposed that the magnetic drug carrier gel is covered with a "camouflage" coat using the *E. coli* membrane, thereby increasing the amount of phagocytosis of the magnetic drug-carrying particles by neutrophils, manipulating the neutrophil microrobot to enrich the brain, and the neutrophil robot that reaches the brain relies on its tendency function, crosses the blood-brain barrier along the inflammatory factors released by the glioma, and finally reaches the glioma patient area and releases the drug, realizing the drive precision target under the exogenous magnetic field. The strategy also improves the biocompatibility of the swimming micro-/nanorobot and also prevents the leakage of drugs contained in the magnetic nanogel (Zhang et al. 2021a) (Fig. 2.2). By binding DNA aptamers outside the nanorobot, nucleolin (a protein specifically expressed on tumor-associated endothelial cells) and thrombin in its lumen can be bound. In this design, the nucleoside targeting aptamer is both a targeting domain and a molecular trigger mechanically opened by nanorobots. Thus, thrombin in the body

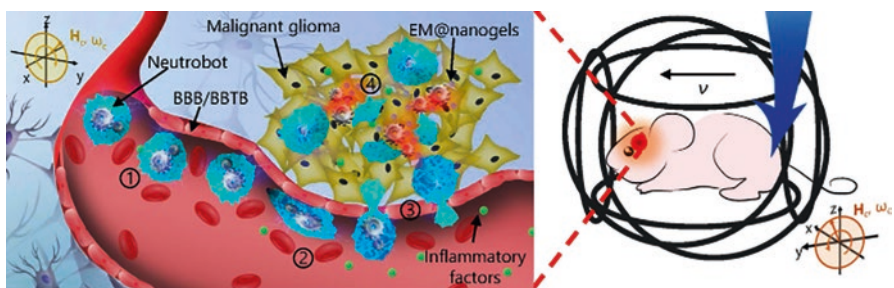


Fig. 2.2 Schematic of active therapeutics of dual-responsive neutroblots in vivo. (Figure was reproduced with permission from Zhang et al. 2021a)

is exposed and activates coagulation at the site of the tumor, thereby inhibiting the growth and exacerbation of the tumor (Li et al. 2018). The white blood cell membrane modified on the surface of the nanorobot can accelerate the entry into cancer cells through specific recognition with cancer cells, while the liquid metal swimming nanorobot loaded with the anti-cancer drug doxorubicin shows good cancer cell drug and photothermal combination therapy ability (Wang et al. 2020).

In nanorobots carrying drug targets into the body, drugs are trapped on the surface of micro-/nanorobots by electrostatic action (Soto et al. 2020). Electrostatics has been reported to act as a positively charged antimicrobial drug by ultrasound into negatively charged polypyrrole-polystyrene sulfonate fragments on nanorobots. Moreover, the electrostatic interaction is stable at pH 7. Under different acid-base conditions, drug release can be carried out. This method proposes a unique trigger release mechanism based on electrochemical stimulation (Manesh et al. 2010; Li et al. 2017). In addition, the use of electrochemical stimulation as a release mechanism is further expanded by loading the therapeutic payload with bismuth coating. The surface of the ultrasonically propulsion porous nanowire is functionally performed with an anionic coating that allows doxorubicin electrostatic loading into a micro-/nanorobot structure. The porous part is responsible for increasing the drug load and promoting the release through the photothermal effect of near-infrared light radiation (Gao et al. 2021).

2.3.2 Surgery

At present, the miniaturized surgical tools or medical devices used in large-scale surgeries in clinical practice, although relatively small in size, still do not have the ability to enter places that catheters and blades cannot reach, hindering the progress of surgery. Surgery using micro-/nanorobots may reach areas of the body that cannot be reached by catheters or invasive surgeries, allowing tissues to be sampled or treatment payloads to be drilled deep into diseased tissues (Xu and Liu 2021; Saravana and Vijayalakshmi 2006). In addition, the potential to reduce the risk of infection and recovery time is a distinct advantage of nanorobots (Agrahari et al. 2020).

Nanorobots can target any tissue part of the body and perform corresponding operations at the cellular level, thus assisting doctors in achieving more accurate, flexible, and controllable minimally invasive surgery (Zhang et al. 2022). The micro-/nanotechnology tools currently used in minimally invasive surgery include nano-drills, micro-clamps, and micro-bullets. Among them, the micro-clamp can pass through the body's narrowest capillaries to capture and move out of the cells in the tissue (Agrahari et al. 2020).

Studies have shown that nanorobots can penetrate thick biological tissues with the help of magnetic fields and ultrasonic waves, and on this basis, nanorobots carrying magnetic fields and ultrasonic control systems have been developed. Magnetically driven microrobot implants have been successful in eye surgery in

animals (Tabatabaei et al. 2016), while ultrasound-driven nanomachines can perform precision surgeries at the single-cell level or even at the subcellular level (Chechetka et al. 2016). Both studies suggest that effective control systems combined with nanorobots can accurately position themselves in surgery and efficiently advance the application of nanorobots in surgery (Nguyen et al. 2017).

Neurosurgery has always had pain points such as small surgical space and difficulty in positioning, and because surgery generally requires operation of specific parts of neural tissue, the operation needs to be very precise. Surgeons generally struggle to achieve the required precision (Bland 2005). In the mid-1980s, PUMA robots were first used in neurosurgery (Zollinger 1991; Barnes 2016). According to the preoperative image of the intracranial lesion, the surgeon enters the coordinates of the lesion into the robot and applies the robot-guided needle for biopsy and other operations. In 1985, Kwoh et al. used the position information obtained from images by the PUMA206 robot for the first time to stereotaxicize patients and perform biopsy surgery (Kwoh et al. 1988). According to the preoperative image of the intracranial lesion, the surgeon enters the coordinates of the lesion into the robot and applies the robot-guided needle for biopsy and other operations. This is the first clinical application of neurosurgical robots.

Therefore, the use of robots to do precise movements on the basis of medical image guidance has become the preferred surgical method of most doctors. Spiral nanorobots made of iron-coated silica capable of being controlled by low-intensity magnetic fields and able to track its movements reach depths during root canal treatment to a depth that is not possible during current clinical treatment, thus helping to completely kill bacteria deep inside the dentin tubules to increase the success rate of root canal treatment (Dasgupta et al. 2022) (Fig. 2.3). A good association of the internal structures of the brain with the external surgical framework can be achieved through medical images. In related clinical applications, such robots are mainly used as an aid to stereoscopic frame positioning, using 3D image guidance and positioning surgical tools to achieve intracranial target targets. At present, neurosurgical robots are mainly used for brain surgery, biopsy, Parkinson's disease targeted stimulation, epilepsy electrode measurement, removal of cysts or hematoma emptying, and other operations (Benabid et al. 1987).

At present, neurosurgery robotic systems have evolved from stereotactic surgery to microsurgery and even remote surgery. With the rapid development of multimedia and information network technology, high-speed networks and virtual reality systems based on effective computer graphics provide technical support for remote human-machine communication, making long-distance surgery a reality, and surgery can be completed by surgeons controlling the robot at the surgical site through remote control operating systems in different places.

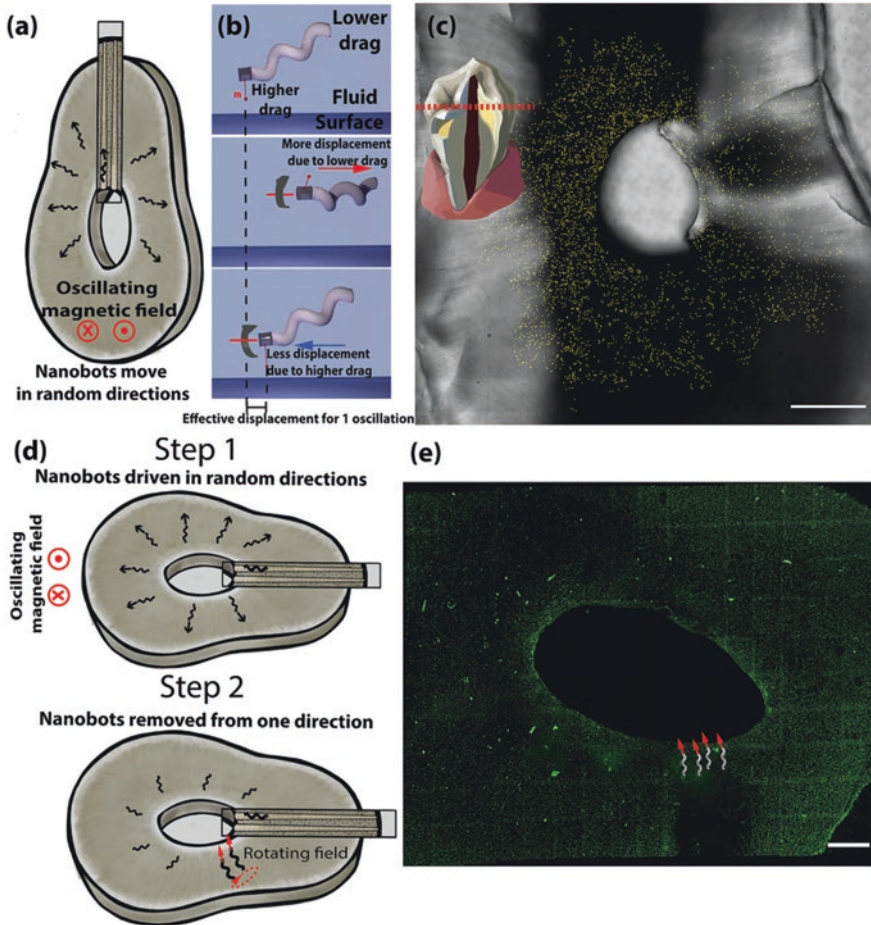


Fig. 2.3 Schematic diagram of the distribution of dental spiral magnetic nanorobots under oscillating field. (Figure was reproduced with permission from Dasgupta et al. 2022)

2.3.3 Biosensing

Recently, nanoporous sensors have become an important tool for solution-based analysis of key components of single-molecule life, including nucleic acids, proteins, polysaccharides, and a large number of biomolecules that play an important role in life and healthcare (Rahman et al. 2021). Nanosensors are nanoscale in shape or sensitivity, or the interaction distance between the sensor and the substance or object to be detected is in the nanometer range (Chinnadayala et al. 2019; Fu and Ma 2020; Ding et al. 2002). Nanosensors have sub-micron sizes, transducers, probes, or nano-/microsystems, their physicochemical properties and their detection sensitivity to biomolecules or cells are greatly improved, the detection reaction

time is also greatly shortened, and high-throughput real-time detection and analysis can be realized (Polidori et al. 2013; Miyashita et al. 2009). Nanosensors mainly use electricity. When materials are physically manipulated, nanosensors change their conductivity, triggering a detectable signal response that ultimately analyzes and measures the response (Liu et al. 2021). Nanotechnology sensors are mainly divided into nanochemical and biological sensors, nano-gas sensors, and other types of nanosensors, such as pressure, temperature, and flow (Lee and Wong 2009; Mishra et al. 2019). At present, nanochemical and biological sensors are clinically diagnosing cancer, cardiovascular disease, etc. in an early stage (Benjaminsen et al. 2011). Due to the attached surface of the gas sensor, a nano-coating is used as a sensitive material to improve the sensitivity and performance of the sensor, usually metal oxide semiconductor nanoparticles, carbon nanotubes, and two-dimensional nanofilms (Forier et al. 2014). The adsorbed gas molecules interact with carbon nanotubes, change their Fermi energy level to cause a significant change in their macroscopic resistance, and detect the gas composition by detecting changes in their resistance, which can be used as a gas sensor (Sondergaard et al. 2014).

Compared with traditional sensors, nanosensors have many significant characteristics, such as high sensitivity, low power consumption, low cost, and multifunctional integration, due to their ability to operate at the atomic and molecular scales, making full use of the unique properties of nanomaterials, Raman spectral effects, catalytic efficiency, conductivity, strength, hardness, toughness, superplasticity, and superparamagnetism (Fulaz et al. 2019; Desai et al. 2013). The sensor made of nanotechnology, the size is reduced, the accuracy is improved, the performance is greatly improved, the nanosensor is standing on the atomic scale, which greatly enriches the theory of the sensor, promotes the production level of the sensor, and broadens the application field of the sensor. Nanosensors have now been widely developed in the fields of biology, chemistry, mechanics, aviation, and military.

Sensors made using nanotechnology can be used for the early diagnosis, monitoring, and treatment of diseases, making early diagnosis of various cancers a display (Aylott 2003). For example, when performing blood tests, when the antibodies to cancer cells present in the sensor encounter the corresponding antigen, the current in the sensor changes, and the type and concentration of cancer cells in the blood can be judged through this current change (Fu and Ma 2020). In the monitoring of ovarian cancer, aromatic ligands capable of reacting with volatile organic compounds associated with ovarian cancer are first selected, forming an integrated cross-reaction induction array with gold nanoparticles and flexible striped polyimide films (Salvati et al. 2015). When a patient with ovarian cancer exhales gas through gold nanoparticles, the specific volatile organic compounds in them react with ligands on the array, causing measurable changes in resistance. This bendable sensor has a high 80% accuracy rate in ovarian cancer diagnosis (Williams et al. 2018). A special odor is produced by human respiration, which consists of specific volatile organic compounds that characterize hypoglycemia. An array of nanosensors was developed to detect this odor and could transmit hypoglycemic signals to relatives for patient safety (Lemmerman et al. 2020). In addition to medical diagnosis, nanosensing is also used in microelectronics information technology and

national defense security (Zhang et al. 2021b). Nano-gold materials are the core materials of nanosensors, which are widely used in test strips, and their size, shape, and self-assembly behavior directly affect the performance of visualization (Wang et al. 2021b). Through the development of bioinformatic chips, nanorobots, and brain-computer interface devices embedded in nanosensors, foreign militaries can effectively improve human memory, reaction ability, and visual and auditory sensitivity and improve the battlefield perception and rapid disposal ability of combatants (Wang 2018).

Nanosensors have revolutionized the need for portable analytical tools with selectivity, stability, and other characteristics in every industry. Nanosensors also have high sensitivity for greater accuracy. They can easily interact at the nanoscale. Small, durable, lightweight, and portable, nanosensors enable better sensitivity, power, speed, and detection range due to the ratio of surface area to volume (Du et al. 2012). Compared to other types of sensors, nanosensors have shorter response times, are faster, and can be analyzed in real time (Li et al. 2018). In addition, nanosensors require a smaller sample volume for analysis and cause minimal interference with the observed material or process. They can also detect multiple things at the same time, making them devices with multiple functions (Fig. 2.4).

2.4 Conclusion

Nanotechnology has provided new ways and means for drug delivery and disease treatment, making significant progress in the treatment of some of the most difficult diseases to overcome. With the help of nanocarriers, drugs can overcome the biological barriers of the human body, directly reach the lesion area through artificial manipulation, and reduce the damage to other tissues, while increasing the local drug concentration to enhance the therapeutic effect, nanorobots are undoubtedly

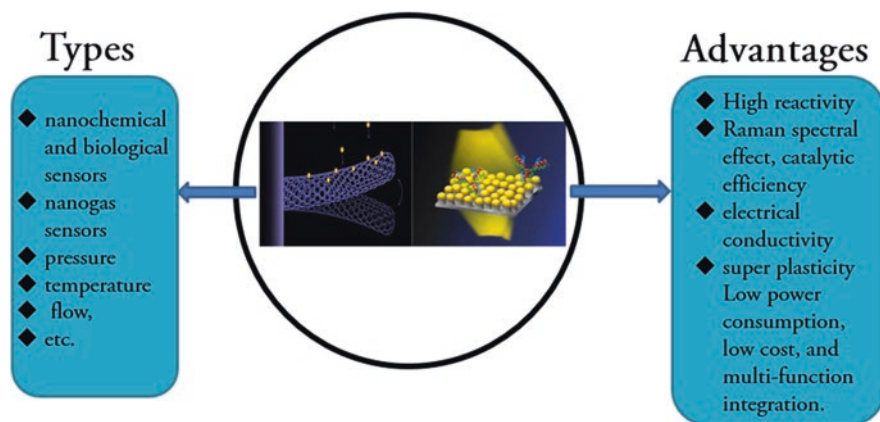


Fig. 2.4 Types and characteristics of nanosensors

the most representative technology for drug delivery with the help of nanocarriers. Nano-scale adjustment kills mutated cancerous cells, through the guidance of external lasers, accurate calculations to find cancerous cells with radiation exceeding standards, and the use of advanced biological cell lysis technology to dissolve possible diseased cells into chemical molecular elements, and through the accurate verification of specific sensor systems, the cell components are successfully entered into healthy cells, completing the conversion of necrotic cells and successful healthy cells. In short, the unique advantages of nanobots with self-driving, in vivo navigation, and intelligent response make it have broad prospects in tumor treatment. In addition, in the future, nanorobots are also expected to shine in medical fields such as in vivo imaging, immunotherapy, and minimally invasive surgery. On the other hand, as a new drug carrier system, nanorobots also face challenges such as low biocompatibility, insufficient in vivo experimental data, and high thresholds for industrial production. At present, most nanorobots are still in the verification stage of in vitro experiments or animal models, and there is still a certain distance from real clinical applications. We expect that with the painstaking research of scientists, nanorobots will be able to overcome these problems and bring revolutionary progress to medicine.

References

- Agrahari V, Agrahari V, Chou ML, Chew CH, Noll J, Burnouf T. Intelligent micro-/nanorobots as drug and cell carrier devices for biomedical therapeutic advancement: promising development opportunities and translational challenges. *Biomaterials*. 2020;260:120163. <https://doi.org/10.1016/j.biomaterials.2020.120163>.
- Ayllott JW. Optical nanosensors--an enabling technology for intracellular measurements. *Analyst*. 2003;128(4):309–12. <https://doi.org/10.1039/b302174m>.
- Barbot A, Tan H, Power M, Seichepine F, Yang GZ. Floating magnetic microrobots for fiber functionalization. *Sci Robot*. 2019;4(34):eaax8336. <https://doi.org/10.1126/scirobotics.aax8336>.
- Barnes SA. Reply to “Women in academic surgery: why is the playing field still not level?” Appearing in the *American Journal of Surgery*, Feb. 2016, volume 211, number 2. *Am J Surg*. 2016;212(2):366. <https://doi.org/10.1016/j.amjsurg.2016.03.002>.
- Bayrac C, Eyidogan F, Avni OH. DNA aptamer-based colorimetric detection platform for salmonella Enteritidis. *Biosens Bioelectron*. 2017;98:22–8. <https://doi.org/10.1016/j.bios.2017.06.029>.
- Benabid AL, Cinquin P, Lavalle S, Le Bas JF, Demongeot J, de Rougemont J. Computer-driven robot for stereotactic surgery connected to CT scan and magnetic resonance imaging. *Technological design and preliminary results. Appl Neurophysiol*. 1987;50(1–6):153–4. <https://doi.org/10.1159/000100701>.
- Benjaminson RV, Sun H, Henriksen JR, Christensen NM, Almdal K, Andresen TL. Evaluating nanoparticle sensor design for intracellular pH measurements. *ACS Nano*. 2011;5(7):5864–73. <https://doi.org/10.1021/nn201643f>.
- Bland KI. Hiram Polk and the American journal of surgery. *Am J Surg*. 2005;190(2):338–43. <https://doi.org/10.1016/j.amjsurg.2005.05.037>.
- Bucolo M, Bucolo G, Buscarino A, Fiumara A, Fortuna L, Gagliano S. Remote ultrasound scan procedures with medical robots: towards new perspectives between medicine and engineering. *Appl Bionics Biomech*. 2022;2022:1072642. <https://doi.org/10.1155/2022/1072642>.

- Ceylan H, Giltinan J, Kozielski K, Sitti M. Mobile microrobots for bioengineering applications. *Lab Chip*. 2017;17(10):1705–24. <https://doi.org/10.1039/c7lc00064b>.
- Chatzipirpiridis G, Ergeneman O, Pokki J, Ullrich F, Fusco S, Ortega JA, et al. Electroforming of implantable tubular magnetic microrobots for wireless ophthalmologic applications. *Adv Healthc Mater*. 2015;4(2):209–14. <https://doi.org/10.1002/adhm.201400256>.
- Chechetka SA, Yuba E, Kono K, Yudasaka M, Bianco A, Miyako E. Magnetically and near-infrared light-powered supramolecular nanotransporters for the remote control of enzymatic reactions. *Angew Chem Int Ed Engl*. 2016;55(22):6476–81. <https://doi.org/10.1002/anie.201602453>.
- Chen Z, Wang Z, Gu Z. Bioinspired and biomimetic nanomedicines. *Acc Chem Res*. 2019a;52(5):1255–64. <https://doi.org/10.1021/acs.accounts.9b00079>.
- Chen F, Zang Z, Chen Z, Cui L, Chang Z, Ma A, et al. Nanophotosensitizer-engineered salmonella bacteria with hypoxia targeting and photothermal-assisted mutual bioaccumulation for solid tumor therapy. *Biomaterials*. 2019b;214:119226. <https://doi.org/10.1016/j.biomaterials.2019.119226>.
- Cheng R, Huang W, Huang L, Yang B, Mao L, Jin K, et al. Acceleration of tissue plasminogen activator-mediated thrombolysis by magnetically powered nanomotors. *ACS Nano*. 2014;8(8):7746–54. <https://doi.org/10.1021/nn5029955>.
- Chinnadayala SR, Park J, Le HTN, Santhosh M, Kadam AN, Cho S. Recent advances in microfluidic paper-based electrochemiluminescence analytical devices for point-of-care testing applications. *Biosens Bioelectron*. 2019;126:68–81. <https://doi.org/10.1016/j.bios.2018.10.038>.
- Chng EL, Zhao G, Pumera M. Towards biocompatible nano/microscale machines: self-propelled catalytic nanomotors not exhibiting acute toxicity. *Nanoscale*. 2014;6(4):2119–24. <https://doi.org/10.1039/c3nr04997c>.
- Dai B, Wang J, Xiong Z, Zhan X, Dai W, Li CC, et al. Programmable artificial phototactic microswimmer. *Nat Nanotechnol*. 2016;11(12):1087–92. <https://doi.org/10.1038/nnano.2016.187>.
- Dasgupta D, Peddi S, Saini DK, Ghosh A. Mobile nanobots for prevention of root canal treatment failure. *Adv Healthc Mater*. 2022;11:e2200232. <https://doi.org/10.1002/adhm.202200232>.
- Deng G, Peng X, Sun Z, Zheng W, Yu J, Du L, et al. Natural-killer-cell-inspired Nanorobots with aggregation-induced emission characteristics for near-infrared-II fluorescence-guided glioma theranostics. *ACS Nano*. 2020;14(9):11452–62. <https://doi.org/10.1021/acsnano.0c03824>.
- Desai AS, Chauhan VM, Johnston AP, Esler T, Aylott JW. Fluorescent nanosensors for intracellular measurements: synthesis, characterization, calibration, and measurement. *Front Physiol*. 2013;4:401. <https://doi.org/10.3389/fphys.2013.00401>.
- Deshpande A, Mailis-Gagnon A, Zoheiry N, Lakha SF. Efficacy and adverse effects of medical marijuana for chronic noncancer pain: systematic review of randomized controlled trials. *Can Fam Physician*. 2015;61(8):e372–81.
- Ding Z, Quinn BM, Haram SK, Pell LE, Korgel BA, Bard AJ. Electrochemistry and electrogenerated chemiluminescence from silicon nanocrystal quantum dots. *Science*. 2002;296(5571):1293–7. <https://doi.org/10.1126/science.1069336>.
- Douglas SM, Bachelet I, Church GM. A logic-gated nanorobot for targeted transport of molecular payloads. *Science*. 2012;335(6070):831–4. <https://doi.org/10.1126/science.1214081>.
- Drinkwater BW. Dynamic-field devices for the ultrasonic manipulation of microparticles. *Lab Chip*. 2016;16(13):2360–75. <https://doi.org/10.1039/c6lc00502k>.
- Du G, Moulin E, Jouault N, Buhler E, Giuseppone N. Muscle-like supramolecular polymers: integrated motion from thousands of molecular machines. *Angew Chem Int Ed Engl*. 2012;51(50):12504–8. <https://doi.org/10.1002/anie.201206571>.
- Ewart L, Dehne EM, Fabre K, Gibbs S, Hickman J, Hornberg E, et al. Application of microphysiological systems to enhance safety assessment in drug discovery. *Annu Rev Pharmacol Toxicol*. 2018;58:65–82. <https://doi.org/10.1146/annurev-pharmtox-010617-052722>.
- Fan F, Jin L, Yang L. pH-sensitive nanoparticles composed solely of membrane-disruptive macromolecules for treating pancreatic cancer. *ACS Appl Mater Interfaces*. 2021;13(11):12824–35. <https://doi.org/10.1021/acsami.0c16576>.

- Forier K, Raemdonck K, De Smedt SC, Demeester J, Coenye T, Braeckmans K. Lipid and polymer nanoparticles for drug delivery to bacterial biofilms. *J Control Release*. 2014;190:607–23. <https://doi.org/10.1016/j.jconrel.2014.03.055>.
- Fournier-Bidoz S, Arsenault AC, Manners I, Ozin GA. Synthetic self-propelled nanorotors. *Chem Commun (Camb)*. 2005;41(4):441–3. <https://doi.org/10.1039/b414896g>.
- Fu Y, Ma Q. Recent developments in electrochemiluminescence nanosensors for cancer diagnosis applications. *Nanoscale*. 2020;12(26):13879–98. <https://doi.org/10.1039/d0nr02844d>.
- Fu X, Chen T, Song Y, Feng C, Chen H, Zhang Q, et al. mRNA delivery by a pH-responsive DNA Nano-hydrogel. *Small*. 2021;17(29):e2101224. <https://doi.org/10.1002/sml.202101224>.
- Fulaz S, Hiebner D, Barros CHN, Devlin H, Vitale S, Quinn L, et al. Ratiometric imaging of the in situ pH distribution of biofilms by use of fluorescent mesoporous silica nanosensors. *ACS Appl Mater Interfaces*. 2019;11(36):32679–88. <https://doi.org/10.1021/acsami.9b09978>.
- Gallego L, Cena V. Nanoparticle-mediated therapeutic compounds delivery to glioblastoma. *Expert Opin Drug Deliv*. 2020;17(11):1541–54. <https://doi.org/10.1080/17425247.2020.1810015>.
- Gao Y, Wei F, Chao Y, Yao L. Bioinspired soft microrobots actuated by magnetic field. *Biomed Microdevices*. 2021;23(4):52. <https://doi.org/10.1007/s10544-021-00590-z>.
- Garcia-Gradilla V, Orozco J, Sattayasamitsathit S, Soto F, Kuralay F, Pourazary A, et al. Functionalized ultrasound-propelled magnetically guided nanomotors: toward practical biomedical applications. *ACS Nano*. 2013;7(10):9232–40. <https://doi.org/10.1021/nn403851v>.
- Guided by the light, nimble nanovehicles make special deliveries. *Nature*. 2022;601(7894):487. <https://doi.org/10.1038/d41586-022-00115-5>.
- Hosseinioust Z, Mostaghaci B, Yasa O, Park BW, Singh AV, Sitti M. Bioengineered and biohybrid bacteria-based systems for drug delivery. *Adv Drug Deliv Rev*. 2016;106(Pt A):27–44. <https://doi.org/10.1016/j.addr.2016.09.007>.
- Hou B, Zhou L, Wang H, Saeed M, Wang D, Xu Z, et al. Engineering stimuli-activatable boolean logic prodrug nanoparticles for combination cancer immunotherapy. *Adv Mater*. 2020;32(12):e1907210. <https://doi.org/10.1002/adma.201907210>.
- Hu M, Ge X, Chen X, Mao W, Qian X, Yuan WE. Micro/nanorobot: a promising targeted drug delivery system. *Pharmaceutics*. 2020;12(7):665. <https://doi.org/10.3390/pharmaceutics12070665>.
- Jager EW, Inganas O, Lundstrom I. Microrobots for micrometer-size objects in aqueous media: potential tools for single-cell manipulation. *Science*. 2000;288(5475):2335–8. <https://doi.org/10.1126/science.288.5475.2335>.
- Karshalev E, Esteban-Fernandez de Avila B, Wang J. Micromotors for “chemistry-on-the-Fly”. *J Am Chem Soc*. 2018;140(11):3810–20. <https://doi.org/10.1021/jacs.8b00088>.
- Khan FA, Narasimhan K, Swathi CSV, Mustak S, Mustafa G, Ahmad MZ, et al. 3D printing technology in customized drug delivery system: current state of the art, prospective and the challenges. *Curr Pharm Des*. 2018;24(42):5049–61. <https://doi.org/10.2174/1381612825666190110153742>.
- Kim S, Qiu F, Kim S, Ghanbari A, Moon C, Zhang L, et al. Fabrication and characterization of magnetic microrobots for three-dimensional cell culture and targeted transportation. *Adv Mater*. 2013;25(41):5863–8. <https://doi.org/10.1002/adma.201301484>.
- Kim E, Jeon S, An HK, Kianpour M, Yu SW, Kim JY, et al. A magnetically actuated microrobot for targeted neural cell delivery and selective connection of neural networks. *Sci Adv*. 2020;6(39):eabb5696. <https://doi.org/10.1126/sciadv.abb5696>.
- Kirui DK, Koay EJ, Guo X, Cristini V, Shen H, Ferrari M. Tumor vascular permeabilization using localized mild hyperthermia to improve macromolecule transport. *Nanomedicine*. 2014;10(7):1487–96. <https://doi.org/10.1016/j.nano.2013.11.001>.
- Kumar SP. Cancer pain: a critical review of mechanism-based classification and physical therapy management in palliative care. *Indian J Palliat Care*. 2011;17(2):116–26. <https://doi.org/10.4103/0973-1075.84532>.
- Kwoh YS, Hou J, Jonckheere EA, Hayati S. A robot with improved absolute positioning accuracy for CT guided stereotactic brain surgery. *IEEE Trans Biomed Eng*. 1988;35(2):153–60. <https://doi.org/10.1109/10.1354>.

- Lee YH, Wong DT. Saliva: an emerging biofluid for early detection of diseases. *Am J Dent.* 2009;22(4):241–8.
- Lee H, Lytton-Jean AK, Chen Y, Love KT, Park AI, Karagiannis ED, et al. Molecularly self-assembled nucleic acid nanoparticles for targeted in vivo siRNA delivery. *Nat Nanotechnol.* 2012;7(6):389–93. <https://doi.org/10.1038/nnano.2012.73>.
- Lee JH, Lee JM, Hwang J, Park JY, Kim M, Kim DH, et al. User perception of medical service robots in hospital wards: a cross-sectional study. *J Yeungnam Med Sci.* 2022;39(2):116–23. <https://doi.org/10.12701/yujm.2021.01319>.
- Lemmerman LR, Das D, Higueta-Castro N, Mirmira RG, Gallego-Perez D. Nanomedicine-based strategies for diabetes: diagnostics, monitoring, and treatment. *Trends Endocrinol Metab.* 2020;31(6):448–58. <https://doi.org/10.1016/j.tem.2020.02.001>.
- Li J, Gao W, Dong R, Pei A, Sattayasamitsathit S, Wang J. Nanomotor lithography. *Nat Commun.* 2014;5:5026. <https://doi.org/10.1038/ncomms6026>.
- Li H, Zhang J, Zhang N, Kershaw J, Wang L. Fabrication and wireless micromanipulation of magnetic-biocompatible microrobots using microencapsulation for microrobotics and microfluidics applications. *J Microencapsul.* 2016;33(8):712–7. <https://doi.org/10.1080/02652048.2016.1234514>.
- Li J, Esteban-Fernandez de Avila B, Gao W, Zhang L, Wang J. Micro/nanorobots for biomedicine: delivery, surgery, sensing, and detoxification. *Sci Robot.* 2017;2(4):eaam6431. <https://doi.org/10.1126/scirobotics.aam6431>.
- Li S, Jiang Q, Liu S, Zhang Y, Tian Y, Song C, et al. A DNA nanorobot functions as a cancer therapeutic in response to a molecular trigger in vivo. *Nat Biotechnol.* 2018;36(3):258–64. <https://doi.org/10.1038/nbt.4071>.
- Li D, Liu C, Yang Y, Wang L, Shen Y. Micro-rocket robot with all-optic actuating and tracking in blood. *Light Sci Appl.* 2020;9:84. <https://doi.org/10.1038/s41377-020-0323-y>.
- Liu M, Qiu JG, Ma F, Zhang CY. Advances in single-molecule fluorescent nanosensors. *Wiley Interdiscip Rev Nanomed Nanobiotechnol.* 2021;13(5):e1716. <https://doi.org/10.1002/wnan.1716>.
- Lu X, Wei Y, Ou H, Zhao C, Shi L, Liu W. Universal control for micromotor swarms with a hybrid Sono-electrode. *Small.* 2021;17(44):e2104516. <https://doi.org/10.1002/smll.202104516>.
- Lueg C, Jungo V. Mobile remote presence robots for medical consultation and social connectedness. *Stud Health Technol Inform.* 2021;281:999–1003. <https://doi.org/10.3233/SHTI210328>.
- Lyu X, Liu X, Zhou C, Duan S, Xu P, Dai J, et al. Active, yet little mobility: asymmetric decomposition of H₂O₂ is not sufficient in propelling catalytic micromotors. *J Am Chem Soc.* 2021;143(31):12154–64. <https://doi.org/10.1021/jacs.1c04501>.
- Mak IW, Evaniew N, Ghert M. Lost in translation: animal models and clinical trials in cancer treatment. *Am J Transl Res.* 2014;6(2):114–8.
- Manesh KM, Cardona M, Yuan R, Clark M, Kagan D, Balasubramanian S, et al. Template-assisted fabrication of salt-independent catalytic tubular microengines. *ACS Nano.* 2010;4(4):1799–804. <https://doi.org/10.1021/nn1000468>.
- Mathesh M, Bhattarai E, Yang W. 2D active nanobots based on soft nanoarchitectonics powered by an ultralow fuel concentration. *Angew Chem Int Ed Engl.* 2022;61(7):e202113801. <https://doi.org/10.1002/anie.202113801>.
- Mei Y, Solovev AA, Sanchez S, Schmidt OG. Rolled-up nanotech on polymers: from basic perception to self-propelled catalytic microengines. *Chem Soc Rev.* 2011;40(5):2109–19. <https://doi.org/10.1039/c0cs00078g>.
- Mertz L. Tiny conveyance: micro- and Nanorobots prepare to advance medicine. *IEEE Pulse.* 2018;9(1):19–23. <https://doi.org/10.1109/MPUL.2017.2772118>.
- Mishra N, Trivedi A, Gajdhar SK, Bhagwat H, Khutwad GK, Mall PE, et al. Correlation of blood glucose levels, salivary glucose levels and oral colony forming units of *Candida albicans* in type 2 diabetes mellitus patients. *J Contemp Dent Pract.* 2019;20(4):494–8.

- Mitra S, Roy N, Maity S, Bandyopadhyay D. Multimodal chemo-/magneto-/phototaxis of 3G CNT-bots to power fuel cells. *Microsyst Nanoeng.* 2020;6:19. <https://doi.org/10.1038/s41378-019-0122-x>.
- Mitragotri S, Burke PA, Langer R. Overcoming the challenges in administering biopharmaceuticals: formulation and delivery strategies. *Nat Rev Drug Discov.* 2014;13(9):655–72. <https://doi.org/10.1038/nrd4363>.
- Miyashita M, Ito N, Ikeda S, Murayama T, Oguma K, Kimura J. Development of urine glucose meter based on micro-planer amperometric biosensor and its clinical application for self-monitoring of urine glucose. *Biosens Bioelectron.* 2009;24(5):1336–40. <https://doi.org/10.1016/j.bios.2008.07.072>.
- Morgado PI, Palacios M, Larrain J. In situ injectable hydrogels for spinal cord regeneration: advances from the last 10 years. *Biomed Phys Eng Express.* 2019;6(1):012002. <https://doi.org/10.1088/2057-1976/ab52e8>.
- Mostaghaci B, Yasa O, Zhuang J, Sitti M. Bioadhesive bacterial microswimmers for targeted drug delivery in the urinary and gastrointestinal tracts. *Adv Sci (Weinh).* 2017;4(6):1700058. <https://doi.org/10.1002/advs.201700058>.
- Nelson BJ, Kaliakatsos IK, Abbott JJ. Microrobots for minimally invasive medicine. *Annu Rev Biomed Eng.* 2010;12:55–85. <https://doi.org/10.1146/annurev-bioeng-010510-103409>.
- Nguyen VD, Zheng S, Han J, Le VH, Park JO, Park S. Nanohybrid magnetic liposome functionalized with hyaluronic acid for enhanced cellular uptake and near-infrared-triggered drug release. *Colloids Surf B Biointerfaces.* 2017;154:104–14. <https://doi.org/10.1016/j.colsurfb.2017.03.008>.
- Olsman N, Goentoro L. There's (still) plenty of room at the bottom. *Curr Opin Biotechnol.* 2018;54:72–9. <https://doi.org/10.1016/j.copbio.2018.01.029>.
- Ongaro F, Scheggi S, Ghosh A, Denasi A, Gracias DH, Misra S. Design, characterization and control of thermally-responsive and magnetically-actuated micro-grippers at the air-water interface. *PLoS One.* 2017;12(12):e0187441. <https://doi.org/10.1371/journal.pone.0187441>.
- Orive G, Hernandez RM, Rodriguez Gascon A, Dominguez-Gil A, Pedraz JL. Drug delivery in biotechnology: present and future. *Curr Opin Biotechnol.* 2003;14(6):659–64. <https://doi.org/10.1016/j.copbio.2003.10.007>.
- Ortiz-Rivera I, Mathesh M, Wilson DA. A supramolecular approach to nanoscale motion: polymersome-based self-propelled nanomotors. *Acc Chem Res.* 2018;51(9):1891–900. <https://doi.org/10.1021/acs.accounts.8b00199>.
- Patel GM, Patel GC, Patel RB, Patel JK, Patel M. Nanorobot: a versatile tool in nanomedicine. *J Drug Target.* 2006;14(2):63–7. <https://doi.org/10.1080/10611860600612862>.
- Peng J, Chen F, Liu Y, Zhang F, Cao L, You Q, et al. A light-driven dual-nanotransformer with deep tumor penetration for efficient chemo-immunotherapy. *Theranostics.* 2022;12(4):1756–68. <https://doi.org/10.7150/thno.68756>.
- Pinan Basualdo FN, Bolopion A, Gauthier M, Lambert P. A microrobotic platform actuated by thermocapillary flows for manipulation at the air-water interface. *Sci Robot.* 2021;6(52):eabf1571. <https://doi.org/10.1126/scirobotics.abd3557>.
- Polidori D, Sha S, Ghosh A, Plum-Morschel L, Heise T, Rothenberg P. Validation of a novel method for determining the renal threshold for glucose excretion in untreated and canagliflozin-treated subjects with type 2 diabetes mellitus. *J Clin Endocrinol Metab.* 2013;98(5):E867–71. <https://doi.org/10.1210/jc.2012-4205>.
- Pourgholi F, Hajivalili M, Farhad JN, Kafil HS, Yousefi M. Nanoparticles: novel vehicles in treatment of glioblastoma. *Biomed Pharmacother.* 2016;77:98–107. <https://doi.org/10.1016/j.biopha.2015.12.014>.
- Rahman M, Sampad MJN, Hawkins A, Schmidt H. Recent advances in integrated solid-state nanopore sensors. *Lab Chip.* 2021;21(16):3030–52. <https://doi.org/10.1039/d1lc00294e>.
- Salvati E, Stellacci F, Krol S. Nanosensors for early cancer detection and for therapeutic drug monitoring. *Nanomedicine (Lond).* 2015;10(23):3495–512. <https://doi.org/10.2217/nmm.15.180>.

- Sanchez S, Soler L, Katuri J. Chemically powered micro- and nanomotors. *Angew Chem Int Ed Engl.* 2015;54(5):1414–44. <https://doi.org/10.1002/anie.201406096>.
- Saravana KR, Vijayalakshmi R. Nanotechnology in dentistry. *Indian J Dent Res.* 2006;17(2):62–5. <https://doi.org/10.4103/0970-9290.29890>.
- Schuerle S, Soleimany AP, Yeh T, Anand GM, Haberli M, Fleming HE, et al. Synthetic and living micropropellers for convection-enhanced nanoparticle transport. *Sci Adv.* 2019;5(4):eaav4803. <https://doi.org/10.1126/sciadv.aav4803>.
- Seeman NC. DNA in a material world. *Nature.* 2003;421(6921):427–31. <https://doi.org/10.1038/nature01406>.
- Sitti M, Ceylan H, Hu W, Giltinan J, Turan M, Yim S, et al. Biomedical applications of untethered mobile milli/microrobots. *Proc IEEE Inst Electr Electron Eng.* 2015;103(2):205–24. <https://doi.org/10.1109/JPROC.2014.2385105>.
- Sobczak JP, Martin TG, Gerling T, Dietz H. Rapid folding of DNA into nanoscale shapes at constant temperature. *Science.* 2012;338(6113):1458–61. <https://doi.org/10.1126/science.1229919>.
- Solovev AA, Xi W, Gracias DH, Harazim SM, Deneke C, Sanchez S, et al. Self-propelled nanotools. *ACS Nano.* 2012;6(2):1751–6. <https://doi.org/10.1021/nn204762w>.
- Sondergaard RV, Henriksen JR, Andresen TL. Design, calibration and application of broad-range optical nanosensors for determining intracellular pH. *Nat Protoc.* 2014;9(12):2841–58. <https://doi.org/10.1038/nprot.2014.196>.
- Soto F, Wang J, Ahmed R, Demirci U. Medical micro/Nanorobots in precision medicine. *Adv Sci (Weinh).* 2020;7(21):2002203. <https://doi.org/10.1002/adv.202002203>.
- Soto F, Karshalev E, Zhang F, Esteban Fernandez de Avila B, Nourhani A, Wang J. Smart materials for microrobots. *Chem Rev.* 2022;122(5):5365–403. <https://doi.org/10.1021/acs.chemrev.0c00999>.
- Suri GS, Kaur A, Sen T. A recent trend of drug-nanoparticles in suspension for the application in drug delivery. *Nanomedicine (Lond).* 2016;11(21):2861–76. <https://doi.org/10.2217/nmm-2016-0238>.
- Tabatabaei SN, Tabatabaei MS, Girouard H, Martel S. Hyperthermia of magnetic nanoparticles allows passage of sodium fluorescein and Evans blue dye across the blood-retinal barrier. *Int J Hyperth.* 2016;32(6):657–65. <https://doi.org/10.1080/02656736.2016.1193903>.
- Teo WZ, Zboril R, Medrik I, Pumera M. Fe(0) Nanomotors in ton quantities (10(20) units) for environmental remediation. *Chemistry.* 2016;22(14):4789–93. <https://doi.org/10.1002/chem.201504912>.
- Torne S, Darandale S, Vavia P, Trotta F, Cavalli R. Cyclodextrin-based nanosponges: effective nanocarrier for tamoxifen delivery. *Pharm Dev Technol.* 2013;18(3):619–25. <https://doi.org/10.3109/10837450.2011.649855>.
- van den Heuvel MG, Dekker C. Motor proteins at work for nanotechnology. *Science.* 2007;317(5836):333–6. <https://doi.org/10.1126/science.1139570>.
- Wan M, Wang Q, Wang R, Wu R, Li T, Fang D, et al. Platelet-derived porous nanomotor for thrombus therapy. *Sci Adv.* 2020;6(22):eaaz9014. <https://doi.org/10.1126/sciadv.aaz9014>.
- Wang H. Plasmonic refractive index sensing using strongly coupled metal nanoantennas: nonlocal limitations. *Sci Rep.* 2018;8(1):9589. <https://doi.org/10.1038/s41598-018-28011-x>.
- Wang F, Yang S, Yuan J, Gao Q, Huang C. Effective method of chitosan-coated alginate nanoparticles for target drug delivery applications. *J Biomater Appl.* 2016;31(1):3–12. <https://doi.org/10.1177/0885328216648478>.
- Wang D, Gao C, Zhou C, Lin Z, He Q. Leukocyte membrane-coated liquid metal nanoswimmers for actively targeted delivery and synergistic chemophotothermal therapy. *Research (Wash D C).* 2020;2020:3676954. <https://doi.org/10.34133/2020/3676954>.
- Wang L, Wang J, Hao J, Dong Z, Wu J, Shen G, et al. Guiding drug through interrupted bloodstream for potentiated thrombolysis by C-shaped magnetic actuation system in vivo. *Adv Mater.* 2021a;33(51):e2105351. <https://doi.org/10.1002/adma.202105351>.

- Wang Z, Murphy A, O'Riordan A, O'Connell I. Equivalent impedance models for electrochemical nanosensor-based integrated system design. *Sensors (Basel)*. 2021b;21(9):3259. <https://doi.org/10.3390/s21093259>.
- Wei T, Liu J, Li D, Chen S, Zhang Y, Li J, et al. Development of magnet-driven and image-guided degradable microrobots for the precise delivery of engineered stem cells for cancer therapy. *Small*. 2020;16(41):e1906908. <https://doi.org/10.1002/sml.201906908>.
- Williams RM, Lee C, Galassi TV, Harvey JD, Leicher R, Sirenko M, et al. Noninvasive ovarian cancer biomarker detection via an optical nanosensor implant. *Sci Adv*. 2018;4(4):eaq1090. <https://doi.org/10.1126/sciadv.aq1090>.
- Wu Z, Li L, Yang Y, Hu P, Li Y, Yang SY, et al. A microrobotic system guided by photoacoustic computed tomography for targeted navigation in intestines in vivo. *Sci Robot*. 2019;4(32):eaax0613. <https://doi.org/10.1126/scirobotics.aax0613>.
- Xie L, Liu T, He Y, Zeng J, Zhang W, Liang Q, et al. Kinetics-regulated interfacial selective super-assembly of asymmetric smart nanovehicles with tailored topological hollow architectures. *Angew Chem Int Ed Engl*. 2022;61(12):e202200240. <https://doi.org/10.1002/anie.202200240>.
- Xing JH, Yin T, Li SM, Xu TT, Ma AQ, Chen Z, et al. Sequential magneto-actuated and optics-triggered biomicrorobots for targeted cancer therapy. *Adv Funct Mater*. 2021;31(11):ARTN 2008262. <https://doi.org/10.1002/adfm.202008262>.
- Xu K, Liu B. Recent progress in actuation technologies of micro/nanorobots. *Beilstein J Nanotechnol*. 2021;12:756–65. <https://doi.org/10.3762/bjnano.12.59>.
- Xuan M, Shao J, Lin X, Dai L, He Q. Self-propelled Janus mesoporous silica nanomotors with sub-100 nm diameters for drug encapsulation and delivery. *ChemPhysChem*. 2014;15(11):2255–60. <https://doi.org/10.1002/cphc.201402111>.
- Yang Y, Arque X, Patino T, Guillerm V, Blersch PR, Perez-Carvajal J, et al. Enzyme-powered porous micromotors built from a hierarchical micro- and mesoporous UiO-type metal-organic framework. *J Am Chem Soc*. 2020;142(50):20962–7. <https://doi.org/10.1021/jacs.0c11061>.
- Yao L, Zhao X, Li Q, Zu Y, Fu Y, Zu B, et al. In vitro and in vivo evaluation of camptothecin nanosuspension: a novel formulation with high antitumor efficacy and low toxicity. *Int J Pharm*. 2012;423(2):586–8. <https://doi.org/10.1016/j.ijpharm.2011.11.031>.
- Yuan S, Holmqvist F, Kongstad O, Jensen SM, Wang L, Ljungstrom E, et al. Long-term outcomes of the current remote magnetic catheter navigation technique for ablation of atrial fibrillation. *Scand Cardiovasc J*. 2017;51(6):308–15. <https://doi.org/10.1080/14017431.2017.1384566>.
- Zelikin AN, Ehrhardt C, Healy AM. Materials and methods for delivery of biological drugs. *Nat Chem*. 2016;8(11):997–1007. <https://doi.org/10.1038/nchem.2629>.
- Zhang Y, Sun C, Kohler N, Zhang M. Self-assembled coatings on individual monodisperse magnetite nanoparticles for efficient intracellular uptake. *Biomed Microdevices*. 2004;6(1):33–40. <https://doi.org/10.1023/b:bmm.0000013363.77466.63>.
- Zhang H, Li Z, Gao C, Fan X, Pang Y, Li T, et al. Dual-responsive biohybrid neutroblots for active target delivery. *Sci Robot*. 2021a;6(52) <https://doi.org/10.1126/scirobotics.aaz9519>.
- Zhang L, Guo Y, Hao R, Shi Y, You H, Nan H, et al. Ultra-rapid and highly efficient enrichment of organic pollutants via magnetic mesoporous nanosponge for ultrasensitive nanosensors. *Nat Commun*. 2021b;12(1):6849. <https://doi.org/10.1038/s41467-021-27100-2>.
- Zhang Z, Wang L, Chan TKF, Chen Z, Ip M, Chan PKS, et al. Micro-/nanorobots in antimicrobial applications: recent Progress, challenges, and opportunities. *Adv Healthc Mater*. 2022;11(6):e2101991. <https://doi.org/10.1002/adhm.202101991>.
- Zhou H, Mayorga-Martinez CC, Pane S, Zhang L, Pumera M. Magnetically driven micro and nanorobots. *Chem Rev*. 2021;121(8):4999–5041. <https://doi.org/10.1021/acs.chemrev.0c01234>.
- Zollinger RM. A salute to the American journal of surgery on its 100th birthday. *Am J Surg*. 1991;161(2):191–3. [https://doi.org/10.1016/0002-9610\(91\)91128-6](https://doi.org/10.1016/0002-9610(91)91128-6).

Chapter 3

Biomolecule-Based Nanorobot for Targeted Delivery of Therapeutics



Keya Ganguly, Sayan Deb Dutta, Dinesh K. Patel, Tejal V. Patil, Rachmi Luthfikasari, and Ki-Taek Lim

3.1 Introduction

Delivery of therapeutics to treat human diseases has greatly been based on *conventional treatments*. These include administering chemical or biological drugs through intravenous, intramuscular, or subcutaneous routes (Langer 1990; Escobar-Chávez et al. 2012; Fenton et al. 2018). Successful therapeutic outcomes have also been realized owing to the potentiality of such medical advancements (Hilt and Peppas 2005). However, these conventional treatments have notable limitations. The limitations are profoundly encountered in treating diseases such as cancer (Senapati et al. 2018; Kratz and Warnecke 2012; Ding et al. 2019), neurodegenerative disorders (Dwivedi et al. 2019; Md et al. 2018; Teixeira et al. 2020), cardiovascular diseases (Khalaj and Douroumis 2022; Aldarondo and Wayne 2022), diabetes (Zaric et al. 2019; Lee et al. 2018), infectious diseases (Paredes et al. 2021; Yeh et al. 2020; Makvandi et al. 2021), and post-surgical scenarios (Bu et al. 2019), among others. A few notable challenges include long-term clinical drawbacks of

K. Ganguly · S. D. Dutta · D. K. Patel · R. Luthfikasari
Department of Biosystems Engineering, Kangwon National University,
Chuncheon, Republic of Korea

T. V. Patil
Interdisciplinary Program in Smart Agriculture, Kangwon National University,
Chuncheon, Republic of Korea

K.-T. Lim (✉)
Department of Biosystems Engineering, Kangwon National University,
Chuncheon, Republic of Korea

Interdisciplinary Program in Smart Agriculture, Kangwon National University,
Chuncheon, Republic of Korea
e-mail: ktlim@kangwon.ac.kr

systemic side effects, toxicity resulting from inexistent targeting, and multiple, indiscriminate damages to non-target tissues and organs (Dostalova et al. 2018). The nanomedicines administered through the conventionally available routes operate through a few common fundamental mechanisms (Siepmann and Siepmann 2008; Li and Mooney 2016). It includes encapsulating therapeutics in a biocompatible nanocarrier system that can move across cellular barriers to ensure targeted delivery with enhanced permeation and retention (EPR) effects (Nakamura et al. 2016; Allen and Cullis 2013; Mitchell et al. 2021). Despite the advancements at the laboratory scale, the percentage of successful clinical applications are relatively sparse (Foulkes et al. 2020). A few causes of such medical failures result from the clearance effect of the mononuclear phagocyte system (MPS) (Huang et al. 2020; Wei et al. 2021), the glomerular filtration of the foreign entity in the kidney (Du et al. 2018; Zhao et al. 2020a), and the impermeability of capillary walls on the administered drug-cargo conjugate (Parakhonskiy et al. 2021). Alternatively, ligands (antibody fragments, peptides, small molecules, antibodies, and several receptor ligands) decorated therapeutic cargos have been employed to achieve ligand-mediated targeted delivery (Parakhonskiy et al. 2021; Oh et al. 2018). Nanomaterials have also been implemented for targeted delivery through active or passive routes, including nanoparticles, liposomes, polymersomes, and dendrimers. However, incapability of the carriers has been the major issue in these situations, leading to drug accumulation at nonspecific locations (Ruenraroengsak et al. 2010).

Moreover, the active delivery of therapeutics is found to be effective only under close proximity between drug carrier and the target tissue, which is $\sim \leq 0.5$ nm (Bae and Park 2011). A careful observation reveals that the fundamental laws of physics along with the physico-chemical aspects of materials, especially in relation to diffusion, adsorption, adhesion, and hydrodynamics behavior, might apply in the successful functioning of a carrier (Forouzandehmehr et al. 2022). Hence, developing intelligent on-demand and site-specific delivery of therapeutics has become a significant objective of modern medical research; this can be possible through developing nanocarriers with self-propulsion and controlled navigation abilities. In this regard, the fabrication of micro-/nanobots appears promising class of delivery carriers toward the targeted delivery of therapeutics. A successful targeted drug delivery using nanobots is anticipated to accelerate pharmacokinetics or pharmacodynamics properties, reducing the off-target toxicity of therapeutics (Luo et al. 2018).

3.2 DNA and Proteins

Attempts are being made to design self-propelling target-specific smart nanobots capable of intrinsic navigation in body fluids with deep tissue-penetrating efficacy. This emerging biomedical engineering frontier heavily relies on outstanding engineering designs, interaction dynamics, and fine-tuning the functional aspects of the nanobots at the biological interfaces. Succeeding in establishing such

biocompatible, controllable, degradable nanobots of high precision is a formidable long-term technological and engineering challenge (Ruenraroengsak et al. 2010). Investigations demonstrate that biomolecules such as DNA and proteins can be programmed to fabricate such intelligent nanobots (Tavassoly and Tavassoly 2021; Chen et al. 2022). The notion of utilizing DNA as a nanomachine was pioneered by Nadrian Seeman in the early 1980s (Seeman 1999). Firstly, bio-based nanobots or *nanorobots* are advantageous over other innovative materials because they are biocompatible and biodegradable. Secondly, DNA strands can be programmed to zip themselves in complex shapes like squares, cubes, octahedrons, or any regular geometric shapes (Winfree et al. 1998; Seeman 2003; Zhang et al. 2022).

Moreover, automated DNA synthesis has enhanced the synthesis of desirable DNA strands (Kosuri and Church 2014) with diverse functionality like stimuli-responsiveness, drug loading, and target specificity, within one rationally designed DNA architecture (Kosuri and Church 2014; Nummelin et al. 2020). Similarly, proteins are also suitable programmable polymers owing to their structure and ability to self-assemble, paving the way toward generating protein-based nanobots. It has even been realized that the number of possible nucleotide and polypeptide sequences for designing nanobots exceeds the number of atoms in the universe (Ulijn and Jerala 2018). To deliver therapeutics to the targeted site, the biomolecule-based nanobots have been equipped with sophisticated abilities. These include systemic circulation and navigation, generation of propulsive forces, cargo transportation, and tissue perforation (Peng et al. 2015; Wu et al. 2015).

Additionally, the nanomotors perform various stimuli-responsive activities, including rotation, rolling, shuttling, and contraction under dynamic body conditions. For instance, DNA and protein origami has been a remarkable strategy to design nanobots with complex shapes and logic switches to attain therapeutic delivery (Chen et al. 2016). Figure 3.1 summarizes the progress in the development of DNA and protein conjugates since the 1980s for disease diagnostics, nanoassembly, drug delivery, and therapeutics, clarifying that the full-fledged emergence of DNA and protein nanobots appeared in the early 2020s (Zhao et al. 2020b). The biomolecular robotic systems generally comprise sensors and actuators coordinated by an information processing unit. An upsurge of these biomolecule-based constructions proved to be a natural modular platform that operates through programmability of the self-assembly of various structural-functional motifs combined in a predetermined order. The biomolecular modules are sophisticatedly organized for sensing, actuation, intra-system communication, and computing, making it a nanorobotic system at the molecular level. DNA nanotechnology has taken DNA molecules into nanobots, owing to several supporting factors. It has been known that DNA molecule acts like an entropic spring, making them suitable for stretching and bending by external forces. The deformed DNA structure can often regain its original form after reversing the environmental condition. Significantly, designing the required kind of DNA nanorobots can utilize the joining of the stiff beams and short oligonucleotides at varying permutations and combinations to constitute a hinge and its analog such as slider, crank-slider, and Bennett linkage, among others. Such compositional variations control the robotic angular, linear, and reversible 3D motion

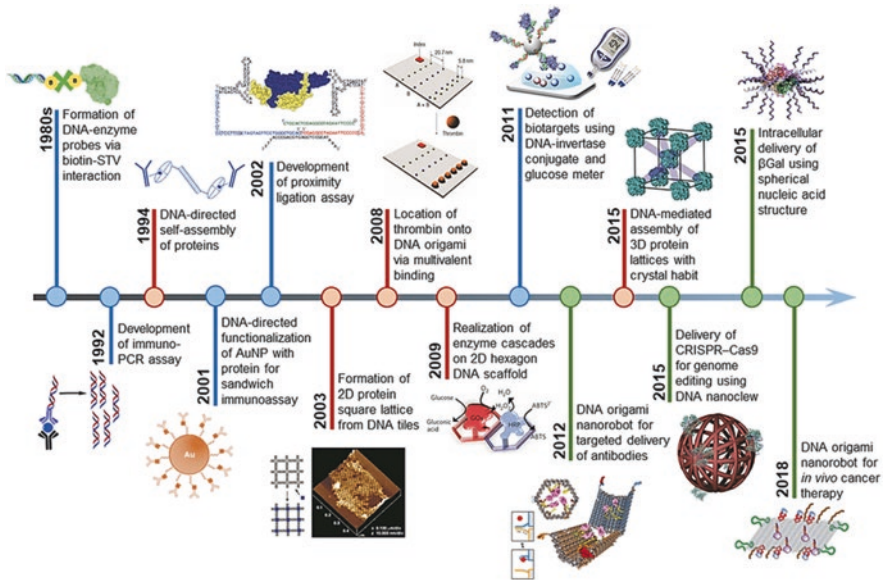


Fig. 3.1 Timeline for developing DNA-protein conjugates from the 1980s through 2018. (Zhao et al. 2020b)

cycle along with other restricted, mechanical motions. One of the significant enhancements in the DNA nanobots has been the integration of various logic gates (AND, OR, XOR, NAND, NOT, CNOT) that can be used to display different drug outputs to living systems from cultured cells to mammals. DNA nanobots are also heavily used as therapeutic cargo in conjugation with targeting aptamer for the accurate delivery of drugs upon molecular triggers. Besides, DNA nanobots are deployed for cascade drug delivery, controlled drug release, and immunotherapy, for instance, using CpG sequence-rich and antigen-modified DNA nanobots.

3.3 CAD Systems for Bio-nanorobotics Simulation

The advancement in the application of virtual reality techniques in bio-nanotechnology is of utmost importance regarding the design of molecular nanobots of DNA or proteins. Moreover, to guarantee the successful utilization of molecular robots in bionic systems, the determination of base sequences is of utmost importance for constructing sophisticated DNA or protein nanobots. Several types of software based on VR and molecular dynamics (MD) simulations can virtually prototype bio-nanorobotic systems and optimize their design considering the dynamic environment in the human body system (Hamdi and Ferreira 2008; Hamdi 2009). MD simulations have also helped determine the potential of DNA nanobots composed of ssDNA w.r.t. dsDNA. It has been estimated that, without covalent

double chains, ssDNA allows facile self-assembly of nanostructures with low valence and directional bonding, making ssDNA-based nanobots more available for modifications w.r.t. its dsDNA counterparts. However, we expect poor stability, increased folding errors, and complicated sequence optimizations concerning ssDNA nanobots. In light of computational calculations into the traditional dsDNA origami, stable 3D structures can be simulated in unprecedented microscopic detail. In an automated fashion, MD simulations allow rapid assemblies of biomolecular nanobot structures with fine control over the geometrical, mechanical, and dynamic properties of the 3D DNA structures (Benson et al. 2019; Shen et al. 2022).

3.4 Biomolecule-Loaded Therapeutic Delivery

3.4.1 *Pharmaceuticals*

Pharmaceutical drugs comprise small synthetic chemicals which demand administration at high dosage to compensate for their short half-life, limited biodistribution, and rapid clearance from the body. However, repeated administration at a high dosage often leads to increased side effects and cytotoxicity. Hence, using nanobots for the targeted drug delivery is a suitable platform to deliver precisely rather than a systemic release of larger therapeutic dosages (Soto et al. 2020). One of the early developments in the DNA-based nanobots was developed as a DNA-based walking device capable of autonomous locomotion along a nucleic acid track, with the light control of initiation, termination, and velocity. The walking system consisted of three parts: a single-stranded DNA tract, our anchorage sites, and a light-sensitive walker. The DNA walker contained two motion legs, a short leg of 7 nucleotides and a long leg of 16 nucleotides, linked by a pyrene moiety that worked as a photosensitizer and was incorporated into a DNA oligomer. The two motion legs are designed to bind the two extender segments, which are connected by a weak disulfide bond. The recognition event between the legs and the anchorage sites brings the pyrene and disulfide moieties together (You et al. 2012).

Autonomous DNA nanobots have also been developed to transport payloads to disease sites such as a tumor in the case of cancer treatment. One of the examples includes the functionalization of DNA nanobots on the outside with a DNA aptamer that binds nucleoli. A protein specifically expressed on tumor-associated endothelial cells and thrombin is the blood-coagulating protease protein within its inner cavity (Li et al. 2018). DNA origami has primarily been used to deliver the cancer drug doxorubicin (DOX). DOX is a well-known anticancer drug, however, with a potent side effect to healthy cells. Hence, the targeted delivery of DOX has been a significant concern in cancer therapy. To confront this challenge, many researchers have developed drug carrier systems based on self-assembled, spatially addressable DNA origami nanostructures. DOX can be non-covalently attached to DNA, leading to a high drug loading level. A non-covalently attached DOX DNA hybrid was

administered against human breast adenocarcinoma cancer cells (MCF 7) with significant enhancement in the cell-killing activity, including doxorubicin-resistant MCF 7 cells. One of the molecular mechanisms associated with this type has primarily been associated with the inhibition of lysosomal acidification, resulting in the cellular redistribution of a drug to the action sites (Jiang et al. 2012). Nie Zhou's team reported for the first time that DNA nanobots, which can walk on the interface of the mobile cell membrane and have the function of driving cells, could regulate cell rearrangement by constantly activating receptor signaling pathways and super-sensitively controlling cell migration behavior.

Additionally, in this design, the conditions of different selective environments can be controlled for the operation of DNA robots by customizing different DNA enzyme-based driving modules. Then the cell behaviors are controlled orthogonally, which further verifies the multi-power of this design strategy. In conclusion, this research provides a new strategy to transform nanoscale molecular manipulation of DNA robots into micro-scale behavior of living cells, which is highly hopeful to promote the development of cell-based nanoscale precision medicine in the future (Guan et al. 2021; Li et al. 2021a) (Fig. 3.2).

DNA origami nanorobots can also recognize specific cell surface protein and deliver payloads such as metal nanoparticles and fluorescently labeled antibody fragments that can ultimately trigger cell signaling. The complex-shaped DNA origami nanorobots are created by manipulating long DNA strands bound to shorter

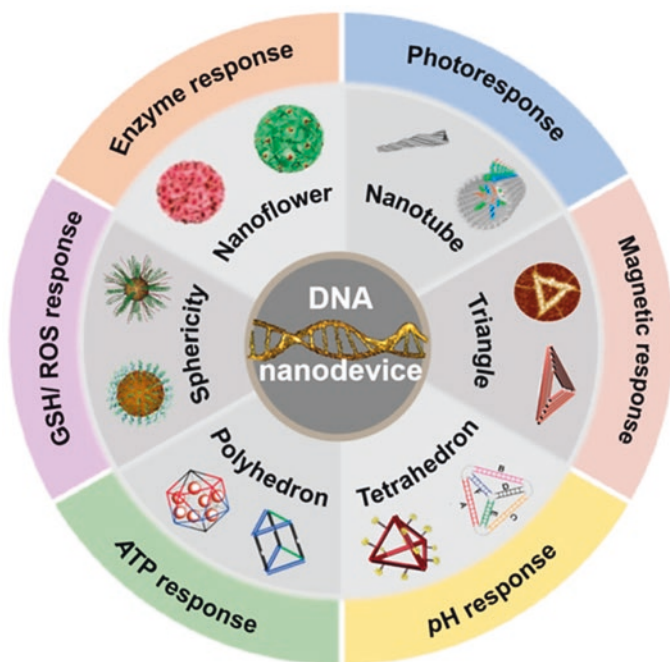


Fig. 3.2 Illustration of the different types of DNA nanodevices. (Guan et al. 2021)

“staple” strands. This DNA origami nanorobot was designed with a computer-aided design tool. For the desired functioning of the device in response to proteins, a DNA aptamer-based lock mechanism was designed that could open in response to binding antigen keys (Fig. 3.3) (Douglas et al. 2012).

3.4.2 *Biologics and Genes*

Gene therapy is a highly researched discipline to treat many gene-related chronic diseases (Wang et al. 2022; Singh et al. 2021; Lostalé-Seijo and Montenegro 2018). RNAi has been a widely used tool for gene therapy for the last few decades using several synthetic gene vectors such as lipid carriers, quantum dots, and nanoparticles, to name a few. Gene delivery strategies could provide a complete and permanent cure for numerous genetic diseases by replacing damaged DNA sequences

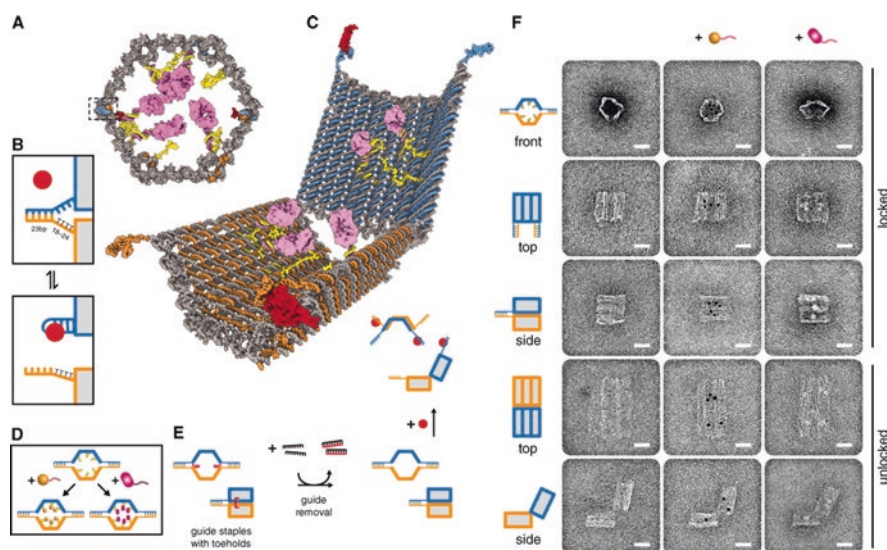


Fig. 3.3 Aptamer-gated DNA nanobot (a) illustrates the orthographic view of a closed nanobot carrying protein payload. (b) The mechanism of the aptamer lock function comprises a DNA aptamer (blue) with its partially complementary strand (orange). The antigen key (red) can stabilize the lock at a dissociated state. (c) Schematic illustration of the nanobot opened by protein displacement of aptamer locks. Blue and orange domains are constrained in the rear by hinges. (d) Payloads can be loaded inside the nanobots, nanoparticles (gold), and antibody Fab' fragments (magenta). (e) Guide staples (red) with eight-base toeholds aid the assembly of nanobot to a 97.5% yield in a closed state. (f) TEM images of the robots in closed and open conformations. Unloaded robots (left column), robots loaded with 5 nm gold nanoparticles (center column), and robots loaded with Fab' fragments (right column). The developed nanodevice can be visualized as an extended version of aptamer beacons and structure-switching aptamer, which typically undergoes target-induced switching between an aptamer-complement duplex and an aptamer-target complex. (Douglas et al. 2012; Nutiu and Li 2003)

with the desired template. In this regard, *chromalloytes*, the hypothetical nanobots capable of chromosomal exchange operation inside living cells, have been envisioned as one of the cell repair nanobots performing chromosome replacement therapy (CRT) (Ahmad et al. 2021).

3.4.3 Living Cell-Based Therapies

Cell-based therapy has become one of the promising approaches for treating several chronic ailments, like cancer, neurodegenerative diseases, diabetes, and wound healing processes (Kimbrel and Lanza 2020; Nourian Dehkordi et al. 2019). It has been a great alternative to the numerous chemical drugs posing severe side effects upon prolonged use. Mesenchymal stem cells (MSCs) are actively used for cell-based therapy owing to their various functionalities and their potency in the replenishment of lost cells through in situ multi-differentiation capability, stimulating in situ cell differentiation, and delivering therapeutic agents (Alipour et al. 2019). New avenues regarding cell therapy for diabetes are at an upsurge through the generation of β -islet cells from human pluripotent stem cells, embryonic stem cells (ESC), and adult mesenchymal stem cells (MSC) (Kondo et al. 2018; P ath et al. 2019; Nair et al. 2020). Strikingly successful outcomes of nanobot-mediated delivery of cells have been observed by researchers worldwide. To accomplish nanobot-mediated transport of therapeutic cells, nanobots are designed to have the desired affinity for the cells. The cell-transport nanorobots had been through various levels of transformational upgradations. One initial nanobot system developed was based on classic bubble-propelled rockets prepared through thin-film rolled-up technology, e-beam evaporation methods, and template-based electrodeposition procedures. Nanobots functionalized with several bio-receptors such as aptamer, oligonucleotides, and antibodies proved advantageous over the classical models. Particular significant challenges in developing such cell-carrying nanobots were the difficulty of releasing cells at the target site; hence, the nanobots' physical features, including their shape and size, were taken into consideration synergistically with the use of biomolecules. The advancement in the fabrication of nanobots has attained the extent that they can carry multiple cell numbers and types (Chen et al. 2022). The type of DNA nanorobot and their mechanism of action and possible applications are summarized in Table 3.1.

Table 3.1 Selected DNA robot types, mechanism of action, characterization techniques, and possible applications (Nummelin et al. 2020)

| Classification/robot type | Mechanism of action | Characterization/imaging | Application |
|--------------------------------|--|---|---|
| <i>Mechanical tools</i> | | | |
| Force clamp | Entropic DNA springs | FRET | Resolving, e.g., DNA conformational changes |
| Pylons | DNA base stacking | Optical tweezers | Resolving DNA base stacking interaction |
| Calipers | DNA hinge + interaction between the investigated species | TEM, FRET, cryo-EM | Measuring, e.g., forces between nucleosomes and nucleosome unwrapping |
| <i>Information relay</i> | | | |
| Networks | Base stacking (depends on ionic strength) | TEM | Large-scale movement |
| Nanoactuator/accordion rack | DNA hybridization | AFM, TEM | Molecular regulation |
| Domino arrays | Base stacking | AFM | Long-distance step-by-step movement |
| <i>Nanomedicine</i> | | | |
| Imaging tools/antibody sensors | Various conformational (e.g., i-tetraplex) and structural transitions, DNA transient binding | FRET, fluorescence microscopy, DNA-PAINT | Diagnostics, studying pathway dynamics, payload delivery, super-resolution imaging, pH mapping (also in vivo) |
| Pliers | Target molecule binding | AFM, spectroscopy | Diagnostics, molecular computing |
| Nanorobots | (logic-gated) aptamer-protein interaction | TEM, AFM, flow cytometry | Targeted and programmable drug delivery, computing (also in vivo) |
| Capsules/cages | Strand displacement/pH-sensitive DNA strands/light/temperature/mRNA | TEM, FRET, fluorescence microscopy, enzyme kinetics | Selective and controlled display/release of molecular cargo |
| <i>Photonics/plasmonics</i> | | | |
| Metamolecules/beacon | Strand displacement/pH-sensitive DNA strands/azobenzene-modified strands/ aptamer binding | CD, FRET, TEM | Sensors, diagnostics |
| AuNR walkers/nanoclock | Strand displacement/DNAzyme | CD, FRET, TEM | Complex nanomachinery |

(continued)

Table 3.1 (continued)

| Classification/robot type | Mechanism of action | Characterization/imaging | Application |
|---------------------------------------|--|---|--|
| <i>External field driven</i> | | | |
| Robotic arms | Electric field | FRET | Nanomachines with rapid and controlled movement |
| Nanohinge/nanorotor | Magnetic field | TIRF | Nanomachines with rapid and controlled movement |
| Swimmers | Magnetic field, thermophoresis | Fluorescence microscopy | Guided drug delivery |
| <i>Autonomous robots</i> | | | |
| Walkers/motors/robots | Strand displacement/toeholds/restriction enzyme driven | AFM, HS-AFM, smFRET, ALEX | Nanoscale assembly lines, cargo sorting, computing |
| Rotary apparatus | Controlled DNA base stacking + Brownian motion | Single-particle fluorescence microscopy | Toward biomimicking nanomachines |
| Interacting dynamic robot populations | Binding through hybridization/toeholds, detection of signals such as miR | Flow cytometry | Toward safe, decision-making robotics |

3.5 Selected Diseases

3.5.1 Cancer

DNA structures have been created in multiple ways to carry drugs or payloads for the selected delivery of therapeutics to the tumor site. The ability to chemically modify DNA with functional groups greatly monitors stoichiometry-regulated loading of molecular cargo (Singh et al. 2018). Aptamer-tethered DNA nanotrains (aptNTrs) have become carriers for targeted drug delivery systems for cancer therapy. Such nanotrains often rely on the property of DNA self-assembly, where long aptNTrs can be self-assembled from two short DNA upon nucleation using modified aptamers. The modified aptamers are locomotives guiding the nanotrains toward the target cancer cells. The nanotrains can be loaded with tandem “boxcars,” delivering the drug payloads to target cells. The antitumor efficiency with reduced side effects has already been realized using the nanotrains in the mouse xenograft tumor model (Fig. 3.4) (Zhu et al. 2013).

DNA origami in conjugation with gold nanoparticles has also demonstrated remarkable effects in treating breast tumor xenografts in mice models. The DNA origami (DO)-gold nanorod (GNR) complex is thus dual-functional theranostic constructed by the decoration of GNR on the surface of DNA origami. Upon incubating with human MCF7 breast cancer cells, such a complex structure can result in higher cellular uptake compared to the GNR itself. Once inside the cells, these structures can undergo photothermolysis in the presence of NIR laser irradiation leading to anticancer therapy (Jiang et al. 2015). GNR-DNA origami can also serve as unique probes for improved imaging quality at low doses while retaining high sensitivity for photothermal therapy (Du et al. 2016). High doxorubicin (Dox) loading and targeted drug delivery can also be achieved by using aptamer probes in a specific self-assembled organization generating DNA nanotriangle-scaffolded multivalent split activatable aptamer probe (NTri-SAAP). Such structural organization shows improved target binding affinity, reduced nonspecific background, and high structural/functional stability in harsh environments, making the complex suitable for *in vitro* and *in vivo* applications for imaging and therapy. The developed aptamer probes have demonstrated ~81.65% tumor inhibition efficiency (Lei et al. 2018). Recently, logic-gated recognition integrated into aptamer-functionalized molecular machines is being developed for fast tumor profiling and safe drug delivery. These DNA logic-gated nanorobots (DLGN) can facilitate precise discrimination between multiple cell lines and kill the target cells (Wang et al. 2021).

3.5.1.1 Diabetes

Diabetes is yet another medical condition having a global impact. It has been classified as type 1 and type 2 based on the nature of pancreatic cell functioning. Type 1 diabetes is the inability of the cells to produce insulin, whereas type 2 diabetes

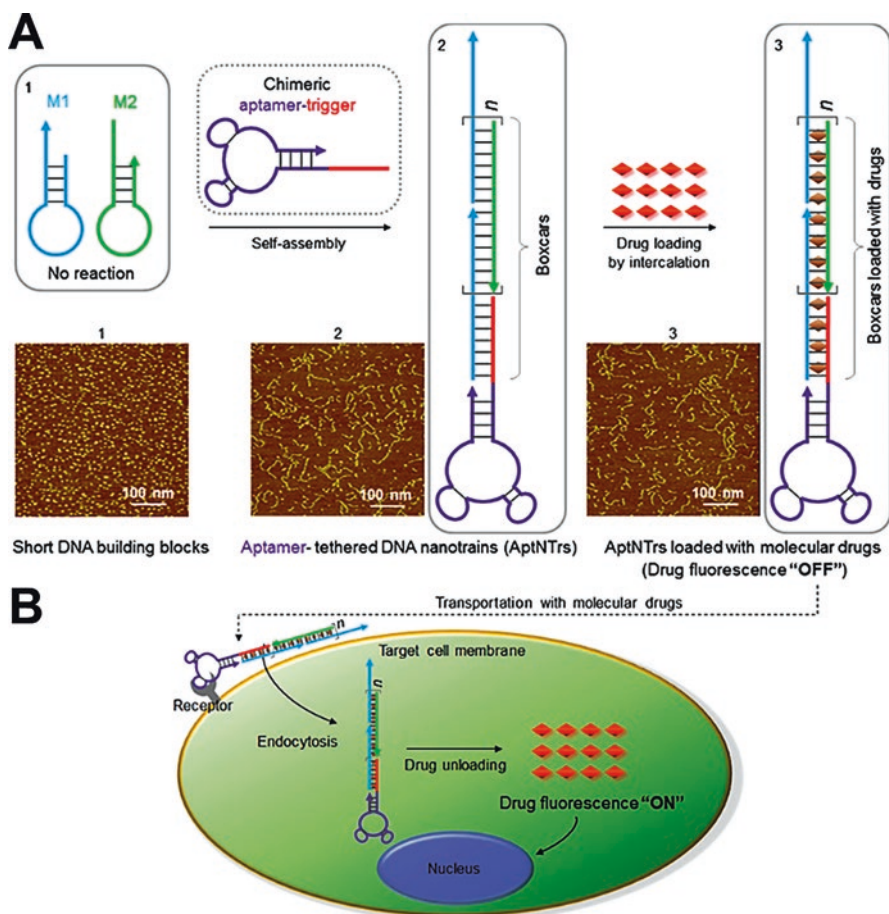


Fig. 3.4 Schematic illustration of the self-assembly of aptamer-tethered DNA nanotrains (aptN-Trs) for the transport of therapeutic drug. (A) Self-assembly of aptNTrs from aptamers: (1) upon initiation from chimeric aptamer-tethered trigger probe, (2) the resulting long trains tethered with aptamers working as locomotives, and (3) multiple loaded “boxcars” to be loaded with molecular drugs. AFM images (1–3) show the corresponding nanostructures’ morphological features. (B) The unloading of the drug to the target cell and subsequent unloading. The different states of fluorescence of the drugs when loaded onto nanotrains (fluorescence OFF); unloaded drug inside cells (fluorescence ON). (Zhu et al. 2013)

marks the inability of the islets to absorb insulin (Joy et al. n.d.). Despite the technological advancements, the delivery of precise drug dosage has not been accurately achieved in many cases, mainly due to the self-administration of drugs leading to various diabetic complications like hyper-/hypoglycemia. Hence, self-regulatory insulin delivery nanobots using biopolymers have been designed to sense the blood glucose level to release insulin (Battistella et al. 2021; Iyer et al. 2022). However, the development of biomolecule-based nanobots for the targeted delivery of insulin

is yet to mark its impression on the development of medical advancements (Cavalcanti et al. 2008; Sindhu et al. 2021). Recently, insulin resistance (IR) has been recognized to play a pathogenic role in developing type 2 diabetes mellitus. IR leads to the failure to respond to insulin in target tissue like the liver. 3D tetrahedral framework nucleic acids (tFNAs) are synthesized from four isometric single-stranded DNA. Researchers have successfully developed tFNA that can ameliorate IR by activating the PI3K/Akt signaling pathway in HepG2 cells (Li et al. 2021b). The tFNAs have also shown successful outcomes in the treatment of type 1 diabetes by inducing T- and B-regulatory immune cells and suppressing autoreactive immune cells (Th1, Th17, and Tfh). Such immunotherapeutic effect is primarily related to cytokine secretion and STAT signaling in the pancreas (Gao et al. 2021).

3.5.1.2 Hemorrhage Treatment

Structurally stable, biocompatible, editable DNA nanobots significantly impact mice models in the cure of intracranial hemorrhage (ICH). ICH is considered the most lethal form of cerebrovascular stroke with a poor prognosis. The neuroinflammation associated with ICH is known to arise from the polarization of microglial cells to the M1 subtype that secretes physiologically threatening chemokines, cytokines, ferrous iron, and prostaglandins. Hence, preventing microglial M1 polarization has been tested by applying certain drugs, like deferoxamine, fingolimod, pinocembrin, rapamycin, and rosuvastatin. However, no effective cure has been achieved, mainly because very few drugs can cross the blood-brain barrier (BBB). DNA nanobots arranged tetrahedrally, often denoted as tetrahedral framework nucleic acids (tFNA), are now designed to carry desired receptor ligands like C-C chemokine receptor 2 (siCCR2) to attenuate the respective expression of the *CCR2* gene. This work by Fu et al. was an intelligent approach to rescuing neurological dysfunction following ICH. The DNA nanobot was utilized for the targeted delivery of siCCR2 to the BV2 cells, causing its M2 polarization and subsequently attenuating inflammatory mediators' release. However, the DNA nanobot was strategically injected into the cerebroventricular system to bypass blood circulation and the BBB (Fu et al. 2021). DNA origami-based aptamer nanoarray can also be helpful in blood coagulation for hemodialysis treatment. DNA origami is often used as a template to incorporate thrombin-binding aptamer at nanometer spatial arrangement. Such a platform can enable the organization of two types of thrombin-binding DNA aptamers to synergistically trigger the recognition and inhibition of thrombin. Moreover, the DNA origami-based anticoagulant could be re-engineered to contain multiple aptamers that can inhibit procoagulation proteases in the coagulation pathway. Such an arrangement can advance the multi-step prevention of blood clotting (Zhao et al. 2021).

3.6 Challenges and Prospects

Despite the numerous successful outcomes of biomolecular nanobots, significant challenges need our undivided attention for the continuous upgradation of the DNA/protein nanobots for intelligent delivery. The foremost concern for the commercial application of DNA/protein nanobots has been their stability and behavior under physiological conditions. The body system's retention rate and biodistribution are also significant concerns. Noticeable efforts have been made to overcome the challenges mentioned above through the introduction of covalent cross-linking, cross-over design, and mineralization; these modifications indeed significantly improved the nanobot's properties, however, without escaping to compromising nanobots' efficiencies. In this context, the immediate challenges claiming our attention appear to be nanobot's stability, cargo loading and release efficiency, analyte's binding potentiality, and dynamic switching. The cost of production of the nanobots at a mass scale can be considered the next challenge in the commercialization of nanobots for the intelligent delivery of therapeutics. As estimated, the typical cost of laboratory-scale DNA-bot synthesis is >1000 dollars. The average amount of DNA bot needed for the successful trial through intravenous administration of the therapeutic cargos into mice was 1 nanomole per dose. Hence, it is estimated that the number of nanobots for an adult human would be about 300 nanomoles per dose, estimated to be over 300,000 dollars per dose. Besides, such biologics have to comply with CMC and GMP standards due to the issue of sterilization, purification, and batch-to-batch consistency, further increasing the production cost. Although DNA nanorobots remain miles away from real-world applications, we can foresee that they would improve human health. This is possible once the few remained challenges are addressed by combining cost-efficient methods of liquid-phase oligonucleotide synthesis, chip-based staple strand production, DNazyme-catalyzed production, and biotechnological "mass production" of DNA nanorobots (Hu 2021).

Acknowledgments This work was supported by the Basic Science Research Program through the "National Research Foundation of Korea" funded by the Ministry of Education (NRF-2018R1A16A1A03025582, NRF-2019R1D1A3A03103828, and NRF-2022R111A3063302).

References

- Ahmad A, Younas M, Santulli C, Kiyani MZ, Ali R, Habbiba O, et al. Nanomedicine and tissue engineering. Nanomedicine manufacturing and applications: Elsevier; 2021. pp. 261–277.
- Aldarondo D, Wayne E. Monocytes as a convergent nanoparticle therapeutic target for cardiovascular diseases. *Adv Drug Deliv Rev.* 2022;114116
- Alipour M, Nabavi SM, Arab L, Vosough M, Pakdaman H, Ehsani E, et al. Stem cell therapy in Alzheimer's disease: possible benefits and limiting drawbacks. *Mol Biol Rep.* 2019;46:1425–46.
- Allen TM, Cullis PR. Liposomal drug delivery systems: from concept to clinical applications. *Adv Drug Deliv Rev.* 2013;65:36–48.

- Bae YH, Park K. Targeted drug delivery to tumors: myths, reality and possibility. *J Control Release*. 2011;153:198.
- Battistella C, Liang Y, Gianneschi NC. Innovations in disease state responsive soft materials for targeting extracellular stimuli associated with cancer, cardiovascular disease, diabetes, and beyond. *Adv Mater*. 2021;33:2007504.
- Benson E, Lolaico M, Tarasov Y, Gådin A, Br H. Evolutionary refinement of DNA nanostructures using coarse-grained molecular dynamics simulations. *ACS Nano*. 2019;13:12591–8.
- Bu L-L, Yan J, Wang Z, Ruan H, Chen Q, Gunadhi V, et al. Advances in drug delivery for post-surgical cancer treatment. *Biomaterials*. 2019;219:119182.
- Cavalcanti A, Shirinzadeh B, Kretly LC. Medical nanorobotics for diabetes control. *Nanomedicine*. 2008;4:127–38.
- Chen H, Zhang H, Pan J, Cha T-G, Li S, Andréasson J, et al. Dynamic and progressive control of DNA origami conformation by modulating DNA helicity with chemical adducts. *ACS Nano*. 2016;10:4989–96.
- Chen W, Zhou H, Zhang B, Cao Q, Wang B, Ma X. Recent Progress of micro/Nanorobots for cell delivery and manipulation. *Adv Funct Mater*. 2022;2110625
- Ding Y, Li W, Zhang F, Liu Z, Zanjanizadeh Ezazi N, Liu D, et al. Electrospun fibrous architectures for drug delivery, tissue engineering and cancer therapy. *Adv Funct Mater*. 2019;29:1802852.
- Dostalova S, Polanska H, Svobodova M, Balvan J, Krystofova O, Haddad Y, et al. Prostate-specific membrane antigen-targeted site-directed antibody-conjugated apoferritin nanovehicle favorably influences in vivo side effects of doxorubicin. *Sci Rep*. 2018;8:1–13.
- Douglas SM, Bachelet I, Church GM. A logic-gated nanorobot for targeted transport of molecular payloads. *Science*. 2012;335:831–4.
- Du Y, Jiang Q, Beziere N, Song L, Zhang Q, Peng D, et al. DNA-nanostructure–gold-nanorod hybrids for enhanced in vivo optoacoustic imaging and photothermal therapy. *Adv Mater*. 2016;28:10000–7.
- Du B, Yu M, Zheng J. Transport and interactions of nanoparticles in the kidneys. *Nat Rev Mater*. 2018;3:358–74.
- Dwivedi N, Shah J, Mishra V, Tambuwala M, Kesharwani P. Nanoneuromedicine for management of neurodegenerative disorder. *J Drug Deliv Sci Technol*. 2019;49:477–90.
- Escobar-Chávez JJ, Díaz-Torres R, Rodríguez-Cruz IM, Dominguez-Delgado CL, Morales RS, Angeles-Anguiano E, et al. Nanocarriers for transdermal drug delivery. *Res Rep Transdermal Drug Deliv*. 2012;1:3.
- Fenton OS, Olafson KN, Pillai PS, Mitchell MJ, Langer R. Advances in biomaterials for drug delivery. *Adv Mater*. 2018;30:1705328.
- Forouzandehmehr M, Ghoytasi I, Shamloo A, Ghosi S. Particles in coronary circulation: a review on modelling for drug carrier design. *Mater Des*. 2022;110511
- Foulkes R, Man E, Thind J, Yeung S, Joy A, Hoskins C. The regulation of nanomaterials and nanomedicines for clinical application: current and future perspectives. *Biomater Sci*. 2020;8:4653–64.
- Fu W, Ma L, Ju Y, Xu J, Li H, Shi S, et al. Therapeutic siCCR2 loaded by tetrahedral framework DNA nanorobotics in therapy for intracranial hemorrhage. *Adv Funct Mater*. 2021;31:2101435.
- Gao S, Zhou M, Li Y, Xiao D, Wang Y, Yao Y, et al. Tetrahedral framework nucleic acids reverse new-onset type 1 diabetes. *ACS Appl Mater Interfaces*. 2021;13:50802–11.
- Guan C, Zhu X, Feng C. DNA nanodevice-based drug delivery systems. *Biomol Ther*. 2021;11:1855.
- Hamdi M. Computational design and multiscale modeling of a nanoactuator using DNA actuation. *Nanotechnology*. 2009;20:485501.
- Hamdi M, Ferreira A. DNA nanorobotics. *Microelectron J*. 2008;39:1051–9.
- Hilt JZ, Peppas NA. Microfabricated drug delivery devices. *Int J Pharm*. 2005;306:15–23.
- Hu Y. Self-assembly of DNA molecules: towards DNA Nanorobots for biomedical applications. *Cyborg Bionic Syst*. 2021;2021
- Huang X, Shang W, Deng H, Zhou Y, Cao F, Fang C, et al. Clothing spiny nanoprobes against the mononuclear phagocyte system clearance in vivo: photoacoustic diagnosis and photothermal

- treatment of early stage liver cancer with erythrocyte membrane-camouflaged gold nanostars. *Appl Mater Today*. 2020;18:100484.
- Iyer G, Dyawanapelly S, Jain R, Dandekar P. An overview of oral insulin delivery strategies (OIDS). *Int J Biol Macromol*. 2022;
- Jiang Q, Song C, Nangreave J, Liu X, Lin L, Qiu D, et al. DNA origami as a carrier for circumvention of drug resistance. *J Am Chem Soc*. 2012;134:13396–403.
- Jiang Q, Shi Y, Zhang Q, Li N, Zhan P, Song L, et al. A self-assembled DNA origami-gold nanorod complex for cancer theranostics. *Small*. 2015;11:5134–41.
- Joy R, Girigoswami A, Prasanna PL, Girigoswami K. The biomedical applications of nanorobots—a mini review (n.d.).
- Khalaj R, Douroumis D. Applications of long-lasting and implantable drug delivery systems for cardiovascular disease treatment, Long-Acting Drug Delivery Systems. Elsevier; 2022. p. 83–127.
- Kimbrel EA, Lanza R. Next-generation stem cells—ushering in a new era of cell-based therapies. *Nat Rev Drug Discov*. 2020;19:463–79.
- Kondo Y, Toyoda T, Inagaki N, Osafune K. iPSC technology-based regenerative therapy for diabetes. *J Diabetes Investig*. 2018;9:234–43.
- Kosuri S, Church GM. Large-scale de novo DNA synthesis: technologies and applications. *Nat Methods*. 2014;11:499–507.
- Kratz F, Warnecke A. Finding the optimal balance: challenges of improving conventional cancer chemotherapy using suitable combinations with nano-sized drug delivery systems. *J Control Release*. 2012;164:221–35.
- Langer R. New methods of drug delivery. *Science*. 1990;249:1527–33.
- Lee H, Song C, Baik S, Kim D, Hyeon T, Kim D-H. Device-assisted transdermal drug delivery. *Adv Drug Deliv Rev*. 2018;127:35–45.
- Lei Y, Qiao Z, Tang J, He X, Shi H, Ye X, et al. DNA nanotriangle-scaffolded activatable aptamer probe with ultralow background and robust stability for cancer theranostics. *Theranostics*. 2018;8:4062.
- Li J, Mooney DJ. Designing hydrogels for controlled drug delivery. *Nat Rev Mater*. 2016;1:1–17.
- Li S, Jiang Q, Liu S, Zhang Y, Tian Y, Song C, et al. A DNA nanorobot functions as a cancer therapeutic in response to a molecular trigger in vivo. *Nat Biotechnol*. 2018;36:258–64.
- Li H, Gao J, Cao L, Xie X, Fan J, Wang H, et al. A DNA molecular robot that autonomously walks on the cell membrane to drive cell motility. *Angew Chem*. 2021a;133:26291–9.
- Li Y, Tang Y, Shi S, Gao S, Wang Y, Xiao D, et al. Tetrahedral framework nucleic acids ameliorate insulin resistance in type 2 diabetes mellitus via the PI3K/Akt pathway. *ACS Appl Mater Interfaces*. 2021b;13:40354–64.
- Lostalé-Seijo I, Montenegro J. Synthetic materials at the forefront of gene delivery. *Nat Rev Chem*. 2018;2:258–77.
- Luo M, Feng Y, Wang T, Guan J. Micro-/nanorobots at work in active drug delivery. *Adv Funct Mater*. 2018;28:1706100.
- Makvandi P, Josic U, Delfi M, Pinelli F, Jahed V, Kaya E, et al. Drug delivery (nano) platforms for oral and dental applications: tissue regeneration, infection control, and cancer management. *Adv Sci*. 2021;8:2004014.
- Md S, Bhattmisra SK, Zeeshan F, Shahzad N, Mujtaba MA, Meka VS, et al. Nano-carrier enabled drug delivery systems for nose to brain targeting for the treatment of neurodegenerative disorders. *J Drug Deliv Sci Technol*. 2018;43:295–310.
- Mitchell MJ, Billingsley MM, Haley RM, Wechsler ME, Peppas NA, Langer R. Engineering precision nanoparticles for drug delivery. *Nat Rev Drug Discov*. 2021;20:101–24.
- Nair GG, Tzanakakis ES, Hebrok M. Emerging routes to the generation of functional β -cells for diabetes mellitus cell therapy. *Nat Rev Endocrinol*. 2020;16:506–18.
- Nakamura Y, Mochida A, Choyke PL, Kobayashi H. Nanodrug delivery: is the enhanced permeability and retention effect sufficient for curing cancer? *Bioconjug Chem*. 2016;27:2225–38.

- Nourian Dehkordi A, Mirahmadi Babaheydari F, Chehelgerdi M, Raeisi DS. Skin tissue engineering: wound healing based on stem-cell-based therapeutic strategies. *Stem Cell Res Ther.* 2019;10:1–20.
- Nummelin S, Shen B, Piskunen P, Liu Q, Kostianen MA, Linko V. Robotic DNA nanostructures. *ACS Synth Biol.* 2020;9:1923–40.
- Nutiu R, Li Y. Structure-switching signaling aptamers. *J Am Chem Soc.* 2003;125:4771–8.
- Oh JY, Kim HS, Palanikumar L, Go EM, Jana B, Park SA, et al. Cloaking nanoparticles with protein corona shield for targeted drug delivery. *Nat Commun.* 2018;9:1–9.
- Parakhonskiy BV, Shilyagina NY, Gusliakova OI, Volovetskiy AB, Kostyuk AB, Balalaeva IV, et al. A method of drug delivery to tumors based on rapidly biodegradable drug-loaded containers. *Appl Mater Today.* 2021;25:101199.
- Paredes AJ, Ramöller IK, McKenna PE, Abbate MT, Volpe-Zanutto F, Vora LK, et al. Microarray patches: breaking down the barriers to contraceptive care and HIV prevention for women across the globe. *Adv Drug Deliv Rev.* 2021;173:331–48.
- Päth G, Perakakis N, Mantzoros CS, Seufert J. Stem cells in the treatment of diabetes mellitus—focus on mesenchymal stem cells. *Metabolism.* 2019;90:1–15.
- Peng F, Tu Y, Van Hest JC, Wilson DA. Self-guided supramolecular cargo-loaded nanomotors with chemotactic behavior towards cells. *Angew Chem Int Ed.* 2015;54:11662–5.
- Ruenraroengsak P, Cook JM, Florence AT. Nanosystem drug targeting: facing up to complex realities. *J Control Release.* 2010;141:265–76.
- Seeman NC. DNA engineering and its application to nanotechnology. *Trends Biotechnol.* 1999;17:437–43.
- Seeman NC. DNA in a material world. *Nature.* 2003;421:427–31.
- Senapati S, Mahanta AK, Kumar S, Maiti P. Controlled drug delivery vehicles for cancer treatment and their performance. *Signal Transduct Target Ther.* 2018;3:1–19.
- Shen X, Ouyang Q, Tan H, Ouyang J, Na N. Computationally designed ssDNA modular nanorobots for cancer recognition, toehold disintegration, visual diagnosis and synergistic gene silencing. 2022.
- Siepmann J, Siepmann F. Mathematical modeling of drug delivery. *Int J Pharm.* 2008;364:328–43.
- Sindhu RK, Kaur H, Kumar M, Sofat M, Yapar EA, Esenturk I, et al. The ameliorating approach of nanorobotics in the novel drug delivery systems: a mechanistic review. *J Drug Target.* 2021;29:822–33.
- Singh HR, Kopperger E, Simmel FC. A DNA nanorobot uprisers against cancer. *Trends Mol Med.* 2018;24:591–3.
- Singh V, Sahebkar A, Kesharwani P. Poly (propylene imine) dendrimer as an emerging polymeric nanocarrier for anticancer drug and gene delivery. *Eur Polym J.* 2021;158:110683.
- Soto F, Wang J, Ahmed R, Demirci U. Medical micro/nanorobots in precision medicine. *Adv Sci.* 2020;7:2002203.
- Tavassoly O, Tavassoly I. Pharmacological functionalization of protein-based nanorobots as a novel tool for drug delivery in cancer. *ACS Pharmacol Transl Sci.* 2021;4:1463–7.
- Teixeira MI, Lopes C, Amaral MH, Costa P. Current insights on lipid nanocarrier-assisted drug delivery in the treatment of neurodegenerative diseases. *Eur J Pharm Biopharm.* 2020;149:192–217.
- Ulijn RV, Jerala R. Peptide and protein nanotechnology into the 2020s: beyond biology. *Chem Soc Rev.* 2018;47:3391–4.
- Wang D, Li S, Zhao Z, Zhang X, Tan W. Engineering a second-order DNA logic-gated Nanorobot to sense and release on live cell membranes for multiplexed diagnosis and synergistic therapy. *Angew Chem Int Ed.* 2021;60:15816–20.
- Wang P, Yang P, Qian K, Li Y, Xu S, Meng R, et al. Precise gene delivery systems with detachable albumin shell remodeling dysfunctional microglia by TREM2 for treatment of Alzheimer's disease. *Biomaterials.* 2022;281:121360.
- Wei Z, Chen Z, Zhao Y, Fan F, Xiong W, Song S, et al. Mononuclear phagocyte system blockade using extracellular vesicles modified with CD47 on membrane surface for myocardial infarction reperfusion injury treatment. *Biomaterials.* 2021;275:121000.

- Winfree E, Liu F, Wenzler LA, Seeman NC. Design and self-assembly of two-dimensional DNA crystals. *Nature*. 1998;394:539–44.
- Wu Z, Lin X, Zou X, Sun J, He Q. Biodegradable protein-based rockets for drug transportation and light-triggered release. *ACS Appl Mater Interfaces*. 2015;7:250–5.
- Yeh Y-C, Huang T-H, Yang S-C, Chen C-C, Fang J-Y. Nano-based drug delivery or targeting to eradicate bacteria for infection mitigation: a review of recent advances. *Front Chem*. 2020;8:286.
- You M, Chen Y, Zhang X, Liu H, Wang R, Wang K, et al. An autonomous and controllable light-driven DNA walking device. *Angew Chem Int Ed*. 2012;51:2457–60.
- Zaric BL, Obradovic M, Sudar-Milovanovic E, Nedeljkovic J, Lazic V, Isenovic ER. Drug delivery systems for diabetes treatment. *Curr Pharm Des*. 2019;25:166–73.
- Zhang C, Zheng M, Ohayon YP, Vecchioni S, Sha R, Seeman NC, et al. Programming DNA self-assembly by geometry. *J Am Chem Soc* 2022.
- Zhao Z, Ukidve A, Kim J, Mitragotri S. Targeting strategies for tissue-specific drug delivery. *Cell*. 2020a;181:151–67.
- Zhao D, Kong Y, Zhao S, Xing H. Engineering functional DNA-protein conjugates for biosensing, biomedical, and nanoassembly applications. *DNA Nanotechnol*. 2020b:83–124.
- Zhao S, Tian R, Wu J, Liu S, Wang Y, Wen M, et al. A DNA origami-based aptamer nanoarray for potent and reversible anticoagulation in hemodialysis. *Nat Commun*. 2021;12:1–10.
- Zhu G, Zheng J, Song E, Donovan M, Zhang K, Liu C, et al. Self-assembled, aptamer-tethered DNA nanotrains for targeted transport of molecular drugs in cancer theranostics. *Proc Natl Acad Sci*. 2013;110:7998–8003.

Chapter 4

Printable Nanorobots and Microswimmers for Therapeutic Advancement: Present Status and Future Opportunities



Sayan Deb Dutta, Keya Ganguly, Dinesh K. Patel, Tejal V. Patil, Rachmi Luthfikasari, and Ki-Taek Lim

4.1 Introduction

Automated tools, such as robotic devices, have gained enormous attention in mankind's history in sensing, manipulating, interacting, and transforming the world. In particular, robotic technology revolutionized the biomedical engineering sector to improve human health. In contrast, industrial robots are dedicated to large-scale manufacturing works. Medical robots are miniature robots that can perform a variety of works, such as drug delivery, biosensing, bioimaging, and many others. Therefore, designing miniature robots (=micro-/nanorobots) with a micro-to-nanometer scale would allow the doctors to monitor the whole human body, including the studies at the molecular level, and offer precise diagnoses with high accuracy (Alemzadeh et al. 2016). However, one significant challenge in micro-/nanorobot development is the precise control of locomotion during active propulsion. The micro-/nanorobots may require a physiologically relevant liquid environment (e.g., low Reynolds number fluids) to peruse their locomotion. The past decade has

S. D. Dutta · K. Ganguly · D. K. Patel · R. Luthfikasari
Department of Biosystems Engineering, College of Agriculture and Life Sciences, Kangwon National University, Chuncheon, Republic of Korea

T. V. Patil
Interdisciplinary Program in Smart Agriculture, Kangwon National University,
Chuncheon, Republic of Korea

K.-T. Lim (✉)
Department of Biosystems Engineering, College of Agriculture and Life Sciences, Kangwon National University, Chuncheon, Republic of Korea

Interdisciplinary Program in Smart Agriculture, Kangwon National University,
Chuncheon, Republic of Korea
e-mail: ktlim@kangwon.ac.kr

developed several micro-/nanorobots with distinct characteristics. Fundamentally, these tiny robots rely on chemical-based propulsion (e.g., pH, peroxide, and other solvents) or biophysical stimulation (e.g., magnetic, ultrasound, electric, and electromagnetic) techniques. The chemically powered nanomotors are usually designed to respond to various pH so that they can swim throughout the body. Besides, the magnetic swimmers rely on external magnetic fields that help them move forward, such as helical or flexible flagella-like nanomotors. To observe the locomotory behavior of those micro-/nanorobots, various micro-/nanofluidic-based devices are often used. Most micro-/nanorobots are used for active and targeted drug delivery with real in vivo applications. This chapter briefly addresses some significant advancements in micro-/nanorobot fabrication based on 3D printing technology and their propulsion mechanism for therapeutic applications. This chapter also highlights the present status, challenges, gaps, limitations, and future outlook of the micro-/nanorobot fabrication for biomedical applications (Fig. 4.1).

4.2 Overview of 3D Printing Techniques for Nanorobot Fabrication

3D printing technology is directly connected to computer-based modeling (CAD) and their visualization and evaluation of the printing quality. The fundamental need for 3D printing relies on the fabrication of printing materials, using biodegradable and biocompatible polymers, and printing at minimal extrusion pressure to obtain high-quality 3D structures for biomedical applications (Zhou et al. 2020; Li and Pumera 2021). The 3D printing process begins with designing CAD structures with pre-determined shape and size, followed by slicing the structure to convert the computer-based code (e.g., raw file) to printable code (SVG or STL file). After transforming the exact file command, the 3D printer recognizes the code and prints layer by layer to form 3D or 4D structures. The printable ink may be composed of liquid resin, powders, emulsion, colloidal materials, or solidified gels (Li and Pumera 2021). The printing technique can be classified into several categories based

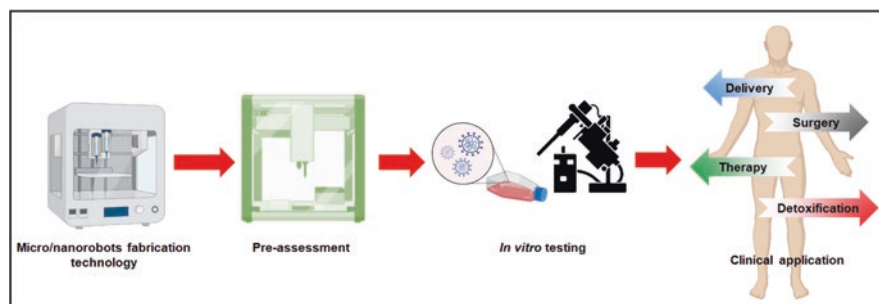


Fig. 4.1 A schematic illustration showing the fabrication of functional medical micro-/nanorobots

on the printing principle. This section will discuss different printing techniques for fabricating microrobots for biomedical applications.

4.2.1 Powder-Bed Fusion

Powder-bed fusion is a kind of additive manufacturing technology where a laser or an electron beam is used as a power source to sinter or melt solid samples or powders. The laser beam followed the path of the designed structure and was printed onto the surface of the platform. This technique is commonly known as selective

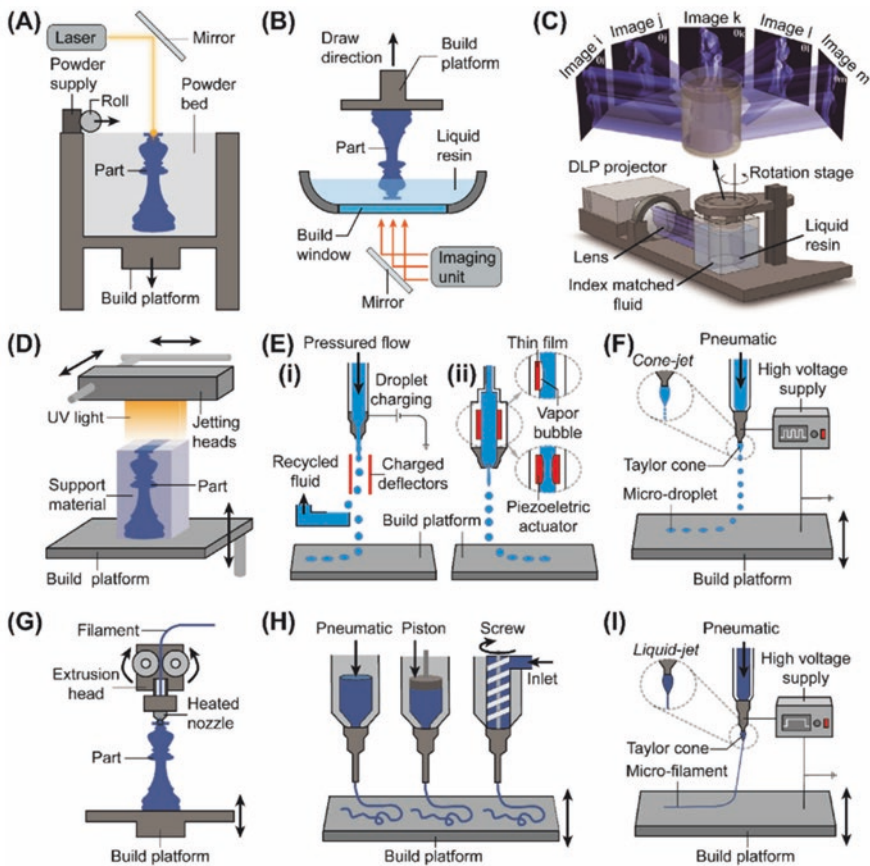


Fig. 4.2 Schematic illustration of various printing techniques used for microrobot fabrication. (a) Powder-bed fusion, (b) vat polymerization, (c) image-guided axial lithography (computed lithography), (d) inkjet printing, (e) CIJ and DOD method of inkjet printing, (f) E-jet printing, (g) FDM printing, and (h, i) DIW-based 3D printing (Zhou et al. 2020). (Reproduced with permission from John Wiley & Sons, Inc., 2020)

laser sintering (SLS) or selective laser melting (SLM) technique (Kinstlinger and Miller 2016). Unlike other printing techniques that use a supporting bath for 3D printing, in SLS printing (Fig. 4.2a), the uncured powder part serves as a supporting material to build high-resolution 3D structures. To improve the printing quality, the built platform temperature is kept slightly higher than the room temperature (Schmid et al. 2014). Therefore, the high-intensity laser beam acts rapidly on the powder material and fastens the sintering process. For accurate printing, the particle size of the powder sample is usually kept between 100 and 120 μm to create high-quality 3D structures (Brandt 2016).

4.2.2 Vat Polymerization

In vat polymerization, the 3D printing was conducted in the presence of a specific light (e.g., ultraviolet or UV light), and the photopolymers were used as a resin vat (Lu et al. 2006). In UV light irradiation, the photopolymers quickly crosslinked to form a highly stable structure through free radical polymerization (Lu et al. 2006). Various types of vat polymerization techniques include stereolithography (SLA), digital light processing (DLP), and continuous liquid interface production (CLIP) printing, respectively. Figure 4.2b represents an overview of the vat polymerization setup, similar to the SLS printing, except for the light source and the printing material.

In SLA-based printing, the printer usually comprises a photopolymer vat for liquid resins (Fig. 4.2c), a UV light source, a digital motorized system allowing the locomotion of the laser beam, and a receiver platform (Mondschein et al. 2017). When the liquid photopolymer resin is irradiated with UV light, the photopolymer absorbs the single photons and transfers them to the photoinitiator (PI) complex. After receiving the absorbed photon from the UV light, the PI initiates crosslinking mechanism via free radical transfer. After crosslinking, the resin solidifies (first layer) onto the platform, and gradually the second layer deposits (Crivello and Reichmanis 2014; Melchels et al. 2010). Following photopolymerization, the unreacted monomers were subsequently removed from the base of the printing platform. It is important to note that UV curing during 3D printing is for a short time, and therefore, an additional post-curing process is required after successful 3D printing of photopolymer resins (Patel et al. 2017). SLA can precisely create micro-/nanoscale structures, which is impossible through SLS-based 3D printing. DLP printing (Fig. 4.2d) is slightly different from SLA printing, where the light source is selectively masked, and each layer is digitally exposed at a time rather than point by point (Kuang et al. 2019). One of the significant advantages of DLP printing is printing high-resolution (1 μm) microscale structures (μCOP) with super-flexibility with minimum time. The μCOP technique allows biofabrication of diverse functional nanoparticles into a single ink to generate simple microrobots for targeted drug delivery (Hribar et al. 2015; Ma et al. 2019). The CLIP-based 3D printing (a modified DLP printing) uses an additional printing window by applying an

oxygen-permeable layer below the plane of UV light at the vat bottom to create a “dead zone” (Tumbleston et al. 2015). CLIP printing enables the formation of large overhangs with tunable mechanical properties. CLIP printing is relatively fast, and maximum printing resolution can be achieved up to 75 μm (Tumbleston et al. 2015; Januszewicz et al. 2016).

4.2.3 Inkjet Printing

Inkjet printing, also known as material jetting, is another additive manufacturing technique where the inks are selectively deposited onto the platform in the form of “ink droplets.” A typical inkjet printer comprises an x - y - z three-axis motion stage and several printing cartridges with auxiliary curing devices, such as a heating or cooling platform and UV curing module (Fig. 4.2e). In inkjet printing, the CAD model is constructed, the low-viscosity ink is directly ejected from the printing nozzle, and each droplet is precisely deposited on the platform and cured as a solid substance (Valot et al. 2019). Recently, three types of inkjet printers have been commercially available: (1) continuous inkjet (CIJ) printer (Fig. 4.2e, i), (2) drop-on-demand (DOD) inkjet printer (Fig. 4.2e, ii), and (3) electrohydrodynamic inkjet (E-jet) printer (Fig. 4.2f) (Li and Pumera 2021; Rosello et al. 2018; Mei et al. 2005; Calvert 2001). The ink is directly pushed from the nozzle in CIJ printing due to the capillary action and current flow. However, in DOD printing, the droplet formation primarily depends on the pressure pulse in the nozzle. There are two methods of DOD printing, for example, thermal- and piezoelectric-based DOD printing (Zhou et al. 2020; Khan et al. 2010; Park et al. 2008).

Inkjet printing is a powerful additive manufacturing tool for printing digital data onto substrates (e.g., papers and transparent films) (Chung et al. 2019; Wu et al. 2016), protein and nucleic acid array chips (e.g., various enzyme assay kits) (Wünscher et al. 2014; Salva et al. 2020; Zhu and Snyder 2003), and micromachines (Singh et al. 2010). Inkjet printing can also be employed for manufacturing chemically or physically powered microswimmers and microstirrers. One major disadvantage of inkjet-based 3D printing is the relatively low printing resolution (50 μm) and printing accuracy, limiting its potential application for microrobot fabrication (Li and Pumera 2021).

4.2.4 Extrusion and Direct-Ink-Writing Printing

Extrusion-based 3D printing is the widely accepted and mainly used 3D printing technique in additive manufacturing. This is also known as fused deposition modeling (FDM) printing. In extrusion printing, the ink is extruded from the printing nozzle due to the mechanical force to form a continuous filament (Hwang et al. 2018). A typical extrusion printer comprises an x - y - z three-axis stage with auxiliary

devices. An extrusion printer generally provides a heating or cooling stage for 3D printing with temperature-responsive or melt-extrusion polymers (Ge et al. 2022). The basic structure and working principle of an ideal extrusion printer are shown in Fig. 4.2g. The extrusion printer is mainly limited to powder or thermoplastic material printing with a maximum printing resolution of 100 μm (Zhou et al. 2020; Sachyani Keneth et al. 2021). However, printing the viscoelastic hydrogels or microgels is difficult through extrusion. To overcome the shortcomings of extrusion-based printing, a new and modified 3D printing was demonstrated recently and is known as direct-ink-writing (DIW) 3D printing (Fig. 4.2h, i). In DIW-based printing, the printing is governed by the air pressure, a piston (either metallic or plastic), or some screw to extrude the polymer hydrogels (Zhou et al. 2020; Rafiee et al. 2020; Kuang 2021). For viscoelastic materials, several printing parameters need to be considered. For example, the printable ink must have a shear-thinning property with higher yield strength and shear recovery properties. A typical shear-thinning ink allows the extrusion process to be smooth and high-resolution 3D printing of the target model. To demonstrate the flow behavior of the printable ink, the power law and Herschel-Bulkley models are described, which can be used to determine the pseudoplastic nature of the hydrogel ink (Lewis 2006; Paxton et al. 2017; Zhou et al. 2019). The rheology analysis can measure the shear-thinning index (n) for a pseudoplastic fluid from the viscosity under increasing shear rate. To evaluate this, the power law equation (Paxton et al. 2017) is applied using the following equation:

$$\eta = k\dot{\gamma}^{n-1}$$

where η is the viscosity, k is the flow consistency index which is defined by the viscosity at a shear rate 1 s^{-1} , and n is the shear-thinning index. The shear-thinning index $n < 1$ indicates the ideal shear-thinning hydrogel, $n > 1$ indicates the shear-thickening hydrogel, and $n = 1$ indicates the Newtonian fluid behavior of the hydrogel. The yield stress (τ_0) of the developed hydrogel can be measured by using the Herschel-Bulkley model (Peak et al. 2018; Schwab et al. 2020) as follows:

$$\tau = \tau_0 + k\dot{\gamma}^n$$

where τ_0 is the yield stress and k and n are the parameters obtained from the power law equation. The UV curable photopolymers use the UV lamp to cure the printed filaments (Layani et al. 2018). Ionically, crosslinked hydrogels can be printed using co-axial printing (Engel et al. 2022), and thermoresponsive hydrogels can be printed through supporting bath or embedded 3D printing (Wang et al. 2015).

4.2.5 Direct Laser Writing Printing

Direct laser writing (DLW) or multiphoton lithography is a newly developed photolithography technique, mostly used for microrobot fabrication. It involves the illumination of a specific light wavelength on a negative- or positive-photoresist compound (Ye et al. 2020; Medina-Sánchez et al. 2018). The basic idea of DLW is

similar to the two-photon printing (TPP), where the sum of the energies of the TP ($2h\nu$) is equal to the energy difference between two energy states (ground state and excited state). Therefore, the TP absorption strength mainly depends on the square of the light intensity (Fig. 4.3a). A DLW 3D printing device is principally equipped with (I) a laser source, (II) a motorized stage, (III) an optical device for focusing beam, and (IV) a device for controlling the intensity of light (Fig. 4.3b, c). This is an efficient technique for fabricating the microswimmers and micromotors with a photoresistive material. This technique is also used in photonic crystals and in situ cell encapsulation. A summary of various fabrication techniques with possible advantages and disadvantages is listed in Table 4.1.

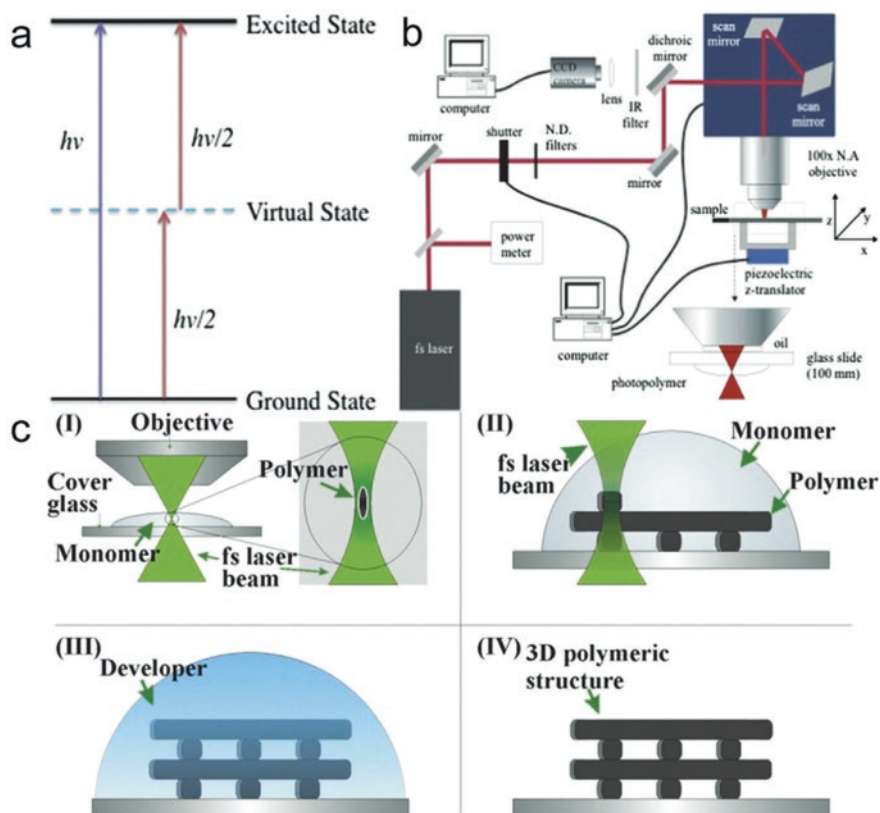


Fig. 4.3 An overview of direct laser writing (DLW) 3D printing. (a) The principle of two-photon absorption. (b, c) A schematic representation of the DLW device shows the various parts used for the 3D printing of macro-/nanorobots (Ye et al. 2020). (Reproduced with permission from John Wiley & Sons, Inc., 2020)

Table 4.1 Summary of various 3D printing techniques used in soft nanorobot fabrication (Zhou et al. 2020; Li and Pumera 2021; Ye et al. 2020)

| Printing techniques | Principle | Build speed | Printing resolution | Build material |
|---------------------|--|-------------|--------------------------|---|
| SLS | Laser-induced or temperature-induced selective sintering | Very high | >100 μm | Thermoplastic polymers, powders |
| SLA | Selective curing of photopolymer resins in a resin vat through light-activated polymerization | High | >5 μm | Photopolymers |
| DLP | Selective curing of photopolymer resins in a resin vat through light-activated polymerization | High | >5 μm | Photopolymers |
| CLIP | Selective curing of photopolymer resins in a resin vat through light-activated polymerization with low oxygen permeability | Very high | >100 μm | Photopolymers |
| TPP | Direct printing of photopolymers via light-activated polymerization | Low | >100 μm | Photopolymers |
| Inkjet | Selective deposition of fluid droplets | Medium | >10 μm | Hydrogel polymers |
| E-jet | Selective deposition of fluid droplets under the influence of electric field | Medium | >100 nm–10 μm | Hydrogel polymers |
| FDM | Temperature-induced direct printing of thermoplastic materials through mechanical force | Medium | >100 μm | Thermoplastic polymers |
| DIW | 3D printing of hydrogels using pneumatic pressure | Medium | >1–100 μm | Photo-curable and other pseudoplastic hydrogels |
| DLW | Two-photon and multiphoton-assisted rapid prototyping | Medium | >20 μm | Thermoplastic or soluble polymers |

4.3 Materials for 3D Printing of Micro-/Nanomotors

Various types of materials are used to fabricate micro-/nanomotors, such as micro-swimmers or nanorobots with different shapes and geometry. A single component of any polymer or powder material is ideal for 3D printing of micromotors; however, the significant disadvantage of this method is poor printability. Therefore, printable micromotors have to meet a few criteria, such as (1) higher shape fidelity of the developed material, (2) mechanically robust, and (3) new functional properties (e.g., chemical, thermal, electrical, magnetic, or electromagnetic). Therefore, composite materials are usually used for 3D printing, combining the matrix and the additives to achieve a hybrid system with better structural integrity and collapse.

Table 4.2 and Fig. 4.4 represent an overview of various types of micromotor fabrication through 3D printing technology for biomedical application.

4.4 Shape Reconfiguration for Tunable Multifunctionality

Shape reconfiguration is an essential parameter for micromotor fabrication under various stimulations. Tabatabaei et al. first used soft hydrogel microrobots (~1 mm) in 2011 with magnetic nanoparticles to demonstrate the stimuli-responsive robots. The magnetic nanorobots respond to the temperature and magnetic field and shrink accordingly to move inside the blood vessel. Several authors have reported in the

Table 4.2 Types of micromotors fabricated through 3D printing as reported in the previous literature

| Categories | Nature | Applications | References |
|--------------------|-----------------|---|--------------------------|
| Geometry | Microbowls | Microsurgery, cargo transport, and drug delivery | Tang et al. (2019) |
| | Microrockets | Cargo transport, targeted drug delivery, pH sensing, bioimaging | Gao et al. (2012) |
| | Microcannons | Micrometer cargo loading and delivery | Soto et al. (2016) |
| | Microbullets | Targeted delivery in deep tissues, non-invasive therapy | Aghakhani et al. (2020) |
| | Microwheels | Targeted transport and delivery | Tasci et al. (2016) |
| Motile | Microswimmers | Targeted delivery of cargo molecules (e.g., drugs, growth factors, etc.) | Alapan et al. (2018) |
| | Microrollers | Robotic fluid transport targeted delivery of drugs and antibodies for cancer theranostics | Driscoll et al. (2017) |
| | Microwalkers | Microscale actuation, muscle movement | Zeng et al. (2015) |
| | Microjets | Load-bearing transport, rapid clot clearance | Sanchez et al. (2011) |
| Stimuli-responsive | Microrobots | Remote actuation and navigation of specific molecules, non-immunogenic properties | Ying et al. (2019) |
| | Micromotors | Targeted delivery of cargo molecules (e.g., drugs, growth factors, etc.) | Maric et al. (2020) |
| | Microengines | Drug delivery, rapid bacteria clearance | Xu et al. (2014) |
| | Micropumps | Targeted delivery of small and active molecules | Sengupta et al. (2014) |
| | Microcarriers | Magnetic tumor targeting and site-specific killing, transport of small objects | Pouponneau et al. (2011) |
| | Microcleaners | Environmental remediation | Soto et al. (2019) |
| | Microscavengers | Rapid vascular clot clearance | Liang et al. (2019) |

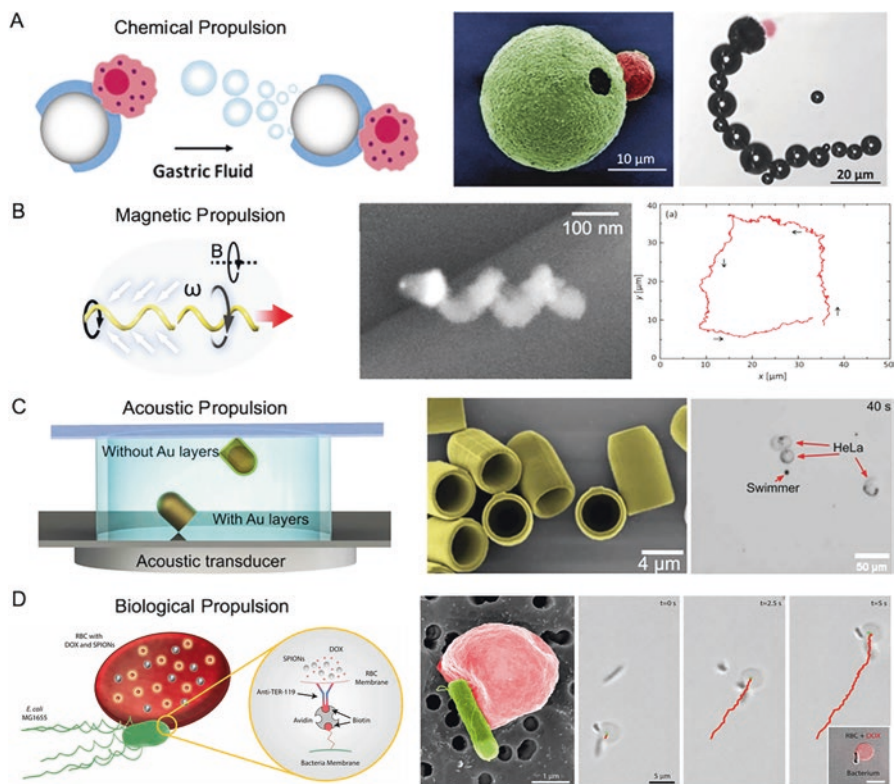


Fig. 4.4 An overview of various types of micro-/nanomotors fabricated through 3D printing or a combination of 3D micro-/nanoprinting for therapeutic advancement. (a) Chemically propelled macrophage-powered magnesium-based Janus micro-/nanorobots, (b) magnetically actuated helical nanorobots, (c) sound-guided conical microrobots for capturing HeLa cells, and (d) engineered biohybrid bacteria-RBC nanorobots for targeted cancer therapy (Wu et al. 2020). (Reproduced with permission from the Royal Society of Chemistry, 2020)

previous literature that hydrogel-based soft robots can be reconfigured using various stimuli, such as temperature, pH, light (e.g., visible, one-photon, two-photon, and multiphoton), pressure, electric field, and magnetic field, and even in the presence of controlled swelling. A soft microgripper, a magnetic hydrogel robot, is usually fabricated using magnetic alginate microbeads and responds to the temperature-dependent opening or closing behavior under near-infrared (NIR) light stimulation. This type of automated tool is widely used for drug delivery in tumor cells. Researchers also reported using temperature-responsive polymer robots, such as gelatin, to immobilize gold nanoparticles (AuNPs) to enhance the light responsiveness, catalytic efficiency, catalytic propulsion, and rapid release of chemotherapeutic drugs. Similarly, the printed microjets are chosen owing to their fast propulsion ability in a diluted hydrogen peroxide medium. Recently, Cabanach et al. reported the fabrication technique of zwitterionic microrobots using 3D microprinting and two-photon polymerization (Cabanach et al. 2020). The fabricated microsystem

allows rapid detection and binding of macrophages and initiates active immune response during various biological processes. Table 4.3 depicts some examples of soft microrobots in which the shape change is mediated through various stimuli. Besides drug delivery ability, the printed soft microrobots are also used to deliver active molecules and are highly biodegradable (Medina-Sánchez et al. 2018). Thus, the shape reconfiguration ability is a crucial parameter for the functional aspects of micromotors during active locomotion.

4.5 Types of Nanomotors and Their Function

4.5.1 Helical Micro-/Nanoswimmers

The helical nanorobots or microswimmers are designed as inspired by the bacterial flagella; a thin filament-like structure helps in the locomotion (Qiu et al. 2015). The 3D printed helical microswimmers can swim and move based on the solvent or in the presence of a magnetic field. Various fabrication techniques have been employed for microswimmers, such as DIW, SLA, DLW, and others (Ceylan et al. 2019). The DLW-based technique offers a high-resolution microstructure with better customizability. Magnetic layers can be deposited after the completion of the printing process. For example, Chen et al. and Tottori et al. reported the fabrication of Ni/Ti double-sandwiched helical microswimmers (Chen et al. 2022; Tottori et al. 2012) through a three-step process to efficiently deliver drugs across the tumor cells under the influence of a magnetic field (Fig. 4.5A). The first step included the writing and polymerization using a negative-tone photoresist (SU-8 or IP-L). The next step involved curing and removing the unpolymerized photoresist using isopropyl alcohol or ethanol. The last step included the electrochemical deposition of Ni/Ti layers on the nanostructure's surface. Similarly, various types of motile microswimmers (Stanton et al. 2015) fabricated through a complex 3D printing process are demonstrated in Fig. 4.5B–D.

Table 4.3 Examples of some stimuli-responsive soft micro-/nanorobots fabricated through 3D printing technology

| Stimulus | Type of soft microrobots | Size (μm) | Speed (μm s ⁻¹) | Solvent | Propulsion mechanism | References |
|----------------------------------|--------------------------------|-----------|-----------------------------|------------------------------------|----------------------|--------------------------|
| Thermally active motion | PNIPAM/PCL/Pt jets | 265 | 300 | 2–5% H ₂ O ₂ | Chemical | Magdanz et al. (2014) |
| pH-induced motion | Cartridge-like soft micromotor | 15 | 90 | 15% H ₂ O ₂ | Chemical | Su et al. (2016) |
| Chemical/light (NIR)/temperature | Gelatin/PPYNP/catalase | 13 | 36 | 2% H ₂ O ₂ | Chemical | Tumbleston et al. (2015) |

PNIPAM poly-N-isopropylacrylamide, PCL polycaprolactone, Pt platinum, NIR near-infrared, PPYNP polypyrrole nanoparticles

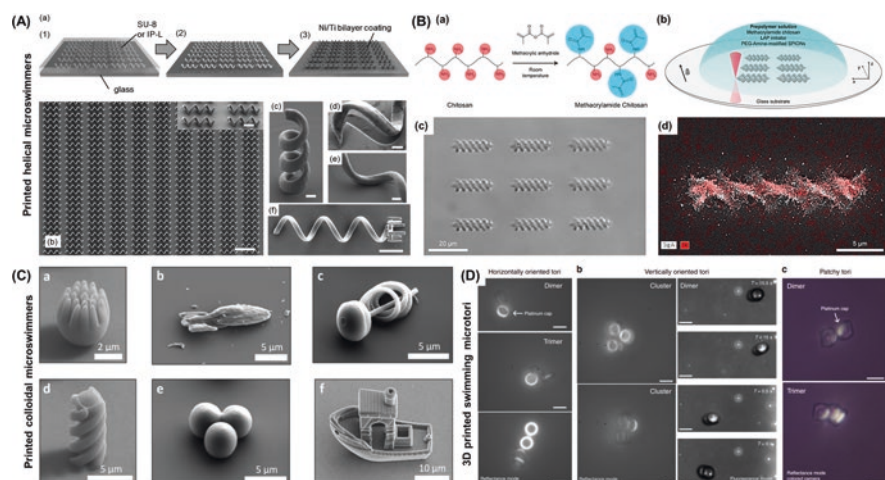


Fig. 4.5 3D printing of functional micromotors. **(A)** Three-step fabrication processes of helical microwimmers. The figure represents an overview of the fabrication process (a), printed horizontal array of microwimmers (b), high-resolution SEM images of 3D printed SU-8 (c), bending and twisting patterns (d, e), and microwimmers with a microholder pocket (f), respectively (Tottori et al. 2012). Reproduced with permission from John Wiley & Sons, Inc., 2012. **(B)** Synthesis of a photo-curable magnetic chitosan-based microwimmers array (a, b), printed image of the microwimmers (c), and EDS elemental mapping (d) showing the presence of iron atoms (Bozuyuk et al. 2018). Reproduced with permission from the American Chemical Society, 2018. **(C)** Photographs showing the colloidal microrobots fabricated through two-photon polymerization. Representative images of the spike-pattern (a), star-ship (b), spiral structure (c), micro-helix (d), micro-trimmer (e), and benchy boat (f), respectively (Doherty et al. 2020). Reproduced with permission from the Royal Society of Chemistry, 2020. **(D)** Fabrication of multi-purpose oriented (horizontally or vertically) Janus micromotor (a–c) for active transport (Baker et al. 2019)). (Reproduced with permission from Springer Nature, 2019)

4.5.2 Tubular Micro-/Nanoswimmers

Mei and Schmidt first reported tubular microwimmers for various applications, such as drug delivery, molecule transport, and facile bioremediation (Campuzano et al. 2011; Kagan et al. 2011; Manesh et al. 2010). The tubular structure also responds to various stimuli with high-efficiency locomotory behavior in biological fluids. The 3D laser lithography exhibits a considerable advantage in micromotor fabrication due to its precise control over shape geometry and high reproducibility (Medina-Sánchez et al. 2016). One of the significant challenges of this technique is that the fabricated microwimmers respond to the higher H_2O_2 concentration, which limits its biomedical application. Therefore, making a biocompatible nanostructure is highly desirable so that the fabricated tubular structure could show motility in

biological fluids (Kunduzova et al. 2002). Recently, a tetrapodal microswimmer consisting of the biocompatible polymer was fabricated through laser lithography and coated with a Fe/Ti layer for enhanced capture, guidance, and release of sperm (Fig. 4.6A). The as-fabricated structure is a four-arm protruder with a curved end.

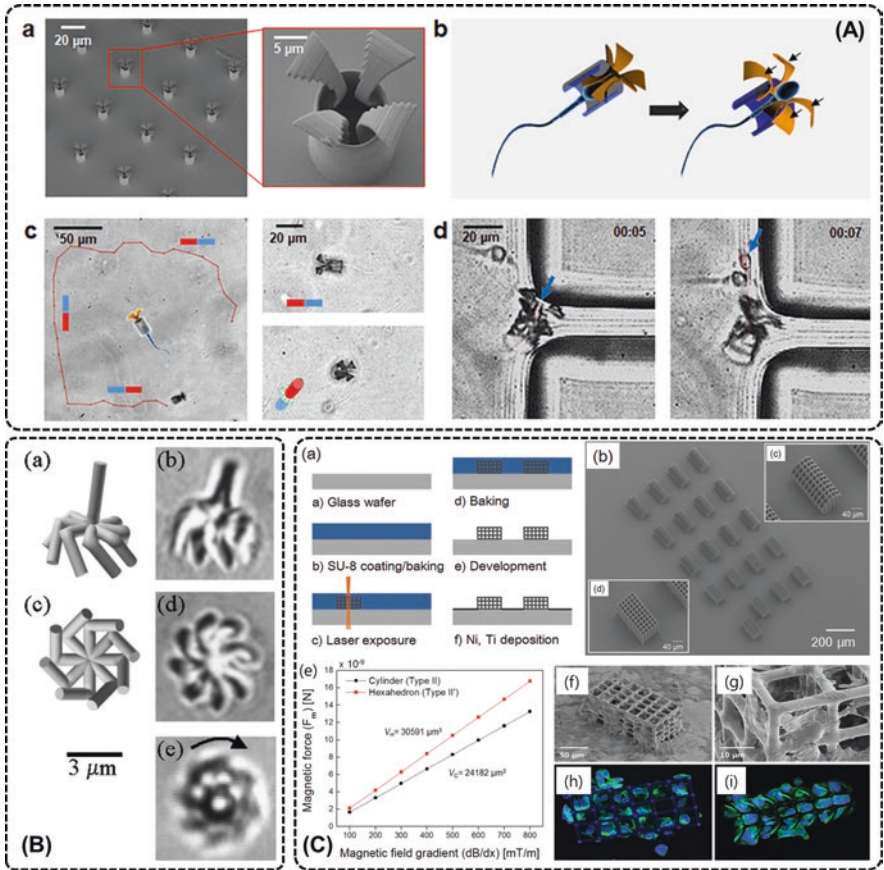


Fig. 4.6 3D printing of various microrobots with diverse functions. (A) Representative SEM morphology of the printed tetrapodal microswimmers (a) and their release mechanism (b), magnetic field-induced locomotion (c), and sperm release process across the PDMS microwell (d). The time-lapse video was recorded to observe the locomotory behavior of the magnetic tetrapods (Xu et al. 2018). Reproduced with permission from the American Chemical Society, 2018. (B) Geometry (a) and image (b) of the light-triggered microrobots (Galajda and Ormos 2001). Reproduced with permission from AIP Publishing, 2001. (C) Schematic overview of the fabrication process of light-induced magnetic microrobots (a) and their SEM morphology (b-d), magnetic force (e), and in vitro biocompatibility of HEK293 cells (f-i), respectively (Kim et al. 2013). (Reproduced with permission from John Wiley & Sons, Inc., 2022)

The tetrapods can respond to the magnetic field and create a driving force to guide the sperm movement (Xu et al. 2018). Therefore, tubular microswimmers have potential therapeutic benefits, especially in gynecological healthcare and disease detection in the reproductive system of humans.

4.5.3 *Micro-/Nanomotors with Mixed Functions*

The 3D printed helical and tubular microswimmers mostly rely on swimming through rotation and bubble propulsion mechanisms. Therefore, high-speed locomotion requires additional stimulation techniques to target more accurately than conventional micromotors (Simpson et al. 1997). Light-triggered propulsion is one of the most useful and recently adopted techniques to achieve the micromotors' controlled and targeted movement. In a study, Ormos and Galajda reported the fabrication technique of light-induced rotating particles with respect to time (Galajda and Ormos 2001). This study reports using a UV light-responsive optical adhesive that can be cured using a 365 nm Ar-ion laser (Fig. 4.6B). This work demonstrates how the microstructure movement can be regulated through light triggering, so-called light-induced particle movement dynamics. Therefore, a combination of two-photon and multiphoton polymerization coupled with light-induced movement may serve as an exciting tool for drug delivery (Bozuyuk et al. 2018; Park et al. 2021; Rajabasadi et al. 2021; Adam et al. 2021) and bioimaging (Fan et al. 2013; Aziz et al. 2020; Gautam et al. 2019) applications. Besides light-induced locomotory behavior, the hybrid micro–nanomotor can also be used as a scaffold for 3D cell culture. A study conducted by Nelson et al. reports using DLW-based magnetic/biocompatible micro-robots capable of in vitro cell culture and in vivo targeted drug delivery applications (Fig. 4.6C). The scaffolding material is made with biocompatible polymers supported with Ni/Ti layer to enhance the magnetic properties (Kim et al. 2013).

4.6 Propulsion Mechanism of Nanomotors

4.6.1 *Chemical and Biological Propulsion*

Understanding the propulsion mechanism in biological fluid is essential before in vitro and in vivo application. Nanoswimmers and nanorobots have the potential to migrate in different biological fluids, such as human serum, blood, and gastrointestinal fluids. In most cases, the fast swimming performance is achieved due to the self-diffusiophoretic and self-electrophoretic nature of the nanorobots triggered by the proteins and electrolytes in the body fluid. Besides, the bubble-based mechanism (which uses the power of classical H_2O_2 fuel instead of biofluid) exhibited considerable performance in terms of speed and directionality in various fluids (Mallouk and Sen 2009; Paxton et al. 2004; Dong et al. 2017; de Ávila et al. 2017).

Figure 4.7 depicts a few examples of chemically and biologically powered nanorobots with tunable functionalities.

4.6.2 Magnetic Propulsion

Magnetic nanorobots are unique nanomotors whose external magnetic field controls the robot’s movement. The magnetic materials can be classified as a function of magnetic susceptibility, denoted by x_m . A ferromagnetic or ferrimagnetic material has $x_m > > 0$, while paramagnetic and diamagnetic materials have $x_m > 0$ and $x_m < 0$, respectively. When a tiny magnetic robot with volume v is placed between two magnetic bars (magnetic field B), the fabricated nanorobot will display the magnetization (M) property. During the movement (in a magnetic gradient (dB)), the nanorobot will experience an attractive force or repulsive force followed by a magnetic torque (T). The magnetic force and torque of a nanorobot are given by Eqs. (4.1) and (4.2):

$$F = v(M \times d)B \tag{4.1}$$

$$T = vM \times B \tag{4.2}$$

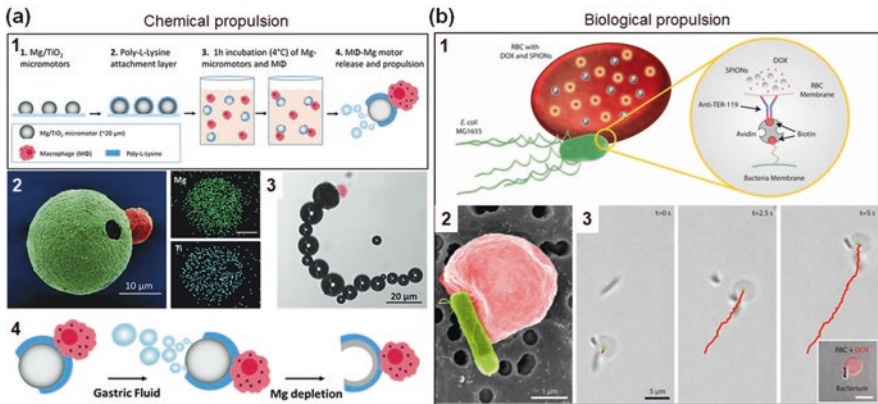


Fig. 4.7 The propulsion mechanism of nanorobots in chemical/biological fluids. (a) Fabrication of macrophage-magnesium (Mq-Mg) nanomotors. Schematic illustration of the nanomotors (1), SEM morphology with EDX mapping image (2), and bright-field image of the Mq-Mg motor displaying active motion in the GI fluid at pH 1.3 (3). Schematic illustration of the propulsion mechanism of the Mq-Mg nanomotors (4). Scale bar: 10 μm (Zhang et al. 2019). Reproduced with permission from John Wiley & Sons, Inc., 2019. (b) Demonstration of red blood cell (RBC)-based magnetic microswimmers for active cargo delivery. The delivery molecule shown here is doxorubicin (DOX). Scale bar: 1 and 5 μm (Alapan et al. 2018). (Reproduced with permission from the American Association for the Advancement of Science, 2018)

Magnetic fields can be classified in three forms based on the direction and time of the magnet. These are static, dynamic, and oscillatory magnetic fields (Yu et al. 2017). To evaluate the swim or motion of the magnetic nanorobots in a given fluid, the Navier-Stokes equation (Eq. 4.3) is applied as follows:

$$Re = \text{inertial forces} / \text{viscous forces} = \rho v L / \eta \quad (4.3)$$

where ρ and η are the density and viscosity of the fluid, v is the time vector, and L is the length or cross-sectional area of the moving object. Re is the Reynolds number for a given fluid. Small-scale devices and organisms have a very small size or length, meaning that the viscous force mainly controls their motion. Therefore, the flow behavior of a tiny magnetic robot can be explained by the “scallop theorem” (Fig. 4.8a), which describes that at a low Reynolds number, the microscopic objects only move back or forward movement. Once the actuation energy is stopped, the scallop object’s movement is immediately halted due to the absence of the external magnetic force. This concept is generally applied for cargo delivery or drug delivery through small-scale nanorobots with helical (Wu et al. 2018; Ceylan et al. 2021), tubular (Yang et al. 2019), or random-shaped morphologies (Vach et al. 2015; Morozov et al. 2017). Figure 4.8b briefly illustrates the propulsion mechanism of classical magnetic nanorobots in the presence of magnetic field stimulation.

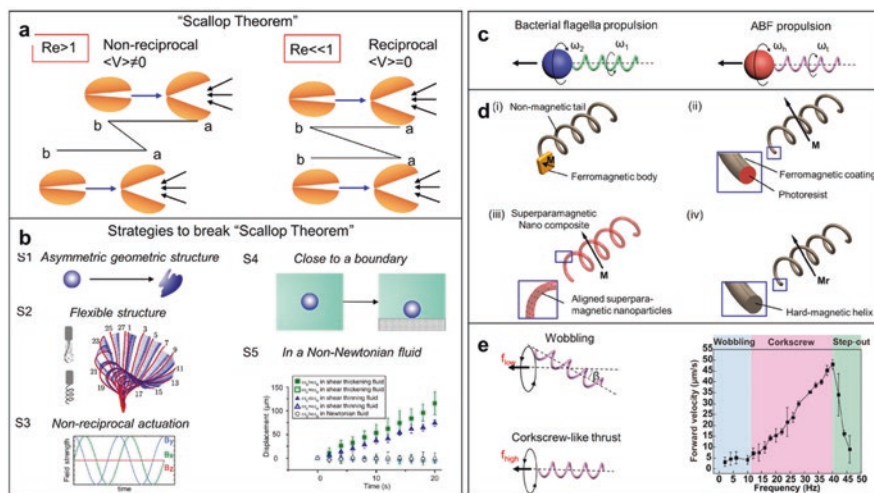


Fig. 4.8 (a, b) “Scallop theorem” demonstrating the nonreciprocal and reciprocal motion of a high and low Reynolds number fluid. (c–e) Flagellar-based propulsion mechanism (ABF propulsion and wobbling mechanism) as a model for magnetic nanorobot manipulation (Zhou et al. 2021). (Reproduced with permission from the American Chemical Society, 2021)

4.6.3 Ultrasonic Propulsion

Ultrasonic-based propulsion is one of the most frequently used stimulation techniques for controlling a nanorobot's movement. Ultrasound therapy with extremely low amplitudes (mostly in MHz frequency) is usually used because the higher amplitude of ultrasound waves is harmful and may damage the living tissues (Veronick et al. 2018). During ultrasound actuation, the micro-/nanorobots receive irradiation from a sound wave (primary sound wave), and together with hydrodynamic flow, the robots drift from one place to another inside the body. It is interesting to note that the reflected sound wave (secondary sound wave) from one particle may help to create motion for another particle during ultrasonication. Therefore, the primary radiation force is only effective for a single particle, and the secondary radiation force mainly controls the particle-particle interplay during active movement and sometimes creates multiparticle structures (Weiser et al. 1984). To understand the mechanism of the nanorobot movement, "particle-fluid hydrodynamics" is often demonstrated. The MHz frequency ultrasound can propel, align, assemble, or rotate the metallic nanorobots in an aqueous solution with high ionic strength (Wang et al. 2012).

4.7 Therapeutic Applications

Micro-/nanomotors can convert ambient energy into mechanical force to achieve movement (Soto et al. 2021). Several reports have demonstrated the use of micro-/nanorobots in therapeutic applications, such as disease diagnosis, drug delivery, surgery, and tumor clearance (Soto et al. 2021; Wang et al. 2022). For example, magnetically propelled nanorobots can easily visualize the immunogenic assays in a short time. A study by Wang et al. reported using rod-like self-propelled magnetic nanorobots (MNRs) via the 3D printing technique (Wang et al. 2022). The MNRs were co-assembled using magnetic field stimulation of Fe_2O_3 nanoparticles. With the help of 3D printing, a thin layer of rigid SiO_2 layer was deposited onto the surface of the MNRs. The biocompatible MNRs can capture antibodies by specific MF stimulation and bind specifically with the target antigen (Fig. 4.9a). Therefore, magnetically propelled MNRs not only are innovative but also reduce the assay time of a standard ELISA. Similarly, various pharmaceutical drugs can be entrapped onto the surface of the printed nanobots via electrostatic interaction at physiological pH (pH 7.4). In a study, ultrasound-guided porous nanowires (NWs) were fabricated using 3D printing and functionalized by anionic polymers (Soto et al. 2020). The anionic polymer helps entrap the doxorubicin into the NW's surface, which can be triggered to release in an acidic pH (pH 6.5–7.0) environment for tumor therapy (Fig. 4.9b).

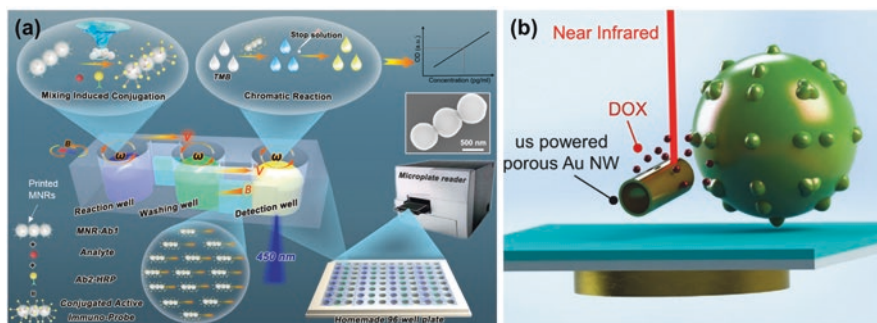


Fig. 4.9 (a) Schematic illustration of a self-propelled magnetic nanorobot enabled high-throughput ELISA assay (Wang et al. 2022). Reproduced with permission from the American Chemical Society, 2022. (b) Demonstration of an ultrasound-guided magnetic nanowire for NIR-triggered delivery of a chemotherapeutic drug (DOX) for tumor therapy (Soto et al. 2020). (Reproduced with permission from John Wiley & Sons, Inc., 2021)

3D printed micro-/nanorobots are also used in cargo delivery and release of several drugs and therapeutic molecules. Biodegradability is one of the crucial factors for micro-/nanorobot fabrication. After delivering suitable products to the target system through nanorobots, it is essential to remove the robot from the body or allow it to degrade for a specific time without showing any adverse effects. On the other hand, using nonbiodegradable robots may result in serious health issues and, to some extent, require surgery. Therefore, most of the micro-/nanorobots fabricated have less biodegradability, hindering their use in clinical trials. A study conducted by Ceylan et al. reported the use of two-photon microprinting of gelatin methacrylate (GelMA)-based hydrogel micro-/nanoswimmer (MNS) (Fig. 4.10a–c) with controlled delivery efficiency and excellent biodegradability (Ceylan et al. 2019). The fabricated MNS with drug coating precisely senses the matrix metalloproteinase-2 (MMP-2) upon swelling (within 0–118 h time frame) and boosts the release of embedded cargo molecule to the target system (Fig. 4.10d). The developed system can also sense and respond to the external magnetic field when incorporated with an anti-Ebr-2 (commonly known as laminin subunit gamma-2 protein/LAMC2) antibody specific to SKBR3 breast cancer cells (Fig. 4.10e). Hence, biodegradable micromotors are intelligent and can be used for cellular imaging and diagnostic applications in the future without any systemic toxicity in the human body (Ceylan et al. 2021).

4.8 Key Challenges and Future Outlook

Although many successful outcomes have been reported in the past 10 years using the micro-/nanorobots, several factors still need to be addressed before clinical application. Some of the significant challenges are listed below:

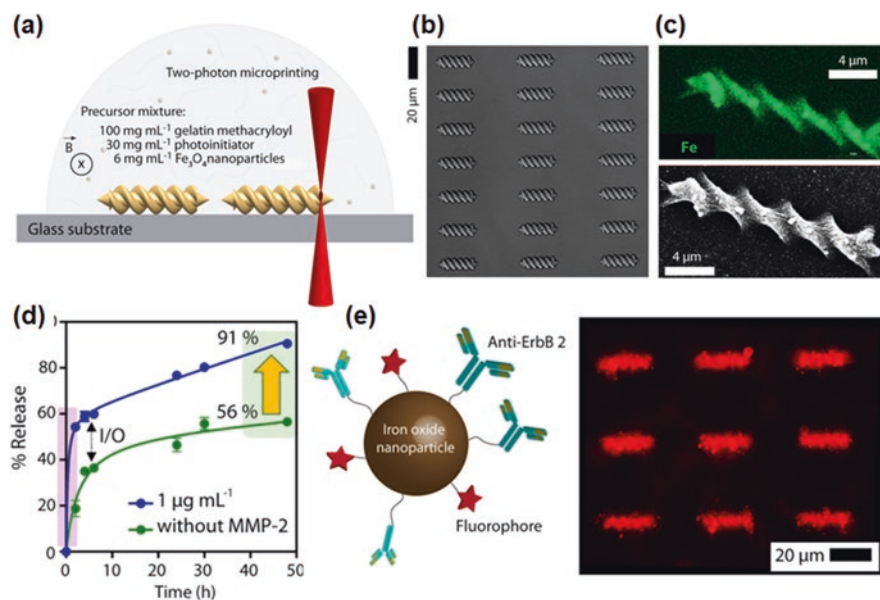


Fig. 4.10 Fabrication of a two-photon enabled microprinting of magnetic nanorobots for cargo delivery, bioimaging, and tumor cell biosensing. (a) Schematic illustration of the nanorobot fabrication process. (b, c) Optical microscopy and EDS elemental mapping image of the fabricated nanorobots. Scale bar: 4 μm and 20 μm . (d) Swelling-induced FITC-dextran release from the nanorobotic system. (e) Construction of an antibody-conjugated nanorobotic system (Fe_2O_3 -Anti Erb2) for breast cancer sensing and drug delivery (Ceylan et al. 2019). (Reproduced with permission from the American Chemical Society, 2019. Scale bar: 20 μm)

1. One of the most crucial parts of nanorobot fabrication is maintaining the proper structure. 3D printing at nanoscale resolution often seems more complicated due to proper viscosity and lack of suitable crosslinking mechanism (Wang and Zhou 2021). In this regard, the two-photon (TP)- and multiphoton (MP)-based printing techniques hold great promises in the future nanorobot development. The smaller the size, the easier it is to control through the blood vessels for targeted cancer therapy.
2. Another key factor of nanorobot fabrication is designing and understanding the propulsion mechanism. Nanomotors fabricated through 3D printing have been claimed to migrate via an active propulsion mechanism in the body system; however, its successful implementation is rather complex. A few reports are available in the existing literature demonstrating the role of chemically powered nanomotors for in vivo therapeutic applications (Wang and Zhou 2021). The exact mechanism governing the motile behavior of these nanomotors is still limited and hinders clinical trials. Moreover, the chemically powered nanomotors are made up of soft polymer materials and display weak motion behavior in the body fluid, also challenging to control the speed or directionality. To some extent, the soft

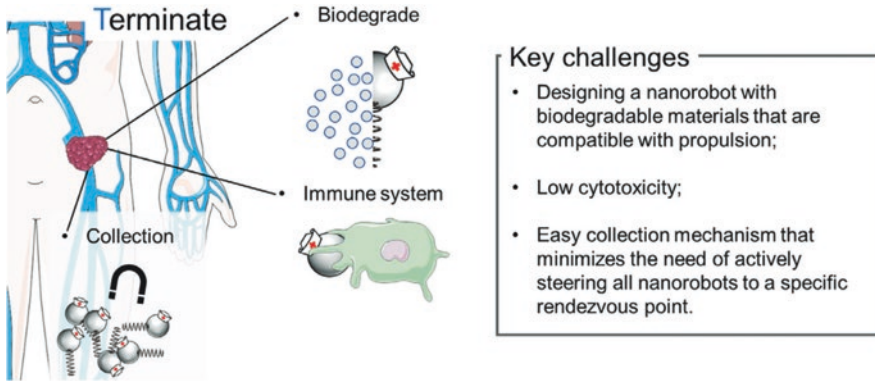


Fig. 4.11 Key challenges and opportunities involved with the termination process of a nanobot after the task is completed (Wang and Zhou 2021). (Reproduced with permission from John Wiley & Sons, Inc., 2020)

polymeric nanorobots shrink and degrade while traveling through the blood vessel; therefore, it is very difficult to control from the outside (de Ávila et al. 2017; Ma et al. 2016; Li et al. 2016). Figure 4.11 depicts some of the major advantages of soft polymeric nanorobots and their possible route of destruction after the mission is completed.

3. Magnetic field (MF)-guided nanorobots have gained enormous attention in the scientific community owing to their unique structure, simplicity, and rapid delivery properties (Soto et al. 2020). Unlike magnetic field stimulation, several other propulsion methods, such as ultrasound, electric field, etc., have been successfully implemented (Wang et al. 2012). Magnetically powered nanomotors mainly consist of magnetic nanorods or nanowires (MNR/MNW). An ideal magnetobot (MagBot) should have active locomotion, a physiologically relevant structure, less cytotoxicity, fast diffusion nature, and precise traceability through existing imaging systems (e.g., magnetic resonance imaging, computed tomography), high immunogenic compatibility, and higher delivery efficiency (e.g., drugs, peptides, nucleic acids, etc.) with controlled biodegradation (Fig. 4.12) (Agrahari et al. 2020). However, the actual clinical application is still unknown. Thus, an ideal MF-powered device integrating all the above functionalities is challenging. The key limitation of MF-powered systems is that they rely on the external MF source, which provides the locomotion of the robot, and once the external MF is removed, the locomotory behavior of the nanorobot is hindered. Furthermore, the sophisticated MF-based controller system requires huge financial investments and is often bulky and unsuitable to carry on (Wang et al. 2012; McNeill et al. 2020; Sun et al. 2022). Therefore, these nanorobots look more hypothetical rather than reality. For example, the condition will be more serious when we need to operate a nanorobot passing through the tumor site (imagine a tiny robot is entered into the tumor cell, destroyed it, and again jumped to another tumor cell), where we need to deliver drugs/cargo.

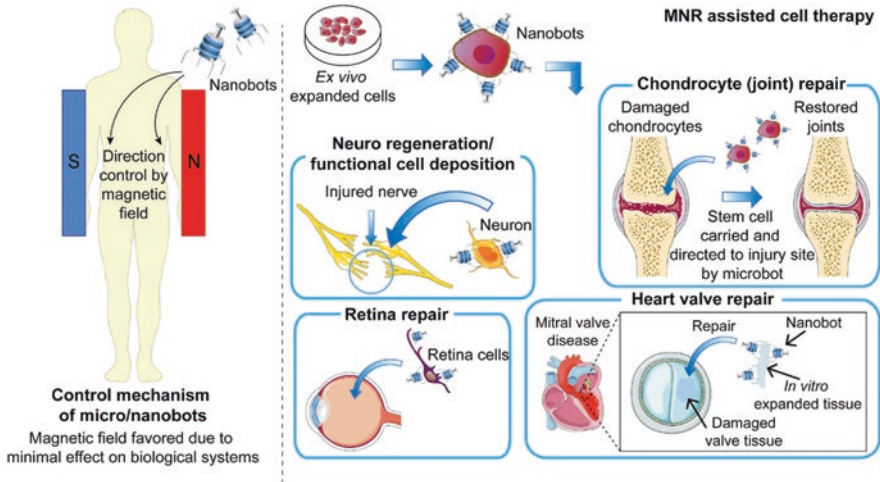


Fig. 4.12 Potential application of functional magnetic nanorobots for clinical applications. A magnetic field-assisted delivery system uses magnetic nanorobots (MagBots) to regenerate the nerves, retina, heart, and cartilage. The MagBots are simple, easy to design, robust, intelligent, and highly biocompatible in the biological system. These nanomotors can be controlled externally and triggered to deliver various components to the target cell or tissue, such as drugs, peptides, proteins, and nucleic acids (Agrahari et al. 2020). (Reproduced with permission from Elsevier Publishing Ltd., 2022)

4. Light-triggered or NIR-responsive nanomotors require precise heating/cooling control when circulating through in vivo system with a suitable tracking system.
5. The biohybrid nanorobots (nanobot fabrication inspired by nature or direct manipulation of nanoscale microorganisms to behave like a functional robot) may solve the problem of cytotoxicity arising from the nonbiodegradable robots after prolonged use in the human body (Wang and Pumera 2020).

4.9 Concluding Remarks

This chapter addressed an overview of recent progress and future opportunities in the 3D printing of micro-/nanorobots and their therapeutic advancements. The 3D printing techniques, especially two-photon (TP) and multiphoton (MP) polymerization techniques, hold many promises to overcome the present challenges of printable nanomotors. The 3D printed medical nanorobots have tremendous application in drug delivery, surgery, and tissue regeneration. Although several factors need to be considered before the practical application of micro-/nanomotors, there is a long way to go when we can serve those nanorobots to medical doctors to combat several diseases, such as cancer, arthritis, sclerosis, etc. Looking forward, a good understanding of the engineering tools and the mechanism of propulsion, precise printing

technique, overall conceptualization, methodology, and actual clinical application is required for the successful application of nano-/microrobots.

Acknowledgments This work was partially supported by the “Basic Science Research Program” through the “National Research Foundation of Korea (NRF)” funded by the Ministry of Education (grant nos. 2018R1A6A1A03025582, 2019R1D1A3A03103828, and 2022R1I1A3063302), Republic of Korea.

References

- Adam G, Benouhiba A, Rabenorosoa K, Clévy C, Cappelleri DJ. 4D printing: enabling technology for microrobotics applications. *Adv Intell Syst.* 2021;3:2000216.
- Aghakhani A, Yasa O, Wrede P, Sitti M. Acoustically powered surface-slipping mobile microrobots. *Proc Natl Acad Sci.* 2020;117:3469–77.
- Agrahari V, Agrahari V, Chou M-L, Chew CH, Noll J, Burnouf T. Intelligent micro-/nanorobots as drug and cell carrier devices for biomedical therapeutic advancement: promising development opportunities and translational challenges. *Biomaterials.* 2020;260:120163.
- Alapan Y, Yasa O, Schauer O, Giltinan J, Tabak AF, Sourjik V, et al. Soft erythrocyte-based bacterial microswimmers for cargo delivery. *Sci Robot.* 2018;3:eaar4423.
- Alemzadeh H, Raman J, Leveson N, Kalbarczyk Z, Iyer RK. Adverse events in robotic surgery: a retrospective study of 14 years of FDA data. *PLoS One.* 2016;11:e0151470.
- Aziz A, Pane S, Iacovacci V, Koukourakis N, Czarske J, Menciassi A, et al. Medical imaging of microrobots: toward in vivo applications. *ACS Nano.* 2020;14:10865–93.
- Baker RD, Montenegro-Johnson T, Sediako AD, Thomson MJ, Sen A, Lauga E, et al. Shape-programmed 3D printed swimming microtori for the transport of passive and active agents. *Nat Commun.* 2019;10:1–10.
- Bozuyuk U, Yasa O, Yasa IC, Ceylan H, Kizilel S, Sitti M. Light-triggered drug release from 3D-printed magnetic chitosan microswimmers. *ACS Nano.* 2018;12:9617–25.
- Brandt M. Laser additive manufacturing: materials, design, technologies, and applications 2016.
- Cabanach P, Pena-Francesch A, Sheehan D, Bozuyuk U, Yasa O, Borros S, et al. Zwitterionic 3D-printed non-immunogenic stealth microrobots. *Adv Mater.* 2020;32:2003013.
- Calvert P. Inkjet printing for materials and devices. *Chem Mater.* 2001;13:3299–305.
- Campuzano S, Kagan D, Orozco J, Wang J. Motion-driven sensing and biosensing using electrochemically propelled nanomotors. *Analyst.* 2011;136:4621–30.
- Ceylan H, Yasa IC, Yasa O, Tabak AF, Giltinan J, Sitti M. 3D-printed biodegradable microswimmer for theranostic cargo delivery and release. *ACS Nano.* 2019;13:3353–62.
- Ceylan H, Dogan NO, Yasa IC, Musaoglu MN, Kulali ZU, Sitti M. 3D printed personalized magnetic micromachines from patient blood-derived biomaterials. *Sci Adv.* 2021;7:eabh0273.
- Chen W, Zhou H, Zhang B, Cao Q, Wang B, Ma X. Recent progress of micro/nanorobots for cell delivery and manipulation. *Adv Funct Mater* 2022;2110625.
- Chung S, Cho K, Lee T. Recent progress in inkjet-printed thin-film transistors. *Adv Sci.* 2019;6:1801445.
- Crivello JV, Reichmanis E. Photopolymer materials and processes for advanced technologies. *Chem Mater.* 2014;26:533–48.
- de Ávila BE-F, Angsantikul P, Li J, Angel Lopez-Ramirez M, Ramírez-Herrera DE, Thamphiwatana S, et al. Micromotor-enabled active drug delivery for in vivo treatment of stomach infection. *Nat Commun.* 2017;8:1–9.
- Doherty RP, Varkevissier T, Teunisse M, Hoecht J, Ketzetzi S, Ouhajji S, et al. Catalytically propelled 3D printed colloidal microswimmers. *Soft Matter.* 2020;16:10463–9.

- Dong R, Hu Y, Wu Y, Gao W, Ren B, Wang Q, et al. Visible-light-driven BiOI-based Janus micro-motor in pure water. *J Am Chem Soc.* 2017;139:1722–5.
- Driscoll M, Delmotte B, Youssef M, Sacanna S, Donev A, Chaikin P. Unstable fronts and motile structures formed by microrollers. *Nat Phys.* 2017;13:375–9.
- Engel KE, Kilmartin PA, Diegel O. Recent advances in the 3D printing of ionic electroactive polymers and core ionomeric materials. *Polym Chem* 2022.
- Fan Q, Hu W, Ohta AT. Light-induced microbubble poration of localized cells. 2013 35th Annual International Conference of the IEEE Engineering in Medicine and Biology Society (EMBC): IEEE; 2013. pp. 4482–4485.
- Galajda P, Ormos P. Complex micromachines produced and driven by light. *Appl Phys Lett.* 2001;78:249–51.
- Gao W, Uygun A, Wang J. Hydrogen-bubble-propelled zinc-based microrockets in strongly acidic media. *J Am Chem Soc.* 2012;134:897–900.
- Gautam R, Xiang Y, Lamstein J, Liang Y, Bezryadina A, Liang G, et al. Optical force-induced nonlinearity and self-guiding of light in human red blood cell suspensions. *Light Sci Appl.* 2019;8:1–9.
- Ge Z, Dai L, Zhao J, Yu H, Yang W, Liao X, et al. Bubble-based microrobots enable digital assembly of heterogeneous microtissue modules. *Biofabrication* 2022.
- Hribar KC, Finlay D, Ma X, Qu X, Ondeck MG, Chung PH, et al. Nonlinear 3D projection printing of concave hydrogel microstructures for long-term multicellular spheroid and embryoid body culture. *Lab Chip.* 2015;15:2412–8.
- Hwang HH, Zhu W, Victorine G, Lawrence N, Chen S. 3D-printing of functional biomedical microdevices via light-and extrusion-based approaches. *Small Methods.* 2018;2:1700277.
- Januszewicz R, Tumbleston JR, Quintanilla AL, Mechem SJ, DeSimone JM. Layerless fabrication with continuous liquid interface production. *Proc Natl Acad Sci.* 2016;113:11703–8.
- Kagan D, Campuzano S, Balasubramanian S, Kuralay F, Flechsig G-U, Wang J. Functionalized micromachines for selective and rapid isolation of nucleic acid targets from complex samples. *Nano Lett.* 2011;11:2083–7.
- Khan MS, Fon D, Li X, Tian J, Forsythe J, Garnier G, et al. Biosurface engineering through ink jet printing. *Colloids Surf B: Biointerfaces.* 2010;75:441–7.
- Kim S, Qiu F, Kim S, Ghanbari A, Moon C, Zhang L, et al. Fabrication and characterization of magnetic microrobots for three-dimensional cell culture and targeted transportation. *Adv Mater.* 2013;25:5863–8.
- Kinstlinger IS, Miller JS. 3D-printed fluidic networks as vasculature for engineered tissue. *Lab Chip.* 2016;16:2025–43.
- Kuang X. Introduction to 4D printing: methodologies and materials. *Additive Manufacturing: Elsevier;* 2021. pp. 303–342.
- Kuang X, Wu J, Chen K, Zhao Z, Ding Z, Hu F, et al. Grayscale digital light processing 3D printing for highly functionally graded materials. *Sci Adv.* 2019;5:eaav5790.
- Kunduzova OR, Bianchi P, Pizzinat N, Escourrou G, Seguelas MH, Parini A, et al. Regulation of JNK/ERK activation, cell apoptosis, and tissue regeneration by monoamine oxidases after renal ischemia-reperfusion. *FASEB J.* 2002;16:1129–31.
- Layani M, Wang X, Magdassi S. Novel materials for 3D printing by photopolymerization. *Adv Mater.* 2018;30:1706344.
- Lewis JA. Direct ink writing of 3D functional materials. *Adv Funct Mater.* 2006;16:2193–204.
- Li J, Pumera M. 3D printing of functional microrobots. *Chem Soc Rev.* 2021;50:2794–838.
- Li J, Thamphiwatana S, Liu W, Esteban-Fernández de Ávila B, Angsantikul P, Sandraz E, et al. Enteric micromotor can selectively position and spontaneously propel in the gastrointestinal tract. *ACS Nano.* 2016;10:9536–42.
- Liang S, Tu Y, Chen Q, Jia W, Wang W, Zhang L. Microscopic hollow hydrogel springs, necklaces and ladders: a tubular robot as a potential vascular scavenger. *Mater Horiz.* 2019;6:2135–42.
- Lu Y, Mapili G, Suhali G, Chen S, Roy K. A digital micro-mirror device-based system for the microfabrication of complex, spatially patterned tissue engineering scaffolds. *J Biomed Mater Res A.* 2006;77:396–405.

- Ma X, Hortelão AC, Patino T, Sanchez S. Enzyme catalysis to power micro/nanomachines. *ACS Nano*. 2016;10:9111–22.
- Ma X, Dewan S, Liu J, Tang M, Miller KL, Yu C, et al. 3D printed micro-scale force gauge arrays to improve human cardiac tissue maturation and enable high throughput drug testing. *Acta Biomater*. 2019;95:319–27.
- Magdanz V, Stoychev G, Ionov L, Sanchez S, Schmidt OG. Stimuli-responsive microjets with reconfigurable shape. *Angew Chem*. 2014;126:2711–5.
- Mallouk TE, Sen A. Powering nanorobots. *Sci Am*. 2009;300:72–7.
- Manesh KM, Cardona M, Yuan R, Clark M, Kagan D, Balasubramanian S, et al. Template-assisted fabrication of salt-independent catalytic tubular microengines. *ACS Nano*. 2010;4:1799–804.
- Maric T, Nasir MZM, Rosli NF, Budanović M, Webster RD, Cho NJ, et al. Microrobots derived from variety plant pollen grains for efficient environmental clean up and as an anti-cancer drug carrier. *Adv Funct Mater*. 2020;30:2000112.
- McNeill JM, Nama N, Braxton JM, Mallouk TE. Wafer-scale fabrication of micro-to nanoscale bubble swimmers and their fast autonomous propulsion by ultrasound. *ACS Nano*. 2020;14:7520–8.
- Medina-Sánchez M, Guix M, Harazim S, Schwarz L, Schmidt OG. Rapid 3D printing of complex polymeric tubular catalytic micromotors. 2016 International Conference on Manipulation, Automation and Robotics at Small Scales (MARSS): IEEE; 2016. pp. 1–6.
- Medina-Sánchez M, Magdanz V, Guix M, Fomin VM, Schmidt OG. Swimming microrobots: soft, reconfigurable, and smart. *Adv Funct Mater*. 2018;28:1707228.
- Mei J, Lovell MR, Mickle MH. Formulation and processing of novel conductive solution inks in continuous inkjet printing of 3-D electric circuits. *IEEE Trans Electron Packag Manuf*. 2005;28:265–73.
- Melchels FP, Feijen J, Grijpma DW. A review on stereolithography and its applications in biomedical engineering. *Biomaterials*. 2010;31:6121–30.
- Mondschein RJ, Kanitkar A, Williams CB, Verbridge SS, Long TE. Polymer structure-property requirements for stereolithographic 3D printing of soft tissue engineering scaffolds. *Biomaterials*. 2017;140:170–88.
- Morozov KI, Mirzae Y, Kenneth O, Leshansky AM. Dynamics of arbitrary shaped propellers driven by a rotating magnetic field. *Phys Rev Fluids*. 2017;2:044202.
- Park J-U, Lee JH, Paik U, Lu Y, Rogers JA. Nanoscale patterns of oligonucleotides formed by electrohydrodynamic jet printing with applications in biosensing and nanomaterials assembly. *Nano Lett*. 2008;8:4210–6.
- Park J, Jy K, Pane S, Nelson BJ, Choi H. Acoustically mediated controlled drug release and targeted therapy with degradable 3D porous magnetic microrobots. *Adv Healthc Mater*. 2021;10:2001096.
- Patel DK, Sakhaei AH, Layani M, Zhang B, Ge Q, Magdassi S. Highly stretchable and UV curable elastomers for digital light processing based 3D printing. *Adv Mater*. 2017;29:1606000.
- Paxton WF, Kistler KC, Olmeda CC, Sen A, St. Angelo SK, Cao Y, et al. Catalytic nanomotors: autonomous movement of striped nanorods. *J Am Chem Soc*. 2004;126:13424–31.
- Paxton N, Smolan W, Böck T, Melchels F, Groll J, Jungst T. Proposal to assess printability of bioinks for extrusion-based bioprinting and evaluation of rheological properties governing bioprintability. *Biofabrication*. 2017;9:044107.
- Peak CW, Stein J, Gold KA, Gaharwar AK. Nanoengineered colloidal inks for 3D bioprinting. *Langmuir*. 2018;34:917–25.
- Pouponneau P, Leroux J-C, Soulez G, Gaboury L, Martel S. Co-encapsulation of magnetic nanoparticles and doxorubicin into biodegradable microcarriers for deep tissue targeting by vascular MRI navigation. *Biomaterials*. 2011;32:3481–6.
- Qiu F, Fujita S, Mhanna R, Zhang L, Simona BR, Nelson BJ. Magnetic helical microswimmers functionalized with lipoplexes for targeted gene delivery. *Adv Funct Mater*. 2015;25:1666–71.
- Rafiee M, Farahani RD, Therriault D. Multi-material 3D and 4D printing: a survey. *Adv Sci*. 2020;7:1902307.
- Rajabasadi F, Schwarz L, Medina-Sánchez M, Schmidt OG. 3D and 4D lithography of untethered microrobots. *Prog Mater Sci*. 2021;120:100808.

- Rosello M, Maîtrejean G, Roux DC, Jay P, Barbet B, Xing J. Influence of the nozzle shape on the breakup behavior of continuous ink jets. *J Fluids Eng* 2018;140.
- Sachyani Keneth E, Kamyshny A, Totaro M, Beccai L, Magdassi S. 3D printing materials for soft robotics. *Adv Mater*. 2021;33:2003387.
- Salva ML, Rocca M, Hu Y, Delamarche E, Niemeyer CM. Complex nucleic acid hybridization reactions inside capillary-driven microfluidic chips. *Small*. 2020;16:2005476.
- Sanchez S, Ananth AN, Fomin VM, Viehrig M, Schmidt OG. Superfast motion of catalytic microjet engines at physiological temperature. *J Am Chem Soc*. 2011;133:14860–3.
- Schmid M, Amado A, Wegener K. Materials perspective of polymers for additive manufacturing with selective laser sintering. *J Mater Res*. 2014;29:1824–32.
- Schwab A, Levato R, D'Este M, Piluso S, Eglin D, Malda J. Printability and shape fidelity of bioinks in 3D bioprinting. *Chem Rev*. 2020;120:11028–55.
- Sengupta S, Patra D, Ortiz-Rivera I, Agrawal A, Shklyav S, Dey KK, et al. Self-powered enzyme micropumps. *Nat Chem*. 2014;6:415–22.
- Simpson N, Dholakia K, Allen L, Padgett M. Mechanical equivalence of spin and orbital angular momentum of light: an optical spanner. *Opt Lett*. 1997;22:52–4.
- Singh M, Haverinen HM, Dhagat P, Jabbour GE. Inkjet printing—process and its applications. *Adv Mater*. 2010;22:673–85.
- Soto F, Martin A, Ibsen S, Vaidyanathan M, Garcia-Gradilla V, Levin Y, et al. Acoustic microcannons: toward advanced microballistics. *ACS Nano*. 2016;10:1522–8.
- Soto F, Lopez-Ramirez MA, Jeerapan I, Esteban-Fernandez de Avila B, Mishra RK, Lu X, et al. Rotibot: use of rotifers as self-propelling biohybrid microcleaners. *Adv Funct Mater*. 2019;29:1900658.
- Soto F, Wang J, Ahmed R, Demirci U. Medical micro/nanorobots in precision medicine. *Adv Sci* 2020;7:2002203.
- Soto F, Karshalev E, Zhang F, Esteban Fernandez de Avila B, Nourhani A, Wang J. Smart materials for microrobots. *Chem Rev* 2021.
- Stanton M, Trichet-Paredes C, Sanchez S. Applications of three-dimensional (3D) printing for microswimmers and bio-hybrid robotics. *Lab Chip*. 2015;15:1634–7.
- Su Y, Ge Y, Liu L, Zhang L, Liu M, Sun Y, et al. Motion-based pH sensing based on the cartridge-case-like micromotor. *ACS Appl Mater Interfaces*. 2016;8:4250–7.
- Sun M, Tian C, Mao L, Meng X, Shen X, Hao B, et al. Reconfigurable magnetic slime robot: deformation, adaptability, and multifunction. *Adv Funct Mater* 2022:2112508.
- Tang S, Zhang F, Zhao J, Talaat W, Soto F, Karshalev E, et al. Structure-dependent optical modulation of propulsion and collective behavior of acoustic/light-driven hybrid microbowls. *Adv Funct Mater*. 2019;29:1809003.
- Tasci T, Herson P, Neeves K, Marr D. Surface-enabled propulsion and control of colloidal micro-wheels. *Nat Commun*. 2016;7:1–6.
- Tottori S, Zhang L, Qiu F, Krawczyk KK, Franco-Obregón A, Nelson BJ. Magnetic helical micro-machines: fabrication, controlled swimming, and cargo transport. *Adv Mater*. 2012;24:811–6.
- Tumbleston JR, Shirvanyants D, Ermoshkin N, Januszewicz R, Johnson AR, Kelly D, et al. Continuous liquid interface production of 3D objects. *Science*. 2015;347:1349–52.
- Vach PJ, Fratzl P, Klumpp S, Faivre D. Fast magnetic micropellers with random shapes. *Nano Lett*. 2015;15:7064–70.
- Valot L, Martinez J, Mehdi A, Subra G. Chemical insights into bioinks for 3D printing. *Chem Soc Rev*. 2019;48:4049–86.
- Veronick JA, Assanah F, Piscopo N, Kutes Y, Vyas V, Nair LS, et al. Mechanically loading cell/hydrogel constructs with low-intensity pulsed ultrasound for bone repair. *Tissue Eng Part A*. 2018;24:254–63.
- Wang H, Pumera M. Coordinated behaviors of artificial micro/nanomachines: from mutual interactions to interactions with the environment. *Chem Soc Rev*. 2020;49:3211–30.
- Wang W, Zhou C. A journey of Nanomotors for targeted cancer therapy: principles, challenges, and a critical review of the state-of-the-art. *Adv Healthc Mater*. 2021;10:2001236.
- Wang W, Castro LA, Hoyos M, Mallouk TE. Autonomous motion of metallic microrods propelled by ultrasound. *ACS Nano*. 2012;6:6122–32.

- Wang X, Sun Y, Peng C, Luo H, Wang R, Zhang D. Transitional suspensions containing thermosensitive dispersant for three-dimensional printing. *ACS Appl Mater Interfaces*. 2015;7:26131–6.
- Wang Y, Liu X, Chen C, Chen Y, Li Y, Ye H, et al. Magnetic nanorobots as maneuverable immunoassay probes for automated and efficient enzyme linked immunosorbent assay. *ACS Nano* 2022.
- Weiser M, Apfel R, Neppiras E. Interparticle forces on red cells in a standing wave field. *Acta Acustica united with Acustica*. 1984;56:114–9.
- Wu L, Dong Z, Li F, Zhou H, Song Y. Emerging progress of inkjet technology in printing optical materials. *Adv Opt Mater*. 2016;4:1915–32.
- Wu Z, Troll J, Jeong H-H, Wei Q, Stang M, Ziemssen F, et al. A swarm of slippery micropropellers penetrates the vitreous body of the eye. *Sci Adv*. 2018;4:eaat4388.
- Wu Z, Chen Y, Mukasa D, Pak OS, Gao W. Medical micro/nanorobots in complex media. *Chem Soc Rev*. 2020;49:8088–112.
- Wünscher S, Seise B, Pretzel D, Pollok S, Perelaer J, Weber K, et al. Chip-on-foil devices for DNA analysis based on inkjet-printed silver electrodes. *Lab Chip*. 2014;14:392–401.
- Xu T, Soto F, Gao W, Garcia-Gradilla V, Li J, Zhang X, et al. Ultrasound-modulated bubble propulsion of chemically powered microengines. *J Am Chem Soc*. 2014;136:8552–5.
- Xu H, Medina-Sánchez M, Magdanz V, Schwarz L, Hebenstreit F, Schmidt OG. Sperm-hybrid micromotor for targeted drug delivery. *ACS Nano*. 2018;12:327–37.
- Yang L, Chen X, Wang L, Hu Z, Xin C, Hippler M, et al. Targeted single-cell therapeutics with magnetic tubular micromotor by one-step exposure of structured femtosecond optical vortices. *Adv Funct Mater*. 2019;29:1905745.
- Ye J, Wilson DA, Tu Y, Peng F. 3D-printed micromotors for biomedical applications. *Adv Mater Technol*. 2020;5:2000435.
- Ying Y, Pourrahimi AM, Zk S, Matějková S, Pumera M. Radioactive uranium preconcentration via self-propelled autonomous microrobots based on metal–organic frameworks. *ACS Nano*. 2019;13:11477–87.
- Yu J, Xu T, Lu Z, Vong CI, Zhang L. On-demand disassembly of paramagnetic nanoparticle chains for microrobotic cargo delivery. *IEEE Trans Robot*. 2017;33:1213–25.
- Zeng H, Wasylczyk P, Parmeggiani C, Martella D, Burrelli M, Wiersma DS. Light-fueled microscopic walkers. *Adv Mater*. 2015;27:3883–7.
- Zhang F, Mundaca-Urbe R, Gong H, Esteban-Fernández de Ávila B, Beltrán-Gastélum M, Karshalev E, et al. A macrophage–magnesium hybrid biomotor: fabrication and characterization. *Adv Mater*. 2019;31:1901828.
- Zhou L-y, Gao Q, Fu J-z, Chen Q-y, Zhu J-p, Sun Y, et al. Multimaterial 3D printing of highly stretchable silicone elastomers. *ACS Appl Mater Interfaces*. 2019;11:23573–83.
- Zhou LY, Fu J, He Y. A review of 3D printing technologies for soft polymer materials. *Adv Funct Mater*. 2020;30:2000187.
- Zhou H, Mayorga-Martinez CC, Pané S, Zhang L, Pumera M. Magnetically driven micro and nanorobots. *Chem Rev*. 2021;121:4999–5041.
- Zhu H, Snyder M. Protein chip technology. *Curr Opin Chem Biol*. 2003;7:55–63.

Chapter 5

Fundamental in Polymer-/Nanohybrid-Based Nanorobotics for Theranostics



Tejal V. Patil and Ki-Taek Lim

5.1 Introduction

Theranostics, also known as theragnostics, is a combination of disease diagnosis and therapy in a single dose. In 2002, Funkhouser used “theranostic” to describe breast cancer detection and treatment (Funkhouser 2002). This technique comprises *in vitro* and *in vivo* investigations that integrate therapeutic procedures such as chemotherapy, photodynamic, nucleic acid delivery, hyperthermia, and radiation treatment with one or more functionality (Kelkar and Reineke 2011). To understand the cellular phenotype(s) and disease heterogeneity, diagnostic imaging is required. Imaging should be performed before treating different diseases, such as cancer. Rather than developing and using different materials for these two goals, theranostics combines both qualities into a single unit, potentially overcoming unfavorable differences in biodistribution and selectivity. The ultimate aim of the theranostics is to detect the diseased tissue and deliver the medicine with the long-term hope of curing and to further adjust the therapy and dose with desirable control (Warenius 2009). Several polymer-based nanohybrid materials (nanorobots) are used for theranostics depending upon the imaging and therapy utilization. Generally, imaging

T. V. Patil
Interdisciplinary Program in Smart Agriculture, Kangwon National University,
Chuncheon, Republic of Korea

K.-T. Lim (✉)
Interdisciplinary Program in Smart Agriculture, Kangwon National University,
Chuncheon, Republic of Korea

Department of Biosystems Engineering, Institute of Forest Science, Kangwon National
University, Chuncheon, Republic of Korea
e-mail: ktlim@kangwon.ac.kr

probes such as quantum dots, contrast agents, organic and inorganic dyes, nuclear imaging agents, and magnetic compounds are used for diagnosis, followed by the treatment strategies of drug delivery (Sharath Kumar et al. 2021), gene delivery (Martins et al. 2021), photodynamic therapy (Loman-Cortes et al. 2021), hyperthermia (Gupta et al. 2021), and radiation therapy (Ruan and Qian 2021). Therefore, theranostics is a solution for the treatment of many diseases, including cancer, Alzheimer's disease, and other genetic disorders such as hereditary hemochromatosis, familial hypercholesterolemia, and ornithine transcarbamylase deficiency and antitrypsin deficiency (Krasia-Christoforou and Georgiou 2013). A schematic presentation of a combination of diagnosis and therapy to form theranostics is shown in Fig. 5.1.

Nanorobots for theranostics are mainly composed of three main components, as depicted in Fig. 5.2: (1) biocompatible polymer (either natural or synthetic), (2) nanomaterial for imaging (e.g., organic dyes, upconversion nanoparticles (UCNPs), quantum dots (QDs)) and enhancing the properties, and (3) a therapeutic component associated with a drug or a gene that encourages treatment (e.g., proteins, ROS-generating agents, hyperthermia-inducing nanoparticles, anticancer drugs, antibiotics, small interfering RNA (siRNA)) (Kelkar and Reineke 2011). Benefits of imaging nanomaterials in theranostics nanorobots include real-time monitoring of drug distribution, analysis of drug delivery at the target site, understanding drug reaction, analysis of drug release, assisting activated drug release, and non-invasively assessing target site accumulation (Lammers et al. 2010a, b). Imaging nanomaterials and drugs should be protected from other reactions during the delivery to the desired targeted site. A therapeutic component (drug) must be delivered to the targeted area, at the right time, and at an appropriate concentration to accomplish the desired therapeutic effect. However, there are many hurdles to obtain a successful drug delivery system. Most of these obstacles are related to poor pharmacokinetics and inappropriate drug distribution. Specifically, enzymatic degradation, the low solubility, nonspecific cytotoxicity, fast clearance rates from the body, and incapability to penetrate the biological barriers (Lammers et al. 2010a; Juillerat-Jeanneret 2008) are difficulties that need to be overcome. This can be accomplished by structurally tailoring polymers, which enables the design and manufacture of effective drug delivery systems by incorporating particular capabilities.

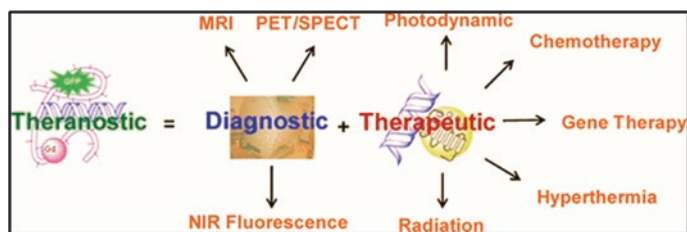


Fig. 5.1 Schematic presentation of the concept of theranostics, which includes disease diagnosis by various bioimaging techniques and its therapeutic approach. (Kelkar and Reineke 2011)

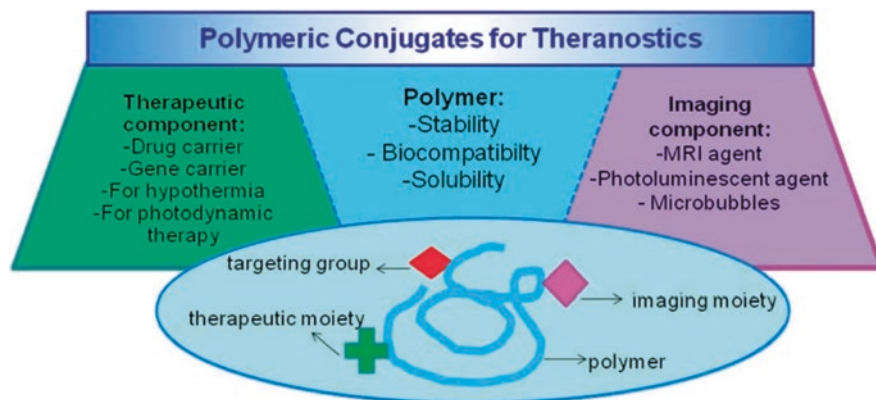


Fig. 5.2 The three main components that are combined for making nanorobots for theranostics. (Krasia-Christoforou and Georgiou 2013)

In recent decades, natural polymers have become increasingly popular in biological applications. They have the benefit of matching the extracellular matrix of natural tissues while keeping biochemical signals and qualities important for biocompatibility. Thus, they promote cellular attachment and behavior while avoiding immunological responses. Furthermore, they degrade quickly through natural enzymatic or chemical mechanisms. On the other hand, natural polymers have little mechanical strength, making modification procedures challenging. Recent breakthroughs in biofabrication, 3D printing, microfluidics, and cell-electrospinning have made it possible to create complex natural polymer matrixes with biophysical and structural features comparable to the extracellular matrix. In addition, these techniques offer the possibility of incorporating different cell lines into the fabrication process, a revolutionary strategy broadly explored in recent years to produce cell-laden scaffolds that can better mimic the properties of functional tissues (Puertas-Bartolomé et al. 2021). This polymeric, artificial matrix needs to provide appropriate biophysical and structural properties (e.g., stiffness, roughness, topography, and alignment) as well as biochemical cues (e.g., signaling, growth factors, and proteins) in order to promote the native capacity of cells to adhere, migrate, proliferate, and differentiate toward the growth of new tissue (Tutar et al. 2019).

Natural polymers are extracted from biological systems such as plants, microorganisms, algae, or animals. These polymers have been used for decades in the biomedical field. These materials retain the biochemical cues and properties necessary to improve their biocompatibility and present similar structures to the extracellular matrix (ECM) of native tissues (Asadi et al. 2020; Nolan et al. 2008; Eiselt et al. 2000). Therefore, they usually present good cellular attachment, improve cellular behavior, and avoid immunological reactions. These properties are sometimes limited due to batch variability within production and purification processes. The most common natural polymers used in biomedical applications include polysaccharides (e.g., alginate (Sanz-Horta et al. 2022; Bauleth-Ramos et al. 2019), cellulose (Patil

et al. 2022), hyaluronic acid (Alijotas-Reig et al. 2010; Felgueiras et al. 2017), and chitosan (Patel et al. 2021; Patel et al. 2022)), proteins (e.g., collagen (Sabir et al. 2019), silk (Ahsan et al. 2018), gelatin (Piao et al. 2021), and fibrin (Park and Woo 2018)), and bacterial polyesters (e.g., bacterial cellulose (Patil et al. 2022)). However, the poor mechanical strength of natural polymers frequently makes the manipulation and biofabrication process difficult. For this reason, using derivatives or blends with different polymers is usually required to obtain appropriate mechanical properties for their use. For example, gelatin was modified with methacrylamide to obtain a photopolymerizable biomaterial that can be used for 3D bioprinting and microfluidics (Aldana et al. 2021; Seeto et al. 2019). Actual biomedical challenges require using complex polymer matrixes that mimic the native ECM and regenerate the lost or damaged tissues (Fabbri et al. 2017; Lee et al. 2008). Recent advances in biofabrication techniques allow the production of a polymer matrix with biophysical and structural properties similar to the ECM, and its combination with different cell lines can proliferate and differentiate into the desired tissue. Moreover, the incorporation of different growth factors or other biomolecules can improve the migration, growth, and differentiation of the cells (Nii et al. 2020; Oliveira et al. 2021). In this context, the recent book chapter will provide an in-depth information of various polymers, including natural and synthetic polymers and nanorobot constructs such as dendrimers, micelles, and conjugates, and their application in theranostics.

5.2 Polymers

In theranostics, several polymers have been utilized to coat inorganic particles to increase their properties, inhibit removal, and minimize toxicity. They can also be used as a base for adding fluorescent chemicals and medications (Zhu et al. 2019). The origin of polymers determines whether they are synthetic or natural. Biodegradable polymers can be broken down enzymatically, non-enzymatically, or both to yield biocompatible, non-toxic by-products that normal metabolic processes can remove. These materials are in great demand in biological applications, such as theranostics. Polymers can be classified based on (1) natural polymers which are originated from plants, animals, and microbes (e.g., nanocellulose, chitosan, alginate, gelatin, silk fibroin) (Vasile et al. 2020) and (2) synthetic polymers which are synthesized (e.g., PCL, PLGA, PVA, PLA, PGA) (Donnalaja et al. 2020).

5.2.1 Natural Polymers

5.2.1.1 Alginate

Alginate is a biopolymer made from many types of microalgae (seaweeds) that grows naturally in numerous coastal places worldwide. Compared to other red or green microalgae, brown seaweed has a large quantity of alginic acid in its cell wall, which is salt insoluble. Several techniques may be used to extract alginate from microalgae in the form of water-soluble alginate, which can then be used in advanced applications. The rheological features of water-soluble alginate (sodium alginate) include gelling, viscosity, and dispersion stability. Alginate is a linear anionic polysaccharide polymer of β -(1-4)-D-mannuronic (M-blocks) and α -L-guluronic acid (G-blocks) (Coleman et al. 2011). The quality of alginate is largely determined by the algae species from which it is derived. This hydrophilic biopolymer is non-toxic, biocompatible, biodegradable, and biostable. These exceptional qualities make them ideal for theranostics and biological applications in polymers. Electrostatic, ionic interactions, covalent bonding, redox reactions, and coordination are easy ways for alginate to connect with metal ions. It is also easily compatible with human tissue. It is utilized as a carrier for drug administration and bioimaging within animals in many forms, such as films, gels, foams, hydrogels, nanofibers, microcapsules, tablets, and nanoparticles (Ahmad Raus et al. 2021; Gheorghita Puscaselu et al. 2020). Figure 5.3 presents the extraction and various applications of alginate.

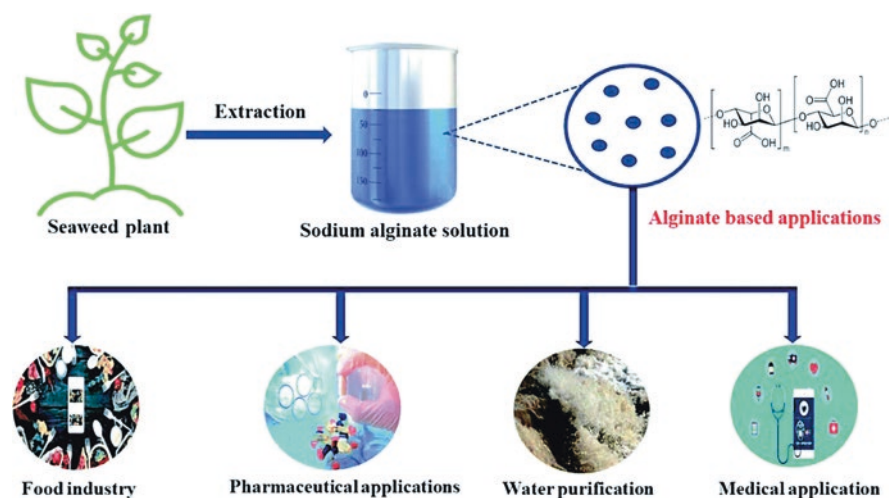


Fig. 5.3 Alginate extraction and its application in diverse fields. (Eltaweil et al. 2022)

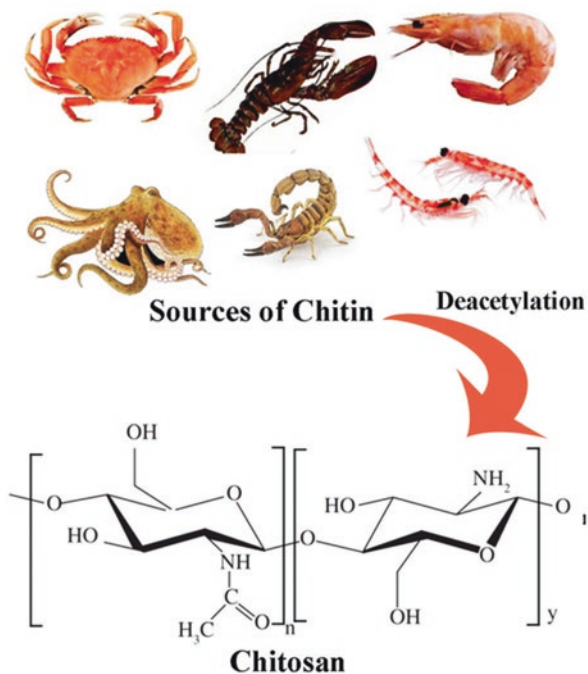
5.2.1.2 Collagen

Collagen fibrils and their combinations form the extracellular matrix (ECM) for hardest and soft tissues, including bone, cartilage, nerve, skin, blood vessels, and tendons in the human body. Collagen exhibits many morphologies in various tissues and is essential for preserving the structural and biological integrity of the ECM architecture. Furthermore, it is extremely dynamic and constantly remodels for appropriate physiological functioning (Sell et al. 2010). There are 28 types of collagen identified to date. Collagen types I, II, III, and V are the primary categories that organize an essential part of collagen in the bone, cartilage, skin, muscle, and tendon. Each type of collagen differs from the other and has its individuality. However, although having a similar triple helical structure, these molecules can be distinguished from one another by the presence of 4-hydroxyproline (Franceschi et al. 1994; Palsson and Bhatia 2004). Collagen type I is found in the bone, skin, dentin, cornea, blood vessels, fibrocartilage, and tendon. It is composed of two $\alpha 1$ chains and one $\alpha 2$ chain forming fibrils of 50 nm in diameter, whereas type II collagen, found in cartilaginous tissues, is composed of three identical $\alpha 1(\text{II})$ chains forming fibrils less than 80 nm in diameter. It is correlated with water, proteoglycans, glycoproteins, and noncollagenous proteins. Our skin, ligaments, blood vessels, and internal organs all contain type III collagen, which is made up of three $\alpha 1(\text{III})$ chains and forms fibrils with a diameter of 30 to 130 nm (Boland et al. 2004; Kumbar et al. 2008). Type IV collagen is composed of $\alpha 1(\text{IV})$ and $\alpha 2(\text{IV})$ chains and is the major skeletal macromolecule of basement membrane in various tissues. The molecular organization of type V collagen, in terms of $\alpha 1(\text{V})$, $\alpha 2(\text{V})$, and $\alpha 3(\text{V})$ chain compositions, remains to be unidentified. However, type V collagen has been well known in many tissues, including the blood vessel walls, synovium, corneal stroma, tendon, lung, bone, cartilage, and skeletal muscle (Lin et al. 2019). Apart from the fact that it is widely distributed naturally in the body, collagen possesses a number of qualities that make it a desirable biomaterial for use in biomedical engineering. These properties include low antigenicity, low inflammatory and cytotoxic responses, biodegradability, high water affinity, and good biocompatibility.

5.2.1.3 Chitosan

Chitosan is the second most abundant natural polymer, produced from the deacetylation of chitin (Fig. 5.4). Chitin is mainly present in fungi and the exoskeleton of crabs, lobster, and shrimps. However, chitosan was also isolated from insects in recent years (Saenz-Mendoza et al. 2020). It is the major part of seafood waste (Yadav et al. 2019). Chitosan is composed of D-glucosamine and, in lower proportion, with N-acetyl-D-glucosamine units randomly connected by β -(1-4)-glycosidic bond linkage. Chitosan can be obtained by two methods: chemical and biological. The chemical method is the most common method on an industrial scale. Strong acid and alkaline treatments are used to obtain chitosan. Biological method involves microbes and enzymes (Pacheco et al. 2011). Jang et al. proposed a new in situ

Fig. 5.4 Fabrication of chitosan from different sources of chitin. (Mallakpour et al. 2021)



crosslinking methodology for fabricating microgels by merging two droplets of different viscosities in an asymmetric cross-junction microfluidic device (Jang et al. 2018). Thus, oxidized dextran and N-carboxymethyl chitosan were mixed with an in situ crosslinking via a Schiff base reaction, resulting in microgel formation. This asymmetric cross-junction geometry was an interesting approach to overcoming the high surface tension of microdroplets of contrasting viscosities, which usually requires significant surfactant concentrations. In addition, the crosslinking methodology allowed the encapsulation of NIH-3 T3 fibroblasts, which showed high viability after 2 days of culture, demonstrating the biocompatibility of the entire process. Mora-Boza et al. reported the fabrication of human mesenchymal stem cell (hMSC)-laden microgels, applying also an in situ crosslinking approach for chitosan lactate, a water-soluble chitosan derivative (Mora-Boza et al. 2021). The ionic gelation was based on a combination of glycerylphosphate (G1Phy) and tripolyphosphate as ionic crosslinkers, obtaining polymeric microgels with homogeneous size distribution between 104 and 127 μm . The authors demonstrated that the presence of G1Phy, which has been recognized as a potent antioxidant and bioactive compound, supported encapsulated hMSC viability over time and modulated hMSC's secretome under adverse conditions, resulting in an appealing cell delivery platform for hMSC's therapy applications.

5.2.1.4 Gelatin

Gelatin is a collagen derivative with great biodegradability and biocompatibility but low mechanical strength (Bello et al. 2020). Nosoudi et al. have demonstrated the successful production of cell-laden nanofibers using a gelatin/pullulan blend (Nosoudi et al. 2020). In this work, the electrospinning ability of gelatin is enhanced by the presence of pullulan, which increases the tensile strength of the blend. An 8 kV voltage and a concentration of 5 mg/mL gelatin/pullulan were used during the process, and adipose-derived stem cells (ADSCs) encapsulated within the fibers presented a 90% viability. This work offers a new area to be studied, since the use of gelatin for CE has been restricted until now by its mechanical properties. Gelatin polymer is a biodegradable and biocompatible material that consists of 85–92% of proteins, mineral salts, and water (Tomić et al. 2021). The triple helical structure of collagen is often irreversibly hydrolyzed to form gelatin through the use of heat and enzymatic denaturation, which results in random coils of collagen. As a result, gelatin and collagen share a similar molecular structure (Fig. 5.5). Gelatin can replace and perform similar biomaterial functions as collagen for cellular development *in vitro*. Gelatin is commercially accessible and can be derived from a variety of sources, including fish, pig skins, cattle bones, and some insects (Noor et al. 2021). Numerous investigations into the biocompatibility of gelatin generated from different sources have demonstrated. The results showed that gelatin does not cause cytotoxicity, antigenicity, or other negative effects in human cells. Gelatin does, however, have significant drawbacks. The fundamental disadvantage of utilizing gelatin is that it lacks thermal stability, has weak mechanical properties, and degrades

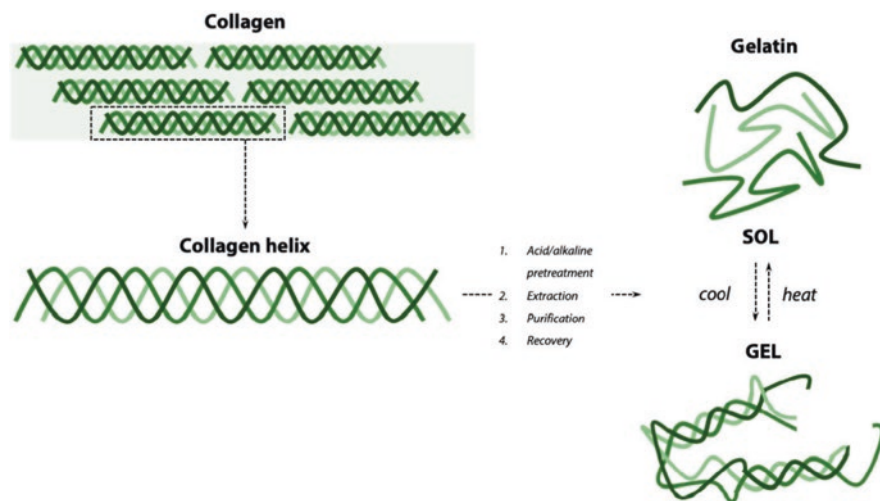


Fig. 5.5 Gelatin obtained through irreversible denaturation of collagen through various treatments. These processes produce linear peptides that can be reassembled in various forms (nanofibers, nanoparticles, microparticles, hydrogels). (Campiglio et al. 2019)

significantly more quickly than other materials (Xing et al. 2014). Gelatin is also much more protease-sensitive than collagen, which could result in quicker breakdown (Bello et al. 2020). However, by altering gelatin and creating gelatin composites, one can easily get around these drawbacks and boost the material's mechanical stability, biocompatibility, and bioactivity.

5.2.1.5 Hyaluronic Acid (HA)

HA or hyaluronan is an anionic, nonsulfated glycosaminoglycan distributed widely in epithelial, connective, and neural tissues. It possesses low toxicity and has been widely utilized in pharmaceutical technology. Derivative forms of HA or its salts are frequently used compared to the pure form of HA to fabricate nanoplatfoms (Siafaka et al. 2021). Zhang et al. performed research by using gadolinium-modified mesoporous silica (GD-MS) as an MRI agent (Li et al. 2022). HA has many biomedical uses, including bone repair, and was first isolated from the vitreous humor of cows. Additionally, it has qualities including flexibility, biocompatibility, antibacterial, and osteoinductive effects (Zhai et al. 2020; Meyer and Palmer 1934). HA participates in important cell signaling pathways and affects cell growth and differentiation (Huang et al. 2003a). CD44 is the receptor of HA, which is found to be overexpressed on many cancer cells (Mattheolabakis et al. 2015). Hence, it is an interesting polymeric material for disease-targeted delivery of drugs or contract agents. Drugs, for example paclitaxel and methotrexate are conjugated to HA with the addition. The conjugate complex is self-assembled to micelles and releases the drug in acidic conditions (Abdullah Al et al. 2013; Goh et al. 2012). Near-infrared (NIR) dye or photosensitizers are also conjugated to HA for enhanced imaging signals to diagnose diseases such as cancer and diabetes (Dai et al. 2021). Various sources of HA and their applications are presented in Fig. 5.6.

5.2.2 Synthetic Biopolymer

5.2.2.1 Polycaprolactone (PCL)

PCL has known a massive rise mainly in the past decade, being immeasurably the most considered polymer in literature dealing with electrospinning. The superior viscoelastic properties of PCL facilitates the electrospinning process (Ghobeira et al. 2018). PCL is a low-cost, bioresorbable polymer with exceptional mechanical qualities, biocompatibility, and a gradual rate of decay (Prasad and Kandasubramanian 2019). Polycaprolactone is an aliphatic polyester composed of hexanoate repeat units. It is a semicrystalline polymer with a degree of crystallinity that can reach 69% (Mark 1999). The molecular weight and degree of crystallinity of PCL affect its physical, mechanical, and thermal properties. PCL is somewhat soluble in acetone, 2-butanone, ethyl acetate, dimethylformamide, and acetonitrile. It is soluble in

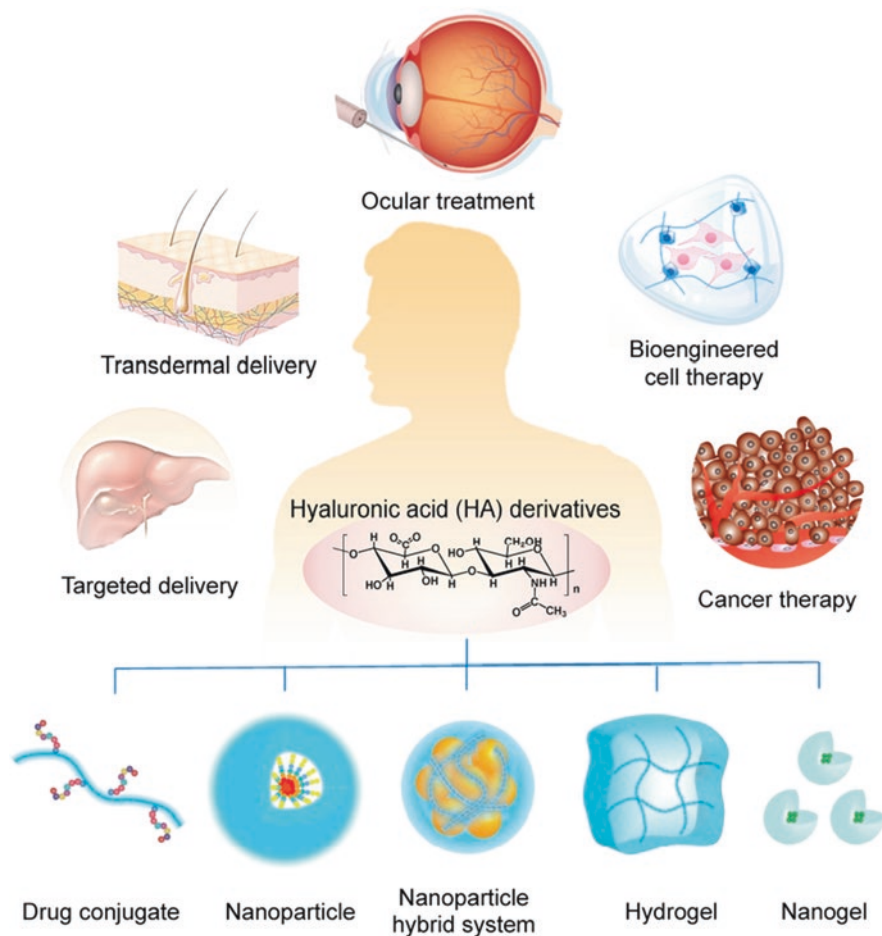


Fig. 5.6 Illustration in schematic form of numerous therapeutic uses of HA-based medications in the form of chemical and biological conjugates, nanoparticles, hybrid systems of nanoparticles, hydrogels, and nanogels. (Kim et al. 2019)

chloroform, dichloromethane, carbon tetrachloride, benzene, toluene, and cyclohexanone and insoluble in alcohols, petroleum ether, and water (Sinha et al. 2004). Depending on the molecular weight, degree of crystallinity, and conditions of breakdown, PCL biodegrades in a few months to a few years. PCL can be totally biodegraded by a variety of natural microorganisms. PCL has a variety of applications, including scaffolds in tissue engineering (Siddiqui et al. 2018), sustained drug delivery systems (Dash and Konkimalla 2012), and packaging (Diken et al. 2022). Its wide applicability and interesting properties such as controlled degradability, miscibility with other polymers, and biocompatibility make PCL a very useful polymer.

5.2.2.2 Poly(D,L-Lactic-co-Glycolic Acid) (PLGA)

PGA and PLA combine to form PLGA. Asymmetric α -carbons found in PLA are frequently referred to as the D or L forms in classical stereochemistry and, on occasion, as the R and S forms (Makadia and Siegel 2011). Poly-L-lactic acid (PLLA) and poly-D-lactic acid (PDLA) are the enantiomeric variants of the PLA polymer (PLLA). The term “PLGA” stands for poly(D,L-lactic-co-glycolic acid), where the amounts of D- and L-lactic acid are equal. The biocompatibility and advantageous mechanical features of PLGA are well known (Huang et al. 2003b). The drawbacks of both PLA and PGA can be overcome by PLGA. By altering the ratio of homopolymers, the copolymerization of PLA and PGA corrects the issues with premature degradation and gives some control over the rates of deterioration. PLGA known to be amorphous and hydrolytically unstable, disintegrating more quickly, contains 75% PGA. Lactic acid and glycolic acid, two common by-products of human metabolism that can be eliminated by urine, are formed as PLGA degrades (Meyer et al. 2012). In addition to medication administration, where it is most commonly utilized, PLGA systems are also used in the regeneration of bone, skin, cartilage, and nerves (Martins et al. 2018).

5.2.2.3 Polyethylene Glycol

PEG is a family of amphiphilic polymers with the same skeleton of repeating ethylene glycol units but with different molecular weights (Lin et al. 2014). The applications of PEG and its derivatives (Fig. 5.7a) are remarkably extensive, ranging from innovative biology, pharmacology, and material science researchers to the massive products of medical supplies and cosmetics. For instance, the derivatives of linear PEG broke through the limitations and expanded the category of its

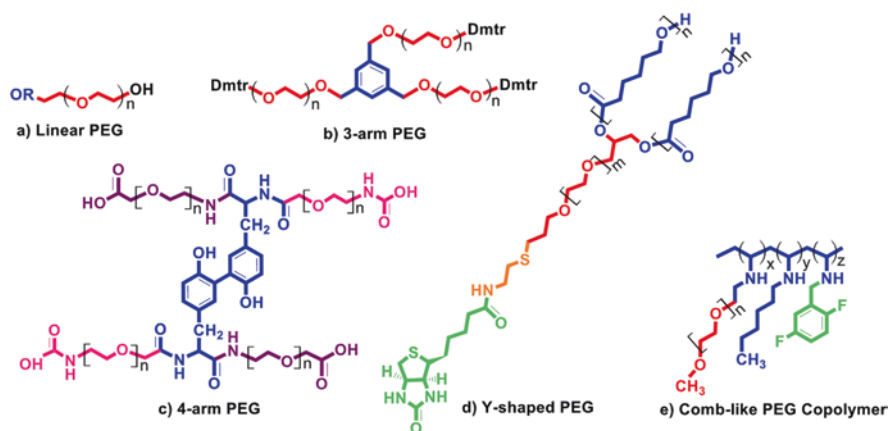


Fig. 5.7 Schematic of PEG derivatives with different structures. (Wang et al. 2019)

functionalization, even if these procedures may cause synthetic challenges (Li et al. 2013). These modified linear PEG chains could form amphiphilic copolymeric chains and other polymers to construct novel DDSs like polymeric micelles (Brandt et al. 2019). Branched PEG structures can shelter peptides or other macromolecules that are vulnerable to proteolysis and reduce immunogenicity like an “umbrella-like” structure (Fig. 5.7b) (Veronese 2001). Multiarmed PEG blocks could function as the polymeric skeleton to build crosslinked networks such as hydrogels. At the same time, comb-like PEGylated copolymers were reported to enable the optimization of gas separation performance (Fig. 5.7c) (Wennink et al. 2013; Yu et al. 2021).

PEG is the most frequently used hydrophilic moiety in biomedical applications. PEG coating or PEGylation method onto various macromolecules is a common approach aiming to improve the blood circulation of drug-loaded nanoparticles. Moreover, PEGylation can reduce the toxicity of nanosystem-enhanced drug protection from degradation and numerous other properties (Siafaka et al. 2016). An amphiphilic semiconducting polymer based on PEG-grafted poly(cyclopentadithiophene-alt-benzothiadiazole) (PEG-PCB) was developed by Jiang et al. The nanoplatforms can be a diagnostic component for NIR fluorescence and photoacoustic imaging as well as a therapeutic agent for photothermal cancer therapy (Jiang et al. 2017).

5.3 Fabrication of Theranostic Nanorobots

5.3.1 Magnetic Nanoparticle-Based Theranostics

Iron-based metal oxide magnetic nanocrystals are synthesized by thermal decomposition of metal-organic precursors. They are good magnetic resonance signal enhancers and can follow cell migration, evaluate tumor response to treatment regimens, and diagnose disease at its early stages (Lee et al. 2007; Song et al. 2005; Sun and Zeng 2002). Their composition, magnetism, size, and crystallinity may all be controlled rather easily (Kim et al. 2008; Lee and Hyeon 2012) compared to previously employed iron oxides. Previously, iron oxides were formed by a coprecipitation method, which does not define nanocrystalline size, stoichiometry, and magnetism of materials. These factors are known to impact the sensitivity of the magnetic resonance signal. Because their intravenously injected nanocrystals have a propensity to aggregate and obstruct blood arteries or induce nonspecific accumulation in organs other than the target, magnetic nanocrystals coated with hydrophobic surfactants are not suitable for direct use in biomedical applications. Many efforts have been made to improve colloidal stability in order to prevent the agglomeration of nanoparticles. One such instance is encapsulation using amphiphilic copolymers (Sulttan and Rohani 2022). Interestingly, magnetic clusters with colloidal stability in which the number of magnetic nanocrystals is trapped inside the polymeric shell could significantly increase the magnetic resonance signals (Xiao

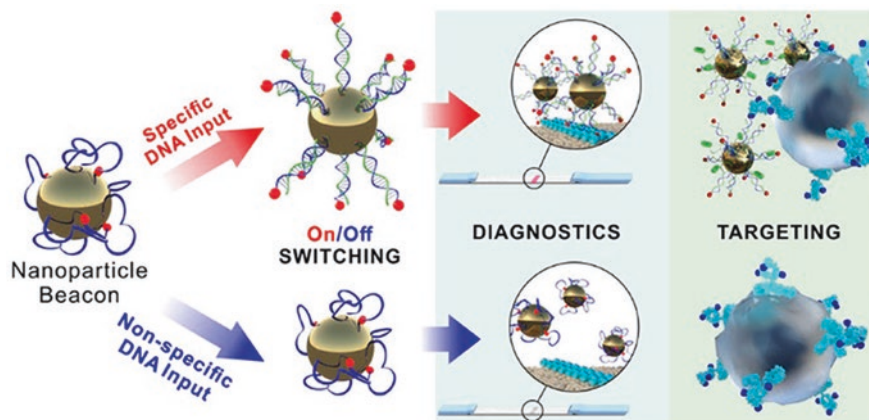


Fig. 5.8 Schematic representation of nanoparticle beacon action showing diagnosis and targeting for therapy. (Cherkasov et al. 2020)

et al. 2022). In addition, molecular probes based on magnetic nanocrystals with high magnetism values exhibit great sensitivity for cancer detection, enabling the in vivo imaging of small tumors (He et al. 2022; Chen et al. 2022; Song et al. 2022). Hyeon et al. developed magnetosome-like ferromagnetic iron oxide nanocubes as an MRI T2 agent (Huang et al. 2010). Magnetic nanoparticles also attract considerable interest due to their ability to mediate heat induction. However, conventional approaches to altering the size and composition of nanoparticles had marginal effects on boosting the magnetic heating power.

As earlier discussed, theranostics is a combination of a single design that should have the capacity to absorb and release a drug, imaging properties, and some enhancing actions (Fig. 5.8). Nanorobots with polymer and magnetic nanoparticles provide an efficient platform where polymer acts as a drug reservoir and a platform for additional functionalization (for cell targeting or imaging). In contrast, magnetic nanoparticles allow for MRI, MPI, and hyperthermia. These are the common treatments for cancer that can be combined with drug action. The major design strategies for fabricating polymer magnetic nanorobots are threefold, focusing on (1) magnetic nanoparticles with an enhanced magnetic response, (2) a combination of magnetic and AuNPs, and (3) sophisticated engineering solutions for the fabrication of shells/containers.

5.3.2 Micelles

Polymeric micelles are self-assembling nano-constructs of amphiphilic copolymers with a core-shell structure widely used for bioimaging and drug delivery. These structures are generally constructed to be 10–100 nm in size, composed of a

hydrophilic shell and hydrophobic core. Polymeric micelles provide a good platform for theranostics consisting of therapeutic agents inside the core and diagnosis agents on the surface to detect the disease (Zhang and Mi 2019). The shell protects the drug inside the core from degradation by enzymes. Targeting moieties such as growth factors, antibodies, aptamer, sugar, and phenylboronic acid are decorated on the surface of the shell to interact with receptors highly expressed on diseased cells to increase the targeting ability. The polymeric micelles are stable in blood circulation, enabling drug delivery to target cells through enhanced permeability and retention effect. The targeting moieties of micelles can specifically interact with epitopes overexpressed on diseased cells to increase the diagnostic selectivity and breakdown therapeutic limitations, which could also reduce their distribution in normal regions. For cancer diagnosis, image-guided therapy, tracking polymeric micelles in the body, and tracking the therapeutic effects, polymeric micelles having theranostic properties may be used. The schematic structure of polymeric micelle is given in Fig. 5.9 with the example of the process of cancer theranostics.

A novel solution to various drug administration problems, including limited water solubility and poor drug permeability through biological barriers, is represented by polymeric micelles (Ghezzi et al. 2021). Compared to other nanorobots, polymeric micelles generally display smaller sizes, easier preparation and sterilization processes, and good solubility properties; unfortunately, they are associated with lower stability in biological fluids and a more complicated characterization. Micelles below a specific concentration, called critical micellar concentration, are present in solution as single molecules. In contrast, they self-assemble into micelles presenting an internal hydrophobic core and hydrophilic shell at a concentration above the critical micellar concentration.

5.3.3 Dendrimers

Dendrimers are highly branched spherical-structured synthetic macromolecules. They have repeated branches of a dendron around a central core, resulting in a near-perfect 3D geometrical shape as shown in Fig. 5.10. The generation can control the size and molecular weight of the dendrimer. They have found applications in material science as sensors, nanoreactors, and green catalyst supports. The most promising application of dendrimers is in biomaterials, where they have emerged as competitive candidates for drug delivery applications. Previously, dendrimers were synthesized from AB_x monomers, resulting in symmetrical dendritic structures that cannot be employed easily in complex applications such as theranostics and drug delivery. For example, materials for theranostics need higher structural complexity because multiple functionalities for solubility, targeting, imaging, and drug delivery are required. The multifunctionalization of dendrimers is crucial for constructing dendrimer-based drug delivery systems. The inner area of the dendrimer is available for the encapsulation of drug molecules. In contrast, the outer functional groups are available for modifying drug molecules through covalent bonds and for complex

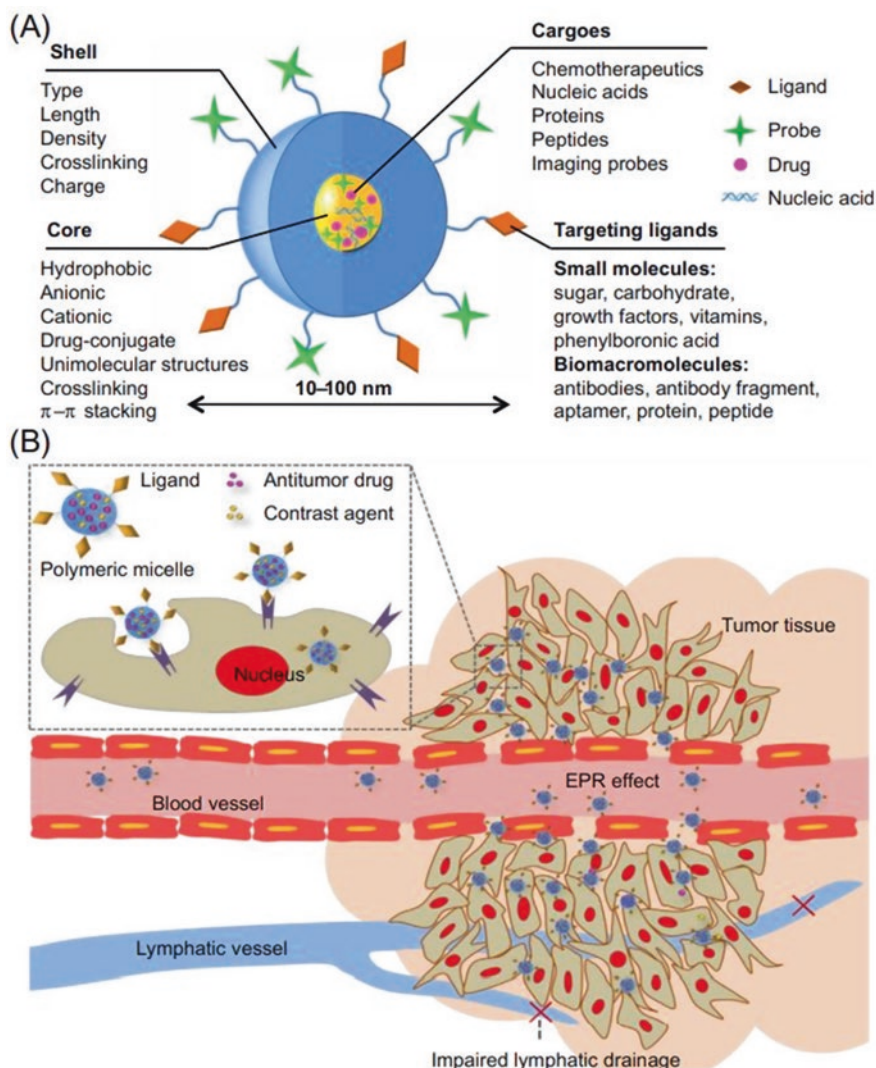


Fig. 5.9 Polymeric micelles for cancer theranostics. (a) Elements found in polymeric micelles. (b) Polymeric micelles target cancer theranostics at tumor tissues. Through the EPR effect, the polymeric micelles might be precisely collected in tumor tissues for cancer diagnosis and treatment. Enhanced permeability and retention or EPR. (Zhang and Mi 2019)

formation. Dendrimers for diagnosis purposes and drug delivery applications are also developed. Various dendrimers have been fabricated to carry a variety of therapeutic drugs with the aim of maximum therapeutic efficacy in cancer treatment. The common anticancer drugs, including doxorubicin, paclitaxel, cisplatin, camptothecin, and methotrexate, have been formulated in dendrimers as drug carriers. Various properties such as biocompatibility can be added to dendrimer-based nanorobots by

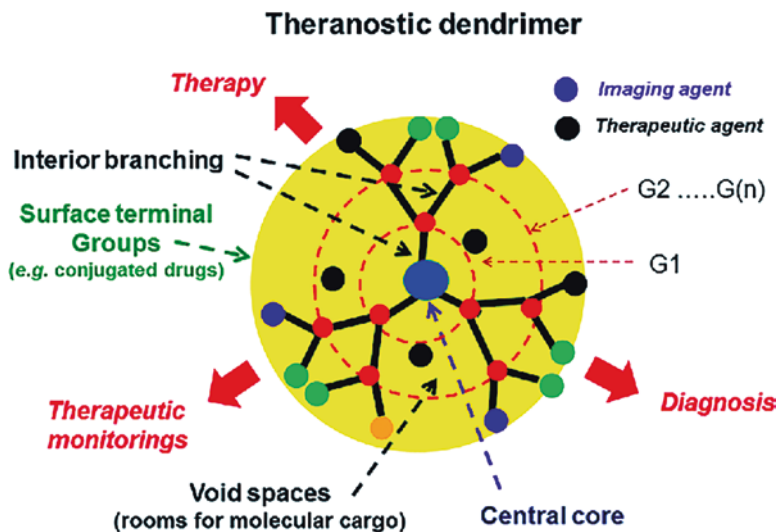


Fig. 5.10 Schematic presentation of dendrimer strategy for application in theranostics. (Mignani et al. 2018)

choosing proper chemical structures and desired functionalization at the periphery. Dendrimers also benefit by facilitating therapeutic transport across various cell membranes or biological barriers via an endocytosis-mediated cellular internalization. Additionally, sustainable and controlled drug release can be achieved by incorporating stimuli-responsive moieties to the dendrimer, which allows administration of lower doses to decrease toxicity against healthy cells. The advantages of dendrimers as nanorobots are their well-defined structures and multifunctionality. This property is of benefit for chemical and biological reproducibility. Dendrimers have been recognized as the most versatile compositionally and structurally controlled nanoscale devices for nanomedicine. Dendrimer nanodevices have often been employed as theranostic platforms and range in size from 10 to 100 nm. The ability to target ligands and imaging agents to a single dendrimer molecule chemically or by a mix of conjugation, encapsulation, and complexation allows dendrimers to carry a high payload of pharmaceuticals and other bioactive compounds. Dendrimers are suitable as nanoplatforms for theranostic devices because of their characteristics.

5.3.4 Nanogels

Nanogels are three-dimensional hydrogel materials in the nanoscale range formed by crosslinked swellable polymer networks with high water-holding capacity without actually dissolving into the aqueous medium. Nanogels are formed by

crosslinked polymer networks with high retention capacity contained within a nanoscale particle and have been employed for controlled release (Parisi et al. 2016). Nanogels can be synthesized via direct polymerization of monomers by heterogeneous free radical polymerization or by hydrophilic copolymers, which carry reactive functional groups with suitable crosslinkers (Chacko et al. 2012; Chambre et al. 2018). The degree of crosslinking can be controlled using surfactants; however, these molecules must be completely removed from the final product due to cytotoxicity concerns. As an alternative to surfactant, the development of click chemistry has proven successful through routes such as azide-alkyne reactions and nucleophilic and radical thiol-ene reactions for producing crosslinked gels (Sepideh and Hamed 2017).

Nanogels are extensively used for drug delivery, tissue engineering, regenerative medicine, bioimaging, biosensors, and wound healing (Sagar et al. 2018; Vashist et al. 2014). Nanogels also found applications in theranostics (Wang et al. 2022). A theranostics nanogel system is comprised of an imaging component, a therapeutic agent, and a targeting ligand. The therapeutic agents are incorporated within the core of nanogel by physical entrapment or chemical conjugation methods (Sindhu et al. 2022). Usually, the diagnostic agents and targeting ligands will be conjugated in the outer corona of a theranostics nanogel. The therapeutic agents loaded inside the nanogels are mainly drugs, genes, or photosensitizers, which, when judiciously delivered with the help of nanogels, exert their therapeutic response on infected cells without affecting the normal cells (Sabir et al. 2019; Debele et al. 2016). Schematic illustration of multifunctionalization of nanogels is shown in Fig. 5.11.

One of the major challenges faced by the theranostics nanogels is the premature leakage of the imaging agent before reaching the target destination. This leads to nonspecific tissue distribution and generates potential toxicity and false results (Li et al. 2019). Therefore, nanogels with innate imaging potential are safer than external imaging agents.

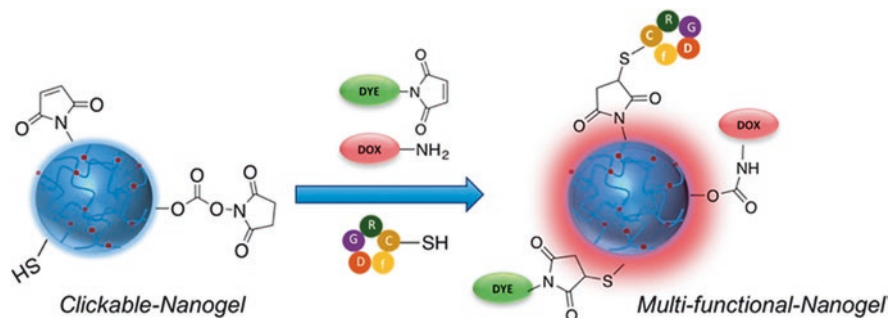


Fig. 5.11 Schematic illustration of multifunctionalization of nanogels. (Chambre et al. 2018)

5.3.5 *Hybrid Conjugates*

The main goal of using polymers in conjugates to produce hybrid materials for theranostics applications lies in stabilizing and improving the therapeutic activity of standalone drugs and bioimaging because there is an urgent demand for the development of effective carrier systems. Combining two or more materials can alter their individual properties and create hybrid materials with new and unique features. Synergistic and hybrid properties derive from the extremely high superficial surface area among the phases, in which the physical and chemical properties of polymers can be transmitted to inorganic materials (or biological polymers); consequently, they can change biodistribution and solubility and improve the system stability.

Attaching synthetic polymers at an atomic level, rather than blending them, is a significant breakthrough in polymer science since it combines the advantageous properties of both polymers without inconveniences such as the separation phase, which is seen when natural polymers get blended. This process has a multifold set of advantages, but its main focus lies on increasing conjugate's solubility and/or stability and, consequently, on decreasing the toxicity of the system (Jiang et al. 2016; Uzunalli and Guler 2020). More specifically, the delivery of cytotoxic drugs, such as antitumor agents, requires advanced therapeutic strategies because, nowadays, these drugs are based on conventional systemic biodistribution and present low specificity and selectivity (Mohammed et al. 2016). For example, although metals have favorable magnetic properties, their high toxicity profile makes them unsuitable for biomedical use without proper and stable surface treatment (Hajba and Guttman 2016). On the other hand, although proteins present high activity and specificity, they have some limitations, such as inherent protein biorecognition and consequently short half-life, poor stability, low solubility, and immunogenicity.

Surface conjugation of polymers in proteins has rectified these shortcomings since protein-polymer conjugates have improved their physical stability, increased their half-life, and made them non-immunogenic. Furthermore, these conjugates show a unique combination of properties derived from biologic and synthetic materials that can be individually used to elicit the desired effect (Pelegri-O'Day et al. 2014). Different synthetic pathways can be used to generate hybrid material; however, the current study focused on the synthesis of hybrid nanoparticles based on the living radical polymerization technique, the so-called reversible-deactivation radical polymerization (RDRP), with emphasis on conjugates enabled through the "grafting-from" approach.

In the synthesis of organic-inorganic hybrid materials, organic polymers are covalently linked to the surface of inorganic precursors such as magnetic nanoparticles (Tian et al. 2018), silica (Xu et al. 2017), and metal-organic frameworks (MOFs) (Yang et al. 2009). The grafting-from method uses polymerization initiators connected by a covalent bond to the surface of the substrate to form polymer chains on organic or inorganic surfaces. This method can be applied to the surface

of several geometric forms, such as nanoparticles and porous materials (e.g., silica), metals, metal oxides, and natural compounds. Additionally, it enables the production of hybrid materials with high grafting density (Flejszar and Chmielarz 2019).

Advances in polymer synthesis have been made possible by the synthesis of macromolecules with controlled sequences and configurations, particularly through the use of reversible-deactivation radical polymerization (RDRP) techniques like atom transfer radical polymerization (ATRP) and reversible addition-fragmentation chain transfer (RAFT). These methods allow for precise and repeatable control of the chain length, the monomer composition, and, to some extent, the monomer sequence (Russell et al. 2018). RDRP techniques are efficient in forming conjugates on organic surfaces such as natural polymers and inorganic surfaces such as silica, iron oxide, and carbon nanotubes.

The development of RDRP techniques has expanded the versatility in synthesizing new hybrid conjugates. Their basic principle is introducing an anchoring layer in a given substrate (organic or inorganic), enabling polymers for grafting-to, grafting-from, or grafting through the substrate. Grafting-from approach is the most efficient and promising strategy (Tebaldi et al. 2017).

5.4 Bioconjugation Process

Bioconjugation is the process of covalently attaching polymers to biomolecules such as proteins, nucleic acids, enzymes, cells, and carbohydrates, which results in hybrid materials that allow nanorobots to interact specifically with biological systems. Covalent binding, nanoextraction, adsorption, electrostatic contact, and non-covalent binding are all strategies used in the bioconjugation of nanorobots. Thiol groups, primary amines, a carboxylic acid, maleimide, and aldehyde groups form covalent bonds. The nanoextraction procedure takes place in the liquid phase, where pharmaceuticals should have a low affinity for solvents but a high affinity for nanocarriers (Yudasaka et al. 2003). Drug molecules travel across a thin layer of a solvent and become adsorbed in the most active centers during the nanoextraction process. Physical adsorption and electrostatic interactions can cause drug agents to collect on the exterior surface of nanocarriers (Lai et al. 2007). Biological conjugation procedures employ a variety of attachment methods, such as (i) direct metal-sulfur or disulfide connections, (ii) functional group crosslinking, (iii) antibody linkers, (iv) streptavidin-biotin, and (v) DNA complementary base pairing (Hermanson 2013). An investigation found that the connection of aniline-functionalized gold nanoparticles (AuNPs) to oligonucleotides, peptides, and proteins demands the oxidative coupling reaction, which is coordinated by potassium ferricyanide (Capehart et al. 2014). According to Politi et al. (Politi et al. 2016), AuNPs are bioconjugated by a ligand exchange in which the surface of AuNPs is

switched with the thiolated peptide. To identify early 6 (E6) oncoproteins in cervical cancer progression, gold nanoparticles with horseradish peroxidase are physically adsorbed with the early 6 antibodies (CIP5) of human papilloma virus 16/18 (Mwai et al. 2020). In another study, the iron oxide particle on the surface was covalently bonded to polyethylene glycol-based ligands via a siloxane group, increasing the colloidal stability of the nanoparticles. An ELISA technique was used to measure the ability of antibody to attach to the surface while simultaneously targeting the plasminogen activator inhibitor-1 (Bloemen et al. 2014). Assembling various organic and inorganic ligands in a nanoscale range via covalent bonds, hydrogen bonds, electrostatic force, etc. is known as surface functionalization of nanomaterials. PEG, hyaluronic acid, polyvinyl alcohol, and other substances are frequently utilized for surface functionalization (Abd Ellah and Abouelmagd 2017).

5.5 Application in Theranostics

5.5.1 Cancer Diagnosis and Therapy

Cancer is currently the second most significant threat to human lives globally. Many effective diagnostic tools and therapies are in clinical trials to achieve a solution to it. Several nanomaterials, including mesoporous silica, metal nanoparticles,

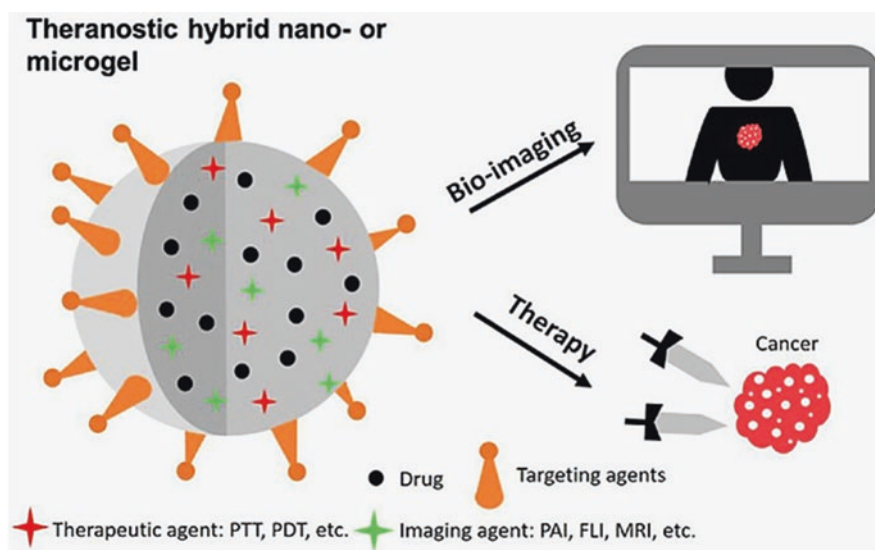


Fig. 5.12 Illustration of theranostics agent based on hybrid microgel encapsulating imaging therapeutic agents for cancer diagnosis and therapy. *FLI* fluorescence imaging, *MRI* magnetic resonance imaging, *PAI* photoacoustic imaging, *PDT* photodynamic therapy, *PTT* photothermal therapy. (Xiao et al. 2021)

carbon-based materials, organic micelles, and liposomes, have been developed for cancer theranostics (Singh et al. 2021). An illustration for cancer theranostics is presented in Fig. 5.12. Targeting the tumor microenvironment is a promising strategy for theranostics of cancer. The tumor microenvironment is composed of cancer cells, stromal cells, immune cells, and extracellular matrices, which help for tumor growth and progression. The tumor microenvironment differs from normal cells by having mildly acidic pH, hypoxia, a high level of reactive oxygen species, and over-expression of specific enzymes. These factors can be considered stimuli to induce specific changes in the nanocarrier structures and hence facilitate specific diagnosis, targeted drug delivery, and immediate treatment (Park et al. 2021). Bioimaging of tumors is possible by high-resolution modalities such as computed tomography (CT), magnetic resonance imaging (MRI), positron emission tomography (PET), and single-photon emission computed tomography (SPECT) (Zhang et al. 2020). Existing diagnosis tools have a few limitations, such as inability to diagnose deep or detect small clusters. Therefore, the techniques fail to identify circulating invasive cell clusters at distant sites for secondary colonization and tumor formation (Dotse et al. 2022). Therefore, assuming that the tumor has been completely removed, conventional treatments are supposedly maintained. Unfortunately, this results in either excessive drug exposure or tumor recurrence due to insufficient cancer cell clearance. Non-invasive imaging modalities can be used to image small cell clusters, which is essential for diagnosis and successful treatment protocols. Target specificity and on-demand drug release are critical aspects for successful theranostics to obtain diagnosis and therapy against the primary and metastatic progression of tumor. They could eventually avoid the routine side effects associated with cytotoxic drugs. Nanorobots with diverse functions such as targeting, imaging, and therapeutics are being developed based on nanotheranostics (Thorat et al. 2019). Integrating imaging modality within the therapeutic entity would be a promising approach to overcoming the limitations of conventional treatments. Nanohybrids integrate organic and inorganic moieties in a single entity presenting synergistic properties of the constituents and new prospects for clinics.

Photoacoustic imaging (PAI) is an emerging non-invasive and inexpensive bioimaging modality for cancer theranostics. PAI is a hybrid imaging technique based on the photoacoustic effect, which combines optical excitation and ultrasound detection. Endogenous absorbing molecules, such as oxy- and deoxyhemoglobin and melanin, have been efficiently used to visualize vessel structures, quantify blood oxygenation, and detect melanoma (Schwarz et al. 2016; Stoffels et al. 2015). However, only a few types of endogenous biomolecules can be exploited for intrinsic PAI, limiting its range of applications. Many efforts have been devoted to overcoming these barriers and boosting PAI specificity by developing exogenous contrast agents. These materials, usually based on NIR absorbing dyes or nanomaterials, can extend the application of PAI in cancer theranostics. For example, metallic, carbon, or semiconducting polymer nanoparticles and molecular dyes have been reported for in vivo PA tumor imaging (Yang et al. 2009). Ren et al. fabricated 2D germanium phosphide (GeP) nanosheets as a biodegradable multifunctional theranostics agent (Ren et al. 2022). The specific applications of material included

photothermal imaging, photoacoustic imaging, stimulative drug delivery, and chemo-photothermal combination therapy. Under 808 nm laser irradiation, the 2D GeP nanosheets have a superior photothermal conversion efficiency of 68.6%, which endows them with promise as high-performance NIR PTA for photoacoustic imaging and photothermal therapy.

5.5.2 Bacterial Infections and Wound Healing

Nanomaterials such as metal nanoparticles and polymeric nanoparticles have been extensively studied in the diagnosis and treatment of diseases that seriously threaten human life and health and are regarded to significantly improve the disadvantages of traditional diagnosis and treatment platforms, such as poor effectiveness, low sensitivity, weak security, and low economy (Zhu et al. 2021). Infectious diseases such as bacterial infection in wounds often delay healing and may seriously threaten human life. Developing wound dressings to detect and treat bacterial infections effectively is important. Nanoparticles have been extensively used in wound dressings because of their specific properties. Nanoparticles have been applied as intrinsic antibacterial agents or drug delivery to treat bacteria in wounds. Moreover, nanoparticles with photothermal or photodynamic properties have also been explored to endow wound dressings with significant optical properties to enhance their bactericidal effect further. More interestingly, nanoparticle-based smart dressings are being recently explored for bacteria detection and treatment, enabling an accurate assessment of bacterial infection and more precise control of on-demand therapy (Xu et al. 2020a). Polymeric nanorobots are widely used for bacteria-infected wound treatment. Polymer embedded with theranostics agents, including antimicrobial agents, growth factors, and nucleic acid, can be delivered to wound sites directly and subsequently released sustainably (Mofazzal Jahromi et al. 2018). A common method for supplying therapeutic chemicals and a moist environment for the treatment of bacteria and wound dressing is nanoparticle-based dressing. However, they are unable to release therapeutic molecules under very tight control, which could result in unwanted side effects and therapies. Additionally, they are unable to keep an eye on bacterial infections as the wound heals. Therefore, it is imperative to create intelligent wound dressing that can detect and cure bacterial infections. The bacteria-infected area differs from the normal cellular environment. Bacteria environment has a change in pH, temperature, enzymes secreted, and toxins present. For example, bacterial infection will cause an inflammatory response, during which the temperature at the wound site will be 1–2 °C higher than normal skin (Bowler et al. 2001). pH will increase during granulation and decrease to 4–6 during the normal healing process, while pH will be more alkaline during the impaired healing process (Jones et al. 2015). Drug-resistant bacteria often secrete specific enzymes, particularly β -lactamase, which are often recognized as drug-resistant bacterial markers (Bajaj et al. 2016). These functions of infections can be used for detection and further treatment. Nanorobots with thermoresponsive

hydrogels are promising candidates for delivering and releasing therapeutic agents precisely to wound sites because they can undergo phase transformations between solid and liquid states with changes in exterior temperature (Xu et al. 2020b).

5.6 Conclusion

In the last few years, the development of novel approaches centered on the discovery of biocompatible nanorobots has produced notable benefits in the biomedical area. These novel approaches are focused on manufacturing new nanorobots capable of accessing specific locations like tumor sites and simultaneously the treatment of disease. Nanorobots are dynamic constructs that perform their function inside the cells. These constructs are usually in the form of micelles, dendrimers, nanogels, and hybrid conjugates. There are three essential components to fabricate nanorobots. Nanorobots used for theranostics include a polymer material, detection probe, and therapeutic agent. Detection probes can be dyes, contrast agents, fluorescent agents, etc., which produce signals when they reach the target. Furthermore, a therapeutic agent is a drug or gene to treat the diseased area. There is still much to learn about the mechanism underlying how these nanorobots function today; thus, more research on this subject is required. Researchers will be able to create better nanohybrid systems because of the benefits afforded by the efficient conjugation of polymers over medications, dyes, and other biocompatible substances. Such hybrids will undoubtedly be able to provide a more efficient targeted distribution of anticancer medications, opening the door for cutting-edge treatments and influencing the existing therapeutic environment.

Acknowledgments This work is financially supported by the Basic Science Research Program through the National Research Foundation of Korea (NRF) funded by the Ministry of Education (NRF-2018R1A6A1A03025582) and the National Research Foundation of Korea (NRF-2019R1D1A3A03103828) and (NRF 2022R111A3063302).

References

- Abd Ellah NH, Abouelmagd SA. Surface functionalization of polymeric nanoparticles for tumor drug delivery: approaches and challenges. *Expert Opin Drug Deliv.* 2017;14(2):201–14.
- Abdullah Al N, Lee J-E, In I, Lee H, Lee KD, Jeong JH, Park SY. Target delivery and cell imaging using hyaluronic acid-functionalized graphene quantum dots. *Mol Pharm.* 2013;10(10):3736–44.
- Ahmad Raus R, Wan Nawawi WMF, Nasaruddin RR. Alginate and alginate composites for biomedical applications. *Asian J Pharm Sci.* 2021;16(3):280–306.
- Ahsan F, Ansari TM, Usmani S, Bagga P. An insight on silk protein Sericin: from processing to biomedical application. *Drug Res (Stuttg).* 2018;68(06):317–27.
- Aldana AA, Valente F, Dilley R, Doyle B. Development of 3D bioprinted GelMA-alginate hydrogels with tunable mechanical properties. *Bioprinting.* 2021;21:e00105.

- Alijotas-Reig J, Hindié M, Kandhaya-Pillai R, Miro-Mur F. Bioengineered hyaluronic acid elicited a nonantigenic T cell activation: implications from cosmetic medicine and surgery to nano-medicine. *J Biomed Mater Res A*. 2010;95A(1):180–90.
- Asadi N, Del Bakshayesh AR, Davaran S, Akbarzadeh A. Common biocompatible polymeric materials for tissue engineering and regenerative medicine. *Mater Chem Phys*. 2020;242:122528.
- Bajaj P, Singh NS, Virdi JS. Escherichia coli β -lactamases: what really matters. *Front Microbiol*. 2016;7:417.
- Bauleth-Ramos T, Shih T-Y, Shahbazi M-A, Najibi AJ, Mao AS, Liu D, Granja P, Santos HA, Sarmento B, Mooney DJ. Acetalated dextran nanoparticles loaded into an injectable alginate Cryogel for combined chemotherapy and cancer vaccination. *Adv Funct Mater*. 2019;29(35):1903686.
- Bello AB, Kim D, Kim D, Park H, Lee S-H. Engineering and functionalization of gelatin biomaterials: from cell culture to medical applications. *Tissue Eng Part B Rev*. 2020;26(2):164–80.
- Bloemen M, Van Stappen T, Willot P, Lammertyn J, Koeckelberghs G, Geukens N, Gils A, Verbiest T. Heterobifunctional PEG ligands for bioconjugation reactions on iron oxide nanoparticles. *PLoS One*. 2014;9(10):e109475.
- Boland E, Espy P, Bowlin G. Tissue engineering scaffolds. In: Wenk GE, Bowlin GL, editors. *Encyclopaedia of biomaterials and biomedical engineering*. Richmng; 2004. p. 1633–5. CRC Press.
- Bowler PG, Duerden BI, Armstrong DG. Wound microbiology and associated approaches to wound management. *Clin Microbiol Rev*. 2001;14(2):244–69.
- Brandt JV, Piazza RD, dos Santos CC, Vega-Chacón J, Amantéa BE, Pinto GC, Magnani M, Piva HL, Tedesco AC, Primo FL, Jafelicci M, Marques RFC. Synthesis and colloidal characterization of folic acid-modified PEG-b-PCL Micelles for methotrexate delivery. *Colloids Surf B: Biointerfaces*. 2019;177:228–34.
- Campiglio CE, Contessi Negrini N, Farè S, Draghi L. Cross-linking strategies for electrospun gelatin scaffolds. *Materials*. 2019;12(15):2476.
- Capehart SL, ElSohly AM, Obermeyer AC, Francis MB. Bioconjugation of gold nanoparticles through the oxidative coupling of ortho-Aminophenols and anilines. *Bioconjug Chem*. 2014;25(10):1888–92.
- Chacko RT, Ventura J, Zhuang J, Thayumanavan S. Polymer nanogels: A versatile nanoscopic drug delivery platform. *Adv Drug Deliv Rev*. 2012;64(9):836–51.
- Chambre L, Degirmenci A, Sanyal R, Sanyal A. Multi-functional Nanogels as Theranostic platforms: exploiting reversible and nonreversible linkages for targeting, imaging, and drug delivery. *Bioconjug Chem*. 2018;29(6):1885–96.
- Chen H, Zhang H, Wang Z. A ratiometric fluorescent probe based on peptide modified MnFe₂O₄ nanoparticles for matrix metalloproteinase-7 activity detection in vitro and in vivo. *Analyst*. 2022;147(8):1581–8.
- Cherkasov VR, Mochalova EN, Babenyshev AV, Vasilyeva AV, Nikitin PI, Nikitin MP. Nanoparticle beacons: supersensitive smart materials with on/off-switchable affinity to biomedical targets. *ACS Nano*. 2020;14(2):1792–803.
- Coleman RJ, Lawrie G, Lambert LK, Whittaker M, Jack KS, Grøndahl L. Phosphorylation of alginate: synthesis, characterization, and evaluation of in vitro mineralization capacity. *Biomacromolecules*. 2011;12(4):889–97.
- Dai H, Shen Q, Shao J, Wang W, Gao F, Dong X. Small molecular NIR-II fluorophores for cancer phototheranostics. *The Innovation*. 2021;2(1):100082.
- Dash TK, Konkimalla VB. Polymeric modification and its implication in drug delivery: poly- ϵ -caprolactone (PCL) as a model polymer. *Mol Pharm*. 2012;9(9):2365–79.
- Debele TA, Mekuria SL, Lin S-Y, Tsai H-C. Synthesis and characterization of bioreducible heparin-polyethyleneimine nanogels: application as imaging-guided photosensitizer delivery vehicle in photodynamic therapy. *RSC Adv*. 2016;6(18):14692–704.

- Diken ME, Koçer Kizilduman B, Doğan S, Doğan M. Antibacterial and antioxidant phenolic compounds loaded PCL biocomposites for active food packaging application. *J Appl Polym Sci*. 2022;139(25):e52423.
- Donnalaja F, Jacchetti E, Sencini M, Raimondi MT. Natural and synthetic polymers for bone scaffolds optimization. *Polymers*. 2020;12(4):905.
- Dotse E, Lim KH, Wang M, Wijanarko KJ, Chow KT. An immunological perspective of circulating tumor cells as diagnostic biomarkers and therapeutic targets. *Life (Basel)*. 2022;12(2):323.
- Eiselt P, Yeh J, Latvala RK, Shea LD, Mooney DJ. Porous carriers for biomedical applications based on alginate hydrogels. *Biomaterials*. 2000;21(19):1921–7.
- Eltaweil AS, Abd El-Monaem EM, Elshishini HM, El-Aqapa HG, Hosny M, Abdelfatah AM, Ahmed MS, Hammad EN, El-Subruiti GM, Fawzy M, Omer AM. Recent developments in alginate-based adsorbents for removing phosphate ions from wastewater: a review. *RSC Adv*. 2022;12(13):8228–48.
- Fabbri M, García-Fernández L, Vázquez-Lasa B, Soccio M, Lotti N, Gamberini R, Rimini B, Munari A, San Román J. Micro-structured 3D-electrospun scaffolds of biodegradable block copolymers for soft tissue regeneration. *Eur Polym J*. 2017;94:33–42.
- Felgueiras HP, Wang LM, Ren KF, Querido MM, Jin Q, Barbosa MA, Ji J, Martins MCL. Octadecyl chains immobilized onto hyaluronic acid coatings by thiol–ene “click chemistry” increase the surface antimicrobial properties and prevent platelet adhesion and activation to polyurethane. *ACS Appl Mater Interfaces*. 2017;9(9):7979–89.
- Flejszar M, Chmielarz P. Surface-initiated atom transfer radical polymerization for the preparation of well-defined organic–inorganic hybrid nanomaterials. *Materials*. 2019;12(18):3030.
- Franceschi RT, Iyer BS, Cui Y. Effects of ascorbic acid on collagen matrix formation and osteoblast differentiation in murine MC3T3-E1 cells. *J Bone Miner Res*. 1994;9(6):843–54.
- Funkhouser J. Reinventing pharma: the theranostic revolution. *Curr Drug Discov*. 2002;2:17–9.
- Gheorghita Puscaselu R, Lobiuc A, Dimian M, Covasa M. Alginate: from food industry to biomedical applications and Management of Metabolic Disorders. *Polymers*. 2020;12(10):2417.
- Ghezzi M, Pescina S, Padula C, Santi P, Del Favero E, Cantù L, Nicoli S. Polymeric micelles in drug delivery: An insight of the techniques for their characterization and assessment in biorelevant conditions. *J Control Release*. 2021;332:312–36.
- Ghobeira R, Asadian M, Verduyck C, Declercq H, De Geyter N, Morent R. Wide-ranging diameter scale of random and highly aligned PCL fibers electrospun using controlled working parameters. *Polymer*. 2018;157:19–31.
- Goh EJ, Kim KS, Kim YR, Jung HS, Beack S, Kong WH, Scarcelli G, Yun SH, Hahn SK. Bioimaging of hyaluronic acid derivatives using nanosized carbon dots. *Biomacromolecules*. 2012;13(8):2554–61.
- Gupta J, Hassan PA, Barick KC. Core-shell Fe₃O₄@ZnO nanoparticles for magnetic hyperthermia and bio-imaging applications. *AIP Adv*. 2021;11(2):025207.
- Hajba L, Guttman A. The use of magnetic nanoparticles in cancer theranostics: toward handheld diagnostic devices. *Biotechnol Adv*. 2016;34(4):354–61.
- He H, Zhang X, Du L, Ye M, Lu Y, Xue J, Wu J, Shuai X. Molecular imaging nanoprobe for theranostic applications. *Adv Drug Deliv Rev*. 2022;186:114320.
- Hermanson GT. Bioconjugate techniques. Academic; 2013.
- Huang L, Cheng YY, Koo PL, Lee KM, Qin L, Cheng JC, Kumta SM. The effect of hyaluronan on osteoblast proliferation and differentiation in rat calvarial-derived cell cultures. *J Biomed Mater Res A*. 2003a;66(4):880–4.
- Huang YC, Connell M, Park Y, Mooney DJ, Rice KG. Fabrication and in vitro testing of polymeric delivery system for condensed DNA. *J Biomed Mater Res A*. 2003b;67(4):1384–92.
- Huang J, Bu L, Xie J, Chen K, Cheng Z, Li X, Chen X. Effects of nanoparticle size on cellular uptake and liver MRI with Polyvinylpyrrolidone-coated iron oxide nanoparticles. *ACS Nano*. 2010;4(12):7151–60.

- Jang Y, Cha C, Jung J, Oh J. Interfacial compression-dependent merging of two miscible microdroplets in an asymmetric cross-junction for In situ microgel formation. *Macromol Res*. 2018;26(12):1143–9.
- Jiang W, Shang B, Li L, Zhang S, Zhen Y. Construction of a genetically engineered chimeric apoprotein consisting of sequences derived from lidamycin and neocarzinostatin. *Anti-Cancer Drugs*. 2016;27(1):24.
- Jiang Y, Cui D, Fang Y, Zhen X, Upputuri PK, Pramanik M, Ding D, Pu K. Amphiphilic semiconducting polymer as multifunctional nanocarrier for fluorescence/photoacoustic imaging guided chemo-photothermal therapy. *Biomaterials*. 2017;145:168–77.
- Jones EM, Cochrane CA, Percival SL. The effect of pH on the extracellular matrix and biofilms. *Adv Wound Care (New Rochelle)*. 2015;4(7):431–9.
- Juillerat-Jeanneret L. The targeted delivery of cancer drugs across the blood–brain barrier: chemical modifications of drugs or drug-nanoparticles? *Drug Discov Today*. 2008;13(23):1099–106.
- Kelkar SS, Reineke TM. Theranostics: combining imaging and therapy. *Bioconjug Chem*. 2011;22(10):1879–903.
- Kim J, Kim KS, Jiang G, Kang H, Kim S, Kim B-S, Park MH, Hahn SK. In vivo real-time bioimaging of hyaluronic acid derivatives using quantum dots. *Biopolymers*. 2008;89(12):1144–53.
- Kim H, Shin M, Han S, Kwon W, Hahn SK. Hyaluronic acid derivatives for translational medicines. *Biomacromolecules*. 2019;20(8):2889–903.
- Krasia-Christoforou T, Georgiou TK. Polymeric theranostics: using polymer-based systems for simultaneous imaging and therapy. *J Mater Chem B*. 2013;1(24):3002–25.
- Kumbar SG, James R, Nukavarapu SP, Laurencin CT. Electrospun nanofiber scaffolds: engineering soft tissues. *Biomed Mater*. 2008;3(3):034002.
- Lai P-S, Lou P-J, Peng C-L, Pai C-L, Yen W-N, Huang M-Y, Young T-H, Shieh M-J. Doxorubicin delivery by polyamidoamine dendrimer conjugation and photochemical internalization for cancer therapy. *J Control Release*. 2007;122(1):39–46.
- Lammers T, Subr V, Ulbrich K, Hennink WE, Storm G, Kiessling F. Polymeric nanomedicines for image-guided drug delivery and tumor-targeted combination therapy. *Nano Today*. 2010a;5(3):197–212.
- Lammers T, Kiessling F, Hennink WE, Storm G. Nanotheranostics and image-guided drug delivery: current concepts and future directions. *Mol Pharm*. 2010b;7(6):1899–912.
- Lee N, Hyeon T. Designed synthesis of uniformly sized iron oxide nanoparticles for efficient magnetic resonance imaging contrast agents. *Chem Soc Rev*. 2012;41(7):2575–89.
- Lee JH, Huh YM, Jun YW, Seo JW, Jang JT, Song HT, Kim S, Cho EJ, Yoon HG, Suh JS, Cheon J. Artificially engineered magnetic nanoparticles for ultra-sensitive molecular imaging. *Nat Med*. 2007;13(1):95–9.
- Lee J, Cuddihy MJ, Kotov NA. Three-dimensional cell culture matrices: state of the art. *Tissue Eng Part B Rev*. 2008;14(1):61–86.
- Li W, Zhan P, De Clercq E, Lou H, Liu X. Current drug research on PEGylation with small molecular agents. *Prog Polym Sci*. 2013;38(3):421–44.
- Li F, Liang Z, Ling D. Smart organic-inorganic Nanogels for Activatable Theranostics. *Curr Med Chem*. 2019;26(8):1366–76.
- Li Z, Guo J, Zhang M, Li G, Hao L. Gadolinium-coated mesoporous silica nanoparticle for magnetic resonance imaging. *Front Chem*. 2022;10:837032.
- Lin X, Zhou M, Wang S, Lou H, Yang D, Qiu X. Synthesis, structure, and dispersion property of a novel lignin-based Polyoxyethylene ether from Kraft lignin and poly(ethylene glycol). *ACS Sustain Chem Eng*. 2014;2(7):1902–9.
- Lin K, Zhang D, Macedo MH, Cui W, Sarmento B, Shen G. Advanced collagen-based biomaterials for regenerative biomedicine. *Adv Funct Mater*. 2019;29(3):1804943.
- Loman-Cortes P, Binte Huq T, Vivero-Escoto JL. Use of polyhedral oligomeric Silsesquioxane (POSS) in drug delivery, photodynamic therapy and bioimaging. *Molecules*. 2021;26(21):6453.
- Makadia HK, Siegel SJ. Poly lactic-co-glycolic acid (PLGA) as biodegradable controlled drug delivery carrier. *Polymers*. 2011;3(3):1377–97.

- Mallakpour S, Azadi E, Hussain CM. Chitosan/carbon nanotube hybrids: recent progress and achievements for industrial applications. *New J Chem*. 2021;45(8):3756–77.
- Mark JE. *The polymer data handbook*. Oxford University Press/University of Cincinnati; 1999.
- Martins C, Sousa F, Araújo F, Sarmento B. Functionalizing PLGA and PLGA derivatives for drug delivery and tissue regeneration applications. *Adv Healthc Mater*. 2018;7(1):1701035.
- Martins I, Tomás H, Lahoz F, Rodrigues J. Engineered fluorescent carbon dots and G4-G6 PAMAM dendrimer Nanohybrids for bioimaging and gene delivery. *Biomacromolecules*. 2021;22(6):2436–50.
- Mattheolabakis G, Milane L, Singh A, Amiji MM. Hyaluronic acid targeting of CD44 for cancer therapy: from receptor biology to nanomedicine. *J Drug Target*. 2015;23(7–8):605–18.
- Meyer K, Palmer JW. The polysaccharide of the vitreous humor. *J Biol Chem*. 1934;107:629–34.
- Meyer F, Wardale J, Best S, Cameron R, Rushton N, Brooks R. Effects of lactic acid and glycolic acid on human osteoblasts: a way to understand PLGA involvement in PLGA/calcium phosphate composite failure. *J Orthop Res*. 2012;30(6):864–71.
- Mignani S, Rodrigues J, Tomas H, Caminade A-M, Laurent R, Shi X, Majoral J-P. Recent therapeutic applications of the theranostic principle with dendrimers in oncology. *Sci China Mater*. 2018;61(11):1367–86.
- Mofazzal Jahromi MA, Sahandi Zangabad P, Moosavi Basri SM, Sahandi Zangabad K, Ghamarypour A, Aref AR, Karimi M, Hamblin MR. Nanomedicine and advanced technologies for burns: preventing infection and facilitating wound healing. *Adv Drug Deliv Rev*. 2018;123:33–64.
- Mohammed L, Ragab D, Goma H. Bioactivity of hybrid polymeric magnetic nanoparticles and their applications in drug delivery. *Curr Pharm Des*. 2016;22(22):3332–52.
- Mora-Boza A, Mancipe Castro LM, Schneider RS, Han WM, García AJ, Vázquez-Lasa B, San Román J. Microfluidics generation of chitosan microgels containing glycerylphosphate crosslinker for in situ human mesenchymal stem cells encapsulation. *Mater Sci Eng C*. 2021;120:111716.
- Mwai LM, Kyama MC, Ngugi CW, Walong E. Bioconjugation of AuNPs with HPV 16/18 E6 antibody through physical adsorption technique. *bioRxiv*. 2020; <https://doi.org/10.1101/2020.01.21.899930>.
- Nii T, Kuwahara T, Makino K, Tabata Y. A co-culture system of three-dimensional tumor-associated macrophages and three-dimensional cancer-associated fibroblasts combined with biomolecule release for cancer cell migration. *Tissue Eng A*. 2020;26(23–24):1272–82.
- Nolan K, Millet Y, Ricordi C, Stabler CL. Tissue engineering and biomaterials in regenerative medicine. *Cell Transplant*. 2008;17(3):241–3.
- Noor NQIM, Razali RS, Ismail NK, Ramli RA, Razali UHM, Bahauddin AR, Zaharudin N, Rozzamri A, Bakar J, Shaarani SM. Application of green Technology in Gelatin Extraction: a review. *Processes*. 2021;9(12):2227.
- Nosoudi N, Oommen AJ, Stultz S, Jordan M, Aldabel S, Hohne C, Mosser J, Archacki B, Turner A, Turner P. Electrospinning live cells using gelatin and pullulan. *Bioengineering*. 2020;7(1):21.
- Oliveira ÉR, Nie L, Podstawczyk D, Allahbakhsh A, Ratnayake J, Brasil DL, Shavandi A. Advances in growth factor delivery for bone tissue engineering. *Int J Mol Sci*. 2021;22(2):903.
- Pacheco N, Garnica-Gonzalez M, Gimeno M, Bárzana E, Trombotto S, David L, Shirai K. Structural characterization of chitin and chitosan obtained by biological and chemical methods. *Biomacromolecules*. 2011;12(9):3285–90.
- Palsson B, Bhatia SN. *Tissue engineering*. Upper Saddle River: Pearson Prentice Hall; 2004.
- Parisi OI, Scrivano L, Sinicropi MS, Picci N, Puoci F. Engineered polymer-based nanomaterials for diagnostic, therapeutic and theranostic applications. *Mini Rev Med Chem*. 2016;16(9):754–61.
- Park CH, Woo KM. Fibrin-based biomaterial applications in tissue engineering and regenerative medicine. In: Noh I, editor. *Biomimetic medical materials: from nanotechnology to 3D bio-printing*. Singapore: Springer Singapore; 2018. p. 253–61.
- Park H, Saravanakumar G, Kim J, Lim J, Kim WJ. Tumor microenvironment sensitive Nanocarriers for bioimaging and therapeutics. *Adv Healthc Mater*. 2021;10(5):2000834.

- Patel DK, Dutta SD, Ganguly K, Lim K-T. Multifunctional bioactive chitosan/cellulose nanocrystal scaffolds eradicate bacterial growth and sustain drug delivery. *Int J Biol Macromol*. 2021;170:178–88.
- Patel DK, Ganguly K, Hexiu J, Dutta SD, Patil TV, Lim K-T. Functionalized chitosan/spherical nanocellulose-based hydrogel with superior antibacterial efficiency for wound healing. *Carbohydr Polym*. 2022;284:119202.
- Patil TV, Patel DK, Dutta SD, Ganguly K, Santra TS, Lim K-T. Nanocellulose, a versatile platform: from the delivery of active molecules to tissue engineering applications. *Bioactive Mater*. 2022;9:566–89.
- Pelegri-O'Day EM, Lin E-W, Maynard HD. Therapeutic protein–polymer conjugates: advancing beyond PEGylation. *J Am Chem Soc*. 2014;136(41):14323–32.
- Piao Y, You H, Xu T, Bei H-P, Piwko IZ, Kwan YY, Zhao X. Biomedical applications of gelatin methacryloyl hydrogels. *Eng Regen*. 2021;2:47–56.
- Politi J, De Stefano L, Rea I, Gravagnuolo AM, Giardina P, Methivier C, Casale S, Spadavecchia J. One-pot synthesis of a gold nanoparticle–Vmh2 hydrophobin nanobiocomplex for glucose monitoring. *Nanotechnology*. 2016;27(19):195701.
- Prasad A, Kandasubramanian B. Fused deposition processing polycaprolactone of composites for biomedical applications. *Polym-Plast Technol Mater*. 2019;58(13):1365–98.
- Puertas-Bartolomé M, Mora-Boza A, García-Fernández L. Emerging biofabrication techniques: a review on natural polymers for biomedical applications. *Polymers*. 2021;13(8):1209.
- Ren X, Liu W, Zhou H, Wei J, Mu C, Wan Y, Yang X, Nie A, Liu Z, Yang X, Luo Z. Biodegradable 2D GeP nanosheets with high photothermal conversion efficiency for multimodal cancer theranostics. *Chem Eng J*. 2022;431:134176.
- Ruan J, Qian H. Recent development on controlled synthesis of Mn-based nanostructures for bioimaging and cancer therapy. *Adv Ther*. 2021;4(5):2100018.
- Russell AJ, Baker SL, Colina CM, Figg CA, Kaar JL, Matyjaszewski K, Simakova A, Sumerlin BS. Next generation protein-polymer conjugates. *AICHE J*. 2018;64(9):3230–45.
- Sabir F, Asad MI, Qindeel M, Afzal I, Dar MJ, Shah KU, Zeb A, Khan GM, Ahmed N, Din F-U. Polymeric nanogels as versatile Nanoplatforms for biomedical applications. *J Nanomater*. 2019;2019:1526186.
- Saenz-Mendoza AI, Zamudio-Flores PB, García-Anaya MC, Velasco CR, Acosta-Muñiz CH, de Jesús Ornelas-Paz J, Hernández-González M, Vargas-Torres A, Aguilar-González MÁ, Salgado-Delgado R. Characterization of insect chitosan films from *Tenebrio molitor* and *Brachystola magna* and its comparison with commercial chitosan of different molecular weights. *Int J Biol Macromol*. 2020;160:953–63.
- Sagar V, Vashist A, Gupta R, Nair M. Chapter 15: Nanogels for biomedical applications: challenges and prospects. In: *Nanogels for biomedical applications*. The Royal Society of Chemistry; 2018. p. 290–300.
- Sanz-Horta R, Matesanz A, Jorcano JL, Velasco D, Acedo P, Gallardo A, Reinecke H, Elvira C. Preparation and characterization of plasma-derived fibrin hydrogels modified by alginate di-aldehyde. *Int J Mol Sci*. 2022;23(8):4296.
- Schwarz M, Buehler A, Aguirre J, Ntziachristos V. Three-dimensional multispectral optoacoustic mesoscopy reveals melanin and blood oxygenation in human skin in vivo. *J Biophotonics*. 2016;9(1–2):55–60.
- Seeto WJ, Tian Y, Pradhan S, Kerscher P, Lipke EA. Rapid production of cell-laden microspheres using a flexible microfluidic encapsulation platform. *Small*. 2019;15(47):1902058.
- Sell SA, Wolfe PS, Garg K, McCool JM, Rodríguez IA, Bowlin GL. The use of natural polymers in tissue engineering: a focus on electrospun extracellular matrix analogues. *Polymers*. 2010;2(4):522–53.
- Sepideh K, Hamed A. Nanogels: chemical approaches to preparation. In: *Concise Encyclopedia of biomedical polymers and polymeric biomaterials*. CRC Press; 2017.
- Sharath Kumar KS, Girish YR, Ashrafizadeh M, Mirzaei S, Rakesh KP, Hossein Gholami M, Zabolian A, Hushmandi K, Orive G, Kadumudi FB, Dolatshahi-Pirouz A, Thakur VK, Zarrabi

- A, Makvandi P, Rangappa KS. AIE-featured tetraphenylethylene nanoarchitectures in biomedical application: bioimaging, drug delivery and disease treatment. *Coord Chem Rev.* 2021;447:214135.
- Siafaka PI, Üstündağ Okur N, Karavas E, Bikiaris DN. Surface modified multifunctional and stimuli responsive nanoparticles for drug targeting: current status and uses. *Int J Mol Sci.* 2016;17(9):1440.
- Siafaka PI, Okur NÜ, Karantas ID, Okur ME, Gündoğdu EA. Current update on nanoplatforms as therapeutic and diagnostic tools: a review for the materials used as nanotheranostics and imaging modalities. *Asian J Pharm Sci.* 2021;16(1):24–46.
- Siddiqui N, Asawa S, Birru B, Baadhe R, Rao S. PCL-based composite scaffold matrices for tissue engineering applications. *Mol Biotechnol.* 2018;60(7):506–32.
- Sindhu RK, Gupta R, Wadhwa G, Kumar P. Modern herbal Nanogels: formulation, delivery methods, and applications. *Gels.* 2022;8(2):97.
- Singh N, Son S, An J, Kim I, Choi M, Kong N, Tao W, Kim JS. Nanoscale porous organic polymers for drug delivery and advanced cancer theranostics. *Chem Soc Rev.* 2021;50(23):12883–96.
- Sinha VR, Bansal K, Kaushik R, Kumria R, Trehan A. Poly-ε-caprolactone microspheres and nanospheres: an overview. *Int J Pharm.* 2004;278(1):1–23.
- Song H-T, Choi J-S, Huh Y-M, Kim S, Jun Y-W, Suh J-S, Cheon J. Surface modulation of magnetic nanocrystals in the development of highly efficient magnetic resonance probes for intracellular labeling. *J Am Chem Soc.* 2005;127(28):9992–3.
- Song B, Li M, Ren J, Liu Q, Wen X, Zhang W, Yuan J. A multifunctional nanoprobe based on europium(iii) complex–Fe₃O₄ nanoparticles for bimodal time-gated luminescence/magnetic resonance imaging of cancer cells in vitro and in vivo. *New J Chem.* 2022; <https://doi.org/10.1039/d2nj00511e>.
- Stoffels I, Morscher S, Helfrich I, Hillen U, Leyh J, Burton NC, Sardella TCP, Claussen J, Poeppel TD, Bachmann HS, Roesch A, Griewank K, Schadendorf D, Gunzer M, Klode J. Metastatic status of sentinel lymph nodes in melanoma determined noninvasively with multispectral opto-acoustic imaging. *Sci Transl Med.* 2015;7(317):317ra199.
- Sulttan S, Rohani S. Controlled drug release of smart magnetic self-assembled micelle, kinetics and transport mechanisms. *J Pharm Sci.* 2022; <https://doi.org/10.1016/j.xphs.2022.03.023>.
- Sun S, Zeng H. Size-controlled synthesis of magnetite nanoparticles. *J Am Chem Soc.* 2002;124(28):8204–5.
- Tebaldi ML, Charan H, Mavliutova L, Böker A, Glebe U. Dual-stimuli sensitive hybrid materials: ferritin–PDMAEMA by grafting-from polymerization. *Macromol Chem Phys.* 2017;218(11):1600529.
- Thorat ND, Tofail SAM, Rechenberg BV, Townley H, Brennan G, Silien C, Yadav HM, Steffen T, Bauer J. Physically stimulated nanotheranostics for next generation cancer therapy: focus on magnetic and light stimulations. *Appl Phys Rev.* 2019;6(4):041306.
- Tian X, Zhang L, Yang M, Bai L, Dai Y, Yu Z, Pan Y. Functional magnetic hybrid nanomaterials for biomedical diagnosis and treatment. *WIREs Nanomed Nanobiotechnol.* 2018;10(1):e1476.
- Tomić SL, Nikodinović-Runić J, Vukomanović M, Babić MM, Vuković JS. Novel hydrogel scaffolds based on alginate, gelatin, 2-hydroxyethyl methacrylate, and hydroxyapatite. *Polymers.* 2021;13(6):932.
- Tutar R, Motealleh A, Khademhosseini A, Kehr NS. Functional nanomaterials on 2D surfaces and in 3D nanocomposite hydrogels for biomedical applications. *Adv Funct Mater.* 2019;29(46):1904344.
- Uzunalli G, Guler MO. Peptide gels for controlled release of proteins. *Ther Deliv.* 2020;11(3):193–211.
- Vashist A, Vashist A, Gupta YK, Ahmad S. Recent advances in hydrogel based drug delivery systems for the human body. *J Mater Chem B.* 2014;2(2):147–66.
- Vasile C, Pamfil D, Stoleru E, Baican M. New developments in medical applications of hybrid hydrogels containing natural polymers. *Molecules.* 2020;25(7):1539.

- Veronese FM. Peptide and protein PEGylation: a review of problems and solutions. *Biomaterials*. 2001;22(5):405–17.
- Wang J-Z, You M-L, Ding Z-Q, Ye W-B. A review of emerging bone tissue engineering via PEG conjugated biodegradable amphiphilic copolymers. *Mater Sci Eng C*. 2019;97:1021–35.
- Wang H, Picchio ML, Calderón M. One stone, many birds: recent advances in functional nanogels for cancer nanotheranostics. *WIREs Nanomed Nanobiotechnol*. 2022;14(4):e1791.
- Warenius HM. Technological challenges of theranostics in oncology. *Expert Opin Med Diagn*. 2009;3(4):381–93.
- Wennink JWH, Signori F, Karperien M, Bronco S, Feijen J, Dijkstra PJ. Introducing small cationic groups into 4-armed PLLA-PEG copolymers leads to preferred micellization over thermo-reversible gelation. *Polymer*. 2013;54(26):6894–901.
- Xiao Y, Gateau J, Silva AKA, Shi X, Gazeau F, Mangeney C, Luo Y. Hybrid nano- and microgels doped with photoacoustic contrast agents for cancer theranostics. *View*. 2021;2(6):20200176.
- Xiao Z, Zhang L, Colvin VL, Zhang Q, Bao G. Synthesis and application of magnetic nanocrystal clusters. *Ind Eng Chem Res*. 2022;61:7613.
- Xing Q, Yates K, Vogt C, Qian Z, Frost MC, Zhao F. Increasing mechanical strength of gelatin hydrogels by divalent metal ion removal. *Sci Rep*. 2014;4(1):4706.
- Xu Z, Ma X, Gao Y-E, Hou M, Xue P, Li CM, Kang Y. Multifunctional silica nanoparticles as a promising theranostic platform for biomedical applications. *Mater Chem Front*. 2017;1(7):1257–72.
- Xu C, Akakuru OU, Ma X, Zheng J, Zheng J, Wu A. Nanoparticle-based wound dressing: recent Progress in the detection and therapy of bacterial infections. *Bioconjug Chem*. 2020a;31(7):1708–23.
- Xu X, Liu Y, Fu W, Yao M, Ding Z, Xuan J, Li D, Wang S, Xia Y, Cao M. Poly(N-isopropylacrylamide)-based Thermoresponsive composite hydrogels for biomedical applications. *Polymers (Basel)*. 2020b;12(3):580.
- Yadav M, Goswami P, Paritosh K, Kumar M, Pareek N, Vivekanand V. Seafood waste: a source for preparation of commercially employable chitin/chitosan materials. *Bioresour Bioprocess*. 2019;6(1):8.
- Yang X, Stein EW, Ashkenazi S, Wang LV. Nanoparticles for photoacoustic imaging. *Wiley Interdiscip Rev Nanomed Nanobiotechnol*. 2009;1(4):360–8.
- Yu Y, Ma Y, Yin J, Zhang C, Feng G, Zhang Y, Meng J. Tuning the micro-phase separation of the PES-g-PEG comb-like copolymer membrane for efficient CO₂ separation. *Sep Purif Technol*. 2021;265:118465.
- Yudasaka M, Ajima K, Suenaga K, Ichihashi T, Hashimoto A, Iijima S. Nano-extraction and nano-condensation for C60 incorporation into single-wall carbon nanotubes in liquid phases. *Chem Phys Lett*. 2003;380(1):42–6.
- Zhai P, Peng X, Li B, Liu Y, Sun H, Li X. The application of hyaluronic acid in bone regeneration. *Int J Biol Macromol*. 2020;151:1224–39.
- Zhang H, Mi P. 12 – polymeric micelles for tumor theranostics. In: Cui W, Zhao X, editors. *Theranostic bionanomaterials*. Elsevier; 2019. p. 289–302.
- Zhang J, Traylor KS, Mountz JM. PET and SPECT imaging of brain tumors. *Semin Ultrasound CT MRI*. 2020;41(6):530–40.
- Zhu W, Zhao J, Chen Q, Liu Z. Nanoscale metal-organic frameworks and coordination polymers as theranostic platforms for cancer treatment. *Coord Chem Rev*. 2019;398:113009.
- Zhu W, Wei Z, Han C, Weng X. Nanomaterials as promising Theranostic tools in nanomedicine and their applications in clinical disease diagnosis and treatment. *Nanomaterials (Basel)*. 2021;11(12):3346.

Chapter 6

Magneto-Responsive Nanohybrids for Bioimaging



S. T. Mhaske, D. A. Patil, and S. U. Mestry

6.1 Introduction

Bioimaging is an aseptic process of visualizing biological activity in a specific period. The various life processes, such as movement, respiration, etc., don't get affected by this method. It helps in observing subcellular structures and all the tissues in multicellular organisms, while it also helps report the 3D structure of specimens other than inferencing physically. From the twentieth century of the X-rays to the ultrasonic, computed tomography (CT), magnetic resonance imaging (MRI), optical, and nuclear modalities of the twenty-first century, medical imaging has revamped the practice of diagnosis (Malik et al. 2019). The relative painless and facile way has dramatically increased the effectiveness of medicines and diagnostics and reduced hospitalization stay.

Furthermore, nanotechnology promises have advanced medical imaging to the next level by increasing the resolution of current techniques. The rapid metabolization and low availability of some drugs always demanded large injection doses but unsatisfactory therapeutic effects (Wang and Kohane 2017). For example, for the desired therapeutic effect, it is generally necessary to enhance the dosage of anti-cancer drugs, which also cause undesirable side effects. In addition, orally administered medicines need to evade the risk of degradation in the acidic/enzymatic environment in the gastrointestinal tract. All of these problems can potentially be addressed with stimulus-responsive nanotechnology (Blum et al. 2015; Liu et al. 2020). There are generally two ways of outlining stimuli-responsive drug delivery nanoparticles that effectively accumulate at the target area of diagnostics. These

S. T. Mhaske (✉) · D. A. Patil · S. U. Mestry
Department of Polymer and Surface Engineering, Institute of Chemical Technology,
Mumbai, Maharashtra, India
e-mail: st.mhaske@ictmumbai.edu.in

methods involve endogenous stimuli (i.e., redox potential, ions, and enzymes), distinctive among target regions, and can effectively enhance drug release. This approach requires carefully selecting materials that can form effective nanocarriers, respond to specific endogenous stimuli, and release enclosed drugs. In the second perspective, exogenous physical stimuli (i.e., electricity, light, magnetic fields, temperature, and ultrasound) are applied to the target area (Hatakeyama 2017; Zuo et al. 2019). Figure 6.1 shows the possible applications of stimuli-responsive materials, their types, and differences between endogenous and exogenous stimuli with examples.

The nanomaterials are obtained from various materials, and there are plenty of such examples as carbon quantum dots, gold nanoparticles, and liposomes. The functionalization of nanomaterials has been studied widely because of their biocompatibility and ease of design and synthesis.

The stimuli-responsive biomaterials, effective for responding on-demand to minute alterations in their local environment, have become an area of focus in medicine and diagnostics. The spatiotemporal manipulation of the nanomaterials by an external magnetic field is known as magneto-responsive materials (Adedoyin and Ekenseair 2018). These materials have emerged as promising for advanced drug delivery and bioimaging applications. Such materials could be developed physically and/or chemically by incorporating magnetic nanoparticles into the polymeric or

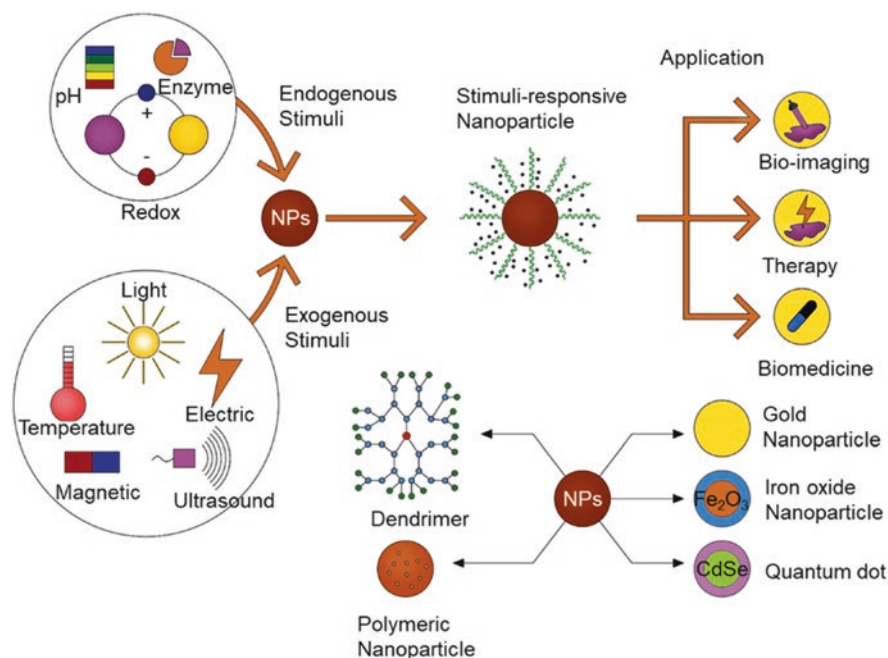


Fig. 6.1 Different types of stimuli, stimuli-responsive materials, and their applications. (Liu et al. 2020)

biomaterial structure (Gupta and Gupta 2005; Ito et al. 2005a, b). Furthermore, multifunctional nanoparticles prepared by integrating multiple properties of single nanostructures have gained much attention because of their combined optical, electronic, magnetic, and thermal properties. One of the studies shows the synthesis of dual-responsive (magnetic and thermal) L-proline nanohybrids (L-Pro-based-TMNHs) by thiol-ene click chemistry through the grafting reaction of thermo-responsive thiol-terminated P(NIPAM-co-L-ProLA)-b-POEGA-SH (PNLPO-SH) and vinyl-functionalized $\text{Fe}_3\text{O}_4@\text{SiO}_2\text{-MPS}$. The obtained material shows the thermal responsiveness of the L-Pro-based-TMNHs, which induced self-assembly to give rise to a hydrophobic microenvironment in aqueous media for catalyzing asymmetric aldol reaction (Wang et al. 2020). Another study introduces different classes of nanomaterials, which gathered notable encouragement as one of the auspicious aspirant materials for biomedical applications due to their quirky structure and properties. The resulted carbon-based nanohybrids could serve only as magnetic resonance and fluorescence imaging contrast agents (Wang and Zhou 2016).

The magneto-responsive composite features could be obtained by merging magnetic and polymer materials. The external magnetic actuating system provides unique operational capabilities as it can be spatially and temporally controlled. The applications in biomedicine, coatings, microelectronics, and microfluidics demand that scientists study magneto-responsive materials more intensely (Li et al. 2021). There are three identified magneto-responsive composite materials depending upon the activation mode and the intended applications, which are defined according to the classified aspects such as i) ability of deformation (bending, stretching, rotation) after exposure to the magnetic field; ii) path-dependent cell or biomolecule guidance, separation, etc., depending upon the ability to drag remotely to the specific area known as magnetic guidance; and iii) the use in controlled drug release and the shape-memory devices through magnetic induction for thermo-responsive polymeric material's actuation (Thévenot et al. 2013).

The current book chapter mainly focuses on nanomaterials responsive to the external magnetic field used for bioimaging and their various applications and characterization techniques. However, to overcome the drawbacks of conventional methods of diagnostics, the dual- and multi-responsive behaviors of nanoparticles have been employed nowadays to improve efficiency from an imaging and diagnostics point of view.

6.2 Nanohybrids

When more than one nanomaterial (NM) of the unique chemical origin or differing dimensionality is conjugated by molecular or macromolecular links or physico-chemical forces or when one nanomaterial overcoats another possessing a unique chemical identity or when complex soft molecules are engineered to chemically bind to NM surfaces, all to enhance the existing functionality or achieve multifunctional usage, can be defined as nanohybrids (NHs). The conjugation of two or more

nanomaterials has recently received much attention to attain increased multifunctionality and create the potential for next-generation materials with improved performance (Aich et al. 2014).

Careful mixing of two or more bimetallic NHs improves their functional performance (Aich et al. 2014). When iron oxide was conjugated with gold to generate core-shell particles, the iron oxide shell retained its natural magnetic properties, while the gold core's surface plasmon resonance was preserved (Shevchenko et al. 2008). These multifunctional bimetallic NHs have been employed as MRI agents with enhanced nanoheating capabilities, making them practical for laser-irradiated drug delivery systems (Fan et al. 2012). Similarly, gold intercalated within layered clay was utilized to immobilize proteins and organic molecules, making it useful for biocatalysis and sensors (Pál et al. 2010; Zhao et al. 2008); paramagnetic iron oxides produced unique drug delivery systems with better drug release and targetability (Ma et al. 2012). Graphene nanosheets have also been coupled with porphyrins, titanium dioxide (TiO₂), carbon nanotubes, quantum dots, and other materials to produce NHs for improved optical emitting (Son et al. 2012) and limiting (D'Souza and Ito 2009) devices, supercapacitors, lithium-ion batteries (Chen et al. 2011), or transparent conductors (Danila et al. 2008). It is clear that the benefits of conjugation and ensembles of various materials are well understood, and as a result, the NH material domain will most certainly expand, affecting a much more extensive application field and in enormous quantities. For example, it is estimated that by 2050, at least 1.0107 kg of platinum-carrying titania-modified multiwalled carbon nanotube (MWNT) NHs will be used in fuel cells for vehicles alone, assuming a platinum content of 20% by mass in the NH (Aich et al. 2014).

When compared to its parent components, an ensemble of multiple materials will most likely act differently. For example, carbonaceous nanomaterials (CNMs), such as fullerenes and carbon nanotubes (CNTs), have a high aggregation propensity due to their inherent hydrophobicity and strong van der Waals interaction forces. In contrast, metallic nanomaterials (MNMs), such as silver or zinc oxide, have unique dissolution and complexation properties. When metal-carbonaceous conjugates are conjugated, the resulting behavior can be either dominating hydrophobicity or dissolution-complexation processes, depending on the nature of the conjugation (Aich et al. 2014). The materials of magneto-responsive nanohybrids can be classified into five types as follows.

6.2.1 Carbon-Carbon NHs

Combinations of three significant carbon nanostructures – zero-dimensional fullerenes, 1D CNTs (single-walled carbon nanotube and multiwalled carbon nanotube (SWCNTs and MWCNTs)), and 2D graphene and carbon nanotubes – make up carbon-based NHs. “Nano-peapods” are fullerenes or graphene (pristine or functionalized) enclosed within CNTs or CNHs via thermal annealing, in situ growth from vapor-based deposition reactions, or dispersion-assisted cavity filling

techniques. A unique multi-layered hybrid fullerene structure known as a “carbon nano-onion” can be created using similar synthesis procedures and the water-assisted electric arc process (Aich et al. 2014).

The oxidation of CNTs and graphene to attach polar carboxyl or hydroxyl surface groups ($-\text{COOH}$ or $-\text{OH}$) and the attachment of chemically active molecules or polymeric assemblies are examples of functionalization. For example, fullerenes functionalized with porphyrin derivatives are refluxed with acid-treated CNT-COOH solutions to produce fullerene-CNT NHs by a reaction between the carboxyl functionality on the CNT and the amine groups on the porphyrin molecules. Catalytic reaction techniques using vapor phase reactant molecules are commonly used to produce seamless exohedral bonding between CNT and graphene or CNT and fullerene (nanobuds) by covalent modification. Furthermore, by electrostatic and non-covalent interactions, these graphitic NMs can build layered assemblies of NH-based thin films using drop-cast, spin-cast, and dipping processes (Aich et al. 2014).

Hybridization among CNMs has been found to be beneficial due to the multifunctional and enhanced features of each species. CNTs have unique electrical, mechanical, optical, and charge-carrying capabilities, whereas graphene has a large reactive surface area, mechanical and thermal durability, and high electrical conductivity. In contrast, fullerenes have a high electron density and photoactivity. Fullerenes conjugated with graphene or CNTs can lead to improved performance of organic photovoltaics and optoelectronic devices. Hybridized graphene could be a promising candidate for transparent conducting films in optoelectronic and solar devices with high surface area. As they conjugate with CNTs or fullerenes, they gain conductivity, transmittance, and a low physical thickness. Such alterations can be used in various ways, including electrochemical and biomolecular sensing, structural health monitoring, and so on (Aich et al. 2014).

6.2.2 Carbon-Metal NHs

The synthesis of carbon-metal nanohybrids (CMNHs) involves combining CNMs (CNTs, graphenes, and fullerenes) with various metallic or metal oxide NMs. CMNHs are made up of metallic NMs (MNHs) ranging from noble metals such as Ag, Au, Pt, Pd, Ru, Rh, and others to lanthanide series metals (La, Sc, Gd, and so on), metal oxide NMs (ZnO , TiO_2 , SiO_2 , Fe_3O_4 , CuO , and so on), and semiconducting quantum dots (CdSe , CdTe , and so on). The formation of unique and synergistic electrical, optical, and mechanical properties results from graphitic and metallic nanostructures. CNTs and graphene with high active surface stability are used to develop Li-ion batteries. The combination of graphitic and metallic nanostructures produces unique and synergistic electrical, optical, and mechanical characteristics (Aich et al. 2014).

When quantum dots are used in conjunction with other materials, they are more effective. Plasmonic (e.g., Fe_3O_4 CdS) or magnetic (e.g., Fe_3O_4 CdS) particles (e.g., Au-CdSe-ZnS) can be employed in bioimaging (Berezin 2015).

6.2.3 *Metal-Metal NHs*

Metal-metal nanohybrids are formed when metal NMs, such as metals and metal oxides, are conjugated to create multimetallic ensembles. The hybrid characteristics and architectures determine the synthesis techniques for conjugated metallic NMs and the applications needed. The most common synthesis strategies are wet chemical reactions utilizing metal salt reduction or heat decomposition. Polyol methods (Aich et al. 2014), photochemical deposition (Wang et al. 1998), electroless plating (Kim et al. 2013a), solvothermal (Sun et al. 2011), sol-gel (Ohno et al. 2009), ion implantation (Cheang-wong 2009), epitaxial growth (Sánchez-Iglesias et al. 2010), and other wet chemical processes are just a few examples. Flame aerosol (Johannessen et al. 2004) and plasma-assisted deposition (Kim et al. 2013b) are two common vapor-gas-phase techniques. Co-reduction or sequential reduction, in which a metal NM previously generated can act as a “seed” for subsequent growth of another NM with a different chemical origin, can be used to create core-shell-based nanostructures (Aich et al. 2014).

Optical lithography is frequently used with other techniques to achieve patterned growth. Hollow spherical, porous (Wang et al. 2008), tubular (Chueh et al. 2006) structures can be created using template-based growth techniques. Matrix-bound approaches, on the other hand, use inorganic silica, the oil-water interface, and polymer or block-co-polymer matrices to build NHs by processes such as coprecipitation (Wu and Lai 2004), ion implantation (Cheang-wong 2009), emulsification (Liu et al. 2013), and reverse micellization (Fan et al. 2011).

Natural products have also been used to generate biogenic or green synthesis techniques for MMNHs. As a solvent or a reducing agent, extracts are used. MMNHs have property synergies that allow them to be used in various applications: photovoltaics and solar cells, biomedical research nanotherapeutics and engineering chemical catalysis, catalysis and antibacterial applications, and sensing and degradation (Aich et al. 2014) (Fig. 6.2).

6.2.4 *Organic Molecule-Coated NHs*

Metallic, carbonaceous, or polymeric NMs coated with organic molecules, biomolecules, or polymers have been identified as NHs in a large body of literature. NHs (layer-by-layer hierarchical thin films) are another name for layer-by-layer hierarchical thin films (Aich et al. 2014).

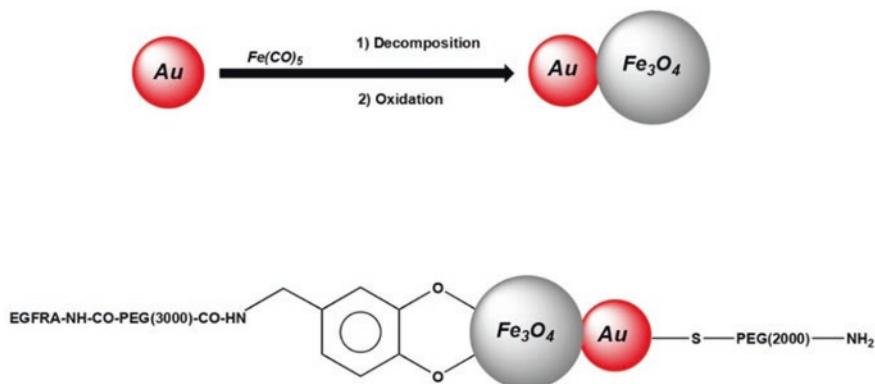


Fig. 6.2 Example of the formation of metal-metal NHs: formation and surface modification of the dumbbell of dumbbell-like Fe₃O₄/Au NPs. (Berezin 2015)

Physisorption of organic molecules (Aich et al. 2014); electrochemical immobilization of protein, enzyme, or DNA molecules (Aich et al. 2014); polymer grafting from or grafting to NM surfaces (Aich et al. 2014); emulsification (Tian et al. 2010); and ion exchange are all described in the literature for OMCNH (Qiu et al. 2012). Nanoelectronics (Qiu et al. 2012), photovoltaics, chemical and bio-sensing (Qiu et al. 2012), bioimaging (Qiu et al. 2012), controlled drug delivery (Qiu et al. 2012), and cancer therapy are among areas where coated NMs are being studied. CNMs are surface-functionalized with porphyrin, phthalocyanine, and other compounds to improve charge transfer efficiency in photovoltaics and dye-sensitized solar cells. Similarly, organic polymers such as polyethylene glycol (PEG) (Wu et al. 2010) and poly(vinyl pyrrolidone) (PVP) (Tagliazucchi et al. 2012) are grafted or coated onto magnetic or plasmonic particles to improve their solubility for bioimaging, drug administration, or sensing. Metallic NMs are also linked to organic fluorophores to improve tagging and contrast (Tagliazucchi et al. 2012). Citrate, PVP, PEG, gum arabic, copolymers, and other substances are commonly adsorbed onto NMs to improve dispersion in a chosen solvent. Recent surface modification of NMs, on the other hand, has been done with relatively complicated supramolecules or heterocyclic structures (e.g., porphyrins) that are covalently bonded to the NM surfaces (Guldi et al. 2005). For example, heterocyclic porphyrins stabilize NH dispersions and have excellent electronic charge transfer properties (Guldi et al. 2005) and antibacterial properties (Guldi et al. 2005). Furthermore, organic compounds or polymers on the NM surface have been shown to have a different destiny, transformation, and toxicity behavior due to conformational variations (Aich et al. 2014) (Fig. 6.3).

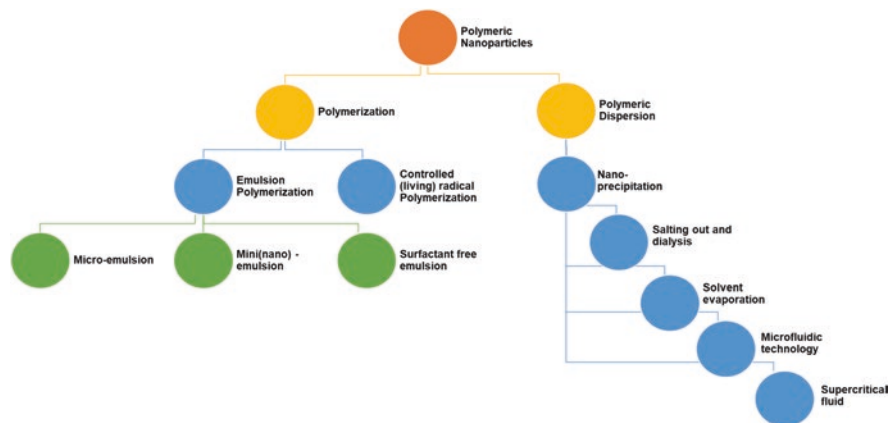


Fig. 6.3 A summary of standard methods for polymeric nanoparticle synthesis used in drug delivery and imaging. (Berezin 2015).

6.2.4.1 Synthesis of Polymeric Nanocapsules (NCs)

NCs can be considered functional and structural models of cells and their organelles. Bioinspired synthetic techniques, not unexpectedly, were successful in creating NCs. The polymerization of hydrophobic monomers dispersed in the hydrophobic interior of bilayers generated by lipids or other surfactants is the basis for vesicle-templated assembly. The bilayer acts as a two-dimensional solvent that arises spontaneously in this manner. The polymer network propagates laterally within the bilayer but not in the dimension orthogonal to the bilayer plane. The polymerization creates a crosslinked network within the bilayer's hydrophobic center. After polymerization, the lipid or surfactant scaffold can be removed to get polymer NCs (Berezin 2015).

Nanopores can be used to alter the permeability of the NC shell (Hentze and Kaler 2003; Dergunov and Pinkhassik 2008; Berezin 2015). Pore-forming templates and monomers and crosslinkers are loaded into the bilayer interior to achieve this purpose. After polymerization, these templates become implanted in the crosslinked polymer network within the bilayer. Chemical degradation or washing NCs with an organic solvent can eliminate these templates, resulting in homogenous nanopores. Molecular imprinting is essentially what this process of pore generation entails. When inert hydrophobic molecules, such as glucose pentaesters, are employed as pore-forming templates, the pore opening has the same chemical composition as the NC shell, a hydrophobic crosslinked polymer. Pore-forming templates with a polymerizable moiety attached to a bulky group with a chemically degradable linker are used to expand the pore-imprinting approach. The monomers and crosslinkers copolymerize with this template. Nanopores having functional group(s) in the pore orifice are created by cleaving the linker and removing the bulky group. Click chemistry can be used to modify embedded functional groups.

This approach allows for precise control of nanopore size and chemical environment, allowing for a wide range of permeability control (Berezin 2015).

The spontaneous assembly of oppositely charged surfactants is an alternate way to manufacture polyelectrolyte hollow spheres (McKelvey et al. 2000; McKelvey and Kaler 2002). Equilibrium vesicles were used to accomplish direct templating without morphological alterations and the utilization of hydrophobic monomers (Dergunov et al. 2010; Richter et al. 2011; Banner et al. 2008). The hollow polymer capsules are stable enough to endure dialysis, vacuum drying, and nonionic surfactant-assisted resuspension in water. The high crosslink density of polystyrene, as well as the compatibility of the aromatics, contributes to the stability of these polymerizable vesicles (Berezin 2015).

The ability of the bilayer to rearrange to accommodate the expanding polymer may be due to surfactants and polymer, as well as the capacity of the bilayer to reorganize to accept the developing polymer. It is possible to construct vesicles with a pretty tight size distribution and diameters ranging from tens of nanometers to tens of micrometers to form polymersomes (Matyjaszewski and Xia 2001; Spanswick 2005). A densely entangled hydrophobic layer and two hydrophilic polymer brushes stabilize the membrane in polymersome membranes. The thickness of the hydrophilic brush and the hydrophobic membrane is usually similar. Polymersomes are self-assembled diblock or triblock copolymers that form spontaneously. A diblock copolymer with a hydrophilic and hydrophobic block typically self-assembles in water to create a vesicle with 10–15-nm-thick shells. LBL assembly begins with a sacrificial core covered with polyelectrolyte layers in sequential order. The core is dissolved in acidic liquid once the necessary layers have been deposited. Hollow microcapsules result from repeated washings. Microcapsules have been extensively explored for a variety of uses, including bioimaging (Berezin 2015) (Fig. 6.4).

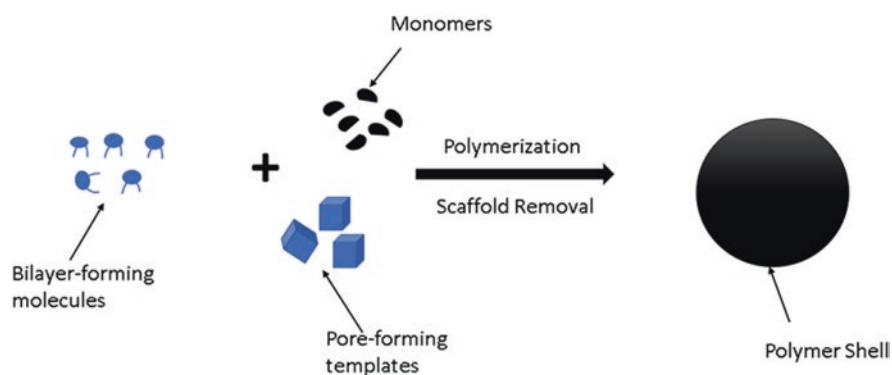


Fig. 6.4 An overview of the vesicle-templated synthesis of NCs. (Berezin 2015)

6.2.4.2 Lipid-Based NHs

Liposomes have been recognized as promising vehicles for delivering a wide range of encapsulated and/or membrane-associated therapeutic or diagnostic agents into the required areas for nearly three decades (Gregoriadis et al. 1974; Papahadjopoulos 1988; Lasic 1998), and micelle-loaded imaging agents have also shown great clinical promise in recent years. These nanocarriers have been exploited to transport diagnostic moieties for all imaging modalities, including gamma scintigraphy, magnetic resonance imaging (MRI), computed tomography (CT) imaging, and sonography (Berezin 2015; Inf 1996).

Liposomes are bilayered phospholipid vesicles with a size range of 50–1000 nm that can be loaded with a variety of water-soluble cargos (into their inner aqueous compartment) and water-insoluble molecules (into the hydrophobic compartment of their phospholipid membrane) and have been considered as promising drug carriers for over three decades. The use of targeted liposomes, or liposomal carriers that accumulate precisely inside the damaged organ or tissue, would improve the efficacy of the liposome-incorporated medicine while reducing the loss of its contents in the reticuloendothelial system (RES) (Torchilin 2007). Micelles are amphiphilic compound-formed colloidal particles with a hydrophobic core and a hydrophilic corona, ranging from 5 to 100 nm (Kakizawa and Kataoka 2002), a remarkable potential to improve the solubility and bioavailability of poorly soluble medicines (Torchilin 2007). The usage of certain amphiphilic compounds as micelle-building components, such as polyethylene glycol (PEG)-phosphatidylethanolamine (PE), can lengthen the micellar carrier's blood half-life.

Furthermore, the micelles might be coupled with various targeting ligands and carefully inserted into the micelle structure to create targeted micelles. For the efficient synthesis of micelle-incorporated medicines and imaging agents, many fundamental micelle properties (size, critical micelle concentration (CMC), and loading capacity of the hydrophobic core of the micelle) are required (Torchilin 2005).

The following criteria were established as the main characteristics of a successful lipid nanovesicle labeling method: sufficient shelf stability of the labeled formulation; (ii) high labeling efficiency; (iii) convenient and efficient labeling at room temperature; (iv) use of readily available isotopes and metals with good physical imaging characteristics, dosimetry, and half-life; and (v) reasonable *in vitro* and *in vivo* label association stability (Berezin 2015) (Table 6.1 and Fig. 6.5).

6.2.4.3 Cellulose-Supported Magnetic NHs

Cellulose is a linear syndiotactic homopolymer of around 1500 D-anhydroglucopyranose rings linked by β -(1–4)-glycosidic linkages. The reasons for cellulose's employment as a support material for CSMN synthesis can be divided into three categories: The C2, C3, and C6 locations on the cellulose backbone are densely packed with secondary and primary hydroxyl groups. As a result, CSMNs can be made by forming covalent bonds between MNPs and the cellulose backbone

Table 6.1 Lipid-based NHs for bioimaging applications

| Sr. no. | Structural nanocomponent | Functional nanocomponent |
|---------|--|---|
| 1 | Phospholipid liposome | Gold nanoparticle (optical imaging) |
| 2 | Phospholipid liposome (calcein) | Gold nanoparticle (photothermal heating-triggered drug release) |
| 3 | Phospholipid liposome (6-carboxyfluorescein) | Gold nanoparticle (photothermal heating-triggered drug release) |
| 4 | Phospholipid liposome (xylenol orange sodium salt) | Magnetic nanocrystal (MRI) |
| 5 | Phospholipid liposome (5,6-carboxyfluorescein) | Magnetic nanocrystal (electromagnetic heating-triggered drug release) |
| 6 | Phospholipid liposome (doxorubicin or cysteine protease inhibitor JPM-565) | Magnetic nanocrystal (MRI and magnetic targeting) |

through stable electrostatic interactions in a homogenous solvent system, whereas cellulose nucleation can be done in a heterogeneous solvent system. The hydroxide groups on cellulose backbones are useful for hybridization with MNPs, but they can also be used to insert chemically crosslinkable functional groups via derivatizing reactions. Covalently functionalized cellulose can be employed alone or crosslinked with other functional macromolecules to form diverse CSMNs.

CSMN synthesis can be divided into three categories:

All forms of cellulose-supported magnetic NHs (CSMNs) are synthesized using a chemical mechanism. Varied CSMN forms, on the other hand, have different designs depending on whether the solvent system is homogenous or heterogeneous. The synthesis of CSMNs consists of four processes, as illustrated schematically in Fig. 6.6: (1) cellulose solubilization, (2) MNP hybridization, (3) isolation of CSMNs from the reaction mixture, and (4) phase transition (drying). The primary and determining stage in the production of distinct CSMNs is the solubilization of cellulose. It's a mechanism in which cellulose in a solvent system dissolves to establish homogeneity, resulting in three-dimensional (3D) CSMNs via MNP encapsulation, or assembles with a heterogeneous surface, resulting in one- and two-dimensional (1D and 2D) CSMNs via MNP nucleation. Micro-/nanocellulose (MCC, CNC, and CNF) creates heterogeneity with water and contributes to the development of 1D and 2D CSMNs due to its weak solubility. On the other hand, cellulose becomes soluble for two reasons:

- (i) When it is submerged in a pre-cooled (between 5 and 20 degrees Celsius) mixture of distilled water, urea, and alkali hydroxide at room temperature. At low temperatures, urea and alkali hydrates have a considerable impact on cellulose dissolution.
- (ii) When it undergoes selective surface modification such as carboxylation, methylation, ethylation, amination, and so on, depending on the temperature of the solvent, the amount of urea, and the hydroxide concentration of the alkaline species. As a result, MNPs are encapsulated using homogenous cellulose mixes that have been created (Haniffa et al. 2021) (Table 6.2).

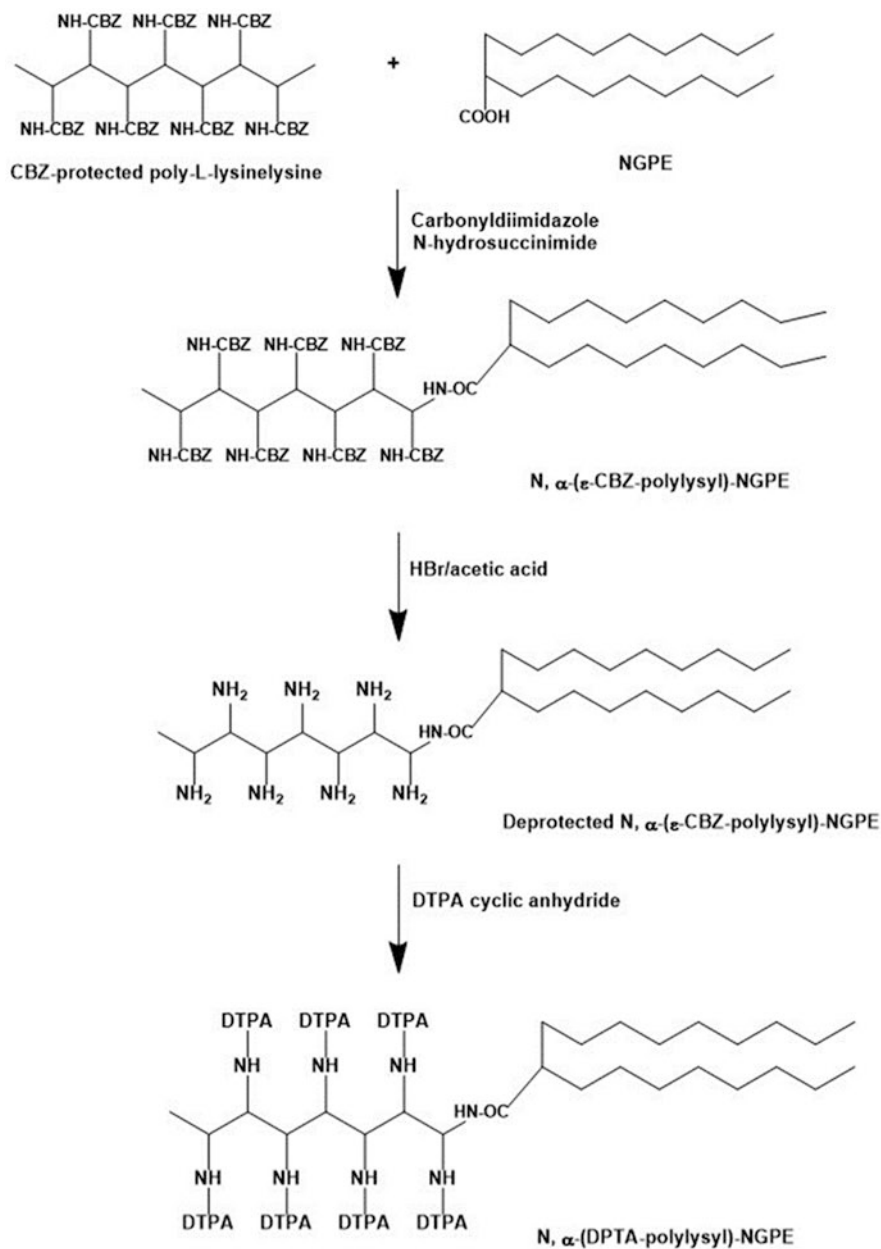


Fig. 6.5 Example of synthesis of amphiphilic polychelator N,N-(diethylene triamine penta-acetic acid, poly-L-lysine)glutaryl phosphatidylethanolamine (DTPA-PLL-NGPE). (Berezin 2015)

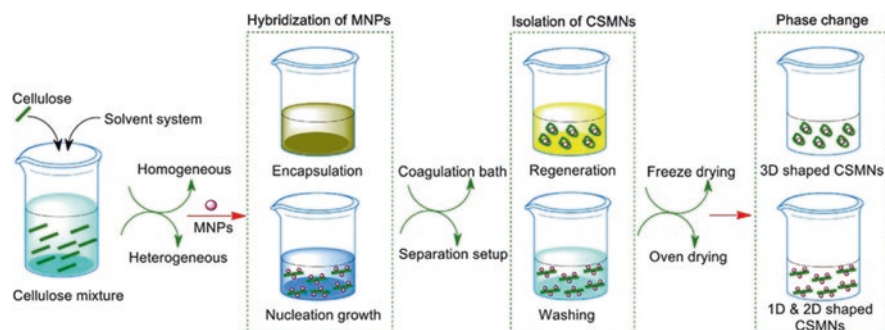


Fig. 6.6 Schematic of the preparation of cellulose-supported magnetic nanohybrids through four basic steps: cellulose solubilization, MNP hybridization, CSMN isolation, and phase change method. (Haniffa et al. 2021)

6.2.5 Virus Nanoparticles (VNPs)

VNPs generated from plants or microorganisms are an excellent starting point for developing targeted imaging agents and drug delivery vehicles (Steinmetz 2010). VLPs are a subset of VNPs that can be created in a heterologous expression system. VNPs and VLPs are systems that self-assemble and are highly symmetrical, dynamic, polyvalent, and monodisperse, allowing them to be used in various applications.

VNPs have been developed and used in medicine for a long time, and each one is unique. The platform can be customized to do specific tasks. Brome mosaic virus (BMV), cowpea chlorotic mottle virus (CCMV), and cowpea mosaic virus are examples of plant-based VNPs. VNPs derived from bacteriophages, such as HK97, M13, and others, are obtained in large amounts from plants, but VNPs derived from bacteriophages, such as MS2 and Q can be made in gramme quantities from the bacteria *Escherichia coli*. Because of their high dynamic character, VNPs can go through transitions that create pores inside the protein capsid, allowing access to the interior. Efforts to encapsulate have been created to introduce guest molecules into the interior of the capsid. As an example, the structure of the CCMV and red protein cages was studied using a technique known as gating. The pH and metal content of the red clover necrotic mosaic virus (RCNMV) can be altered. Ion concentration is used to manage the loading or release of cargo molecules from the inside. Encapsulation can also be performed by disassembling and reassembling components. VNP protein subunits can be biochemically changed or genetically engineered for specific functionalization due to their structure and physicochemical properties. Many bio-orthogonal chemistries have been discovered and created to allow pharmacological cargos, targeting ligands, and/or imaging moieties

Table 6.2 Cellulose-supported magnetic nano hybrids for bioimaging

| Matrix | MNPs | Solvents | Technique | Shape | Size |
|-------------------------------|--|--|--------------------------------|--|------------------|
| Carboxymethyl cellulose | Co _{0.25} Cu _{0.25} Mn _{0.5} Fe ₂ O ₄ | Deionized water | Co-precipitation | Nanorods | – |
| Reduced graphite oxide | NiCl ₂ ·6H ₂ O | Deionized water | Grafting and doping techniques | Nanocomposite (ferromagnetic material) | 10–60 nm |
| Bacterial cellulose pellicles | Fe ₃ O ₄ | Deionized water | In situ precipitation | Magnetic hydrogel | 49.81 ± 20.77 nm |
| Cellulose nanocrystals | Fe ₃ O ₄ /Ag | [Bmm]Cl/AgNO ₃ solution (30 ml, 250 mM) | In situ co-precipitation | Nanocomposite films | 18–30 nm |

to be loaded. Genetic engineering involves adding amino acids to the viral capsid to act as ligation handles, introduction of peptide-based affinity tags for purification and bioconjugation, and the use of cell-specific targeting ligands for delivery (Berezin 2015).

Because humans are not the natural hosts for viruses, VNPs generated from plants and bacteriophages are safe to employ in humans. Plant-derived CPMV, CCMV, and PVX nanoparticles and Q and M13 bacteriophage particles are found in a range of tissues throughout the body, with accumulation and clearance occurring through the liver and spleen (RES organs) (Prasuhn et al. 2008). Despite their widespread biodistribution, no toxicity or clinical signs have been reported in mice after VNPs were given at doses of up to 100 mg/kg body weight (Singh et al. 2007; Kaiser et al. 2007). The immunogenicity of the protein coat is a potential disadvantage of using VNPs. The conjugation of PEG, an FDA-approved polymer that is nontoxic, neutrally charged, and strongly hydrophilic, can lower the chance of an immunogenic reaction. PEGylation is a widely utilized technique for improving the solubility and stability of nanocarriers containing hydrophobic medicines, minimizing biospecific interactions and nonspecific absorption, and lengthening the time spent in the bloodstream (Steinmetz 2010; Van Vlerken et al. 2007). Most of the studies of these VNP contrast compounds have been done in test tubes in the laboratory setting rather than in vivo.

However, because these VNP constructions have been proven safe and biocompatible, there is definite potential for their translation into the clinic. Direct binding at the interface between coat protein subunits, covalent attachment to the exterior and inner surface, and complexation with RNA molecules within the capsid are potentials for Gd³⁺ incorporation into VNPs. These approaches resulted in

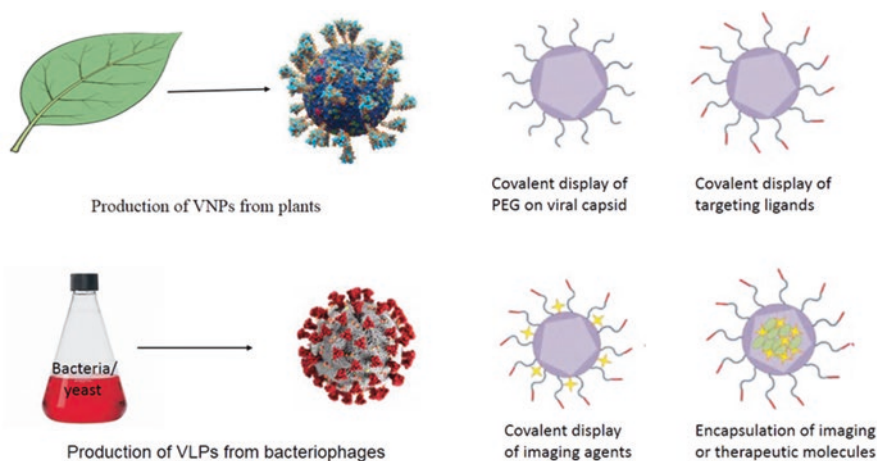


Fig. 6.7 Production and chemical engineering of VNPs. (Berezin 2015)

formulations with considerable increases in relaxivity that are highly promising for clinical usage in the future (Van Vlerken et al. 2007; Berezin 2015) (Fig. 6.7).

6.3 Characterizations of Nanohybrids

The expeditious evolution of nanoparticles for biomedical applications is hugely dependent on the theoretical and instrumental analytical fundamentals augmented in the past decade. The electron microscopy methods existed before the escalation of nanoparticles, such as scanning electron microscopy (SEM) and transmission electron microscopy (TEM) along with inductively coupled plasma mass spectrometry (ICP-MS), which are then embraced by bioimaging bodies. Together with nanoparticle analysis, the biocompatibility of the imaging nanoparticles to humans has to be studied in terms of absorption, biodistribution, etc., before implementation in actual applications for which hydrodynamic size, toxicity, and surface charge were employed. Furthermore, to evaluate the mechanisms of magnetic nanoparticle's cellular uptake and transport, advances in instrumentation have emerged several methods such as elemental analysis, size analysis, biological impacts, and magnetic properties. Table 6.3 summarizes the common methods for analysis for the bioimaging nanoparticles and their output in terms of different results. The specific and important characterization techniques for identifying elements and their quantification, morphology, and magnetic properties are briefly discussed here.

6.3.1 ICP-MS and ICP-OES

ICP-MS uses an inductively coupled plasma to ionize the sample, unlike the common mass spectroscopy technique. The small atomic and polyatomic ions are created through the atomization of the sample, which are then analyzed. It is prevalent because of its accuracy in detecting low concentrations of metals and non-metals in liquid samples. It is also used in isotopic labeling, where it can detect the isotopes of the same elements. The ICP-MS is not valid for the analysis of the elements which produce negative ions. Also, it cannot be utilized to detect noble gases or the elements like oxygen, carbon, nitrogen, and hydrogen. The organic nanoparticles are also one of the exceptions for being analyzed by ICP-MS as during analysis, all compounds are broken down into constituent elements. But, if the molecule persists a characteristic element or any tracer which ICP-MS could detect, the sample can be analyzed (e.g., sulfur in the thiols).

On the other hand, ICP-OES is a straightforward and powerful atomic spectroscopy technique that provides a harmonizing tool to ICP-MS. A liquid sample is drawn out and injected into argon plasma, breaking the sample down into constituent atoms, similar to ICP-MS. Nevertheless, ICP-OES uses optical emissions emitted from the excited atoms in the sample to detect the elements and not the

Table 6.3 Bioimaging magnetic nanoparticles and common methods of analysis

| Sr. no. | Method | Particle and hydrodynamic size | Concentration | Elemental analysis and composition | Surface charge | Shape | Quality control | Reporting activity |
|---------|--|--------------------------------|---------------|------------------------------------|----------------|-------|-----------------|--------------------|
| 1 | Inductively coupled plasma mass spectrometry (ICP-MS) | | ✓✓✓ | ✓✓✓ | | | ✓ | |
| 2 | Inductively coupled plasma optical emission spectroscopy (ICP-OES) | | | ✓✓✓ | | | | |
| 3 | Energy-dispersive X-ray spectroscopy (EDS) | | | ✓✓✓ | | | | |
| 4 | Scanning electron microscopy (SEM) | ✓✓✓ | | | | | | |
| 5 | Transmission electron microscopy (TEM) | ✓✓✓ | | | | | | |
| 6 | Dynamic light scattering (DLS) Zeta potential | ✓✓✓ | | | ✓✓✓ | | ✓ | |
| 7 | X-ray diffraction (XRD) | ✓✓ | ✓ | ✓✓✓ | ✓ | | ✓ | ✓✓✓ |
| 8 | Steady-state absorption | | ✓✓✓ | | | | ✓✓✓ | ✓✓✓ |
| 9 | Steady-state emission | | ✓✓✓ | | | | ✓✓✓ | ✓✓✓ |
| 10 | Fluorescence anisotropy Fluorescence lifetime (FLT) | ✓✓ | | | | ✓ | ✓ | ✓✓ |
| 11 | Fluorescence correlation spectroscopy (FCS) | ✓✓ | ✓✓✓ | | | | | |
| 12 | Raman spectroscopy | | | ✓✓ | | | | |
| 13 | Fourier transform near-infrared spectroscopy (FT-NIRS) | | | ✓✓ | | | | |
| 14 | Nuclear magnetic resonance (NMR) | ✓ | | ✓✓✓ | | | ✓ | ✓✓ |

(continued)

Table 6.3 (continued)

| Sr. no. | Method | Particle and hydrodynamic size | Concentration | Elemental analysis and composition | Surface charge | Shape | Quality control | Reporting activity |
|---------|-------------------------------------|--------------------------------|---------------|------------------------------------|----------------|-------|-----------------|--------------------|
| 15 | Quartz crystal microbalances | | ✓ | | | | | |
| 16 | Electrophoresis, gel, and capillary | ✓✓ | ✓ | | ✓ | | ✓✓✓ | |
| 17 | Radiography | | ✓✓✓ | | | | ✓✓✓ | |

Note: ✓✓✓ extensively used, ✓✓ used, ✓ rarely used

mass-to-charge ratio like MS. The magnitudes of the detection limits are always one order higher than that of the ICP-MS, which cannot even determine the isotopic ratios. At the same time, the concentration limits for ICP-OES are higher than ICP-MS, which can tolerate the concentrated buffer and saline solutions. In an ICP-OES, the full spectrum of emissions is gathered through a viewing window from each element, releasing the emissions at specific characteristic wavelengths. These wavelengths are then eventually divided with the help of gratings, followed by the detection using CCD. It is very challenging to discriminate between the mass of an element in particle form and the mass of the same element suspended in the liquid, being the disadvantage of atomic spectroscopy analysis.

In one of the studies, Zhang et al. produced a magnetic nanohybrid involving the non-steroid anti-inflammatory drug diclofenac (DIC) intercalated Mg-Al layered double hydroxides (LDH) coated on magnesium ferrite particles via a one-step co-precipitation self-assembly method. The chemical formula of the magnesium ferrite ($\text{MgFe}_{1.03}\text{O}_{2.54}$) was derived from the ICP analysis (Zhang et al. 2009). Moreover, Kutzesnova et al. used ICP-MS to understand serum protein-mediated transformations of magnetic nanoparticles (Kuznetsova et al. 2021). Figure 6.8 shows the general schematic representation of the ICP spectrophotometer (Fernández-Sánchez 2019).

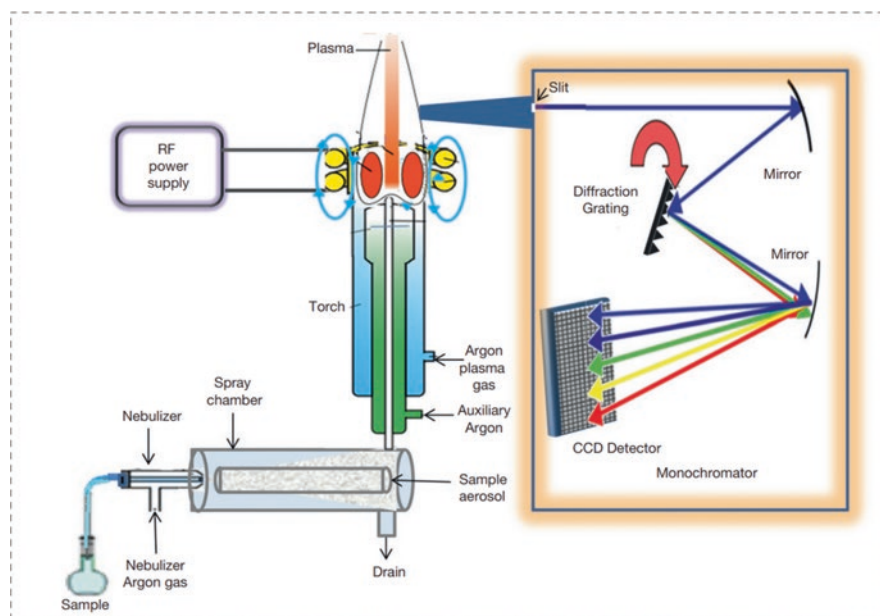


Fig. 6.8 Schematic representation of ICP spectrophotometer. (Reproduced from Fernández-Sánchez (2019) with permission from Elsevier)

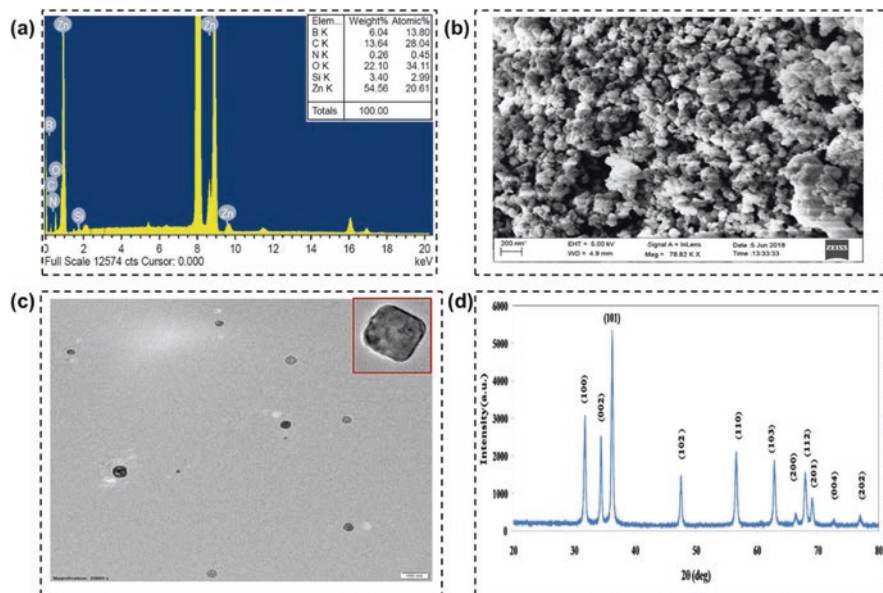


Fig. 6.9 (a) TEM, (b) SEM, and (c) EDX of ZnO-PBA-curcumin nanohybrids and (d) XRD analysis of ZnO NPs. (Reproduced from Kundu et al. (2019) with permission from Elsevier)

6.3.2 EDS

Energy-dispersive X-ray spectroscopy (EDS) is a very distinct technique frequently used jointly with electron microscopy where the electron beam from scanning electron microscope (SEM) or transmission electron microscope (TEM) is employed to excite the sample and emitted X-rays are detected as an electric signal. The characteristic element composed within the sample gets detected depending upon the associated energy of the X-rays. Unlike other atomic spectroscopy techniques, EDS has high detection limits. The elements with a concentration of more than 10% of the sample's weight are identifiable in EDS. Furthermore, this technique is capable of determining most of the elements heavier than beryllium like nitrogen, carbon, or oxygen. Hence, the quantitative analysis data from EDS offers the percent relative compositions of the samples. Figure 6.10c depicts the schematic representation of EDS, and Fig. 6.9a shows the X-ray spectrograph of curcumin-loaded ZnO nanoparticles (ZnO-PBA-curcumin) (Kundu et al. 2019). Studies have concluded that the EDS signals are delicate to sample height, where polished surfaces are preferred. In the case of amorphous powders or particles, the samples should be uniformly distributed over the flat surface for analysis. The multidimensional resolution achieved in EDS is in microns, and hence, the technique is occasionally used for the nanoparticles' study.

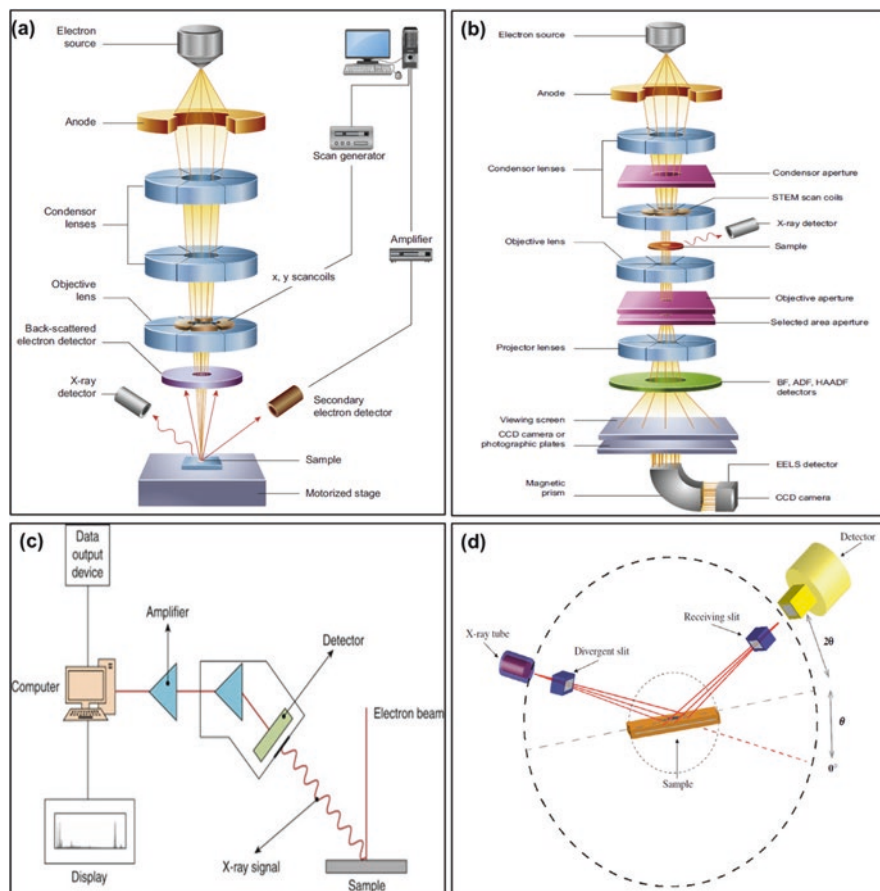


Fig. 6.10 Schematic representations of setups of (a) SEM, (b) TEM, (c) EDS, and (d) XRD. (Reproduced from Inkson (2016), Colpan et al. (2018), and Falsafi et al. (2020) with permission from Elsevier)

6.3.3 SEM and TEM

SEM is a surface imaging technique commonly used to determine the size and form of nanoparticles. In a SEM, electrons are fired at voltages ranging from less than 1 kV to about 30 kV into a sample in a vacuum chamber. The electrons hit the sample and are reflected toward detectors above and to the sides of the sample, where a CCD camera records an image. Figure 6.10a depicts an example of the instruments. The signal from low-energy secondary electrons is collected for most SEM imaging. Contrast is formed primarily by contours and surface features of the sample that modify the trajectory of the reflected secondary light, giving these images a three-dimensional (3D) look. Securing particles to a flat, conductive substrate is an essential element of particle sample preparation for SEM.

Carbon tape is frequently used to attach particles in a dry powder form to a standard aluminum stub. Drop-cast or spin-coated particles in liquid suspensions are commonly placed on a piece of the silicon wafer and allowed to dry before imaging. Because charging effects in SEM are sensitive, non-conductive materials that might build charge are routinely sputter-coated with a tiny layer of conductive material like gold. Charging effects on non-conductive samples can be mitigated by utilizing lower accelerating voltages or the low-vacuum or ambient mode available on some SEMs when sputter coating is not desired. Charging effects on non-conductive samples are avoided in low-vacuum mode by adding water or solvent vapor into the sample chamber, although at some resolution and contrast.

The transmission electron microscope (TEM) is one of the most widely used methods for characterizing nanoparticles because it can produce high-resolution images of particles ranging in size from a few nanometers to hundred nanometers. In a TEM, electrons have been fired at voltages ranging from 20 kV to about 120 kV toward a fragile specimen (hundreds of nanometers or more minor) within a high vacuum. The electrons interact with the specimen, and an impression is established from the electrons that are transmitted through the specimen and concentrated onto a focal plane situated below the specimen holder. Figure 6.4 depicts an example of a TEM instrument. A CCD camera collects the focused image in most current TEMs. Because this approach uses electrons that have passed through a sample, the picture generated is a two-dimensional (2D) profile, which enables straightforward measurement of particle diameter or edge length in multiple particle samples. However, because TEM is a high-resolution technology, the field of view is restricted, making gathering statistically significant numbers of particle sizes time-consuming. As a result, TEM is frequently used to corroborate morphology and sizing data acquired through other approaches.

Drop casting or dip coating of particles in a solution onto a typical carbon-coated copper grid and leaving them to dry is a standard method of particle sample preparation for TEM. A negative staining technique frequently follows the drop casting or dip coating of organic particles. A cryogenic sample holder can be used to photograph particles frozen in liquid nitrogen for particles that cannot resist drying. Intracellular characteristics of cell and tissue samples are also imaged using TEM. Nanoparticles in cell and tissue specimens may occasionally be imaged; however, this involves significant sample processing, comprising fixation, polymerization, ultrathin slicing, and negative staining. Finding nanoparticles can be time-consuming because most tissues and cell specimens are evaluated in microns or millimeters. Similarly, this method is ineffective for particles that are difficult to identify from naturally produced organelles and biological characteristics.

The study mentioned earlier by Kundu et al. (2019) also reports the SEM and TEM analysis (Fig. 6.9a, b) of the ZnO-PBA-curcumin nanohybrids to determine the size and shape. The nanoparticles had a tetragonal shape with an average of 30–40 nm size. According to the TEM investigation, there was no substantial variation between ZnO and ZnO-PBA-curcumin.

6.3.4 XRD

Constructive interference between monochromatic X-rays and a crystalline sample is the foundation of X-ray diffraction (Fig. 6.10d). A cathode-ray tube produces the X-rays, filtered to create monochromatic radiation, collimated to focus the beam, and aimed onto the sample. When Bragg's law ($n = 2d \sin$) is satisfied, constructive interference (and a diffracted ray) results from the interaction of incident rays with the specimen. This rule relates the wavelength of electromagnetic radiation to the diffraction angle and lattice spacing in a crystalline specimen. Following that, the diffracted X-rays are detected, analyzed, and tallied. Caused by random alignment of the powders, scanning the specimen across a range of two angles should provide all conceivable lattice diffraction patterns. Since each material has a set of different d-spacings, converting the diffraction peak to d-spacings permits recognition of the material. D-spacings are often compared to conventional reference patterns to accomplish this.

The most common use of X-ray powder diffraction is the detection of unidentified crystal structures (e.g., minerals, inorganic compounds). Determining unfamiliar solids is crucial in geology, earth sciences, material science, engineering, and biology. Other uses include (i) crystalline substance characterization, (ii) unit cell dimension measurement, (iii) detection of perfectly all right materials such as clays and mixed layer clays that are difficult to discern visually, and (iv) sample purity testing. One of the studies mentioned above also mentions the XRD analysis for ZnO NPs, as shown in Fig. 6.9d. All of the peaks found suggest that ZnO NPs have a hexagonal crystalline structure free of contaminants.

6.3.5 Magnetic Properties of Nanohybrids

The magnetic resonance imaging (MRI) system comprises several elements that make it possible to create the required results. The magnet, shim coils, gradient coils, radio-frequency (RF) coils, amplifier systems, RF transmission and receiving electronics, and computer systems that synchronize the elements, operate the electronics, and analyze the image data are all examples of these aspects. The MRI magnet generates a vast, homogenous magnetic field, represented by B_0 . The highest current field strength in clinical imaging is 3.0 T, while prototype scanners may reach 7 T.

The magnetic resonance imaging (MRI) system consists of various components working together to form the desired images. These components include the magnet, shim coils, gradient coils, radio-frequency (RF) coils, amplifier systems, RF transmission and receiving electronics, and computer systems that synchronize the components, control the electronics, and process the imaging data. The MRI magnet produces a large uniform magnetic field, denoted as B_0 . The maximum field strength currently used in clinical imaging is 3.0 T, whereas experimental scanners may

exceed 7 T. Gradient coils within the magnet's bore provide non-static magnetic fields that disturb B_0 in the x -, y -, and z -axes. The RF coil is also situated inside the magnetic bore to produce an oscillatory magnetic field B_1 perpendicular to B_0 . To have a simple example, the RF coil functions as an antenna, generating and receiving the signals that'll be utilized to form the image.

Vibrating Sample Magnetometry (VSM)

The VSM uses Faraday's law of induction to detect the emf,

$$\varepsilon = N \frac{d}{dt} (BA \cos \vartheta)$$

with N equaling the count of wire turns and A equaling the area and where ϑ is the angle between the coil's standard and the B field. However, if the VSM is appropriately calibrated, N and A are frequently unneeded. The external magnetic field is swept from high to low and returned to high by adjusting the intensity of the electromagnet using computer software. Typically, this is done using a software program, and a data cycle is written out. The electromagnet is usually mounted on a revolving base so that measurements may be made as a function of angle.

As the sample is dragged up and down, the magnetic dipole moment of the sample produces a magnetic field, which varies over time (Fig. 6.11(i)). A piezoelectric substance is often used to accomplish this. Inside the receiver coils of the VSM, the oscillating magnetism causes an electric field. The induced current is proportionate to the sample's magnetism; the higher the current, the higher the magnetization.

Narayanan et al. (2012) have utilized green chemistry to make magnetite/gold ($\text{Fe}_3\text{O}_4/\text{Au}$) hybrid nanoparticles from a single iron precursor (ferric chloride) utilizing grape seed proanthocyanidin as the reducing agent. Researchers determined their magnetization properties by measuring the magnetic saturation of bare and hybrid $\text{Fe}_3\text{O}_4/\text{Au}$ nanoparticles at room temperature. The magnetization curves for bare Fe_3O_4 and $\text{Fe}_3\text{O}_4/\text{Au}$ nanoparticles are shown in Fig. 6.11(ii). The hysterical, sigmoidal curve confirms the superparamagnetic character of the as-synthesized bare and hybrid samples without coercivity and remanence in magnetism. At 25 °C, the saturation magnetization (M_s) of Fe_3O_4 nanoparticles was 56.57 emu/g. The magnetism of the nanohybrids, on the other hand, was lowered to 48.6 emu/g, attributable to the diamagnetic characteristic of Au.

Relaxation

The method by which protons relax back to equilibrium along the z -axis after a revolution of the proton's magnetization more toward the x - y plane is known as longitudinal relaxation or spin-lattice relaxation. Longitudinal relaxation is a condition characterized by proliferation.

$$M_z = M_z^0 \left(1 - e^{-t/T_1}\right)$$

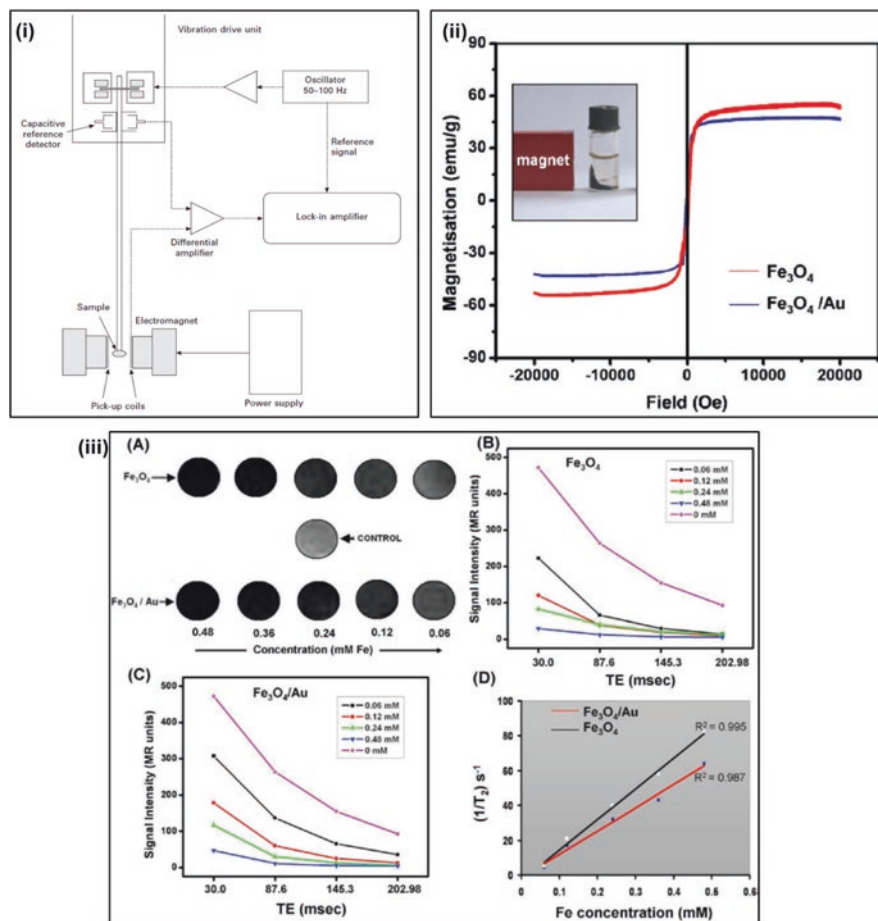


Fig. 6.11 (i) Schematic of the setup of VSM, (ii) magnetization curve of Fe_3O_4 and $\text{Fe}_3\text{O}_4/\text{Au}$ hybrid nanoparticles, and (iii) MR imaging. (a) T2-weighted MR phantom images of Fe_3O_4 and $\text{Fe}_3\text{O}_4/\text{Au}$ hybrid nanoparticles with reference to control. (b, c) Signal intensity vs. TE plots for Fe_3O_4 and $\text{Fe}_3\text{O}_4/\text{Au}$ hybrid nanoparticles, respectively, and (d) T2 relaxation rate ($1/T_2$) plotted against varying Fe concentrations. (Reproduced from Narayanan et al. (2012) and Thomson (2013) with permission from Elsevier)

where M_z^0 is the equilibrium proton magnetization, M_z is the magnetization along the z-axis at time t , and T_1 is the time constant for longitudinal relaxation. Another relaxation process is called transverse relaxation or spin-spin relaxation. This process occurs when protons exchange energy but do not lose energy to their surroundings. This results in loss of proton magnetization in the transverse plane but does not necessarily generate magnetization along the z-axis.

$$M_{xy} = M_{xy}^0 \times e^{-t/T_2}$$

M_{xy}^0 denotes the starting transverse magnetism, M_{xy} denotes the transverse magnetic polarity at time t , and T_2 is the transverse relaxation constant value. Imperfections in the main magnetic field, in conjunction with T_2 relaxation, have a role in transverse magnetization degradation. T_2^* is the time constant for the interaction of these two components, and it is given by

$$\frac{1}{T_2^*} = \frac{1}{T_2} + \frac{1}{T_2^{\text{inhomo}}}$$

The results from the study as mentioned earlier by Narayanan et al. (2012) showed that with increasing Fe concentrations, an unusual darkening (with decreasing signal strength) and hence negative contrast were detected in the T_2 -weighted pictures of bare and hybrid $\text{Fe}_3\text{O}_4/\text{Au}$ nanoparticles in the phantom gels (Fig. 6.11(iii) a–c). Although the concentration vs. signal intensity curves for both hybrid and bare nanoparticles had a similar trend, the latter had a more excellent dark contrast when compared to the control agar gel. The relaxation rate ($1/T_2$) was also shown to vary linearly with iron concentration (as shown in Fig. 6.11(iii) d).

6.4 Conclusion

Conjugation and overcoating have already produced novel features that are changing fundamental physicochemical parameters. As a result of these variations, NHs' behavior will be altered, necessitating careful study and strategizing for systematic evaluation. When NH-landed, real-world applications are marketed in electronics (e.g., silicon oxycarbide-CNTs and CNF-lithium titanate NHs for Li-ion electrodes), dentistry-related products, antimicrobial coatings and protective devices (e.g., Ag-TiO₂), and bioimaging or graphene-based MRI contrast agents, their environmental exposure appears to be more. The main question is how the NHs' distinctive affects environmental health and safety (EHS) (Aich et al. 2014).

The next generation of NHs will have more complex hierarchical structures, with NMs from more than two chemical origins coupled, for example, CdS/ZnS-Au, MWNT/Ag-TiO₂, or CdS-TiO₂-Fe₃O₄ (Aich et al. 2014). As a result, there is a possibility of endless combinations and functionalization of NMs. It is possible to formulate a strategy during the selection of material qualities and structural integrity exposure to the environment or targeting specific groups based on increased danger potential as a result of the component behavior. Such methods, on the other hand, demand precise and well-thought-out plans. Prior to formalization, systematic research considering EHS need to be conducted.

References

- Adedoyin AA, Ekenseair AK. Biomedical applications of magneto-responsive scaffolds. *Nano Res.* 2018;11:5049–64. <https://doi.org/10.1007/s12274-018-2198-2>.
- Aich N, Plazas-Tuttle J, Lead JR, Saleh NB. A critical review of nanohybrids: synthesis, applications and environmental implications. *Environ Chem.* 2014;11:609–23. <https://doi.org/10.1071/EN14127>.
- Banner LT, Danila DC, Sharpe K, et al. Controlled loading of building blocks into temporary self-assembled scaffolds for directed assembly of organic nanostructures. *Langmuir.* 2008;24:11464–73. <https://doi.org/10.1021/la801755b>.
- Berezin MY. *Nanotechnology for biomedical imaging and diagnostics: from nanoparticle design to clinical applications.* Hoboken: Wiley; 2015.
- Blum AP, Kammeyer JK, Rush AM, et al. Stimuli-responsive nanomaterials for biomedical applications. *J Am Chem Soc.* 2015;137:2140–54. <https://doi.org/10.1021/ja510147n>.
- Cheang-wong JC. Formation of Au – Ag core – shell nanostructures in silica matrix by sequential ion. *J Phys Chem C.* 2009;113:2296–300.
- Chen S, Chen P, Wang Y. Carbon nanotubes grown in situ on graphene nanosheets as superior anodes for Li-ion batteries. *Nanoscale.* 2011;3:4323–9. <https://doi.org/10.1039/c1nr10642b>.
- Chueh YL, Chou LJ, Wang ZL. SiO₂/Ta₂O₅ core-shell nanowires and nanotubes. *Angew Chem Int Ed.* 2006;45:7773–8. <https://doi.org/10.1002/anie.200602228>.
- Colpan CO, Nalbant Y, Ercelik M. Fundamentals of fuel cell technologies. *Compr Energy Syst.* 2018;4–5:1107–30. <https://doi.org/10.1016/B978-0-12-809597-3.00446-6>.
- D'Souza F, Ito O. Supramolecular donor-acceptor hybrids of porphyrins/phthalocyanines with fullerenes/carbon nanotubes: electron transfer, sensing, switching, and catalytic applications. *Chem Commun.* 2009:4913–28. <https://doi.org/10.1039/b905753f>.
- Danila DC, Banner LT, Karimova EJ, et al. Directed assembly of sub-nanometer thin organic materials with programmed-size nanopores. *Angew Chem Int Ed.* 2008;47:7036–9. <https://doi.org/10.1002/anie.200801814>.
- Dergunov SA, Pinkhassik E. Functionalization of imprinted nanopores in nanometer-thin organic materials. *Angew Chem Int Ed.* 2008;47:8264–7. <https://doi.org/10.1002/anie.200803261>.
- Dergunov SA, Schaub SC, Richter A, Pinkhassik E. Time-resolved loading of monomers into bilayers with different curvature. *Langmuir.* 2010;26:6276–80. <https://doi.org/10.1021/la904054f>.
- Falsafi SR, Rostamabadi H, Jafari SM. X-ray diffraction (XRD) of nanoencapsulated food ingredients. Elsevier; 2020.
- Fan JW, Tseng TT, Chen CN, et al. Preparation of ITO/Ag nanohybrid particles by a reverse micellar layer-by-layer coating. *Ceram Int.* 2011;37:43–7. <https://doi.org/10.1016/j.ceramint.2010.08.006>.
- Fan Z, Shelton M, Singh AK, et al. Multifunctional plasmonic shell-magnetic core nanoparticles for targeted diagnostics, isolation, and photothermal destruction of tumor cells. *ACS Nano.* 2012;6:1065–73. <https://doi.org/10.1021/nn2045246>.
- Fernández-Sánchez ML. *Atomic emission spectrometry | inductively coupled plasma.* 3rd ed. Elsevier; 2019.
- Gregoriadis G, Putman D, Louis L, Neerunjun D. Comparative effect and fate of non-entrapped and liposome entrapped neuraminidase injected into rats. *Biochem J.* 1974;140:323–30. <https://doi.org/10.1042/bj1400323>.
- Guldi DM, Taieb H, Rahman GMA, et al. Novel photoactive single-walled carbon nanotube-porphyrin polymer wraps: efficient and long-lived intracomplex charge separation. *Adv Mater.* 2005;17:871–5. <https://doi.org/10.1002/adma.200400641>.
- Gupta AK, Gupta M. Synthesis and surface engineering of iron oxide nanoparticles for biomedical applications. *Biomaterials.* 2005;26:3995–4021. <https://doi.org/10.1016/j.biomaterials.2004.10.012>.

- Hatakeyama H. Recent advances in endogenous and exogenous stimuli-responsive nanocarriers for drug delivery and therapeutics. *Chem Pharm Bull.* 2017;65:612–7. <https://doi.org/10.1248/cpb.c17-00068>.
- Hentze HP, Kaler EW. Polymerization of and within self-organized media. *Curr Opin Colloid Interface Sci.* 2003;8:164–78. [https://doi.org/10.1016/S1359-0294\(03\)00018-9](https://doi.org/10.1016/S1359-0294(03)00018-9).
- Inkson BJ. Scanning electron microscopy (SEM) and transmission electron microscopy (TEM) for materials characterization. Elsevier; 2016.
- Ito A, Hibino ERI, Kobayashi C, et al. *Ten.* 2005a;11:489.
- Ito A, Ino K, Hayashida M, et al. Novel methodology for fabrication of tissue-engineered tubular constructs using magnetite nanoparticles and magnetic force. *Tissue Eng.* 2005b;11:1553–61. <https://doi.org/10.1089/ten.2005.11.1553>.
- Johannessen T, Jensen JR, Mosleh M, et al. Flame synthesis of nanoparticles: applications in catalysis and product/process engineering. *Chem Eng Res Des.* 2004;82:1444–52. <https://doi.org/10.1205/cerd.82.11.1444.52025>.
- Kaiser CR, Flenniken ML, Gillitzer E, Harmsen AL, Harmsen AG, Jutila MA, Douglas T, Young MJ. Biodistribution studies of protein cage nanoparticles demonstrate broad tissue distribution and rapid clearance in vivo. *Int J Nanomedicine.* 2007;2(4):715–33.
- Kakizawa Y, Kataoka K. Block copolymer micelles for delivery of gene and related compounds. *Adv Drug Deliv Rev.* 2002;54:203–22. [https://doi.org/10.1016/S0169-409X\(02\)00017-0](https://doi.org/10.1016/S0169-409X(02)00017-0).
- Kim SD, Choe WG, Jeong JR. Environmentally friendly electroless plating for Ag/TiO_2 -coated core-shell magnetic particles using ultrasonic treatment. *Ultrason Sonochem.* 2013a;20:1456–62. <https://doi.org/10.1016/j.ultsonch.2013.03.011>.
- Kim SH, Jung CH, Sahu N, et al. Catalytic activity of Au/TiO_2 and Pt/TiO_2 nanocatalysts prepared with arc plasma deposition under CO oxidation. *Appl Catal A Gen.* 2013b;454:53–8. <https://doi.org/10.1016/j.apcata.2012.12.049>.
- Kundu M, Sadhukhan P, Ghosh N, et al. pH-responsive and targeted delivery of curcumin via phenylboronic acid-functionalized ZnO nanoparticles for breast cancer therapy. *J Adv Res.* 2019;18:161–72. <https://doi.org/10.1016/j.jare.2019.02.036>.
- Kuznetsova OV, Jarosz M, Keppler BK, Timerbaev AR. Toward a deeper and simpler understanding of serum protein-mediated transformations of magnetic nanoparticles by ICP-MS. *Talanta.* 2021;229:122287. <https://doi.org/10.1016/j.talanta.2021.122287>.
- Lasic DD. Novel applications of liposomes. *Trends Biotechnol.* 1998;16:307–21. [https://doi.org/10.1016/S0167-7799\(98\)01220-7](https://doi.org/10.1016/S0167-7799(98)01220-7).
- Li Y, Gong X, Liu Y, Wu J. Editorial: synthesis, characterization, and applications of magneto-responsive functional materials. *Front Mater.* 2021;8:2020–1. <https://doi.org/10.3389/fmats.2021.710474>.
- Liu H, Wu J, Min JH, et al. Tunable synthesis and multifunctionalities of Fe_3O_4 - ZnO hybrid core-shell nanocrystals. *Mater Res Bull.* 2013;48:551–8. <https://doi.org/10.1016/j.materresbull.2012.11.051>.
- Liu G, Lovell JF, Zhang L, Zhang Y. Stimulus-responsive nanomedicines for disease diagnosis and treatment. *Int J Mol Sci.* 2020;21:1–44. <https://doi.org/10.3390/ijms21176380>.
- Ma X, Tao H, Yang K, et al. A functionalized graphene oxide-iron oxide nanocomposite for magnetically targeted drug delivery, photothermal therapy, and magnetic resonance imaging. *Nano Res.* 2012;5:199–212. <https://doi.org/10.1007/s12274-012-0200-y>.
- Malik N, Arfin T, Khan AU. Graphene nanomaterials: chemistry and pharmaceutical perspectives. Elsevier; 2019.
- Matyjaszewski K, Xia J. Atom transfer radical polymerization. *Chem Rev.* 2001;101:2921–90. <https://doi.org/10.1021/cr940534g>.
- McKelvey CA, Kaler EW. Characterization of nanostructured hollow polymer spheres with small-angle neutron scattering (SANS). *J Colloid Interface Sci.* 2002;245:68–74. <https://doi.org/10.1006/jcis.2001.7999>.

- McKelvey CA, Kaler EW, Zasadzinski JA, et al. Templating hollow polymeric spheres from cationic equilibrium vesicles: synthesis and characterization. *Langmuir*. 2000;16:8285–90. <https://doi.org/10.1021/la000569d>.
- Narayanan S, Sathy BN, Mony U, et al. Biocompatible magnetite/gold nanohybrid contrast agents via green chemistry for MRI and CT bioimaging. *ACS Appl Mater Interfaces*. 2012;4:251–60. <https://doi.org/10.1021/am201311c>.
- Ohno T, Tagawa S, Itoh H, et al. Size effect of TiO₂-SiO₂ nano-hybrid particle. *Mater Chem Phys*. 2009;113:119–23. <https://doi.org/10.1016/j.matchemphys.2008.07.034>.
- Pál E, Hornok V, Sebik D, et al. Optical and structural properties of protein/gold hybrid bio-nanofilms prepared by layer-by-layer method. *Colloids Surf B Biointerfaces*. 2010;79:276–83. <https://doi.org/10.1016/j.colsurfb.2010.04.010>.
- Papahadjopoulos D. Liposome formation and properties: an evolutionary profile. *Biochem Soc Trans*. 1988;16:910–2. <https://doi.org/10.1042/bst0160910>.
- Prasuhn DE, Jr Pratik SS, Strable E, Brown S, Manchester M, Finn MG. Plasma Clearance of Bacteriophage Q β Particles as a Function of Surface Charge, *J Am Chem Soc* 2008;130(4):1328–1334. <https://doi.org/10.1021/ja075937f>
- Qiu L, Peng Y, Liu B, et al. Polypyrrole nanotube-supported gold nanoparticles: an efficient electrocatalyst for oxygen reduction and catalytic reduction of 4-nitrophenol. *Appl Catal A Gen*. 2012;413–414:230–7. <https://doi.org/10.1016/j.apcata.2011.11.013>.
- Richter AG, Dergunov SA, Ganus B, et al. Scattering studies of hydrophobic monomers in liposomal bilayers: an expanding shell model of monomer distribution. *Langmuir*. 2011;27:3792–7. <https://doi.org/10.1021/la105094z>.
- Sánchez-Iglesias A, Carbó-Argibay E, Glaria A, et al. Rapid epitaxial growth of Ag on Au nanoparticles: from Au nanorods to core-shell Au@Ag octahedrons. *Chem A Eur J*. 2010;16:5558–63. <https://doi.org/10.1002/chem.201000144>.
- Shevchenko EV, Bodnarchuk MI, Kovalenko MV, et al. Gold/iron oxide core/hollow-shell nanoparticles. *Adv Mater*. 2008;20:4323–9. <https://doi.org/10.1002/adma.200702994>.
- Singh P, Prasuhn D, Yeh RM, Destito G, Rae CS, Osborn K, Finn MG, Manchester M. Bio-distribution, toxicity and pathology of cowpea mosaic virus nanoparticles in vivo. *J Control Release*. 2007;120(1–2):41–50. <https://doi.org/10.1016/j.jconrel.2007.04.003>.
- Son DI, Kwon BW, Park DH, et al. Emissive ZnO-graphene quantum dots for white-light-emitting diodes. *Nat Nanotechnol*. 2012;7:465–71. <https://doi.org/10.1038/nnano.2012.71>.
- Spanswick J. Controlled/living radical polymerization. *Mater Today*. 2005;8:26–33.
- Steinmetz NF, Manchester M. PEGylated Viral Nanoparticles for Biomedicine: The Impact of PEG Chain Length on VNP Cell Interactions In Vitro and Ex Vivo, *Biomacromolecules* 2009, 2010;4:784–792. <https://doi.org/10.1021/bm801274z>
- Sun M, Fu W, Yang H, et al. One-step synthesis of coaxial Ag/TiO₂ nanowire arrays on transparent conducting substrates: enhanced electron collection in dye-sensitized solar cells. *Electrochem Commun*. 2011;13:1324–7. <https://doi.org/10.1016/j.elecom.2011.08.003>.
- Tagliazucchi M, Blaber MG, Schatz GC, et al. Optical properties of responsive hybrid Au@polymer nanoparticles. *ACS Nano*. 2012;6:8397–406. <https://doi.org/10.1021/nn303221y>.
- Thévenot J, Oliveira H, Sandre O, Lecommandoux S. Magnetic responsive polymer composite materials. *Chem Soc Rev*. 2013;42:7099–116. <https://doi.org/10.1039/c3cs60058k>.
- Thomson T. Magnetic properties of metallic thin films. In: *Metallic films for electronic, optical and magnetic applications*; 2013. <https://doi.org/10.1533/9780857096296.2.454>.
- Tian J, Jin J, Zheng F, Zhao H. Self-assembly of gold nanoparticles and polystyrene: a highly versatile approach to the preparation of colloidal particles with polystyrene cores and gold nanoparticle coronae. *Langmuir*. 2010;26:8762–8. <https://doi.org/10.1021/la904519j>.
- Torchilin VP. Liposomes as delivery agents for medical imaging. *Mol Med Today*. 1996;2(6):242–249. [https://doi.org/10.1016/1357-4310\(96\)88805-8](https://doi.org/10.1016/1357-4310(96)88805-8).
- Torchilin V. Lipid-Core micelles for targeted drug delivery. *Curr Drug Deliv*. 2005;2:319–27. <https://doi.org/10.2174/156720105774370221>.

- Torchilin VP. Micellar nanocarriers: pharmaceutical perspectives. *Pharm Res.* 2007;24:1–16. <https://doi.org/10.1007/s11095-006-9132-0>.
- van Vlerken LE, Vyas TK, Amiji MM. Poly(ethylene glycol)-modified Nanocarriers for Tumor-targeted and Intracellular Delivery. *Pharm Res* 2007;24:1405–1414. <https://doi.org/10.1007/s11095-007-9284-6>
- Wang Y, Kohane DS. External triggering and triggered targeting strategies for drug delivery. *Nat Rev Mater.* 2017;2:17020. <https://doi.org/10.1038/natrevmats.2017.20>.
- Wang H, Zhou S. Magnetic and fluorescent carbon-based nanohybrids for multimodal imaging and magnetic field/NIR light responsive drug carriers. *Biomater Sci.* 2016;4:1062–73. <https://doi.org/10.1039/c6bm00262e>.
- Wang CY, Liu CY, Zheng X, et al. The surface chemistry of hybrid nanometer-sized particles. I. Photochemical deposition of gold on ultrafine TiO₂ particles. *Colloids Surf A Physicochem Eng Asp.* 1998;131:271–80. [https://doi.org/10.1016/S0927-7757\(97\)00086-1](https://doi.org/10.1016/S0927-7757(97)00086-1).
- Wang X, Mitchell DRG, Prince K, et al. Gold nanoparticle incorporation into porous titania networks using an agarose gel templating technique for photocatalytic applications. *Chem Mater.* 2008;20:3917–26. <https://doi.org/10.1021/cm703509f>.
- Wang Q, Tang Y, Wu L, et al. Thermal and magnetic dual-responsive L-proline nanohybrids for aqueous asymmetric aldol reaction. *React Funct Polym.* 2020;149:104508. <https://doi.org/10.1016/j.reactfunctpolym.2020.104508>.
- Wu ML, Lai LB. Synthesis of Pt/Ag bimetallic nanoparticles in water-in-oil microemulsions. *Colloids Surf A Physicochem Eng Asp.* 2004;244:149–57. <https://doi.org/10.1016/j.colsurfa.2004.06.027>.
- Wu W, Shen J, Banerjee P, Zhou S. Core-shell hybrid nanogels for integration of optical temperature-sensing, targeted tumor cell imaging, and combined chemo-photothermal treatment. *Biomaterials.* 2010;31:7555–66. <https://doi.org/10.1016/j.biomaterials.2010.06.030>.
- Zhang H, Pan D, Zou K, et al. A novel core-shell structured magnetic organic-inorganic nanohybrid involving drug-intercalated layered double hydroxides coated on a magnesium ferrite core for magnetically controlled drug release. *J Mater Chem.* 2009;19:3069–77. <https://doi.org/10.1039/b820176e>.
- Zhao X, Mai Z, Kang X, et al. Clay-chitosan-gold nanoparticle nanohybrid: preparation and application for assembly and direct electrochemistry of myoglobin. *Electrochim Acta.* 2008;53:4732–9. <https://doi.org/10.1016/j.electacta.2008.02.007>.
- Zuo Y, Gou Z, Zhang Y, et al. Thermally responsive materials for bioimaging. *Chem Asian J.* 2019;14:67–75. <https://doi.org/10.1002/asia.201801305>.

Chapter 7

Photothermal Nanomaterials for Wound Monitoring and Cancer Biomedicine



Ashwini Shinde, Kavitha Illath, Sayan Deb Dutta, Ki-Taek Lim,
and Tuhin Subhra Santra

7.1 Introduction

The interaction between light and tissue is essential to cognize either during more minor invasive imaging diagnostics or during high-energy laser for lesion removal. The phenomenon of light similar to an external environment like scattering, transmission, absorption, and reflection may also occur during light penetration in tissue (Walsh 2010). Due to changes in enzyme activity, various biological activities are affected by light, such as oxygen consumption (Sarna and Sealy 1984), thermal effect (Walsh 2010), catalysis effect (Hanf et al. 2012), etc. Thus, it is essential to consider all these realities before considering the light on clinical treatments.

The wavelength of light and optical property of tissue is mainly responsible for the light-tissue interaction (Fig. 7.1). But the optical properties of tissue and biomolecules cannot be modified. Thus, the primary focus should be on selecting a particular wavelength of light that can be used for medical purposes. As reported, the accumulated energy due to absorption of light can be used for lesion ablation during surgery, but the thermal effect generated along with this would cause harm to normal cells as well (Sarna and Sealy 1984; Walsh 2010; Hanf et al. 2012). Moreover, scattering, reflection, and absorption are the primary optical activities detected and used in diagnostics.

The study of light-tissue interaction is carried out for three frequently used lights in various wavelengths: X-ray, ultraviolet (UV) light, and near-infrared (NIR) light. Since the 1970s, X-rays ($\lambda = 0.001$ to 10 nm) have been used under strict guidelines

A. Shinde · K. Illath · T. S. Santra (✉)

Department of Engineering Design, Indian Institute of Technology Madras, Chennai, India

S. D. Dutta · K.-T. Lim

Department of Biosystem Engineering, Institute of Forest Science, Kangwon National University, Chuncheon, Republic of Korea

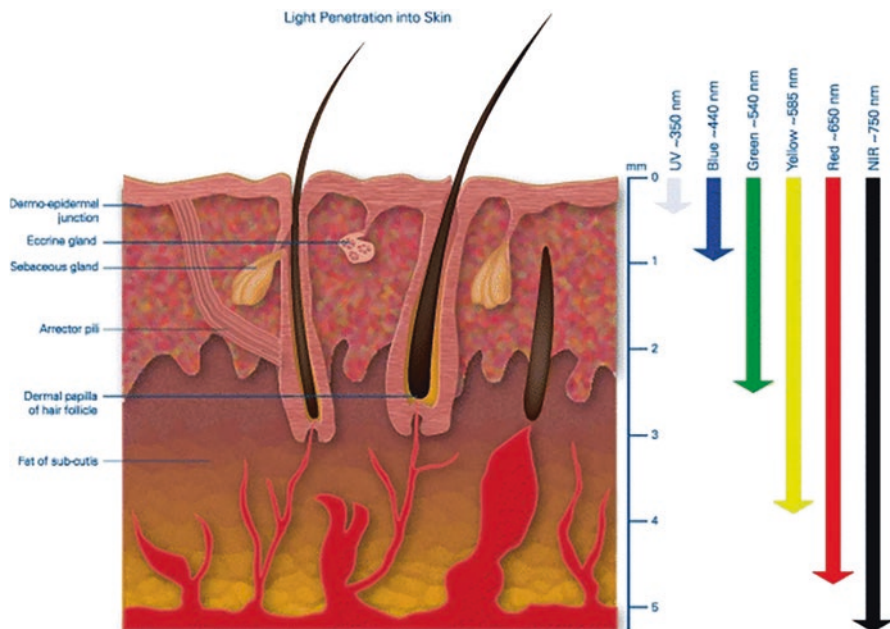


Fig. 7.1 Illustration of various light sources penetrating the skin depth showing different wavelengths penetrating the human skin. [Reproduced with permission from Ash et al. (2017)]

as it provides 3D views of deep body structure. They have high energy and high frequency, which leads to high penetrability. The X-ray with dual energy produces high and low X-rays, which measure muscle mass (Visser et al. 1999) and bone density (Johnson and Dawson-Hughes 1991). High-density metal also can be detected using X-rays. It can be thus used to observe and analyze ablation agents (e.g., gold nanomaterials) (Huang et al. 2011; Tian et al. 2015). However, during tissue-X-ray interaction, primary and secondary electrons are formed by high-energy X-rays. Further, radicals are produced by these excited electrons, resulting in DNA damage and thus cancer development (Cheng and Caffrey 1996; Zhongli Cai et al. 2005).

In the case of UV light, high-affinity absorption is observed by water. This indicates that UV does not penetrate through tissues. Thus, protection from and application of UV are mainly studied on eyes and human skin. The properties of UV light depend on its wavelength. The ozone layer does not filter UV-A (320–400 nm) because of its low energy and long wavelength (Ju et al. 2015). Thus, it reaches the earth's surface and penetrates deep into the skin. The UV-B (280–320 nm) can penetrate only the upper layer of the epidermis. While UV-C (200–280 nm) can barely pass through the ozone layer, its high energy can lead to eye or skin burns. Long-term exposure to UV light can cause aging, erythema, skin wrinkling, sunburn, immune system suppression, cancer, etc. Yet, UV light has been used in phototherapy. It is reported that neuropeptides, cytokines, and some different natural

molecules are induced *in vivo* due to UV light exposure, which helps in the improvement of the immunosuppressive or anti-inflammatory effect of human skin (M. Maestro et al. 2011; Ju et al. 2015). Unlike visible and UV light, NIR light is regarded as an acceptable candidate as a stimulation source. This is because the NIR light with low power can penetrate tissues deeply without causing severe damage or absorption by body fluids (Fig. 7.2) (M. Maestro et al. 2011; Ju et al. 2015). The penetration level of the NIR light is higher for tumor tissues than that of normal cells. For example, 630 nm wavelength penetrates about 0.9 mm in normal brain tissue while about 1.6 mm through lung carcinoma (Stolik et al. 2000). Thus, selective phototherapy can be achieved using NIR light.

The laser power has great significance in the light-tissue interaction along with the wavelength. When an external laser source is applied, laser irradiation produces heat that burns both lesions and surrounding healthy cells. This restricted its clinical use. Thus, local heating induced by the photothermal effect has attracted significant attention. Photothermal-influenced increase in body temperature could be advantageous for recuperation from certain diseases (Huang et al. 2007; Ramasamy et al. 2014; Matteini et al. 2014; Tang et al. 2014). Upon elevation in body temperature, the growth of the pathogens slows down, and enzymes become inactive due to the unfavorable internal temperature. Thus, the thermal effect has been used in various medical treatments. Ablation agents such as nanomaterials (NMs) absorb light irradiation that converts it into heat, initiating the photothermal effect. These ablation agents help to generate heat in the selective lesion itself, and thus the surrounding tissues remain unharmed. According to the American National Standard for Safe Use of Lasers, the most commonly used NIR light with a safe power density limit is $\sim 0.726 \text{ Wcm}^{-2}$ for 980 nm and $\sim 0.33 \text{ Wcm}^{-2}$ for 808 nm (Robinson et al. 2010; Li et al. 2014b). Focal spot size and exposure time are essential points to consider as it affects the interaction.

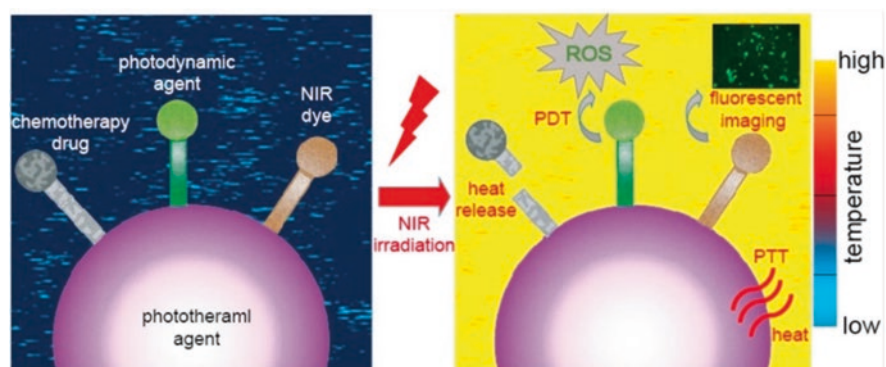


Fig. 7.2 Schematics depicting photothermal therapy and its medical applications combined with different light-induced treatments. The background color designates the temperature change during treatment as per the color map on the right. [Reproduced with permission from Chen et al. (2019)]

This book chapter reviews the development of photothermal nanomaterials for skin wound healing and monitoring, bone regeneration, and cartilage damage treatment. Their photothermal and photodynamic activity for wound healing is discussed with essential examples. Also, various nanomaterials, including semiconductors, noble metals, conducting polymers, and carbon-based NMs for photothermal therapy in cancer treatment, are discussed, along with the photothermal mechanism and their effect. At the end of this chapter, we enlist a few limitations and future prospects for photothermal nanomaterials, emphasizing synergistic light-responsive systems and composite nanomaterials for better photothermal effect in wound healing and anti-cancer effect.

7.2 Photothermal Nanomaterials: Application for Wound Healing and Monitoring

A wound is an injury to the skin, which lowers the skin's protective function. It may lead to the loss of continuity of epithelial tissue with further loss or damage of connective tissue under the skin like muscle, bone, nerves, etc. A wound can also be a result of surgery or trauma (Leaper and Harding 1998). Treatment of wounds was a major clinical issue in the past, and its diagnosis mainly relies on continuous monitoring of wound healing or its status. Expertise and experience are required for accurate and timely treatment of the wound by assessing the wound status (Loizou et al. 2012). Wound healing consists of four phases: hemostasis, inflammation (response phase), proliferation (re-epithelialization phase), and remodeling or scar formation (maturation phase) (Morton and Phillips 2016). Hemostasis occurs through the combined action of platelets and fibrin to stop the bleeding. Damage to endothelial cells exposes collagen, and it stimulates platelets. Platelets produce two growth factors that can attract essential components for the proceeding steps of wound healing. Inflammation begins with the adhesion of neutrophils to the endothelium. After migrating into the extracellular space, neutrophils phagocytose bacteria, degrade matrix proteins, and attract additional neutrophils and macrophages. Macrophages are the most important inflammatory cells, and they phagocytose pathogenic organisms, degrade wound debris, and stimulate granulation tissue formation and angiogenesis. Proliferation phase consists of formation of fibrous tissue, granulation tissue, epithelial tissue, and new blood vessels and begins within 24 hours of the wound occurrence in normal healing, and it may last for 4–24 days. Weeks to years will take for remodeling process. During this time, new tissues form, and they gain strength. A crucial step in wound healing is neovascularization. Any alteration or failure at this stage may result in chronic ulcer, which is very difficult to heal (Shanmugapriya and Kang 2019). A wound can also be observed on bone or cartilage that requires more attention as it is difficult to treat compared to skin. The key goal of wound management is to kill or inhibit the pathogens which cause wound infection in order to fasten wound healing process with minimal pain and scars.

Researchers have utilized *in vivo* and *in vitro* animal evaluation with the help of NMs for wound healing and management applications. Animal model systems such as a rat, mouse, chicken embryo, rabbit, and pig have been used with incision or excision models through spray method, laser therapy, intraperitoneal injection, intradermal, intravenous, topical liquid, and ointment application to study wound healing (Shanmugapriya and Kang 2019). Also, various studies explored the properties of NMs, which are helpful in different stages of wound healing and wound management process. Polymeric, ceramic, and zinc oxide NMs are useful for hemostasis, whereas gold (Au), silver (Ag), liposome, polymer, silica, fullerenes, carbon-based, metal oxide, ceramic, and nanocomposites were used for the inflammation stage. The proliferation phase uses liposome, polymer, solid lipid NMs, polymer micelle, polymer vesicles, Ag, Au, copper (Cu), magnetic NMs, carbon-based NMs, ceramics, and dendrimers. In contrast, remodeling uses iron oxide, nanoceria, and nanoscaffolds (Shanmugapriya and Kang 2019). Nowadays, NM-based new strategies have evolved, such as gene therapy, photostimulation, stem cell therapy, photodynamic therapy, and photothermal therapy. These modalities involve the application of therapeutic agents from NMs to enhance complicated wound treatment in wound care.

7.2.1 Photothermal and Photodynamic Therapy for Wound Healing

Photothermal nanomaterial-based therapies, namely, photodynamic therapy (PDT) and photothermal therapy (PTT), are gaining attention due to their non-invasive nature and low risk of multidrug-resistant bacteria effect (Cheng and Li 2020; Xu et al. 2020). To enhance wound healing through anti-bacterial activity, researchers incorporated PTT and PDT. In NM-based PDT, NMs act as a photosensitizer, and the photochemical reaction with oxygen produces reactive oxygen species (ROS) that eventually cause cell death. In PTT, exposure to NIR laser converts light photons into heat, increases local heat, and finally leads to cell ablation (Cheng and Li 2020). Compared to cancer PDT and PTT, wound treatment requires mild temperature increment, i.e., usage of laser light at lower energy densities. This gentle temperature stimulation helps develop resistance to thermal stress (or thermo-resistance) that aids cell survival during repeated exposures. In addition, mild temperature increment assists in cell proliferation and expression of heat shock proteins (HSP), which inhibit the unfolding and denaturing of cellular protein at mild temperature. Also, it has been found that HSPs 27, 47, 70, and 90 effectively produce thermo-resistance to overheated cells and could help wound healing *in vivo* (Cheng and Li 2020). The parameters that dictate PDT and PTT efficiency are laser power, exposure time and concentration, morphology, surface modification, size, and incubation time of NMs. It has been observed a positive relationship between laser power and cell damage. Laser power should be lower than the threshold density, which could

damage severe cell death. Longer exposure time increases the temperature and cell damage.

The concentration of NMs and their morphology, size, and surface modification can alter the internalization of NMs within the cells. Moreover, it has been found that longer incubation time helped improve the internalization of NMs and thereby improved their efficiency (Xu et al. 2020). The physical properties such as size, shape, and surface charge of NMs have significantly impacted PTT- and PDT-based therapy in wound healing applications (Cheng and Li 2020). Once the NMs enter the body, they must be cleared through the renal system or excretory system. The final concentration and clearance of NMs from the body depend mainly on the size of NMs. If the size of NMs is very small ($\sim <6$ nm), it usually secretes through the renal system. But, if it is very large (>200 nm), it accumulates in the spleen and liver, while moderate (6–200 nm) size accumulates in the kidney, bone marrow, heart, and stomach. However, the size of the NMs should be small enough for easy clearance through the excretory system. Few studies attempted to find the relation between ROS generation and rate of metal ion production with size of NMs. Most of the cell surface is negatively charged due to the presence of phosphate and anionic carboxyl groups; hence, positively charged NM's surface can be easily attracted, while blood plasma contains calcium and proteins that attracts negatively charged NMs. Hence, it can be easily uptaken and cleared by the liver. Therefore, NMs of neutral charges are favorable to avoid liver uptake and extended blood circulation. Sometimes, small molecules can be conjugated or immobilized on NM's surface to target specific wound locations. Antibody-conjugated NMs were extensively studied and reduced the passive accumulation of NMs on surrounding wound tissues. Further, it helps to increase the photothermal activity in the wound area due to the accumulated NMs (Du et al. 2017).

7.2.2 Photothermal Nanomaterials for Skin Wound Healing

Diverse NMs have been used for PDT and PTT in skin wound healing and management: metallic, carbon-based, organic, metal-organic framework (MOF), etc. In general, they comprise either inorganic or organic NMs. Inorganic NMs include metal, metal oxides, and their hybrid combinations. Organic NMs include polymers, liposomes, micelles, etc. that comprise carbon (Cheng and Li 2020). Most of the NMs used for skin wound healing are nanohybrid composed of two or more individual components; one component provides photothermal heat, while others may help produce ROS to kill the bacteria to fasten the wound healing process.

Au NMs have been used in wound healing applications due to their excellent plasmonic behavior, chemical inertness, and biocompatibility (Santra et al. 2015a, b; Santra 2020; Illath et al. 2020a, b). Surface plasmon resonance (SPR) is defined as the collective oscillation of electrons of NMs due to its size restrictions (Illath et al. 2021). Au NMs possess shape- and size-dependent plasmonic behavior, and their plasmonic peak can be tuned to NIR easily. Au nanorod, triangular Au

nanoplates, Au shell, and Au-based core-shell nanocomplexes have been investigated in detail by the research community for wound healing (Santra et al. 2016; Xu et al. 2018; Shanmugapriya and Kang 2019; Wentao et al. 2019; Li et al. 2021; Yan et al. 2021). Metallic NMs are usually coated or doped with hydrogels to release ROS and kill the bacteria, thereby improving biocompatibility and biostability. For example, N-acryloyl glycinamide mixing with polydopamine-coated Au nanorods treated wound has shown 98% bacterial killing efficiency and photothermal activity against both gram-positive and gram-negative bacteria within 5 min of NIR irradiation (808 nm, 2 Wcm⁻²) (Li et al. 2021). In addition, it was able to facilitate the infected wound healing and avoid injury during peeling when it was coated with a specific bacteria-activated macrophage membrane. In another study, the photocatalytic activity of polydopamine-coated hydroxyapatite Au nanorods was used to produce hydroxyl radicals, manifesting the bacteria more at temperature change (Xu et al. 2018). At a controlled temperature of 45 °C, the observed anti-bacterial efficiency was 96.8% and 95.2% against *S. aureus* and *E. coli*, respectively, under laser irradiation at 808 nm for 10 min. Also, the treatment promoted the formation of granulation tissue and collagen, thereby aiding the tissue repair. Triangular Au nanoplates (50 µgmL⁻¹) combined with hydrogen peroxide (H₂O₂) of low concentration (0.1 mM) revealed excellent anti-bacterial activity and infected wound healing activity with laser exposure at 808 nm (1 Wcm⁻²) for 3 min (Yan et al. 2021).

Cu NMs have an excellent SPR effect similar to Au NMs. In addition, dose-dependent therapy using Cu NMs stimulates the proliferation and angiogenesis of endothelial cells in vitro and aids wound healing through the expression of vascular endothelial growth factors (Tao et al. 2019). By incorporating hydrogels, Cu NM's biocompatibility can be enhanced, and their photothermal efficiency can be improved. For example, Cu NMs of 8 mM embedded into hydrogel showed a considerable increment in temperature (raised by 40 °C) within 10 min of laser exposure (Tao et al. 2019). Tao et al. developed a nanocomposite consisting of Cu NMs embedded into the hydrogel (Fig. 7.3) to improve the anti-bacterial capability by producing ROS and enhancing wound healing simultaneously (Tao et al. 2019). In vivo wounds infected with *S. aureus* bacteria were treated with Cu NM-hydrogel complex and exposed under laser light at 808 nm. A power density of 1.2 Wcm⁻² showed complete wound healing after 14 days. The local temperature was raised from 25 to 49.8 °C after 10 min of exposure time, which was sufficient to kill the bacteria. The remaining bacteria were killed easily due to the sustained production of ROS on subsequent days, and they were quickly released through the degraded hydrogel. Compared to pure hydrogel, Cu NM-hydrogel composite produced 3.1 times higher ROS upon laser irradiation and 1.6 times ROS without laser treatment. In addition, the viabilities of *E. coli* and *S. aureus* bacteria were reduced to 9% and 9.8%, respectively, after performing PDT and PTT using Cu NM-hydrogel composite.

PTT can be combined with metallic NMs, metal ions, or antibiotics to improve anti-bacterial activity. The anti-bacterial efficiency of Ag NMs was well established; it disrupts cell wall and plasma membrane components, decreases adenosine triphosphate (ATP) level, collapses membrane potential, induces pits and gaps in the

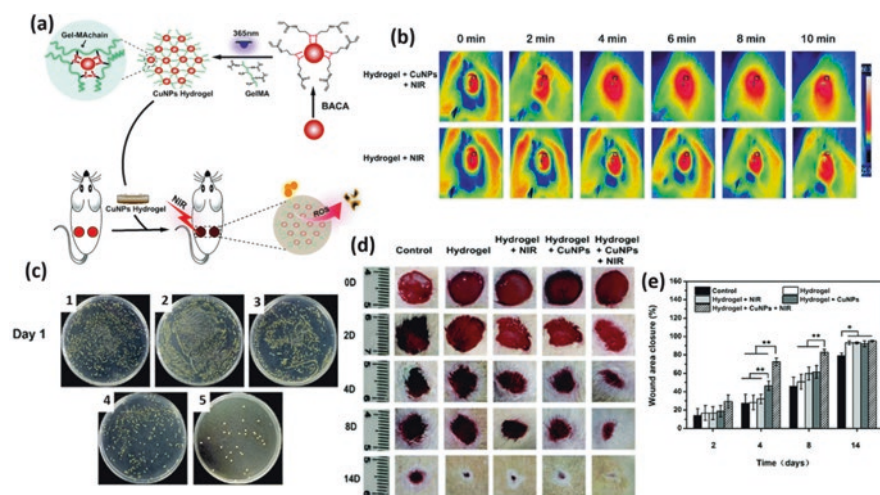


Fig. 7.3 Wound healing and anti-bacterial control using Cu-hydrogel nanocomposite: (a) schematic illustration of the fabrication of Cu NM-hydrogel complex and its anti-bacterial activity through PTT and PDT; (b) thermographic image of mice wound tissue after laser exposure at 808 nm with various exposure times; (c) photograph of the *S. aureus* bacteria obtained from wound tissue in control (1), hydrogel (2), hydrogel + NIR (3), hydrogel + Cu NPs (4), and hydrogel + Cu NPs + NIR (5) during day 1 after exposure; (d) photograph of the wound area in mice on 0, 2, 4, 8, and 10 days after laser exposure; and quantitative analysis of wound area closure as a function of time; (e) quantitative information of corresponding wound area closure (%) at varying time points ($n = 4$). [Reproduced with permission from Tao et al. (2019)]

cell wall, affects DNA replication and halts cell cycle, leads to loss of proton motive force, and interacts with thiol groups (Shanmugapriya and Kang 2019; Chen et al. 2021). It has been found that compared to other shapes, triangular Ag NMs have excellent anti-bacterial activity. In addition, it has a strong absorbance peak at NIR, and irradiation at this wavelength elevates the temperature, which is adequate to kill the bacteria in the wound (Xu et al. 2020). Metallic nanocomposite formed by combining Au and Ag showed excellent photothermal efficiency and a high wound healing rate by simultaneously releasing Ag upon NIR irradiation (Fig. 7.4) (He et al. 2020a). Au-Ag nanoshells possess photothermal properties due to Au and Ag's presence, while Ag NMs provide high anti-bacterial properties. It has been found that Au-Ag nanoshells treated for chronic wounds under NIR exposure were capable of sensitively detecting the bacteria and inhibiting the gram-positive and gram-negative bacteria and their multidrug-resistant bacteria strains. In general, multidrug-resistant bacteria strains arise due to the abusive usage of antibiotics. Most of the wounds infected with multidrug-resistant bacteria demand accurate residual bacteria assessment methods to provide further treatment information. Surface-enhanced Raman scattering (SERS) imaging is a powerful tool to image residual bacteria with the help of plasmonic NMs like Ag NMs. A chronic wound treated with Au-Ag hollow nanoshells under the exposure of 808 nm and power density of 1 Wcm^{-2} showed that a nanoshell suspension of $37.5 \mu\text{g mL}^{-1}$ was needed

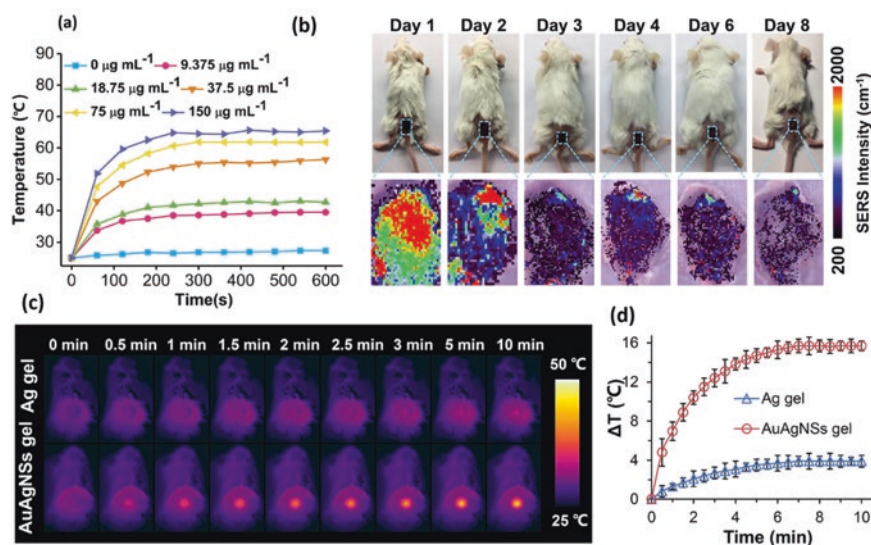


Fig. 7.4 Au-Ag nanoshell (AuAgNS)-based PTT for chronic wound healing and bacterial monitoring: (a) temperature variation as time progresses after the exposure of laser at 808 nm (1 W cm^{-2}) for 10 min with various concentrations of AuAgNSs, (b) photographs and corresponding pseudo-color-coded SERS signal image up to 8 days after exposure and Ag NPs for 10 min after irradiation at 808 nm, (c) in vivo photothermal images captured at different time durations after laser exposure, and (d) corresponding quantitative representation of temperature evolution. [Reproduced with permission from He et al. (2020a)]

to heat the bacteria above $44 \text{ }^\circ\text{C}$. SERS-based detection of extended-spectrum beta-lactamase (ESBL) *E. coli* and MRSA (methicillin-resistant *Staphylococcus aureus*) bacteria was analyzed by performing both in vivo and in vitro studies in mice. It has been found that there exists a correlation between the abundance of bacteria and the intensity of SERS signals. On day 1, SERS intensity was very high, and it gradually decreased as the day progressed, which showed the successive elimination of bacteria. Further, it was observed that the bacterial survival rate with Ag NMs alone was 80%, irrespective of the laser. In comparison, Au-Ag nanoshells exhibited 40% bacteria survival, and in the presence of a laser, all the bacteria were eliminated. The minimum concentration of Au-Ag nanoshell required for anti-bacterial activity was $25 \mu\text{g mL}^{-1}$ without a laser and $18.7 \mu\text{g mL}^{-1}$ in the presence of a laser. After 10 min of laser exposure at 808 nm, Au-Ag nanoshell-treated bacteria showed only less than 5% bacteria colonization. The photothermal activity of Au-Ag nanoshells was enhanced by mixing the nanocomplex with sodium hyaluronate gel, which increased the temperature by $20 \text{ }^\circ\text{C}$ within 500 s after laser irradiation with the same absorbance response. The elevated photothermal activity and anti-bacterial activity helped shrink the wound area by 50% after 6 days of treatment, and complete removal of the wound was observed after 8 days (He et al. 2020a).

The anti-bacterial property of Ag NMs was also utilized in healing MRSA-infected diabetic wounds (Tong et al. 2020). Prussian blue@polydopamine@Ag

NM-treated diabetic wounds upon NIR irradiation led to cell integrity damage, produced ROS, lowered the ATP, and disrupted the bacterial metabolism. Specifically, the vascular endothelial growth factor expression rate was higher in *in vivo* mice model of the diabetic wound, and hence, the healing rate was also increased. Cu, zinc (Zn), and cobalt (Co) also possess anti-bacterial properties (Chen et al. 2021); Cu disrupts DNA structure and damages vital enzymes, while Co promotes cell aggregation, and Zn helps in plasma membrane disorganization. A combination of Co and Zn can generate ROS, whereas Cu and Zn together promote cellular internalization. Similarly, the hybrid of Ag and Co affects the correction function of plasma protein, and that of Ag and Cu induces intracellular substance leakage. Moreover, the accumulation of Ag, Cu, and Zn in the cell wall can decrease cell membrane permeability.

Due to high photocatalytic performance, TiO₂ (titanium oxide) NMs have been used in wound healing through infection control (Xu et al. 2020). Upon illumination, it generates electrons and holes in the conduction and valence band, respectively. They further produce enough ROS to destroy the gram-positive and gram-negative bacteria. By properly bonding with metallic NMs such as Cu, Au, Ag, etc., photocatalytic efficiency can be increased. For example, Zhang and co-workers increased the photocatalytic efficiency of TiO₂ NMs by adding Ag NMs. They found that the higher the concentration of Ag NMs, the higher the number of produced ROS under light irradiation under 660 nm (Wang et al. 2019). By incorporating hydrogel, generated ROS were quickly released through the porous hydrogel, thereby improving anti-bacterial efficiency. Like metallic NMs, upconversion NMs (UPCNMs) can indirectly convert NIR light into visible or UV light triggering ROS production (Sun et al. 2019). But UPCNMs@TiO₂ alone is not sufficient to kill the bacteria for wound healing. Hence, a nanosized photothermal agent like graphene oxide (GO) was doped, and the surface was further modified using poly(vinylidene fluoride). UPCNMs@TiO₂-produced ROS were easily transferred through GO due to the excellent electrical conductivity possessed by GO. It can collect and transfer electrons, inhibit the electron-hole recombination, and increase ROS production. Also, upon NIR exposure (980 nm, 2.5 Wcm⁻²), the temperature was raised by ~20 °C within 5 min and effectively restrained the inflammatory reaction, improving wound healing. In another recent study, black nano-TiO₂ synthesized by magnesium (Mg) reduction of TiO₂ followed by chitosan incorporation was found to possess excellent wound healing performance upon NIR irradiation. The Mg²⁺ released from nanocomposites was responsible for wound healing; it stimulated normal skin adhesion, proliferation, and migration in chronic ulcer closure.

Metal-organic frameworks (MOF) are hybrid nanocomplex formed by organic linkers to connect inorganic materials. MOFs' chemical and physical properties can be varied by controlling the metal ion center or manipulating organic connectors, thereby aiding in the easy release of metal ions. Compared to metal and metal-organic NMs, MOFs can prevent metal oxidation and aggregation. Also, MOFs fabricated from biologically active ligands offer sustained anti-bacterial properties even with structural and chemical variability of MOF (Chen et al. 2021). The

majority of MOFs perform anti-bacterial activity by releasing Cu^{2+} and Zn^{2+} . For example, MOF formed by wrapping anti-bacterial polymer (polyvinyl alcohol, PVA) film on ZnO@CuO@Au core-shell NMs showed combined PTT and PDT activity along with the release of Cu^{2+} and Zn^{2+} under laser exposure at 635 nm for 10 minutes (Wentao et al. 2019). In addition, the release rates of Cu^{2+} and Zn^{2+} were varied by changing the polymer film thickness to control the disinfection. It showed 99.8% and 97.5% anti-bacterial efficiency against *S. aureus* and *E. coli* bacteria, respectively. Another essential MOF is Prussian blue, which is biosafe and possesses excellent biocompatibility for wound healing (Cheng and Li 2020; Tong et al. 2020). Table 7.1 lists the important recent works in NM-based PTT and PDT for skin wound healing.

7.2.3 Photothermal Nanomaterials for Bone and Cartilage Defects

Apart from healing skin wounds, PTT and nanomaterials incorporated in PDT can also treat bone and cartilage defects. In general, bone damage is caused by arthritis, trauma, tumor ablation, etc. and is a significant cause of disability in older people. As NIR exposure can penetrate the soft skin tissue, it can easily absorb on bone. Compared to skin wound healing, laser exposure time and power density should be higher as it has to penetrate the skin and reaches the bone (Cheng and Li 2020). By combining the photothermal activity of black phosphorus (BPs) and biocompatibility of poly(lactic-co-glycolic acid) (PLGA) NMs, BPs@PLGA NMs under NIR exposure showed excellent temperature elevation and osteogenesis (Fig. 7.5) (Tong et al. 2019). BPs are biodegradable, and the end products CO_2 , H_2O , and PO_4^{3-} are non-toxic and may help osteogenesis in stem cells. Acidic by-product H_3PO_4 is responsible for degradation by lowering the pH. As an example, in vivo bone regeneration was observed in a rat tibia defect model with laser exposure at 808 nm for 450 s for 5 weeks continuously after incubating with BPs@PLGA NMs. It has been observed that power density as low as 0.5 Wcm^{-2} was sufficient to elevate the temperature from $32 \text{ }^\circ\text{C}$ to $41 \pm 1 \text{ }^\circ\text{C}$ within 150 s after exposure. The thermographic image revealed that BPs@PLGA+NIR could cross the tissue barrier and heat the bone in vivo, whereas the heated area zone in PLGA+NIR was outside the path or on the skin. Hence, it is clear that PLGA+NIR alone cannot penetrate the skin to perform hyperthermia of bone. The osteogenesis action is the upregulation of osteogenic genes expressed due to HSP47 and HSP70 production after heat generation. Micro-CT imaging confirmed the successful tibia bone regeneration. The tibia's BV/TV (bone volume/total volume) increased very highly, whereas the BV/TV of PLGA-implanted bone was low. New bone and osteoid were observed in abundance under blue staining, which was in consistent with fluorescent and micro-CT imaging.

In another example, porous Au-Pd NMs were used as a hyperthermia agent in PTT, producing mild localized heat ($40\text{--}43 \text{ }^\circ\text{C}$) that accelerated cell proliferation

Table 7.1 Recent works in photothermal NM-based wound healing and monitoring

| Nanomaterials | Shape | Size (nm) | Laser wavelength (nm) | Power density (Wcm^{-2}) | Exposure time | Type of therapy | Ref. |
|-------------------------------|------------------|-------------------------------------|------------------------|-------------------------------------|---------------|-----------------|------------------------|
| PB@PDA@Ag | Cube | 123 | 808 | 1 | 5 min | PTT and PDT | Tong et al. (2020) |
| Ag/TiO ² -hydrogel | Spherical | <100 | 660 | 0.6 | 5 min | PTT | Wang et al. (2019) |
| PDA@Au-hydroxyapatite | Rod | 4.9 (Au) 80–100 (Hap) | 808 | 1 | 10 min | PTT | Xu et al. (2018) |
| Au | Triangular plate | 132 (side length) 10 (thickness) | 808 | 1 | 3 min | PTT | Yan et al. (2021) |
| Carbon-hydrogel | Branched | 30 | – | 0.15 | 10 min | PTT | Xie et al. (2021) |
| BPs@Carbon dot | Sheet | 8–13 (BPs) | 808 | 1.5 | 5 min | PTT and PDT | Zhang et al. (2021b) |
| Cu ₂ S | Flower | 200–600 | – | 0.5 | 5 min | PTT | Wang et al. (2017) |
| CuS | – | – | 980 | 0.5 | 15 min | PTT | Yuan et al. (2019) |
| BSA-CuS | Sphere | 16.08 | 808 | 3 | 10 min | PTT | Zhao et al. (2018) |
| CuS | Dot | 6 | 808 | 2.5 | 10 min | PTT | Qiao et al. (2019) |
| BPs | Sheet | 155 | 808 | 0.65 | 5 min | PTT | Xue et al. (2021) |
| Reduced graphene oxide-CG | Porous | – | 980 | 1 | 10 min | PTT | Rosselle et al. (2020) |
| Graphene hybrid | Sheet | – | 808 | 2 | 5 s | PTT | Zhang et al. (2021a) |
| Graphene-quantum dots | Sheet | <25 | 450 | 0.0142 | 10 min | PTT + PDT | Mei et al. (2020) |
| Graphene oxide | Sheet | 1.61 | 450 (PTT) 680 (PDT) | 0.0142 | 10 min | PTT + PDT | Mei et al. (2021) |
| MnO ₂ | Sheet | 5.6 | 808 | 1 | 5 min | PTT and PDT | Wang et al. (2020) |
| Hydrogel (Bio) | – | – | 808 | 2 | 3 min | PTT | Yao et al. (2020) |

| Nanomaterials | Shape | Size (nm) | Laser wavelength (nm) | Power density (Wcm^{-2}) | Exposure time | Type of therapy | Ref. |
|---------------------------------------|--------------|--------------------|-----------------------|-------------------------------------|---------------|-----------------|-----------------------|
| Hydrogel composite | - | - | 808 | 2 | 3 min | PTT | Ma et al. (2021) |
| CuS | Sphere | 40 | 808 | 0.4 | 5 min | PTT | Zhou et al. (2021) |
| Hydrogel | - | - | 808 | 2 | 10 min | PTT | Liu et al. (2020) |
| Chitosan-hydrogel | - | - | - | 1.4 | 10 min | PTT | He et al. (2020b) |
| Chitosan | - | - | 808 | 0.85 | 10 min | PTT | Sheng et al. (2021) |
| Polymer hybrid- hydrogel | Sphere | 5-6 | 550 + 808 | - | 10 min | PTT and PDT | Wang et al. (2021) |
| $\text{Ag}_3\text{PO}_4/\text{MoS}_2$ | Sphere/Sheet | 10-30 (sphere) | 660 + 808 | 0.6 | 5 min | PTT and PDT | Zhang et al. (2019b) |
| GO | Sheet | 0.81 (spacing) | 808 | 1 and 1.5 | 10 min | PTT | Huang et al. (2020) |
| PDA-hydrogel | Sphere | 179 (hydrodynamic) | 808 | 1 | 10 min | PTT | Zeng et al. (2021) |
| PdH | Cube | 20 | 808 | 1.5 | 5 min | PTT and PDT | Yu et al. (2019) |
| Pd | - | 30.2 | 808 | 1 | 10 min | PTT | Phan et al. (2019) |
| Silicon | Fiber | - | - | 0.71 | 10 min | PTT | Anti-in et al. (2020) |

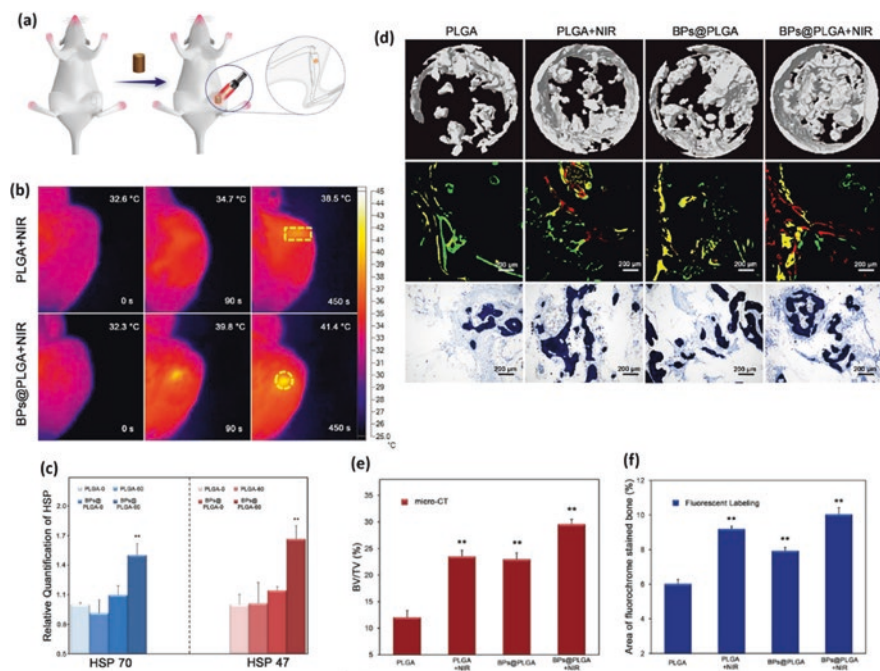


Fig. 7.5 Bone regeneration using BPs@PLGA-based therapy: (a) schematic diagram of progress of rat tibia implantation and NIR irradiation; (b) infrared thermographic images of PLGA- and BPs@PLGA-treated tibia damage after NIR exposure with different exposure times; (c) quantification of produced HSP70 and HSP47 proteins after treatment; (d) in vivo bone regeneration evaluation using micro-CT (top row), corresponding fluorescent labeling of new bone formation (middle row), and histological micrographs stained using toluidine blue (bottom row); (e) BV/TV (bone volume/total volume) of tibia based on micro-CT images; and (f) area of the percentage of fluorochrome-stained bone. [Reproduced with permission from Tong et al. (2019)]

and bone regeneration (Zhang et al. 2019a). Six weeks after treatment, the complete cranial defect was replaced with new bone; almost 97% of the bone area was recovered. Carbon-based NMs such as carbon nitride sheets and carbon nanotubes (CNTs) also exhibit bone regeneration under PTT. Carbon nitride sheets under red light illumination activated human bone marrow-derived mesenchymal stem cells and achieved a recovery of 91% after 4 weeks (Tiwari et al. 2017). Carbon nanotube-based therapy-induced photothermal stress and PDT triggered the stimulus for the expression of osteogenic genes, thereby activating bone deposition (Yanagi et al. 2015). This is due to the contribution of HSP70 expressed after heat generation that eventually promoted osteogenesis.

Cartilage damage is challenging to treat as its self-regeneration is not so easy compared to skin and bone. For regeneration of cartilage, Ag or carbon NMs have been used as photosensitizers in PDT to produce ROS, which is needed for chondrogenic differentiation and cartilage regeneration (Cheng and Li 2020). As an example, Lu et al. studied the chondrogenesis activity of carbon dot-doped collagen

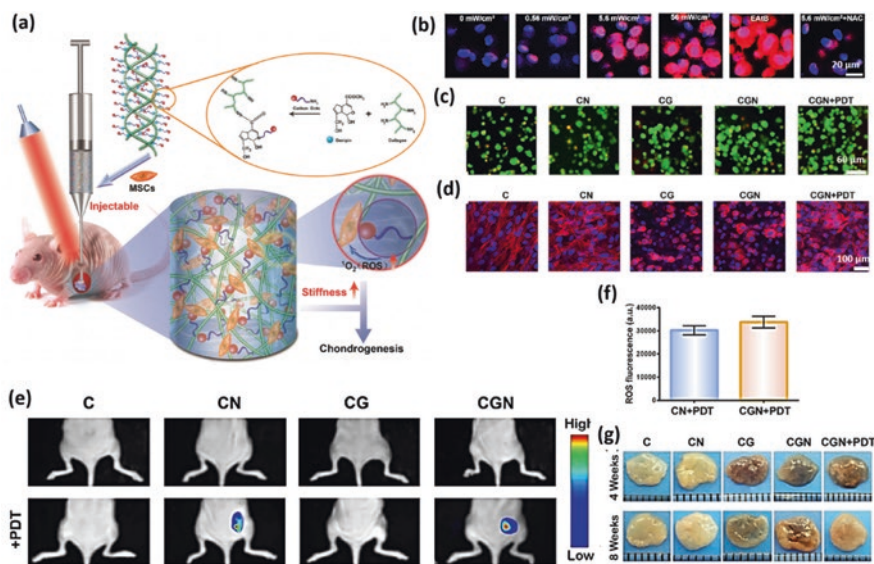


Fig. 7.6 Cartilage regeneration using carbon dot-embedded collagen hydrogel under PDT: (a) schematic illustration of the synthesis of CGN and its activity under NIR irradiation; (b) ROS generation with exposure of various laser power densities for 3 min (scale bar = 20 μm); (c) cell viability of cells treated with C (collagen), CN (collagen + carbon dot), CG (collagen + genipin), and CGN (collagen+ genipin + carbon dot) under the presence or absence of laser exposure; (d) corresponding skeletal-stained image; (e) in vivo imaging of temperature evolution in mice treated with C, CN, CG, and CGN with or without PDT; (f) quantification of ROS fluorescence signal generated for CN and CGN under PDT; and (g) evolution of cartilage formation for C, CN, CG, CGN, and CGN + PDT during 4 and 8 weeks after treatment. [Reproduced with permission from Lu et al. (2019)]

hydrogel NMs (CGN) in the presence or absence of NIR exposure for a short time (Fig. 7.6) (Lu et al. 2019). Compared to pure hydrogel, stiffness of CGN was improved and produced ROS during PDT, thereby promoting chondrogenic marker expression of bone marrow-derived stem cells (BMSC). This, in turn, enhanced the cartilage regeneration through transforming growth factors and mammalian target of rapamycin pathways. Combining CGN with PDT resulted in an increased cell proliferation rate of BMSCs by 50.3%, thereby enhancing the expression of cartilage-specific genes by multiple folds and promoting glycosaminoglycan by 205.1% on the 21st day after therapy.

7.3 Photothermal Nanomaterials: Applications for Cancer Biomedicine

One of the greatest enigmas in the field of modern medicine is to cure cancer. Compared to chemotherapy and radiotherapy, PTT has been acknowledged as one of the most favorable for the reduced side effects in cancer treatments. Ablation agents used in PTT are NMs having a photothermal effect, which helps to convert light into heat energy (Santra and Tseng 2022; Jia et al. 2015). Thus, the temperature elevation would kill the cancer cells, creating minimum side effects on the normal cells. The current theory can be applied only because cancer cells have minimum heat tolerance than normal cells. Irreversible damage is caused to the membranes of cancer cells, and thus protein denaturation is initiated (Melamed et al. 2015). Unlike visible and UV light, NIR light penetrates deep tissues with minimum damage (André M. Gobin et al. 2007). NIR region is also known as the biological window (Tsai et al. 2013). Here, biomolecules and water absorb minimum light amounts and make NIR favorable to PTT. Thus, NMs having photothermal effects in the NIR region and passive localization in tumors have fascinated vast attention due to their non-invasive, efficient, and selectivity characteristics. Thus, in the following section, we will discuss the current status of NMs used to create a photothermal effect for anti-cancer treatment. Also, the mechanism and various factors affecting the performance of the photothermal effect shall be discussed. Moreover, PTT merging with other potential methods of cancer therapies is even discussed as a future trend (Chen et al. 2019).

In the current research, NMs are the main focus as ablation agents. Nanoscale properties of materials play an essential role in the photothermal effect. As mentioned previously, Au NMs can convert excited state photon energy into heat due to the SPR (Xiaohua Huang et al. 2006). During cancer treatment, nanomedicines target with the mechanism nanoparticle-induced endothelial leakiness (NanoEL) for immature tumors (Tay et al. 2017) or enhanced permeability and retention of NMs for mature tumors. In NanoEL, NMs interact with the adherent's protein junction of endothelial cells, which helps to induce micro-sized gaps between endothelial cells. This helps nanomedicine to penetrate into the cell and accumulate (Chen et al. 2019). Many NMs such as noble metals and nanoarchitecture conducting polymers have been developed for the PTT application.

7.3.1 Photothermal Therapy Using Metal Nanomaterials

Noble metal NMs have been the main focus for PTT agents in the last few decades, such as Au-based (Wang et al. 2013b) and platinum-based (Manikandan et al. 2013) NMs. Noble metal NMs have comparatively high efficiency for photothermal conversion and optical solid absorption properties without generating quick photobleaching problems, which is the frequently encountered phenomenon in the usage

of organic dyes as ablation agents (Jiang et al. 2013; Barik et al. 2021; Santra and Mohan 2021; Shinde et al. 2021b). M. Manikandan et al. studied the PT effect of Pt-NPs with 5–6 nm size range from that is used as ablation agents for PT ablation of Neuro 2A cells. In some studies, Au NMs have sought attention in PTT. Even without surface modifications, they have an SPR effect in the visible light region (Pitsillides et al. 2003). However, according to the Mie theory, the shape and size of the Au NMs are essential aspects of the SPR effect. This makes it possible to shift the wavelength of the SPR effect in the NIR region. Various Au NM variants were developed to increase photothermal performance, including Au nanohexapods (Wang et al. 2013b), Au nanoshells (Vankayala et al. 2014), and Au nanorods (Tsai et al. 2013). Apart from these shape variants, dendritic Au NMs have also been studied for PTT applications (Qiu et al. 2016).

Additionally, apart from PTT, Au NMs are the multi-functional medical agent used as image contrast agents and drug carriers (Santra 2020). The Au nanocage possesses significant NIR absorption for PTT and can carry drugs within or act as contrast agents for imaging (Li et al. 2015). In a study conducted by Yavuz et al., Au nanocage was enveloped with a poly(N-isopropyl acrylamide)-co-polyacrylamide polymer coating (Yavuz et al. 2009). This polymer would undergo phase transition when heated during PTT, creating pores and allowing inside drugs from gold nanocage to diffuse into the environment. Au nanorods loaded with doxorubicin (DOX) were designed for combinatorial chemo-photothermal therapy against cancer by Wang et al. (2014). DNA was coated over the Au nanorods via the self-assembly technique of electrostatic interaction for efficient loading of DOX (Figure 7.7a). Also, some other variants like Au-shelled iron oxide black (Fe_3O_4) NMs (Mohammad et al. 2010) and Au-shelled silica NMs (Liu et al. 2011a) were fabricated for cancer therapy. These hybrids further can play an essential function in medical applications with high optical absorption in the NIR region due to the hollow Au nanoshells with

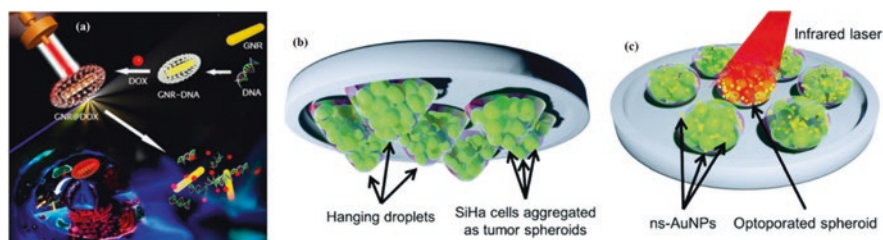


Fig. 7.7 (a) Schematic representation of DNA-coated Au nanorods (GNRs) loaded with DOX and cell mechanism for chemo-PT cancer therapy (Wang et al. 2014). (b, c) Illustration of the optoporation-mediated cargo delivery in 3D SiHa tumor spheroids. SiHa cancer cells (green) mixed with ns-Au NPs were pipetted on the petri plate lid as in the form of droplets which were then inverted and allowed to incubate. Thus, formation of 3D spheroids at the apex of the hanging droplets. The 3D spheroids were then exposed to a pulsed infrared laser, resulting in the formation of photothermal cavitation bubbles causing transient plasma membrane disruption and rapid entry of biomolecules into the cell's cytosol. [Reproduced with permission from Pallavi Gupta et al. (2021)]

improved thermal performance using Fe_3O_4 magnetic NMs and high thermal stability using silica nanocores.

Gupta et al. demonstrated pulsed laser-assisted optoporation-based high-throughput intracellular delivery of propidium iodide (PI) dye within 3D SiHa human cervical cancer spheroids (Figure 7.7b, c) (Kar et al. 2020; Shinde et al. 2021a; Pallavi Gupta et al. 2021). This technique used synthesized nano-spiked core-shell gold-coated polystyrene nanoparticles (ns-Au NPs). The excitation wavelength of 680 nm with a laser fluence of 45 mJcm^{-2} and pulse frequency of 10 Hz was used to deliver PI dye into the cells successfully. This technique ensured high delivery efficiency ($89.6 \pm 2.8\%$) while maintaining high cellular viability ($97.4 \pm 0.4\%$).

Noble metal NMs have extraordinary PTT for cancer treatment, but some issues are still to be worked out. After treatment, the detection of Au NMs is most necessary due to the non-biodegradable phenomenon. Also, Au NMs are concerned with photostability issues, as some relatively weak structures cause melting effects (Vankayala et al. 2014). Due to prolonged NIR irradiation exposure, Au NMs deform, further causing a decrease in PTT. Thus, much further experimental work is needed for noble metal NM's viability.

7.3.2 *Photothermal Therapy Using Semiconductor Nanomaterials*

Some semiconductor NMs like Cu chalcogenide have been used as an ablation agent in PTT due to low cytotoxicity and low cost (Huang et al. 2015). However, these Cu-based NMs have low photothermal conversion efficiency and may require higher NIR power over 808 nm to achieve ablation of the tumor. For some Cu-based NPs, NIR light of 980 nm is often used as an alternative, demonstrating a high limit for skin exposure in humans. It penetrates through biological tissues in about several centimeters (Chen et al. 2009). The treatment effects can be retained while reducing the power NIR laser concerning this aspect.

The photothermal performance of Cu-based NMs could be improved by adjusting their size and shape. Hu's group has synthesized uniform 3D flower-shaped CuS NMs with better PT conversion efficiency (Tian et al. 2011b). The superstructures of about $1 \mu\text{m}$ in size could serve as exceptional laser cavity mirrors at 980 nm, further enhancing the absorption and reflection potentiality of laser. Thus, subsequent improvement in an efficient photothermal conversion. The same group also achieved photothermal conversion efficiency up to 25.7% by synthesizing Cu_9S_5 plate-like structure (Tian et al. 2011a). This PT conversion efficiency is slightly higher than the Au NRs at 980 nm NIR. Also, shuttle-like CuS bundle nanostructures with a self-assembly process were developed for better PT conversion efficiency (Fig. 7.8a, b) (Bu et al. 2014). Here, the CuS NMs would first form CuS nanorods primarily with final undergoing shuttle-like bundles due to interparticle

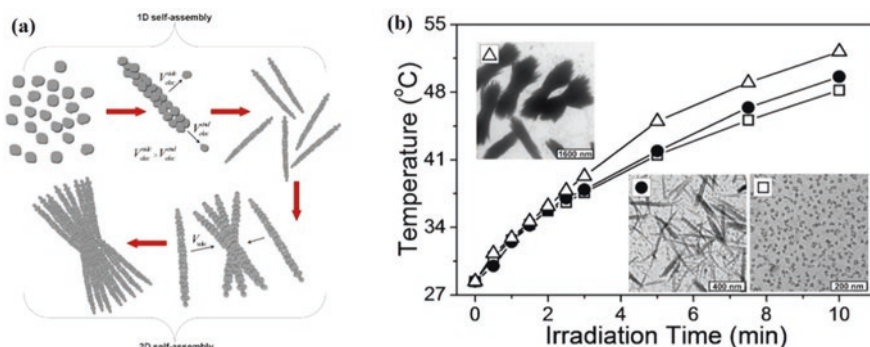


Fig. 7.8 (a, b) Schematic representation of the self-assembly of CuS NMs to primary nanorods and finally shuttle-like bundles and accordingly the improvement in photothermal effect. [Reproduced with permission from Bu et al. (2014)].

distance change and new electronic structure generation. The studies suggested that Cu-based nanoarchitectures play a significant role in PTT performance.

CuS NMs have found their practical use in the research involving the PTT effects on HeLa cervical cancer cells (Li et al. 2010). The dependent effect of CuS NMs concentration and laser dose was observed. The research showed that the application of an 808 nm NIR laser with even 24 Wcm^{-2} killed specific cancer cells. The effect of CuS NMs and NIR laser individually showed a minimum impact on killing cells. Furthermore, up to 56.7% PT conversion efficiency was achieved with $\text{Cu}_{7.5}\text{S}_4$ -modified nanocrystals (Li et al. 2014a). These nanocrystals effectively killed cancer cells even at the low power 980 nm laser and low dose concentration. Thus, low cytotoxicity, low cost, and specific ablation effect have made CuS NMs an ablation agent in PTT (Li et al. 2010, 2014a).

Yet, there are a few concerns regarding the use of CuS NMs in PTT. Studies have started focusing on NIR with 980 nm for PTT, as few Cu-based NMs have stimulation wavelength at 808 nm and still need a high-powered NIR laser. Nevertheless, NIR with wavelength of 980 nm can be absorbed by water, resulting in temperature elevation in exposed tissues, healthy or not, and even without an ablation agent. Thus, this needs to be explored before its implementation in PTT.

Mohan et al. have studied how TiO_2 nanotubes (TNT) can be used as an efficient platform for intracellular delivery using nanosecond pulse laser photoporation (Mohan et al. 2019, 2021a, b, c; Shinde et al. 2020). The technique was successful for intracellular delivery of PI dye and dextran into HeLa cells with high transfection efficiency and cell viability. The illustrations for the mechanisms and the associated results are schematically shown in Fig. 7.9. However, all these mentioned techniques still have the need of single-cell selectivity along with high-throughput methodologies which has not yet fulfilled, making it as the main objective for further application purposes (Shinde et al. 2021a).

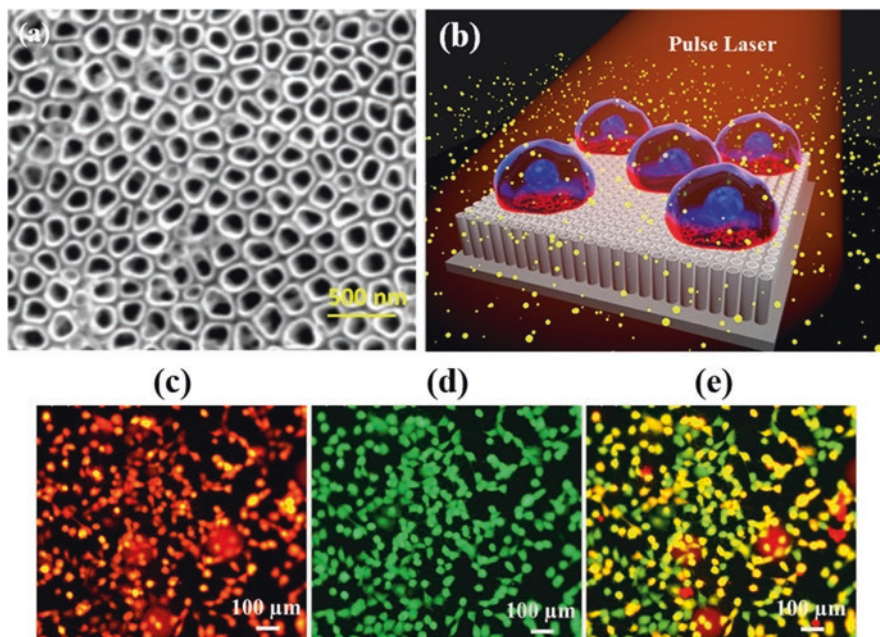


Fig. 7.9 (a) FESEM top view image of TNTs formed. (b) Pictorial presentation of massively parallel photoporation using an array of nanotube surface and pulse laser interaction. (c–e) Fluorescence images of HeLa cells after photoporation on TNTs at 10X magnification – PI dye (red-delivered cells); Calcein AM (green-live cells); and merged image of PI and Calcein AM (yellow, delivered live cells; red, delivered dead cells). [Reproduced with permission from Mohan et al. (2021c)]

7.3.3 Photothermal Therapy Using Carbon-Based Nanomaterials

CNTs have been used frequently in the optoelectronics industry (Consales et al. 2007). CNTs have also been studied in the medical field for PTT due to their thermal behavior and optical properties (Neves et al. 2013). They have been used as drug carriers (Dhar et al. 2008) and bioimaging probes (Zavaleta et al. 2008). CNTs can also be modified by binding (noncovalently or covalently) or wrapping with different functionalized biomolecules (Arsawang et al. 2011), like anti-cancer drugs (Wang et al. 2013a) and magnetic NMs (Vasilios Georgakilas et al. 2005). Though it can be modified with various surface chemical properties, there is a possibility that CNTs can bring out a high dose of toxic molecules (Wang et al. 2011). Thus, surface functionalization should be studied with extra detail to minimize the toxicity.

In particular, polyethylene glycol (PEG) coatings are used to functionalize the carbon-based NMs. This helps enhance biocompatibility, extend blood circulation time, and circumvent aggregation (Liu et al. 2013). Liu et al. coated PEG-poly(maleic anhydride-alt-1-octadecene) (PMHC₁₈) on single-walled carbon nanotubes

(SWNTs) and studied its effect on PTT (Liu et al. 2011b). It was found that coating increased the half-life blood circulation of SWNTs. Thus, enhanced uptake of the SWNTs by the tumors showed positive treatment. But it also showed increased uptake of SWNTs by the skin, which may cause skin damage and decrease treatment efficiency. Therefore, it was focused on controlling the blood circulation half-time, which would balance the uptake of SWNTs. Burke et al. illustrated the PTT-mediated CNT's mechanism by characterizing the response of breast cancer stem cells (BCSCs) (Burke et al. 2012). They used a water bath to create hyperthermia or multi-walled carbon nanotubes (MWNTs) to induce the PT effect. They found out that the BCSCs were resistant to hyperthermia, while MWNTs generated PT effect promoting necrotic cell death.

Graphene, a new carbon NM, has exceptional physical and mechanical properties (Korkut et al. 2011). Graphene-based NMs have found their application in anti-tumor activity due to high surface activity and strong optical absorption in the NIR region. Thus, it is favorable for PTT as an ablation agent along with the use of other synergistic therapies. Markovic et al. studied the mechanism and cell death type resulting from graphene NMs inducing PTT (Markovic et al. 2011). The characterization showed cell death by both apoptosis and necrosis. Apart from PTT-triggered cell death, superoxide/oxidative stress was produced potentiated by hyperthermia, which concluded in causing apoptosis.

Also, metal-filled CNTs represent a novel class of photothermal NMs. When illuminated by visible light, they strongly enhance the metal sites' temperature due to the enhanced plasmonic light absorption at the metal surface, which behaves as a heat radiator. Potential applications include nanomedicine, heat-assisted magnetic recording, and light-activated thermal gradient-driven devices (Rossella et al. 2012).

7.3.4 Photothermal Therapy Using Conducting Polymers

Polypyrrole (PPy) (Ghanbari et al. 2008) and polyaniline (PANI) (Guo et al. 2009) are the conducting polymers (CPs) used in bioelectronics and biomedical applications. CPs have shown optical absorption capabilities and better biocompatibility than inorganic NMs and are cheaper than noble metal NMs, making them employable for use in PTT (Zhou et al. 2013). To induce the PT effect, CP-based NMs are excited by light stimulation forming a bio-polaron which further decays into a photon band producing heat (Di et al. 2011). Moreover, during the doping process, nanoarchitecture CPs shift their optical absorption peak by generating an interband gap resulting in excitation-energy level change. This helps improve the conductivity of the polymer and changes its optical properties. In one of the studies, the doping-dedoping process and oxidative chemical polymerization were used to synthesize water-soluble PANI NMs resulting in tumor ablation under irradiation of NIR dependent on its pH (Zhou et al. 2013). During the NIR stimulation, the PANI NMs transform from the emeraldine base state to the emeraldine salt state reporting to convert NIR light energy into heat (Fig. 7.10) (Di et al. 2011; Zhou et al. 2013).

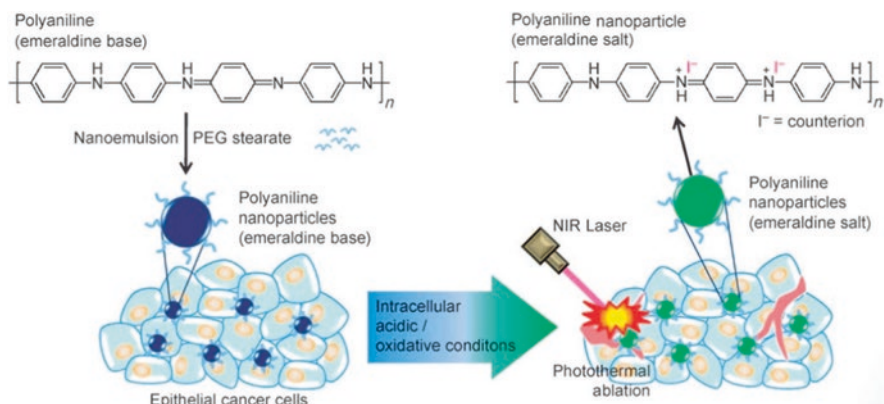


Fig. 7.10 Schematic representation of the synthesizing polyaniline nanoparticles, an organic photothermal agent, and their application in photothermal ablation of epithelial cancer cells by NIR laser irradiation. [Reproduced with permission from Yu et al. (2020)]

Even so, some studies showed that the PANI NMs have comparatively low PT conversion efficiency. Also, bare poly(3,4-ethylenedioxythiophene):poly(styrene sulfonate) (PEDOT:PSS) NMs were found to be toxic to cells. Cheng's group has coated PEDOT:PSS NMs with PEG to enhance its functionality by prolonged blood circulation half lifetime (about 21 hrs) with 28% tumor uptake (Di et al. 2011). According to the in vivo experiments, this resulted in a spectacular effect on tumor ablation.

Recently, PPy NMs have been considered for their better biocompatibility compared to other CPs and utilized as PTT ablation agents and in other medical fields such as neural probes and biosensors (Ramanaviciene et al. 2010). PPy NMs (sub-100 nm) have shown high PT conversion efficiency, about 44.7% photostability, and strong optical absorption at 808 nm (Chen et al. 2012). Dai's group synthesized PPy NMs uniformly with a mean size of 46 nm using aqueous dispersion polymerization and studied its PT ablation effects on HeLa cells in vitro (Zha et al. 2013). The research showed that the PPy NMs could be used as an ablation agent for selective therapy with minimum side effects.

PPy could also be considered an excellent candidate for coating other nano-drugs due to its comparative ease of synthesis, stability, and biocompatibility. Though Au NMs have a strong SPR effect in the visible light region, yet not precisely in the NIR window without any modifications. This has limited its use in PTT. Thus, PPy is used to coat chainlike Au NM's architectures to tune the responsive NIR region (Lin et al. 2014). These PPy-coated Au NMs have better PT transduction in the NIR region and result in specificity to inhibit the growth of cancer cells (Fig. 7.11).

In conclusion, CP-based NMs and their developing use in PTT have shown exceptional photothermal abilities and high photostability. Along with Au-based NMs, and PPy nanoarchitecture, NMs can be utilized as a carrier for drugs. Various synthesis procedures, like electrochemical deposition (Singh et al. 2013) and chemical oxidation (Zha et al. 2013), were used to synthesize PPy nanoscale

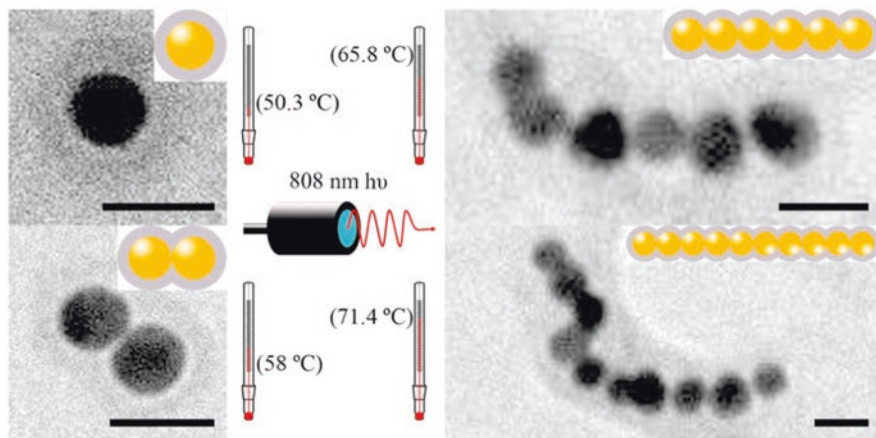


Fig. 7.11 Schematic representation of the photothermal effect of PPy-coated chainlike gold nanoparticles (scale bar = 50 nm). [Reproduced with permission from Lin et al. (2014)]

functionalized coating for enhanced medical systems. Thus, PPy NMs could work as excellent ablation agents and accessories for modified medical systems involving synergistic therapies.

Overall, the NMs used as ablation agents cover semiconductors, noble metals, conducting polymers, carbon-based materials, etc. (Table 7.2 Such diverse ablation agents are made possible for the fabrication of composites with various NMs for a more significant PT effect.

7.4 Limitations and Future Prospect

Even though NM-based PTT and PDT showed significant bacterial killing efficiency and wound healing, few limitations are observed. First is the cytotoxicity introduced by the NMs. The majority of the NMs for wound healing applications are based on inorganic NMs, such as Au, Ag, Cu, etc., that are not biodegradable. They quickly accumulate inside the cells due to the interaction between the cell membrane and NMs. Therefore, new materials have to be fabricated that are biodegradable and should give the same photothermal properties as inorganic NMs. Also, NM's uptake must be maintained to control the accumulation, which is possible by tuning the laser power density. Most of the studies were conducted using a power density of $1\text{--}2\text{ Wcm}^{-2}$, which is not within the minimum threshold's safe range. Therefore, power density should be less than $330\text{--}350\text{ mWcm}^{-2}$ to reduce the NM's accumulation on the skin (Cheng and Li 2020). Also, Ag NM-based PTT shows cytotoxicity at relatively higher Ag concentration due to the uncontrolled release of Ag^+ . As the anti-bacterial activity depends on the concentration of Ag NMs, it is not possible to perform the therapy at a low dosage. Hence, several NM's matrixes were

Table 7.2 Nanomaterials used as ablation agent for PTT in cancer therapy

| Nanomaterials | Size (nm) | Shape | Wavelength (nm) | Cancer type | Reference |
|---------------|-----------|------------------|-----------------|-----------------------------|---|
| Au NPs | 10–50 | Nanospheres | 528 | Cervical carcinoma | Prashant K. Jain et al. (2006) |
| | | Nanorods | 695 | | Vankayala et al. (2014) |
| | | Nanoshells | 800 | Breast epithelial carcinoma | Hirsch et al. (2003) |
| | | Nanohehexapods | 805 | | Wang et al. (2013b) |
| Pt NPs | 1–20 | Nanospheres | 1064 | Neuroblastoma | Manikandan et al. (2013) |
| CuS NPs | 1–20 | Nanospheres | 808 | Cervical carcinoma | Li et al. (2010) |
| | 500–800 | Flower-like | 980 | Glioblastoma | Tian et al. (2011b) and Li et al. (2014a) |
| C NPs | 50–500 | Multi-walled | 1064 | Breast cancer | Burke et al. (2012) |
| | | Single-walled NT | 808 | | Liu et al. (2011b) |
| Graphene | 50–360 | Nanospheres | 808 | Glioblastoma | Markovic et al. (2011) |
| PANI | 100–150 | Nanospheres | 808 | Epidermoid carcinoma | Yang et al. (2011) |
| PEDOT:PSS | 80–130 | Nanospheres | 808 | Breast cancer | Cheng et al. (2012) |
| PPy | 40–60 | Nanospheres | 808 | Breast cancer | Chen et al. (2012) and Zha et al. (2013) |

introduced to control the Ag^+ release by immobilizing the Ag NMs (Tong et al. 2020). However, achieving higher anti-bacterial efficiency with a low Ag dosage is still challenging. Second, very few papers successfully addressed tracing the ROS or by-products during ROS production and other by-product generation. Also, most of the research was focused on in vitro analysis, which inhibited their clinical usage. Recently, very few works demonstrated in vivo and cytotoxicity analysis in inorganic metal-based NM's therapy. In addition, PDT-based wound healing shows low skin penetration compared to PTT. Hence, the fabrication of hybrid NMs that can convert NIR into heat with high penetration is required, which is beneficial for bone and cartilage regeneration.

Apart from every functional use, PTT has its limitations also in cancer therapy. NMs can pass through the cell membrane of the cancer cells, which leads to its accumulation in lesions and intensifies treatment efficacy. Nonetheless, accumulation of the NMs is also possible inside the healthy cells during and after PTT. Thus, the possibility of causing long-term cytotoxicity of aggregated NMs needs further research. It is pretty strenuous to detect, locate, and eradicate nanoscale materials.

The surface properties of the NMs play an essential role in the physicochemical properties and photothermal effect (Prashant K. Jain et al. 2006; Wang et al. 2013b). To meet the demands of PTT and make it biocompatible, surface modifications are necessary. This modification process can make NMs better biocompatible and increased NIR conversion efficacy for PTT. This would also avoid any side effects; using NMs and a large density laser would be unnecessary.

7.5 Conclusion

Photothermal nanomaterial-based therapy and photodynamic therapy are gaining attention in skin wound healing and monitoring, bone regeneration, cartilage damage treatment, and selective and non-invasive cancer treatment. Most of the nanomaterials for this purpose incorporate an inorganic nanomaterial that shows excellent photothermal behavior and biocompatibility in nature or biodegradable nanomaterials. Though the mechanism is different, its photothermal effect could be tuned by varying the size and shape of the photothermal agent. In wound healing, upon near-infrared irradiation, these materials elevate mild local temperature in selected areas that are adequate to kill most of the bacteria. The generated reactive oxygen species or the presence of metal ions kills the remaining bacteria, and through biodegradation of nanomaterials, it can be easily eliminated. Compared to skin wounds, bone and cartilage defect healing requires near-infrared exposure for longer due to soft tissue penetration. For osteogenesis and chondrogenesis, photothermal nanomaterial-based therapy upregulates osteogenic and chondrogenic factors that efficiently promote bone and cartilage regeneration.

While continuous efforts are taken in photothermal therapeutic development for the anti-tumor treatment and its clinical applications, photothermal therapy-integrated synergistic therapies should be focused on improving its curative effects. Photothermal ablation agents are needed to be multi-functional, i.e., drug carriers as well as contrast agents. Thus, real-time imaging with photothermal therapy or synergistic with chemotherapy could be achieved. These synergistic therapies can help us to monitor the over-dosing concerns and secondary treatments, resulting in better anti-cancer potentiality.

References

- Anti-in B, Xi Y, Ge J, et al. Anti-inflammatory, antibacterial, Antioxidative silicon-based Nanofibrous dressing enables cutaneous tumor Photothermo-chemo therapy and infection-induced wound healing. *ACS Nano*. 2020;14:2904–16.
- Arasawang U, Saengsawang O, Rungrotmongkol T, et al. How do carbon nanotubes serve as carriers for gemcitabine transport in a drug delivery system? *J Mol Graph Model*. 2011;29:591–6. <https://doi.org/10.1016/J.JMGM.2010.11.002>.

- Ash C, Dubec M, Donne K, Bashford T. Effect of wavelength and beam width on penetration in light-tissue interaction using computational methods. *Lasers Med Sci.* 2017;32:1909–18. <https://doi.org/10.1007/S10103-017-2317-4/FIGURES/8>.
- Barik TK, Maity GC, Gupta P, et al. Nanomaterials: an introduction. In: *Nanomaterials: an introduction. Nanomaterials and their biomedical applications.* Singapore: Springer; 2021 p 1–27.
- Bu X, Zhou D, Li J, et al. Copper sulfide self-assembly architectures with improved Photothermal performance. *Langmuir.* 2014;30:1416–23. <https://doi.org/10.1021/LA404009D>.
- Burke AR, Singh RN, Carroll DL, et al. The resistance of breast cancer stem cells to conventional hyperthermia and their sensitivity to nanoparticle-mediated photothermal therapy. *Biomaterials.* 2012;33:2961–70. <https://doi.org/10.1016/J.BIOMATERIALS.2011.12.052>.
- Zhongli C, Pierre C, Darel H, Sanche L. Comparison between X-ray photon and secondary electron damage to DNA in vacuum. *J Phys Chem B.* 2005;109:4796–800. <https://doi.org/10.1021/JP0459458>.
- Chen Z, Zhang L, Sun Y, et al. 980-nm laser-driven photovoltaic cells based on rare-earth up-converting phosphors for biomedical applications. *Adv Funct Mater.* 2009;19:3815–20. <https://doi.org/10.1002/ADFM.200901630>.
- Chen M, Fang X, Tang S, Zheng N. Polypyrrole nanoparticles for high-performance in vivo near-infrared photothermal cancer therapy. *Chem Commun.* 2012;48:8934–6. <https://doi.org/10.1039/C2CC34463G>.
- Chen J, Ning C, Zhou Z, et al. Nanomaterials as photothermal therapeutic agents. *Prog Mater Sci.* 2019;99:1–26.
- Chen S, Lu J, You T, Sun D. Metal-organic frameworks for improving wound healing, vol. 439. *Coord. Chem. Rev.* 2021. p. 213929.
- Cheng A, Caffrey M. Free radical mediated x-ray damage of model membranes. *Biophys J.* 1996;70:2212–22.
- Cheng G, Li B. Nanoparticle-based photodynamic therapy: new trends in wound healing applications. *Mater Today Adv.* 2020;6:100049. <https://doi.org/10.1016/j.mtadv.2019.100049>.
- Cheng L, Yang K, Chen Q, Liu Z. Organic stealth nanoparticles for highly effective in vivo near-infrared photothermal therapy of cancer. *ACS Nano.* 2012;6:5605–13. <https://doi.org/10.1021/NN301539M>.
- Consales M, Cutolo A, Penza M, et al. Carbon nanotubes coated acoustic and optical VOCs sensors: towards the tailoring of the sensing performances. *IEEE Trans Nanotechnol.* 2007;6:601–11. <https://doi.org/10.1109/TNANO.2007.907843>.
- Dhar S, Liu Z, Thomale J, et al. Targeted Single-Wall carbon nanotube-mediated Pt(IV) prodrug delivery using folate as a homing device. *J Am Chem Soc.* 2008;130:11467–76. <https://doi.org/10.1021/JA803036E>.
- Di B, Meng Y, Wang YD, et al. Electroluminescence enhancement in polymer light-emitting diodes through inelastic scattering of oppositely charged Bipolarons. *J Phys Chem B.* 2011;115:9339–44. <https://doi.org/10.1021/JP2006342>.
- Du B, Ma C, Ding G, et al. Cooperative strategies for enhancing performance of photothermal therapy (PTT) agent: optimizing its photothermal conversion and cell internalization ability. *Small.* 2017;13:19–24. <https://doi.org/10.1002/sml.201603275>.
- Georgakilas V, Tzitzios V, Gournis D, Petridis D. Attachment of magnetic nanoparticles on carbon nanotubes and their soluble derivatives. *Chem Mater.* 2005;17:1613–7. <https://doi.org/10.1021/CM0483590>.
- Ghanbari K, Bathaie SZ, Mousavi MF. Electrochemically fabricated polypyrrole nanofiber-modified electrode as a new electrochemical DNA biosensor. *Biosens Bioelectron.* 2008;23:1825–31. <https://doi.org/10.1016/J.BIOS.2008.02.029>.
- Gobin AM, Lee MH, Halas NJ, et al. Near-infrared resonant nanoshells for combined optical imaging and photothermal cancer therapy. *Nano Lett.* 2007;7:1929–34. <https://doi.org/10.1021/NL070610Y>.
- Guo S, Dong S, Wang E. Polyaniline/Pt hybrid nanofibers: high-efficiency nanoelectrocatalysts for electrochemical devices. *Small.* 2009;5:1869–76. <https://doi.org/10.1002/SMLL.200900190>.

- Gupta P, Kar S, Kumar A, et al. Pulsed laser assisted high-throughput intracellular delivery in hanging drop based three dimensional cancer spheroids. *Analyst*. 2021;146:4756–66. <https://doi.org/10.1039/D0AN02432E>.
- Hanf R, Fey S, Schmitt M, et al. Catalytic efficiency of a photoenzyme—an adaptation to natural light conditions. *ChemPhysChem*. 2012;13:2013–5. <https://doi.org/10.1002/CPHC.201200194>.
- He J, Qiao Y, Zhang H, et al. Gold–silver nanoshells promote wound healing from drug-resistant bacteria infection and enable monitoring via surface-enhanced Raman scattering imaging. *Biomaterials*. 2020a;234:119763. <https://doi.org/10.1016/j.biomaterials.2020.119763>.
- He J, Shi M, Liang Y, Guo B. Conductive adhesive self-healing nanocomposite hydrogel wound dressing for photothermal therapy of infected full-thickness skin wounds. *Chem Eng J*. 2020b;394:124888. <https://doi.org/10.1016/j.cej.2020.124888>.
- Hirsch LR, Stafford RJ, Bankson JA, et al. Nanoshell-mediated near-infrared thermal therapy of tumors under magnetic resonance guidance. *Proc Natl Acad Sci*. 2003;100:13549–54. <https://doi.org/10.1073/PNAS.2232479100>.
- Huang X, El-Sayed IH, Qian W, El-Sayed MA. Cancer cell imaging and photothermal therapy in the near-infrared region by using gold Nanorods. *J Am Chem Soc*. 2006;128:2115–20. <https://doi.org/10.1021/JA057254A>.
- Huang X, Jain PK, El-Sayed IH, El-Sayed MA. Plasmonic photothermal therapy (PPTT) using gold nanoparticles. *Lasers Med Sci*. 2007;23:217–28. <https://doi.org/10.1007/S10103-007-0470-X>.
- Huang P, Bao L, Zhang C, et al. Folic acid-conjugated silica-modified gold nanorods for X-ray/CT imaging-guided dual-mode radiation and photo-thermal therapy. *Biomaterials*. 2011;32:9796–809. <https://doi.org/10.1016/J.BIOMATERIALS.2011.08.086>.
- Huang Y, Lai Y, Shi S, et al. Copper sulfide nanoparticles with phospholipid-PEG coating for in vivo near-infrared Photothermal cancer therapy. *Chem – An Asian J*. 2015;10:370–6. <https://doi.org/10.1002/ASIA.201403133>.
- Huang S, Liu H, Liao K, et al. Functionalized GO Nanovehicles with nitric oxide release and Photothermal activity-based hydrogels for bacteria-infected wound healing. *ACS Appl Mater Interfaces*. 2020;12:28952–64. <https://doi.org/10.1021/acsami.0c04080>.
- Illath K, Narasimhan AK, Nagai M, et al. Microfluidics-based metallic nanoparticle synthesis and applications. In: *microfluidics and Bio-MEMS*. Jenny Stanford Publishing; 2020a. p 429–501.
- Illath K, Narasimhan AK, Shinde P, et al. Intracellular delivery using anisotropic gold nanocrystals synthesized by microfluidic device. In: *IEEE nano/micro engineered and molecular systems; 2020b*. p 448–52.
- Illath K, Wankhar S, Mohan L, et al. Metallic nanoparticles for biomedical applications. In: *nano-materials and their biomedical applications*. Singapore: Springer; 2021. p. 29–81.
- Jain PK, Lee KS, El-Sayed IH, El-Sayed MA. Calculated absorption and scattering properties of gold nanoparticles of different size, shape, and composition: applications in biological imaging and biomedicine. *J Phys Chem B*. 2006;110:7238–48. <https://doi.org/10.1021/JP057170O>.
- Jia GZ, Lou WK, Cheng F, et al. Excellent photothermal conversion of core/shell CdSe/ bi 2 se 3 quantum dots. *Nano Res*. 2015;8:1443–53. <https://doi.org/10.1007/s12274-014-0629-2>.
- Jiang R, Cheng S, Shao L, et al. Mass-based Photothermal comparison among gold nanocrystals, PbS nanocrystals, organic dyes, and carbon Black. *J Phys Chem C*. 2013;117:8909–15. <https://doi.org/10.1021/JP400770X>.
- Johnson J, Dawson-Hughes B. Precision and stability of dual-energy X-ray absorptiometry measurements. *Calcif Tissue Int*. 1991;49:174–8. <https://doi.org/10.1007/BF02556113>.
- Ju Q, Chen X, Ai F, et al. An upconversion nanoprobe operating in the first biological window. *J Mater Chem B*. 2015;3:3548–55. <https://doi.org/10.1039/C5TB00025D>.
- Kar S, Shinde P, Nagai M, Santra TS. Optical manipulation of cells. In: *microfluidics and Bio-MEMS: Devices and Applications*. New York: Jenny Stanford Publishing; 2020. p 49–94.
- Korkut S, Roy-Mayhew JD, Dabbs DM, et al. High surface area tapes produced with functionalized graphene. *ACS Nano*. 2011;5:5214–22. <https://doi.org/10.1021/NN2013723>.
- Leaper D, Harding K. *Wounds: biology and management*. Oxford University Press; 1998.

- Li Y, Lu W, Huang Q, et al. Copper sulfide nanoparticles for photothermal ablation of tumor cells. *Nanomedicine*. 2010;5:1161–71. <https://doi.org/10.2217/NNM.10.85>.
- Li B, Wang Q, Zou R, et al. Cu₇S₄ nanocrystals: a novel photothermal agent with a 56.7% photothermal conversion efficiency for photothermal therapy of cancer cells. *Nanoscale*. 2014a;6:3274–82. <https://doi.org/10.1039/C3NR06242B>.
- Li B, Zhang Y, Zou R, et al. Self-assembled WO₃-x hierarchical nanostructures for photothermal therapy with a 915 nm laser rather than the common 980 nm laser. *Dalt Trans*. 2014b;43:6244–50. <https://doi.org/10.1039/C3DT53396D>.
- Li S, Zhang L, Wang T, et al. The facile synthesis of hollow au nanoflowers for synergistic chemophotothermal cancer therapy. *Chem Commun*. 2015;51:14338–41. <https://doi.org/10.1039/C5CC05676D>.
- Li J, Wang Y, Yang J, Liu W. Bacteria activated-macrophage membrane-coated tough nanocomposite hydrogel with targeted photothermal antibacterial ability for infected wound healing. *Chem Eng J*. 2021;420:127638.
- Lin M, Guo C, Li J, et al. Polypyrrole-coated chainlike gold nanoparticle architectures with the 808 nm photothermal transduction efficiency up to 70%. *ACS Appl Mater Interfaces*. 2014;6:5860–8. <https://doi.org/10.1021/AM500715F>.
- Liu H, Chen D, Li L, et al. Multifunctional gold Nanoshells on silica nanorattles: a platform for the combination of photothermal therapy and chemotherapy with low systemic toxicity. *Angew Chemie Int Ed*. 2011a;50:891–5. <https://doi.org/10.1002/ANIE.201002820>.
- Liu X, Tao H, Yang K, et al. Optimization of surface chemistry on single-walled carbon nanotubes for in vivo photothermal ablation of tumors. *Biomaterials*. 2011b;32:144–51. <https://doi.org/10.1016/J.BIOMATERIALS.2010.08.096>.
- Liu X, Huang N, Wang H, et al. The effect of ligand composition on the in vivo fate of multidentate poly(ethylene glycol) modified gold nanoparticles. *Biomaterials*. 2013;34:8370–81. <https://doi.org/10.1016/J.BIOMATERIALS.2013.07.059>.
- Liu H, Zhu X, Guo H, et al. Nitric oxide released injectable hydrogel combined with synergistic photothermal therapy for antibacterial and accelerated wound healing. *Appl Mater Today*. 2020;20:100781. <https://doi.org/10.1016/j.apmt.2020.100781>.
- Loizou CP, Kasparis T, Mitsi O, Polyviou M. Evaluation of wound healing process based on texture analysis. *IEEE 12th Int Conf Bioinforma Bioeng BIBE*. 2012;2012:709–14. <https://doi.org/10.1109/BIBE.2012.6399754>.
- Lu Z, Liu S, Le Y, et al. An injectable collagen-genipin-carbon dot hydrogel combined with photodynamic therapy to enhance chondrogenesis. *Biomaterials*. 2019;218:119190. <https://doi.org/10.1016/j.biomaterials.2019.05.001>.
- Ma M, Zhong Y, Jiang X. An injectable photothermally active antibacterial composite hydroxypropyl chitin hydrogel for promoting the wound healing process through photobiomodulation. *J Mater Chem B*. 2021;9:4567–76. <https://doi.org/10.1039/d1tb00724f>.
- Maestro L, Ramírez-Hernández J, Bogdan N, et al. Deep tissue bio-imaging using two-photon excited CdTe fluorescent quantum dots working within the biological window. *Nanoscale*. 2011;4:298–302. <https://doi.org/10.1039/C1NR11285F>.
- Manikandan M, Hasan N, Wu HF. Platinum nanoparticles for the photothermal treatment of neuro 2A cancer cells. *Biomaterials*. 2013;34:5833–42. <https://doi.org/10.1016/J.BIOMATERIALS.2013.03.077>.
- Markovic ZM, Harhaji-Trajkovic LM, Todorovic-Markovic BM, et al. In vitro comparison of the photothermal anticancer activity of graphene nanoparticles and carbon nanotubes. *Biomaterials*. 2011;32:1121–9. <https://doi.org/10.1016/J.BIOMATERIALS.2010.10.030>.
- Matteini P, Tatini F, Cavigli L, et al. Graphene as a photothermal switch for controlled drug release. *Nanoscale*. 2014;6:7947–53. <https://doi.org/10.1039/C4NR01622J>.
- Mei L, Gao X, Shi Y, et al. Augmented graphene quantum dot-light irradiation therapy for bacteria-infected wounds. *ACS Appl Mater Interfaces*. 2020;12:40153–62. <https://doi.org/10.1021/acsaami.0c13237>.

- Mei L, Shi Y, Cao F, et al. PEGylated phthalocyanine-functionalized graphene oxide with ultrahigh-efficient photothermal performance for triple-mode antibacterial therapy. *ACS Biomater Sci Eng.* 2021;7:2638–48. <https://doi.org/10.1021/acsbiomaterials.1c00178>.
- Melamed JR, Edelstein RS, Day ES. Elucidating the fundamental mechanisms of cell death triggered by photothermal therapy. *ACS Nano.* 2015;9:6–11. <https://doi.org/10.1021/ACSNANO.5B00021>.
- Mohammad F, Balaji G, Weber A, et al. Influence of gold Nanoshell on hyperthermia of superparamagnetic iron oxide nanoparticles. *J Phys Chem C.* 2010;114:19194–201. <https://doi.org/10.1021/JP105807R>.
- Mohan L, Kar S, Nandhini B, et al. Fabrication of TiO₂ micro-spikes and micro-flowers for massively parallel intracellular delivery. In: 23rd International conference on miniaturized systems for chemistry and life sciences, MicroTAS; 2019.
- Mohan L, Kar S, Mahapatra PS, et al. Fabrication of TiO₂ microspikes for highly efficient intracellular delivery by pulse laser-assisted photoporation. *RSC Adv.* 2021a;11:9336–48. <https://doi.org/10.1039/D0RA09785C>.
- Mohan L, Kar S, Nagai M, Santra TS. Electrochemical fabrication of TiO₂ micro-flowers for an efficient intracellular delivery using nanosecond light pulse. *Mater Chem Phys.* 2021b;267:124604. <https://doi.org/10.1016/j.matchemphys.2021.124604>.
- Mohan L, Kar S, Hattori R, et al. Can titanium oxide nanotubes facilitate intracellular delivery by laser-assisted photoporation? *Appl Surf Sci.* 2021c;543:148815. <https://doi.org/10.1016/j.apsusc.2020.148815>.
- Morton LM, Phillips TJ. Wound healing and treating wounds. *J Am Acad Dermatol.* 2016;74:589–605.
- Neves LFF, Kraiss JJ, Van RBD, et al. Targeting single-walled carbon nanotubes for the treatment of breast cancer using photothermal therapy. *Nanotechnology.* 2013;24:375104. <https://doi.org/10.1088/0957-4484/24/37/375104>.
- Phan TTV, Huynh TC, Oh J. Photothermal responsive porous membrane for treatment of infected wound. *Polymers.* 2019;11:1679. <https://doi.org/10.3390/polym11101679>.
- Pitsillides CM, Joe EK, Wei X, et al. Selective cell targeting with light-absorbing microparticles and nanoparticles. *Biophys J.* 2003;84:4023–32. [https://doi.org/10.1016/S0006-3495\(03\)75128-5](https://doi.org/10.1016/S0006-3495(03)75128-5).
- Qiao Y, Ping Y, Zhang H, et al. Laser-activatable CuS nanodots to treat multidrug-resistant bacteria and release copper ion to accelerate healing of infected chronic nonhealing wounds. *ACS Appl Mater Interfaces.* 2019;11:3809–22. <https://doi.org/10.1021/acsami.8b21766>.
- Qiu P, Yang M, Qu X, et al. Tuning photothermal properties of gold nanodendrites for in vivo cancer therapy within a wide near infrared range by simply controlling their degree of branching. *Biomaterials.* 2016;104:138–44. <https://doi.org/10.1016/J.BIOMATERIALS.2016.06.033>.
- Ramanaviciene A, Kausaite A, Tautkus S, Ramanavicius A. Biocompatibility of polypyrrole particles: an in-vivo study in mice. *J Pharm Pharmacol.* 2010;59:311–5. <https://doi.org/10.1211/JPP.59.2.0017>.
- Ramasamy M, Lee SS, Yi DK, Kim K. Magnetic, optical gold nanorods for recyclable photothermal ablation of bacteria. *J Mater Chem B.* 2014;2:981–8. <https://doi.org/10.1039/C3TB21310B>.
- Robinson JT, Welscher K, Tabakman SM, et al. High performance in vivo near-IR (>1 μm) imaging and photothermal cancer therapy with carbon nanotubes. *Nano Res.* 2010;3:779–93. <https://doi.org/10.1007/s12274-010-0045-1>.
- Rossella F, Soldano C, Bellani V, Tommasini M. Metal-filled carbon nanotubes as a novel class of photothermal nanomaterials. *Adv Mater.* 2012;24:2453–8. <https://doi.org/10.1002/adma.201104393>.
- Rosselle L, Cantelmo AR, Barras A, et al. An “on-demand” photothermal antibiotic release cryogel patch: evaluation of efficacy on an ex vivo model for skin wound infection. *Biomater Sci.* 2020;8:5911–9. <https://doi.org/10.1039/d0bm01535k>.
- Santra TS. Bio-MEMS and Bio-NEMS: devices and applications. Jenny Stanford Publishers; 2020.
- Santra T, Mohan L. Nanomaterials and their biomedical applications. Singapore: Springer; 2021.
- Santra TS, Tseng F-G. Handbook of single cell technologies. Singapore: Springer; 2022.

- Santra TS, Tseng F-G(K), Barik TK. Biosynthesis of silver and gold nanoparticles for potential biomedical applications—a brief review. *J Nanopharm Drug Deliv.* 2015a;2:249–65. <https://doi.org/10.1166/jnd.2014.1065>.
- Santra TS, Tseng F-G, Barik TK. Green biosynthesis of gold nanoparticles and biomedical applications. *Am J nano res Appl.* 2015b;2(6–2):5–12.
- Santra TS, Wu TH, Chiou EPY. Photothermal microfluidics. In: optical MEMS for chemical analysis and iomedicine. London: The Institute of Engineering and Technology (IET); 2016. p 289–323.
- Santra TS, Kar S, Chen TC, et al. Near-infrared nanosecond-pulsed laser-activated highly efficient intracellular delivery mediated by nano-corrugated mushroom-shaped gold-coated polystyrene nanoparticles. *Nanoscale.* 2020;12:12057–67. <https://doi.org/10.1039/d0nr01792b>.
- Sarna T, Sealy RC. Photoinduced oxygen consumption in melanin systems. Action spectra and quantum yields for eumelanin and synthetic melanin. *Photochem Photobiol.* 1984;39:69–74. <https://doi.org/10.1111/J.1751-1097.1984.TB03406.X>.
- Shanmugapriya K, Kang HW. Engineering pharmaceutical nanocarriers for photodynamic therapy on wound healing: review. *Mater Sci Eng C.* 2019;105:110110. <https://doi.org/10.1016/j.msec.2019.110110>.
- Sheng L, Zhang Z, Zhang Y, et al. A novel “hot spring”-mimetic hydrogel with excellent angiogenic properties for chronic wound healing. *Biomaterials.* 2021;264:120414. <https://doi.org/10.1016/j.biomaterials.2020.120414>.
- Shinde P, Kar S, Loganathan M, et al. Infrared pulse laser-activated highly efficient intracellular delivery using titanium microdish device. *ACS Biomater Sci Eng.* 2020;6:5645–52. <https://doi.org/10.1021/acsbiomaterials.0c00785>.
- Shinde A, Kar S, Nagai M, et al. Light-induced cellular delivery and analysis. In: handbook of single cell technologies; 2021a. p 1–29.
- Shinde AS, Shinde PS, Santra TS. Nanomaterials: versatile drug carriers for nanomedicine. In: nanomaterials and their biomedical applications; 2021b. p 253.
- Singh S, Jain DVS, Singla ML. One step electrochemical synthesis of gold-nanoparticles–polypyrrole composite for application in catechin electrochemical biosensor. *Anal Methods.* 2013;5:1024–32. <https://doi.org/10.1039/C2AY26201K>.
- Stolik S, Delgado JA, Pérez A, Anasagasti L. Measurement of the penetration depths of red and near infrared light in human “ex vivo” tissues. *J Photochem Photobiol B Biol.* 2000;57:90–3. [https://doi.org/10.1016/S1011-1344\(00\)00082-8](https://doi.org/10.1016/S1011-1344(00)00082-8).
- Sun J, Song L, Fan Y, et al. Synergistic photodynamic and photothermal antibacterial nanocomposite membrane triggered by single NIR light source. *ACS Appl Mater Interfaces.* 2019;11:26581–9. <https://doi.org/10.1021/acsami.9b07037>.
- Tang S, Chen M, Zheng N. Sub-10-nm Pd Nanosheets with renal clearance for efficient near-infrared photothermal cancer therapy. *Small.* 2014;10:3139–44. <https://doi.org/10.1002/SMLL.201303631>.
- Tao B, Lin C, Deng Y, et al. Copper-nanoparticle-embedded hydrogel for killing bacteria and promoting wound healing with photothermal therapy. *J Mater Chem B.* 2019;7:2534–48. <https://doi.org/10.1039/C8TB03272F>.
- Tay CY, Setyawati MI, Leong DT. Nanoparticle density: a critical biophysical regulator of endothelial permeability. *ACS Nano.* 2017;11:2764–72. <https://doi.org/10.1021/ACS.NANO.6B07806>.
- Tian Q, Jiang F, Zou R, et al. Hydrophilic Cu₉S₅ nanocrystals: a photothermal agent with a 25.7% heat conversion efficiency for photothermal ablation of cancer cells in vivo. *ACS Nano.* 2011a;5:9761–71. <https://doi.org/10.1021/NN203293T>.
- Tian Q, Tang M, Sun Y, et al. Hydrophilic flower-like CuS superstructures as an efficient 980 nm laser-driven photothermal agent for ablation of cancer cells. *Adv Mater.* 2011b;23:3542–7. <https://doi.org/10.1002/ADMA.201101295>.
- Tian Y, Luo S, Yan H, et al. Gold nanostars functionalized with amine-terminated PEG for X-ray/CT imaging and photothermal therapy. *J Mater Chem B.* 2015;3:4330–7. <https://doi.org/10.1039/C5TB00509D>.

- Tiwari JN, Seo YK, Yoon T, et al. Accelerated bone regeneration by two-photon photoactivated carbon nitride nanosheets. *ACS Nano*. 2017;11:742–51. <https://doi.org/10.1021/acs.nano.6b07138>.
- Tong L, Liao Q, Zhao Y, et al. Near-infrared light control of bone regeneration with biodegradable photothermal osteoimplant. *Biomaterials*. 2019;193:1–11. <https://doi.org/10.1016/j.biomaterials.2018.12.008>.
- Tong C, Zhong X, Yang Y, et al. PB@PDA@Ag nanosystem for synergistically eradicating MRSA and accelerating diabetic wound healing assisted with laser irradiation. *Biomaterials*. 2020;243:119936. <https://doi.org/10.1016/j.biomaterials.2020.119936>.
- Tsai M-F, Chang S-HG, Cheng F-Y, et al. Au nanorod design as light-absorber in the first and second biological near-infrared windows for in vivo photothermal therapy. *ACS Nano*. 2013;7:5330–42. <https://doi.org/10.1021/NN401187C>.
- Vankayala R, Lin CC, Kalluru P, et al. Gold nanoshells-mediated bimodal photodynamic and photothermal cancer treatment using ultra-low doses of near infra-red light. *Biomaterials*. 2014;35:5527–38. <https://doi.org/10.1016/J.BIOMATERIALS.2014.03.065>.
- Visser M, Fuerst T, Lang T, et al. Validity of fan-beam dual-energy X-ray absorptiometry for measuring fat-free mass and leg muscle mass. *J Appl Physiol*. 1999;87:1513–20. <https://doi.org/10.1152/JAPPL.1999.87.4.1513>.
- Walsh JT. Basic interactions of light with tissue. In: *Optical-thermal response of laser-irradiated tissue*. Dordrecht: Springer; 2010. https://doi.org/10.1007/978-90-481-8831-4_2.
- Wang R, Mikoryak C, Li S, et al. Cytotoxicity screening of single-walled carbon nanotubes: detection and removal of cytotoxic contaminants from Carboxylated carbon nanotubes. *Mol Pharm*. 2011;8:1351–61. <https://doi.org/10.1021/MP2001439>.
- Wang L, Shi J, Jia X, et al. NIR-/pH-responsive drug delivery of functionalized single-walled carbon nanotubes for potential application in cancer chemo-Photothermal therapy. *Pharm Res*. 2013a;30(30):2757–71. <https://doi.org/10.1007/S11095-013-1095-3>.
- Wang Y, Black KCL, Luehmann H, et al. Comparison study of gold nanohexapods, nanorods, and nanocages for photothermal cancer treatment. *ACS Nano*. 2013b;7:2068–77. <https://doi.org/10.1021/NN304332S>.
- Wang D, Xu Z, Yu H, et al. Treatment of metastatic breast cancer by combination of chemotherapy and photothermal ablation using doxorubicin-loaded DNA wrapped gold nanorods. *Biomaterials*. 2014;35:8374–84. <https://doi.org/10.1016/J.BIOMATERIALS.2014.05.094>.
- Wang X, Lv F, Li T, et al. Electrospun micropatterned nanocomposites incorporated with Cu2S Nanoflowers for skin tumor therapy and wound healing. *ACS Nano*. 2017;11:11337–49. <https://doi.org/10.1021/acs.nano.7b05858>.
- Wang J, Zhang C, Yang Y, et al. Poly (vinyl alcohol) (PVA) hydrogel incorporated with ag/TiO2 for rapid sterilization by photoinspired radical oxygen species and promotion of wound healing. *Appl Surf Sci*. 2019;494:708–20.
- Wang S, Zheng H, Zhou L, et al. Injectable redox and light responsive MnO2 hybrid hydrogel for simultaneous melanoma therapy and multidrug-resistant bacteria-infected wound healing. *Biomaterials*. 2020;260:120314.
- Wang J, Li Y, Han X, et al. Light-triggered antibacterial hydrogels containing recombinant growth factor for treatment of bacterial infections and improved wound healing. *ACS Biomater Sci Eng*. 2021;7:1438–49. <https://doi.org/10.1021/acsbiomaterials.0c01588>.
- Wentao W, Tao Z, Bulei S, et al. Functionalization of polyvinyl alcohol composite film wrapped in am-ZnO@CuO@Au nanoparticles for antibacterial application and wound healing. *Appl Mater Today*. 2019;17:36–44.
- Xie G, Zhou N, Gao Y, et al. On-demand release of CO2 from photothermal hydrogels for accelerating skin wound healing. *Chem Eng J*. 2021;403:126353.
- Xu X, Liu X, Tan L, et al. Controlled-temperature photothermal and oxidative bacteria killing and acceleration of wound healing by polydopamine-assisted Au-hydroxyapatite nanorods. *Acta Biomater*. 2018;77:352–64.
- Xu C, Akakuru OU, Ma X, et al. Nanoparticle-based wound dressing: recent progress in the detection and therapy of bacterial infections. *Bioconjug Chem*. 2020;31:1708–23. <https://doi.org/10.1021/acs.bioconjugchem.0c00297>.

- Xue C, Sutrisno L, Li M, et al. Implantable multifunctional black phosphorus nanoformulation-deposited biodegradable scaffold for combinational photothermal/ chemotherapy and wound healing. *Biomaterials*. 2021;269:120623. <https://doi.org/10.1016/j.biomaterials.2020.120623>.
- Yan L, Mu J, Ma P, et al. Gold nanoplates with superb photothermal efficiency and peroxidase-like activity for rapid and synergistic antibacterial therapy. *Chem Commun*. 2021;57:1133–6. <https://doi.org/10.1039/d0cc06925f>.
- Yanagi T, Kajiya H, Kawaguchi M, et al. Photothermal stress triggered by near infrared-irradiated carbon nanotubes promotes bone deposition in rat calvarial defects. *J Biomater Appl*. 2015;29:1109–18. <https://doi.org/10.1177/0885328214556913>.
- Yang J, Choi J, Bang D, et al. Convertible organic nanoparticles for near-infrared photothermal ablation of cancer cells. *Angew Chemie*. 2011;123:461–4. <https://doi.org/10.1002/ANGE.201005075>.
- Yao Q, Lan QH, Jiang X, et al. Bioinspired biliverdin/silk fibroin hydrogel for antiangioma photothermal therapy and wound healing. *Theranostics*. 2020;10:11719–36. <https://doi.org/10.7150/thno.47682>.
- Yavuz MS, Cheng Y, Chen J, et al. Gold nanocages covered by smart polymers for controlled release with near-infrared light. *Nat Mater*. 2009;8:935–9. <https://doi.org/10.1038/nmat2564>.
- Yu S, Li G, Zhao P, et al. NIR-laser-controlled hydrogen-releasing PdH nanohydride for synergistic hydrogen-photothermal antibacterial and wound-healing therapies. *Adv Funct Mater*. 2019;29:1905697.
- Yu C, Xu L, Zhang Y, et al. Polymer-based nanomaterials for noninvasive cancer photothermal therapy. *ACS Appl Polym Mater*. 2020;2:4289–305. https://doi.org/10.1021/ACSAPM.0C00704/ASSET/IMAGES/LARGE/APOC00704_0009.JPEG.
- Yuan Z, Zhang K, Jiao X, et al. A controllable local drug delivery system based on porous fibers for synergistic treatment of melanoma and promoting wound healing. *Biomater Sci*. 2019;7:5084–96. <https://doi.org/10.1039/c9bm01045a>.
- Zavaleta C, Zerda A d l, Liu Z, et al. Noninvasive Raman spectroscopy in living mice for evaluation of tumor targeting with carbon nanotubes. *Nano Lett*. 2008;8:2800–5. <https://doi.org/10.1021/NL801362A>.
- Zeng Q, Qian Y, Huang Y, et al. Polydopamine nanoparticle-dotted food gum hydrogel with excellent antibacterial activity and rapid shape adaptability for accelerated bacteria-infected wound healing. *Bioact Mater*. 2021;6:2647–57.
- Zha Z, Yue X, Ren Q, Dai Z. Uniform Polypyrrole nanoparticles with high photothermal conversion efficiency for photothermal ablation of cancer cells. *Adv Mater*. 2013;25:777–82. <https://doi.org/10.1002/ADMA.201202211>.
- Zhang X, Cheng G, Xing X, et al. Near-infrared light-triggered porous AuPd alloy nanoparticles to produce mild localized heat to accelerate bone regeneration. *J Phys Chem Lett*. 2019a;10:4185–91. <https://doi.org/10.1021/acs.jpcclett.9b01735>.
- Zhang X, Zhang C, Yang Y, et al. Light-assisted rapid sterilization by a hydrogel incorporated with Ag₃PO₄-MoS₂ composites for efficient wound disinfection. *Chem Eng J*. 2019b;374:596–604.
- Zhang H, Zheng S, Chen C, Zhang D. A graphene hybrid supramolecular hydrogel with high stretchability, self-healable and photothermally responsive properties for wound healing. *RSC Adv*. 2021a;11:6367–73. <https://doi.org/10.1039/d0ra09106e>.
- Zhang P, Sun B, Wu F, et al. Wound healing acceleration by antibacterial biodegradable black phosphorus nanosheets loaded with cationic carbon dots. *J Mater Sci*. 2021b;56:6411–26. <https://doi.org/10.1007/s10853-020-05766-1>.
- Zhao Y, Cai Q, Qi W, et al. BSA-CuS nanoparticles for photothermal therapy of diabetic wound infection in vivo. *ChemistrySelect*. 2018;3:9510–6.
- Zhou J, Lu Z, Zhu X, et al. NIR photothermal therapy using polyaniline nanoparticles. *Biomaterials*. 2013;34:9584–92. <https://doi.org/10.1016/j.biomaterials.2013.08.075>.
- Zhou L, Chen F, Hou Z, et al. Injectable self-healing CuS nanoparticle complex hydrogels with antibacterial, anti-cancer, and wound healing properties. *Chem Eng J*. 2021;409:128224.

Chapter 8

Polymer Nanohybrid-Based Smart Platforms for Controlled Delivery and Wound Management



Dinesh K. Patel, Tejal V. Patil, Keya Ganguly, Sayan Deb Dutta, Rachmi Luthfikasari, and Ki-Taek Lim

8.1 Introduction

Millions of people suffer from wounds globally every year. Rapid wound healing has social and economic importance in the personalized healthcare sector (Nam and Mooney 2021). Wound healing is a complex process and involves several steps, including hemostasis, inflammation, cell proliferation, and dermal remodeling (Zeng et al. 2022). Different factors, such as reactive oxygen species (ROS), infection, inflammation, and other diseases, significantly influence wound healing (Zhu et al. 2018; Gao et al. 2020). Therefore, developing ideal platforms for rapid wound healing is necessary. Biocompatible and biodegradable materials with adequate mechanical strength, hydrophilic, and suitable antibacterial potentials have been widely explored for wound healing applications (Li et al. 2020; Guo et al. 2021). Different synthetic and naturally derived polymer materials, such as polyurethane (PU), polyvinyl pyrrolidone (PPD), polycaprolactone (PCL), polyethylene glycol

D. K. Patel · K. Ganguly · S. D. Dutta · R. Luthfikasari
Department of Biosystems Engineering, Institute of Forest Science, Kangwon National University, Chuncheon, Republic of Korea

T. V. Patil
Interdisciplinary Program in Smart Agriculture, Kangwon National University, Chuncheon, Republic of Korea

K.-T. Lim (✉)
Department of Biosystems Engineering, Institute of Forest Science, Kangwon National University, Chuncheon, Republic of Korea
Interdisciplinary Program in Smart Agriculture, Kangwon National University, Chuncheon, Republic of Korea
e-mail: ktlim@kangwon.ac.kr

(PEG), poly (lactic-co-glycolic acid) (PLGA), polysaccharides or their derivatives, collagen, silk fibroin, and gelatin, are often used as a wound dressing (Mogoşanu and Grumezescu 2014). Rapid development in nanotechnology has facilitated the formation of nanostructured materials within the dimension range of 0.1–100 nm. Nanostructured materials have received considerable attention from researchers due to their size-dependent structural properties, which have broad applicability in tissue engineering, drug delivery, sensing, and more (Li et al. 2021b). Different techniques, such as electrospinning and three-dimensional (3D) printing, are frequently utilized to prepare smart platforms for wound care (Wang et al. 2021b). Electrospinning is a widely used technique to generate nanofiber platforms by charging and ejecting the desired polymer solution through a syringe under a high voltage electric field. The electrospun nanofibers are categorized into ultrafine 1D fibers, 2D non-woven membranes, and 3D scaffolds (Min et al. 2015; Jiang et al. 2015). The physicochemical properties of the prepared nanofibers are profoundly affected by the applied voltage, the distance between the syringe to the collector, rotor speed, and polymer solution (Li et al. 2021b). Poly (lactic acid) (PLA), PU, PCL, PLGA, collagen, chitosan, and poly (vinylidene fluoride) (PVDF) are commonly used to prepare electrospun platforms for different applications (Meireles et al. 2018; Nezarati et al. 2013; Vidotti et al. 2015).

The 3D printing technique is another fascinating method used to prepare customized platforms based on computer-aided design (CAD) software for different applications, including medicine, pharmaceuticals, automobiles, and tissue engineering (Jain et al. 2021). The 3D printing technique enables accurate and cost-effective development of polymer platforms for new possibilities. Different 3D printing techniques, including stereolithography (SLA), selective laser sintering (SLS), fused deposition modeling (FDM), digital light process (DLP), polyjet, electron beam melting (EBM), direct metal laser sintering (DMLS), and multi-jet fusion (MJF) are used to develop the required platforms for different applications (Ambrosi and Pumera 2016). Each technique has advantages and disadvantages. PCL, PLA, PLGA, gelatin, and more are commonly used in 3D printing to construct the desired structures. The 3D-printed constructs demonstrated enhanced wound healing potential (Jahan et al. 2019).

Micro- and nano-robotic platforms constructed of smart materials have also paid wide attention in tissue engineering applications for the controlled release of the loaded active molecules (drugs, genes, DNA, and RNA) and wound healing due to their mimicking potential with biological systems, and accurate targeting ability (Chen et al. 2017). The local conditions of the targeted sites, such as pH and temperature, have a vast influence on releasing the loaded materials from these constructs. Biocompatible hydrogels are considered suitable materials for developing soft robotic constructs due to their favorable properties such as biocompatibility, stretchability, and stimuli responsiveness (Cheng et al. 2019). However, the broad applicability of the constructed platforms is restricted due to the weak mechanical strength and chance of damage (Sun et al. 2012). Therefore, enhancement in the mechanical strength is required to construct desirable platforms for tissue engineering.

Various nanomaterials, such as carbon nanotubes (CNTs), graphene, metals, nanocellulose, zeolite, and more in different forms (1D, 2D, and 3D), are widely used to enhance the mechanical strength of the native polymers (Lau et al. 2013; Adhikari et al. 2017; Lee et al. 2014). The addition of nanomaterials in the polymer matrix also facilitates the stimuli responsiveness in nanohybrids. The physicochemical properties of nanomaterials are profoundly affected by their shape and size. The nanomaterial properties can be easily altered through surface medication (Zhu et al. 2012). Thus, it is possible to choose an appropriate nanomaterial in the polymer matrix for specific stimuli responsiveness. Herein, we concisely discussed the potential application of polymeric nanohybrid-based smart platforms for tissue engineering, primarily controlled drug delivery, and wound healing. The advantages and disadvantages of commonly used synthetic and naturally derived polymers were briefly mentioned. The physicochemical properties of different nanomaterials (zero-dimensional (0D), one dimensional (1D), two dimensional (2D), and three dimensional (3D)) were concisely illustrated. The effects of the different stimuli were also discussed.

8.2 Classification of the Polymers

The demands for polymeric materials (macromolecules) are increasing in the controlled delivery and wound healing applications owing to their desirable properties. The physicochemical properties of the polymers are profoundly affected by their composition, structure, and arrangement of the repeating units (Reddy et al. 2021). Depending on the origin of the polymeric materials, they are further categorized into natural and synthetic polymers. We briefly discussed the advantages and disadvantages of naturally derived and synthetic polymers by considering some attractive examples.

8.2.1 *Natural Polymers*

These polymers are derived from natural resources and frequently applied in drug delivery and wound healing applications. These materials are categorized into three categories depending on their monomer units and structures. These are polypeptide, polysaccharide, and polynucleotide-based polymers. The polypeptide-based polymers include gelatin, silk fibroin, collagen, keratin, elastin, and fibrinogen. The polysaccharide-derived polymers involve chitosan, alginate, cellulose, chitin, agarose, hyaluronic acid, and chitin. The DNA, RNA, and plasmid are categorized as polynucleotide-based polymers (Reddy et al. 2021; Prasad and Wong 2018). The superior bioactivity, biocompatibility, and nontoxic byproducts after degradation make naturally derived polymers suitable candidates for developing smart polymeric platforms for biomedical applications. The vast applicability of naturally

derived polymers is restricted due to their weak mechanical strength, decreased tunability, immunogenic reaction, undesired degradation, and being prone to microbial contamination (Reddy et al. 2021). However, these drawbacks can be overcome by using suitable nanofillers or crosslinkers in the polymer matrix.

8.2.2 Synthetic Polymers

The synthetic polymers are prepared from their monomer units through different methods, such as in situ polymerization, condensation, and addition for different applications. The physicochemical properties of the synthetic polymers are profoundly affected by the degree of polymerization, structure, and orientation of repeating units, molecular weight (Mogoşanu and Grumezescu 2014). It is easy to modify the physicochemical properties of synthetic polymers over natural polymers. Synthetic polymers have improved mechanical strength and controlled degradability than natural polymers. However, most synthetic polymers lack cell adhesion sites and need some chemical modifications to improve their cellular activity. PLA, PU, PCL, PLGA, PVA, and PEG are widely used synthetic polymers in tissue engineering. The advantages and disadvantages of some naturally derived and synthetic polymers are summarized in Table 8.1.

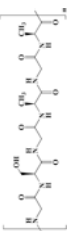
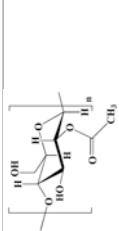
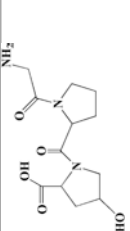
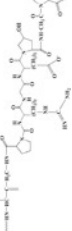
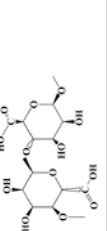
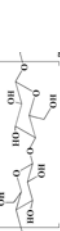
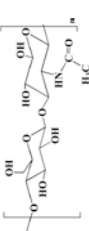
8.3 Kinds of Nanomaterials

The rapid growth in nanotechnology provides an opportunity to modify the chemical composition and dimension of nanomaterials for desired applications. The nanomaterials are further categorized into different groups, depending on the material dimensions. These are 0D, 1D, 2D, and 3D. Each material has different physicochemical properties. The brief discussions of these materials are given here.

8.3.1 0D and 1D Nanomaterials

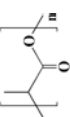


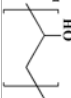
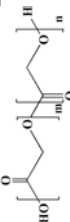

Materials whose all dimensions occur within the nanoscale are categorized into 0D nanomaterials. They have ultra-small sizes and a greater surface-to-volume ratio providing the significant active sites per unit mass. Nanomaterials have been extensively explored in materials science, sensing, biomedicine, catalysis, energy, and nano-devices. Carbon quantum dots (CQDs), graphene quantum dots (GQDs), fullerenes, metal nanoparticles, and polymer dots are categorized as 0D nanomaterials (Wang et al. 2020c). The carbon-based 0D nanomaterials exhibited superior electrical and thermal conductivity, optical property, high quantum yield, and biocompatibility. Due to these attractive properties, these materials are widely applied

Table 8.1 Advantages and disadvantages of commonly used natural and synthetic polymers in tissue engineering

| Polymers | Chemical structure | Advantages | Disadvantages | References |
|-------------------------|---|--|---|--|
| <i>Natural polymers</i> | | | | |
| Silk fibroin |  | Biocompatible, bioactive, lightweight, good elasticity, and promote cellular activities, | Immunogenic reaction after prolonged degradation | Tandon et al. (2020) and Santi et al. (2021) |
| Chitosan |  | Bioactive, anti-inflammatory, hemostatic, and facilitates cellular activities | Weak mechanical strength with low solubility in physiological pH and fast in vivo degradation | Gnavi et al. (2013) and Pita-López et al. (2021) |
| Collagen |  | Biodegradable, biocompatible, minor immunogenic responses with enhanced cellular activities | Poor mechanical strength and aqueous stability | Yu and Wei (2021) |
| Gelatin |  | Biodegradable, stable in a wide range of pH, biocompatible, and facilitates cell adhesion, proliferation | Weak stability in physiological conditions | Aldana and Abraham (2017) and Kang and Park (2021) |
| Alginate |  | Hydrophilic, biocompatible, biodegradable, and able to mimic the extracellular matrix (ECM) of host tissue | Weak mechanical strength, with low cellular adhesion | Valente et al. (2012) |
| Cellulose |  | Better mechanical strength, hydrophilic, bioactive, and biocompatible | Nondegradable or slow degradable in human tissues | Müller et al. (2006) and Salmoria et al. (2009) |
| Hyaluronic acid |  | Biocompatible, non-immunogenic, and promotes cellular activities | Brittle mechanical strength | Castro et al. (2021) and Wang and Spector (2009) |

(continued)

Table 8.1 (continued)

| Polymers | Chemical structure | Advantages | Disadvantages | References |
|--------------------------------|---|---|---|-----------------------------|
| <i>Synthetic polymers</i> | | | | |
| Poly (lactic acid) |  | Good mechanical strength, biodegradable, and biocompatible | Hydrophobic, brittleness, and lack of sites for cell adhesion | Hyon et al. (1997) |
| Polyurethane |  | Good mechanical strength, biodegradable, non-allergic, bio-, and hemocompatible | Limited in vivo stability | Wang et al. (2021a) |
| Poly (caprolactone) |  | Suitable mechanical strength, biocompatible, and promotes cell proliferation and angiogenesis | Hydrophobic and weak bioactivity | Joseph et al. (2019) |
| Polyvinyl alcohol |  | Good mechanical strength, nontoxic, noncarcinogenic, and biocompatible | Lack of sites for cell adhesion | Liao et al. (2011) |
| Poly (lactic-co-glycolic acid) |  | Suitable mechanical strength, biodegradable, biocompatible, and facilitates cellular activities | Weak osteoconductivity | Reddy et al. (2021) |
| Poly (ethylene glycol) |  | Hydrophilic, non-immunogenic, biocompatible, and promotes cell adhesion | Bio-inertness | Sheikholeslam et al. (2018) |

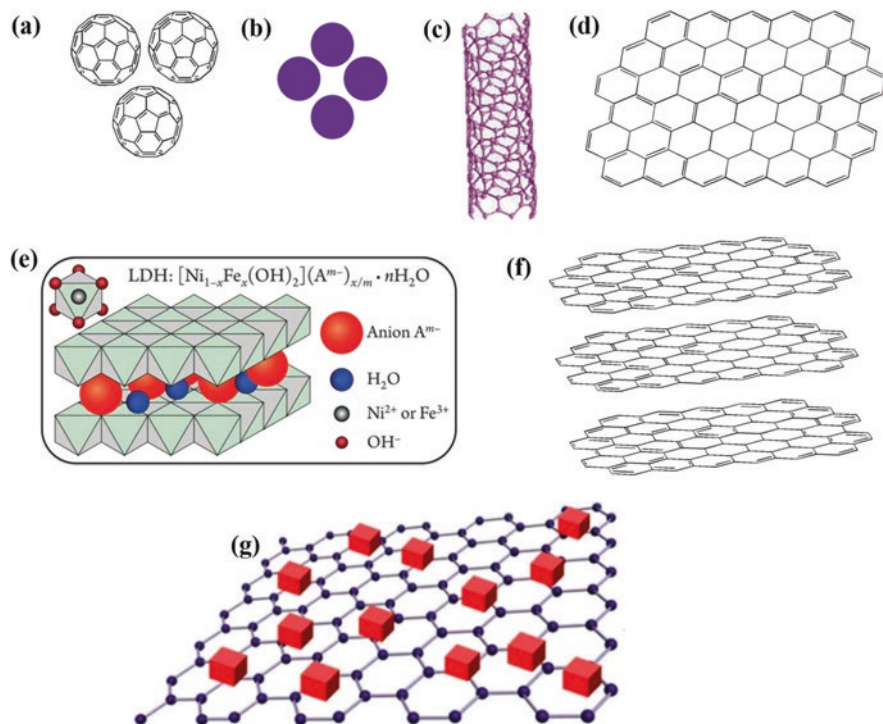


Fig. 8.1 The schematic presentation of 0D nanomaterials: (a) carbon dots and (b) metal nanoparticles. (c) 1D, CNTs (Geim and Novoselov 2007); (d, e) 2D, graphene and LDH (Hunter et al. 2016); and (f, g) 3D, graphite and metal oxide-based nanocubes. (Wang et al. 2014b)

in controlled drug release, wound healing, sensing, and imaging. The metallic nanoparticles are also considered promising materials in developing smart polymeric nanohybrids for tissue engineering applications due to their appealing physicochemical properties (Wang et al. 2019b). The morphologies of some 0D nanomaterials are shown in Fig. 8.1a, b.

The materials in which one dimension occurs within 1–100 nm are considered 1D nanomaterials. These are classified as tubes, rods, oxides, and ribbons, depending on the morphologies and composition. Different advanced techniques, such as hydrothermal reaction, chemical vapor deposition, microemulsion system, and reduction method, have been applied to prepare the morphological and chemically controlled 1D nanomaterials for desired applications (Lu et al. 2009). Due to their superior inheritance properties, these materials are widely explored in different fields, including cargo delivery, wound healing, sensing, and energy (Geim and Novoselov 2007). Carbon nanotubes and metal nanorods are most extensively utilized to develop smart polymeric nanohybrid platforms for drug delivery and wound healing applications. The morphologies of some 1D nanomaterials are presented in Fig. 8.1c. Their one dimensions occur within 1–100 nm.

8.3.2 2D and 3D Nanomaterials

2D nanomaterials have received considerable attention in biomedicine, energy, and tissue engineering due to their remarkable physicochemical properties. Different 2D nanomaterials, such as graphene, transition metal dichalcogenides (TMDs), black phosphorus (BP), layered double hydroxides (LDH), MXene, and metal-organic frameworks (MOFs), are commonly used in the preparation of smart polymeric nanohybrid platforms for diverse applications. Different approaches such as chemical vapor deposition and chemical and mechanical exfoliations are explored to prepare 2D nanomaterials (Halim et al. 2021). In addition to the high aspect ratio, the 2D nanomaterials demonstrated superior biocompatibility and biodegradability making them attractive candidates for the delivery of small molecules, such as drugs, nucleic acids, and genes. Graphene, an allotrope of carbon with sp^2 hybridization, is often explored to synthesize smart polymeric platforms owing to its remarkable properties, such as high surface area, high electrical and thermal conductivity, superior mechanical strength, and biocompatibility (Geim and Novoselov 2007). TMDs and BPs have been widely explored in device fabrication due to their material compositions and electronic structures. LDHs are another attractive 2D nanomaterial used to prepare smart polymeric nanohybrid platforms for tissue engineering applications. LDHs are clays with brucite-like cationic layers having anions in the hydrated interlayer. LDHs have numerous attractive potentials, such as ion exchange and catalytic activity (Hunter et al. 2016). MXenes and MOFs are emerging groups of 2D nanomaterials and are often used in gas separation, sensing, catalysis, and more, due to their superior porosity, high surface area, and structural and chemical tunability (Wu et al. 2019). MOFs are commonly synthesized by coordination reactions between inorganic metal salts and organic ligands in polar media. The MXenes have also been utilized as metal sources to synthesize MOFs. The morphologies of different 2D nanomaterials are given in Fig. 8.1d, e. The one dimension of all 2D nanomaterials occurs within 1–100 nm.

The 3D nanomaterials are generally formed by the spatial assembly of 1D materials (nanowires/nanotubes/nanorods) and/or 2D nanomaterials (nanosheets/nanoflakes). The 3D nanomaterials provide a fascinating platform for integrating and manipulating multiple units on a nanoscale. It is believed that the assembly of multiple nano-units might cause the alternation in the physicochemical properties of the formed 3D nanomaterials from their precursors. The 3D nanomaterials exhibited high surface area and superior electrical, magnetic, and optical properties owing to the interactions and coupling among nanoscale units. The 3D nanomaterials have been widely explored in sensing, energy, and other fields (Zhao and Lei 2020). Graphite and metallic nanocubes or nanostars are typical examples of 3D nanomaterials. Mahmoud et al. synthesized silver nanocubes and gold nanocages through a sulfur-mediated reduction process for photo-thermal applications (Mahmoud and El-Sayed 2012). The structure of some 3D nanomaterials is given in Fig. 8.1f, g (Wang et al. 2014b).

8.4 Application of Polymer Nanohybrid-Based Smart Platforms

Due to the desired physicochemical properties, polymer nanohybrid-based smart platforms have various applications, including drug delivery and wound healing. Different polymers (natural and synthetic) have been widely explored in developing these platforms. Here, we briefly discussed the drug delivery and wound healing potentials of polymer nanohybrid-based smart platforms by considering some attractive works.

8.4.1 Delivery of Active Molecules

The controlled delivery of the loaded drugs in the desired area has been paid considerable attention over the conventional delivery systems. The targeted drug delivery exhibited improved therapeutic effects than conventional delivery systems. Hossieni-Aghdam and coworkers developed carboxymethyl cellulose/halloysite nanotube (CMC/HNT) hydrogels for pH-responsive delivery of atenolol (AT) drug. They have added AT drugs through the co-precipitation method in the lumen of HNTs. The polymer nanohybrids exhibited a lower swelling potential than pure polymer hydrogel. The drug release behavior of the developed nanohybrids was profoundly affected by the pH of the media. Enhanced drug release occurred at pH 6.8 than another pH (1.2 and 4.5) due to the more significant swelling of nanohybrids at this pH (Hossieni-Aghdam et al. 2018). Jamshidzadeh et al. prepared HNTs modified with chitosan (CTS) and pectin (PCN) nanohybrid platforms for pH-responsive delivery of phenytoin sodium (PHT) drug through the layer-by-layer (LBL) method. The nanohybrids demonstrated enhanced drug loading efficiency (34.6 mg/g) than pure HNTs (18.3 mg/g). The pH-responsive release of loaded PHT under-simulated intestinal fluid (SIF) and simulated gastric fluid (SGF) is shown in Fig. 8.2a, b. The pH responsiveness behavior in the developed nanohybrids originated due to the abundant active functional groups on the surface of CTS and PCN. A slow release of the PHT drug occurred in the SGF media, whereas a fast release was observed in SIF media due to the partial degradation of the last PCN layer under an acidic environment (Jamshidzadeh et al. 2020).

In another study, Kakwere and coworkers developed temperature-responsive hydrogel of poly (*N*-isopropylacrylamide-co-polyethylene glycol methyl ether acrylate)/iron oxide nanocubes for hyperthermia and heat-assisted drug delivery applications. They have used doxorubicin (DOX) as a model drug for their study. The release profile of the loaded DOX is shown in Fig. 8.2c. The developed nanohybrids demonstrated a phase transition potential above 37 °C. A slow release of the loaded DOX was observed at lower temperatures (4, 25, and 37 °C). However, a burst release occurred at above the lower critical solution temperature (LCST, >37 °C) due to the phase transition in developed nanohybrids showed

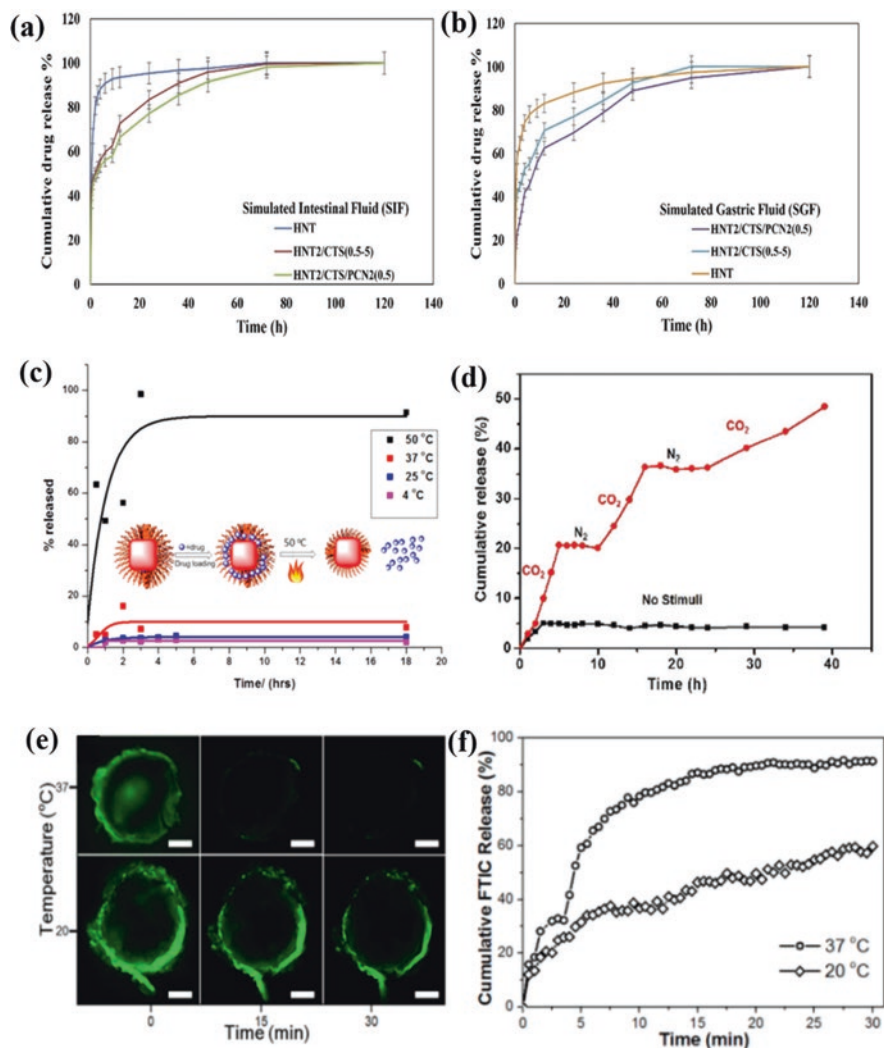


Fig. 8.2 The release profile of PHT. (a) Simulated intestinal fluid and (b) simulated gastric fluid (Jamshidzadeh et al. 2020). (c) Drug release from thermo-responsive PNIPAAm-co-PEGA/iron oxide nanocubes at indicated temperatures (Kakwere et al. 2015). (d) The DOX release behavior from PDMAEMA/core-shell corona-like structure in the presence of CO₂ and N₂ conditions (Che et al. 2015). (e) Fluorescent images indicate the drug release from the Mg/Pt-PNIPAM Janus micro-motor (scale bar = 10 μm) and (f) the normalized average cumulative release profiles at indicated temperatures. (Mou et al. 2014)

temperature-responsive drug delivery potential. The drug-free platform did not exhibit cytotoxic effects even at a high concentration (1 g/L of iron) (Kakwere et al. 2015).

The superparamagnetic iron oxide nanoparticles (SPIONs) have also paid wide attention to drug delivery, gene therapy, and tissue engineering because of their superior stability, good biocompatibility, and stimuli responsiveness (Hao et al. 2010; Zhou et al. 2012). Che et al. prepared carbon dioxide (CO₂) responsive Fe₃O₄@SiO₂/poly (*N,N*-dimethyl aminoethyl methacrylate) (PDMAEMA) core-shell corona-like structure as an efficient drug carrier system. The hydrodynamic volume of the developed hybrid magnetic nanoparticles (MNPs) was controlled by adjusting the levels of CO₂ and N₂. They have loaded DOX as a model drug in their study. The developed structure exhibited superparamagnetic, biocompatible, and gas-responsive properties. The DOX release profile from the developed system is given in Fig. 8.2d. A rapid drug release was observed under CO₂ conditions from the developed structure due to the protonation of the polymer shell, whereas a slow release occurred in the absence of CO₂ condition demonstrated gas-assisted drug delivery behavior of the systems. No significant cytotoxicity was observed with the developed platform in the presence of A549 cells, showing their good biocompatibility (Che et al. 2015).

Mou et al. developed Mg/Pt-poly (*N*-isopropylacrylamide) (PNIPAM) Janus micro-robotic platform for temperature-assisted drug delivery. They have used fluorescein isothiocyanate (FITC) as a model drug in their study. The developed micro-robotic platform was self-propelled in blood plasma without external supports. The fluorescence images of drug release from the developed micro-robotic platform and the cumulative release of the loaded drug are shown in Fig. 8.2e, f. A greater release of the loaded drug occurred with increasing the temperature (>37 °C) due to the shrinking of the polymer structure above the LCST, showing the temperature-triggered release efficiency of the developed micro-robotic platform. The physico-chemical properties of developed micro-motors can be easily modified with other desired polymers or antibodies through a surface medication approach, showing their promising potential for various applications (Mou et al. 2014).

Inorganic minerals have a significant influence on the metabolic process of the living organism, and their deficiency causes severe problems to human health. Iron is considered an essential mineral for human health and plays a vital role in oxygen transport. Its deficiency causes anemia, and excess supplement is responsible for gut inflammation and constipation (Armstrong 2017). Karshalev and coworkers developed a micro-robotic platform for the controlled delivery of iron in an anemic mouse. The micro-robot has consisted of Mg and TiO₂ as core, followed by the wrapping of PLGA polymer. The developed micro-motors were further coated with chitosan solution, followed by the desired minerals loading. The schematic representation for the formation of micro-motors and minerals loading is shown in Fig. 8.3a. SEM and EDX images of the developed micro-motors are given in Fig. 8.3b. The developed motor exhibited a nearly spherical shape, and the distribution of different elements Mg, Ti, Fe, and Se occurred in the micro-motor. They examined the toxicity of the mineral-loaded micro-motor after 30 days of oral

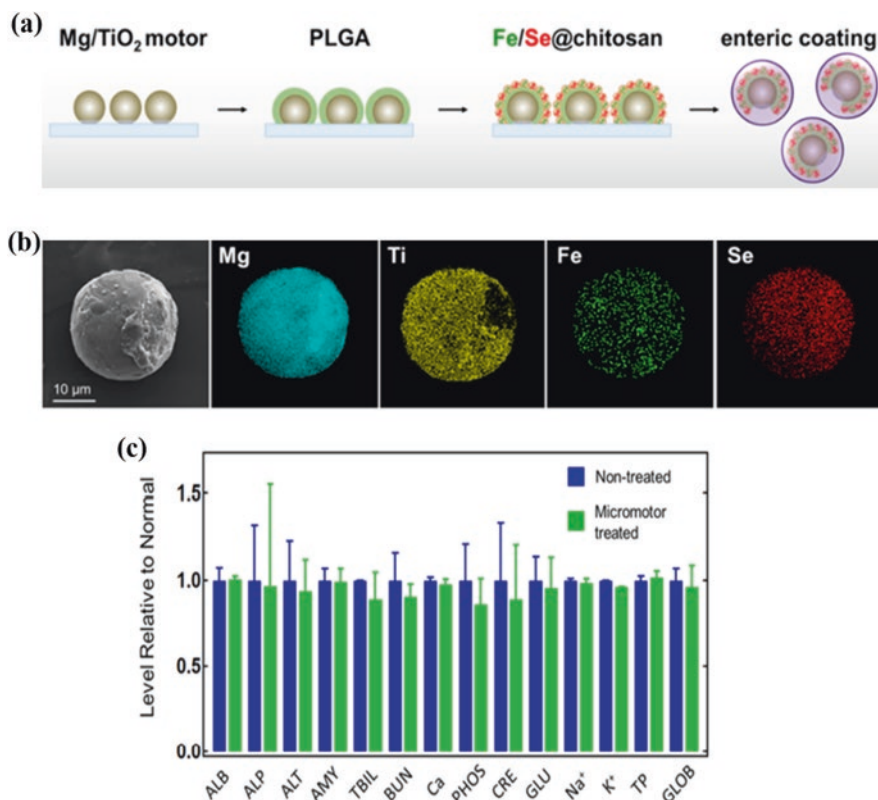


Fig. 8.3 Micro-motor preparation and its characterization. (a) Schematic representation of the micro-motor preparation, (b) SEM and EDX analysis of the developed micro-motors, and (c) comprehensive blood chemistry panel taken from non-treated and treated mice after 30 days ($n = 3$). *ALB* albumin, *ALP* alkaline phosphatase, *ALT* alanine transaminase, *AMY* amylase, *TBIL* total bilirubin, *BUN* blood urea nitrogen, *Ca* calcium, *PHOS* phosphorus, *CRE* creatinine, *GLU* glucose, *Na⁺* sodium, *K⁺* potassium, *TP* total protein, *GLOB* globulin. (Karshalev et al. 2019)

administration in the mice, and the comprehensive chemical analysis of the blood is presented in Fig. 8.3c. No significant difference in the blood composition and blood cell parameters was observed in micro-motor-administrated mice than the control, showing their potential for active delivery of minerals (Karshalev et al. 2019).

Tu and coworkers developed a self-propelled and temperature-responsive supra-molecular nano-motor using a PNIPAM polymer brush through the surface-initiated atom transfer radical polymerization (SI-ATRP) method to deliver the active molecules. The schematic representation of the developed nano-motor is shown in Fig. 8.4a (i–iii). They prepared a self-assembled nano-motor based on a bowl-shaped polymeric platform, called stomatocytes. The catalytic platinum nanoparticles (PtNPs) were entrapped inside the developed stomatocytes. The bowl-shaped polymeric structure was made of poly(ethylene glycol)-grafted polystyrene (PEG-*b*-PS). The developed nano-motor can convert chemical energy (hydrogen

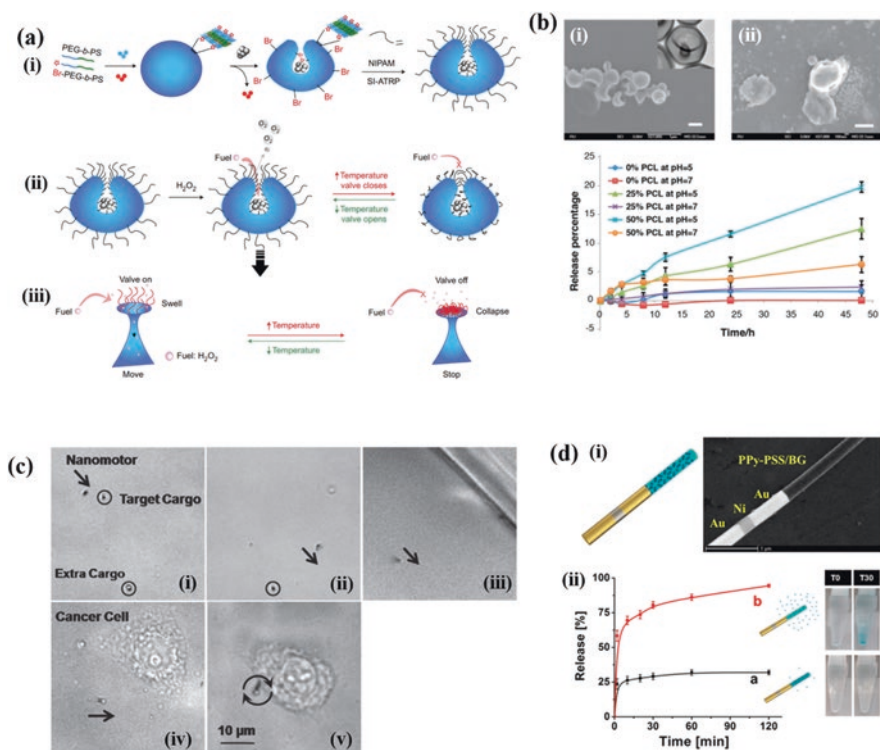


Fig. 8.4 (a) Design of polymeric stomatocytes nano-motors with thermosensitive polymers: (i) schematic representation of the formation of PtNP-loaded stomatocytes with ATRP of styrene starting from a PEG PNIPAM brushes by SI-ATRP on the surface of the stomatocytes, (ii) schematic representation of the reversible control over the speed of PNIPAM-modified stomatocytes motors by changing the temperature, (iii) the collapse of PNIPAM brushes takes place and so the opening of the stomatocytes is covered when the temperature is increased above the LCST of PNIPAM (Tu et al. 2016). (b) Pore formation of stomatocytes before and after degradation: (i) SEM images of stomatocytes with 50% PEG-*b*-PCL before acidic degradation (inset is a TEM image of a single stomatocyte with a small opening), (ii) SEM images of stomatocytes with 50% PEG-*b*-PCL after acidic degradation, (iii) Release of DOX from a stomatocyte with different percentages of PCL at different pH (scale bars are 400 nm) (Tu et al. 2017). (c) Drug delivery to HeLa cells using flexible magnetic nano-swimmers in cell-culture media: (i) captures the drug-loaded magnetic polymeric particle in the loading reservoir, (ii) transports it through the channel, (iii) approaches the target cell, (iv) sticks onto the target cell, (v) releases the drug (Gao et al. 2012). (d) Characterization of ultrasound-propelled nano-wire motor containing the pH-responsive drug-loaded polymeric segment: (i) SEM image of the Au/Ni/Au/PPy-PSS nanowire, (ii) Time-dependent release of BG at pH 7.4 (a) and 4.0 (ii). Right: optical images of the release of BG particles at 0 and 30 min (left and right) using pH 4.0 (top) and 7.4 (bottom). (Garcia-Gradilla et al. 2013)

peroxide) into mechanical motion. A fixed LCST characterizes the PNIPAM polymer. The collapse of PNIPAM polymer brushes occurred above its LCST led to a hydrophobic layer on the top of stomatocyte opening and blocked the passage of hydrogen peroxide inside the developed system. Thus, the self-propelling motion of

the developed nano-motor stopped in the absence of chemical fuel (Tu et al. 2016). In another study, they prepared self-propelled and biodegradable PtNPs embedded stomatocyte nano-motors having PEG-*b*-PCL and PEG-*b*-PS to deliver DOX drug. The developed nano-motor can convert the chemical energy into mechanical motion and achieve a speed of 39 $\mu\text{m/s}$. Biodegradable motor systems have advantages over nondegradable systems (Wu et al. 2014). The developed nano-motor exhibited pH-responsive drug delivery property. A higher drug release was observed under the acidic conditions than the physiological condition due to the pore structure formation in the nano-motor. The SEM morphologies of the developed nano-motor under acidic conditions are given in Fig. 8.4b (i, ii). The pore structure was visualized in the developed nano-motor under acidic conditions, which accelerated the release of the loaded drug. The release profiles of loaded DOX at different pH are shown in (Fig. 8.4b (iii)). It is well known that cancerous cells have a lower pH (acidic micro-environment) than normal cells. Thus, a higher drug release occurred at a low pH (5) than the high pH (7) from different compositions of the developed nano-motors due to pore structure formation (Tu et al. 2017). The fuel-free nano-motors are considered attractive platforms for delivering loaded active molecules in the desired area. To achieve this target, the proper understanding and performance of nano-motors are essential for biomedical applications, such as drug delivery and gene therapy (Mei et al. 2011). Gao et al. developed fuel-free magnetic nano-swimmers for the targeted drug delivery application. The developed nano-swimmers were composed of magnetic PLGA nanoparticles and Ni-Ag. The schematic binding of drug-loaded magnetic PLGA nanoparticles with Ni-Ag for drug delivery is presented in Fig. 8.4c. The flexible Ni-Ag motor approached the targeted drug-loaded magnetic PLGA nanoparticles via controlled magnetic guidance and bound them. The bound motor moved toward cancer cells media through a channel and then attached with targeted cells. The attached motors released the encapsulated drug. Nonspecific binding of the motor was also observed in some cases due to the noncontrolled movement of the motors. Therefore, modification in the motor is required for specific binding with the targeted cells (Gao et al. 2012).

The ultrasound wave is also considered a significant stimulus and has been extensively explored in medicine. It can be applied to the motion of micro-/nano-motors in biological conditions. Gold (Au)-based nanowire motors have often been propelled through ultrasound waves owing to their concave geometry at one side (Garcia-Gradilla et al. 2014). Garcia-Gradilla et al. developed functionalized ultrasound-propelled and magnetically assisted nano-motors for drug delivery application. The developed systems were composed of Au-Ni-Au nanowire motors and polypyrrole-polystyrene sulfonate (PPy-PSS) polymers. Au segments facilitated the ultrasound-mediated motion, whereas Ni segments assisted magnetically controlled motion. The PPy-PSS polymers have pH responsiveness potential. The SEM image clearly illustrated that PPy-PSS polymers were well-connected with Au-Ni-Au nanowire motors. The SEM image is given in Fig. 8.4d (i). The ultrasound-propelled drug delivery from the developed systems is shown in Fig. 8.4d (ii). They have incorporated the brilliant green (BG) model antiseptic drug in the polymeric part of the system. The BG drug has positively charged centers and is bound with a

Table 8.2 The drug delivery application of some smart polymer platforms

| System | Condition | Application | References |
|---|---|---|----------------------------|
| Pluronic F127 modified with polyethyleneimine/citrate stabilized mixed ferrite nanoparticles | Temperature and pH-responsive | Enhanced DOX release at a higher temperature and low pH | Bhattacharya et al. (2016) |
| N-(2-hydroxypropyl) methacrylamide (HPMA) co-polymer/SiO ₂ | pH-responsive nanohybrids | Fast drug release under acidic conditions | Li et al. (2017) |
| PEG-PLA/laponite | pH-responsive nanohybrids | Fast drug release under acidic conditions | Wang et al. (2014a) |
| Polypyrrole coated PCL/palmitoxel | Temperature and pH-responsive | NIR and pH-triggered drug release | Tiwari et al. (2018) |
| Hyaluronic acid/graphene oxide | pH-responsive nanohybrids | Enhanced drug release occurred in the acidic conditions | Song et al. (2014) |
| Poly(<i>N</i> -isopropylacrylamide)-based <i>N</i> -butyl imidazolium copolymer/gold functionalized silica shell | Temperature and pH-responsive nanohybrids | Fast drug release occurred under acidic and high-temperature conditions | Baek et al. (2016) |
| Magnetic nanoclusters@Au@PDA/PEG/FA | Temperature and pH-responsive nano-robots | Fast drug release occurred under acidic and high temperature conditions | Jin et al. (2019) |
| PLGA/Na ₂ CO ₃ /perfluorocarbon/DOX | Ultrasound-triggered nano-robot | Enhanced drug release occurred with ultrasound stimulus | Meng et al. (2020) |

negatively charged PPy-PSS polymeric backbone through electrostatic interactions. A higher drug release was observed at a low pH (4) than the higher pH (7) in the developed systems. The higher drug release at low pH was attributed to the protonation of the polymer backbone, which caused the greater release of the loaded drug (Garcia-Gradilla et al. 2013).

The smart drug release from other polymeric nanohybrids is also summarized in Table 8.2.

8.4.2 Wound Management

Wound care is a billion-dollar problem across the globe, and approximately 5.7 million people are suffering from different kinds of wound problems at an estimated cost of US\$20 billion in the USA (Järbrink et al. 2017). Different approaches, including autografts, allografts, and artificial implants, are explored to regenerate lost tissues. Autografts are associated with a limited resource availability problem, whereas allografts have immune rejection and pathogenic risk. Naturally derived

polymeric grafts such as chitosan, fibrin, gelatin, etc., have been explored for wound dressing at the clinical level. However, uncontrolled structures and mechanical weakness restricted their broad applicability (Lin et al. 2020). Thus, we need to design smart platforms that trigger wound healing without exhibiting adverse effects. Wound healing is a complex process, and several processes, such as vasoconstriction, thrombogenesis, angiogenesis, collagen synthesis, ECM formation, and remodeling, occur during wound healing. Materials with desired physicochemical properties, including flexibility, durability, adequate mechanical strength, bioactivity, and biocompatibility, are considered ideal platforms for wound dressing (Pereira et al. 2013). Mai et al. developed a multifunctional hydrogel patch of photosensitizing sinoporphyrin sodium (DVDMS)/PLGA-encapsulated with basic fibroblast growth factor (bFGF), carboxymethyl chitosan (CMCS), and sodium alginate for wound management. The fabricated patch was indicated by CSDP. The developed platform was portable and photo-dynamically active and demonstrated antimicrobial potential. The developed platform eradicated approximately 99.9% *Staphylococcus aureus* (*S. aureus*) and inhibited biofilm formation under mild photo-irradiation (intensity, 30 J/cm²; time, 5 min; and concentration, 10 µg/mL). The wound healing efficiency of the developed platform at different periods with 30 J/cm² light irradiation is shown in Fig. 8.5a. The developed platform exhibited superior wound healing potential than the control without showing any scar in the defected site (Mai et al. 2020). The quantitative value of wound healing rate is presented in Fig. 8.5b. The enhanced healing rate was observed with the developed platform under 30 J/cm² light irradiation, demonstrating better healing efficiency. Hu and coworkers developed the dual-crosslinked pH-responsive smart patch of quaternary ammonium functionalized chitosan and aldehyde functionalized dextran-dopamine for chronically infected diabetic wound management. They have encapsulated silver nanoparticles (AgNPs) and proangiogenic drug deferoxamine (DFO) in the developed patch for antibacterial and angiogenic potentials. The wound healing efficiency of the developed smart patch is given in Fig. 8.5c. An accelerated wound healing was observed with the developed patch than control, showing superior tissue regeneration efficiency. The better wound healing potential of the developed patch was due to the sustained and controlled release of the loaded drug, which accelerated diabetic wound healing. It is well established that lactic acid and acetic acid production occur from bacteria at wounded sites, causing the locally acidic microenvironment (pH: 4.5–6.5). Relatively fast drug release (DFO) was observed from the developed smart patch under acidic conditions (pH ~5.0) than the physiological condition (pH ~7.4) due to the dissociation of the crosslinked structure under acidic conditions. The quantitative value for wound closure is given in Fig. 8.5d. The percentage of wound closure area was higher in the developed smart patch than control, demonstrating their superior wound healing efficiency (Hu et al. 2021). Restoration of skin functions is required for normal human activities. Chronic wound requires a long time for their healing process due to the oxidative stress within the wounded area, which causes the extensive accumulation of reactive oxygen species (ROS). These ROS cause acute inflammation and destroy the endogenous stem cells and macrophage activities for wound healing. These ROS also

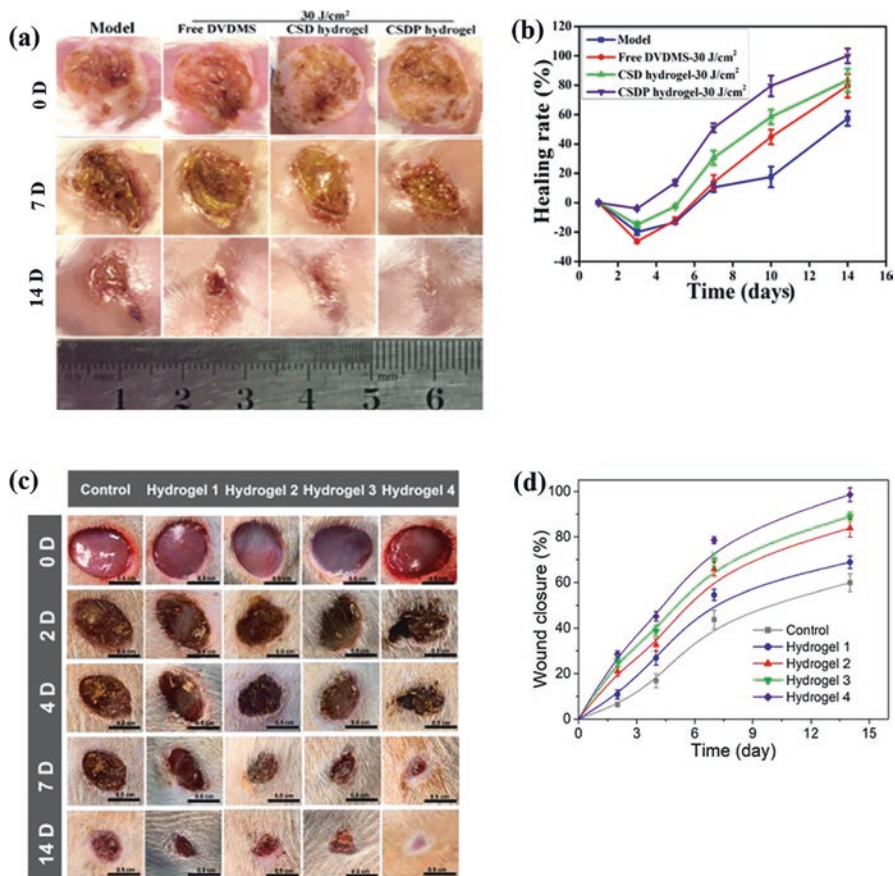


Fig. 8.5 Effect of CSDP hydrogel-PACT on burn infection. (a) In vivo study of the treatment of burn infections by hydrogels and the corresponding wound photographs of the rate at days 1, 3, 5, 7, 10, and 14. (b) Measurement of the wound size as shown as a percentage normalized to that of the initial wound size at day 0 (Mai et al. 2020). (c) Photographs of wound closure with different treatments on 0th, second, fourth, seventh, and 14th day ($n = 8$). (d) In vivo wound closure rates during the 14 days (mean \pm SD, $n = 6$, $**P < 0.001$). (Hu et al. 2021)

inhibit the neovascularization process leading to the failure of endodermis functions (Yuan et al. 2021).

The delivery of the desired materials into interesting cells or tissues is still a challenging task for regenerative applications. Le and coworkers developed a bioinspired pH- and temperature-responsive injectable hydrogel for wound healing application. The developed hydrogel was composed of water-soluble PEG, pH-, and temperature-responsive poly(sulfamethazine ester urethane) (PSMEU) polymers. The developed hydrogel demonstrated a sol-like property at high pH and room temperature (pH 8.5, 23 °C), and the sol-gel transition occurred at physiological conditions (pH 7.4, 37 °C). It showed excellent adhesive potential on a wide range of surfaces, such as skin, glass, and plastic, and can be easily injected at the desired

sites. The developed hydrogel effectively covered the wounded site and triggered the healing process (Le et al. 2018). The loss in the properties of implanted materials occurs at wounded sites due to the destruction of materials through several factors, causing prolonged wound healing. Therefore, it is essential to develop materials which can restore their functions after destroying the structure. These can be classified into extrinsic and intrinsic self-healing materials. The microcapsules or microvascular structures are occurred in extrinsic self-healing materials, whereas reversible associations occur in intrinsic self-healing materials. The extrinsic self-healing materials can easily cover the smaller wound, and problems are occurred for larger wounds due to the smaller size and concentration of microcapsules or microvascular structures. However, the intrinsic self-healing materials can be explored to heal the larger wound (Xu et al. 2017). Zhu et al. developed an intrinsic self-healing polymer patch through host-guest interactions for wound healing application. The developed patch has consisted of temperature-responsive PNIPAM polymer and beta-cyclodextrin (β -CD). The developed material can be smoothly applied to large wound sites. Initially, the swelling was observed within the implanted patch, which covered the large open wound. The original size of the implanted patch was regained by volume construction. The design of a developed patch with intrinsic self-healing potential for large wound care through host-guest interactions is given in Fig. 8.6a (Zhu et al. 2020). In another study, Zhang et al. synthesized the temperature-responsive, stretchable, conductive, and self-healable polymer patch for chronic wound treatment. The synthesized patch consisted of zinc functionalized chitosan, poly(vinyl alcohol) (PVA), and poly(pyrrole) (PPy) and was crosslinked with borax. The PPy component facilitated the conductivity and temperature responsiveness in the developed patch, whereas zinc remarkably increased the antibacterial potential of the developed patch. The developed patch was termed by PCPZ. The wound healing efficiency of the developed patch with and without electrical stimulation (ES) is shown in Fig. 8.6b. An accelerated wound healing was observed in PCPZ-treated groups than in control, and commercially available Hydrosorb dressing showed their wound healing potential. This was significantly higher in electrically stimulated (3 V) groups than in all groups, demonstrating improved healing affinity. The improved healing under ES was attributed to the rapid migration of fibroblasts, and angiogenesis, which accelerated wound healing. The enhanced wound healing under ES may also be attributed to the enhancement of cutaneous current, which accelerated the healing process (Zhang et al. 2020).

The layer-by-layer (LBL) self-assembly method is commonly applied to develop the multifunctional film for different applications. It is anticipated that developing a self-powered electric field and ROS scavenging efficiency into a single film would be suitable for wound healing applications. Yuan and coworkers developed pH-responsive and anti-inflammatory film through the LBL method for wound management. The developed film was composed of 2-hydroxypropyltrimethyl ammonium chloride chitosan (HTCC), alginate, poly-dopamine functionalized iron nanoparticles (PFNs), and a self-powered nano-generator (SN). The developed film was indicated by HAP/SN-NR. Enhanced cell proliferation, migration, and neovascularization were observed with the developed film. The wound healing efficiency of the

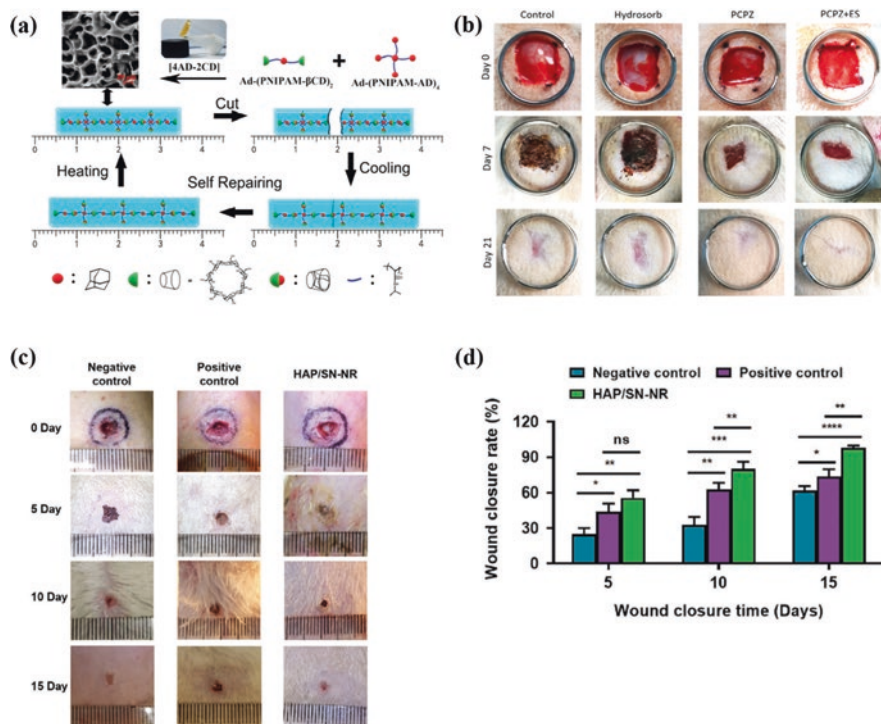


Fig. 8.6 (a) Schematic design of the hydrogel with synergetic repeatable self-closing and intrinsic self-healing of large wounds through the host-guest orthogonal assembly of well-defined temperature-sensitive PNIPAM units (Zhu et al. 2020). (b) Photos of the wounds of the different groups at indicate periods with and without electrical stimulation (ES) (Zhang et al. 2020). (c) Representative images of rat wounds with no treatment (negative control), Tegaderm film (positive control), and HAP/SN-NR (experimental group) in 15 days. (d) The wound closure rate of rats in the treated groups (Yuan et al. 2021). In another study, Preman et al. synthesized a biodegradable temperature and pH dual responsive supramolecular hydrogels using sodium alginate and poly(*N*-vinyl caprolactam) via free radical polymerization followed by chemical and ionic crosslinking. They have added tannic acid (TA) as a natural therapeutic agent. TA-added hydrogel demonstrated free radical scavenging, anti-inflammatory, and antibacterial potentials. The developed hydrogels accelerated 3 T3 fibroblast cell proliferation. The improved wound healing was observed with the developed system, showing their potential for skin regeneration and rapid wound healing (Preman et al. 2020). The nanofibrous hydrogels are considered attractive for wound healing applications due to their superior cell adhesion and proliferation potential. Additionally, accelerated mass transport can be achieved in these systems. Zhang and coworkers prepared a temperature-responsive nanofibrous hydrogel platform for improved wound healing application. The nanofibrous hydrogel was composed of a methacrylate gelatin (GelMA) polymer. They have added fatty acids/ aspirin (ASP) encapsulated polydopamine (PDA) in the nanofibrous hydrogel. No cytotoxicity was observed with the developed nanofibrous hydrogel, which showed their biocompatibility. An accelerated wound healing occurred with the developed system, demonstrating their wound healing potential. (Zhang et al. 2021)

developed film is shown in Fig. 8.6c. Improved wound healing was observed with developed film than control, which showed their superior healing ability. The developed film also exhibited ROS scavenging potential, and no inflammatory signs were observed with the developed film in wounded rats. The quantitative value of wound closure at different periods is also given in Fig. 8.6d. This finding indicated that the developed film could promote wound healing process (Yuan et al. 2021).

Furthermore, micro-/nanorobotics platforms have received considerable attention due to their desirable biomedical engineering properties and environmental remediation. The micro-robot size is less than 1 mm, whereas the nano-robot has a dimension of less than 1 μm . These structures can be actuated and localized within the human body to diagnose and cure different diseases. Different biological challenges, such as the blood-brain barrier, vascular endothelial barrier, and glomeruli filter, have wide influences on the transportation of specific sizes of robotic structures. The small-sized nano-robots may be quickly discharged from the body, whereas the larger robots may be stored in the monocytes, leukocytes, platelets, dendritic cells, and other tissues (Wang et al. 2020a). Therefore, developing a suitable size of robotic platforms is necessary for biomedical applications. He and coworkers developed the magnetic field and NIR-responsive thermoplastic Janus robotic systems for wound welding applications. The formation of Janus composite and their wound management is shown in Fig. 8.7a, b. The Janus composite particles were developed through the LBL method. The temperature of the wounded area was increased with irradiation of NIR light, which melted the collagen fiber. The melted fiber reformed the collagen film after reducing the temperature, closing the open wound. They have applied the developed system to beef liver, beef meat, and chicken meat to observe their wound welding efficiency. The developed platform with NIR-assisted wound healing potential is shown in Fig. 8.7c. In addition, the developed platform exhibited improved wound welding potential on NIR irradiation (He et al. 2016). Cell-based therapy using suitable carriers has also drawn considerable attention in the regenerative tissue field. Go et al. developed a micro-robot platform for rabbit knee cartilage healing/regeneration using human adipose-derived mesenchymal stem cells (MSCs). The developed platform was composed of ferumoxylol (an iron source), chitosan, and PLGA polymers. The developed micro-robot platform has an electromagnetic actuation (EMA) system (for targeting the micro-robot) and magnet (for fixing the micro-robot in the desired area). They have examined the cartilage regeneration in control and MSC-loaded micro-robot injected groups after 3 weeks of treatment via hematoxylin and eosin (H&E) and Col II staining methods. The expression of Col II was higher in MSC-loaded micro-robot injected groups than in control. This was more significantly high in magnetically fixed micro-robot than in the unfixed system. This finding indicated that the developed system has potential and could be applied for cartilage regeneration using MSCs (Go et al. 2020).

Inhibition of fungal infections at the wounded sites is one of the critical challenges in the regenerative tissue field. Fungi can form biofilms under the protective skin layer, causing inflammation. The therapeutic efficiency of the common antifungal drugs is restricted at the infected sites due to the non-skin penetration ability of

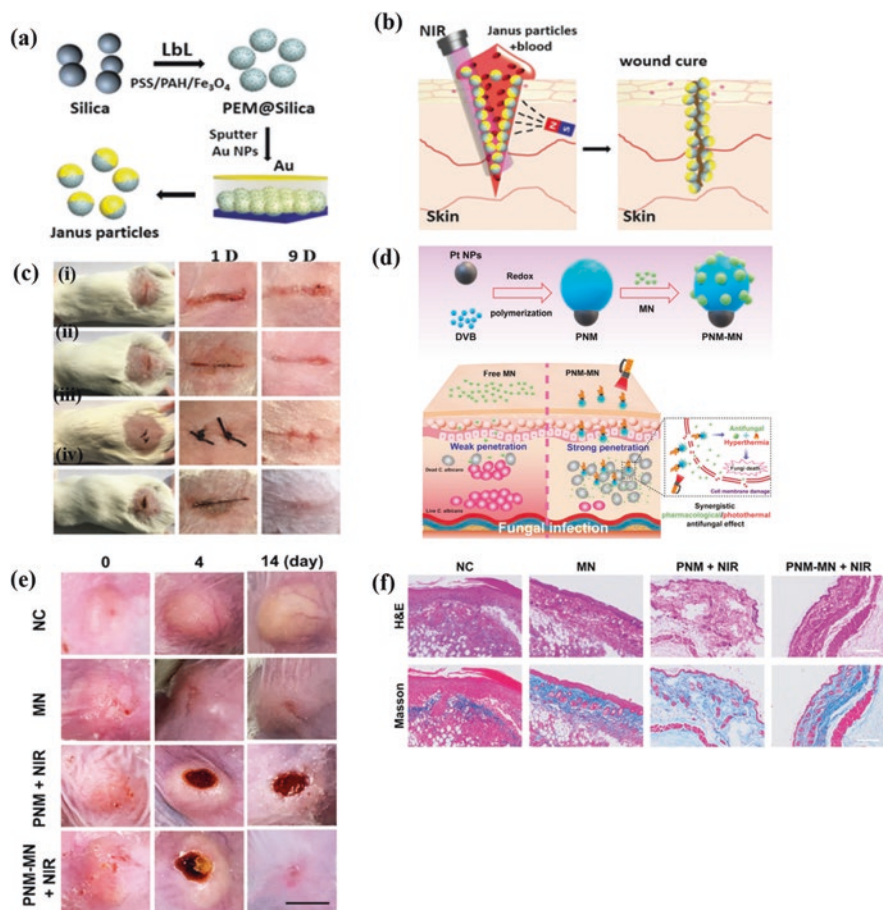


Fig. 8.7 (a) Production of Janus composite particles by LbL self-assembly of PEM and magnetite nanoparticles followed by sputter coating with gold and resuspension in water. (b) Laser tissue welding with magnetic assistance, due to magnetite particles being homogeneously distributed in the particles, the particle orientation is random during welding. (c) The wound healing potential of the developed composites at indicated periods: (i) control, (ii) laser tissue welding, (iii) medical suturing, and (iv) nanoparticle glue (He et al. 2016). (d) The schematic representation for NIR active parachute-like nano-motor (PNM) loaded with miconazole nitrate (MN) and its antifungal effects. (e) The images of *Candida albicans*-infected mice treated with PBS, free MN, PNM + NIR, and PNM-MN + NIR at indicated periods (scale bar = 1 cm). (f) H&E (upper) and Masson trichrome (lower) analyses of infected skin tissues after 14 days of treatment (scale bar = 100 μ m). (Ji et al. 2021)

the drugs. Azoles, echinomycines, and polyenes are the major antifungal drugs used in clinical treatment (Berman and Krysan 2020; Osanloo et al. 2019). Ji and coworkers developed NIR-responsive multifunctional parachute-like nano-motors (PNM) to treat fungal-infected skin. The developed PNM was composed of platinum nanoparticles (Pt NPs) and poly (divinylbenzene) (PDVB). The schematic

representation for the synthesis of PNM is given in Fig. 8.7d. The synthesis of PNM was achieved through the in situ polymerization method. The Pt NPs were used owing to their superior photo-thermal affinity. They have used miconazole nitrate (MN) as an antifungal drug. The MN drugs were effectively loaded within PNM through strong hydrophobic interaction. The developed system was termed PNM-MN. The photographs of *Candida albicans*-infected mice treated with the developed system are shown in Fig. 8.7e. A large white pustule was observed in the negative groups than in MN-treated groups after 14 days of treatment. On the other hand, rupturing of pustule and scab formation occurred in PNM + NIR treated groups with swollen wounds, demonstrating that only NIR treatment is not capable of eradicating fungal skin infection. However, complete wound healing was observed in PNM-MN + NIR-treated mice groups, showing their wound-healing ability. The scab also disappeared in PNM-MN + NIR-treated mice groups after 14 days of treatment. The hematoxylin and eosin (H&E) and Masson trichrome analysis of the PNM-treated mice are shown in Fig. 8.7f. The intact histological structures were observed in PNM-MN + NIR-treated mice groups, showing their improved therapeutic effects on bacterial eradication and skin regeneration (Ji et al. 2021). In another study, Cui et al. self-propelled NIR-responsive nano-swimmer (HSMV) for deep layered removal of biofilm developed by *Staphylococcus aureus*. The developed nano-swimmer consisted of a polystyrene sphere (PS), polydopamine (PDA), and gold nanoparticles (AuNPs). The AuNPs were in situ growth on the surface of PS@PDA. They have encapsulated the vancomycin (Van) drug to eliminate biofilm. An enhancement in the local temperature (45 °C) and thermal-induced Van release occurred from the developed nano-swimmers, demonstrating photothermal therapy and chemotherapy potentials in one system. Above 90% biofilm elimination was achieved within 10 min of NIR irradiation without affecting the healthy tissues (Cui et al. 2020).

The wound healing potential of some other smart platforms under different conditions is also summarized in Table 8.3.

8.5 Conclusion

Polymer nanohybrid-based smart platforms have paid broad interest in delivering active agents and wound healing owing to their desirable physicochemical properties. Natural and synthetic polymers are often explored for the synthesis of the required platforms. The naturally derived polymer patches have superior biocompatibility over synthetic polymers, making them suitable candidates to develop required platforms. However, the weak mechanical strength restricts their broad applicability. The physicochemical properties of the synthetic and naturally derived polymers can be altered by adding suitable nanomaterials in their matrix or chemical functionalization. Different nanomaterials, including metal oxides, nanocellulose, carbon nanotubes, and graphene, have been profoundly explored to develop smart polymer nanohybrid platforms for different applications. The smart polymer

Table 8.3 The wound healing potential of indicated systems under different conditions

| System | Stimulus | Application | References |
|---|--------------|--|---|
| Catechol functionalized chitosan/MnO ₂ hybrid Hydroxybutyl modified chitosan/L-3, 4-dihydroxyphenylalanine (L-DOPA)/ ϵ -Poly-L-lysine | Light | Melanoma therapy and multidrug-resistant bacteria-infected wound management Improved wound healing | Wang et al. (2020b) and Tian et al. (2021) |
| Agarose/iron functionalized tannic acid Hydroxypropyl chitin/iron functionalized tannic acid ϵ -Polylysine-stabilized agarose/polydopamine hybrid | Photothermal | Improved wound healing with antibacterial potential Enhanced wound healing with antibacterial potential Improved wound healing | Deng et al. (2020), Ma et al. (2021) and Qi et al. (2021) |
| Poly (<i>N</i> -acryloyl glycinamide) (PNAGA)/gold functionalized polydopamine (Au@PDA) | Photothermal | Enhanced wound healing with antibacterial property | Li et al. (2021a) |
| Adipic dihydrazide modified hyaluronic acid/benzaldehyde functionalized poly(ethylene glycol)-co-poly(glycerol sebacate) and cuttlefish-derived melanin nanoparticles | Photothermal | Superior wound healing in methicillin-resistant <i>Staphylococcus aureus</i> (MRSA) in rat | Li et al. (2022) |
| Polysaccharide/exosomes (FEP@exo) platform | pH | Enhanced angiogenesis and wound healing under diabetic condition | Wang et al. (2019a) |
| Carboxylated agarose/zinc modified with tannic acid | pH | Accelerated wound healing with antibacterial property | Ninan et al. (2016) |
| Gelatin/tannic acid | pH | Radical scavenging and hemostatic abilities with accelerated wound healing | Ahmadian et al. (2020) |
| Alginate/CaCO ₃ | pH | Improved wound healing | Shi et al. (2019) |
| Hydroxypropyl chitin/iron functionalized tannic acid | pH | Accelerated wound healing with antibacterial property | Ma et al. (2020) |

nanohybrid platforms have additional advantages compared to the conventional systems, and their properties can be modified by applying different stimuli, such as light, pH, and electric and magnetic fields. The smart polymer nanohybrids platforms with smaller dimensions have received considerable attention in delivering active molecules and wound healing. These systems have the potential to move from one site to another site with or without applying external stimuli.

They are classified as micro- and nano-motors depending on their size. However, these platforms exhibited superior healing and delivery of the loaded molecules on the targeted sites. The elimination of the small motors is possible through the excretory system, whereas big motors can accumulate in monocytes, leukocytes, platelets, dendritic cells, and other tissues. Therefore, the fabrication of the suitable size of the motors is required for desired applications. Additionally, the precise injection and fixation of these motors in the targeted area are still critical challenges for researchers.

Acknowledgments The Basic Science Research Program supported this work through the National Research Foundation of Korea (NRF), funded by the Ministry of Education (No. 2018R1A6A1A03025582, 2019R1D1A3A03103828 & 2022R111A3063302), Republic of Korea.

References

- Adhikari J, Biswas B, Chabri S, Bandyopadhyay NR, Sawai P, Mitra BC, Sinha A. Effect of functionalized metal oxides addition on the mechanical, thermal and swelling behaviour of polyester/jute composites. *Int J Eng Sci Technol.* 2017;20:760–74.
- Ahmadian Z, Correia A, Hasany M, Figueiredo P, Dobakhti F, Eskandari MR, Hosseini SH, Abiri R, Khorshid S, Hirvonen J, Santos HA, Shahbazi MA. A hydrogen-bonded extracellular matrix-mimicking bactericidal hydrogel with radical scavenging and hemostatic function for pH-responsive wound healing acceleration. *Adv Healthc Mater.* 2020;10:2001122.
- Aldana AA, Abraham GA. Current advances in electrospun gelatin-based scaffolds for tissue engineering applications. *Int J Pharm.* 2017;523:441–53.
- Ambrosi A, Pumera M. 3D-printing technologies for electrochemical applications. *Chem Soc Rev.* 2016;45:2740–55.
- Armstrong GR. The lucky iron fish: a simple solution for iron deficiency. *Blood Adv.* 2017;1:330.
- Baek S, Singh RK, Kim T-H, Seo J-W, Shin US, Chrzanowski W, Kim H-W. Triple hit with drug carriers: pH- and temperature-responsive theranostics for multimodal chemo- and photothermal therapy and diagnostic applications. *ACS Appl Mater Interfaces.* 2016;8:8967–79.
- Berman J, Krysan DJ. Author correction: drug resistance and tolerance in fungi. *Nat Rev Microbiol.* 2020;18:539.
- Bhattacharya D, Behera B, Sahu SK, Ananthakrishnan R, Maiti TK, Pramanik P. Design of dual stimuli responsive polymer modified magnetic nanoparticles for targeted anti-cancer drug delivery and enhanced MR imaging. *New J Chem.* 2016;40:545–57.
- Castro KC, Campos MGN, Mei LHI. Hyaluronic acid electrospinning: challenges, applications in wound dressings and new perspectives. *Int J Biol Macromol.* 2021;173:251–66.
- Che H, Huo M, Peng L, Ye Q, Guo J, Wang K, Wei Y, Yuan J. CO₂-switchable drug release from magneto-polymeric nanohybrids. *Polym Chem.* 2015;6:2319–26.
- Chen X-Z, Hoop M, Shamsudhin N, Huang T, Özkale B, Li Q, Siringil E, Mushtaq F, Di Tizio L, Nelson BJ, Pané S. Hybrid magnetoelectric nanowires for nanorobotic applications: fabrication, magnetoelectric coupling, and magnetically assisted in vitro targeted drug delivery. *Adv Mater.* 2017;29:1605458.
- Cheng Y, Chan KH, Wang X-Q, Ding T, Li T, Lu X, Ho GW. Direct-ink-write 3D printing of hydrogels into biomimetic soft robots. *ACS Nano.* 2019;13:13176–84.
- Cui T, Wu S, Sun Y, Ren J, Qu X. Self-propelled active photothermal nanoswimmer for deep-layered elimination of biofilm in vivo. *Nano Lett.* 2020;20:7350–8.

- Deng H, Yu Z, Chen S, Fei L, Sha Q, Zhou N, Chen Z, Xu C. Facile and eco-friendly fabrication of polysaccharides-based nanocomposite hydrogel for photothermal treatment of wound infection. *Carbohydr Polym.* 2020;230:115565.
- Gao W, Kagan D, Pak OS, Clawson C, Campuzano S, Chuluun-Erdene E, Shipton E, Fullerton EE, Zhang L, Lauga E, Wang J. Cargo-towing fuel-free magnetic nanoswimmers for targeted drug delivery. *Small.* 2012;8:460–7.
- Gao B, Guo M, Lyu K, Chu T, He B. Intelligent silk fibroin based microneedle dressing (i-SMD). *Adv Funct Mater.* 2020;31:2006839.
- Garcia-Gradilla V, Orozco J, Sattayasamitsathit S, Soto F, Kuralay F, Pourazary A, Katzenberg A, Gao W, Shen Y, Wang J. Functionalized ultrasound-propelled magnetically guided nanomotors: toward practical biomedical applications. *ACS Nano.* 2013;7:9232–40.
- Garcia-Gradilla V, Sattayasamitsathit S, Soto F, Kuralay F, Yardımcı C, Wiitala D, Galarnyk M, Wang J. Ultrasound-propelled nanoporous gold wire for efficient drug loading and release. *Small.* 2014;10(20):4154–9.
- Geim AK, Novoselov KS. The rise of graphene. *Nat Mater.* 2007;6:183–91.
- Gnavi S, Barwig C, Freier T, Haastert-Talini K, Grothe C, Geuna S. The use of chitosan-based scaffolds to enhance regeneration in the nervous system. *Int Rev Neurobiol.* 2013;109:1–62.
- Go G, Jeong S-G, Yoo A, Han J, Kang B, Kim S, Nguyen KT, Jin Z, Kim C-S, Seo YR, Kang JY, Na JY, Song EK, Jeong Y, Seon JK, Park J-O, Choi E. Human adipose-derived mesenchymal stem cell-based medical microrobot system for knee cartilage regeneration in vivo. *Sci Robot.* 2020;5:eay6626.
- Guo Y, Wang Y, Zhao X, Li X, Wang Q, Zhong W, Mequanint K, Zhan R, Xing M, Luo G. Snake extract-laden hemostatic bioadhesive gel cross-linked by visible light. *Sci Adv.* 2021;7:eabf9635.
- Halim A, Qu K-Y, Zhang X-F, Huang N-P. Recent advances in the application of two-dimensional nanomaterials for neural tissue engineering and regeneration. *ACS Biomater Sci Eng.* 2021;7:3503–29.
- Hao R, Xing R, Xu Z, Hou Y, Gao S, Sun S. Synthesis, functionalization, and biomedical applications of multifunctional magnetic nanoparticles. *Adv Mater.* 2010;22:2729–42.
- He W, Frueh J, Hu N, Liu L, Gai M, He Q. Guidable thermophoretic janus micromotors containing gold Nanocolorifiers for infrared laser assisted tissue welding. *Adv Sci.* 2016;3:1600206.
- Hossieni-Aghdam SJ, Foroughi-Nia B, Zare-Akbari Z, Mojarad-Jabali S, Motasadizadeh H, Farhadnejad H. Facile fabrication and characterization of a novel oral pH-sensitive drug delivery system based on CMC hydrogel and HNT-AT nanohybrid. *Int J Biol Macromol.* 2018;107:2436–49.
- Hu C, Long L, Cao J, Zhang S, Wang Y. Dual-crosslinked mussel-inspired smart hydrogels with enhanced antibacterial and angiogenic properties for chronic infected diabetic wound treatment via pH-responsive quick cargo release. *Chem Eng J.* 2021;411:128564.
- Hunter BM, Heringer W, Winkler JR, Gray HB, Müller AM. Effect of interlayer anions on [NiFe]-LDH nanosheet water oxidation activity. *Energy Environ Sci.* 2016;9:1734–43.
- Hyon S-H, Jamshidi K, Ikada Y. Synthesis of polylactides with different molecular weights. *Biomaterials.* 1997;18:1503–8.
- Jahan I, George E, Saxena N, Sen S. Silver-nanoparticle-entrapped soft GelMA gels as prospective scaffolds for wound healing. *ACS Appl Bio Mater.* 2019;2:1802–14.
- Jain K, Shukla R, Yadav A, Ujjwal RR, Flora SJS. 3D printing in development of nanomedicines. *Nano.* 2021;11:420.
- Jamshidzadeh F, Mohebbali A, Abdouss M. Three-ply biocompatible pH-responsive nanocarriers based on HNT sandwiched by chitosan/pectin layers for controlled release of phenytoin sodium. *Int J Biol Macromol.* 2020;150:336–43.
- Järbrink K, Ni G, Sönnergren H, Schmidtchen A, Pang C, Bajpai R, Car J. The humanistic and economic burden of chronic wounds: a protocol for a systematic review. *Syst Rev.* 2017;6:15.

- Ji X, Yang H, Liu W, Ma Y, Wu J, Zong X, Yuan P, Chen X, Yang C, Li X, Lin H, Xue W, Dai J. Multifunctional parachute-like nanomotors for enhanced skin penetration and synergistic antifungal therapy. *ACS Nano*. 2021;15:14218–28.
- Jiang S, Liu F, Lerch A, Ionov L, Agarwal S. Unusual and superfast temperature-triggered actuators. *Adv Mater*. 2015;27:4865–70.
- Jin Z, Nguyen KT, Go G, Kang B, Min H-K, Kim S-J, Kim Y, Li H, Kim C-S, Lee S, Park S, Kim K-P, Huh KM, Song J, Park J-O, Choi E. Multifunctional nanorobot system for active therapeutic delivery and synergistic chemo-photothermal therapy. *Nano Lett*. 2019;19:8550–64.
- Joseph B, Augustine R, Kalarikkal N, Thomas S, Seantier B, Grohens Y. Recent advances in electrospun polycaprolactone based scaffolds for wound healing and skin bioengineering applications. *Mater Today Commun*. 2019;19:319–35.
- Kakwere H, Leal MP, Materia ME, Curcio A, Guardia P, Niculaes D, Marotta R, Falqui A, Pellegrino T. Functionalization of strongly interacting magnetic nanocubes with (thermo) responsive coating and their application in hyperthermia and heat-triggered drug delivery. *ACS Appl Mater Interfaces*. 2015;7:10132–45.
- Kang JI, Park KM. Advances in gelatin-based hydrogels for wound management. *J Mater Chem B*. 2021;9:1503–20.
- Karshalev E, Zhang Y, Esteban-Fernández De Ávila B, Beltrán-Gastélum M, Chen Y, Mundaca-Uribe R, Zhang F, Nguyen B, Tong Y, Fang RH, Zhang L, Wang J. Micromotors for active delivery of minerals toward the treatment of iron deficiency anemia. *Nano Lett*. 2019;19:7816–26.
- Lau K-T, Wong T-T, Leng J, Hui D, Rhee KY. Property enhancement of polymer-based composites at cryogenic environment by using tailored carbon nanotubes. *Compos Part B*. 2013;54:41–3.
- Le TMD, Duong HTT, Thambi T, Giang Phan VH, Jeong JH, Lee DS. Bioinspired pH- and temperature-responsive injectable adhesive hydrogels with polyplexes promotes skin wound healing. *Biomacromolecules*. 2018;19:3536–48.
- Lee K-Y, Aitomäki Y, Berglund LA, Oksman K, Bismarck A. On the use of nanocellulose as reinforcement in polymer matrix composites. *Compos Sci Technol*. 2014;105:15–27.
- Li L, Sun W, Li L, Liu Y, Wu L, Wang F, Zhou Z, Zhang Z, Huang Y. A pH-responsive sequential-disassembly nanohybrid for mitochondrial targeting. *Nanoscale*. 2017;9:314–25.
- Li S, Chen A, Chen Y, Yang Y, Zhang Q, Luo S, Ye M, Zhou Y, An Y, Huang W, Xuan T, Pan Y, Xuan X, He H, Wu J. Lotus leaf inspired antiadhesive and antibacterial gauze for enhanced infected dermal wound regeneration. *Chem Eng J*. 2020;402:126202.
- Li J, Wang Y, Yang J, Liu W. Bacteria activated-macrophage membrane-coated tough nanocomposite hydrogel with targeted photothermal antibacterial ability for infected wound healing. *Chem Eng J*. 2021a;420:127638.
- Li Y, Zhu J, Cheng H, Li G, Cho H, Jiang M, Gao Q, Zhang X. Developments of advanced electrospinning techniques: a critical review. *Adv Mater Technol*. 2021b;6:2100410.
- Li M, Liang Y, Liang Y, Pan G, Guo B. Injectable stretchable self-healing dual dynamic network hydrogel as adhesive anti-oxidant wound dressing for photothermal clearance of bacteria and promoting wound healing of MRSA infected motion wounds. *Chem Eng J*. 2022;427:132039.
- Liao H, Qi R, Shen M, Cao X, Guo R, Zhang Y, Shi X. Improved cellular response on multiwalled carbon nanotube-incorporated electrospun polyvinyl alcohol/chitosan nanofibrous scaffolds. *Colloids Surf B: Biointerfaces*. 2011;84:528–35.
- Lin X, Li Y, Luo W, Xiao L, Zhang Z, Zhao J, Liu C, Li Y. Leucine-activated nanohybrid biofilm for skin regeneration via improving cell affinity and neovascularization capacity. *J Mater Chem B*. 2020;8:7966–76.
- Lu X, Wang C, Wei Y. One-dimensional composite nanomaterials: synthesis by electrospinning and their applications. *Small*. 2009;5:2349–70.
- Ma M, Zhong Y, Jiang X. Thermosensitive and pH-responsive tannin-containing hydroxypropyl chitin hydrogel with long-lasting antibacterial activity for wound healing. *Carbohydr Polym*. 2020;236:116096.

- Ma M, Zhong Y, Jiang X. An injectable photothermally active antibacterial composite hydroxypropyl chitin hydrogel for promoting the wound healing process through photobiomodulation. *J Mater Chem B*. 2021;9:4567–76.
- Mahmoud MA, El-Sayed MA. Metallic double shell hollow nanocages: the challenges of their synthetic techniques. *Langmuir*. 2012;28:4051–9.
- Mai B, Jia M, Liu S, Sheng Z, Li M, Gao Y, Wang X, Liu Q, Wang P. Smart hydrogel-based DVDMS/bFGF nanohybrids for antibacterial phototherapy with multiple damaging sites and accelerated wound healing. *ACS Appl Mater Interfaces*. 2020;12:10156–69.
- Mei Y, Solovev AA, Sanchez S, Schmidt OG. Rolled-up nanotech on polymers: from basic perception to self-propelled catalytic microengines. *Chem Soc Rev*. 2011;40:2109.
- Meireles AB, Corrêa DK, Da Silveira JW, Millás ALG, Bittencourt E, De Brito-Melo GEA, González-Torres LA. Trends in polymeric electrospun fibers and their use as oral biomaterials. *Exp Biol Med*. 2018;243:665–76.
- Meng X, Xu Y, Lu Q, Sun L, An X, Zhang J, Chen J, Gao Y, Zhang Y, Ning X. Ultrasound-responsive alkaline nanorobots for the treatment of lactic acidosis-mediated doxorubicin resistance. *Nanoscale*. 2020;12:13801–10.
- Min L-L, Yuan Z-H, Zhong L-B, Liu Q, Wu R-X, Zheng Y-M. Preparation of chitosan based electrospun nanofiber membrane and its adsorptive removal of arsenate from aqueous solution. *Chem Eng J*. 2015;267:132–41.
- Mogoşanu GD, Grumezescu AM. Natural and synthetic polymers for wounds and burns dressing. *Int J Pharm*. 2014;463:127–36.
- Mou F, Chen C, Zhong Q, Yin Y, Ma H, Guan J. Autonomous motion and temperature-controlled drug delivery of Mg/Pt-Poly(N-isopropylacrylamide) janus micromotors driven by simulated body fluid and blood plasma. *ACS Appl Mater Interfaces*. 2014;6:9897–903.
- Müller FA, Müller L, Hofmann I, Greil P, Wenzel MM, Staudenmaier R. Cellulose-based scaffold materials for cartilage tissue engineering. *Biomaterials*. 2006;27:3955–63.
- Nam S, Mooney D. Polymeric tissue adhesives. *Chem Rev*. 2021;121:11336–84.
- Nezarati RM, Eifert MB, Cosgriff-Hernandez E. Effects of humidity and solution viscosity on electrospun fiber morphology. *Tissue Eng Part C Methods*. 2013;19:810–9.
- Ninan N, Forget A, Shastri VP, Voelcker NH, Blencowe A. Antibacterial and anti-inflammatory pH-responsive tannic acid-carboxylated agarose composite hydrogels for wound healing. *ACS Appl Mater Interfaces*. 2016;8:28511–21.
- Osanloo M, Assadpour S, Mehrvaran A, Abastabar M, Akhtari J. Niosome-loaded antifungal drugs as an effective nanocarrier system: a mini review. *Curr Med Mycol*. 2019;4(4):31–6.
- Pereira R, Carvalho A, Vaz DC, Gil MH, Mendes A, Bártolo P. Development of novel alginate based hydrogel films for wound healing applications. *Int J Biol Macromol*. 2013;52:221–30.
- Pita-López ML, Fletes-Vargas G, Espinosa-Andrews H, Rodríguez-Rodríguez R. Physically cross-linked chitosan-based hydrogels for tissue engineering applications: a state-of-the-art review. *Eur Polym J*. 2021;145:110176.
- Prasadh S, Wong RCW. Unraveling the mechanical strength of biomaterials used as a bone scaffold in oral and maxillofacial defects. *Oral Sci Int*. 2018;15:48–55.
- Preman NK, Sindhu Priya ES, Prabhu A, Shaikh SB, Vipin C, Barki RR, Bhandary YP, Rekha PD, Johnson RP. Bioresponsive supramolecular hydrogels for hemostasis, infection control and accelerated dermal wound healing. *J Mater Chem B*. 2020;8:8585–98.
- Qi X, Pan W, Tong X, Gao T, Xiang Y, You S, Mao R, Chi J, Hu R, Zhang W, Deng H, Shen J. ϵ -Polylysine-stabilized agarose/polydopamine hydrogel dressings with robust photothermal property for wound healing. *Carbohydr Polym*. 2021;264:118046.
- Reddy MSB, Ponnamma D, Choudhary R, Sadasivuni KK. A comparative review of natural and synthetic biopolymer composite scaffolds. *Polymers*. 2021;13:1105.
- Salmoria GV, Klauss P, Paggi RA, Kanis LA, Lago A. Structure and mechanical properties of cellulose based scaffolds fabricated by selective laser sintering. *Polym Test*. 2009;28:648–52.
- Santi S, Mancini I, Dirè S, Callone E, Speranza G, Pugno N, Migliaresi C, Motta A. A bio-inspired multifunctionalized silk fibroin. *ACS Biomater Sci Eng*. 2021;7:507–16.

- Sheikholeslam M, Wright MEE, Jeschke MG, Amini-Nik S. Biomaterials for skin substitutes. *Adv Healthc Mater.* 2018;7:1700897.
- Shi M, Zhang H, Song T, Liu X, Gao Y, Zhou J, Li Y. Sustainable dual release of antibiotic and growth factor from pH-responsive uniform alginate composite microparticles to enhance wound healing. *ACS Appl Mater Interfaces.* 2019;11:22730–44.
- Song E, Han W, Li C, Cheng D, Li L, Liu L, Zhu G, Song Y, Tan W. Hyaluronic acid-decorated graphene oxide nanohybrids as nanocarriers for targeted and pH-responsive anticancer drug delivery. *ACS Appl Mater Interfaces.* 2014;6:11882–90.
- Sun J-Y, Zhao X, Illeperuma WRK, Chaudhuri O, Oh KH, Mooney DJ, Vlassak JJ, Suo Z. Highly stretchable and tough hydrogels. *Nature.* 2012;489:133–6.
- Tandon S, Kandasubramanian B, Ibrahim SM. Silk-based composite scaffolds for tissue engineering applications. *Ind Eng Chem Res.* 2020;59:17593–611.
- Tian M-P, Zhang A-D, Yao Y-X, Chen X-G, Liu Y. Mussel-inspired adhesive and polypeptide-based antibacterial thermo-sensitive hydroxybutyl chitosan hydrogel as BMSCs 3D culture matrix for wound healing. *Carbohydr Polym.* 2021;261:117878.
- Tiwari AP, Hwang TI, Oh J-M, Maharjan B, Chun S, Kim BS, Joshi MK, Park CH, Kim CS. pH/NIR-responsive polypyrrole-functionalized fibrous localized drug-delivery platform for synergistic cancer therapy. *ACS Appl Mater Interfaces.* 2018;10:20256–70.
- Tu Y, Peng F, Sui X, Men Y, White PB, Van Hest JCM, Wilson DA. Self-propelled supramolecular nanomotors with temperature-responsive speed regulation. *Nat Chem.* 2016;9:480–6.
- Tu Y, Peng F, André AAM, Men Y, Srinivas M, Wilson DA. Biodegradable hybrid stomatocyte nanomotors for drug delivery. *ACS Nano.* 2017;11:1957–63.
- Valente JFA, Valente TAM, Alves P, Ferreira P, Silva A, Correia JJ. Alginate based scaffolds for bone tissue engineering. *Mater Sci Eng C.* 2012;32:2596–603.
- Vidotti HA, Manso AP, Leung V, Do Valle AL, Ko F, Carvalho RM. Flexural properties of experimental nanofiber reinforced composite are affected by resin composition and nanofiber/resin ratio. *Dent Mater.* 2015;31:1132–41.
- Wang T-W, Spector M. Development of hyaluronic acid-based scaffolds for brain tissue engineering. *Acta Biomater.* 2009;5:2371–84.
- Wang G, Maciel D, Wu Y, Rodrigues J, Shi X, Yuan Y, Liu C, Tomás H, Li Y. Amphiphilic polymer-mediated formation of laponite-based nanohybrids with robust stability and pH sensitivity for anticancer drug delivery. *ACS Appl Mater Interfaces.* 2014a;6:16687–95.
- Wang R, Xu C, Sun J, Gao L. Three-dimensional Fe₂O₃ nanocubes/nitrogen-doped graphene aerogels: nucleation mechanism and lithium storage properties. *Sci Rep.* 2014b;4:7171.
- Wang M, Wang C, Chen M, Xi Y, Cheng W, Mao C, Xu T, Zhang X, Lin C, Gao W, Guo Y, Lei B. Efficient angiogenesis-based diabetic wound healing/skin reconstruction through bioactive antibacterial adhesive ultraviolet shielding nanodressing with exosome release. *ACS Nano.* 2019a;13:10279–93.
- Wang W, Lu K-J, Yu C-H, Huang Q-L, Du Y-Z. Nano-drug delivery systems in wound treatment and skin regeneration. *J Nanobiotechnol.* 2019b;17:82.
- Wang B, Kostarelos K, Nelson BJ, Zhang L. Trends in micro-/nanorobotics: materials development, actuation, localization, and system integration for biomedical applications. *Adv Mater.* 2020a;33:2002047.
- Wang S, Zheng H, Zhou L, Cheng F, Liu Z, Zhang H, Zhang Q. Injectable redox and light responsive MnO₂ hybrid hydrogel for simultaneous melanoma therapy and multidrug-resistant bacteria-infected wound healing. *Biomaterials.* 2020b;260:120314.
- Wang Z, Hu T, Liang R, Wei M. Application of zero-dimensional nanomaterials in biosensing. *Front Chem.* 2020c;8:320.
- Wang H, Liu X, Christiansen DE, Fattahpour S, Wang K, Song H, Mehraeen S, Cheng G. Thermoplastic polyurethane with controllable degradation and critical anti-fouling properties. *Biomater Sci.* 2021a;9:1381–96.

- Wang Z, Wang Y, Yan J, Zhang K, Lin F, Xiang L, Deng L, Guan Z, Cui W, Zhang H. Pharmaceutical electrospinning and 3D printing scaffold design for bone regeneration. *Adv Drug Deliv Rev.* 2021b;174:504–34.
- Wu Z, Li T, Li J, Gao W, Xu T, Christianson C, Gao W, Galarnyk M, He Q, Zhang L, Wang J. Turning erythrocytes into functional micromotors. *ACS Nano.* 2014;8:12041–8.
- Wu H, Almalki M, Xu X, Lei Y, Ming F, Mallick A, Roddatis V, Lopatin S, Shekhah O, Eddaoudi M, Alshareef HN. MXene derived metal–organic frameworks. *J Am Chem Soc.* 2019;141:20037–42.
- Xu F, Li X, Li Y, Sun J. Oil-repellent antifogging films with water-enabled functional and structural healing ability. *ACS Appl Mater Interfaces.* 2017;9:27955–63.
- Yu L, Wei M. Biominalization of collagen-based materials for hard tissue repair. *Int J Mol Sci.* 2021;22:944.
- Yuan R, Yang N, Fan S, Huang Y, You D, Wang J, Zhang Q, Chu C, Chen Z, Liu L, Ge L. Biomechanical motion-activated endogenous wound healing through LBL self-powered nanocomposite repairer with pH-responsive anti-inflammatory effect. *Small.* 2021;17:2103997.
- Zeng Q, Qi X, Shi G, Zhang M, Haick H. Wound dressing: from nanomaterials to diagnostic dressings and healing evaluations. *ACS Nano.* 2022;16:1708–33.
- Zhang J, Wu C, Xu Y, Chen J, Ning N, Yang Z, Guo Y, Hu X, Wang Y. Highly stretchable and conductive self-healing hydrogels for temperature and strain sensing and chronic wound treatment. *ACS Appl Mater Interfaces.* 2020;12:40990–9.
- Zhang K, Lv H, Zheng Y, Yao Y, Li X, Yu J, Ding B. Nanofibrous hydrogels embedded with phase-change materials: temperature-responsive dressings for accelerating skin wound healing. *Compos Commun.* 2021;25:100752.
- Zhao H, Lei Y. 3D nanostructures for the next generation of high-performance nanodevices for electrochemical energy conversion and storage. *Adv Energy Mater.* 2020;10:2001460.
- Zhou L, Wu J, Zhang H, Kang Y, Guo J, Zhang C, Yuan J, Xing X. Magnetic nanoparticles for the affinity adsorption of maltose binding protein (MBP) fusion enzymes. *J Mater Chem.* 2012;22:6813.
- Zhu M, Nie G, Meng H, Xia T, Nel A, Zhao Y. Physicochemical properties determine nanomaterial cellular uptake, transport, and fate. *Acc Chem Res.* 2012;46:622–31.
- Zhu Y, Cankova Z, Iwanaszko M, Lichtor S, Mrksich M, Ameer GA. Potent laminin-inspired antioxidant regenerative dressing accelerates wound healing in diabetes. *Proc Natl Acad Sci.* 2018;115:6816–21.
- Zhu DY, Chen XJ, Hong ZP, Zhang LY, Zhang L, Guo JW, Rong MZ, Zhang MQ. Repeatedly intrinsic self-healing of millimeter-scale wounds in polymer through rapid volume expansion aided host–guest interaction. *ACS Appl Mater Interfaces.* 2020;12:22534–42.

Chapter 9

Development of Efficient Strategies for Physical Stimuli-Responsive Programmable Nanotherapeutics



Pravin P. Upare, Hyung Sub Shin, Jun Hak Lee, and Byung Gyu Park

9.1 Introduction

Stimuli-responsive nanomaterials can change their properties and functions upon exposure to external or internal factors, such as pH, light, electric field, magnetic field, and temperature. Due to these desired properties of these nanomaterials, they are intended to be applied as controlled and targeted delivery of various therapeutic agents (Bhuchar et al. 2012; Du et al. 2010, Hoare et al. 2012a). The most dangerous diseases such as cancer, neurodegenerative diseases, metabolic disorders, and other serious diseases are often found in the human society, which has intensified the necessity of an efficient alternative drug delivery system that can efficiently release a sufficient quantity of drugs to the target site of the body. The development of nanomedicine is an emerging research field. The term nanorobotics refers to molecular robotics, in which related technology of device development is near the nanoscale range (>150 nm). The nanotherapeutics outcome from the merging of nanoscience, nanomedicine, and nanoengineering and the resultant nanotechnology or nanodevices derived from life and chemical sciences showed an outstanding application in biomedical science (Gil et al. 2012; Müller et al. 2000). Among the different nanomedicine platforms, research has shown great interest in developing new nanotechnology-based drug delivery systems and imaging nano-agents (Hua et al. 2011). The nanomedicine of theragnostic involves the combination of nano-sized theragnostic with several important functions which can contribute to targeted drug delivery, sustained release, and greater transport efficiency via endocytosis; however, they are highly functional for stimuli-responsive systems, and their

P. P. Upare (✉) · H. S. Shin · J. H. Lee · B. G. Park (✉)
C.T. (Core Technology) Team, ACTIVON R&D CENTER,
Cheongju-si, Chungcheongbuk-do, Republic of Korea
e-mail: pravin2112@activon.kr; bgpark1503@activon.kr

combination of therapeutic approaches included diagnosis and therapy (Poß et al. 2017). The term “nanotherapeutics” represents the nanosystem or nanodevices that can be applied as therapeutics and imaging agents (Gil et al. 2012; Landon et al. 2011; Bulbake et al. 2017). Different strategies of nanotherapeutics are summarized in Fig. 9.1. These efficient nanotheranostics can be derived from polymeric nanoparticles (NPs), liposomes, nanocrystal, micelles, microemulsion, polymersomes, nanorods, nanowires, nanofluid devices, carbon materials (graphene oxide, carbon nanotubes, quantum dots, fullerenes), inorganic nanosized materials (metal-based), dendrimers, and polymer-coated nanocarriers (Colombo et al. 2017; Xuan et al. 2012; Sahle et al. 2012; Sahle et al. 2017); these nanomaterials have been intensively utilized for controlled drug delivery. However, these nanotheranostics have been employed for detecting drugs in biological samples and also emphasized in related detection tools as conductive devices (Zhang et al. 2011; Chen et al. 2017). Nanomedicine lesser than 150 nm can be easily entrapped in the liver and spleen; however, nanomaterials with sizes <5 nm can be easily filtered out by the kidneys (Zhang et al. 2017a; Stejskalová et al. 2016). As per studies related to targeting

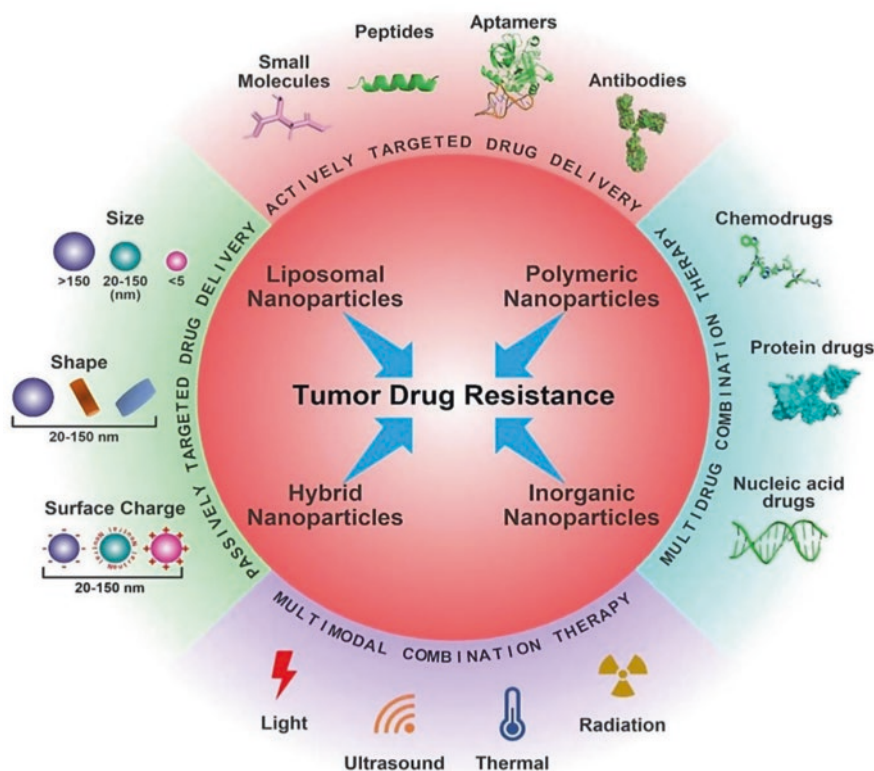


Fig. 9.1 Different strategies of nanotherapeutics to overcome cancer drug resistance. (Bukhari 2022)

various tumors, nanoparticles in the range of 100–200 nm were very efficient in tumor targeting.

So far, the desired amount of drug to target and for controlled release is yet to be achieved using traditional nanoformulations. However, few nanoformulations have reached the market (Stejskalová et al. 2016; Li et al. 2013). Hence, there are a lot of scope and demands in developing program nanomaterials with more appropriate structures and properties for effective therapeutic effects. Among the potential drug delivery platforms, nanotechnology contributes to the much-needed targeted drug delivery. In literature, a variety of studies are available on the development of nano-carriers which could assume a variety of bulk and surface chemistry, functionalization, modifications, sizes, shapes, and architectures, for improved drug release, targeting, and blood circulation time. This book chapter systematically discusses the design strategies for easy and systematic programmable physical stimuli-responsive nanotherapeutics.

9.2 Stimuli-Responsive Nanomaterials

Stimuli-responsive nanomaterials are specifically developed to respond to various physical stimuli such as light, temperature, ultrasound, magnetic field, electric field, and X-ray. However, external stimuli are easier to control and are associated with less variability than internal stimuli. Different nanomaterial types can be developed by considering several factors such as intended application, target, target site, cost, recovery, side effects, etc. Mostly, the nanomaterials have been designed based on chemical stimuli-responsive nanomaterials. However, several attempts have been made to enhance the programmability of various stimuli-responsive nanomaterials for improved therapeutic effects. These nanomaterials are responsive to different external physical stimuli such as temperature, light, ultrasound, magnetic field, and X-ray. In addition, functionalization of the surfaces of nanomaterials could significantly improve drug targeting.

9.2.1 *Temperature-Responsive Nanomaterial*

Temperature-responsive nanomaterials are denoted as thermo-responsive nanomaterials. These types of material exhibit the properties of phase transition in response to temperature change.

Critical solution temperature (CST) is the temperature point where phase transition occurs. Lower CST (LCST) and upper CST (UCST) are the temperature state where phase changes happen. In the case of LCST, material properties change from a hydrophilic and swollen state into the hydrophobic and collapsed state with the increase in temperature. In contrast, the hydrophobic and collapsed state change into the hydrophilic and swelling state which is known as UCST. Generally, these

temperature-responsive nanomaterials have been investigated for biomedical applications and usually have an LCST. Before the programming of various biomedical applications, these types of nanomaterials can modify through chemical modification, LCST, architecture, and targeting moieties as per requirements or demands. The related strategies for the programming are discussed below.

9.2.1.1 Programming with Different Thermoresponsive Chemical Compounds

As discussed above, a variety of thermoresponsive polymers have been utilized in the development of thermoresponsive nanomaterials. Here, a few potential examples are briefly discussed. PNIPAAm (poly(N-isopropylacrylamide)) is the most recognized and highly investigated thermoresponsive polymer that exhibits LCST near the physiological temperature of 37 °C. Interestingly, the LCST of PNIPAAm is independent of their molecular weight, amount, and nature conditions (Rahikkala et al. 2015; Lutz et al. 2006). However, LCST of N,N-diethyl acrylamide depends on the tacticity of the polymer, which could restrict their use (Gandhi et al. 2015). Other polymers such as poly(N-vinylalkyl-amide)s are investigated as thermoresponsive polymers due to their LCST range between 60 °C and 50 °C (Rejinold et al. 2011). Nevertheless, poly(N-vinylcaprolactam) can be well-tolerated by human intestinal Caco-2 and bronchial Calu-3 cell lines due to their efficient thermoresponsive properties; however, these polymers are not investigated as much as PNIPAAm investigated as a thermoresponsive polymer (Vihola et al. 2005). The thermoresponsive properties of poly(N-vinylcaprolactam) such as Flory-Huggins thermoresponsive phase behaviors in water with lowering and raising LCST with enlarging the length of polymers and concentration. It can also be used as temperature-responsive nanogel for controlled drug delivery and grafting on another polymer. For instance, N-vinylcaprolactam grafted on chitosan produced chitosan-g-poly(N-vinylcaprolactam) nanoparticles; these nanoparticles are found to be efficient in releasing the drug 5-fluorouracil (4% to 50%) over three days below and above its LCST.

Polyoxazolines, due to their variable chain length, exhibit a broad range of solubilities in water such as reactivity (Diehl and Schlaad 2009; Kurzhals et al. 2017; Pánek et al. 2012). Polyoxazoline polymers are well-known as nanostructure surface-grafting agents. In addition, these polymers have other important functions such as low immunogenicity, biodegradability, and easy penetrability through porcine gastric mucosa (Viegas et al. 2011; Ulbricht et al. 2014; Mansfield et al. 2015). Interestingly, Kurzhals and coworkers have nicely investigated the applicability of poly(2-isopropyl-2-oxazoline) after grafting on the surface of magnetic nanoparticles, in which LCST is near the physiological temperature (Kurzhals et al. 2017). For example, poly(2-isopropyl-2-oxazoline) (LCST in cell culture medium = 32.5 °C) and poly(2-ethyl-oxazoline) (LCST in cell culture medium = 37 °C). The permeability of poly(2-isopropyl-oxazoline)-grafted nanoparticles was four times higher than the permeability of poly(2-ethyl-oxazoline)-grafted nanoparticles in HeLa cells at

37 °C. The difference is attributed to the hydrophobicity of the former, with LCST below 37 °C. Pluronics® is another class of thermoresponsive polymers (block copolymers of poly(ethylene oxide) and poly(propylene oxide)); these polymers have a large range of LCST between 20 and 85 °C. These LCSTs can be easily controlled by the lengths of the hydrophilic poly(ethylene oxide) and the hydrophobic poly(propylene oxide) segments and their ratios.

These polymers exhibit amphiphilic polymer properties, which can be applied as food additives and pharmaceutical ingredients (Wang et al. 2013). Their amphiphilic nature undoubtedly intended them to be used as thermoresponsive grafting agents (Chen et al. 2007). Tian and coworkers have nicely developed nanomaterials based on the fabrication of doxorubicin-loaded dual thermo- and redox-responsive nanogels using poly(oligo ethylene glycol methacrylate) and 2-(2-methoxyethoxy) ethyl methacrylate using the disulfide-containing crosslinker N,N'-bis(acryloyl)cystamine; these polymers' LCST changed from 25.7 to 42.8 °C by thermal variation (Tian et al. 2016). However, there are several polymers, such as poly(N-alkyloxazolines)(polyoxazolines) based, which are thermoresponsive and utilized for biomedical applications (Diehl and Schlaad 2009; Kurzhals et al. 2017).

There are some other classes of natural and synthetic thermoresponsive polymers such as polypeptides or lipids that have been utilized. The peptide such as Elastin-like polypeptides and random copolypeptoids are commonly used for thermoresponsive nanomaterial synthesis (Sicilia et al. 2014; Bessa et al. 2010). Elastin-like polypeptides are composed of multiple repeating pentapeptide units of Val-Pro-Gly-Xaa-Gly (Xaa is any amino acid except proline), which shows significant transition at 2–3 °C (Kowalczyk et al. 2014; Kracke et al. 2015). In addition, Elastin-like polypeptides are useful in the synthesis of composite nanoparticles and vesicular nanostructures. Recently, Bessa et al. have synthesized bone morphogenetic protein (BMP)-2- and BMP-14-loaded nanomaterials by thermoresponsive self-assembly of the elastin-like polypeptide (VPAVG)₂₂₀ (transition temperature = 33 °C) at 37 °C. These nanoparticles efficiently work in the release of cytokines for 2 weeks in vitro at 37 °C (Sicilia et al. 2014; Bessa et al. 2010). In another case, Kurzhals and coworker have designed magnetic nanoparticles by grafting poly(N-methyl glycine)–poly(N-butyl glycine) polypeptide with different percentages of N-methyl glycine and N-butyl glycine from 61 to 73%. These developed nanopolymers showed great amphiphilic and biodegradable properties. Thermoresponsive liposomes are among the pioneering stimuli-responsive nanocarriers of which few have advanced to clinical trial stages (Landon et al. 2011; Bulbake et al. 2017).

9.2.1.2 LCST Programming for Thermal Targeting and Controlled Release

Thermoresponsive nanomaterials with LCST properties can be offered the controlled release of drugs at a target point (Kim et al. 2006, 2018). These thermoresponsive nanomaterials are composed of a variety of temperature-sensitive polymers, exhibiting different LCSTs that are higher or lower than body temperature.

Nanomaterial with lower LCST than 37 °C can work efficiently without being affected by biological barriers owing to their inbuilt sol-gel transition at body temperature, which enhances efficiencies such as drug permeability and dosage retention period. Wang et al. have developed the thermoresponsive self-assembled poloxamer 407 nanogels, which was found to be very active on the corneal surface, and showed enhancement in the permeability of muscone across the cornea around three- to fourfold (Wang et al. 2016a). Wu et al. have examined Pluronics® as an efflux protein inhibitor; they designed micelles containing Pluronic® F127 and Plasdone™ S630, which were increased in oral bioavailability of biochanin A2 16-fold in SD rats compared with the free drug (Wu et al. 2017). However, Mung et al. nicely studied self-assembled micelles of segments of Pluronics® (hydrophilic poly(ethylene oxide) segments as well as hydrophobic poly(propylene oxide) segments) with D- α -tocopheryl PEG succinate at 50 °C, which showed enhancement in the permeability of the small molecular-model drug Rho123 in Sprague–Dawley (SD) rats after intravenous administration; interestingly, it can work across the blood–brain barrier (Meng et al. 2017).

In the case of materials with higher LSCT than 37 °C, these materials can easily disperse in the physiological fluid and freely circulate in the whole body at 37 °C. When the target point or decess point is heated up to 40–42 °C by different treatments, the thermoresponsive nanomaterials in the body can change their behaviors and become hydrophobic, which can be easily captured by the surrounding cells and tissue; in that way, controlled drug delivery to target site can be achieved (Han et al. 2013; Kim et al. 2013). Few studies of 5-fluorouracil (Rejinold et al. 2011), doxorubicin (Dicheva et al. 2014), and 17-(allylamino)-17-demethoxygeldanamycin (Sanyal et al. 2011) were incorporated into chitosan-g-poly(N-vinylcaprolactam) nanoparticles, cationic liposomes, and core-shell composite nanoparticles, respectively; these carriers showed improvement in the cellular uptake of the drugs for tumor cell lines upon hyperthermia. However, these nanocarriers were more cytotoxic than the free drugs.

Han et al. and Kim et al. have observed the response changes in behaviors of gold nanorods and inorganic magnetic nanoparticles (Han et al. 2013; Kim et al. 2013). These gold nanoparticles can absorb NIR light at ~800 nm and generate heat, whereas magnetic nanoparticles exchange magnetic fields into heat. These types of nanomaterials can be modified within the core of such thermoresponsive devices. Interestingly, the drug release can be easily controlled by turning “on” or “off” by applying and removing NIR or the magnetic field, by which drug demand can induce significant “on-demand drug release.” However, such types of smart nanocarriers are well designed with important drugs such as doxorubicin (Kim et al. 2013; Yildiz and Sizerici Yildiz 2015), vascular endothelial growth factor (Dionigi et al. 2014), or curcumin (Al-Ahmady et al. 2012) reported in the literature (Yassine et al. 2016; Cunliffe et al. 2003; Nykänen et al. 2012). However, drug release efficiency controlled the LCST in nanoparticles, and their incorporation into other components such as thermoresponsive polymers have been achieved by copolymerization, conjugation, and grafting (Dionigi et al. 2014).

Nevertheless, hydrophilic components increase the LCST, and hydrophobic components decrease the LCST. In literature, various thermosensitive nanoparticles are designed, and their efficiencies are investigated in drug delivery systems (Hoare et al. 2012a). Vesicular nanostructures such as ammonium bicarbonate, nitric oxide, carbon monoxide, and hydrogen sulfide can also be utilized as thermoresponsive for controlled drug release and diagnosis purposes using bubble-generating agents (Schwarz et al. 2016; Lin et al. 2017). Ammonium bicarbonate, known as CO₂ bubble-generating agent, was well incorporated into thermoresponsive liposomes.

Programming with Different Architecture

The parameters including shape, size, and surface properties such as porosity, surface area, and nature (acidic or basic) of thermoresponsive nanomaterials can affect the targeting and therapeutic efficiency of the drug-loaded nanomaterials (Sahle et al. 2017; Nykänen et al. 2012). Several polymers are designed and redesigned to form composite nanoparticles such as nanogels and micelles of Pluronics® (Wang et al. 2016a). Nevertheless, many polymers and copolymers can be self-assembled into thermoresponsive supramolecular nanostructures with well-known morphologies like lamella and gyroid, which offer drug release functions. For instance, Rahikkala et al. prepared 1-anilinonaphthalene-8-sulfonic acid-loaded nanoparticles of the triblock polymer polystyrene–PNIPAAm–polystyrene with three different morphological architectures, namely, polystyrene spheres in PNIPAAm matrix, polystyrene gyroids in PNIPAAm matrix, and polystyrene–PNIPAAm lamellar structure (Rahikkala, 2015). Micellar aggregates are utilized after crosslinking, resulting in thermodynamically stable vesicular systems with thermoresponsive cores (Bhuchar et al. 2012). Thermoresponsive liposomes are a special type of vesicle formed by hydrophobic lipid bilayers and an aqueous core.

Programming with Additional Functional Groups

Effective functionalization of nanomaterials is possible through their functional modifications, such as acidic group, ionic, metal sites, incorporation of ligand and polymers, crosslinkers, and the thermoresponsive material modified with more advanced properties which are desired for particular treatment and disease recovery. However, the thermoresponsive materials can be easily functionalized with charge ions, cell-binding ligands, and functional groups (-OH, -COOH, -C=O, -CHO, etc.) through different chemical and physical treatments. In the case of ion/charge modification, the resultant charged nanomaterials can enhance the drug loading and sustain the release of the drug, which is oppositely charged. Hoare et al. have successfully incorporated 20 mole% of anions of acrylic acid into PNIPAAm nanogels, and the results showed a huge enhancement in drug loading efficiency (Hoare et al. 2012b). In addition, it could efficiently sustain the release of cations of local anesthetic bupivacaine through their ionic interactions. However, effective action

and duration were found to be increased threefold (Hoare et al. 2012a). In another study by Bhuchar et al., 2-aminoethyl methacrylamide hydrochloride is successfully incorporated into nanomaterials and generated cationic nanoparticles, which showed improvement in encapsulation efficiency and could limit the release of the anionic proteins, insulin, BSA, and β -galactosidase (Bhuchar et al. 2012). Du et al. have developed nanogel with a variable pH-responsive charge which transformed an anionic medium into a cationic medium in a slightly acidic tumor extracellular environment (Du et al. 2010). These types of charge variable functions of nanogels can improve their cellular uptake, which results controlled release of doxorubicin to improve the cytotoxic release of the drug. However, few studies have been found where researchers have modified the nanomaterials by cell-binding ligands such as peptides, aptamers, and antibodies which results in an improvement in cell targeting and cellular loading/consumptions by endocytosis.

Folic acid and folate receptors are widely used as a tumor-targeting ligand for different tumor cells, which can be easily incorporated into thermoresponsive material for a particular treatment of tumors (Kim et al. 2013; Liang et al. 2017). Integrin β 4 was nicely fabricated on the surface of hybrid core-shell thermoresponsive nanoparticles; this resultant nanomaterial homogenously dispersed on the surface of squamous head and neck carcinoma cells, on which A9 antigen was overexpressed (Kim et al. 2013). Interestingly, biodegradable nanoparticles (bio-monomer and bio-polymer based, enzyme-based) were utilized in a controlled drug delivery system (Huang et al. 2008; Cubero et al. 2006). For instance, HEMA–lactate–dextran (Lanier and Bermudez 2015; Samanta and Medintz 2016), poly(L-lactic acid) (Kim et al. 2018), bis(2-methacryloyloxyethyl) disulfide (Jiang et al. 2009), and disulfide-containing crosslinker N,N'-bis(acryloyl) cystamine (Tian et al. 2016) or enzymes (e.g., dextran-methacrylate (Aguirre et al. 2013)) have been added or incorporated with temperature-responsive nanomaterials.

PNIPAAm-co-polymethacrylate was found to increase the circulation time in the body at various temperatures and was effective in nanotherapeutics (Sahle et al. 2018). However, more advanced thermoresponsive nanomaterials have been developed using thermoresponsive polymers and peptides, which could show enhancement in the therapeutic effects of the nanosystem. Fig. 9.2 presents a hybrid nanomaterial system of thermoresponsive amphiphilic leucine zipper peptide and thermoresponsive liposomes, where thermoresponsive amphiphilic leucine zipper peptide showed phase transition at 42 °C, which could effectively enhance the uptake of drug doxorubicin almost three times in the heated tumor site in SW480 tumor-bearing mice compared with lysolipid-modified thermoresponsive liposomes (Sahle et al. 2018; Chen et al. 2013).

Photo-responsive Nanomaterials

Photo-responsive materials can undergo physicochemical changes in response to light stimuli. Usually, UV range of 200–400 nm and NRI of 650–900 nm has been employed as effective exogenous stimuli for biomedical applications because the

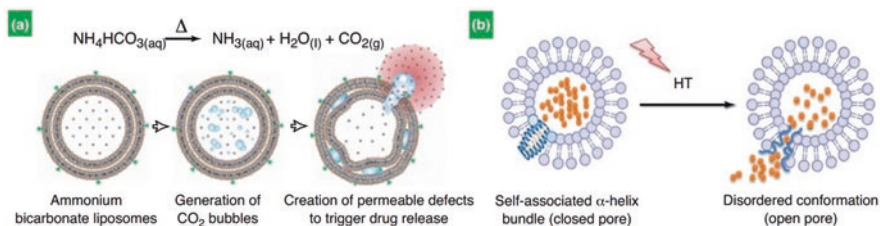


Fig. 9.2 Thermoresponsive system, smart nanomaterial with amphiphilic leucine zipper peptide and thermoresponsive liposomes, (a) thermoresponsive bubble-generating liposomes, designed by adding bubble generating agents, (b) liposome–peptide hybrid thermoresponsive vesicles, designed by adding a thermoresponsive amphiphilic leucine zipper peptide into thermoresponsive liposomes and their response to hyperthermia. (Chen et al. 2013; Al-Ahmady et al. 2012)

light in the wavelength range of UV and NIR can be easily absorbed by tissues and skin with high spatial and temporal precision (Zhou et al. 2006; Xiao et al. 2012). However, the controlled release of the desired drug can be regulated by physico-chemical modifications to the light-responsive nanomaterials. In addition, it can be regulated by adjusting the light wavelength, intensity, and duration of exposure (Fomina et al. 2012). The various efficient strategies to design program or device photosensitive nanomaterials for particular disease treatment is presented below.

Programming with Different Basic Chemistry That Is Light-Responsive

Photosensitive chemical compounds such as azobenzene, stilbene, spiropyran, dithienylethene, diazonaphthoquinone, and pheophorbide A are widely utilized organic compounds for the development or design of light-responsive nanomaterials. However, these smart materials can exhibit irreversible photoisomerization upon exposure to light (Fig. 9.3). As per their chemistry, these light-sensitive materials can be easily bound to the nanomaterials. Cis-trans isomerization of azobenzene and stilbene is very common whenever they are exposed to 300–380 nm. Noteworthy, the dipole movement of cis-isomer is much greater as compared to the dipole moment of trans-isomers. Patnaik et al. (2007) have developed the self-assembled micelles using hydrophobic azobenzene to the hydrophilic dextran. These resultant micelles were found to be very active, which could efficiently release the dosages of loaded acetylsalicylic acid and rhodamine upon UV irradiation, where hydrophobic trans-azobenzene changes into the hydrophilic cis-azobenzene. Other compounds, such as natural spiropyran, can easily isomerize to charged merocyanine, whereas reversible transition of diethylene is very common; it can easily go through the transition from the ring-open isomer to ring-closed isomer. In addition, diazonaphthoquinone compounds exhibit irreversible transition when exposed to UV light through photoinduced Wolff rearrangement (Zhao 2012). Pyrene, o-nitrobenzyl, coumarin, and thymine are widely used photosensitive groups (Sahle et al. 2018). Pyrene molecules can be easily gone through solvolysis in the presence of protic

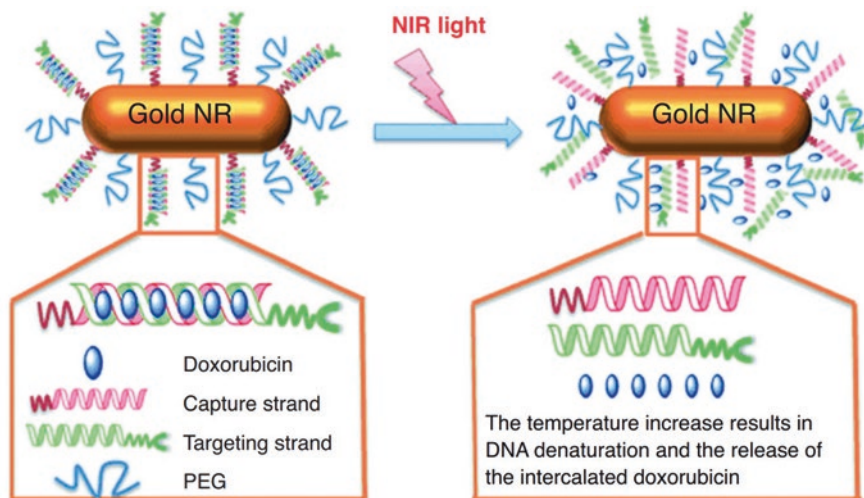


Fig. 9.3 NIR (near-infrared) responsive nanotherapeutics based on gold nanorods modified with doxorubicin and folic acid-modified DNA nanoaggregates. The gold NR generates heat under the exposure with NIR light that dehybridizes the DNA aggregates and releases the loaded doxorubicin. (Xiao et al. 2012)

solvents. However, the *o*-nitrobenzyl group is very responsive to UV light, which can undergo intramolecular rearrangement in the presence of water and can also be activated by NIR light through proton absorption. Pheophorbide A molecule is very sensitive to light. Pheophorbide-A incorporated with polyethyleneimine nanoparticles is developed that could have shown enhancement in cellular uptake of FITC-labeled ovalbumin by murine dendritic cells by ~2.8-fold, which was very effective in the cytoplasm, indicating protein release from the endocytic vesicles to the cytoplasm (Zhang et al. 2017b). The nanogel of *o*-nitrobenzyl and crosslinker was found to be very sensitive to light; it was irradiated with 365 nm of UV rays, and more interestingly, it was degraded to release the loaded protein alkaline phosphatase; the related study was well conducted by Azagarsamy and coworkers (Azagarsamy et al. 2012). Recently, Huu and coworkers (Huu et al. 2015) designed nintedanib-loaded, photosensitive nanoparticles using the polymers with surface *o*-nitrobenzyl groups, the resultant polymers are robust for more than 10 weeks before intravitreal injection but rapidly released the nintedanib when exposed to 365 nm light, which suppress the choroidal neovascularization in Brown Norway rats. However, there are many reports where the researcher utilized a variety of light-sensitive compounds and designed the light-sensitive nanomaterials for the treatments of various therapies (Azagarsamy et al. 2012; He et al. 2012; Itoh et al. 2004). However, few photo-responsive inorganic materials are also utilized to design photosensitive materials such as metal oxides TiO₂, ZnO, and CuO and metals such as gold and other noble and precious metals. Wand and coworkers have designed surface-grafted polyethyleneimine paclitaxel-loaded porous TiO₂ nanoparticles by an amide linkage to close

the pores (Wang et al. 2015). After their modification with folic acid, these materials were applied for tumor targeting. However, it has efficiently released (3.2%) the amount of paclitaxel from the nanomaterials. When these nanoparticles were exposed to the UV for 5–15 min, the polyethyleneimine moieties from the surface were successfully cleaved by the free radicals ($\text{OH}\cdot$ and $\text{O}_2\cdot^-$), which were generated on TiO_2 , and it could release up to 73.4% of the paclitaxel over 3 h. Gold nanoparticles with different shapes and carbon nanotubes can absorb NIR light and generate the heat for light and thermal-responsive drug delivery at targeting sites (Alibolandi et al. 2017). This technology has been used to deliver drugs in deep tissues because the NIR rays can easily penetrate 10 cm with minimal absorption of water and tissues (Karimi et al. 2016; You et al. 2012). In other studies, doxorubicin-loaded hollow gold nanospheres were employed to target mice bearing Hey tumors, and irradiation to the tumor area using 808 nm NIR laser light was conducted, which resulted in rapid release of the doxorubicin in the treated area.

Programming with Additional Functional Groups

As discussed in the thermoresponsive materials section, the functioning of light-sensitive materials can be enhanced by their functionalization with different functional groups such as folic acid (Liang et al. 2017), antibodies (Gandhi et al. 2015), aptamer (Chuang et al. 2016), and other thermoresponsive materials for targeted and efficient drug delivery systems. Liang et al. have developed folic acid functionalized photo-responsive material and investigated the targeting of tumor sites for cytotoxicity in the human body. These folic acid nanoparticles showed superior cytotoxicity than nontargeted nanoparticles in human nasopharyngeal epidermoid carcinoma cell lines (Liang et al. 2017). When they induced cancerous model by injecting human nasopharyngeal epidermoid carcinoma cells, and check the growth tumor volume after targeting the folic acid nanoparticles, that was found to be 35% lesser than nontargeted one owing to targeted photothermal ablation.

In another study by Xiao and coworkers, they developed a light-responsive nanocarrier based on DNA strands. This excellent material was very efficient and offered the loading platform for doxorubicin by owing to CG base pairs (Fig. 9.3) (Xiao et al. 2012). In addition, the light-responsive nanoparticles are functionalized at one end of DNA strands, which was supposed to be capturing strands functionalized with thiol group modified with gold nanorods, whereas another end of DNA strand (i.e., targeting strand) was functionalized with folic acid-specific cell targeting. These well-designed nanoparticles functioned as NIR light-to-heat transducers when exposed to 808 nm NIR irradiation. The resultant heat organized by gold nanoparticles can rehybridize the DNA strands, which results from the efficient release of loaded doxorubicin in a BALB/c nude mice xenograft tumor site. Interestingly, these nanoparticles were nicely PEGylated, which showed improvement in their performance for blood circulation half-life. Lee and coworkers successfully functionalized Herceptin (a drug; antihuman epidermal growth factor receptor 2 (HER2) antibody) with polylactic-co-glycolic acid gold-based core-shell

nanomaterials by aiming to generate multiple functions such as binding, NIR irradiation effects, and enhancement in the accumulations of light-sensitive nanoparticles (Lee et al. 2011).

Interestingly, the resulting programming offers moderate doxorubicin to breast cancer cells in mice. However, doxorubicin loading effectively sustained the tumor growth rate by 28%. In the detail of treatment, in mice with tumors treated with doxorubicin in the presence of targeted nanoparticles and compared the drug efficiency in the absence of nanoparticles without NIR irradiations, the related tumor growth rate was lower than in control groups. At the same time, the tumor growth was reduced by 68–75% when they were treated with nanoparticles without doxorubicin in the presence of NIR irradiation (for 10 min exposure). However, tumors proliferate without any treatments. Interestingly, the same tumor effectively recurred within a week by treatment of the targeted doxorubicin-loaded nanoparticles followed by 10 min NIR irradiations.

Chuang et al. have designed ammonium bicarbonate-loaded bubble-generating and mucin-1 aptamer surface-modified thermoresponsive liposomes modified with gold nanocages (Chuang et al. 2016), which increased the drug delivery efficiency at the targeted disease sites. The resultant gold nanoparticles can easily convert NIR irradiation into heat, by which ammonium bicarbonate gets decomposed and generates carbon dioxide bubbles which produced permeable defects on the wall of the lipid membrane that could trigger doxorubicin release (Fig. 9.3). Chuang et al. have also observed that treatment with free doxorubicin did not become effective in reducing the tumor volume. However, administration of the loaded liposomal systems effectively reduced the relative tumor volume to ~60% over 12 days in the presence of NIR irradiation. The energy transfer mechanism allows the luminescent materials such as ytterbium and erbium to convert low-energy NIR light into UV/visible light. These photoluminescent materials can be applied to release the drug from UV and visible photo-responsive nanomaterials. Liang et al. nicely (Liang et al. 2017) incorporated the luminescent ytterbium- and erbium-co-loaded sodium yttrium fluoride nanoparticles with folic acid and loaded doxorubicin drug. The resultant multifunctional nanosystem showed higher cytotoxicity in folate receptor-positive KB cells due to higher uptake of the nanoparticle by receptor-mediated endocytosis, which is higher than the folate-receptor negative A549 cells. The most crucial point is that most of the nanoparticles converted NIR light of 980 nm into the different emission peaks of lesser wavelength (512 nm, 541 nm, 656 nm), which can be a good signal for cell image therapies.

9.2.2 *Ultrasound-Responsive Materials*

The nanomaterial which can undergo physicochemical changes in response to the ultrasound stimulus is called ultrasound-responsive nanomaterials. Ultrasound-sensitive materials are a class of smart materials that can be utilized in drug delivery

and targeting of disease sites and a variety of biomedical applications using ultrasound-related therapies.

For biomedical application/or utilization, high-intensity focused ultrasound has been employed as the most effective exogenous stimulus due to the most critical functions such as its noninvasiveness, reliable accessibility, lower cost, availability, ion-free radiation residues, controllable spatiotemporal effect, and ease of patient acceptability (Sirsi and Borden 2014; Lee et al. 2015; Yildirim et al. 2017). The strategies for developing programmable ultrasound-responsive nanomaterials for specific therapeutic effects are discussed.

9.2.2.1 Programming Using Basic Chemistry for Ultrasound-Responsive Materials

Generally, mechanophores (ultrasound-labeled moieties) incorporated or fabricated with polymeric nanomaterials turn into ultrasound-responsive nanomaterials such as tetrahydropyranyl (Paris et al. 2015). Ultrasound labile such as tetrahydropyranyl incorporated with methacrylic monomer through chemical reactions/bonding and generate ultrasound-responsive materials, from which tetrahydropyranyl group (predominantly hydrophobic) dissociate and released by insonation, and hydrophilic group (acidic) retain on the polymer material (Fig. 9.4). These types of the critical transition phenomenon through ultrasound stimulus are beneficial for a controllable drug delivery system. Paris and coworkers have designed the polymer grafted mesoporous silica nanoparticles that acted as ultrasound-responsive drug carriers (model dye fluorescein) (Paris et al. 2015). The crosslinking polymer such as tetrahydropyranyl methacrylate copolymerized with monomer 2-(2-methoxyethoxy) ethyl methacrylate (temperature-responsive polymer) and

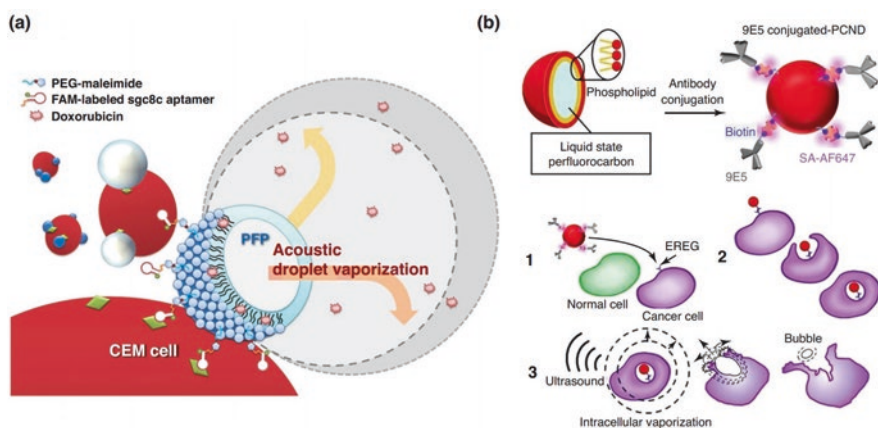


Fig. 9.4 Ultrasound-responsive nanodroplets conjugated with (a) aptamer and (b) antibody for tumor-targeted therapy and their interaction and degradation with cancerous cells by ultrasound. (Wang et al. 2012b; Ishijima et al. 2017)

generated a polymeric gatekeeper. In another study by Xuan et al., they synthesized micelles at room temperature, which are composed of 2-tetrahydropyranyl methacrylate and amphiphilic di-block copolymer comprising poly(ethylene oxide) and poly(2-(2-methoxyethoxy) ethyl methacrylate) (Xuan et al. 2012). The resultant micelles efficiently cleaved the tetrahydropyranyl group and released the loaded model hydrophobic compound such as Nile red upon insonation. Nevertheless, ultrasound can function to generate intense acoustic cavitation as well as disarray various drug-loaded nanoaggregates such as Pluronic® micelles (Jo and Ban 2016), nanobubbles (Xie et al. 2016), nanodroplets (Lee et al. 2015), and liposomes (Xin et al. 2017). Undoubtedly, these essential facilities can be beneficial to release the drug at the disease site in response to ultrasound therapies.

Recently, Yildirim et al. have observed the related phenomenon of muddle in their solid inelastic polymeric nanoparticles, which are ultrasound responsive (Yildirim et al. 2017). The polymeric nanoparticles were synthesized from 3,4-dihydro-2H-pyran-co-2-((tetrahydro-2H-pyran-2-yl)oxy)ethyl methacrylate-co-2-(dimethylamino)ethyl methacrylate copolymer. In addition to this vesicular distorting effect, these nanocarriers allow the mechanical cavitation of tissues using ultrasound. These nanocarriers can easily circulate across blood capillaries and penetrability across cell membranes (Sirsi and Borden 2014; Zhao et al. 2013). Marin and coworkers designed the aptamer–nanoparticle complexes as powerful diagnostic and therapeutic tools based on Pluronic® micelles and doxorubicin drug (Zhao et al. 2013). The resultant tools were found to be efficient in uptakes of doxorubicin from Pluronic® micelles by HL-60 cells in response to the continuous ultrasound waves of 20 kHz, which is due to the releasing/disruption facility of synthesized nanomaterials and easy perturbation of the cell membrane in the presence of ultrasound waves.

Ultrasound-responsive PLGA nanoparticles incorporation liposomes were synthesized by Xin et al. (2017). The resultant nanomaterials were efficient, which can quickly release the PLGA nanoparticles and loaded mitoxantrone drug upon insonation. However, drug encapsulation increased its half-life 6.7-fold in adult SD rats, which was again reduced to 1.7-fold upon insonation. However, these ultrasound-responsive nanomaterials can be used to design a broader range of ultrasound contrast agents by incorporating drugs (Paris et al. 2017). For instance, Wang et al. investigated ultrasound-induced hyperthermia to produce gas bubbles for vascular occlusion and ablation of cancer cells (Wang et al. 2012a). The nanomaterial using doxorubicin fabricated with perfluorocarbon nanodroplets was developed and observed to be very stable in the bloodstream. Interestingly, ultrasound-induced hyperthermia starts generating perfluorocarbon gas bubbles in response to the ultrasound (this phenomenon is described as the acoustic droplet vaporization effect); this active function turns into a decrease in human acute lymphoblastic leukemia cell viability by 5.6% *in vitro* after 6 hours of incubation.

9.2.2.2 Programming with Functional Groups on Nanomaterials

As discussed above, controlled drug release from drug-loaded ultrasound-responsive nanoparticles is monitored by the ultrasound actions. However, appropriate functionalizing of nanomaterials with reactive ligands such as antibodies, peptides, or aptamers can enhance the efficiencies in biodistribution and targeting of disease sites in response to the ultrasound.

In the same study by Wang et al. (2012a), they have designed the nanoparticles and drug-loaded nanomaterials such as sgc8c aptamer-conjugated, doxorubicin-loaded acoustic droplets composed of a liquid perfluoropentane core, and lipid shell for tumor theragnostic and therapies (Fig. 9.4a).

The resultant nanomaterial (aptamer-conjugated droplets) efficiently reduced (around 56.8%) the cell viability *in vitro*, which was significantly higher (around 4.5 times) than that of the nonconjugated one. Figure 9.4b was captured from the report of Ishijima et al. (Ishijima et al. 2017). They have developed an anticancer monoclonal antibody 9E5-conjugated phase-change nanodroplets composed of perfluorocarbon liquid core (perfluorobutane and perfluorohexane mixture) and a phospholipid shell, which was utilized for intracellular vaporization and drug release. The resultant nanomaterial with epiregulin receptor effectively works on the colonic adenocarcinoma cell line DLD1, which showed around 97.8% accumulation of the nanoparticles into the cell lines, which was significantly higher than the value obtained without the antibody. As discussed, perfluorocarbon liquid in the nanodroplets produced intracellular vaporization generated under ultrasound waves, which could kill 57% of the targeted DLD1 cells.

Paris et al. have designed an intelligent nanoparticle by grafting porous silica nanoparticles using the ultrasound-responsive copolymer, poly(2-(2-methoxyethoxy) ethyl methacrylate-co-2-tetrahydropyranyl methacrylate) which can act as a gate-keeper. The designed nanomaterial allows the loading of doxorubicin together with polyethyleneimine modification to enhance their permeation into the mesenchymal stem cells. The resultant nanoparticle with mesenchymal stem cells was then co-cultured with N-nitroso-N-methyl urea-induced tumor cells obtained from SD rats (female). Interestingly, a more negligible effect was observed in stem cell migration by adding nanoparticle loading, which could sustain the tumor cell viability by ~60% owing to doxorubicin release by insonation (Paris et al. 2017). An advanced approach was designed by Lee et al. by combining magnetic nanoparticles with ultrasound-responsive protein-polymer nanodroplet core to achieve trio magnetic field-receptor and ultrasound-mediated targeted drug delivery. This advanced approach performed well and has enhanced the cancer cell-killing efficiency by 40% (Lee et al. 2015).

9.2.3 *Magnetic Field-Responsive Nanomaterials*

The nanomaterials that can respond to magnetic field stimuli are called magnetic field-responsive nanomaterials. Alike thermoresponsive, photo-responsive, and ultrasound-responsive materials, magnetic field-responsive nanomaterial has been utilized in biomedical applications such as nanotherapeutics for diagnostic and therapeutic applications (Yang et al. 2011). This class of materials is easy to synthesize (organic and inorganic); however, these materials have been highly recognized as biocompatible and can be easily controlled by a magnetic field. By owning the critical property of generating hyperthermia in a magnetic field, these materials can be utilized to improve blood cell permeability, control drug release, and destroy the cancerous cells (McGill et al. 2009). The unique human body cannot absorb the frequency below 400 Hz magnetic field, which can be easily directed toward desired tissue (Prijic et al. 2012).

9.2.3.1 **Programming Using the Magnetic Field-Responsive Chemical Compounds**

Superparamagnetic iron oxide nanoparticles (SPIONs) such as Fe_3O_4 and Fe_2O_3 have been recognized as magnetic field-responsive nanomaterials constructed in core-shell-type systems (Hua et al. 2011). Various shell materials such as polymers, mesoporous silica, squalene–gemcitabine, and lipids have been used to core iron oxide nanoparticles and produce magnetic field-responsive nanomaterials (Zhang et al. 2012). SPIONs are nanomaterials that can attribute quantum effect at the nanoscale. Due to the vital phenomenon, these materials can be remotely directed to the target site without any modification related to the magnetic field.

Cation of polyethylenimine can easily interconnect with anions of the sugar-phosphate backbone of the nucleic acid and generate a very stable complex. The resultant phosphate offers a proton sponge effect to the nanoparticles, which allows the controllable release of nanoparticles from end lysosomes into the cytoplasm. SPIONs incorporated with polyethyleneimine have been used for gene transfection and DNA magnetoreception (Prijic et al. 2012). In the study of Prijic et al., they developed a nanomaterial composed of cytokine interleukin 12A–encoded plasmid DNA loaded in polyethyleneimine and acrylic acid-coated SPIONs (Prijic et al. 2012). The resultant nanomaterial effectively stimulated an immune response and sustained/delayed the tumor growth rate in murine mammary adenocarcinoma-transfected female BALB/c mice for 9 days in the present magnetic field.

However, free plasmid and gene electrotransfer can delay tumor growth for 7 days, which means gene magnetoreception is as effective as gene electrotransfer. The same author has designed the material using 3,4-dihydroxy-L-phenylalanine-conjugated, branched polyethyleneimine coated on SPIONs. The resultant SPION nanocluster exhibits superior magneto-responsive properties than separate magnetite materials and efficiently delivers siRNA into cancer cells (Draz et al. 2014).

Magnetic nanoparticles were also exploited to produce localized hyperthermia and remotely drug release from thermoresponsive and lipid nanomaterials (Huang et al. 2012; Katagiri et al. 2011).

For example, Ruiz-Hernandez et al. have designed the DNA strand as a gate-keeper, where DNA hybridization caused by altering the magnetic field induced hyperthermia, which can efficiently release loaded model compound fluorescein on demand from mesoporous silica nanoparticles (Fig. 9.5) (Ruiz-Hernández et al. 2011). Pluronic® F127 micelles (thermoresponsive material) were decorated with SPIONs, and ethosuximide was loaded on them; the resultant nanomaterial was stabilized by poly(vinyl acetate), which owned LCST of around 38 °C. In response to the magnetic field, these nanomaterials generate heat, irreversibly deform the structure, rupture the micelle-like structure, and remote the drug release (Huang

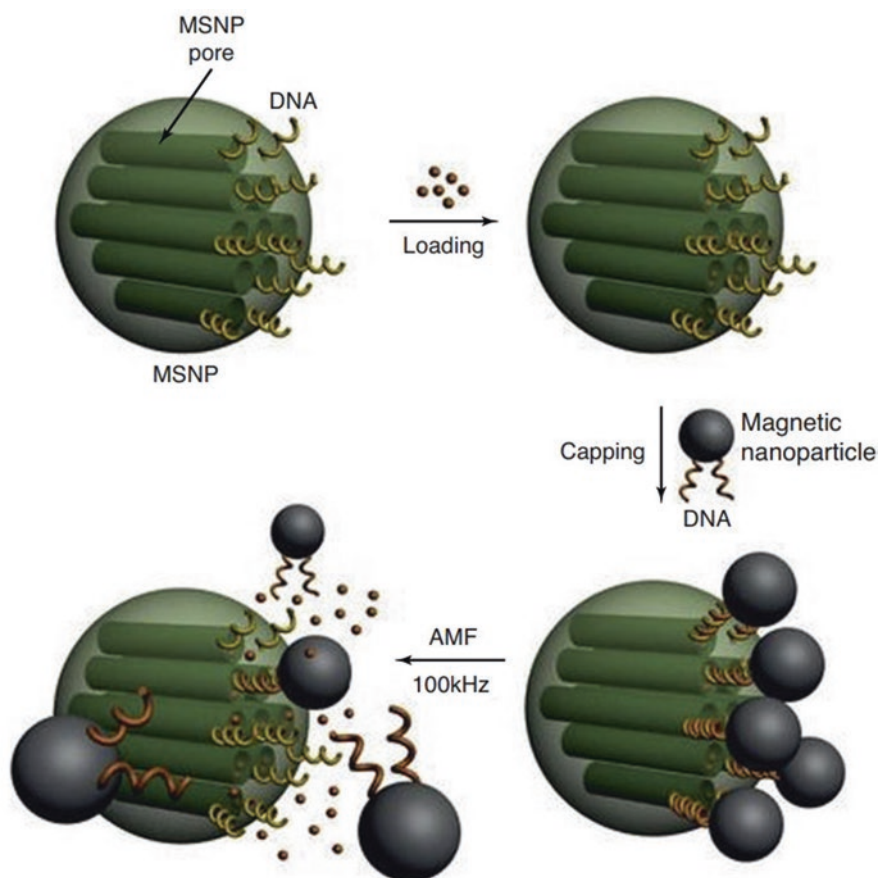


Fig. 9.5 Magnetic nanoparticles based on mesoporous silica nanoparticles modified with DNA worked as gatekeepers. On the exposure to a magnetic field, these hybrid nanoparticles generated hyperthermia through DNA dehybridization, pore opening, and on-demand drug release from the silica nanoparticles. (Mura et al. 2013)

et al. 2012). Katagiri et al. have designed the material composed of liposomes (thermo-responsive, LCST 35 °C) loaded with pyranine dye and iron oxide phosphatidylcholine, PEG-modified phosphatidylethanolamine, and a thermosensitive block copolymer of (2-ethoxy) ethoxy ethyl vinyl ether and octadecyl vinyl ether (Katagiri et al. 2011). However, the iron oxide-loaded nanoparticles released >80% of the dye *in vitro*. The resultant magnetic-responsive material released >95% of dye in response to the magnetic field, whereas liposomes release a negligible amount of dye for the nanomaterials.

Apart from drug delivery and gene therapy applications discussed above, SPIONs have been utilized to localize micelles at target tissues and induce drug release. For a similar purpose, Qin et al. encapsulated SPIONs in ferrogel-based Pluronic® F127 micelles, loaded with lipophilic drug indomethacin, to form injectable Ferro gets (Qin et al. 2009). This ferrogel efficiently works and releases the indomethacin where half-life decreased from 3195 to 1500 min *in vitro*. Jayant et al. have significantly investigated using SPIONs as core to produce layer-by-layer assembled magnetic nanoformulations. The developed smart nanomaterial has easily crossed an *in vitro* blood–brain barrier model in response to the magnetic field and released the loaded drugs for over 8 da.

9.2.3.2 Programming After Modification with Different Functional Groups

In order to achieve better results, magnetic-responsive materials have been modified with functional groups and compounds such as cell-targeting ligands and other stimuli-responsive materials like aptamers. Wang and coworkers have developed a material using conjugated A10 RNA aptamer bonded to the extracellular domain of the prostate-specific membrane antigen and crosslinked with SPIONs for prostate cancer therapy and imaging (Wang et al. 2008). In brief, RNA aptamer was encapsulated with doxorubicin. As SPIONs are nonconjugated, the aptamer-conjugated nanoparticles were uptake by prostate-specific-membrane antigen-expressing prostate cancer cells *in vitro*. However, the aptamer-conjugated nanoparticles were not uptake by non-prostate-specific membrane antigen-expressing prostate cancer cells.

Electroresponsive Nanomaterials

The innovative nanomaterials which can respond to the weak electric field are recognized as electro-responsive materials, which can be applied to control diagnostic and therapeutic effects (Yang et al. 2011). Electro-responsive nanomaterials are desirable materials that be synthesized easily. The electrical stimulus is quickly produced and remotely controllable without sophisticated instruments. Due to easy availability and low generation cost, electro-responsive nanocarriers are desirable drug delivery systems. Controllable drug release from electro-responsive nanomaterials can be easily monitored by chemical modification of electroconductive

materials and changing electric voltage, current, and exposure duration. The representative strategies for designing electro-responsive nanomaterials for desired therapeutic effects are discussed.

Programming Using Different Chemical Modification

Electro-responsive nanomaterials are composed of electroconductive materials such as montmorillonite, ferrocene, polypyrrole, multiwalled carbon nanotubes, polyelectrolytes, etc. (Samanta et al. 2016; Im et al. 2010). Samantha and coworkers successfully designed fluorescein-, piroxicam-, and insulin-loaded electro-responsive nanoparticles using polypyrrole (Samanta et al. 2016). The resultant nanomaterial efficiently released fluorescein from the nanoparticles in response to the electrical environments. The release was linearly increased when the applied current increased from 0 to $-300 \mu\text{A}$. However, the dye release from nanoparticles was increased by at least 50% in the presence of electrical current. In addition, these developed nanoparticles have improved the efficiency of releasing the drugs piroxicam and insulin from the nanoparticles in an electrical environment. Phenytoin sodium-loaded electro-responsive nanogels were developed by Ying et al. (2014); they used sodium 4-vinylbenzene sulfonate-based polyelectrolyte for the synthesis. The resultant nanogel (particle size) swelled from 102.3 to 388.0 nm when exposed to $500 \mu\text{A}$ for 1 min. However, phenytoin sodium release from the resultant nanogels was enhanced from 34.6% to 87.3% in response to the electrical current of $200 \mu\text{A}$ current for 4 hours. In other examples, Yan and coworkers (Yan et al. 2010) developed a reasonable electro-responsive nanomaterial composed of self-assembled micellar nanostructures (amphiphilic block copolymer comprising two end-functionalized polymers), PEG-ferrocene, and polystyrene- β -cyclodextrin (Fig. 9.6). The chemistry behind the synthesis and formation has been thoroughly discussed by Yan et al., they obtained micelle-like vesicles containing hydrophobic ferrocene on the hydrophilic end of the PEG to the β -cyclodextrin cavity of the hydrophobic styrene polymer. Interestingly, when the nanomaterial is exposed with an electric field, the ferrocene turns hydrophilic; moves from the β -cyclodextrin cavity, which results in reversible disassemble of the micelle-like vesicle; and efficiently releases rhodamine B (encapsulated model compound). However, rhodamine B release was controlled by electric voltage, and it takes 450 min to release the loaded compound +1 V. Noteworthy, without electric stimuli, more than 25% of the loaded dye was released within 600 min.

Epilepsy is an intelligent technique that has been used for recurrent, abrupt, and unpredicted seizures. Generally, the epileptic seizure has been recommended to overcome or reduce the side effects of prolonged treatment of high doses of drugs. Interestingly, electro-sensitive nanomaterials have been utilized in epilepsy treatments. In brief, the treatment “epileptic seizure” can act as an internal stimulus, which can effectively induce the demanded drug release from electro-responsive nanoparticles. In the study of Wang and coworkers, they designed an electro-responsive nanogel (phenytoin sodium-loaded nanogel), which was produced from

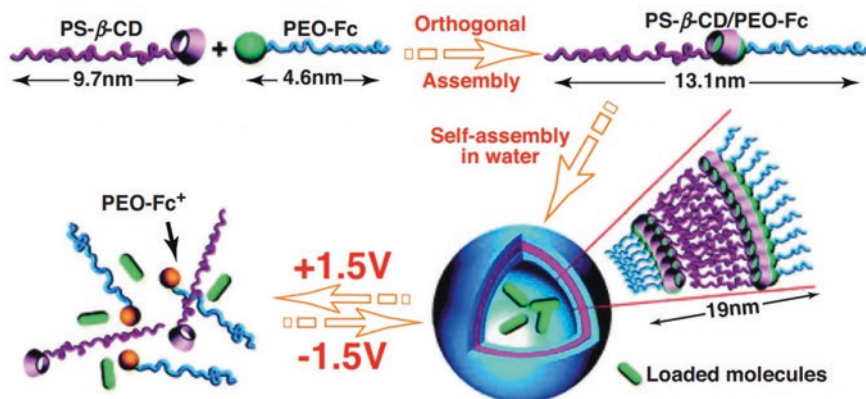


Fig. 9.6 A schematic representation of electro-responsive nanomaterials: it presents drug-loaded, micelle-like vesicles formed through self-assembly of an electro-responsive amphiphilic molecule, which was generated by the inclusion complexation of the hydrophobic ferrocene (Fs) group of the hydrophilic polyethylene oxide moiety (PEO-Fs) and a β -CD group of hydrophobic polystyrene moiety (PS- β -CD). On exposure to electric stimuli, the Fs became hydrophilic. They left the β -54 groups to disrupt the vesicle and release the loaded cargo on demand. (Reproduced, with permission, from Yan et al. 2010)

2-(dimethylamino)ethyl methacrylate, styrene, and electro-responsive monomer 4-vinylbenzene sulfonate with N,N' -methylenebisacrylamide (crosslinker) (Wang et al. 2016b). The resultant nanogel was found to be very efficient in pentylenetetrazole-induced epileptic seizures for rapid drug release when it was tested on rats.

Electroresponsive nanomaterials are extensively used as nanocarriers in the areas of transdermal drug delivery. The treatment “iontophoresis” (low voltages to enhance the penetration of charged compounds across the skin) has been recommended to enhance drug penetration from nanocarriers across the skin and sclera. Similarly, electroporation (relatively high transmembrane voltage to create the desired pores in cell membranes) has been recommended to enhance the permeability of drugs together with nanocarriers across biological membranes.

For instance, PEG-coated silica nanoparticles were developed by Kim et al. It was further modified with positively charged and negatively charged surface ions of 5-propyl sulfonyl oxyimino-5H-thiophene-2-ylidene-(2-methyl phenyl) acetonitrile and poly(4-methyl-2-pentyne), respectively (Kim and Lee 2011). The resultant nanoparticles were investigated as gene transporters after labeling fluorescent dye rhodamine B isothiocyanate, and the negatively charged pEGFP-N1 was loaded on the nanoparticles. When combined with electroporation, these negatively charged nanoparticles have improved gene transfection in HeLa cells. However, Wang et al. have seen the enhancement in permeability of antisense oligonucleotide-loaded transferrin-decorated liposomes across leukemia cells after electroporation (Wang et al. 2010).

Programming After Modification with Different Functional Groups

The efficiency of performance of electro-responsive material can be tuned by surface functionalization in drugs targeting the target tissue. In the study of Ying et al., the surfaces of phenytoin sodium-loaded electro-responsive nanogels were modified with brain-targeting angiopep-2 peptide (a ligand with low-density lipoprotein-receptor-related protein), the resultant material performed well and have significantly improved the blood–brain barrier penetration of the nanogels for the treatment of epilepsy (Ge et al. 2012). The programming efficiency of electro-responsive nanomaterials can be improved after combining electro stimuli nanoparticles with other stimuli systems. Ge and coworkers developed an injectable conductive hydrogel using daunorubicin-loaded polypyrrole nanoparticles in the thermoresponsive and biodegradable PLGA–PEG–PLGA polymer (Ying et al. 2014). The resultant hydrogel was injected into the dorsal sites of FVB mice to conduct the pulsatile drug release.

9.3 Concluding Remarks and Future Perspectives

Various strategies have been explored for programming the physical stimuli-responsive nanomaterials for the controllable release of drugs and targeting the infected site in the body in response to the physical stimuli (light, temperature, ultrasound, and magnetic and electric field). Many essential strategies have been recommended for programming nanomaterials and devices after their modification with multiple functionalities, such as chemical and physical. The related strategies have been discussed above (Ying et al. 2014); the chemical modification includes a change of nanomaterial surface modification with functionalities and surface targeting ligands (antibody, peptides, aptamers, etc.), change of nanomaterial architecture, surface properties, and parameters of the physical stimuli. No doubt, improvements in drug release efficiency have been observed with these modifications. However, the biomedical field always appeals to developing more advanced devices, programs, and treatments for effective drug delivery at the target site for fast and efficient recovery. Several research studies and academic documents have been found for effective drug delivery systems (Ying et al. 2014). Before the clinical practice, several significant obstacles related to biological barriers, side effects and related issues, clinical approvals, and government approvals must be overcome. In addition to these hurdles, a few other essential challenges must be overcome. These challenges include:

1. To limit the remote and uncontrolled cellular uptake of physical stimuli-responsive nanomaterials by nontarget tissues (Soni et al. 2016; Bobo et al. 2016). These uncontrolled cellular uptakes are mainly observed due to random adsorption of proteins on nanomaterial surfaces (forming a protein corona) in the biological milieu.

2. The limited and unclear studies related to the clearance of the nanotherapeutics from the treated body after or during recovery progress can be observed due to stimuli-responsive nanomaterials shared with conventional nanotherapeutics. In this case, nanotherapeutics should have sizes below the renal threshold and can be easily removed from the body via the kidneys. In the case of biodegradable nanomaterials, they can be easily removed from the body. However, their degraded fragments might be sequestered in lysosomal compartments to cause toxicity and side effects in the case of few biodegradable nanomaterials (Soni et al. 2016).
3. In the case of targeting, most of the targeting moieties are not specific to the targeting sites. The receptors for the targeting compounds can target the other organs together with the target sites.
4. Responsiveness or tolerances level of the human body for some physical stimuli. These physical stimuli might not be safer for or fully tolerated by the body. In brief, UV-responsive nanotherapeutics should not be used to treat mucosal surfaces of the human body, eyes, and skin (Yang et al. 2009); cavitation caused by ultrasound stimulus can create cavitation, which could enhance vessel permeability of cancer cells.
5. Due to the low tissue penetration efficiency of electrical stimuli, it can be responsible for tissue damage, which could restrict the use of electrical-responsive nanomaterials in clinical applications despite the nanoparticle flexibility and low cost. Magnetic field stimulus has been considered a high-cost device or therapy due to their complexity and necessity of specific arrangement for good focusing and deep penetration into disease sites with enough strength. In the case of temperature-sensitive nanomaterials, these systems need a longer duration and precise temperature control that results in uncontrolled drug release at the target site without causing tissue damage (Zardad et al. 2016).

Owing to the limitation, these restricted physical stimuli-responsive nanotherapeutics have been designed to a more advanced level for the advanced level of clinical studies. Hence, more advanced nanotherapeutics must be developed for the treated human body. In this regard, future advanced design improvement, more in vivo toxicology and efficacy evaluations, and more reliable techniques and mass-scale production studies on these nanomaterials are required.

References

- Hoare T, Young S, Lawlor MW, Kohane DS. Thermoresponsive nanogels for prolonged duration local anesthesia. *Acta Biomater.* 2012a;8(10):3596–605.
- Bhuchar N, Sunasee R, Ishihara K, Thundat T, Narain R. Degradable thermoresponsive nanogels for protein encapsulation and controlled release. *Bioconjug Chem.* 2012;23(1):75–83.
- Du J-Z, Sun T-M, Song W-J, Wu J, Wang J. A tumor-acidity-activated charge-conversional nanogel as an intelligent vehicle for promoted tumoral-cell uptake and drug delivery. *Angew Chem Int Ed.* 2010;49(21):3621–6.

- Gil ES, Wu L, Xu L, Lowe TL. β -Cyclodextrin-poly(β -amino ester) nanoparticles for sustained drug delivery across the blood-brain barrier. *Biomacromolecules*. 2012;13(11):3533–41.
- Müller RH, Mäder K, Gohla S. Solid lipid nanoparticles (SLN) for controlled drug delivery – a review of the state of the art. *Eur J Pharm Biopharm*. 2000;50(1):161–77.
- Hua M-Y, Liu H-L, Yang H-W, Chen P-Y, Tsai R-Y, Huang C-Y, Tseng IC, Lyu L-A, Ma C-C, Tang H-J, Yen T-C, Wei K-C. The effectiveness of a magnetic nanoparticle-based delivery system for BCNU in the treatment of gliomas. *Biomaterials*. 2011;32(2):516–27.
- Poß M, Tower RJ, Napp J, Appold LC, Lammers T, Alves F, Glüer C-C, Boretius S, Feldmann C. Multimodal [GdO]⁺[ICG]⁻ nanoparticles for optical, photoacoustic, and magnetic resonance imaging. *Chem Mater*. 2017;29(8):3547–54.
- Landon CD, Park JY, Needham D, Dewhirst MW. Nanoscale drug delivery and hyperthermia: the materials design and preclinical and clinical testing of low temperature-sensitive liposomes used in combination with mild hyperthermia in the treatment of local cancer. *Nanomed J*. 2011;3:38–64.
- Bulbake U, Doppalapudi S, Kommineni N, Khan W. Liposomal formulations in clinical use: an updated review. *Pharmaceutics*. 2017;9(2):12.
- Colombo M, Staufenbiel S, Rühl E, Bodmeier R. In situ determination of the saturation solubility of nanocrystals of poorly soluble drugs for dermal application. *Int J Pharm*. 2017;521(1):156–66.
- Xuan J, Boissière O, Zhao Y, Yan B, Tremblay L, Lacelle S, Xia H, Zhao Y. Ultrasound-responsive block copolymer micelles based on a new amplification mechanism. *Langmuir*. 2012;28(47):16463–8.
- Sahle FF, Metz H, Wohlrab J, Neubert RHH. Polyglycerol fatty acid ester surfactant-based microemulsions for targeted delivery of ceramide AP into the stratum corneum: formulation, characterisation, in vitro release and penetration investigation. *Eur J Pharm Biopharm*. 2012;82(1):139–50.
- Sahle FF, Giubudagian M, Bergueiro J, Lademann J, Calderón M. Dendritic polyglycerol and N-isopropylacrylamide based thermoresponsive nanogels as smart carriers for controlled delivery of drugs through the hair follicle. *Nanoscale*. 2017;9(1):172–82.
- Zhang W, Zhang Z, Zhang Y. The application of carbon nanotubes in target drug delivery systems for cancer therapies. *Nanoscale Res Lett*. 2011;6(1):555.
- Chen W, Ouyang J, Liu H, Chen M, Zeng K, Sheng J, Liu Z, Han Y, Wang L, Li J, Deng L, Liu Y-N, Guo S. Black phosphorus Nanosheet-based drug delivery system for synergistic photodynamic/photothermal/chemotherapy of cancer. *Adv Mater*. 2017;29(5):1603864.
- Zhang P, Ye J, Liu E, Sun L, Zhang J, Lee S-J, Gong J, He H, Yang VC. Aptamer-coded DNA nanoparticles for targeted doxorubicin delivery using pH-sensitive spacer. *Front Chem Sci Eng*. 2017a;11(4):529–36.
- Stejskalová A, Kiani MT, Almquist BD. Programmable biomaterials for dynamic and responsive drug delivery. *Exp Biol Med (Maywood)*. 2016;241(10):1127–37.
- Li J, Fan C, Pei H, Shi J, Huang Q. Smart drug delivery nanocarriers with self-assembled DNA nanostructures. *Adv Mater*. 2013;25(32):4386–96.
- Bukhari SNA. Emerging nanotherapeutic approaches to overcome drug resistance in cancers with update on clinical trials. *Pharmaceutics*. 2022;14(4):866.
- Rahikkala A, Aseyev V, Tenhu H, Kauppinen EI, Raula J. Thermoresponsive nanoparticles of self-assembled block copolymers as potential carriers for drug delivery and diagnostics. *Biomacromolecules*. 2015;16(9):2750–6.
- Lutz J-F, Akdemir Ö, Hoth A. Point by point comparison of two thermosensitive polymers exhibiting a similar LCST: is the age of poly(NIPAM) over? *J Am Chem Soc*. 2006;128(40):13046–7.
- Gandhi A, Paul A, Sen SO, Sen KK. Studies on thermoresponsive polymers: phase behaviour, drug delivery and biomedical applications. *Asian J Pharm Sci*. 2015;10(2):99–107.
- Rejinold NS, Chennazhi KP, Nair SV, Tamura H, Jayakumar R. Biodegradable and thermosensitive chitosan-g-poly(N-vinylcaprolactam) nanoparticles as a 5-fluorouracil carrier. *Carbohydr Polym*. 2011;83(2):776–86.

- Vihola H, Laukkanen A, Valtola L, Tenhu H, Hirvonen J. Cytotoxicity of thermosensitive polymers poly(N-isopropylacrylamide), poly(N-vinylcaprolactam) and amphiphilically modified poly(N-vinylcaprolactam). *Biomaterials*. 2005;26(16):3055–64.
- Diehl C, Schlaad H. Thermo-responsive polyoxazolines with widely tuneable LCST. *Macromol Biosci*. 2009;9(2):157–61.
- Kurzahls S, Gal N, Zirbs R, Reimhult E. Controlled aggregation and cell uptake of thermoresponsive polyoxazoline-grafted superparamagnetic iron oxide nanoparticles. *Nanoscale*. 2017;9(8):2793–805.
- Pánek J, Filippov SK, Hrubý M, Rabyk M, Bogomolova A, Kučka J, Štěpánek P. Thermoresponsive nanoparticles based on poly(2-alkyl-2-Oxazolines) and Pluronic F127. *Macromol Rapid Commun*. 2012;33(19):1683–9.
- Viegas TX, Bentley MD, Harris JM, Fang Z, Yoon K, Dizman B, Weimer R, Mero A, Pasut G, Veronese FM. Polyoxazoline: chemistry, properties, and applications in drug delivery. *Bioconjug Chem*. 2011;22(5):976–86.
- Ulbricht J, Jordan R, Luxenhofer R. On the biodegradability of polyethylene glycol, polypeptoids and poly(2-oxazoline)s. *Biomaterials*. 2014;35(17):4848–61.
- Mansfield EDH, Sillence K, Hole P, Williams AC, Khutoryanskiy VV. POZylation: a new approach to enhance nanoparticle diffusion through mucosal barriers. *Nanoscale*. 2015;7(32):13671–9.
- Wang N, Guan Y, Yang L, Jia L, Wei X, Liu H, Guo C. Magnetic nanoparticles (MNPs) covalently coated by PEO–PPO–PEO block copolymer for drug delivery. *J Colloid Interface Sci*. 2013;395:50–7.
- Chen S, Li Y, Guo C, Wang J, Ma J, Liang X, Yang L-R, Liu H-Z. Temperature-responsive magnetite/PEO–PPO–PEO block copolymer nanoparticles for controlled drug targeting delivery. *Langmuir*. 2007;23(25):12669–76.
- Tian Y, Bian S, Yang W. A redox-labile poly(oligo(ethylene glycol)methacrylate)-based nanogel with tunable thermosensitivity for drug delivery. *Polym Chem*. 2016;7(10):1913–21.
- Sicilia G, Grainger-Boulby C, Francini N, Magnusson JP, Saeed AO, Fernández-Trillo F, Spain SG, Alexander C. Programmable polymer-DNA hydrogels with dual input and multiscale responses. *Biomater Sci*. 2014;2(2):203–11.
- Bessa PC, Machado R, Nürnberger S, Dopler D, Banerjee A, Cunha AM, Rodríguez-Cabello JC, Redl H, van Griensven M, Reis RL, Casal M. Thermoresponsive self-assembled elastin-based nanoparticles for delivery of BMPs. *J Control Release*. 2010;142(3):312–8.
- Kowalczyk T, Hnatuszko-Konka K, Gerszberg A, Kononowicz AK. Elastin-like polypeptides as a promising family of genetically-engineered protein based polymers. *World J Microbiol Biotechnol*. 2014;30(8):2141–52.
- Kracke B, Cole JT, Kaiser CJO, Hellenkamp B, Krysiak S, Ghoorchian A, Braun GB, Holland NB, Hugel T. Thermoswitchable nanoparticles based on elastin-like polypeptides. *Macromolecules*. 2015;48(16):5868–77.
- Kim YS, Gultam M, Lowe TL. Thermoresponsive-co-biodegradable linear–dendritic nanoparticles for sustained release of nerve growth factor to promote neurite outgrowth. *Mol Pharm*. 2018;15(4):1467–75.
- Kim YS, Gil ES, Lowe TL. Synthesis and characterization of thermoresponsive-co-biodegradable linear–dendritic copolymers. *Macromolecules*. 2006;39(23):7805–11.
- Wang G, Nie Q, Zang C, Zhang B, Zhu Q, Luo G, Wang S. Self-assembled thermoresponsive Nanogels prepared by reverse micelle → positive micelle method for ophthalmic delivery of muscone, a poorly water-soluble drug. *J Pharm Sci*. 2016a;105(9):2752–9.
- Wu X, Ge W, Shao T, Wu W, Hou J, Cui L, Wang J, Zhang Z. Enhancing the oral bioavailability of biochanin A by encapsulation in mixed micelles containing Pluronic F127 and Pladone S630. *Int J Nanomedicine*. 2017;12:1475–83.
- Meng X, Liu J, Yu X, Li J, Lu X, Shen T. Pluronic F127 and D- α -tocopheryl polyethylene glycol succinate (TPGS) mixed micelles for targeting drug delivery across the blood brain barrier. *Sci Rep*. 2017;7(1):2964.

- Han H, Lee JY, Lu X. Thermoresponsive nanoparticles + plasmonic nanoparticles = photoresponsive heterodimers: facile synthesis and sunlight-induced reversible clustering. *Chem Commun.* 2013;49(55):6122–4.
- Kim D-H, Vitol EA, Liu J, Balasubramanian S, Gosztola DJ, Cohen EE, Novosad V, Rozhkova EA. Stimuli-responsive magnetic nanomicelles as multifunctional heat and cargo delivery vehicles. *Langmuir.* 2013;29(24):7425–32.
- Dicheva BM, ten Hagen TLM, Schipper D, Seynhaeve ALB, van Rhoon GC, Eggermont AMM, Koning GA. Targeted and heat-triggered doxorubicin delivery to tumors by dual targeted cationic thermosensitive liposomes. *J Control Release.* 2014;195:37–48.
- Sanyal S, Huang HC, Rege K, Dai LL. Thermo-responsive core-shell composite nanoparticles synthesized via one-step Pickering emulsion polymerization for controlled drug delivery. *J Nanomed Nanotechnol.* 2011;2:1–7.
- I. Yildiz, B. Sizirici Yildiz, Applications of thermoresponsive magnetic nanoparticles, *journal of nanomaterials* 2015 (2015).
- Dionigi C, Lungaro L, Goranov V, Riminucci A, Piñeiro-Redondo Y, Bañobre-López M, Rivas J, Dediu V. Smart magnetic poly(N-isopropylacrylamide) to control the release of bio-active molecules. *J Mater Sci Mater Med.* 2014;25(10):2365–71.
- Yassine O, Zaher A, Li EQ, Alfadhel A, Perez JE, Kavaldzhiev M, Contreras MF, Thoroddsen ST, Khashab NM, Kosel J. Highly efficient thermoresponsive nanocomposite for controlled release applications. *Sci Rep.* 2016;6(1):28539.
- Cunliffe D, C. de las Heras Alarcón, Peters V, Smith JR, Alexander C. Thermoresponsive surface-grafted poly(N-isopropylacrylamide) copolymers: effect of phase transitions on protein and bacterial attachment. *Langmuir.* 2003;19(7):2888–99.
- Nykänen A, Rahikkala A, Hirvonen S-P, Aseyev V, Tenhu H, Mezzenga R, Raula J, Kauppinen E, Ruokolainen J. Thermally sensitive block copolymer particles prepared via aerosol flow reactor method: morphological characterization and behavior in water. *Macromolecules.* 2012;45(20):8401–11.
- Schwarz M, Buehler A, Aguirre J, Ntziachristos V. Three-dimensional multispectral optoacoustic mesoscopy reveals melanin and blood oxygenation in human skin in vivo. *J Biophotonics.* 2016;9(1–2):55–60.
- Lin YJ, Huang CC, Wan WL, Chiang CH, Chang Y, Sung HW. Recent advances in CO(2) bubble-generating carrier systems for localized controlled release. *Biomaterials.* 2017;133:154–64.
- A. Rahikkala, Self-assembly of block and graft copolymers in DNA nanoparticles, (2015).
- Hoare T, Sivakumaran D, Stefanescu CF, Lawlor MW, Kohane DS. Nanogel scavengers for drugs: local anesthetic uptake by thermoresponsive nanogels. *Acta Biomater.* 2012b;8(4):1450–8.
- Liang X, Fan J, Zhao Y, Cheng M, Wang X, Jin R, Sun T. A targeted drug delivery system based on folic acid-functionalized upconversion luminescent nanoparticles. *J Biomater Appl.* 2017;31(9):1247–56.
- Huang X, Misra GP, Vaish A, Flanagan JM, Sutermeister B, Lowe TL. Novel nanogels with both thermoresponsive and hydrolytically degradable properties. *Macromolecules.* 2008;41(22):8339–45.
- Cubero E, Luque FJ, Orozco M. Theoretical study of the Hoogsteen–Watson-Crick Junctions in DNA. *Biophys J.* 2006;90(3):1000–8.
- Lanier LA, Bermudez H. DNA nanostructures: a shift from assembly to applications. *Curr Opin Chem Eng.* 2015;7:93–100.
- Samanta A, Medintz IL. Nanoparticles and DNA – a powerful and growing functional combination in bionanotechnology. *Nanoscale.* 2016;8(17):9037–95.
- Jiang X, Liu S, Narain R. Degradable thermoresponsive core cross-linked micelles: fabrication, surface functionalization, and biorecognition. *Langmuir.* 2009;25(23):13344–50.
- Aguirre G, Ramos J, Forcada J. Synthesis of new enzymatically degradable thermo-responsive nanogels. *Soft Matter.* 2013;9(1):261–70.
- Sahle FF, Gulfam M, Lowe TL. Design strategies for physical-stimuli-responsive programmable nanotherapeutics. *Drug Discov Today.* 2018;23(5):992–1006.

- Chen K-J, Liang H-F, Chen H-L, Wang Y, Cheng P-Y, Liu H-L, Xia Y, Sung H-W. A thermoresponsive bubble-generating liposomal system for triggering localized extracellular drug delivery. *ACS Nano*. 2013;7(1):438–46.
- Al-Ahmady ZS, Al-Jamal WT, Bossche JV, Bui TT, Drake AF, Mason AJ, Kostarelou K. Lipid-peptide vesicle nanoscale hybrids for triggered drug release by mild hyperthermia in vitro and in vivo. *ACS Nano*. 2012;6(10):9335–46.
- Zhou H, Gan X, Liu T, Yang Q, Li G. Electrochemical study of photovoltaic effect of nano titanium dioxide on hemoglobin. *Bioelectrochemistry*. 2006;69(1):34–40.
- Xiao Z, Ji C, Shi J, Pridgen EM, Frieder J, Wu J, Farokhzad OC. DNA self-assembly of targeted near-infrared-responsive gold nanoparticles for cancer thermo-chemotherapy. *Angew Chem Int Ed*. 2012;51(47):11853–7.
- Fomina N, Sankaranarayanan J, Almutairi A. Photochemical mechanisms of light-triggered release from nanocarriers. *Adv Drug Deliv Rev*. 2012;64(11):1005–20.
- Patnaik S, Sharma AK, Garg BS, Gandhi RP, Gupta KC. Photoregulation of drug release in azo-dextran nanogels. *Int J Pharm*. 2007;342(1):184–93.
- Zhao Y. Light-responsive block copolymer micelles. *Macromolecules*. 2012;45(9):3647–57.
- Zhang C, Zhang J, Shi G, Song H, Shi S, Zhang X, Huang P, Wang Z, Wang W, Wang C, Kong D, Li C. A light responsive nanoparticle-based delivery system using Pheophorbide a graft polyethylenimine for dendritic cell-based cancer immunotherapy. *Mol Pharm*. 2017b;14(5):1760–70.
- Azagarsamy MA, Alge DL, Radhakrishnan SJ, Tibbitt MW, Anseth KS. Photocontrolled nanoparticles for on-demand release of proteins. *Biomacromolecules*. 2012;13(8):2219–24.
- Huu VAN, Luo J, Zhu J, Zhu J, Patel S, Boone A, Mahmoud E, McFearin C, Olejniczak J, de Gracia Lux C, Lux J, Fomina N, Huynh M, Zhang K, Almutairi A. Light-responsive nanoparticle depot to control release of a small molecule angiogenesis inhibitor in the posterior segment of the eye. *J Control Release*. 2015;200:71–7.
- He D, He X, Wang K, Cao J, Zhao Y. A light-responsive reversible molecule-gated system using thymine-modified mesoporous silica nanoparticles. *Langmuir*. 2012;28(8):4003–8.
- Itoh H, Tahara A, Naka K, Chujo Y. Photochemical assembly of gold nanoparticles utilizing the photodimerization of thymine. *Langmuir*. 2004;20(5):1972–6.
- Wang T, Jiang H, Wan L, Zhao Q, Jiang T, Wang B, Wang S. Potential application of functional porous TiO₂ nanoparticles in light-controlled drug release and targeted drug delivery. *Acta Biomater*. 2015;13:354–63.
- Alibolandi M, Taghdisi SM, Ramezani P, Hosseini Shamili F, Farzad SA, Abnous K, Ramezani M. Smart AS1411-aptamer conjugated pegylated PAMAM dendrimer for the superior delivery of camptothecin to colon adenocarcinoma in vitro and in vivo. *Int J Pharm*. 2017;519(1):352–64.
- Karimi M, Ghasemi A, Sahandi Zangabad P, Rahighi R, Moosavi Basri SM, Mirshekari H, Amiri M, Shafaei Pishabad Z, Aslani A, Bozorgomid M, Ghosh D, Beyzavi A, Vaseghi A, Aref AR, Haghani L, Bahrami S, Hamblin MR. Smart micro/nanoparticles in stimulus-responsive drug/gene delivery systems. *Chem Soc Rev*. 2016;45(5):1457–501.
- You J, Zhang R, Xiong C, Zhong M, Melancon M, Gupta S, Nick AM, Sood AK, Li C. Effective photothermal chemotherapy using doxorubicin-loaded gold Nanospheres that target EphB4 receptors in Tumors. *Cancer Res*. 2012;72(18):4777–86.
- Chuang E-Y, Lin C-C, Chen K-J, Wan D-H, Lin K-J, Ho Y-C, Lin P-Y, Sung H-W. A FRET-guided, NIR-responsive bubble-generating liposomal system for in vivo targeted therapy with spatially and temporally precise controlled release. *Biomaterials*. 2016;93:48–59.
- Lee SM, Park H, Choi JW, Park YN, Yun CO, Yoo KH. Multifunctional nanoparticles for targeted chemophotothermal treatment of cancer cells. *Angew Chem Int Ed Engl*. 2011;50(33):7581–6.
- Sirsi SR, Borden MA. State-of-the-art materials for ultrasound-triggered drug delivery. *Adv Drug Deliv Rev*. 2014;72:3–14.
- Lee JY, Carugo D, Crake C, Owen J, de Saint Victor M, Seth A, Coussios C, Stride E. Nanoparticle-loaded protein-polymer nanodroplets for improved stability and conversion efficiency in ultrasound imaging and drug delivery. *Adv Mater*. 2015;27(37):5484–92.

- Yildirim T, Yildirim I, Yañez-Macias R, Stumpf S, Fritzsche C, Hoepfner S, Guerrero-Sanchez C, Schubert S, Schubert US. Dual pH and ultrasound responsive nanoparticles with pH triggered surface charge-conversional properties. *Polym Chem.* 2017;8(8):1328–40.
- Paris JL, Cabañas MV, Manzano M, Vallet-Regí M. Polymer-grafted mesoporous silica nanoparticles as ultrasound-responsive drug carriers. *ACS Nano.* 2015;9(11):11023–33.
- Jo H, Ban C. Aptamer–nanoparticle complexes as powerful diagnostic and therapeutic tools. *Exp Mol Med.* 2016;48(5):e230.
- Xie X, Lin W, Liu H, Deng J, Chen Y, Liu H, Fu X, Yang Y. Ultrasound-responsive nanobubbles contained with peptide–camptothecin conjugates for targeted drug delivery. *Drug Deliv.* 2016;23(8):2756–64.
- Xin Y, Qi Q, Mao Z, Zhan X. PLGA nanoparticles introduction into mitoxantrone-loaded ultrasound-responsive liposomes: in vitro and in vivo investigations. *Int J Pharm.* 2017;528(1):47–54.
- Zhao YZ, Du LN, Lu CT, Jin YG, Ge SP. Potential and problems in ultrasound-responsive drug delivery systems. *Int J Nanomedicine.* 2013;8:1621–33.
- Paris JL, de la Torre P, Victoria Cabañas M, Manzano M, Grau M, Flores AI, Vallet-Regí M. Vectorization of ultrasound-responsive nanoparticles in placental mesenchymal stem cells for cancer therapy. *Nanoscale.* 2017;9(17):5528–37.
- Wang CH, Kang ST, Lee YH, Luo YL, Huang YF, Yeh CK. Aptamer-conjugated and drug-loaded acoustic droplets for ultrasound theranosis. *Biomaterials.* 2012a;33(6):1939–47.
- Wang C-H, Kang S-T, Lee Y-H, Luo Y-L, Huang Y-F, Yeh C-K. Aptamer-conjugated and drug-loaded acoustic droplets for ultrasound theranosis. *Biomaterials.* 2012b;33(6):1939–47.
- Ishijima A, Minamihata K, Yamaguchi S, Yamahira S, Ichikawa R, Kobayashi E, Iijima M, Shibasaki Y, Azuma T, Nagamune T, Sakuma I. Selective intracellular vaporisation of antibody-conjugated phase-change nano-droplets in vitro. *Sci Rep.* 2017;7(1):44077.
- Yang HW, Hua MY, Liu HL, Huang CY, Tsai RY, Lu YJ, Chen JY, Tang HJ, Hsien HY, Chang YS, Yen TC, Chen PY, Wei KC. Self-protecting core-shell magnetic nanoparticles for targeted, traceable, long half-life delivery of BCNU to gliomas. *Biomaterials.* 2011;32(27):6523–32.
- McGill SL, Cuylear CL, Adolphi NL, Osinski M, Smyth HDC. Magnetically responsive nanoparticles for drug delivery applications using low magnetic field strengths. *IEEE Trans Nanobioscience.* 2009;8(1):33–42.
- Prijic S, Prosen L, Cemazar M, Scancar J, Romih R, Lavrencak J, Bregar VB, Coer A, Krzan M, Znidarsic A, Sersa G. Surface modified magnetic nanoparticles for immuno-gene therapy of murine mammary adenocarcinoma. *Biomaterials.* 2012;33(17):4379–91.
- Zhang F, Braun GB, Pallaoro A, Zhang Y, Shi Y, Cui D, Moskovits M, Zhao D, Stucky GD. Mesoporous multifunctional upconversion luminescent and magnetic “Nanorattle” materials for targeted chemotherapy. *Nano Lett.* 2012;12(1):61–7.
- Draz MS, Fang BA, Zhang P, Hu Z, Gu S, Weng KC, Gray JW, Chen FF. Nanoparticle-mediated systemic delivery of siRNA for treatment of cancers and viral infections. *Theranostics.* 2014;4(9):872–92.
- Huang H-Y, Hu S-H, Chian C-S, Chen S-Y, Lai H-Y, Chen Y-Y. Self-assembling PVA-F127 thermosensitive nanocarriers with highly sensitive magnetically-triggered drug release for epilepsy therapy in vivo. *J Mater Chem.* 2012;22(17):8566–73.
- Katagiri K, Imai Y, Koumoto K, Kaiden T, Kono K, Aoshima S. Magneto-responsive on-demand release of hybrid liposomes formed from Fe₃O₄ nanoparticles and thermosensitive block copolymers. *Small.* 2011;7(12):1683–9.
- Ruiz-Hernández E, Baeza A, Vallet-Regí M. Smart drug delivery through DNA/magnetic nanoparticle gates. *ACS Nano.* 2011;5(2):1259–66.
- Qin J, Asemphah I, Laurent S, Fornara A, Muller RN, Muhammed M. Injectable superparamagnetic ferrogels for controlled release of hydrophobic drugs. *Adv Mater.* 2009;21(13):1354–7.
- Mura S, Nicolas J, Couvreur P. Stimuli-responsive nanocarriers for drug delivery. *Nat Mater.* 2013;12(11):991–1003.
- Wang AZ, Bagalkot V, Vasilliou CC, Gu F, Alexis F, Zhang L, Shaikh M, Yuet K, Cima MJ, Langer R, Kantoff PW, Bander NH, Jon S, Farokhzad OC. Superparamagnetic iron oxide nanoparticle-

- aptamer bioconjugates for combined prostate cancer imaging and therapy. *ChemMedChem*. 2008;3(9):1311–5.
- Samanta D, Hosseini-Nassab N, Zare RN. Electroresponsive nanoparticles for drug delivery on demand. *Nanoscale*. 2016;8(17):9310–7.
- Im JS, Bai BC, Lee Y-S. The effect of carbon nanotubes on drug delivery in an electro-sensitive transdermal drug delivery system. *Biomaterials*. 2010;31(6):1414–9.
- Ying X, Wang Y, Liang J, Yue J, Xu C, Lu L, Xu Z, Gao J, Du Y, Chen Z. Angiopep-conjugated electro-responsive hydrogel nanoparticles: therapeutic potential for epilepsy. *Angew Chem Int Ed*. 2014;53(46):12436–40.
- Yan Q, Yuan J, Cai Z, Xin Y, Kang Y, Yin Y. Voltage-responsive vesicles based on orthogonal assembly of two homopolymers. *J Am Chem Soc*. 2010;132(27):9268–70.
- Wang Y, Ying X, Chen L, Liu Y, Wang Y, Liang J, Xu C, Guo Y, Wang S, Hu W, Du Y, Chen Z. Electroresponsive nanoparticles improve antiseizure effect of phenytoin in generalized tonic-clonic seizures. *Neurotherapeutics*. 2016b;13(3):603–13.
- Kim JA, Lee WG. Role of weakly polarized nanoparticles in electroporation. *Nanoscale*. 2011;3(4):1526–32.
- Wang S, Zhang X, Yu B, Lee RJ, Lee LJ. Targeted nanoparticles enhanced flow electroporation of antisense oligonucleotides in leukemia cells. *Biosens Bioelectron*. 2010;26(2):778–83.
- Ge J, Neofytou E, Cahill TJ, Beygui RE, Zare RN. Drug release from electric-field-responsive nanoparticles. *ACS Nano*. 2012;6(1):227–33.
- Soni KS, Desale SS, Bronich TK. Nanogels: an overview of properties, biomedical applications and obstacles to clinical translation. *J Control Release*. 2016;240:109–26.
- Bobo D, Robinson KJ, Islam J, Thurecht KJ, Corrie SR. Nanoparticle-based medicines: a review of FDA-approved materials and clinical trials to date. *Pharm Res*. 2016;33(10):2373–87.
- Yang J, Lee J, Kang J, Oh SJ, Ko H-J, Son J-H, Lee K, Suh J-S, Huh Y-M, Haam S. Smart drug-loaded polymer gold nanoshells for systemic and localized therapy of human epithelial cancer. *Adv Mater*. 2009;21(43):4339–42.
- Zardad A-Z, Choonara YE, Du Toit LC, Kumar P, Mabrouk M, Kondiah PPD, Pillay V. A review of thermo- and ultrasound-responsive polymeric systems for delivery of chemotherapeutic agents. *Polymers*. 2016;8(10):359.

Chapter 10

The Flexible and Wearable Pressure Sensing Microsystems for Medical Diagnostics



Hui Li, Ronghua Lan, Jing Chen, and Lin Li

10.1 Introduction

In recent years, with the advancement in science and technology, a great number of new applications have appeared in many domains. For instance, artificial intelligence (Shi et al. 2020a, b; Dong et al. 2020; Wang 2020) and smart electronics (Kaichen et al. 2019; Ding et al. 2019; Liang et al. 2020; Tao et al. 2017) have changed the world a lot and have improved the living conditions of human beings in many ways. Particularly in the healthcare monitoring field, it provides equipment foundation for cardiovascular disease and diabetes (Chung et al. 2019; Meng et al. 2019; Park et al. 2017; Yang et al. 2017; Schüssler-Fiorenza Rose et al. 2019). The life expectancy will increase since people's living conditions have improved. In the future, wearable electronic equipment will have a great market prospect. As one of the core components, sensor will affect the functional design and the development of wearable devices in the future. Flexible wearable electronics are often used in human-machine interaction interface (Tang et al. 2021), electronic skin (e-skin) (Zhang et al. 2019), wearable healthcare monitoring devices, etc. The flexible electronics can withstand compression, pulling, twisting, and distortion, compared with traditional rigid silicon-based electronics. In recent years, with the rapid development of new material synthesis and processing technology, it also provides the foundation for flexible pressure sensors. The flexible pressure sensors have become one of the most concerned electronic sensors because of their certain characteristics such as high sensitivity, low cost, low weight, portability, outstanding flexibility, high tensile strength, and high integration (Wan et al. 2017).

H. Li (✉) · R. Lan · J. Chen · L. Li
Shenzhen Institute of Advanced Technology, Chinese Academy of Sciences, Shenzhen, China
e-mail: hui.li1@siat.ac.cn

Wearable sensors which are used in medical detection can play an important role in people's daily life. It is well-known that the surface of the human skin is irregular and complex. With the advantages of fast response, portability, and wearability, the flexible pressure sensor has a great potential in continuous vital sign monitoring. Traditional centralized healthcare services require patients to travel to hospitals, which means that the patients' needs may not be addressed in time, especially for individuals who require emergency treatment. Flexible sensing electronics will transform traditional diagnostic methods, by giving a portable, wearable, real-time characteristic for medical diagnosis. Moreover, flexible sensors can measure physiological abnormalities in real time for early detection, which could provide a safer and more comfortable way to protect human health. Flexible pressure sensors can be attached to the human body to capture different physiological parameters such as blood pressure (Wang et al. 2017), heart rate (Shin et al. 2016), breath detection (Ghosh et al. 2021), and pulse rate (Kim et al. 2019a). Various internal pressures such as intracranial pressure (Wang et al. 2019a) and intraocular pressure (Zou et al. 2019) are important health indicators and can also be measured by flexible pressure sensors (Shin et al. 2019). In addition, some new wearable devices, for instance, gait analysis (Song et al. 2018), tactile perception (Xiong et al. 2020), and voice recognition (Wang et al. 2019b), are widely used in medical diagnostics. Figure 10.1 shows some flexible pressure sensors with the above applications.

In the last few years, by attaching sensors to a patient's arm, leg, or other organs for continuous monitoring, wearable pressure sensors have become a popular medical aid. Especially for elderly patients with low physical strength and immunity, the pressure sensor can respond quickly in emergency situations. Based on the feedback of pressure sensor, we can know our body's state in real time and make adjustments to let our lives become healthier. Therefore, research on flexible pressure sensors used in medical diagnostic is meaningful for the development of sensor technology. We summarize in this review the latest development of flexible pressure sensors for medical healthcare applications. In Sect. 10.2, we introduce the commonly used materials in fabrication. In Sect. 10.3, we review the transduction mechanisms of sensor and analyzed the property of the pressure sensor, for instance, sensitivity, power consumption, and linearity. In Sect. 10.4, we mainly focus on the recent progress in medical diagnostics applications. Conclusion and future perspectives are described in the final section.

10.2 Materials

The difference between a flexible sensor and a traditional sensor is that it has a certain degree of plasticity on the basis of realizing the function of the traditional sensor to adapt to irregular surfaces and can withstand deformations, such as contraction, extrusion, bending, and torsion. The materials commonly used in traditional sensors are silicon semiconductor materials (Jayathilaka et al. 2019; Jeon et al. 2019; Li et al. 2020a), metal oxides, and other rigid materials (Jayathilaka et al. 2019; Yang

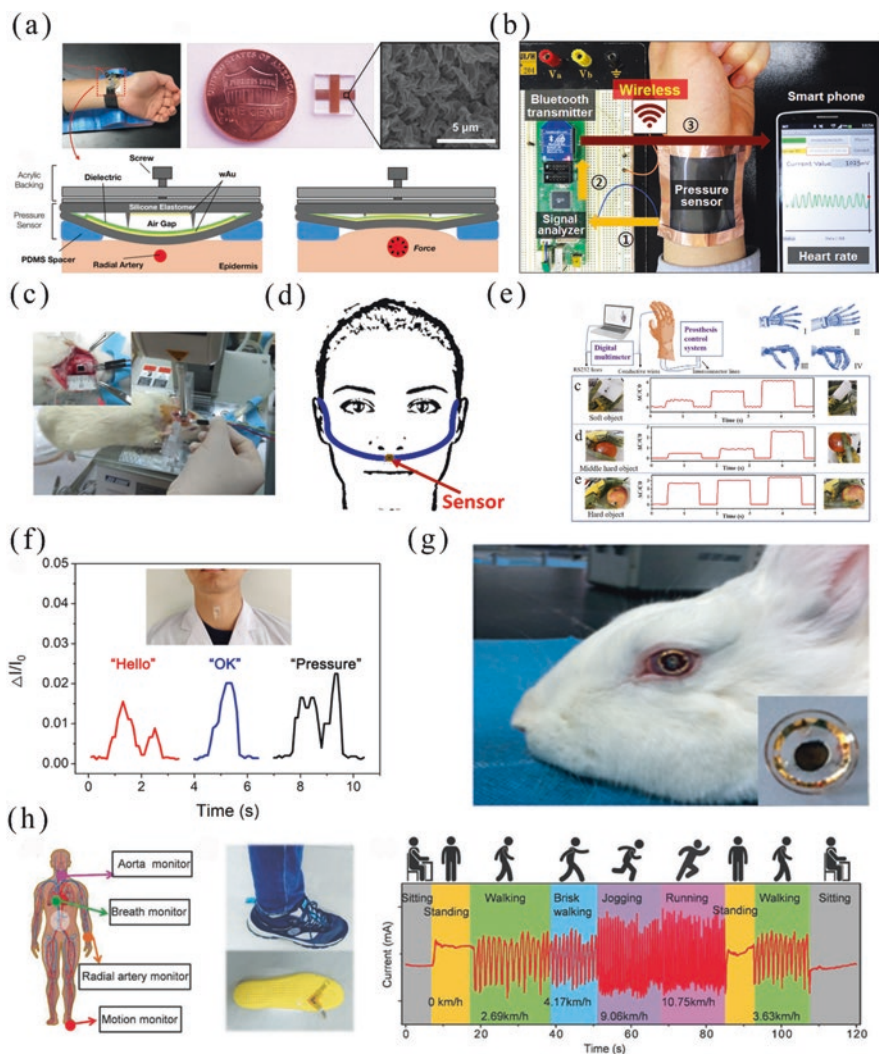


Fig. 10.1 (a) Image of how the pressure sensor is attached to the wrist. Photograph image of the parallel wAu electrodes (Kim et al. 2019a). (b) Photograph of wearable and wireless pressure sensor for heart rate monitoring (Shin et al. 2016). (c) Real-time photograph of intracranial surgery of a rat with the fabricated PEDOT:PSS/GO pressure sensor. R–P curve of the fabricated pressure sensor on the rat’s brain surface without creating any major damage (Wang et al. 2019a). (d) Schematic of breath detection, indicating the sensor’s placement on the philtrum (Ghosh et al. 2021). (e) Real-time monitoring of robotic hand grabbing objects (Xiong et al. 2020). (f) Relative current change of Ti₃C₂/NMC flexible sensor in terms of various sound stimuli, such as “hello,” “Ok,” and “pressure” (Wang et al. 2019b). (g) Intraocular biosensor made from GC–COOH worn on a rabbit’s cornea. The inset shows the working side of the intraocular biosensor (Zou et al. 2019). (h) Schematic illustration of the pressure sensor for monitoring human vital signs, and real-time recording of the whole motion process, including sitting, standing, walking, brisk walking, jogging, and running (Song et al. 2018)

et al. 2019). These materials have poor plasticity, which is likely to cause irreversible damage during the application process if used in large deformation scene or irregular object surface. For the sensor, to endow deformable properties, flexible materials are required. After years of research, people have made outstanding achievements in the field of flexible sensors and have a relatively complete understanding of flexible sensors. In order to create a flexible wearable sensor with good sensing capabilities, the option of appropriate material is very vital. Here, we summarized some of the most commonly used functional materials, for instance, substrate materials and active materials.

10.2.1 Substrate Materials

The substrate material constitutes the base part of the flexible sensor, and the deformability of the flexible sensor is mainly determined by it. To meet the deformability requirements of a flexible sensor, the substrate material needs to have the characteristics of high flexibility and high ductility. In some special cases, the substrate material is also required to have other characteristics, such as water resistance, heat resistance, and biocompatibility, to allow the sensor to work normally under severe conditions. Many commercially available polymers and elastomers including polydimethylsiloxane (PDMS), polyimide (PI), polyethylene (PEN), polyethylene terephthalate (PET), and polyurethane (PU) can serve as substrates for flexible and stretchable electronics (Li et al. 2020a; Tan et al. 2022). PDMS, a product widely used in the market, is a silicon rubber with a low Young's modulus that can be prepared with readily accessible laboratory techniques (YuHao and JunPing 2022; Kang et al. 2021). The intrinsic flexibility and extensibility of PDMS make corresponding devices respond readily to torsion and compressive and tensile strain (Li et al. 2017a, 2019a; Wang et al. 2019c; Gong et al. 2021; Shi et al. 2018). Furthermore, the extensibility of PDMS can be improved by geometric structuring such as the formation of nets and bucking structures to meet the requirements of applications for coplanar devices (Mao et al. 2019). It should also be noted that PDMS possesses many other advantages such as high transparency and excellent stability over a large temperature range. These advantages broaden its applicability as a large-area substrate for transparent electronics and thermally stable devices (Rajitha and Dash 2018; Hwang et al. 2021; Mengdi et al. 2018).

PI has excellent stability, insulating property, and mechanical performance. This material can sustain a large temperature range, from -100 to 300 °C, without obvious property changes (Xiaohe et al. 2020; Xiaoyu Chen et al. 2019). It is also invulnerable to corrosion by commonly used chemical solvents, which is vital in the subsequent device process steps. Furthermore, even ultrathin PI films are not damaged by high mechanical forces, and its excellent bending stability makes it a suitable candidate for compliant devices (Kwak et al. 2017; Liu et al. 2020). A very thin catheter was thus prepared for measuring the spatial distribution of pressure,

demonstrating its potential application in medical diagnosis (Cui et al. 2019; Fan et al. 2019; Bi et al. 2019).

PET has a good mechanical property, excellent tensile strength and creep resistance, good electrical insulation performance, and little influence by temperature. PEN's excellent performance is mainly reflected in its relatively high heat resistance, with a glass transition temperature of 113 °C, higher than PET which is 65 °C. The physical and mechanical properties of PEN are also better than PET, and it can be widely used in fabrication of sensors. For instance, an ultralightweight plastic electronic device (3 g cm^{-2}) has been produced with an ultrathin PEN foil 1 μm thick that can withstand repeated bending to a 5 mm radius and paperlike crumpling (Rui et al. 2019; Zhao et al. 2017; Lin et al. 2019; Yuan et al. 2017; Lamanna et al. 2019; Lee et al. 2019; Wang et al. 2018a). By combining pressure-sensitive rubbers with organic field-effect transistors (OFETs) on a PEN substrate, pressure-sensing matrices have been produced and demonstrated their encouraging potentials in e-skin (Shuaidi Zhang et al. 2019; Gao et al. 2019a, 2020; Cai et al. 2017; Seyedin et al. 2020; Ma et al. 2018).

10.2.2 Active Materials

The active material is the core part of the flexible sensor. Its physical properties change under the action of pressure, usually involving changes in the resistance, piezoelectricity and capacitance. It achieves the function of converting pressure signals into electrical signals on this basis. Commonly used active materials for making flexible sensors include carbon nanotubes (CNTs), which have well-charge carrier mobility, steady chemical property, and excellent elasticity. For example, benefiting from these material properties, as shown in Fig. 10.2a, Qin et al. presented a pressure sensor by integrating hydrophobic CNTs into hydrophobically associated polyacrylamide hydrogel and exhibited high linear sensitivity (0.127 kPa^{-1}) in a large-pressure region within 0–50 kPa (Qin et al. 2020). Graphene (GR) has lots of carrier mobility, good mechanical performance, great light transmittance, chemical stability, thermal conductivity, and low-cost mass-production potential (Xiaoyu Chen et al. 2019; He et al. 2019a; Cai et al. 2018; Li et al. 2018, 2021). Based on its good electrical conductivity, intrinsic and structural flexibility, high chemical and thermal stability, etc., He et al. presented and developed a novel material design strategy to fabricate a self-assembled graphene sensing film, in which the conductivity and thickness can be well balanced (Fig. 10.2c). The sensor showed high sensitivity (1875.53 kPa^{-1}) and wide linear detection range (0–40 kPa) (He et al. 2019b). Metal materials and their nanowires, such as silver nanowires (AgNWs) and gold films, have excellent conductivity, light transmittance, flexibility, and stability. Chu et al. reported a sensing system based on a fluorinated ethylene propylene (FEP)/Ecoflex/FEP/Au sandwich-structured piezoelectret for piezoelectric-like detections and showed high precision and stability (Fig. 10.2b) (Chu et al. 2018). As shown in Fig. 10.2e, the pressure sensor was based on Au/

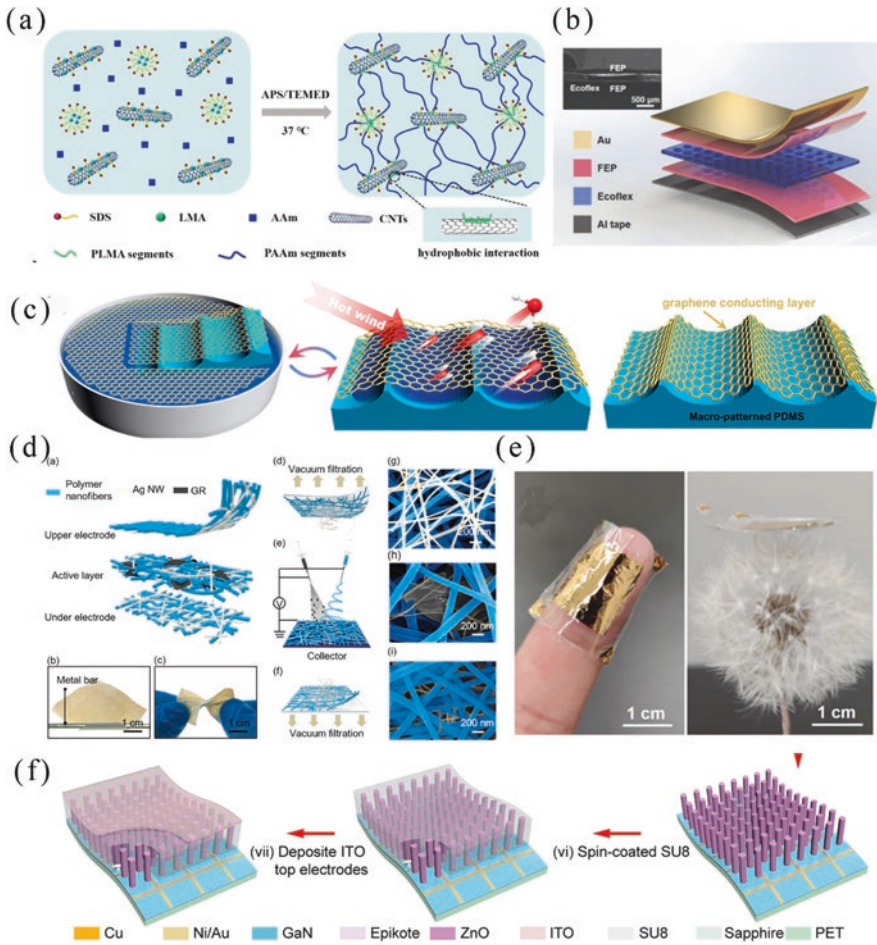


Fig. 10.2 (a) Schematic illustration of the preparation process for the CNTs/HAPAAm hydrogel (Qin et al. 2020). (b) Schematic diagram of the pulse sensing device using the FEP/Ecoflex/FEP sandwich-structured piezoelectric film (Chu et al. 2018). (c) Schematic of the fabrication process of PDMS-Gr (He et al. 2019b). (d) Structure and fabrication process of the AgNWs/GR/PANF pressure sensor (Li et al. 2020b). (e) Photo of a sensor surrounding a finger depicting its super flexibility, and photo illustrating the super lightness of the sensor (Zhong et al. 2022). (f) Schematic diagram of the device fabrication consisting of GaN LLO process and the synthesis of ZnO nanowire array (Peng et al. 2019)

parylene/Teflon AF films, and a sensor surrounding a finger depicting its super flexibility (Zhong et al. 2022). Li et al. presented a piezoresistive sensor based on hierarchical nanonetwork structured pressure sensitive material, including AgNWs, GR, and polyamide nanofibers (PANFs), and showed the sensitivity of 134 kPa^{-1} (0–1.5 kPa) (Fig. 10.2d) (Li et al. 2020b). And common piezoelectric materials such as ZnO have excellent optical properties, good reliability, and excellent stability and are environment friendly. Based on its properties, Peng et al. presented a pressure

sensor, composed of a GaN/ZnO nanowire heterostructure light-emitting diode (LED), which can be enhanced by the local compressive strain based on piezophototronic effect (Fig. 10.2f) (Peng et al. 2019). Active materials with excellent performance are the most important component for the stable and accurate operation of sensors. Developing better materials and optimizing the performance of active materials is the key to our research on flexible sensors.

10.3 Fundamentals of Pressure Sensors

Firstly, in order to better understand the overall sensing equipment, we first outlined the basic principles of pressure sensors here. Next, we will discuss the conduction mechanism and key parameters of the pressure sensor in detail.

10.3.1 Sensing Mechanisms

When a force is applied to a sensor, the physical properties of the sensor can change. Changes in different physical properties correspond to different working principles of the sensor. According to the sensing principle, sensors can be classified into the following categories: piezoresistive, capacitive, piezoelectric, and triboelectric. Different working principles also have different working characteristics and structural characteristics. Here, a brief introduction and schematic illustrations of four typical transduction mechanisms are provided.

10.3.1.1 Piezoresistivity

A piezoresistive sensor exhibits resistance changes under pressure. A piezoresistive sensor has the characteristics of high sensitivity, big measurement range, long lifetime, simple construction, and easy manufacturing and realization of subminiaturization and integration, but the resistance is easily affected by the environment, especially temperature, and this nonlinear error under large strain is obvious. It is not suitable for working in temperature-unstable environment. The resistance of a piezoresistive pressure sensor is usually determined by its material, shape, temperature, and other elements. The resistivity is usually determined by the material of the resistor. It is also affected by temperature. We can change the resistance by changing the resistance length or the cross-sectional area. As shown in Fig. 10.3a, Yang et al. designed a hierarchically microstructure-bioinspired flexible piezoresistive sensor consisting of a hierarchical polyaniline/polyvinylidene fluoride nanofiber (HPPNF) film sandwiched between two interlocking electrodes with microdome structure. The sensor exhibited an ultrahigh sensitivity of 53 kPa^{-1} , a pressure detection range from 58.4 to 960 Pa, and excellent cycle stability over 50,000 cycles (Yang et al. 2021).

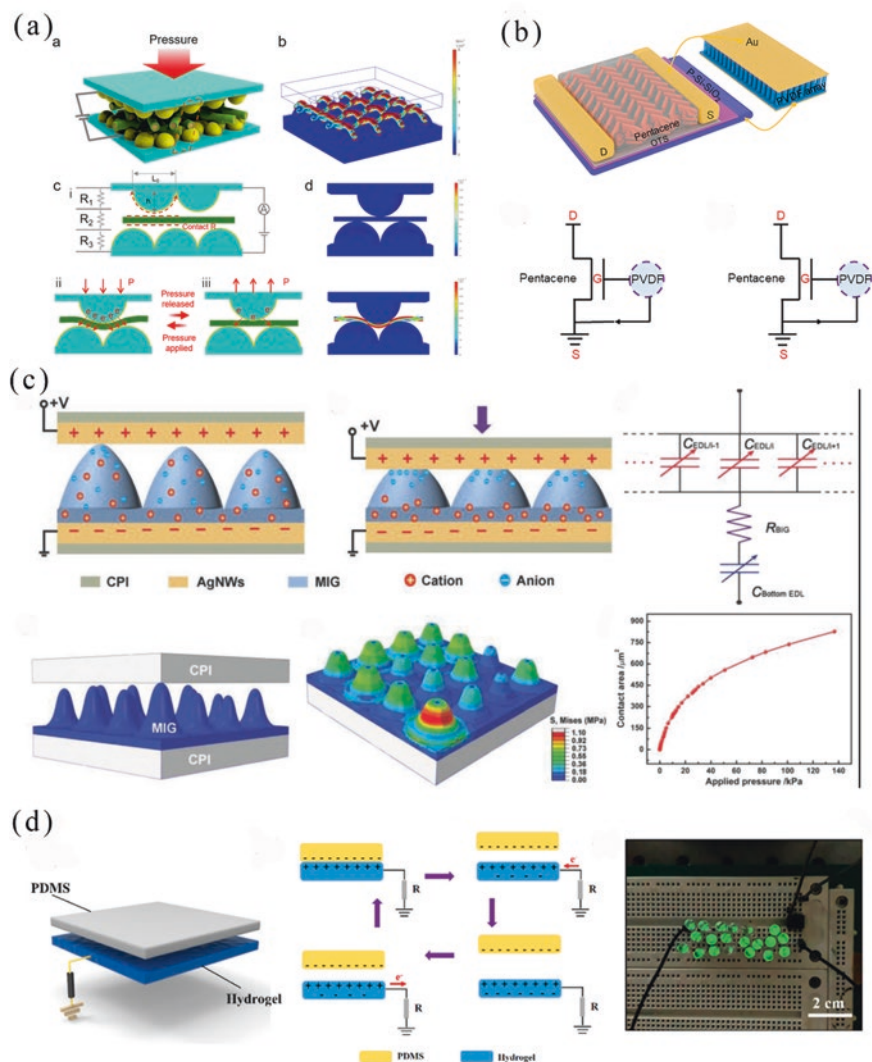


Fig. 10.3 (a) Schematic of flexible piezoresistive sensor under the normal pressure. And simulation results of the stress distribution of the flexible sensor under an applied pressure using the COMSOL software (Yang et al. 2021). (b) Working mechanism of the pentacene piezoelectric transistor (Wang et al. 2020). (c) Graphical explanation of the sandwiched structure and charge distribution in the capacitive sensor (Qiu et al. 2018). (d) Working principle of the triboelectric nanogenerators (He et al. 2020)

10.3.1.2 Capacitance

Capacitive sensors can convert perceived pressure changes into changes in capacitance, and changes in capacitance can also directly cause changes in electrical signals. A capacitive sensor has the performance of a simple structure, high sensitivity, less temperature effect, low power dissipation, and short dynamic response time. It can work under high-frequency conditions and is especially suitable for dynamic measurement. However, the capacitive sensor is highly susceptible to parasitic influence and electromagnetic interference. Therefore, it is not suitable for working in strong electric and magnetic fields. The definition formula of the capacitance is $C = \epsilon S / 4\pi kd$, where ϵ is the relative permittivity, k is the electrostatic force constant, S is the overlapping area of the two panels, and d is the distance between the two panels. The capacitance is mainly affected by the area of the plates, the distance between the plates, and the insulating medium between the two plates. The change of the distance between the plates and the material composition will lead to the increase or decrease of capacitance value. We can also detect shear stress by changing the overlap area of the capacitor plates. As shown in Fig. 10.3c, Qiu et al. presented a low-cost microstructured ionic gel (MIG) with uniform cone-like surface microstructures for high-performance capacitive e-skins. The device exhibited a low limit of detection down to 0.1 Pa, a ultrahigh sensitivity of 54.31 kPa⁻¹ in the low-pressure regime (<0.5 kPa), and a sensitivity that is kept larger than 1 kPa⁻¹ over a broad-range pressure from 0.1 Pa to 115 kPa (Qiu et al. 2018).

10.3.1.3 Piezoelectricity

The physical basis of a piezoelectric sensor is the piezoelectric effect. The piezoelectric effect refers to some dielectric being deformed by the action of an external force along a certain direction, and a polarization phenomenon will occur inside it. Opposite positive and negative charges appear on its opposite surfaces at the same time. As the outer force is removed, the dielectric will return to an uncharged state. The commonly used piezoelectric materials include the following: ZnS, ZnO, and CaS with semiconductive and piezoelectric properties, as well as polyvinyl fluoride, nylon, polyvinylidene fluoride (PVDF), etc. The advantage of a piezoelectric pressure sensor is that it has a self-generated signal, large output signal, high-frequency response, and small size. The disadvantage is that it can only be used for dynamic measurement, and because the amount of charge of the piezoelectric material is fixed, special attention should be given to avoiding leakage when connecting it. In addition, when it is subjected to sudden vibrations or excessive pressure, self-recovery is slower. As shown in Fig. 10.3b, Wang et al. constructed a high-performance, energy-efficient, and fully flexible piezoelectric tactile sensor based on piezoelectric effect. The sensor exhibited excellent pressure sensitivity, detection limit, and response time of 5.17 kPa⁻¹, 175 Pa, and 150 ms, respectively (Wang et al. 2020).

10.3.1.4 Triboelectricity

The operating principle of a TES (triboelectric sensor) is the triboelectric effect. After two different objects are rubbed together, electrons are transferred from one object to the other such that the two different objects are charged. The polarity and strength of the charge generated in the process vary depending on the material, surface roughness, temperature, and other elements. Triboelectric sensors are usually made of two different materials. Selecting suitable materials and increasing the contact area between the two films are effective methods for enhancing the performance of flexible TES. Piezoelectric sensors and TES have self-powered characteristics, which provide a basis for the development of self-powered sensor system. But the output of the TES usually contains noncontinuous pulses with irregular magnitude. On the other hand, the relatively high voltage output and low current output greatly hinder the TES for practical applications. So, it is targeted to harvest “random” and possibly low-frequency mechanical signals. He et al. presented a pressure sensor, designed by proportionally mixing silk fibroin, polyacrylamide, graphene oxide, and poly(3,4-ethylenedioxythiophene)/poly(styrenesulfonate). The assembled sensor exhibited a wide sensing range (strain, 2–600%; pressure, 0.5–119.4 kPa) and reliable stability (Fig. 10.3d) (He et al. 2020).

10.3.2 Key Parameters of Pressure Sensor

Pressure sensors can convert the applied force into an electrical signal or other signal output. To estimate the property of pressure sensors, we need to evaluate key parameters such as the sensitivity, detection limit, response time, and durability.

10.3.2.1 Sensitivity

Sensitivity, which is commonly defined as the magnitude of electrical response upon pressure stimuli, is the most important parameter that can determine the measuring effect and accuracy of the pressure sensor. In general, the pressure sensor sensitivity is defined as $S = dX/dP$, where S represents the sensitivity, X represents the quantitative output signals, and P is the imposed external pressure. Various strategies have been reported to enhance the sensitivity of pressure sensors. Herein, we presented two typical optimization ways, which may be useful for the design and production of highly sensitive pressure sensors.

We may improve the sensitivity of sensors by choosing better active materials. In the above, we briefly introduced some common active materials used for fabrication of sensors; herein, we will further introduce the effect of these active materials for sensor's sensitivity. For example, as for the piezoresistive pressure sensors, Gao et al. used silver nanowires (AgNWs) as active material and a nanocellulose paper (NCP) as a bottom substrate, which showed a high sensitivity of 1.5 kPa^{-1} in the

range of 0.03–30.2 kPa and retained excellent performance in the bending state (Gao et al. 2019b). As for the capacitive pressure sensors, Li et al. reported a novel capacitive flexible pressure sensor by using silver nanowire (AgNWs)-paper substrates as electrodes and polydimethylsiloxane (PDMS) as dielectrics, which showed dynamic ranges of the as-prepared sensor of 1.05 kPa^{-1} and 1 Pa to 2 kPa, respectively (Li et al. 2019a). As for the piezoelectric pressure sensor, Chen et al. reported a pressure sensor for static measurements and nanowires/graphene as active materials, based on the synergistic mechanisms between strain-induced polarization charges in piezoelectric nanowires and the caused change of carrier scattering in graphene. Compared to the conventional piezoelectric nanowire or graphene pressure sensors, this sensor is capable of measuring static pressures with a sensitivity up to $9.4 \times 10^{-3} \text{ kPa}^{-1}$ (Chen et al. 2017). As for the triboelectric pressure sensor, Ning et al. reported a pressure sensor by using AgNWs/CNT as active materials and PDMS as the substrate materials, which can reach 3.627 kPa^{-1} in the pressure range of 0–8 kPa and still keep 1.264 kPa^{-1} in the range of 8–80 kPa (Ning et al. 2020).

Another approach to realize high sensitivity relies on the utilization of micro- and nanostructures such as multilevel structure (Tang et al. 2019), pyramid structure (Li et al. 2020c), patterned structure (Shi et al. 2018), porous structures (Mahanty et al. 2017), and microdome structure (Park et al. 2018a). For example, Tang et al. reported a pressure sensor by combining a sandpaper-molded multilevel microstructured PDMS and a reduced oxide graphene film, which showed an ultrahigh sensitivity ($2.5\text{--}1051 \text{ kPa}^{-1}$) (Tang et al. 2019). Li et al. reported a sensor by adding elastic pyramidal microstructures on one side of the electrode, and the sensitivity of the proposed device has been improved from 3.1 to 70.6 kPa^{-1} compared to no microstructure of sensor (Li et al. 2020c). Shi et al. fabricated a flexible transparent capacitive pressure sensor based on patterned microstructured silver nanowires (AgNWs)/polydimethylsiloxane (PDMS) composite dielectrics. Compared with the pure PDMS dielectric layer with planar structures, the patterned microstructured sensor exhibits a higher sensitivity (0.831 kPa^{-1} , $<0.5 \text{ kPa}$) (Shi et al. 2018). Hwang et al. reported a capacitive pressure sensor using hierarchically porous structured PDMS composites, which exhibited a sensitivity 22.5 times higher (0.18 kPa^{-1}) than the sensors using bulk PDMS (Hwang et al. 2021). Park et al. reported a pressure sensor using microdome structure in fabricating sensor, which exhibited extremely high pressure sensitivities over broad pressure ranges ($47,062 \text{ kPa}^{-1}$ in the range of $<1 \text{ kPa}$, $90,657 \text{ kPa}^{-1}$ in the range of 1–10 kPa, and $30,214 \text{ kPa}^{-1}$ in the range of 10–26 kPa) (Park et al. 2018a).

10.3.2.2 Power Consumption

The power consumption of flexible pressure sensors is a significant obstacle for practical integrated sensing systems. Various strategies have been demonstrated to reduce the power consumption of flexible sensors.

The first approach relies on the reduction of both operating voltage and operating current of the sensor (Jiang et al. 2019a). For example, Ai et al. demonstrated a flexible resistive pressure sensor based on polystyrene ball@reduced graphene-oxide (PS ball@rGO) core-shell microball composite materials (Ai et al. 2018). The PS ball@rGO-based wearable pressure sensors exhibit a high sensitivity of 50.9 kPa^{-1} at 3–1000 Pa with a low power consumption of 1 mW at an operating voltage of 1 V. Zhu and co-workers designed a novel flexible resistive pressure sensor by conformal coating of vertically aligned gold nanowires (v-AuNWs) on pyramid microarrays on PDMS elastomer (Zhu et al. 2019). The hierarchical structured pressure sensor can achieve a high sensitivity of 23 kPa^{-1} in a low regime (<600 Pa) and a rapid response time (<10 ms). Furthermore, owing to the high conductivity of v-AuNWs, the operation voltage of the pressure sensor was only 0.1 V, and the current during operation was less than 2 mA, resulting in a low power consumption below 0.2 mW.

Another approach to resolve the power consumption issues for the sensing unit is the fabrication of self-powered pressure sensors. Therefore, piezoelectric and triboelectric pressure sensors have attracted increasing attention in recent years (Yang et al. 2020; Li et al. 2017b). Hosseini et al. fabricated a flexible piezoelectric pressure sensor based on biodegradable glycine and chitosan piezoelectric films (Hosseini et al. 2020). The β -glycine/chitosan (β -Gly/CS)-based pressure sensor could produce an output voltage of 190 mV under 60 kPa pressure with a sensitivity of $2.82 \pm 0.2 \text{ mV kPa}^{-1}$. Wang's group reported a self-powered thin-film-based triboelectric tactile sensor. They produced a highly triboelectric-negative fluorinated ethylene propylene (FEP) film with nanowire-structured surface applied as the contact electrification layer, which can generate triboelectric charges upon contact with a foreign object. Ouyang and co-workers reported a novel flexible and self-powered triboelectric nanogenerator (TEENG)-based pulse sensor, which can directly acquire voltage signal that is consistent with second derivative of conventional pulse signal without complex mathematical operations and circuit design (Ouyang et al. 2017). The flexible self-powered ultrasensitive pulse sensor (SUPS) is composed of two friction layers, electrode layers, a spacer, and an encapsulating PDMS layer. The pulse wave velocity can be measured by using two SUPS simultaneously, which can be used to indicate the degree of arteriosclerosis.

10.3.2.3 Other Key Parameters

The sensing range of flexible pressure sensors is an important parameter, which refers to the minimum and maximum pressure that can be detected. Jiang et al. constructed by introducing a knoll-like microstructured surface into a percolative thermoplastic polyurethane/carbon black sensitive film, which exhibited an ultrawide sensing range of 0–1500 kPa (Jiang et al. 2019b). Response time, another key parameter, is defined as the time consumption of the flexible wearable pressure sensor from applying stimuli to applying a steady signal output. It is related to the contact conditions between the active material and the electrode as well as the

viscoelastic property of the elastomeric materials (Lee et al. 2017). Some practical applications of pressure sensors such as real-time pulse monitoring device and instant-response displays have the requirement of short response time. Chen et al. presented a microfluidic flexible strain sensor by introducing liquid metal eutectic gallium-indium (EGaIn) embedded into a wave-shaped microchannel elastomeric matrix (300 μm width \times 70 μm height), which showed quick response time ($t = 116$ ms) and exhibited a good response in pulse monitoring (Chen et al. 2020a).

Linearity is typically defined as the degree of deviation between the calibration curve and the selected fitting line and is represented as a percentage (Chen et al. 2018). In the linear range, the output signals of pressure sensors are more precise and credible. Furthermore, high linearity is beneficial to the calibration process and data processing. Therefore, developing pressure sensors with good linearity is highly desired. For example, Pang et al. proposed a special surface morphology with spinosum microstructure of random distribution via the combination of an abrasive paper template and reduced graphene oxide, which exhibited a wide linearity range of 0–2.6 kPa (Pang et al. 2018). Hysteresis of a pressure sensor refers to the phenomenon that the sensing performance is inconsistent between loading and unloading. The performance of hysteresis is mostly affected by the viscoelasticity of the active materials. Hysteresis is usually defined as the maximum difference between the output signals under the same pressure in a loading-unloading cycle by the full-scale output (Ray et al. 2019). Chen et al. presented a pressure sensor by the wave-patterned structure, which improved the hysteresis performance from 6.79 to 1.02% and achieved the accurate measurement (Chen et al. 2020a). Durability represents the ability to maintain stable electrical functionality during reciprocating deformation. Flexible sensors with high durability can sustain various applied pressures and strains (Park et al. 2018a). Fan et al. reported a wearable liquid-capsule sensor platform, which exhibited high durability over 30,000 loading cycles (Fan et al. 2018). Herein, some typical flexible pressure sensors are compared and summarized in Table 10.1 “Summary of materials/structure, sensing mechanism, sensitivity/linearity range, power consumption, detection range, and duration of recently reported pressure sensors.”

10.4 Applications for Flexible Pressure Sensors

The wearable flexible sensors can be widely used in various areas of society. They can be used to detect various force signals and behavioral signals of the human body, such as blood pressure, heart rate, and pulse rate, intracranial pressure, intra-ocular pressure, tactile perception, and gait monitoring. Based on the feedback of wearable sensor, we can know our body's state in real time and make adjustments to let our lives become healthier.

Table 10.1 Summary of recently reported pressure sensors and their performance parameters

| Materials/structure | Sensing mechanism | Sensitivity(kPa ⁻¹)/linearity range | Power consumption | Detection range | Duration (cycles) |
|--|-------------------|---|-------------------|-----------------|-------------------|
| Au/PDMS (Wang et al. 2018b) | Piezoresistivity | 196/0–10 kPa | – | 0–100 kPa | >10,000 |
| Ecoflex/graphene (Qi et al. 2020) | Piezoresistivity | 12.3/– | – | 0–200 kPa | 5000 |
| SF/PAN I (Mengting et al. 2021) | Piezoresistivity | 2.54/0–100 kPa | – | – | >2000 |
| ZnOEP/CNTs/PDMS (Xia et al. 2017) | Piezoresistivity | 39.4/0–10 kPa | <30 μ W | – | 5000 |
| PDMS/PEDOT:PSS (Wang et al. 2016) | Piezoresistivity | 851/0–3 kPa | 100 nW | 34 Pa–20 kPa | – |
| PEN/@rGO (Ai et al. 2018) | Piezoresistivity | 4.2/– | 35 nW | 0–50 kPa | >30,000 |
| PANI@silica (Kim et al. 2019b) | Piezoresistivity | 17.5/– | – | 0.008–120 kPa | >6000 |
| GO/KGM (Xianzhang et al. 2018) | Capacitance | 0.28/– | – | 0–10 kPa | >1000 |
| Ag/PVDF/micro-arrayed (Xiong et al. 2020) | Capacitance | 30.2/0–130 Pa | – | – | >100,000 |
| MXene (Ti3C2Tx)/PVA (Zhang et al. 2019) | Capacitance | 0.4/– | – | – | 10,000 |
| AgNWs/PDMS | Capacitance | 20.08/0–0.8 kPa | – | – | >5000 |
| Ag/PET/FEP (Chen et al. 2020b) | Capacitance | 7.989/– | – | 0.1–60 kPa | 10,000 |
| PDA@BTO/PVDF (Yang et al. 2020) | Piezoelectricity | – | 0.122 μ W | – | >5000 |
| PbTiO ₃ nanowires/PI (Chen et al. 2017) | Piezoelectricity | 9.4×10^{-3} /– | – | – | 10,000 |

(continued)

Table 10.1 (continued)

| Materials/structure | Sensing mechanism | Sensitivity(kPa ⁻¹)/linearity range | Power consumption | Detection range | Duration (cycles) |
|--|-------------------|---|-------------------|-----------------|-------------------|
| Ag/PVDF/PDMS (Lin et al. 2021) | Piezoelectricity | 7.7 mV/– | – | – | 80,000 |
| Au/PET (Park et al. 2017) | Piezoelectricity | 0.018/– | – | – | 5000 |
| PDMS/bamboo structures (Lei et al. 2022) | Triboelectricity | 3.627/0–8 kPa | – | 0–80 kPa | – |
| AgNWs/CTT/PDMS (Ning et al. 2020) | Triboelectricity | – | – | – | 15,000 |
| rGO/PI (Xia et al. 2022) | Triboelectricity | 30.3/– | – | – | >4000 |

10.4.1 Detecting Heart Rate or Pulse

Heart rate is defined as the frequency of the cardiac cycle, and long-term heart rate monitoring during daily life can provide important information about human health status for noninvasive medical diagnosis. The heart rate or pulse can be commonly measured from radial artery at the wrist or carotid artery at the neck (Kaisti et al. 2019).

Recently, various flexible pressure sensors have demonstrated the capability of accurate pulse or heart rate measurement in real time. He et al. presented a novel material design strategy developed to fabricate a self-assembled graphene sensing film (He et al. 2019b). Figure 10.4a shows the schematic illustration of artery pulse detection on the skin surface. The applied pressure forces the sensor close to the artery, which maximizes the signal from the artery pulse. Although there is a prominent progress in wearable health monitoring electronics, long-term monitoring weak pulse signal during daily activities remains a challenge owing to their sensitivity and vulnerability to body movement. The pulse wave is a significant physiological phenomenon detectable along the arterial system during blood circulation, containing numerous and reliable signals. Wu et al. demonstrated a flexible pressure sensor with a positive resistance–pressure response based on laser scribing graphene, and the sensor exhibited an ultrahigh sensitivity and a broad detection range (Qi et al. 2020). By collecting the pulse strength, frequency, and reflection, professional medical professionals can infer a variety of information, providing a diagnosis and prophylaxis of relevant diseases. In addition to detecting the weak signals such as pulse directly, the sensor with amplification ability is able to amplify the pulse signal by applying external pressure, making detection more accurate (Fig. 10.4b). Chen et al. presented a flexible hierarchical elastomer tuned self-powered pressure sensor, which achieves both high sensitivity (7.989 V kPa⁻¹) and

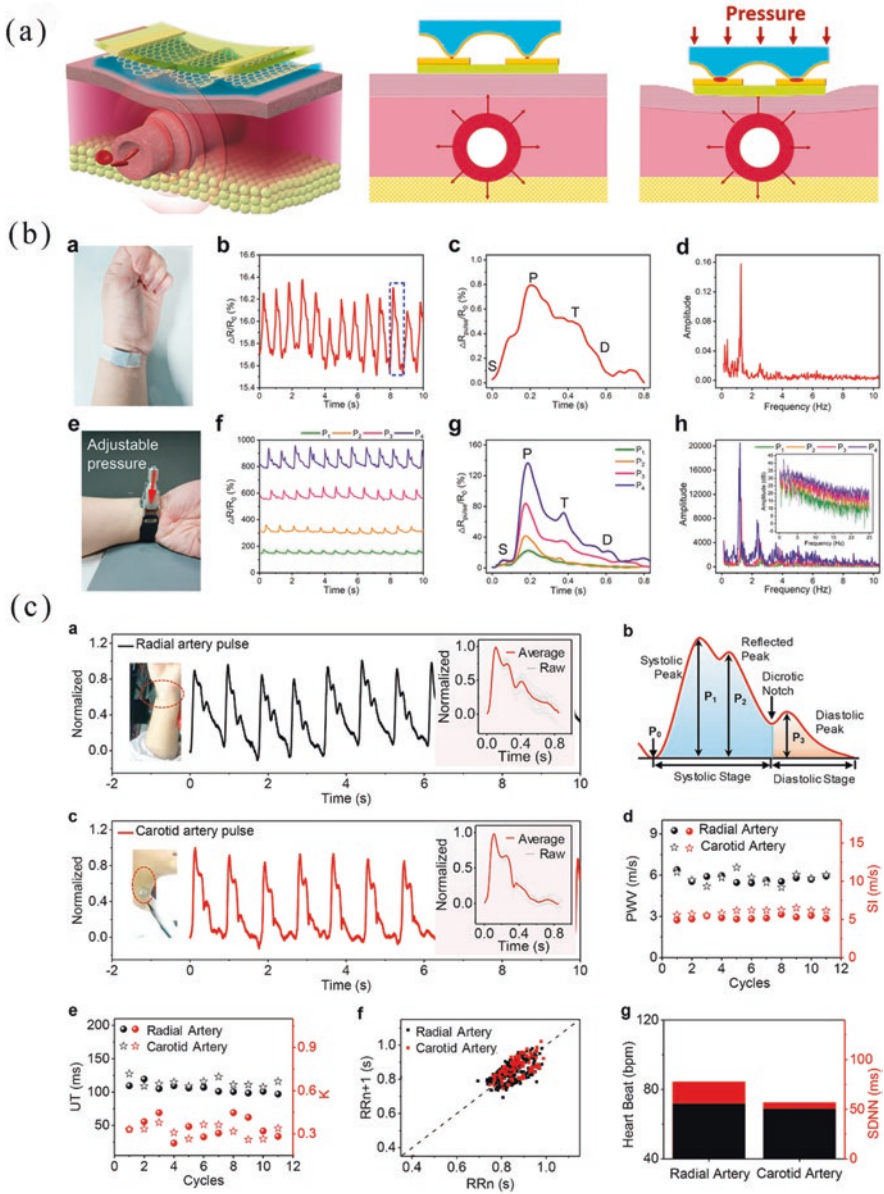


Fig. 10.4 (a) Schematic illustration of artery pulse detection on the skin surface. The applied pressure forces the sensor close to the artery, which maximizes the signal from the artery pulse (He et al. 2019b). (b) Photograph of the TMPGPS attached to the wrist by medical tape and the corresponding real-time, pulse signal detected, single pulse wave, and frequency spectrum (Qi et al. 2020). (c) HSPS for CVD monitoring. The radial and carotid arterial pulse waves of a 30-year-old healthy female. Inset is the enlarged view of each cycle (Chen et al. 2020b)

wide pressure range (Chen et al. 2020b). As shown in Fig. 10.4c, the sensor is used in monitoring radial artery pulse and carotid artery pulse. They studied the pulse wave and cardiovascular conditions of different adults, such as diastolic blood pressure (DBP), systolic blood pressure (SBP), pulse transit time (PTT), etc. By using an easier way to know about our body state such as heart rate and pulse signal information, it can make people live a healthier life. And the device could obtain accurate arterial pulse signal information from the sensor output even under the strong interference of body movement such as running and cycling.

10.4.2 *Detecting Pressure In Vivo*

Intracranial hypertension is an acute and chronic condition with a variety of causes that include traumatic brain injury, aneurysms, brain tumors, hydrocephalus, stroke, and meningitis. Accurate measurement of intracranial pressure can provide useful information for clinical diagnosis and management of such diseases. Karmakar et al. developed a pressure sensor that can be used to monitor the applied pressure during surgery for intraoperative care (Karmakar et al. 2020). As shown in Fig. 10.5a, it exhibits real-time photograph of pressure sensor placement along with the (intracranial pressure) ICP catheter on a live rodent model. In this study, it has been proven that real-time intraoperative pressure monitoring is important to save the complication and risks of patients (especially older patients), and our fabricated flexible pressure sensor can be an ideal candidate for this. Besides, Lee et al. presented a pressure sensor that is used for detecting the intracranial pressure of sheep (Fig. 10.5b) (Lee et al. 2020). The fixed sheep brain did not come with the skull or intact meninges; a sheep brain tends to be easily deformed, causing a technical challenge to implant the valve. Thus, they cast the entire brain in PDMS to form a watertight seal with the valve implanted. Pressure sensors measured the inlet and outlet pressure of fluidic ports. It also provides a method for better measurement of intracranial pressure.

As for intraocular pressure, Kim et al. developed a pressure sensor to monitor the intraocular pressure and applied this for noninvasive monitoring in association with the intraocular islet transplantation in diabetes (Fig. 10.5c) (Kim et al. 2019c). A strain sensor inside the lens can detect detailed changes in intraocular pressure by focusing the strain only in the desired, selective area of the contact lens. In addition, this smart sensor can transmit the real-time value of the intraocular pressure wirelessly using an antenna. This type of monitoring will provide important information on potential changes in the intraocular pressure associated with the transplantation procedure, and it enables appropriate clinical safety steps to be taken, if needed. Savariraj et al. presented a intraocular pressure sensor by using graphene-AgNWs hybrid electrodes (Fig. 10.5d) (Savariraj et al. 2021). In this work, only in vitro wireless monitoring of intraocular pressure was carried out on bovine eyeballs, and the sensor exhibited transparency adequately on the bovine or mannequin eye, ensuring clear vision. At lower pressure (>50 mmHg), the frequency response is

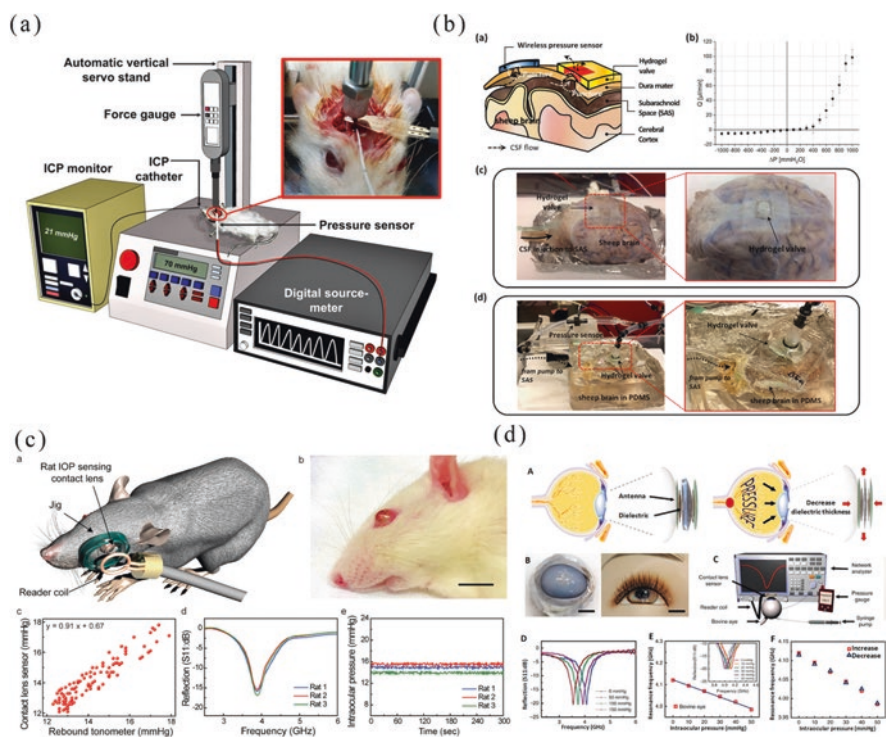


Fig. 10.5 (a) Schematic diagram of the measurement setup for in vivo pressure monitoring. Real-time photograph of pressure sensor placement along with the ICP catheter on a live rodent model is shown in the inset fig (Karmakar et al. 2020). (b) Actual configuration of the experimental setup. A syringe pump injects CSF to the cavity formed by SAS and the valve. The excess portion of manual cut was sealed by PDMS to prevent any leakage. The pressure sensor measures the differential pressure across the valve (Lee et al. 2020). (c) Correlation between the IOP measurements using the contact lens sensor and the rebound tonometer. Real-time continuous monitoring of the IOP in the rats (Kim et al. 2019c). (d) Graphene-AgNWs hybrid electrodes incorporated IOP sensor, fabrication, working principle, and results. Schematic showing the mechanism of AgNWs spiral coil-based intraocular pressure sensor. Photographs of the sensor transferred onto the contact lens worn by a bovine eyeball (left) and a mannequin eye (right). Scale bar, 1 cm (Savariraj et al. 2021)

linear, with a high sensitivity, and the sensor was noninvasive so that it can be well used in monitoring intraocular pressure.

10.4.3 Gait Monitoring

Accurate gait monitoring, which could be used in various health-related applications such as dynamic monitoring of Parkinson's disease, early diagnosis, and rehabilitation assessment, has attracted more and more attention in recent years (Park

et al. 2018b). Generally, the gait status could be monitored by measuring the force applied by the periodic foot stepping, and as a consequence, pressure sensors with suitable sensitivity in a wide pressure range are highly desired. Zhu et al. reported a highly flexible, compressible, and conductive PEDOT:PSS-@MS-based piezoresistive sensors for human motion detection. The conductive sponge was fabricated by dip-coating the melamine sponge (MS) in an aqueous dispersion of PEDOT:PSS. Owing to the highly porous and interconnected open-cell structure of MS, the PEDOT:PSS@MS exhibits excellent compressibility and flexibility. As a demonstration, three pressure sensors were fixed at three different positions (heel, arch, and forefoot) of an insole to collect different walking signals simultaneously. The fabricated pressure sensors can recognize gait and speed of walking, which may be useful in physical therapy such as helping stroke patients recover using gait training method.

Based on piezoelectric effect, Ahn et al. presented a new wearable multi-local strain sensor (MLS sensor) based on 3D textile structure with prestrained monofilament (Ahn et al. 2020). It detects signals from body movement based on pressure of the fingertip and gait, four movements of the neck, and joint movement (elbow and knee). Figure 10.6a presents the analysis result of the difference in gait pressure and stride length between the normal gait (5°) and toe-out angle gait (25°) using the output voltage. An MLS sensor was attached to the insole such that the output voltage (normal gait, 50 V; toe-out angle gait, 80 V) that varies based on the pressure on the heel and the one that varies based on the stride length (normal gait, 1.56 s; toe-out angle gait, 1.89 s) are analyzed to identify the difference between the toe-out angle and normal gaits. This enables the detection of pattern change in the gait due to dementia. In addition, the Bluetooth module is linked to a mobile phone in order to monitor the number of steps in real time. This suggests the possibility of its application in remote medical care.

Moreover, gait monitoring pressure sensors can be utilized in sports training to improve the performance of athletes (Zhu et al. 2019; Li et al. 2019b). Wu et al. demonstrated a low-cost flexible pressure sensor with a positive resistance-pressure response based on laser scribing graphene (Fig. 10.6b) (Qi et al. 2020). To perform human gait monitoring, they first attached a triode-mimicking graphene pressure sensor (TMPGPS) onto the heel to detect plantar pressure of various movements. And due to the good sensitivity of sensors under high pressure, different motion modes such as standing, walking, and jumping can be distinguished easily not only from the waveform but also from the intensity. Furthermore, several TMPGPSs were attached to a sponge insole with a flexible printed circuit board (PCB) to fabricate a pressure sensing array shoe pad. After processing, the data will be wirelessly transmitted to terminals such as mobile phones and laptops using Bluetooth modules and antennas. Finally, according to the feedback data, athletes can judge their own body state, so that they can achieve better protection in the following training.

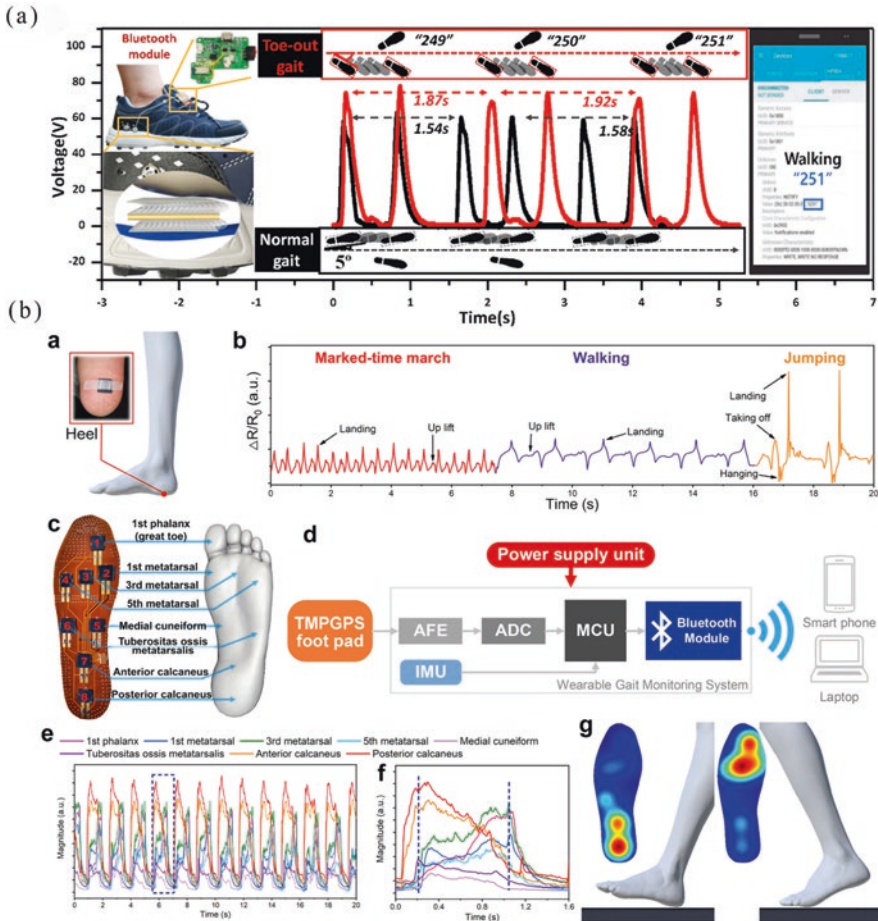


Fig. 10.6 (a) Output voltage change when on normal gait and toe-out gait. MLS sensor attached to the insole and illustration of smartphone application showing gait using Bluetooth (Ahn et al. 2020). (b) Schematic illustration and photograph of the sensor attached under the testing object’s heel. Signal of foot pressure detected during various movements of marked-time march, walking, and jumping. Photograph of the shoe pad with TMPGPSs and corresponding anatomy in the schematic diagram of a human foot. Block diagram of the wearable gait monitoring system (Qi et al. 2020)

10.4.4 Recognition of Sound Signal

The sound signal, which is defined as the process of producing a certain sound through quasiperiodic vibration of vocal cords, is the most vital way of communication between people. In general, pressure changes across the larynx during the voicing process can induce oscillation of vocal folds. The characteristic signals of different throat motions can be used to record the word or speech. Recently,

different kinds of flexible wearable pressure sensors have been used for word recognition. While the flexible pressure sensor is attached to the human neck, the subtle pressure changes induced by the muscle movements around the throat during speech will be captured by the device.

Zhang et al. proposed a piezoresistive pressure sensor by forming a cobweb-like network made of a zinc octaethylporphyrin (ZnOEP)/carbon nanotube (CNT) hybrid on an array of polydimethylsiloxane (PDMS) microposts (Zhang et al. 2020). The sensor exhibited an ultrahigh sensitivity of 39.4 kPa^{-1} , a superfast response time of 3 ms, a low detection limit of 10 Pa, and a reproducible response without degradation after 5000 cycles of pressure loading/unloading. With the rapid response, the sensor could also recognize fast rhythms from light music, as shown in Fig. 10.7a. It can be noted that the response curve of the sensor at the bottom of the figure matches well with the acoustic spectrum of the music depicted in the

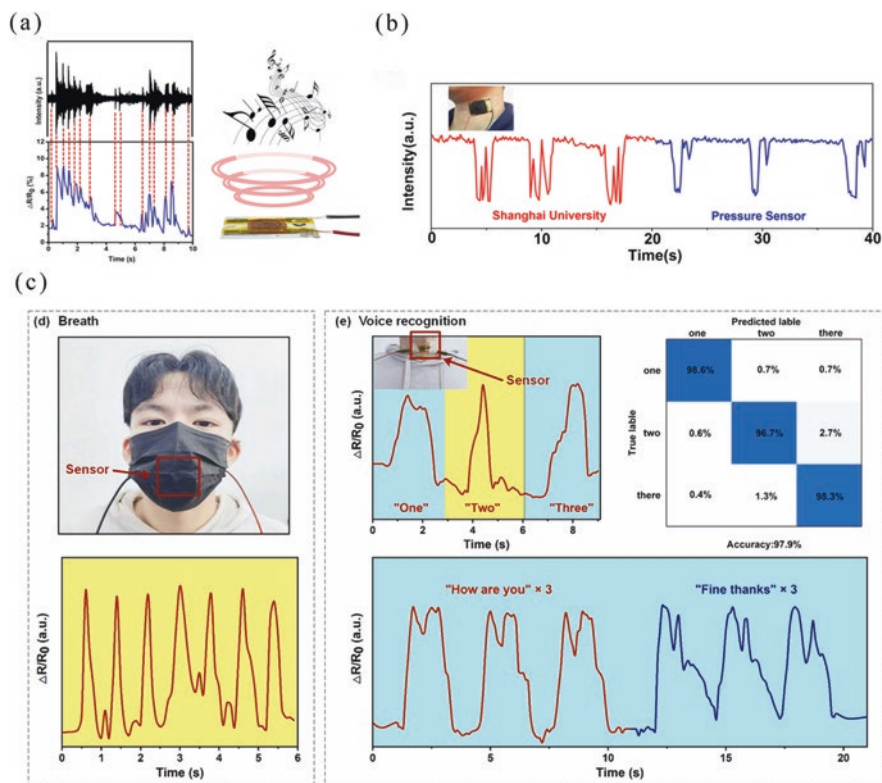


Fig. 10.7 (a) Acoustic spectrum of a light music and sensor response curve matches well, showing that the pressure sensor can also recognize the rhythm of music (Zhang et al. 2020). (b) Real-time recording of current changes for detecting the acoustic vibration (inset: photograph of the pressure sensor attached onto the neck of a speaker) (Zhao et al. 2019). (c) Applications of the rGO-cloth/LIG pressure sensor. Breath and response of rGO-cloth/LIG pressure sensor for voice recognition and confusion matrix of the deep learning outcome (Xia et al. 2022)

upper part of the figure, proving its great potential for use in electronic skin systems. Zhao et al. presented a highly sensitive flexible piezoresistive pressure sensor based on hybrid porous microstructures (HPM) (Zhao et al. 2019). The HPM combines the advantages of hybrid structures, which increase the contact area because of stress concentration and reduce Young's modulus, and the porous structure, which introduces an additional pore resistance. Consequently, the pressure sensor had a high sensitivity of 83.9 kPa^{-1} at an applied pressure $< 140 \text{ Pa}$. As shown in Fig. 10.7b, a pressure sensor device was attached to the neck of a speaker directly. When the speaker spoke different words such as "Shanghai University" and "pressure sensor" repeatedly, the output current signal changed correspondingly, indicating that the device was able to discriminate the voice through the vibration patterns.

However, the high performance of pressure sensors mainly powered by external batteries cannot meet the needs of ultra-long standby and portability. Hence, the self-powered sensors are emerging. Herein, Xia et al. presented a reduced graphene oxide (rGO)-cloth-based pressure sensor with laser-induced graphene (LIG) prepared by a simple and low-cost preparation process (Xia et al. 2022). LIG not only contribute to the sensitivity of pressure sensors (from 20.6 to 30.3 kPa^{-1}) but also improve the transfer charge density of triboelectric nanogenerator (TENG) (from 160 to $270 \text{ } \mu\text{C}/\text{m}^2$). The resistance variation response for different words and sentences is displayed in Fig. 10.7c, which shows that this sensor has excellent repeatability and distinguishability in recognizing voices. Moreover, the BP neural networks are employed to further detecting the accuracy of voice recognition, and the results suggest the total recognition accuracy reaches 97.9% . Given these advantages, a high-performance self-powered measurement-control combined system consisting of the LIG-based pressure sensors and TENG is constructed, which bears huge potential to support the development of wearable devices, smart skin, and human-computer interaction. Based on these advantages, the application of our sensor could potentially be used to detect vocal fold vibration for mute and deaf people.

10.4.5 *Breath Detection*

Respiratory rate, as a physiological parameter, is a sensitive indicator of acute respiratory dysfunction. Both doctors and nursing staff take it as one of the vital signs. The respiratory rate sensor can reflect the respiratory status in real time, record the number of breaths per unit time, and display the current respiratory rate. It can help doctors and researchers to grasp the patient's condition in real time and make effective treatment in time to save patient's life. Zhong et al. presented a wireless smart face mask by integrating an ultrathin self-powered pressure sensor and a compact readout circuit with a normal face mask (Zhong et al. 2022). The wireless breath monitoring by a smart face mask was successfully developed by combining an ultrathin self-powered pressure sensor as a breathing sensor, a power supply unit with a lithium battery, a voltage boost circuit, and a measuring circuit based on an Arduino board, as shown in Fig. 10.8a. Based on the average breath rate and

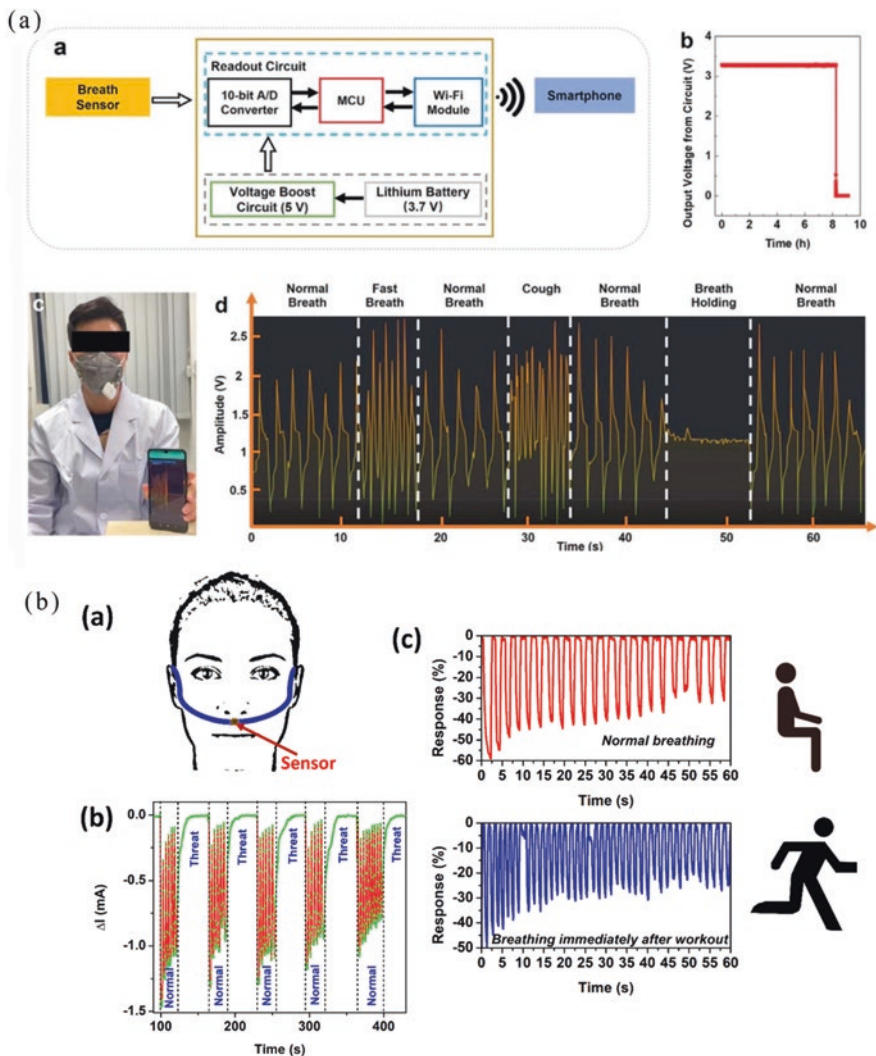


Fig. 10.8 (a) Photos showing the measured continuous and successive breath conditions of normal breath, fast breath, normal breath, cough, normal breath, breath-holding, and normal breath of tester 1 (Zhong et al. 2022). (b) Schematic of breath detection, indicating the sensor’s placement on the philtrum. Pressure response for NB and intermittent breathing (threat) condition in a regular interval. Comparison of breathing pattern before (upper panel) and after (lower panel) a physical workout (Ghosh et al. 2021)

amplitude (peak-peak voltage) for normal breath, different breath conditions, including normal breath, fast breath, cough, and breath-holding, were recognized by the wireless breath-monitoring system. The sensor responds sensitively to breathing airflow owing to its ultrathin/light structure and high electrostatic induction efficiency; unlike breath measurement using a non-embedded device, it is completely

portable and wearable, making it easy to use in daily life; and it can easily achieve an efficient breath information process including data measurement, transmission, storage, and analysis. Finally, the smart face mask has potential applications in maintaining personal health and preventing breath-related epidemic diseases.

Besides, Ghosh et al. presented a highly sensitive piezoresistive sensor by using Si nanorod (NR) arrays (Ghosh et al. 2021). The sensor exhibited an ultralow-pressure detection, and excellent ambient stability (>several months) for detecting breath signals. As shown in Fig. 10.8b, the sensor can efficiently detect the difference between the normal breathing (NB) and the states of hold breathing/stop breathing (SB) for some moments and provide an alarm in the case of risky events for an individual with breathing disorders such as sleep apnea. It is more convenient for those patients with respiratory diseases to know about real-time physical condition, which also provides guarantee for their safety. Wireless integration of the sensors, having the portable and smart platform, can enhance the utility of the breath sensor as a routine-life workout partner and can be considered to realize next-generation breath-sensing gadgets. We believe that this work provides guidance to develop next-generation breath-sensing gadgets and other leading-edge applications in electronic and healthcare devices.

10.4.6 Tactile Perception

Tactile sense plays a critical role in enabling human beings to interact with the surrounding environments. Humans can feel and manipulate diverse objects by applying precisely controlled forces, which is important for accomplishing fundamental activities of daily life. Moreover, tactile perception is extremely significant in various applications, containing the control of prosthetic limb, tactile reconstruction of patients with neurological diseases, clinical rehabilitation therapies after trauma (Boutry et al. 2018), robotic manipulation (Sundaram et al. 2019), and artificial intelligence (Wan et al. 2018).

With extensive investigation in recent years, various types of flexible tactile sensors that can mimic the tactile sensory features of the human skin have been developed. Inspired by the human skin as a highly sensitive biological sensor, Cheng et al. fabricated a highly sensitive MXene-based piezoresistive sensor with microspinous microstructures formed by a simple abrasive paper stencil printing process (Cheng et al. 2020). Importantly, the randomly distributed spinous microstructures can effectively promote increased contact area of the conductive channels with improved performance of the pressure sensor: high sensitivity (151.4 kPa^{-1}), fast response time ($<130 \text{ ms}$), small pressure detection limit (4.4 Pa), and excellent stability over 10,000 cycles. As shown in Fig. 10.8a, flexible sensor could be attached onto the robot joint surface with the aid of a PI tape. The obvious changes of the peak shape indicate that the sensor can easily detect the robot movement. In practice, the sensor shows great performance in monitoring human physiological signals, tactile sensing, and remote monitoring of intelligent robot motion in real time.

Besides, Lin et al. presented a skin-inspired piezoelectric tactile sensor array with real-time differentiation ability of diverse external stimuli (Lin et al. 2021). As shown in Fig. 10.8b, the manipulator with tactile sensor array was used to grab tofu and observe whether the tofu was damaged. It turned out that the former was intact and the latter damaged. Integrated with a signal processor and a logical algorithm, the tactile sensor array achieves to sense and distinguish the magnitude, positions, and modes of diverse external stimuli, including gentle slipping, touching, and bending, in real time. Herein, the proposed tactile sensor array possesses the characteristics of high sensitivity (7.7 mV kPa^{-1}), long-term durability (80,000 cycles), and rapid response time (10 ms) (less than human skin). And this research provides a new strategy for tactile sensor design and would broadly benefit many fields, especially for electronic skins, health monitoring, animal movement detection, and robotics (Fig. 10.9).

10.5 Conclusions and Perspectives

In this article, we have provided a state-of-the-art review of the emerging flexible pressure sensors for biomedical applications. In the past few years, advances in new materials, power supplies, sensing modalities, and assembly techniques provide important foundations for the development of new classes of skin-like flexible sensors. Among these sensors, some basic parameters such as stretchability, spatial resolution, and sensitivity even exceed those of the biological skin. Herein, based on the rapid development of science and technology, we have summarized some applications of flexible pressure sensors in medical diagnostic in recent years. It is obvious that flexible wearable sensors have greatly improved our medical conditions and have provided safer social environment.

While numerous basic and applied research results have been translated from the laboratory to the real world, many important challenges still exist in practical applications. For instance, due to the viscoelastic performance of the polymers, response delay existed in all polymers based on pressure sensors, which limits the application of these sensors. The hysteresis of elastic materials will affect the accuracy of collected physiological signals and bring inconvenience to the doctor's analysis. Moreover, when measuring pulse signals, blood pressure, or other data by wearable sensors, in order to get accurate data, we usually need to improve the high sensitivity and linearity of sensor. It requires us to select appropriate substrates and active materials in the fabrication. Also, standard everlasting electronic implants used in modern clinical medicine usually acts as a nidus for infection, with the potential to provoke pathological tissue reactions. In the meantime, the associated surgical removal can cause patients' reoperating-related pain. Consequently, developing materials that can naturally resorb via metabolic and/or hydrolysis action might be an important trend for implantable devices. These are all we need to put forward higher requirements for material synthesis technology.

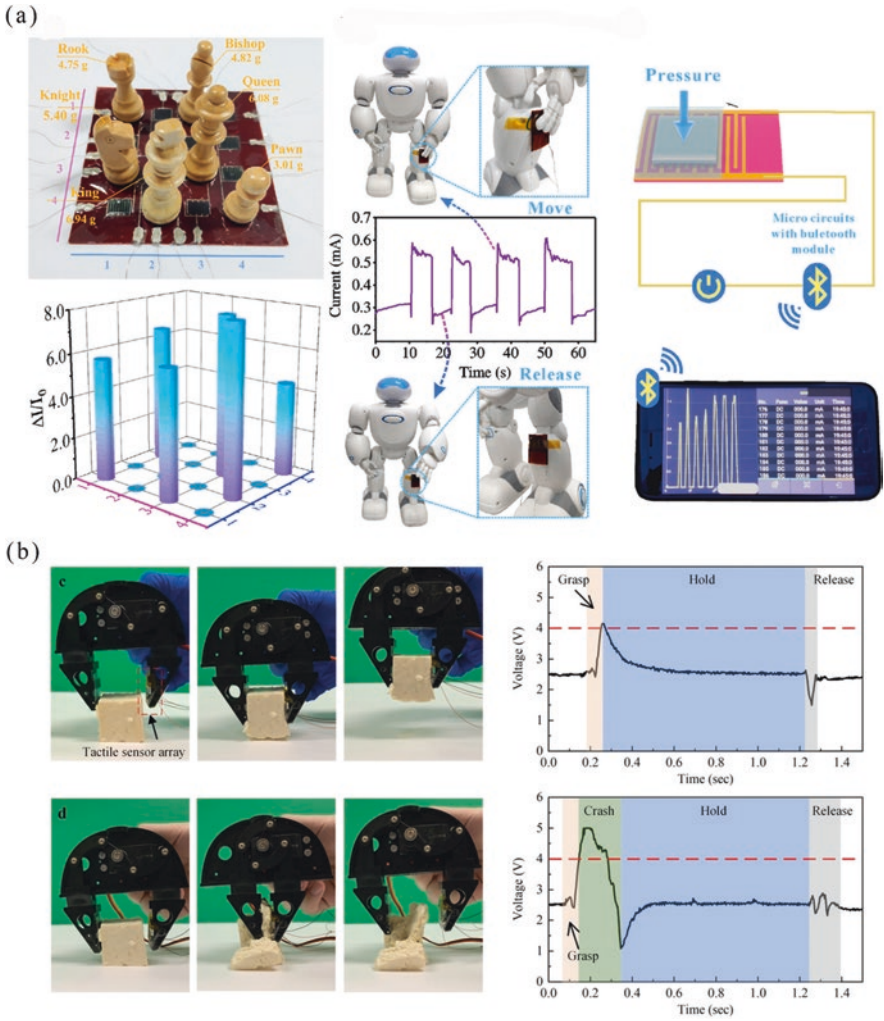


Fig. 10.9 (a) Photograph of the 4×4 array of MXene-based piezoresistive sensor and detection of the corresponding pressure distributions. Photograph of the pressure sensor assembled on a robot (inset: enlarged view of the sensing position) and detection of its response to the motion behavior. Piezoresistive sensor with a Bluetooth circuit module converts its current signal to a portable mobile device display (Cheng et al. 2020). (b) Demonstration of grasping objects using a robotic hand with a feedback module. The tactile sensor is mounted on the robotic hand and used as real-time feedback. A piece of soft and fragile tofu keeps integrity during the movement of the robotic hand. And demonstration of grasping objects using a robotic hand without the proposed sensor array. A piece of soft and fragile tofu damaged during the movement of the robotic hand (Lin et al. 2021)

Another important challenge is the power supply of sensors, for instance, some physiological signals (pulse, blood pressure, etc.) require continuous monitoring, which is vital for long-term operations. Thus, continued progress in energy harvesting and energy storage technologies will be needed to support increasing requirements for communication bandwidth, operating distance, sampling frequencies, and operating lifetimes. Developing self-powered sensing devices represents a promising candidate to achieve sustainability in pressure sensors. By combining the sensing components with various energy harvest units (such as thermoelectric devices, organic solar cells, piezoelectric electronics, etc.), self-powered pressure sensor that can operate continuously without external power supply might be fabricated. In particular, triboelectric and piezoelectric phenomena could be applied to external pressure sensing in the self-powered flexible devices. However, uninterrupted supply of energy from sources including mechanical motions, ambient light, and others is typically not possible. Therefore, combinations of self-power devices together with some other energy storage components such as batteries and supercapacitors may provide an attractive solution.

In the future, a complete sensor system should have the following foundations. Firstly, the sensor tends to be integrated. The system contains batteries, circuits, and sensors so that users can wear it comfortably for a long time. The sensor can be multifunctional. When we put sensor in some extreme circumstances, it still can measure various body signals (blood pressure, pulse signal, etc.) accurately. Moreover, the sensor can achieve intelligence. It can achieve signal acquisition in real-time analysis and get health report and feedback to users. In addition, in terms of the recycle mechanism of wearable sensors, we should try to use degradable materials in fabrication for the *in vivo* sensors, so as to minimize the harm to human. As for the *ex vivo* sensors, we should choose greener materials to protect the environment.

References

- Ahn S, Cho Y, Park S, Kim J, Sun J, Ahn D, Lee M, Kim D, Kim T, Shin H, Park J-J. Wearable multimode sensors with amplified piezoelectricity due to the multi local strain using 3D textile structure for detecting human body signals [J]. *Nano Energy*. 2020;74:104932.
- Ai Y, Hsu TH, Wu DC, Lee L, Chen J-H, Chen Y-Z, Wu S-C, Wu C, Wang ZM, Chueh Y-L. An ultrasensitive flexible pressure sensor for multimodal wearable electronic skins based on large-scale polystyrene ball@reduced graphene-oxide core-shell nanoparticles [J]. *J Mater Chem C*. 2018;6(20):5514–20.
- Bi P, Liu X, Yang Y, Wang Z, Shi J, Liu G, Kong F, Zhu B, Xiong R. Silver-nanoparticle-modified polyimide for multiple artificial skin-sensing applications [J]. *Adv Mater Technol*. 2019;4:1900426.
- Boutry CM, Wang Z, Chang J, Kaizawa Y, Schroeder BC, Fox P, Bao Z. A stretchable and biodegradable strain and pressure sensor for orthopaedic application [J]. *Nat Electron*. 2018;1(5):314–21.

- Cai G, Yang M, Zhenglin X, Liu J, Tang B, Wang X. Flexible and wearable strain sensing fabrics [J]. *Chem Eng J*. 2017;325:396–403.
- Cai Y, Shen J, Ge G, Zhang Y, Jin W, Huang W, Shao J, Yang J, Dong X. Stretchable Ti₃C₂T_x MXene/carbon nanotube composite based strain sensor with ultrahigh sensitivity and tunable sensing range [J]. *ACS Nano*. 2018;12(1):56–62.
- Chen Z, Wang Z, Li X, Lin Y, Luo N, Long M, Zhao N, Jian-Bin X. Flexible piezoelectric-induced pressure sensors for static measurements based on nanowires/graphene heterostructures [J]. *ACS Nano*. 2017;11(5):4507–13.
- Chen J, Zheng J, Gao Q, Zhang J, Zhang J, Omisore OM, Wang L, Li H. Polydimethylsiloxane (PDMS)-based flexible resistive strain sensors for wearable applications [J]. *Appl Sci*. 2018;8(3):345.
- Chen J, Zhang J, Luo Z, Zhang J, Li L, Yi S, Gao X, Li Y, Tang W, Cao C, Liu Q, Wang L, Li H. Superelastic, sensitive, and low hysteresis flexible strain sensor based on wave-patterned liquid metal for human activity monitoring [J]. *ACS Appl Mater Interfaces*. 2020a;12(19):22200–11.
- Chen S, Nan W, Lin S, Duan J, Zisheng X, Pan Y, Zhang H, Zheheng X, Huang L, Bin H, Zhou J. Hierarchical elastomer tuned self-powered pressure sensor for wearable multifunctional cardiovascular electronics [J]. *Nano Energy*. 2020b;70:104460.
- Cheng Y, Ma Y, Li L, Zhu M, Yue Y, Liu W, Wang L, Jia S, Li C, Qi T, Wang J, Gao Y. Bioinspired microspines for a high-performance spray Ti₃C₂T_x MXene-based piezoresistive sensor [J]. *ACS Nano*. 2020;14(2):2145–55.
- Chu Y, Zhong J, Liu H, Ma Y, Nathaniel Liu Y, Song JL, Zhichun Shao Y, Sun YD, Wang X, Lin L. Human pulse diagnosis for medical assessments using a wearable piezoelectret sensing system [J]. *Adv Funct Mater*. 2018;28(40):1803413.
- Chung H, Kim BH, Lee JY, Lee J, Xie Z, Ibler EM, Lee KH, Banks A, Jeong JY, Kim J, Ogle C, Grande D, Yu Y, Jang H, Assem P, Ryu D, Kwak JW, Namkoong M, Park JB, Lee Y, Kim DH, Ryu A, Jeong J, You K, Ji B, Liu Z, Huo Q, Feng X, Deng Y, Xu Y, Jang K-I, Kim J, Zhang Y, Ghaffari R, Rand CM, Schau M, Hamvas A, Weese-Mayer DE, Huang Y, Lee SM, Lee CH, Shanbhag NR, Paller AS, Xu S, Rogers JA. Binodal, wireless epidermal electronic systems with in-sensor analytics for neonatal intensive care [J]. *Science*. 2019;363(6430):eaau0780.
- Cui Z, Poblete F, Zhu Y. Tailoring the temperature coefficient of resistance of silver nanowire nanocomposites and their application as stretchable temperature sensors [J]. *ACS Appl Mater Interfaces*. 2019;11(19):17836–42.
- Ding Y, Xu T, Onyilagha O, et al. Recent advances in flexible and wearable pressure sensors based on piezoresistive 3D monolithic conductive sponges [J]. *ACS Appl Mater Interfaces*. 2019;11(7):6685–704.
- Dong K, Peng X, Wang ZL. Fiber/fabric-based piezoelectric and triboelectric nanogenerators for flexible/stretchable and wearable electronics and artificial intelligence [J]. *Adv Mater*. 2020;32(5):e1902549.
- Fan X, Huang Y, Ding X, Luo N, Li C, Zhao N, Chen S-C. Alignment-free liquid-capsule pressure sensor for cardiovascular monitoring [J]. *Adv Funct Mater*. 2018;28(44):1805045.
- Fan S, Meng L, Dan L, Zheng W, Wang X. Polymer microelectromechanical system-integrated flexible sensors for wearable technologies [J]. *IEEE Sensors J*. 2019;19(2):443–50.
- Gao J, Li B, Huang X, Wang L, Lin L, Wang H, Xue H. Electrically conductive and fluorine free superhydrophobic strain sensors based on SiO₂/graphene-decorated electrospun nanofibers for human motion monitoring [J]. *Chem Eng J*. 2019a;373:298–306.
- Gao L, Zhu C, Li L, Zhang C, Liu J, Hai-Dong Y, Huang W. All paper-based flexible and wearable piezoresistive pressure sensor [J]. *ACS Appl Mater Interfaces*. 2019b;11(28):25034–42.
- Gao J, Wang L, Guoa Z, Lia B, Wanga H, Luo J, Huang X, Xue H. Flexible, superhydrophobic, and electrically conductive polymer nanofiber composite for multifunctional sensing applications [J]. *Chem Eng J*. 2020;2:122778.

- Ghosh R, Song MS, Park JB, Tchoe Y, Guha P, Lee W, Lim Y, Kim B, Kim S-W, Kim M, Yi G-C. Fabrication of piezoresistive Si nanorod-based pressure sensor arrays: a promising candidate for portable breath monitoring devices [J]. *Nano Energy*. 2021;80:105537.
- Gong H, Cai C, Hongjun G, Jiang Q, Zhang D, Cheng Z. Flexible and wearable strain sensor based on electrospun carbon sponge/polydimethylsiloxane composite for human motion detection [J]. *RSC Adv*. 2021;11(7):4186–93.
- He Z, Zhou G, Byun J-H, Lee S-K, Um M-K, Park B, Kim T, Lee SB, Chou T-W. Highly stretchable multi-walled carbon nanotube/thermoplastic polyurethane composite fibers for ultrasensitive, wearable strain sensors [J]. *Nanoscale*. 2019a;11(13):5884–90.
- He J, Xiao P, Wei L, Shi J, Zhang L, Liang Y, Pan C, Kuo S-W, Chen T. A universal high accuracy wearable pulse monitoring system via high sensitivity and large linearity graphene pressure sensor [J]. *Nano Energy*. 2019b;59:422–33.
- He F, You X, Gong H, Yang Y, Bai T, Wang W, Guo W, Liu X, Ye M. Stretchable, biocompatible, and multifunctional silk fibroin-based hydrogels toward wearable strain/pressure sensors and triboelectric nanogenerators [J]. *ACS Appl Mater Interfaces*. 2020;12(5):6442–50.
- Hosseini ES, Manjakkal L, Shakthivel D, Dahiya R. Glycine-chitosan-based flexible biodegradable piezoelectric pressure sensor [J]. *ACS Appl Mater Interfaces*. 2020;12(8):9008–16.
- Hwang J, Kim Y, Yang H, Oh JH. Fabrication of hierarchically porous structured PDMS composites and their application as a flexible capacitive pressure sensor [J]. *Compos Part B Eng*. 2021;4:108607.
- Jayathilaka WADM, Qi K, Qin Y, Chinnappan A, Serrano-García W, Baskar C, Wang H, He J, Cui S, Thomas SW, Ramakrishna S. Significance of nanomaterials in wearables: a review on wearable actuators and sensors [J]. *Adv Mater*. 2019;31(7):e1805921.
- Jeon S, Lim S-C, Trung TQ, Jung M, Lee N-E. Flexible multimodal sensors for electronic skin: principle, materials, device, array architecture, and data acquisition method [J]. *Proc IEEE Inst Electr Electron Eng*. 2019;107(10):2065–83.
- Jiang C, Cheng X, Nathan A. Flexible ultralow-power sensor interfaces for E-skin [J]. *Proc IEEE Inst Electr Electron Eng*. 2019a;107(10):2084–105.
- Jiang S, Jiangtao Y, Xiao Y, Zhu Y, Zhang W. Ultrawide sensing range and highly sensitive flexible pressure sensor based on a percolative thin film with a knoll-like microstructured surface [J]. *ACS Appl Mater Interfaces*. 2019b;11(22):20500–8.
- Kaichen X, Yuyao L, Takei K. Multifunctional skin-inspired flexible sensor systems for wearable electronics [J]. *Adv Mater Technol*. 2019;4:1800628.
- Kaisti M, Panula T, Leppänen J, Punkkinen R, Tadi MJ, Vasankari T, Jaakkola S, Kiviniemi T, Airaksinen J, Kostiaainen P, Meriheinä U, Koivisto T, Pänkäälä M. Clinical assessment of a non-invasive wearable MEMS pressure sensor array for monitoring of arterial pulse waveform, heart rate and detection of atrial fibrillation [J]. *NPJ Digit Med*. 2019;2:39.
- Kang B-C, Park S-J, Ha T-J. Wearable pressure/touch sensors based on hybrid dielectric composites of zinc oxide nanowires/poly(dimethylsiloxane) and flexible electrodes of immobilized carbon nanotube random networks [J]. *ACS Appl Mater Interfaces*. 2021;13(35):42014–23.
- Karmakar RS, Wang J-C, Huang Y-T, Lin K-J, Wei K-C, Hsu Y-H, Huang Y-C, Lu Y-J. Real-time intraoperative pressure monitoring to avoid surgically induced localized brain injury using a miniaturized piezoresistive pressure sensor [J]. *ACS Omega*. 2020;5(45):29342–50.
- Kim J, Chou E-F, Le J, Wong S, Chu M, Khine M. Soft wearable pressure sensors for beat-to-beat blood pressure monitoring [J]. *Adv Healthc Mater*. 2019a;8(13):e1900109.
- Kim S, Amjadi M, Lee T-I, Jeong Y, Kwon D, Kim MS, Kim K, Kim T-S, Yong Suk O, Park I. Wearable, ultrawide-range, and bending-insensitive pressure sensor based on carbon nanotube network-coated porous elastomer sponges for human interface and healthcare devices [J]. *ACS Appl Mater Interfaces*. 2019b;11(26):23639–48.
- Kim J, Kim J, Minjae K, Cha E, Seoyoung J, Park WY, Kim KH, Kim DW, Berggren P-O, Park J-U. Intraocular pressure monitoring following islet transplantation to the anterior chamber of the eye [J]. *Nano Lett*. 2019c;20(3):1517–25.

- Kwak YH, Kima W, Parka KB, Kima K, Seo S. Flexible heartbeat sensor for wearable device [J]. *Biosens Bioelectron.* 2017;94:250–5.
- Lamanna L, Rizzi F, Guido F, Algeri L, Marras S, Mastronardi VM, Quattieri A, De Vittorio M. Flexible and transparent aluminum-nitride-based surface-acoustic-wave device on polymeric polyethylene naphthalate [J]. *Adv Electron Mater.* 2019;5:1900095.
- Lee K, Lee J, Kim G, Kim Y, Kang S, Cho S, Kim SG, Kim J-K, Lee W, Kim D-E, Kang S, Kim DE, Lee T, Shim W. Rough-surface-enabled capacitive pressure sensors with 3D touch capability [J]. *Small.* 2017;13(43) <https://doi.org/10.1002/smll.201700368>.
- Lee Y, Kim J, Jang B, Kim S, Sharma BK, Kim J-H, Ahn J-H. Graphene-based stretchable/wearable self-powered touch sensor [J]. *Nano Energy.* 2019;62:259–67.
- Lee S, Bristol RE, Preul MC, Chae J. Three-dimensionally printed microelectromechanical-system hydrogel valve for communicating hydrocephalus [J]. *ACS Sens.* 2020;5(5):1398–404.
- Lei H, Xiao J, Chen Y, Jiang J, Renjie X, Wen Z, Dong B, Sun X. Bamboo-inspired self-powered triboelectric sensor for touch sensing and sitting posture monitoring [J]. *Nano Energy.* 2022;91:106670.
- Li Y-Q, Huang P, Zhu W-B, Shao-Yun F, Ning H, Liao K. Flexible wire-shaped strain sensor from cotton thread for human health and motion detection [J]. *Sci Rep.* 2017a;7:45013.
- Li T, Zou J, Xing F, Zhang M, Cao X, Wang N, Wang ZL. From dual-mode triboelectric nanogenerator to smart tactile sensor: a multiplexing design [J]. *ACS Nano.* 2017b;11(4):3950–6.
- Li H, Han C, Huang Y, Huang Y, Zhu M, Pei Z, Xue Q, Wang Z, Liu Z, Tang Z, Wang Y, Kang F, Li B, Zhi C. An extremely safe and wearable solid-state zinc ion battery based on a hierarchical structured polymer electrolyte [J]. *Energy Environ Sci.* 2018;11(4):941–51.
- Li W, Xiong L, Yueming P, Quan Y, Li S. High-performance paper-based capacitive flexible pressure sensor and its application in human-related measurement [J]. *Nanoscale Res Lett.* 2019a;14(1):183.
- Li Z, Li HY, Fan Y, Lu L, Chen YH, Zhang C, Zhu G. Small-sized, lightweight, and flexible triboelectric nanogenerator enhanced by PTFE/PDMS nanocomposite electret [J]. *ACS Appl Mater Interfaces.* 2019b;11(22):20370–7.
- Li L, Zheng J, Chen J, Luo Z, Yi S, Tang W, Gao X, Li Y, Cao C, Liu Q, Kang X, Wang L, Li H. Flexible pressure sensors for biomedical applications: from ex vivo to in vivo [J]. *Adv Mater Interfaces.* 2020a;7:2000743.
- Li X, Fan YJ, Li HY, Cao JW, Xiao YC, Wang Y, Liang F, Wang HL, Yang J, Wang ZL, Zhu G. Ultracomfortable hierarchical nanonetwork for highly sensitive pressure sensor [J]. *ACS Nano.* 2020b;14(8):9605–12.
- Li M, Liang J, Wang X, Zhang M. Ultra-sensitive flexible pressure sensor based on microstructured electrode [J]. *Sensors.* 2020c;20(2):371.
- Li H, Chen J, Chang X, Youquan X, Zhao G, Zhu Y, Li Y. A highly stretchable strain sensor with both an ultralow detection limit and an ultrawide sensing range [J]. *J Mater Chem A.* 2021;9(3):1795–802.
- Liang C, Ruan K, Zhang Y, Junwei G. Multifunctional flexible electromagnetic interference shielding silver nanowires/cellulose films with excellent thermal management and joule heating performances [J]. *ACS Appl Mater Interfaces.* 2020;12(15):18023–31.
- Lin S, Cheng Y, Mo X, Chen S, Zisheng X, Zhou B, Zhou H, Bin H, Zhou J. Electrospun polytetrafluoroethylene nanofibrous membrane for high-performance self-powered sensors [J]. *Nanoscale Res Lett.* 2019;14(1):251.
- Lin W, Wang B, Peng G, Shan Y, Hong H, Yang Z. Skin-inspired piezoelectric tactile sensor array with crosstalk-free row+column electrodes for spatiotemporally distinguishing diverse stimuli [J]. *Adv Sci.* 2021;8(3):2002817.
- Liu W, Huang Y, Peng Y, Walczak MS, Dong W, Chen Q, Zhu L, Li L. Stable wearable strain sensors on textiles by direct laser writing of graphene [J]. *ACS Appl Nano Mater.* 2020;3(1):283–93.
- Ma Z, Wei A, Ma J, Shao L, Jiang H, Dong D, Ji Z, Wang Q, Kang S. Lightweight, compressible and electrically conductive polyurethane sponges coated with synergistic multiwalled carbon nanotubes and graphene for piezoresistive sensors [J]. *Nanoscale.* 2018;10(15):7116–26.

- Mahanty B, Ghosh SK, Garain S, Mandal D. An effective flexible wireless energy harvester/sensor based on porous electret piezoelectric polymer [J]. *Mater Chem Phys*. 2017;186:327–32.
- Mao Y, Ji B, Chen G, Hao C, Zhou B, Tian Y. Robust and wearable pressure sensor assembled from AgNW-coated PDMS micropillar sheets with high sensitivity and wide detection range [J]. *ACS Appl Nano Mater*. 2019;2(5):3196–205.
- Meng K, Chen J, Li X, Wu Y, Fan W, Zhou Z, He Q, Xue W, Fan X, Zhang Y, Yang J, Wang ZL. Flexible weaving constructed self-powered pressure sensor enabling continuous diagnosis of cardiovascular disease and measurement of cuffless blood pressure [J]. *Adv Funct Mater*. 2019;29:1806388.
- Mengdi X, Gao Y, Guohui Y, Cong L, Tan J, Xuan F. Flexible pressure sensor using carbon nanotube-wrapped polydimethylsiloxane microspheres for tactile sensing [J]. *Sens Actuator A Phys*. 2018;284:260–5.
- Mengting X, Cai H, Liu Z, Chen F, Chen L, Chen X, Cheng X, Dai F, Li Z. Breathable, degradable piezoresistive skin sensor based on a sandwich structure for high-performance pressure detection [J]. *Adv Electron Mater*. 2021;7(10):2100368.
- Ning C, Dong K, Cheng R, Yi J, Ye C, Peng X, Sheng F, Yang J, Wang ZL. Flexible and stretchable fiber-shaped triboelectric nanogenerators for biomechanical monitoring and human-interactive sensing [J]. *Adv Funct Mater*. 2020;31(4):2006679.
- Ouyang H, Tian J, Sun G, Yang Z, Liu Z, Hu L, Zhao L, Shi B, Fan Y, Fan Y, Wang ZL, Li Z. Self-powered pulse sensor for antidiastole of cardiovascular disease [J]. *Adv Mater*. 2017;29(40):1703456.
- Pang Y, Wang D, Jian M, Zhang Y, Liang R, Tian H, Yang Y, Ren T-L. Epidermis microstructure inspired graphene pressure sensor with random distributed spinosum for high sensitivity and large linearity [J]. *ACS Nano*. 2018;12(3):2346–54.
- Park DY, Joe DJ, Kim DH, Park H, Han JH, Jeong CK, Park H, Park JG, Joung B, Lee KJ. Self-powered real-time arterial pulse monitoring using ultrathin epidermal piezoelectric sensors [J]. *Adv Mater*. 2017;29:1702308.
- Park J, Kim J, Hong J, Lee H, Lee Y, Cho S, Kim S-W, Kim JJ, Kim SY, Ko H. Tailoring force sensitivity and selectivity by microstructure engineering of multidirectional electronic skins [J]. *NPG Asia Mater*. 2018a;10(4):163–76.
- Park SW, Das PS, Park JY. Development of wearable and flexible insole type capacitive pressure sensor for continuous gait signal analysis [J]. *Org Electron*. 2018b;53:213–20.
- Peng Y, Que M, Leed HE, Bao R, Wang X, Lu J, Yuan Z, Li X, Tao J, Sun J, Zhai J, Leed KJ, Pan C. Achieving high-resolution pressure mapping via flexible GaN/ZnO nanowire LEDs array by piezo-phototronic effect [J]. *Nano Energy*. 2019;58:633–40.
- Qi W, Qiao Y, Guo R, Naveed S, Hirtz T, Li X, Yixin F, Wei Y, Deng G, Yang Y, Xiaoming W, Ren T-L. Triode-mimicking graphene pressure sensor with positive resistance variation for physiology and motion monitoring [J]. *ACS Nano*. 2020;14(8):10104–14.
- Qin Z, Sun X, Qingyu Y, Zhang H, Xiaojun W, Yao M, Liu W, Yao F, Li J. Carbon nanotubes/hydrophobically associated hydrogels as ultrastretchable, highly sensitive, stable strain, and pressure sensors [J]. *ACS Appl Mater Interfaces*. 2020;12(4):4944–53.
- Qiu Z, Wan Y, Zhou W, Yang J, Yang J, Huang J, Zhang J, Liu Q, Huang S, Bai N, Wu Z, Hong W, Wang H, Guo CF. Ionic skin with biomimetic dielectric layer templated from calathea zebrine leaf [J]. *Adv Funct Mater*. 2018;28(37):1802343.
- Rajitha G, Dash RK. Optically transparent and high dielectric constant reduced graphene oxide (RGO)-PDMS based flexible composite for wearable and flexible sensors [J]. *Sens Actuator A Phys*. 2018;277:26–34.
- Ray TR, Choi J, Bandodkar AJ, Krishnan S, Gutruf P, Tian L, Ghaffari R, Rogers JA. Bio-integrated wearable systems: a comprehensive review [J]. *Chem Rev*. 2019;119(8):5461–533.
- Rui FENG, Tang F, Zhang N, Wang X. Flexible, high-power density, wearable thermoelectric nanogenerator and self-powered temperature sensor [J]. *ACS Appl Mater Interfaces*. 2019;11(42):38616–24.

- Savariraj AD, Salih A, Alam F, Elsherif M, AlQattan B, Khan AA, Yetisen AK, Butt H. Ophthalmic sensors and drug delivery [J]. *ACS Sens.* 2021;6(6):2046–76.
- Schüssler-Fiorenza Rose SM, Contrepois K, Moneghetti KJ, Zhou W, Mishra T, Mataraso S, Dagan Rosenfeld O, Ganz AB, Dunn J, Hornburg D, Rego S, Perelman D, Ahadi S, Sailani MR, Zhou Y, Leopold SR, Chen J, Ashland M, Christle JW, Avina M, Limcaoco P, Ruiz C, Tan M, Butte AJ, Weinstock GM, Slavich GM, Sodergren E, McLaughlin TL, Haddad F, Snyder MP. A longitudinal big data approach for precision health [J]. *Nat Med.* 2019;25(5):792–804.
- Seyedin S, Uzun S, Levitt A, Anasori B, Dion G, Gogotsi Y, Razal JM. MXene composite and coaxial fibers with high stretchability and conductivity for wearable strain sensing textiles [J]. *Adv Funct Mater.* 2020;3:1910504.
- Shi R, Lou Z, Chen S, Shen G. Flexible and transparent capacitive pressure sensor with patterned microstructured composite rubber dielectric for wearable touch keyboard application [J]. *Sci China Mater.* 2018;61(12):1587–95.
- Shi J, Liu S, Zhang L, Yang B, Shu L, Yang Y, Ren M, Wang Y, Chen J, Chen W, Chai Y, Tao X. Smart textile-integrated microelectronic systems for wearable applications [J]. *Adv Mater.* 2020a;32(5):e1901958.
- Shi Q, Dong B, He T, Sun Z, Zhu J, Zhang Z, Lee C. Progress in wearable electronics/phonics—moving toward the era of artificial intelligence and internet of things [J]. *InfoMat.* 2020b;2:1131–62.
- Shin K-Y, Lee JS, Jang J. Highly sensitive, wearable and wireless pressure sensor using free-standing ZnO nanoneedle/PVDF hybrid thin film for heart rate monitoring [J]. *Nano Energy.* 2016;22:95–104.
- Shin J, Yan Y, Bai W, Xue Y, Gamble P, Tian L, Kandela I, Haney CR, Spees W, Lee Y, Choi M, Ko J, Ryu H, Chang J-K, Pezhoh M, Kang S-K, Won SM, Yu KJ, Zhao J, Lee YK, MacEwan MR, Song S-K, Huang Y, Ray WZ, Rogers JA. Bioresorbable pressure sensors protected with thermally grown silicon dioxide for the monitoring of chronic diseases and healing processes [J]. *Nat Biomed Eng.* 2019;3(1):37–46.
- Shuaidi Zhang H, Liu SY, Shi X, Zhang D, Shan C, Mi L, Liu C, Shen C, Guo Z. Ultrasensitive and highly compressible piezoresistive sensor based on polyurethane sponge coated with a cracked cellulose nanofibril/silver nanowire layer [J]. *ACS Appl Mater Interfaces.* 2019;11(11):10922–32.
- Song Z, Weiyang Li Y, Bao WW, Liu Z, Han F, Han D, Niu L. Bioinspired microstructured pressure sensor based on a Janus graphene film for monitoring vital signs and cardiovascular assessment [J]. *Adv Electron Mater.* 2018;4:1800252.
- Sundaram S, Kellnhofer P, Li Y, Zhu J-Y, Torralba A, Matusik W. Learning the signatures of the human grasp using a scalable tactile glove [J]. *Nature.* 2019;569(7758):698–702.
- Tan Y, Liu X, Tang W, Chen J, Zhu Z, Li L, Zhou N, Kang X, Dongliang X, Wang L, Wang G, Tan H, Li H. Flexible pressure sensors based on bionic microstructures: from plants to animals [J]. *Adv Mater Interfaces.* 2022;9:2101312.
- Tang X, Wu C, Lin G, Zhang T, Zhou T, Huang J, Wang H, Xie C, Zeng D. Multilevel microstructured flexible pressure sensors with ultrahigh sensitivity and ultrawide pressure range for versatile electronic skins [J]. *Small.* 2019;15(10):e1804559.
- Tang G, Shi Q, Zhang Z, He T, Sun Z, Lee C. Hybridized wearable patch as a multi-parameter and multi-functional human-machine interface [J]. *Nano Energy.* 2021;81:105582.
- Tao L-Q, Tian H, Liu Y, Zhen-Yi J, Pang Y, Chen Y-Q, Wang D-Y, Tian X-G, Yan J-C, Deng N-Q, Yang Y, Ren T-L. An intelligent artificial throat with sound-sensing ability based on laser induced graphene [J]. *Nat Commun.* 2017;8:14579.
- Wan Y, Wang Y, Guo CF. Recent progresses on flexible tactile sensors [J]. *Mater Today Phys.* 2017;1:61–73.
- Wan C, Chen G, Yangming F, Wang M, Matsuhisa N, Pan S, Pan L, Yang H, Wan Q, Zhu L, Chen X. An artificial sensory neuron with tactile perceptual learning [J]. *Adv Mater.* 2018;30(30):e1801291.

- Wang ZL. Triboelectric nanogenerator (TENG)—sparking an energy and sensor revolution [J]. *Adv Energy Mater.* 2020;10:2000137.
- Wang Z, Wang S, Zeng J, Ren X, Chee AJY, Yiu BYS, Chung WC, Yang Y, Yu ACH, Roberts RC, Tsang ACO, Chow KW, Chan PKL. High sensitivity, wearable, piezoresistive pressure sensors based on irregular microhump structures and its applications in body motion sensing [J]. *Small.* 2016;12(28):3827–36.
- Wang X, Liu Z, Zhang T. Flexible sensing electronics for wearable/attachable health monitoring [J]. *Small.* 2017;13:1602790.
- Wang J, Jeevarathinam AS, Jhunjunwala A, Ren H, Lemaster J, Luo Y, Fenning DP, Fullerton EE, Jokerst JV. A wearable colorimetric dosimeter to monitor sunlight exposure [J]. *Adv Mater Technol.* 2018a;2018:1800037.
- Wang Z, Zhang L, Liu J, Jiang H, Li C. Flexible hemispheric microarrays of highly pressure-sensitive sensors based on breath figure method [J]. *Nanoscale.* 2018b;10(22):10691–8.
- Wang J-C, Karmakar RS, Lu Y-J, Chan S-H, Wu M-C, Lin K-J, Chen C-K, Wei K-C, Hsu Y-H. Miniaturized flexible piezoresistive pressure sensors: poly(3,4-ethylenedioxythiophene);poly(styrenesulfonate) copolymers blended with graphene oxide for biomedical applications [J]. *ACS Appl Mater Interfaces.* 2019a;11(37):34305–15.
- Wang K, Lou Z, Wang L, Zhao L, Zhao S, Wang D, Han W, Jiang K, Shen G. Bioinspired interlocked structure-induced high deformability for two-dimensional titanium carbide (MXene)/natural microcapsule-based flexible pressure sensors [J]. *ACS Nano.* 2019b;13(8):9139–47.
- Wang L, Chen Y, Lin L, Wang H, Huang X, Xue H, Gao J. Highly stretchable, anti-corrosive and wearable strain sensors based on the PDMS/CNTs decorated elastomer nanofiber composite [J]. *Chem Eng J.* 2019c;362:89–98.
- Wang J, Jiang J, Zhang C, Sun M, Han S, Zhang R, Liang N, Sun D, Liu H. Energy-efficient, fully flexible, high-performance tactile sensor based on piezotronic effect: piezoelectric signal amplified with organic field-effect transistors [J]. *Nano Energy.* 2020;76(18):105050.
- Xia K, Wang C, Jian M, Wang Q, Zhang Y. CVD growth of fingerprint-like patterned 3D graphene film for an ultrasensitive pressure sensor [J]. *Nano Res.* 2017;11(2):1124–34.
- Xia S-Y, Long Y, Huang Z, Zi Y, Tao L-Q, Li C-H, Sun H, Li J. Laser-induced graphene (LIG)-based pressure sensor and triboelectric nanogenerator towards high-performance self-powered measurement-control combined system [J]. *Nano Energy.* 2022;96:107099.
- Xianzhang W, Hou K, Huang J, Wang J, Yang S. Graphene-based cellular materials with extremely low density and high pressure sensitivity based on self-assembled graphene oxide liquid crystals [J]. *J Mater Chem C.* 2018;6(32):8717–25.
- Xiaohe H, Jiang Y, Ma Z, He Q, He Y, Zhou T, Zhang D. Highly sensitive P(VDF-TrFE)/BTO nanofiber-based pressure sensor with dense stress concentration microstructures [J]. *ACS Appl Polym Mater.* 2020;2(11):4399–404.
- Xiaoyu Chen H, Liu YZ, Zhai Y, Liu X, Liu C, Mi L, Guo Z, Shen C. Highly compressible and robust polyimide/carbon nanotube composite aerogel for high-performance wearable pressure sensor [J]. *ACS Appl Mater Interfaces.* 2019;11(45):42594–606.
- Xiong Y, Shen Y, Tian L, Yougen H, Zhu P, Sun R, Wong C-P. A flexible, ultra-highly sensitive and stable capacitive pressure sensor with convex microarrays for motion and health monitoring [J]. *Nano Energy.* 2020;2020:104436.
- Yang T, Jiang X, Zhong Y, Zhao X, Lin S, Li J, Li X, Jianlong X, Li Z, Zhu H. A wearable and highly sensitive graphene strain sensor for precise home-based pulse wave monitoring [J]. *ACS Sens.* 2017;2(7):967–74.
- Yang JC, Mun J, Kwon SY, Park S, Bao Z, Park S. Electronic skin: recent progress and future prospects for skin-attachable devices for health monitoring, robotics, and prosthetics [J]. *Adv Mater.* 2019;31(48):e1904765.
- Yang Y, Pan H, Xie G, Jiang Y, Chen C, Yuanjie S, Wang Y, Tai H. Flexible piezoelectric pressure sensor based on polydopamine-modified BaTiO₃/PVDF composite film for human motion monitoring [J]. *Sens Actuator A Phys.* 2020;301:111789.

- Yang T, Deng W, Chu X, Wang X, Yeting H, Fan X, Song J, Gao Y, Zhang B, Tian G, Xiong D, Zhong S, Tang L, Yonghe H, Yang W. Hierarchically microstructure-bioinspired flexible piezoresistive bioelectronics [J]. *ACS Nano*. 2021;15(7):11555–63.
- Yuan Z, Zhou T, Yin Y, Cao R, Li C, Wang ZL. Transparent and flexible triboelectric sensing array for touch security applications [J]. *ACS Nano*. 2017;11(8):8364–9.
- YuHao Q, JunPing Z. An Azo-PDMS-based wearable UV sensor with the optimized photo response mode for dual sensing and synchronous detection [J]. *Sci China Technol Sci*. 2022;65:179–90.
- Zhang J, Wan L, Gao Y, Fang X, Ting L, Pan L, Xuan F. Highly stretchable and self-healable MXene/polyvinyl alcohol hydrogel electrode for wearable capacitive electronic skin [J]. *Adv Electron Mater*. 2019;5:1900285.
- Zhang W, Yan Xiao Y, Duan NL, Linlin W, Lou Y, Wang H, Peng Z. A high-performance flexible pressure sensor realized by overhanging cobweb-like structure on a micropost array [J]. *ACS Appl Mater Interfaces*. 2020;12(43):48938–47.
- Zhao J, Guo H, Pang YK, Xi F, Yang ZW, Liu G, Guo T, Dong G, Zhang C, Wang ZL. Flexible organic triboelectric transistor for pressure and magnetic sensing [J]. *ACS Nano*. 2017;11(11):11566–73.
- Zhao T, Li T, Chen L, Yuan L, Li X, Zhang J. Highly sensitive flexible piezoresistive pressure sensor developed using biomimetically textured porous materials [J]. *ACS Appl Mater Interfaces*. 2019;11(32):29466–73.
- Zhong J, Li Z, Takakuwa M, Inoue D, Hashizume D, Jiang Z, Shi Y, Lexiang O, Nayeem MOG, Umezu S, Fukuda K, Someya T. Smart face mask based on an ultrathin pressure sensor for wireless monitoring of breath conditions [J]. *Adv Mater*. 2022;34(6):e2107758.
- Zhu B, Ling Y, Yap LW, Yang M, Lin F, Gong S, Wang Y, An T, Zhao Y, Cheng W. Hierarchically structured vertical gold nanowire array-based wearable pressure sensors for wireless health monitoring [J]. *ACS Appl Mater Interfaces*. 2019;11(32):29014–21.
- Zou R, Shan S, Huang L, Chen Z, Lawson T, Lin M, Yan L, Liu Y. High-performance intraocular biosensors from chitosan-functionalized nitrogen-containing graphene for the detection of glucose [J]. *ACS Biomater Sci Eng*. 2019;6(1):673–9.

Chapter 11

Microfluidics and Lab-on-a-Chip for Biomedical Applications



Dinesh K. Patel, Maria Mercedes Espinal, Tejal V. Patil, Keya Ganguly,
Sayan Deb Dutta, Rachmi Luthfikasari, and Ki-Taek Lim

11.1 Introduction

The development and testing of new drugs have significant concerns worldwide. The main challenges are that development costs are very high, it takes a very long time for these drugs to become available to those who need them, and drug development ultimately fails more often than it succeeds. The traditional tools (cell culture and animal model) used for drug development and testing are one of the major factors for low productivity. The cell culture involves transplanting of cells from their native environment to a foreign flat condition, leading to poor results in cell responsiveness experiments. In contrast, animal models fail to predict the influences of a particular drug on humans. Therefore, the development of personalized in vitro tools is required for cell cultures, providing the dynamically reactive environment to the cells as in vivo conditions. However, the manipulations of the fluids flow at milli- to nanoscopic scales are critical challenges for developing such tools.

D. K. Patel · M. M. Espinal · K. Ganguly · S. D. Dutta · R. Luthfikasari
Department of Biosystems Engineering, Institute of Forest Science, Kangwon National
University, Chuncheon, Republic of Korea

T. V. Patil
Interdisciplinary Program in Smart Agriculture, Kangwon National University,
Chuncheon, Republic of Korea

K.-T. Lim (✉)
Department of Biosystems Engineering, Institute of Forest Science, Kangwon National
University, Chuncheon, Republic of Korea

Interdisciplinary Program in Smart Agriculture, Kangwon National University,
Chuncheon, Republic of Korea
e-mail: ktlim@kangwon.ac.kr

Microfluidics and related concepts have provided a new platform to design, build, and engineer a suitable area for cell cultivation and experimentation for advancing drug development and personalized medicine and reducing the need for animal testing (TED 2013). It is well established that fluid flow behavior is widely affected by the design of the developed platforms (Preetam et al. 2022). The origins of microfluidics and its related counterparts began in 1960 with the development of microelectromechanical systems (MEMS) technology. In 1965, the development of the inkjet printer further accelerated this technology.

The first lab-on-a-chip (LoC) was developed in 1979. The soft lithographical technique was introduced to fabricate microfluidic channels in 1995. George McClelland Whitesides developed polydimethylsiloxane (PDMS)-based microfluidic chips in 1998. The droplet microfluidic system was developed in 2000, followed by the development of microfluidic cell culture systems. The first organ-on-a-chip (OoC) was fabricated in 2005, followed by the development of paper-based microfluidics through the soft lithography technique. The three-dimensional (3D) printing techniques were utilized to develop more sophisticated microfluidics in 2008. Developing “open-space” microfluidics became a crucial step in related bioanalytical technologies toward personalized medicine (2021) (Delamarche 2018). The origin of the Drop-Seq technology enables biologists to analyze RNA expression genome-wide in thousands of individual cells at once via a droplet-based system (Goldman et al. 2022). The benefits of microfluidics have been acknowledged worldwide. Several efforts are being made to develop microfluidics applications for end-user systems and mass production (Chen et al. 2021a). The history of microfluidics development is represented in Fig. 11.1.

In 1990, the Defense Advanced Research Projects Agency (DARPA) of the US Department of Defense supported a series of programs to develop field-deployable microfluidic systems for chemical and biological threats (Whitesides 2006). These technological advancements in microfluidics have prompted high-tech uprisings in

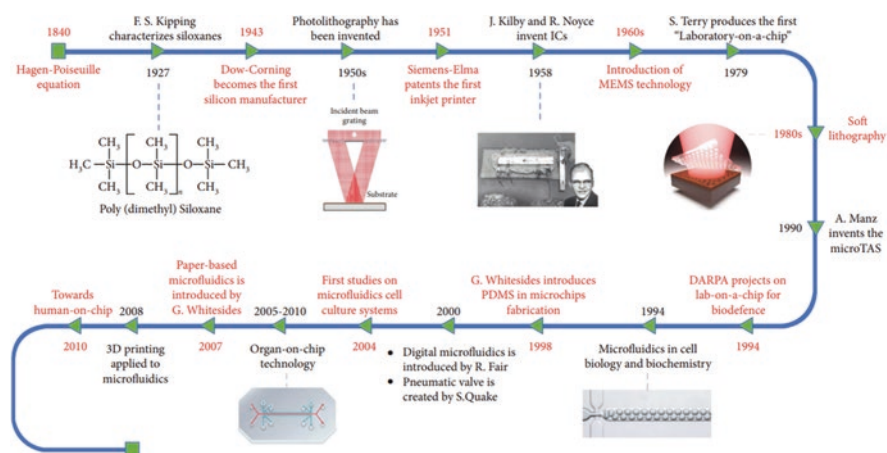


Fig. 11.1 Timeline showing the progress in the microfluidic technology. (Khorsandi et al. 2021)

numerous biomedical disciplines, including diagnostics, single-cell analysis, micro- and nanodevice fabrication, organ-in-chip platforms, and med-tech applications (Preetam et al. 2022). Microfluidic devices have significant roles in biomedical applications involving the advancement of nanomedicine. Nanomedicine involves the utilization of nanoscale or nanostructured materials in medical applications, such as biosensing and imaging, disease diagnosis, and therapeutic delivery. The nanomaterials used in nanomedicine have unique medical effects according to their structures. Thus, the combination of microfluidic technologies and nanomedicine provides numerous benefits, including improved bioavailability, targeting ability, delivery efficacy, dose-response, and personalization compared to conventional medicines (Chen et al. 2021b). Traditionally, animal models have been widely exploited to assess nanomedicine potentials. However, the tracking of nanomedicine in vivo and physiological responses between animals and humans have seriously misunderstood such drugs' efficacy and toxicity (Chen et al. 2021b). Thus, microfluidic technology has proven to be effective in analyzing and synthesizing molecules and these nanomedicines by way of a microfluidic device known as a LoCs (Whitesides 2006). The LoC devices have been utilized for biomedical applications with more realistic pharmacokinetics, toxicity, and metabolic modeling capabilities (Fritschen and Blaeser 2021). These advancements allow the development of in vitro human models that are more predictive of human responses as opposed to resorting to live animal models (Chen et al. 2021b). This effectivity has been augmented through coupling with computational modeling and LoCs (Nathanael et al. 2022). The LoC enables one or multiple laboratory functions such as sample preparation, assay, and detection on a single integrated system (Whitesides et al. 2006; Park et al. 2011). Fluid mechanics plays a critical role at the microscale, especially in healthcare applications. The fluid flows in microfluidic devices usually occur on a small scale and at a slow speed (Battat et al. 2022). The flow dynamics, including laminar, transitional, and turbulent flow, enable efficient and faster reactions, significantly minimizing chemical wastes (Mathur and Roy 2022). The LoC devices can provide several benefits, including less reagent consumption, fast response time, effective process control, and low-cost chip fabrication (Namgung et al. 2020; Cho et al. 2021). The laminar flow is smooth, and even motion of the particles occurs across pathways. Fluids move in regular layers with minimal mixing between layers due to a lack of random fluctuations in velocity. The turbulent flow is irregular, and particles are mixed across a pathway. The fluid velocities fluctuate at random and chaotic intervals, causing chaotic particle movement and swirling regions in the medium. A transitional flow occurs during the transition from laminar to turbulent flow and vice versa. During this transition, particles flow along a smooth pathway and occasionally disperse in bursts of random motion (Engineer 2020). A schematic representation of these concepts is shown in Fig. 11.2.

Despite these, the primary challenge in developing microfluidic devices is specific flow dynamics in the designing and fabricating such device platforms. The rapid advancements in materials science and micro/nanofabrication methodologies have enabled the development and analysis of large numbers of point-of-care and

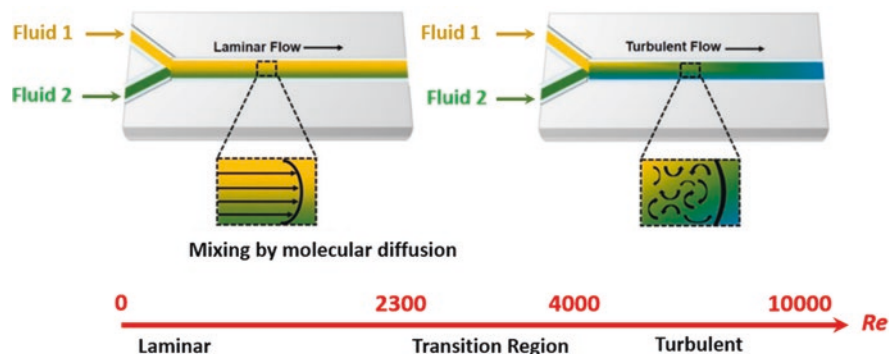


Fig. 11.2 The schematic presentation for laminar and turbulent flow. The Reynolds number (Re) indicates the physical properties of the fluid flow in microfluidic channel. In laminar flow ($Re < 2300$), the two streams move in parallel to the flow direction and mixed based on the diffusion (left). In turbulent flow ($Re > 4000$), fluids move in all three dimensions without correlation with the flow direction (right). The transition region ($2300 < Re < 4000$) shares the features of laminar and turbulent flow. (Saliba et al. 2018)

LoC devices for the promotion of a variety of applications, including chemical synthesis (Jing et al. 2018; Yen et al. 2005; Visaveliya and Kohler 2014; Nathanael et al. 2022), pharmaceutical research in drug development (Pihl et al. 2005; Wu et al. 2010; Bendre et al. 2022), energy conversion and storage (Ibrahim et al. 2022; Zeng et al. 2020), environmental monitoring (Pol et al. 2017), and various other applications (Mathur and Roy 2022).

An OoC is a subset of a LoC. It is a 3D microfluidic cell culture chip that contains continuously perfused chamber(s) inhabited by living cells. The purpose of these devices is to accurately simulate the activities, functionality, mechanics, and physiological response of entire organs and organ systems (Chen et al. 2021b). The fabrication of OoCs combines bioengineering and mechanical engineering concepts, thus representing biotechnology's cutting edge (Piergiovanni et al. 2021). They offer enormous potential to bridge the gap between scalable production desired by industry and the cell biological complexity required for efficient and predictive use (Fritschen and Blaeser 2021). The OoCs have the potential to revolutionize many fields, including biomedical research, drug discovery, and cost reduction in preclinical trials. OoCs aid in this through the possibility of accurate, high-throughput, systematic, and repetitive quantitative investigations via extensive qualification processes (Piergiovanni et al. 2021). Additionally, with these favorable prospects, OoCs have the potential to reduce or even stop the need for in vivo animal testing by replacing the traditional translational animal model with a microfluidic model. This chapter highlights the various aspects of microfluidics, including the fabrication of healthcare-oriented microfluidic and LoC devices and their biomedical applications.

11.2 Fabrication of Microfluidic System

Depending on the requirements, the microfluidic devices are developed using different materials, as shown in Fig. 11.3a. Polymer, silicon, glass, stainless steel, metal, and plastic are used to develop millifluidic, microfluidic, and nanofluidic devices (Hao et al. 2018). Silicon-based devices are the most advantageous because they offer broader flexibilities to various experimental conditions and have the advantage of low cost (Yen et al. 2005). Engineering techniques have allowed the accurate and precise fabrication of various microfluidic-enabled LoC models. These techniques are broadly categorized into two major categories: additive manufacturing and non-additive manufacturing. The conventional preparation techniques are classified into top-down and bottom-up approaches (Luo et al. 2019). Additive manufacturing is commonly known as three-dimensional (3D) printing, which includes stereolithography, fused deposition modeling (FDM), hydrogel inkjet printing, etc. (Zeng et al. 2020). In stereolithography, a high-intensity laser is focused into a spot, which selectively polymerizes the photopolymerizable resins or monomers at the spot, as

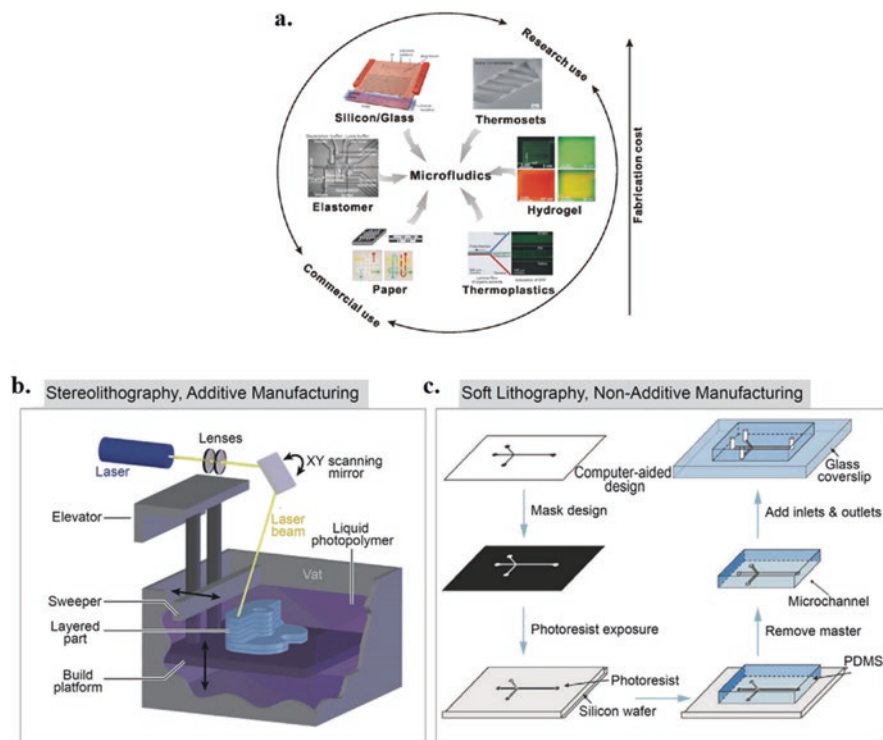


Fig. 11.3 (a) Microfluidic chip fabrication materials and cost based on intention of use (Ren et al. 2013). Fabrication methods for millifluidic, microfluidic, and nanofluidic devices. (b) Stereolithography, an additive manufacturing method, and (c) soft lithography, a nonadditive manufacturing method, for millifluidic and microfluidic devices. (Chen et al. 2021a)

seen in Fig. 11.3b. Therefore, the stereolithographic resolution is dependent on the size of the spot. A 3D structure can be generated through a *layer-by-layer* polymerization process by scanning of laser spot in the x-y plane via the x-y scanning mirror and moving the model along the z-axis via the elevator. Projections of digital light spots from light-emitting diode (LED) sources are exploited to simultaneously polymerize an entire layer of resins or monomers at each time. The resolution of the constructed structure depends on the pixel size of LED sources. Selective laser sintering is similar to stereolithography, where the sinter powders of metals, ceramics, or polymers are generally used to construct complex objects (Chen et al. 2021a). FDM and hydrogel inkjet printing are other forms of additive manufacturing techniques. These techniques have features of extruding precursors out of a nozzle, which is subsequently solidified. In FDM, the thermoplastic materials are heated up to their melting point in the printer head and then extruded out of the nozzle, which becomes hard on cooling in the air (Chen et al. 2021a). In hydrogel inkjet printing, the hydrogels are extruded from the nozzle and subsequently polymerized or cross-linked (Yang et al. 2021).

Nonadditive manufacturing techniques include soft lithography, direct laser writing, and glass capillary (Zhang et al. 2020; Yu et al. 2018). Among these, soft lithography is most widely used in microfluidics. In soft lithography, the master pattern is prepared on a silicon wafer using a photomask and photoresist, followed by replication using PDMS, which eventually bonds to a glass coverslip or a PDMS slab, as schematically illustrated in Fig. 11.3c. In contrast to glass capillary microfluidic devices, PDMS devices have the advantages of flexible design, good biocompatibility, and high gas permeability. However, some drawbacks include their two-dimensional (2D) channel geometry, poor chemical resistance, and the difficulty of fabrication (Chen et al. 2021a).

The top-down approach involves a mechanical breakdown of large materials through sonication, ball milling, plasma, homogenization, and pyrolysis (Hatzor and Weiss 2001), whereas the bottom-up approach involves atomic or molecular condensation to assemble particles via polymerization, sol-gel reaction, microemulsion, coprecipitation, laser vaporization, and metal evaporation (Visaveliya and Kohler 2014). A high-resolution microfluidic device can be fabricated with these techniques. However, soft lithography is most widely used in microfluidics and LoC fabrication (Chen et al. 2021a). A summary of these techniques is given in Table 11.1.

11.3 Significance of Nonlinear Process in Microfluidics

To better understand fluid dynamics at smaller scales, we must consider the importance of nonlinear phenomena in microfluidic devices. Nonlinear microfluidics involves inertial flows, stimuli-responsive materials in microfluidic devices, and non-Newtonian fluids. Most fluid flows in microfluidic devices occur at low Reynolds numbers (Re). The Reynolds number is a dimensionless parameter that describes the ratio of inertial forces ($\rho v^2/L$) to viscous forces ($\mu v/L^2$) acting on a

Table 11.1 A summary of the techniques, resolution, materials, advantages, and disadvantages of millifluidics-, microfluidics-, and nanofluidics-based devices (Chen et al. 2021a)

| | Techniques | Resolution | Materials | Advantages | Disadvantages |
|---------------------------------|----------------------------------|--------------------------|---|--|--|
| Millifluidics and microfluidics | <i>Additive manufacturing</i> | | | | |
| | Stereolithography | 25–300 μm | Photopolymerized resins or monomers | Easy to process, flexible design | Limited materials, small volume |
| | Selective laser sintering | 1–150 μm | Metals, ceramics, or polymeric powders | Favorable for ceramics, and metals | Easy clogging, and time consuming |
| | Fused deposition modeling | 100–400 μm | Polystyrene, polyamide, polylactic acid, acrylonitrile butadiene styrene, and polymethyl methacrylate | Easy to process, low cost, and flexible design | Fragile, and low resolution |
| | Hydrogel inkjet printing | 5–100 μm | Cross-linking hydrogels | Biocompatible, and flexible design | Expensive, and restricted to limited materials |
| | <i>Nonadditive manufacturing</i> | | | | |
| | Direct laser writing | 100 nm–1 μm | Polymers, and glasses | Easy to design, and high resolution | Easy clogging, and time consuming |
| | Soft lithography | 100 nm–100 μm | Polydimethylsiloxane | Flexible design, gas permeable, and biocompatible | Low chemical resistance, two-dimensional channel, and time consuming |
| | Glass capillary | 10–100 μm | Glass capillaries | Low cost, chemical resistance, and three-dimensional channel | Fragile, and limited design |

(continued)

Table 11.1 (continued)

| | Techniques | Resolution | Materials | Advantages | Disadvantages |
|--------------|-------------------------|------------|---|------------------------------|------------------------------|
| Nanofluidics | <i>Top-down method</i> | | | | |
| | Nanomachining | 10–100 nm | Silica and their derivatives | Good resolution | Expensive and time consuming |
| | Nanoimprint lithography | 10–100 nm | Photopolymerized resins or monomers | Easy to process | Restricted design |
| | <i>Bottom-up method</i> | | | | |
| | Self-assembly | 0.1–10 nm | Different nanomaterials, such as graphene, carbon nanotubes, zeolite, boron nitrile, etc. | Highly ordered nanostructure | Restricted design |

volume element of fluid. The equation for the determination of Re is mentioned below:

$$Re = \frac{\rho v L}{\mu}$$

where Re , ρ , v , L , and μ are Reynolds numbers, the density of the fluid, characteristic velocity of the fluid, characteristic linear dimension, and dynamic viscosity of the fluid, respectively (Stone et al. 2004; Anna 2016; Ajaev and Homsy 2006).

The Stokes equation (below) approximates the Navier-Stokes equation in the limit of low Reynolds numbers for incompressible, single-phase Newtonian fluids:

$$0 = -\nabla p + \mu \nabla^2 U$$

where p , μ , and U are the pressure, dynamic viscosity of the fluid, and velocity field, respectively.

The continuity equation gives the conditions for the conservation of mass of incompressible fluids:

$$\nabla \cdot U = 0$$

This provides better information about the nonlinear phenomena in microfluidics to develop more streamlined devices for biomedical applications, such as LoC models (Battat et al. 2022).

Fluid flow, such as blood or interstitial flow, is crucially important for the functions of all tissues, with cells responding to flow-through mechanisms such as differentiation and metabolic adaptation (Chen et al. 2021b). In comparison to the static culture models, microfluidics permits continuous nutrient exchange, better oxygen perfusion, and physiological shear stress, which provide a better emulation of conditions in living organisms, including readily mimicking the complex dynamic microscale 3D environments found *in vivo*; ability to control features such as gas exchange, nutritional composition, and metabolite and waste removal; and integration of multiple steps, such as cell culture, sampling, capture, lysis, imaging, and detection within a single device (Mehling and Tay 2014; Halldorsson et al. 2015).

11.4 Significance of Microfluidic Systems

Understanding the cellular behavior and its interactions with the extracellular matrices (ECM) is essential to designing new engineering tools to perturb local cell mechanics and guide its growth, differentiation, and regeneration (Li et al. 2022). The advantages of microfluidic systems are that they allow a great deal of freedom in fabrication. This, in turn, permits the customization of conditions within the device to mimic cellular and ECM conditions for accurate biomimetic cell behavior.

Cells require a sufficient exchange of nutrients and gases, which is mediated by convection and diffusive transport through liquid media (Filippi et al. 2022). Microchips can also precisely control the spatiotemporal oxygen distribution in 3D cell cultures (Rexius-Hall et al. 2014; Brennan et al. 2014).

It is essential to investigate the hypoxic microenvironment, a crucial pathological feature in many diseases, including cancer (Jiang et al. 2019; Filippi et al. 2019; Yang et al. 2020). Hypoxic tissue models can be produced by recreating physiologically relevant low and cycling oxygen levels that are not attainable in traditional macroscopic cell culture (Brennan et al. 2014). The additional advantages of the microfluidic systems are that they need minimum amounts of samples and reagents in *in vivo*-like environments (Filippi et al. 2022). A schematic representation of cellular behavior under different conditions is presented in Fig. 11.4. Miniaturization ensures a homogeneous reaction environment, efficient heat and mass transfer associated with the large surface-to-volume ratio, and controlled kinetic parameters within a continuous flow regime (Atencia and Beebe 2005). Miniaturization also reduces the consumption of chemicals, particularly with toxic, flammable, and potentially explosive properties, and therefore assists a safer operation with particular emphasis on environmental friendliness and green chemistry metrics (Tu et al. 2010). The microfluidic systems reduce costs due to the lesser use of expensive reagents. The continued focus on developing more optimized microfluidic systems has led to the ability of these systems to feature high resolution and sensitivity in the detection and separation of molecules. The microfluidic systems also reduce the footprint of analytical and diagnostic systems compared to the huge machines traditionally required to accomplish the lab. The microfluidic devices provide a sustainable operation control during automating multiple syntheses, facilitating fast

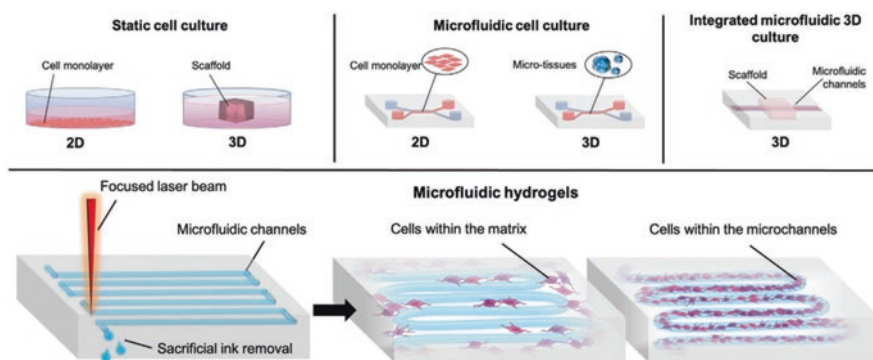


Fig. 11.4 Cellular approaches. Static culture of cell monolayers and 3D tissue constructs in plastic dishes (top, left). Microfluidic platforms for cell monolayers and microtissue culture (top, middle). Integrated microfluidic tissue culture (top, right), where scaffolds inserted in the microfluidic platform are crossed by microfluidic channels. Microfluidic flows can support integrated heterocellular cultures while regulating the nutrients' diffusion and the biomechanical cell stimulation. Microfluidic hydrogels can be generated by photo patterning of hydrogel matrices or removal of sacrificial inks from pre-designed channel networks (bottom, left). Cells can be seeded in the matrix or the microchannel space (bottom, right). (Filippi et al. 2022)

screening, and optimization of the parameters for multistep reaction processing. It enables shorter analysis times and faster results (Luo et al. 2019). The laminar flow of fluids in tiny channels allows a greater flow control (Filippi et al. 2022). The microfluidic systems aid a greater control of experimental parameters and sample concentration at the microscopic scale. Soft robotics development has advanced to promote the evolution of soft machines that can interact safely with natural environments and humans and adapt effectively to complex, dynamic situations (Filippi et al. 2022). Mechanically active OoC microdevices that reconstitute tissue-tissue interfaces facilitate cell culture models. The OoC provides low-cost alternatives to animal and clinical studies for drug screening and toxicology applications (Huh et al. 2010).

11.5 Biomedical Applications

11.5.1 *Organs-on-Chips (OoCs)*

The OoCs are multichannel analytical microfluidic devices used to study cell-nanoparticle interactions. The cell cultures present within these devices allow them to mimic various organs' bioactive and physiochemical properties (Bendre et al. 2022; Lin et al. 2022). Thus, they are an important tool for research on cell-cell interaction matrix influence and an organ's response to drug delivery (Fritschen and Blaeser 2021). Additionally, these microfluidics-based OoC techniques offer a promising way to resolve the challenges of a slow lab-to-clinic translation of nanomedicine. These devices allow for a complete understanding, evaluation, and ability to predict nanomaterial behaviors within the complex environment of human beings. A schematic design of OoCs is represented in Fig. 11.5. The sophisticatedly designed device biomimetics in vivo microenvironments provides robust platforms for evaluating nanomedicine (Chen et al. 2021b).

The OoCs approach has rapidly expanded in the past decade (2012–2022) to simulate organ tissues that can serve as physiological organ biomimetics for fundamental biological studies, drug development, and testing. A slight manipulation of fluid flow in microfluidic channels can further establish concentration gradients of biological cues directing cell migration or differentiation or provides shear forces analogous to the flow of blood and other fluids in the body (Wan et al. 2022). Before designing and fabricating OoCs, careful consideration must be taken to selecting cell types and biomaterials suitable to mimic the desired tissue of interest. The type, origin, and spatial distribution of tissue-specific stromal and parenchymal cells need to be analyzed (Fritschen and Blaeser 2021). These factors control cellular microenvironments with high spatiotemporal precision and present cells with mechanical and biochemical signals in a more physiologically relevant context (Meyvantsson and Beebe 2008; El-Ali et al. 2006; Whitesides et al. 2001).

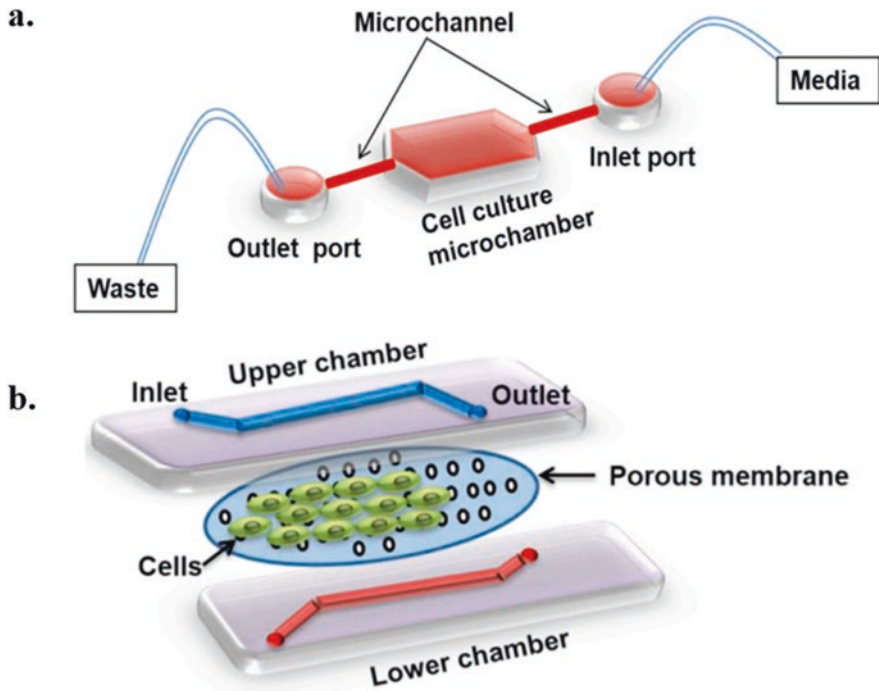


Fig. 11.5 A simple microfluidic OoC device. (a) Cells cultured inside the microchamber and (b) cells cultured on the surface of the porous membrane. (Syama and Mohanan 2021)

11.5.2 Lung-on-a-Chip (LuoC)

The lung is a highly complex organ with a treelike branched structure of highly specialized cells. The LuoC has emerged as a promising tool for modeling the complexity of human lung structure and function (Sone et al. 2021; Benam et al. 2016; Huh et al. 2010, 2012; Tavakol et al. 2021; Liu et al. 2021; Si et al. 2021). The LuoC structure mimics the physiological characteristic of lungs and natural airflow. It can be used to reveal the intrinsic interactions between lung tissue and materials. This knowledge can provide new insights into the effect of the toxicology of environmental particles on human lungs. In addition, LuoC devices can be used for the health assessment of air pollution and accurate methods for drug screening and toxicity testing (Lin et al. 2022). The LuoC gives significant information related to the movement of the pollutants from the respiratory tract to the alveolar tissues, and their deposition in lung tissues (Lin et al. 2022). A multifunctional LuoC mimics the interface found in the lungs. A dynamic air-liquid interface culture, tissue barrier function, and cilia and mucus and polar proteins and directional mucociliary clearance are the four major parts of a LuoC. The biologically inspired design of a human-breathing LuoC microdevice and its function is given in Fig. 11.6.

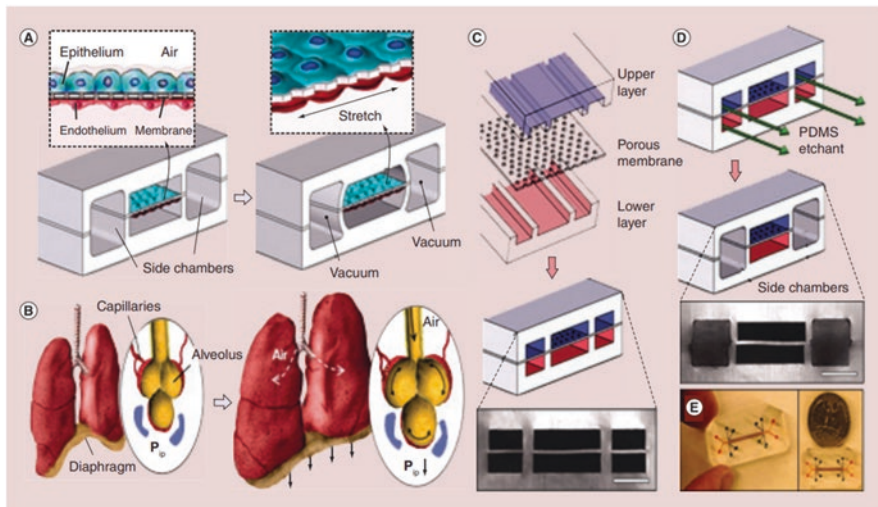


Fig. 11.6 Biologically inspired design of a human-breathing lung-on-a-chip microdevice. (a) The microfabricated lung mimic device uses compartmentalized PDMS microchannels to form an alveolar-capillary barrier on a thin, porous, flexible PDMS membrane coated with ECM. The device recreates physiological breathing movements by applying vacuum to the side chambers and causing mechanical stretching of the PDMS membrane forming the alveolar-capillary barrier. (b) During inhalation in the living lung, contraction of the diaphragm causes a reduction in intrapleural pressure (P_{ip}), leading to distension of the alveoli and physical stretching of the alveolar-capillary interface. (c) Three PDMS layers are aligned and irreversibly bonded to form two sets of three parallel microchannels separated by a 10-mm-thick PDMS membrane containing an array of through-holes with an effective diameter of 10 mm. Scale bar, 200 mm. (d) After permanent bonding, PDMS etchant is flowed through the side channels. Selective etching of the membrane layers in these channels produces two large side chambers to which vacuum is applied to cause mechanical stretching. Scale bar, 200 mm. (e) Images of an actual lung-on-a-chip microfluidic device viewed from above. (Bhattacharjee and Brayden 2015)

The dynamic air-liquid interface culture allows the mechanical distortion to the alveolar-capillary interface caused by breathing movements to develop a biomimetic device suitable for accurate *in vitro* testing (Huh et al. 2010). The alveolar-capillary tissue barrier assists the permeability and transport in the fabricated microsystem. The alveolar-capillary tissue barrier primarily refers to the components of barrier thickness, cellular composition, lack of alveolar macrophages, and changes in air pressure and flow. The cilia, mucus, and polar proteins and directional mucociliary clearance also play significant roles in the LuoC device. The microarchitecture of the LuoC allows for nanoparticle translocation, which is an asset in drug delivery applications (Huh et al. 2010).

The LuoC device has often been utilized to assess air pollution toxicity. However, LuoC devices proved their significance and effectiveness in diagnosing the coronavirus disease in 2019, showing the importance of microdevices in relieving the burden of the urgent demand for quick detections with a low cost and high sensitivity (Xing et al. 2020). The successful development of a human-breathing LuoC microdevice proves a proof of a biomimetic strategy's concept.

11.5.3 *Brain-on-a-Chip (BoC)*

The human brain is a highly dynamic and complex organ composed of 100 billion neurons and 1 trillion supportive glial cells arranged in a highly ordered manner. The structural and functional integrity maintenance of the human brain depends on a delicate balance between substrate delivery through blood flow and energy demands from neural activities (Abbott et al. 2010; Zlokovic 2011). The BoC devices have also been developed to culture the blood-brain barrier (BBB), neurons, and brain organoids in vitro (Sivandzade and Cucullo 2018). The mechanistic study of neural activity and the interactions between neurons, glial cells, and blood vessels in BoC devices is still limited. In addition, recent advances in microfluidic-integrated neural probes focus primarily on drug delivery (Pongrácz et al. 2013).

In contrast to blood that flows inside blood vessels, cerebrospinal fluid (CSF) is a clear, plasma-like fluid that surrounds the brain and spinal cord and bathes the central nervous system (CNS) (Adigun 2021). CSF is known as a cushion and a shock absorber during head trauma and contributes to the maintenance of intracranial pressure (ICP) and cerebral perfusion (Oshio et al. 2005; Bothwell et al. 2019). The capability of microfluidics to implement the spatial arrangement of cells or tissues during culture is particularly advantageous because most organs are structural tissues with a specific spatial organization of different cell types (Krausgruber et al. 2020). Recent advances in OoC technology provide an opportunity to control and simulate microenvironments in cell culture to construct 3D ex vivo microtissues/organs mimicking their in vivo counterparts (Mittal et al. 2019; Caballero et al. 2017). The microfluidic-based brain models have been developed to culture and guide the neural cells in micrometer-sized chambers, aiming to replicate the in vivo microenvironment better. Patterns are typically etched into flexible silicon or biocompatible polymeric molds, such as PDMS (Duffy et al. 1998). PDMS surface can be functionalized for cell culture by coating it with ECM molecules (Toepke and Beebe 2006). Small hollow chambers (1 mm × 1 mm) with openings at both ends of the PDMS for the inputs and outputs of culture media are created by inverting the mold and sealing it to a flat smooth substrate. Cells are loaded into the microchambers and cultured with regular medium exchange from the inlet and outlet reservoirs (Tan et al. 2021). In vivo, mechano-biological and biochemical factors can be mimicked by precision engineering and manipulating geometrical factors in microfluidic devices (Haring et al. 2017). The microgrooves connected with compartmentalized channels and assisted neurite growth across compartments while maintaining fluid isolation (Taylor et al. 2005). Owing to high fluid resistance in the microgrooves, the localized physical and chemical species could be contained in one compartment without leakage to other compartments (Taylor et al. 2005, 2010). Furthermore, the BoC accelerated the growth length, growth rate, the retraction rate of axons and dendrites, and factors for modulating growth (Taylor et al. 2005; Hengst et al. 2009; Riviaccio et al. 2009).

The design of a compartment channel enables the co-culturing of cells nearby or in direct contact, separated by a porous membrane or micropillars (Kilic et al. 2016;

Achyuta et al. 2013). Micropillars facilitated the independent analysis of different tissue while permitting the parametric control of microenvironment factors (Booth and Kim 2012). Hence, tissue-specific media can be maintained and sampled in separate compartments while supporting diverse cell populations. Analyzing of metabolites and other secretory products from separate cell populations also becomes possible in such systems. The BoC devices have been explored for reconstituting BBB by culturing endothelial cells or by co-culturing them with pericytes, glial cells (astrocytes and microglia), and neurons (Booth and Kim 2012; Achyuta et al. 2013; Adriani et al. 2017; Park et al. 2019; Walter et al. 2016). The BoC could aid the identification and development of new toxicity biomarkers and of disease processes and can act as an excellent test bed for therapeutic drug efficacy and toxicity (Park et al. 2019). The compartmentalized microfluidic-based devices have the leverage to differentiate human pluripotent stem cells (hPSCs). Kilic et al. differentiated hPSCs into a mixed neuronal-glial mixture in one chamber and cultured endothelial cells separately in another chamber, which permitted better mimicking of brain tissue (Kilic et al. 2016). The BoC device also opens new possibilities for integrating biochemical and bioelectronics sensors for real-time measurements, including transepithelial electrical resistance (TEER) electrodes to monitor the endothelial permeability of the BBB, or microelectrode arrays to monitor the electrical activity of neurons (Booth and Kim 2012; Park et al. 2019). Furthermore, BoC devices have advantages over animal models owing to their optical transparency, allowing the real-time visualization and high-resolution quantitative analyses of biological processes (Tan et al. 2021).

The microfluidic devices can be scaled up to achieve high-throughput measurements while reducing costs and using a lesser biological resource. Shi et al. reported a compartment-sensitive synapse microarray device that can be incorporated into a multi-well format, which enabled the screening of synaptogenic small molecules (Shi et al. 2011). The array of micro-holes permitted the precise positioning of non-neuronal cells expressing synaptic proteins, which allowed neurites to grow freely around these cells while encouraging synaptic formation at specific sites.

11.5.4 Joint/Muscle-on-a-Chip (JoC) and Human-on-a-Chip (HoC)

A JoC device is a multi-organ-on-chip platform that incorporates a range of engineered features to match essential aspects and functions of the human joint and recapitulates the joint's physiological responses. These features include biomimetically fabricated versions of articular cartilage, subchondral bone, synovial membrane, ligaments, and the meniscus. A schematic presentation for the preparation and organization of osteochondral and synovial membrane units of the JoC device is represented in Fig. 11.7a–b.

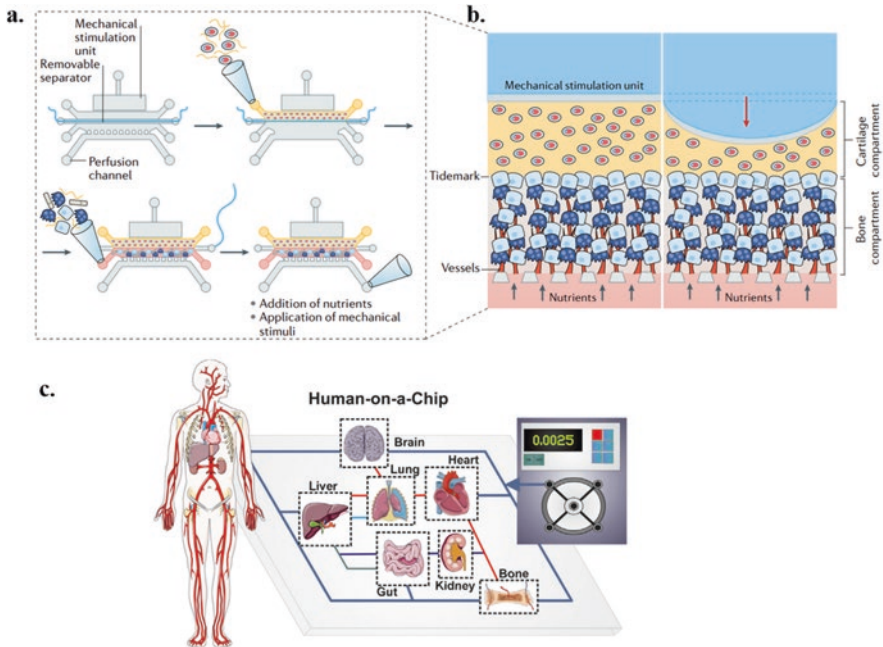


Fig. 11.7 A schematic presentation for the preparation and organization of osteochondral and synovial membrane units of the JoC platform. (a) Overview of the steps for preparing the osteochondral unit (side view), (b) side view of the osteochondral unit in static conditions (left) and with mechanical stimulation (right). The system includes upper and lower layers of 3D hydrogels of different properties, separated by a porous membrane. The upper cartilage compartment contains chondrocytes, and the lower bone compartment contains osteoblasts, osteoclasts, and endothelial cells (to form a microvasculature). The hydrogel used for the bone compartment could also be supplied with neural cells to mimic innervation. Nutrients are supplied to the entire system via a perfusion channel, and the entire tissue is exposed to mechanical actuation. Alternatively, the perfusion channel can be used to introduce immune cells into the system (Paggi et al. 2022), and (c) human-on-a-chip philosophy is by integrating different organ-on-a-chip devices in a single plate. (Piccollet-D'hahan et al. 2021)

The JoC device has potential and provides a next-generation caliber of *in vitro* models for studying the pathophysiology of rheumatoid arthritis (RA) and osteoarthritis (OA) and might prove indispensable for drug development (Paggi et al. 2022). The HoC microfluidic device is also known as me-on-a-chip. It is a specialized device with multiple OoC models on a single chip. A schematic presentation for different organ models (brain, liver, lung, heart, kidney, bone, and gut) in a single platform is shown in Fig. 11.7c. In conjunction, this HoC can simulate the functions of various human systems, including the respiratory, digestive, lymphatic, and excretory systems, from one microfluidic model (Chen et al. 2021b). The integrating multiple sensors and coupling other spectroscopic tools in the HoC device opens new possibilities for identifying the side effects of drugs, and patient responses.

11.6 Conclusion and Future Perspectives

Here, we discussed the progress of microfluidic devices, development methods, and biomedical applications. The precise control of fluid behavior in microfluidic devices makes them an attractive platform for multidisciplinary applications. Different characteristics, millifluidics, microfluidics, and nanofluidics have demonstrated different trends in their applications. The additive manufacturing methods make plenty of materials amenable to millifluidics and microfluidics, whereas non-additive manufacturing approaches provide more alternatives with low cost and flexible processing. Nanofluidic devices are often developed using the top-down method, which is expensive and complex. The advancement of technologies allows the inclusion of patient-derived cells in constructing disease-on-a-chip or tumor-on-a-chip for preclinical medical diagnosis, which is crucial for designing patient-specific therapies. The millifluidics, microfluidics, and nanofluidics possess unique advantages at their different length scales. They could jointly be applied to meet specific demands. The continuous progress in fundamental fluid sciences and developments of device fabrication techniques will inspire more innovative applications and make fluidic systems more and more important in the future. Despite the advantages, these systems need to overcome the barrier of low throughput, which result from their sophisticated structure and channel design. One promising solution is to combine these systems with 3D printing, such as the microfluidic 3D printing technique, which will further implement microfluidics with more powerful capabilities and make new functions or materials accessible.

Acknowledgments The Basic Science Research Program supported this work through the National Research Foundation of Korea (NRF) funded by the Ministry of Education (No. 2018R1A6A1A03025582, 2019R1D1A3A03103828, and 2022R111A3063302), Republic of Korea.

References

- Abbott NJ, Patabendige AA, Dolman DE, Yusof SR, Begley DJ. Structure and function of the blood-brain barrier. *Neurobiol Dis.* 2010;37:13–25.
- Achyuta AK, Conway AJ, Crouse RB, Bannister EC, Lee RN, Katnik CP, Behensky AA, Cuevas J, Sundaram SS. A modular approach to create a neurovascular unit-on-a-chip. *Lab Chip.* 2013;13:542–53.
- Adigun O. Anatomy, head and neck, cerebrospinal fluid [Online]. 2021. StatPearls.com. Available <https://www.statpearls.com/articlelibrary/viewarticle/19195/>
- Adriani G, Ma D, Pavesi A, Kamm RD, Goh EL. A 3D neurovascular microfluidic model consisting of neurons, astrocytes and cerebral endothelial cells as a blood-brain barrier. *Lab Chip.* 2017;17:448–59.
- Ajaev VS, Homsy GM. Modeling shapes and dynamics of confined bubbles. *Annu Rev Fluid Mech.* 2006;38:277–307.
- Anna SL. Droplets and bubbles in microfluidic devices. *Annu Rev Fluid Mech.* 2016;48:285–309.
- Atencia J, Beebe DJ. Controlled microfluidic interfaces. *Nature.* 2005;437:648–55.

- Battat S, Weitz DA, Whitesides GM. Nonlinear phenomena in microfluidics. *Chem Rev.* 2022;122:6921–37.
- Benam KH, Villenave R, Lucchesi C, Varone A, Hubeau C, Lee HH, Alves SE, Salmon M, Ferrante TC, Weaver JC, Bahinski A, Hamilton GA, Ingber DE. Small airway-on-a-chip enables analysis of human lung inflammation and drug responses in vitro. *Nat Methods.* 2016;13:151–7.
- Bendre A, Bhat MP, Lee K-H, Altalhi T, Alruqi MA, Kurkuri M. Recent developments in microfluidic technology for synthesis and toxicity-efficiency studies of biomedical nanomaterials. *Mater Today Adv.* 2022;13:100205.
- Bhattacharjee S, Brayden DJ. Development of nanotoxicology: implications for drug delivery and medical devices. *Nanomedicine.* 2015;10:2289–305.
- Booth R, Kim H. Characterization of a microfluidic in vitro model of the blood-brain barrier (muBBB). *Lab Chip.* 2012;12:1784–92.
- Bothwell SW, Janigro D, Patabendige A. Cerebrospinal fluid dynamics and intracranial pressure elevation in neurological diseases. *Fluids Barriers CNS.* 2019;16:9.
- Brennan MD, Rexus-Hall ML, Elgass LJ, Eddington DT. Oxygen control with microfluidics. *Lab Chip.* 2014;14:4305–18.
- Caballero D, Kaushik S, Correlo VM, Oliveira JM, Reis RL, Kundu SC. Organ-on-chip models of cancer metastasis for future personalized medicine: from chip to the patient. *Biomaterials.* 2017;149:98–115.
- Chen L, Yang C, Xiao Y, Yan X, Hu L, Eggersdorfer M, Chen D, Weitz DA, Ye F. Millifluidics, microfluidics, and nanofluidics: manipulating fluids at varying length scales. *Mater Today Nano.* 2021a;16:100136.
- Chen X, Zhang YS, Zhang X, Liu C. Organ-on-a-chip platforms for accelerating the evaluation of nanomedicine. *Bioact Mater.* 2021b;6:1012–27.
- Cho AN, Jin Y, An Y, Kim J, Choi YS, Lee JS, Kim J, Choi WY, Koo DJ, Yu W, Chang GE, Kim DY, Jo SH, Kim J, Kim SY, Kim YG, Kim JY, Choi N, Cheong E, Kim YJ, Je HS, Kang HC, Cho SW. Microfluidic device with brain extracellular matrix promotes structural and functional maturation of human brain organoids. *Nat Commun.* 2021;12:4730.
- Delamarque E. Open-space microfluidics: concepts, implementations, applications. Weinheim: Wiley-VCH; 2018.
- Duffy DC, McDonald JC, Schueller OJA, Whitesides GM. Rapid prototyping of microfluidic systems in poly(dimethylsiloxane). *Anal Chem.* 1998;70:4974–84.
- El-Ali J, Sorger PK, Jensen KF. Cells on chips. *Nature.* 2006;442:403–11.
- Engineer TE. Understanding laminar and turbulent flow [Online]. 2020. YouTube. Available <https://youtu.be/9A-uUGOWR0w>
- Filippi M, Nguyen DV, Garello F, Perton F, Begin-Colin S, Felder-Flesch D, Power L, Scherberich A. Metronidazole-functionalized iron oxide nanoparticles for molecular detection of hypoxic tissues. *Nanoscale.* 2019;11:22559–74.
- Filippi M, Buchner T, Yasa O, Weirich S, Katzschmann RK. Microfluidic tissue engineering and bio-actuation. *Adv Mater.* 2022;34:e2108427.
- Fritschen A, Blaeser A. Biosynthetic, biomimetic, and self-assembled vascularized organ-on-a-chip systems. *Biomaterials.* 2021;268:120556.
- Goldman M, Nemes J, Macoska E, Wysoker A, Mccarroll S. Drop-seq [Online]. 2022. Available <https://mccarrolllab.org/dropseq/>
- Halldorsson S, Lucumi E, Gomez-Sjoberg R, Fleming RMT. Advantages and challenges of microfluidic cell culture in polydimethylsiloxane devices. *Biosens Bioelectron.* 2015;63:218–31.
- Hao N, Nie Y, Zhang JXJ. Microfluidic synthesis of functional inorganic micro-/nanoparticles and applications in biomedical engineering. *Int Mater Rev.* 2018;63:461–87.
- Haring AP, Sontheimer H, Johnson BN. Microphysiological human brain and neural systems-on-a-chip: potential alternatives to small animal models and emerging platforms for drug discovery and personalized medicine. *Stem Cell Rev Rep.* 2017;13:381–406.
- Hatzor A, Weiss PS. Molecular rulers for scaling down nanostructures. *Science.* 2001;291:1019–21.

- Hengst U, Deglincerti A, Kim HJ, Jeon NL, Jaffrey SR. Axonal elongation triggered by stimulus-induced local translation of a polarity complex protein. *Nat Cell Biol.* 2009;11:1024–30.
- Huh D, Matthews BD, Mammoto A, Montoya-Zavala M, Hsin HY, Ingber DE. Reconstituting organ-level lung functions on a chip. *Science.* 2010;328:1662–8.
- Huh D, Leslie DC, Matthews BD, Fraser JP, Jurek S, Hamilton GA, Thorneloe KS, McAlexander MA, Ingber DE. A human disease model of drug toxicity-induced pulmonary edema in a lung-on-a-chip microdevice. *Sci Transl Med.* 2012;4:159ra147.
- Ibrahim OA, Navarro-Segarra M, Sadeghi P, Sabate N, Esquivel JP, Kjeang E. Microfluidics for electrochemical energy conversion. *Chem Rev.* 2022;2022 <https://doi.org/10.1021/acs.chemrev.1c00499>.
- Jiang X, Wang J, Deng X, Xiong F, Ge J, Xiang B, Wu X, Ma J, Zhou M, Li X, Li Y, Li G, Xiong W, Guo C, Zeng Z. Role of the tumor microenvironment in PD-L1/PD-1-mediated tumor immune escape. *Mol Cancer.* 2019;18:10.
- Jing X, Mi H-Y, Lin Y-J, Enriquez E, Peng X-F, Turng L-S. Highly stretchable and biocompatible strain sensors based on mussel-inspired super-adhesive self-healing hydrogels for human motion monitoring. *ACS Appl Mater Interfaces.* 2018;10:20897–909.
- Khorsandi D, Nodehi M, Waqar T, Shabani M, Kamare B, Zare EN, Ersoy S, Annabestani M, Çelebi MF, Kafadenk A, Yin J. Manufacturing of microfluidic sensors utilizing 3D printing technologies: a production system. *J Nanomater.* 2021;2021:1–16.
- Kilic O, Pamies D, Lavell E, Schiapparelli P, Feng Y, Hartung T, Bal-Price A, Hogberg HT, Quinones-Hinojosa A, Guerrero-Cazares H, Levchenko A. Brain-on-a-chip model enables analysis of human neuronal differentiation and chemotaxis. *Lab Chip.* 2016;16:4152–62.
- Krausgruber T, Fortelny N, Fife-Gernedl V, Senekowitsch M, Schuster LC, Lercher A, Neme A, Schmidl C, Rendeiro AF, Berghaler A, Bock C. Structural cells are key regulators of organ-specific immune responses. *Nature.* 2020;583:296–302.
- Li Y, Wong IY, Guo M. Reciprocity of cell mechanics with extracellular stimuli: emerging opportunities for translational medicine. *Small.* 2022;2022:e2107305.
- Lin KC, Yen CZ, Yang JW, Chung JHY, Chen GY. Airborne toxicological assessment: the potential of lung-on-a-chip as an alternative to animal testing. *Mater Today Adv.* 2022;14:100216.
- Liu X, Fang J, Huang S, Wu X, Xie X, Wang J, Liu F, Zhang M, Peng Z, Hu N. Tumor-on-a-chip: from bioinspired design to biomedical application. *Microsyst Nanoeng.* 2021;7:50.
- Luo X, Su P, Zhang W, Raston CL. Microfluidic devices in fabricating nano or micromaterials for biomedical applications. *Adv Mater Technol.* 2019;4:1900488.
- Mathur A, Roy S. 10 – microfluidics and lab-on-a-chip. In: Maruccio G, Narang J, editors. *Electrochemical sensors.* Woodhead Publishing; 2022.
- Mehling M, Tay S. Microfluidic cell culture. *Curr Opin Biotechnol.* 2014;25:95–102.
- Meyvantsson I, Beebe DJ. Cell culture models in microfluidic systems. *Annu Rev Anal Chem (Palo Alto, Calif).* 2008;1:423–49.
- Mittal R, Woo FW, Castro CS, Cohen MA, Karanxha J, Mittal J, Chhibber T, Jhaveri VM. Organ-on-chip models: implications in drug discovery and clinical applications. *J Cell Physiol.* 2019;234:8352–80.
- Namgung B, Lee T, Tan JKS, Poh DKH, Park S, Chng KZ, Agrawal R, Park SY, Leo HL, Kim S. Vibration motor-integrated low-cost, miniaturized system for rapid quantification of red blood cell aggregation. *Lab Chip.* 2020;20:3930–7.
- Nathanael K, Pico P, Kovalchuk NM, Lavino AD, Simmons MJH, Matar OK. Computational modelling and microfluidics as emerging approaches to synthesis of silver nanoparticles – a review. *Chem Eng J.* 2022;436:135178.
- Oshio K, Watanabe H, Song YL, Verkman AS, Manley GT. Reduced cerebrospinal fluid production and intracranial pressure in mice lacking choroid plexus water channel Aquaporin-1. *FASEB J.* 2005;19:76–8.
- Paggi CA, Teixeira LM, Le Gac S, Karperien M. Joint-on-chip platforms: entering a new era of in vitro models for arthritis. *Nat Rev Rheumatol.* 2022;18:217–31.

- Park SY, Wu TH, Chen Y, Teitell MA, Chiou PY. High-speed droplet generation on demand driven by pulse laser-induced cavitation. *Lab Chip*. 2011;11:1010–2.
- Park TE, Mustafaoglu N, Herland A, Hasselkus R, Mannix R, Fitzgerald EA, Prantil-Baun R, Watters A, Henry O, Benz M, Sanchez H, Mccrea HJ, Goumnerova LC, Song HW, Palecek SP, Shusta E, Ingber DE. Hypoxia-enhanced blood-brain barrier chip recapitulates human barrier function and shuttling of drugs and antibodies. *Nat Commun*. 2019;10:2621.
- Picollet-D'hahan N, Zuchowska A, Lemeunier I, Le Gac S. Multiorgan-on-a-chip: a systemic approach to model and decipher inter-organ communication. *Trends Biotechnol*. 2021;39:788–810.
- Piergiovanni M, Leite SB, Corvi R, Whelan M. Standardisation needs for organ on chip devices. *Lab Chip*. 2021;21:2857–68.
- Pihl J, Karlsson M, Chiu DT. Microfluidic technologies in drug discovery. *Drug Discov Today*. 2005;10:1377–83.
- Pol R, Céspedes F, Gabriel D, Baeza M. Microfluidic lab-on-a-chip platforms for environmental monitoring. *TrAC Trends Anal Chem*. 2017;95:62–8.
- Pongrácz A, Fekete Z, Márton G, Bérces Z, Ulbert I, Fürjes P. Deep-brain silicon multielectrodes for simultaneous in vivo neural recording and drug delivery. *Sensors Actuators B Chem*. 2013;189:97–105.
- Preetam S, Nahak BK, Patra S, Toncu DC, Park S, Syväjärvi M, Orive G, Tiwari A. Emergence of microfluidics for next generation biomedical devices. *Biosens Bioelectron X*. 2022;10:100106.
- Ren K, Zhou J, Wu H. Materials for microfluidic chip fabrication. *Acc Chem Res*. 2013;46:2396–406.
- Rexius-Hall ML, Mauleon G, Malik AB, Rehman J, Eddington DT. Microfluidic platform generates oxygen landscapes for localized hypoxic activation. *Lab Chip*. 2014;14:4688–95.
- Rivieccio MA, Brochier C, Willis DE, Walker BA, D'annibale MA, McLaughlin K, Siddiq A, Kozikowski AP, Jaffrey SR, Twiss JL, Ratan RR, Langley B. HDAC6 is a target for protection and regeneration following injury in the nervous system. *Proc Natl Acad Sci U S A*. 2009;106:19599–604.
- Saliba J, Daou A, Damiati S, Saliba J, El-Sabban M, Mhanna R. Development of microplatforms to mimic the in vivo architecture of CNS and PNS physiology and their diseases. *Gene*. 2018;9:285.
- Shi P, Scott MA, Ghosh B, Wan D, Wissner-Gross Z, Mazitschek R, Haggarty SJ, Yanik MF. Synapse microarray identification of small molecules that enhance synaptogenesis. *Nat Commun*. 2011;2:510.
- Si LL, Bai HQ, Oh CY, Jin L, Prantil-Baun R, Ingber DE. Clinically relevant influenza virus evolution reconstituted in a human lung airway-on-a-chip. *Microbiol Spectr*. 2021;9:e00257–21.
- Sivandzade F, Cucullo L. In-vitro blood-brain barrier modeling: a review of modern and fast-advancing technologies. *J Cereb Blood Flow Metab*. 2018;38:1667–81.
- Sone N, Konishi S, Igura K, Tamai K, Ikeo S, Korogi Y, Kanagaki S, Namba T, Yamamoto Y, Xu Y, Takeuchi K, Adachi Y, Chen-Yoshikawa Toyofumi F, Date H, Hagiwara M, Tsukita S, Hirai T, Torisawa Y-S, Gotoh S. Multicellular modeling of ciliopathy by combining iPS cells and microfluidic airway-on-a-chip technology. *Sci Transl Med*. 2021;13:eabb1298.
- Stone HA, Stroock AD, Ajdari A. Engineering flows in small devices: microfluidics toward a lab-on-a-chip. *Annu Rev Fluid Mech*. 2004;36:381–411.
- Syama S, Mohanan PV. Microfluidic based human-on-a-chip: a revolutionary technology in scientific research. *Trends Food Sci Technol*. 2021;110:711–28.
- Tan HY, Cho H, Lee LP. Human mini-brain models. *Nat Biomed Eng*. 2021;5:11–25.
- Tavakol DN, Fleischer S, Vunjak-Novakovic G. Harnessing organs-on-a-chip to model tissue regeneration. *Cell Stem Cell*. 2021;28:993–1015.
- Taylor AM, Blurton-Jones M, Rhee SW, Cribbs DH, Cotman CW, Jeon NL. A microfluidic culture platform for CNS axonal injury, regeneration and transport. *Nat Methods*. 2005;2:599–605.
- Taylor AM, Dieterich DC, Ito HT, Kim SA, Schuman EM. Microfluidic local perfusion chambers for the visualization and manipulation of synapses. *Neuron*. 2010;66:57–68.

- TED, Geraldine Hamilton: body parts on a chip [Online]. 2013. YouTube. Available <https://youtu.be/CpkXmtJOH84>
- Toepke MW, Beebe DJ. PDMS absorption of small molecules and consequences in microfluidic applications. *Lab Chip*. 2006;6:1484–6.
- Tu ST, Yu X, Luan W, Löwe H. Development of micro chemical, biological and thermal systems in China: a review. *Chem Eng J*. 2010;163:165–79.
- Visaveliya N, Kohler JM. Single-step microfluidic synthesis of various nonspherical polymer nanoparticles via in situ assembling: dominating role of polyelectrolytes molecules. *ACS Appl Mater Interfaces*. 2014;6:11254–64.
- Walter FR, Valkai S, Kincses A, Petneházi A, Czeller T, Veszelka S, Ormos P, Deli MA, Dér A. A versatile lab-on-a-chip tool for modeling biological barriers. *Sensors Actuators B Chem*. 2016;222:1209–19.
- Wan J, Zhou S, Mea HJ, Guo Y, Ku H, Urbina BM. Emerging roles of microfluidics in brain research: from cerebral fluids manipulation to brain-on-a-chip and neuroelectronic devices engineering. *Chem Rev*. 2022;122:7142–81.
- Whitesides GM. The origins and the future of microfluidics. *Nature*. 2006;442:368–73.
- Whitesides GM, Ostuni E, Takayama S, Jiang XY, Ingber DE. Soft lithography in biology and biochemistry. *Annu Rev Biomed Eng*. 2001;3:335–73.
- Whitesides GM, Janasek D, Franzke J, Manz A, Psaltis D, Quake SR, Yang C, Craighead H, Demello AJ, El-Ali J, Sorger PK, Jensen KF, Yager P, Edwards T, Fu E, Helton K, Nelson K, Tam MR, Weigi BH. Lab on a chip. *Nature*. 2006;442
- Wu MH, Huang SB, Lee GB. Microfluidic cell culture systems for drug research. *Lab Chip*. 2010;10:939–56.
- Xing W, Liu Y, Wang H, Li S, Lin Y, Chen L, Zhao Y, Chao S, Huang X, Ge S, Deng T, Zhao T, Li B, Wang H, Wang L, Song Y, Jin R, He J, Zhao X, Liu P, Li W, Cheng J. A high-throughput, multi-index isothermal amplification platform for rapid detection of 19 types of common respiratory viruses including SARS-CoV-2. *Engineering (Beijing)*. 2020;6:1130–40.
- Yang X, Biswas SK, Han J, Tanpichai S, Li MC, Chen C, Zhu S, Das AK, Yano H. Surface and interface engineering for nanocellulosic advanced materials. *Adv Mater*. 2020;33:2002264.
- Yang C, Wu B, Ruan J, Zhao P, Chen L, Chen D, Ye F. 3D-printed biomimetic systems with synergistic color and shape responses based on oblate cholesteric liquid crystal droplets. *Adv Mater*. 2021;33:e2006361.
- Yen BK, Gunther A, Schmidt MA, Jensen KF, Bawendi MG. A microfabricated gas-liquid segmented flow reactor for high-temperature synthesis: the case of CdSe quantum dots. *Angew Chem Int Ed Eng*. 2005;44:5447–51.
- Yu Y, Shang L, Guo J, Wang J, Zhao Y. Design of capillary microfluidics for spinning cell-laden microfibers. *Nat Protoc*. 2018;13:2557–79.
- Zeng L, Li P, Yao Y, Niu B, Niu S, Xu B. Recent progresses of 3D printing technologies for structural energy storage devices. *Mater Today Nano*. 2020;12:100094.
- Zhang J, Sun J, Li B, Yang C, Shen J, Wang N, Gu R, Wang D, Chen D, Hu H, Fan C, Zhang H, Liu K. Robust biological fibers based on widely available proteins: facile fabrication and suturing application. *Small*. 2020;16:e1907598.
- Zlokovic BV. Neurovascular pathways to neurodegeneration in Alzheimer's disease and other disorders. *Nat Rev Neurosci*. 2011;12:723–38.

Chapter 12

Lab-on-a-Chip Devices for Medical Diagnosis II: Strategies for Pathogen Detection



Rachmi Luthfikasari, Tejal V. Patil, Dinesh K. Patel, Keya Ganguly, Sayan Deb Dutta, and Ki-Taek Lim

12.1 Introduction

The rapid advances in micro and nanofabrication in combination with the synthesis and discovery of new materials have pushed the drive to develop new technologies in biomedical devices (Castillo-León 2015). The global risk of viral disease outbreaks (Zhu et al. 2020) and diseases caused by foodborne pathogens represents an increasing problem to public health and safety worldwide (Tsougeni et al. 2019), emphasizing the need for accurate, fast, and sensitive detection techniques to speed up diagnostics for early intervention.

Lab-on-a-chip (LoC) technology implies to the technology that performs a variety of lab operations on a miniaturized scale, such as chemical synthesis and analysis on a single chip which enables to be a handheld and portable device. In other words, LoC is a device that is capable of scaling single or multiple laboratory functions down to chip format. The size of this chip ranges from millimeters to a few square centimeters (Volpatti and Yetisen 2014). LoC is basically the integration of

R. Luthfikasari · D. K. Patel · K. Ganguly · S. D. Dutta
Department of Biosystems Engineering, Institute of Forest Science, Kangwon National University, Chuncheon, Republic of Korea

T. V. Patil
Interdisciplinary Program in Smart Agriculture, Kangwon National University, Chuncheon, Republic of Korea

K.-T. Lim (✉)
Department of Biosystems Engineering, Institute of Forest Science, Kangwon National University, Chuncheon, Republic of Korea
Interdisciplinary Program in Smart Agriculture, Kangwon National University, Chuncheon, Republic of Korea
e-mail: ktlim@kangwon.ac.kr

fluidics, electronics, optics, and biosensors (Giannitsis and Min 2010). The main motive of LoC is the need for state-of-the-art pathological analysis on the go. LoC has proven to help find ways to diagnose fatal and chronic illnesses early. LoC has proven to help find ways to diagnose fatal and chronic illnesses early with the advent of advanced technologies such as microelectromechanical systems (MEMS), nano-electromechanical systems (NEMS), and the integration of many interdisciplinary modules into a single chip. The LoC process started by collecting the physiological sample, and then from this sample, the extraction of a particular analyte/biomarker is done. Depending on the biomedical application, the transducer will act based on analyte electrically, optically, electromechanically, or mechanically. The next step includes counting, sorting, and amplification of the transducer output and finally processing the amplified sample using microelectronics techniques (Gupta et al. 2016).

12.2 LoC Fabrication for Medical Diagnosis

Research on microfluidic systems for more than two decades led to the advancement of lab-on-a-chip devices that play important roles in biochemical, biomedical, and future healthcare systems particularly in point-of-care (PoC) devices (Nguyen et al. 2020; van den Berg 2013). Cheap, easy-to-handle process, rapid sample-to-answer results, and no need of technical operators are some of the essential advantages. However, there are three most important factors to play the essential roles in successfully making commercially viable PoC pathogen-detection devices in advanced of biomedical application. Those three insights are (1) the utilizations of disposable polymer (microfluidic) chips, (2) the enforcement of surface-bound (or solid-phase) nucleic acid amplification techniques, and (3) the development of open-source hardware and software (Nguyen et al. 2020). The PoC devices generally consist of three components: (a) sample handling, (b) detecting, and (c) signal reading.

1. Sample Handling

In the early days of the LoC era, based on silicon technology and microelectronic processes, the microfluidic chips (from here on referred to simply as chips) were made from silicon and glass such as borofloat and fused silica. However, for glass and fused silica, there are also challenging circumstances. Glass such as Pyrex has low signal-to-noise fluorescent intensity due to limited transmission of deep UV light for applications related to tryptophan fluorescence. In general, that leaves us the last option of using fused silica (also called quartz). Fused silica is transparent for a wide range of UV wavelengths (Burke 1996). This material is, however, expensive and difficult to process, for instance, bonding and etching steps (Reisner et al. 2009; Waldauer et al. 2012; Izadi et al. 2017), both in a lab and at industrial scale. In 1998, Whitesides group introduced the soft-lithography technique (Duffy et al. 1998) which made use of (cheap) poly(dimethylsiloxane) (PDMS) material, giving

rise to a burst of development in the LoC research, especially in the biology and medicine areas. However, this material can be used only in cases of low flow rate or low-pressure LoC measurements, is not ideal for fabrication of high-aspect-ratio structures (Bakajin et al. 2006), and can be damaged from high-energy light (Bakajin et al. 2006) and high pressure (Nguyen et al. 2020), so PDMS cannot be used in this kind of experiments. Therefore, materials with simple and low-cost fabrication processes, such as polymer injection molding, are needed for mass production of cyclic olefin copolymer (COC) micro- and nanofluidic chips suitable for fluorescent biomedical-physical experiments. COC has a better UV transparency compared to PDMS, polymethyl methacrylate (PMMA), and polycarbonate (PC) and has extremely low water absorption (Ahn et al. 2004; Khanarian 2001). Besides, polymer injection molding is a high-throughput and easily scalable technique, hence providing faster and cheaper possibilities for production compared to fused silica and elastomer casting PDMS. The inexpensive high-throughput fabrication of LoC devices can yield broad distribution of the devices, enabling access to personalized diagnosis and hence PoC devices. Furthermore, COC being a thermoplastic with high thermostability up to 130 °C makes it a perfect candidate for PCR-based applications in PoC devices (Nguyen et al. 2020).

2. Sample Detecting

Revolution in molecular analysis of nucleic acids (NA) has focused the scientific research on the development of new miniaturized and easy-to-use technologies, such as PoC technologies, interfaced with advanced molecular techniques. Ideally, such PoC systems should allow rapid NA analysis in decentralized environments, with all the steps necessary for sample preparation and detection automated, to make the test accessible and manageable by unskilled personnel (Petralia and Conoci 2017). Recently, a number of the advanced molecular techniques, such as polymerase chain reaction (PCR), loop-mediated isothermal amplification (LAMP), etc., have been integrated into PoC systems for rapid detection of pathogens in food and clinical samples (Craw and Balachandran 2012). However, there is still a requirement for efficient sample preparation and its integration into the microfluidic-based PoC systems.

Sample preparation is the greatest challenge in the rapid detection of pathogenic microorganisms in the area of clinical diagnostics. While developing a robust sample preparation method with capacity for automation and integration, one should keep in mind the complexities of the clinical and environmental samples. The complexity and heterogeneity of biological matrices, such as whole blood, urine, saliva, swab, and fecal materials, in particular, the nonuniform distribution of pathogens, as well as the low abundance of target pathogens, are the main challenges for rapid and ultrasensitive detection of pathogens. In addition, the analytical performance of advanced pathogen detection strategies also suffers from the interference from indigenous microflora (Mandal et al. 2011). Although microfluidic-based PoC systems have emerged as promising tools in recent years, limited measurement volumes and low abundance of target pathogens are an obvious bottleneck in the applications of such devices. In most of the cases, the microbial load can be even

less than 1 CFU/mL in blood. The recoverable NA concentration from such samples may far exceed the capacity of most of the sample preparation methods (Afshari et al. 2012). The low operational sample volume in the microfluidic channels might render difficulties in attaining high sensitivity and required selectivity (Kant et al. 2018). Hence, we believe that additional efforts are required to integrate efficient sample handling strategies with microfluidic systems to implement them for real-time pathogen detection in biological samples.

Sample concentration and growth-based enrichment of microorganisms have been key steps in current methodologies. The basic intention of the sample preparation may not be limited to concentrate the target pathogens. It may also be desirable to eliminate the adverse effects of biological matrices on the analytical/bioanalytical performances and to reduce the heterogeneity of food or clinical samples, but they also may fail to eliminate the biological matrices. These traces of biological matrices, if they remain in the sample, may interfere or inhibit the downstream analytical performance. Biochemical principle of sample preparation has advantages in this regard, as the method can concentrate the target pathogens selectively, thereby eliminating the interference from indigenous microflora of the food samples. The possibility of separating and eliminating the biological matrices from the samples is an added advantage when the biorecognition ligands used for the pathogen capturing are immobilized on a solid support, such as microfluidic channels or magnetic beads. A magnetic bead-based approach enables sample concentration and sample purification, simultaneously, by concentrating pathogens from large sample volumes besides eliminating matrix and PCR inhibitors. Therefore, this strategy is ideally suited for designing sample preparation integrated PoC devices (Nguyen et al. 2020).

Detection and differentiation of pathogens at genus, subspecies, or serotype level is very much important to analyze food, clinical, or environmental samples accurately. However, as mentioned above, the capacity of online multiplexing with qPCR-based microfluidic systems is limited due to the interferences between different primer and probe sets. Replacement of conventional PCR with solid-phase PCR (SP-PCR) in the PoC systems may be a possible alternative solution. Despite real-time PCR being an advanced molecular technique, a requirement of precise and repeated thermocycling necessitates an instrumental design with complex thermal control mechanisms. The invention of isothermal amplification strategies has provided a positive advancement for overcoming the thermal limitations of a PCR-based method (Nguyen et al. 2020).

Isothermal amplification techniques emerged in the 1990s and have been verified as a simple, rapid, and efficient method of nucleic acid amplification. Unlike PCR that requires distinct thermal steps for denaturation, annealing, and extension, the entire process of isothermal amplification is conducted at a constant temperature. In the past decades, microfluidic systems and PoC devices that employed PCR as the detection technique have been extensively studied. However, the thermal cycling requirement for PCR remains the main challenge for designing handheld devices for on-site testing of pathogens. Besides rapidity and high efficiency, the simple thermal requirement of isothermal amplification techniques was considered as a

proper alternative for PCR for implementation in PoC device. Various LAMP-integrated PoC devices have been reported for on-site pathogen detection. Oh et al. reported a centrifugal microfluidic device that is capable of identifying multiple foodborne pathogens using LAMP- and colorimetric-based rapid and simple test, without the need for an additional instrument for detection (Oh et al. 2016) Yi et al. have reported a LAMP-based LOC system for real-time quantitative detection of *Salmonella*. The system was integrated with a magnetic bead for sample preparation. LAMP was employed for rapid and quantitative detection of *Salmonella* in enriched pork meat samples (Sun et al. 2015). The whole process, including DNA isolation, isothermal amplification, and real-time detection, was completed in a single chamber. These examples demonstrated the advantages of the integration of LAMP into microfluidic chips and PoC for rapid real-time or at-site pathogen detection (Nguyen et al. 2020). Although LAMP is a well-developed method, multiplexed analysis using LAMP is challenging because LAMP amplicons are very complicated in structure. Unlike PCR, LAMP amplicons do not have a defined structure and target gene amplicon-specific definite molecular size. Normally, LAMP generates amplicons with various lengths irrespective of the length of the template. Therefore, in order to develop multiplexed LAMP, it is necessary to discriminate target-specific amplicons from the mixture of LAMP products originating from simultaneous amplification of multiple target genes (Liang et al. 2012). LAMP-based PoC systems may be in the complex engineering challenges, but integrating and automating LAMP assays with both upstream sample processing and downstream detection schemes is the bottleneck in developing multiplexed LAMP-based PoC devices. LAMP can be considered as a potential technique in future generations of PoC devices due to its sensitivity (10–100-fold greater than conventional PCR and 500–1000 times more sensitive than antigen detection), rapidness, robustness, and specificity, as well as simplicity in practical implementations. Besides traditional optical- and electrochemical-based detection modalities, novel techniques, e.g., giant magnetoresistance (GMR) (Zhi et al. 2014), have been adapted for LAMP in PoC devices. The next generation of PoC may be fully integrated systems which are portable, fast, low cost, easy to use, sensitive, and specific. To integrate LAMP as a powerful detection tool in PoC devices, it needs to be combined with an appropriate monitoring method. In general, monitoring methods are defined as the methods adapted for real-time or endpoint recognition of signals from a biochemical reaction (Zhang et al. 2014). The field of integration of monitoring methods within PoC devices is currently an ongoing developing field. Figure 12.1 shows the microfluidic structures that were fabricated based on the sensor chip using photolithography of SU-8 photoresist.

3. Signal Reading

The open hardware solutions that are relevant for PoC systems generally consists of two things: mechanics, for sample handling and interaction, and electronics, for controlling functions, and possibly, for running user interaction/interface processes (Nguyen et al. 2018). Furthermore, once the desired hardware solution that fulfills the task, e.g., performing the desired PoC test, has been developed, the system needs

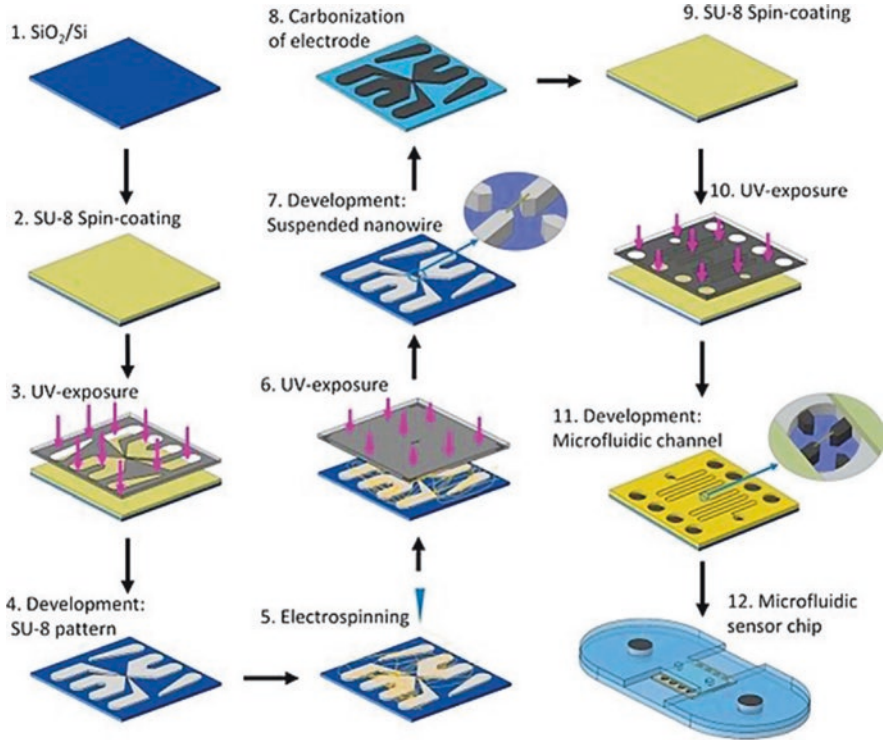


Fig. 12.1 Schematic illustration of the fabrication steps of the carbon nanowire LOC biosensor using electrospinning and photolithography. (Reprinted from Ref. (Thiha et al. 2018) with permission from Elsevier)

to be packaged, that is, put in an enclosure. Custom-made parts for the mechanics of the system, as well as the enclosure, are usually designed using CAD software and fabricated using fast-prototyping tools, e.g., tabletop laser cutters, CNCs, and/or 3D printers. Interestingly, even they are needed to fabricate these custom-made parts can also be made from readily available open-source hardware resources, provided by the ever-growing community of makers (Wittbrodt et al. 2013). To be able to perform any tests with PoC systems, these systems need to include some micro-controllers or other control circuitry, to run the necessary procedure for the test (Nguyen et al. 2018). The basis for developing a PoC device could, for instance, be some newly developed technology, e.g., an experimental setup in a lab such as a sensor or lab-on-a-chip system. An overall tactic for the development of such (an open-source) PoC device would be (1) identifying the core function(s) of the system and how they could be automated; (2) replacing any commercial tools necessary to run the function with self-made solutions, developed either from scratch or open-source resources, (3) developing a user interface for the system, as well as the necessary functions to control and operate the system; and finally, (4) figuring out how the developed solution(s) could be packaged into a fully integrated device.

Fluorescent PoC detection using open-source hardware is also needed, and in general, the platform includes (1) an excitation module (M1) consisting of a light source (LEDs or laser) and excitation filters; (2) a sample chamber module (M2, which accommodates a microscope slide, nitrocellulose membrane, microfluidic chip or cassette); (3) an emission filter and signal readout module (M3), consisting of emission filters, photodiodes, and charge integration readout electronics, for multiplexed fluorescence detection (Obahiagbon et al. 2018; Nikkhoo et al. 2016), or a camera, for fluorescence image array detection (Nikkhoo et al. 2016; Maia Chagas et al. 2017; Nasseri et al. 2018; Wang et al. 2018); (4) a microcontroller module (M4), for control of the sequence, power, and data processing; and (5) a display and connectivity module (M5), including an optional mini display for prompting and presenting results to the user. Alternatively, a smartphone, with a user interface, which established a connection via Bluetooth or Wi-Fi, could be used to show device status and displays results. Other possibilities are uploading of information for cloud processing and providing interpretation feedback to the operator, i.e., a primary care physician (Obahiagbon et al. 2018).

12.3 Pathogen Diagnosis

Recent advances in the LoC technology and design strategies lead to the development of universal sample-to-result microfluidic devices that are beneficial and efficient for pathogen detection with high specificity and sensitivity. The concept of microfluidics investigates the behavior and manipulation of small volumes of liquids at nano- and micrometer scales. This concept has been consistently further developed over the last two decades as a result of the advent of microelectromechanical systems (Sin et al. 2011). Here we presented LoC device grouping based on the types of pathogens detected.

1. Bacteria

Increasing concerns of diseases caused by foodborne pathogens are threatening public health and food product safety. Rapid and reliable pathogen detection is needed in utmost importance. Therefore, well-designed lab-on-a-chip (LOC) devices (Foudeh et al. 2012; Lafleur et al. 2016) can further achieve rapid, sensitive, and specific bacterial detection due to their unique property of the short diffusion path and high surface-to-volume ratios that are combined with other advantages (Kovarik et al. 2013), such as small sample volume, portability, and shortened assay time. Real-time biosensors, portable biosensors, and LOC biosensors show great potential in food safety. Core performance characteristics are the detection time, detection range, the limit of detection (LOD), and the specificity. In the LOC biosensors, the LOD ranges from 10^2 to 10^5 cells/mL and the detection time from 20 min to 6 h (Tsougeni et al. 2019).

Sun et al. (2015) developed a lab-on-a-chip system integrated with sample preparation and loop-mediated isothermal amplification for rapid and quantitative

detection of *Salmonella* spp. in food samples. Salmonellosis is one of the most common foodborne diseases causing major public health threat worldwide. They, for the first time, developed an integration of eight-chamber lab-on-a-chip (LOC) system and magnetic bead-based sample preparation and loop-mediated isothermal amplification (LAMP) for rapid and accurate detection of *Salmonella* spp. in food samples. The whole general diagnostic procedures involve DNA isolation, isothermal amplification, and real-time detection and were accomplished in a single chamber. The devices can handle up to eight samples simultaneously, and the system was able to effectively detect *Salmonella* at concentration of 50 cells per test within 40 min. The practical ability of the LOC system for rapid on-site screening of *Salmonella* in food safety control, environmental surveillance, and clinical diagnostics will significantly increase by the simple design, together with high level of integration, using isothermal amplification, and quantitative analysis of multiple samples in a short time (Sun et al. 2015).

For the first time also, Nguyen et al. (2019) developed a supercritical angle fluorescence (SAF) structures in polymer microfluidic chips which are fabricated using a combination of micro-milling and polymer injection molding (Nguyen et al. 2019). Together with theoretical modeling, they experimentally fabricated microarrays of SAF structures with various heights from zero to the order of 300 μm in cyclic olefin copolymer (COC) microfluidic chips. The results show that in the case of fluorophores at the air and COC interface, the highest fluorescence intensities are obtained with a SAF structure with a 163 μm height on a milling machine with a diameter of 97.4 μm , which is very consistent with the modeling. Using a SAF structure, a fluorescence LOD of 5.42×10^4 molecules is achieved. The solid-phase polymerase chain reaction (SP-PCR) with these SAF structures enables high pathogen detection (3.37×10^2 copies of the *E. coli* genome per μL) on-chip. These results are particularly interesting for applications in hypersensitive pathogen detection as well as in assisting the design of devices for point-of-care applications. The findings on the height optimization of SAF structures provide better understanding on SAF detection techniques and provide insights into the development of fluorescence microscopy.

Ma et al. (2020) did a detection of *Campylobacter* spp. in food samples such as whole milk and raw chicken meat because the consumption of these food commodities is the major route of human campylobacteriosis. They developed an array of bacterial incubation chambers in the microfluidic device, where chromogenic medium and antibiotics were loaded. The growth of *Campylobacter* spp. was visualized by color change due to chromogenic reactions. This platform achieved 100% specificity for *Campylobacter* identification. Sensitive detection of multiple *Campylobacter* species (*C. jejuni*, *C. coli*, and *C. lari*) was obtained in artificially contaminated milk and poultry meat, with detection limits down to 1×10^2 CFU/ml and 1×10^4 CFU/25 g, respectively. On-chip AST determined *Campylobacter* antibiotic susceptibilities by the lowest concentration of antibiotics that can inhibit bacterial growth (i.e., no color change observed). High coincidences (91–100%) of on-chip AST and the conventional agar dilution method were achieved against several clinically important antibiotics. For a presumptive colony, on-chip

identification and AST were completed in parallel within 24 h, whereas standard methods, including biochemical assays and traditional culture-based AST, take several days for multiple sequential steps (Ma et al. 2020).

Cabibbe et al. evaluate the performance of a molecular lab-on-a-chip-based VerePLEX Biosystem for detection for the multidrug-resistant tuberculosis (MDR-TB) with a diagnostic accuracy of 97.8% or higher compared to sequencing and MTBDRplus assay for *Mycobacterium tuberculosis* complex and rifampin and isoniazid resistance detection on clinical isolates and smear-positive specimens. The speed, user-friendly interface, and versatility make it suitable for routine laboratory use.

2. Protozoa

Malaria is a disease caused by blood-borne protozoan parasite called *Plasmodium* sp., and microscopic examination, if available, is the gold standard for diagnosing malaria, but in health centers with limited resources, patients with fever may be diagnosed with malaria (Murray et al. 2008). These practices lead to overtreatment and misdiagnosis of potentially fatal bacterial infections and are becoming less feasible in the face of emerging drug resistance and costly new therapies (Amexo et al. 2004; O'Dempsey et al. 1993; Breman et al. 2004). Therefore, new sensitive diagnostics will play a key role in surveillance to identify sporadic outbreaks and asymptomatic reservoirs of infection (The malERA Consultative Group on Diagnoses and Diagnostics 2011) and are urgently needed. Taylor et al. (2014) developed a plastic hydrogel chip and a portable real-time PCR machine for malaria diagnosis (Taylor et al. 2014).

Few have overcome the barriers of sample preparation, refrigeration, cost, complexity, and infrastructure requirements for use in resource-poor environment (Yager et al. 2008). The recent clinical evaluations of a commercially available LAMP (loop-mediated isothermal amplification) kit that amplify parasite DNA with a minimum of extraction steps address many of these issues and enable on-site molecular testing (Watanabe et al. 2011; Polley et al. 2013; Hopkins et al. 2013). However, while the innovations present in field-ready LAMP kits are commendable, a distinctive sample preparation process still remains as an important part of the procedure. This step, even in optimized and self-contained form provided by commercial kits, can pose a significant obstacle to the implementation of diagnostic tests in resource-constrained areas. Lab-on-a-chips were manufactured on MEMS-based silicon wafers and mounted on printed circuit boards (PCBs) that provide mechanical, thermal, and electrical connectivity (Teo et al. 2011; Petralia et al. 2013). It encompassed two silicon microreactors (12 mL) connected to a microarray chamber. The microarray chamber (3.5 mm, 69.0 mm) contains 126 spots consisting of duplicate oligo-probes spotted onto the surface through a piezo-array system (Petralia et al. 2013) to ensure that differential signals do not occur by chance. The enzymatic thermal cycling and hybridization reactions on the lab-on-a-chip are performed by the electronic TCS. Tropical pathogen detection was split into two chip versions to be subjected to two different multiplex reactions: DNA chip with a

customized microarray layout specific for DNA pathogens and RNA chip specialized for RNA pathogen detection.

3. Virus

Tan et al. (2014) research about tropical pathogens that often cause febrile illnesses in humans and are responsible for considerable morbidity and mortality. The similarities in clinical symptoms provoked by these pathogens make diagnosis difficult. Thus, early, rapid, and accurate diagnosis will be crucial in-patient management and in the control of these diseases. In this study, a microfluidic lab-on-a-chip integrating multiplex molecular amplification and DNA microarray hybridization was developed for simultaneous detection and species differentiation of 26 globally important tropical pathogens. Lab-on-a-chip analytical performance for each pathogen ranged from 10² to 10³ DNA or RNA copies. Assay performance was further verified with human whole blood spiked with Chikungunya virus that yielded a range of detection from 200 to 4 × 10⁵ each pathogen ranged from 250 to 4 × 10⁷ PFU. This lab-on-a-chip was subsequently assessed and evaluated using 170 retrospective patient specimens in Singapore and Thailand. The lab-on-a-chip had a detection sensitivity of a positive 90.0% agreement and a specificity of 100% for Chikungunya virus, and a positive 85.0% agreement and a specificity of 100% for dengue virus serotype 3 with reference methods conducted on the samples. Results suggested the practicality of an amplification microarray-based approach in a field setting for high-throughput detection and identification of tropical pathogens (Tan et al. 2014). Schematic illustration of the detection of tropical pathogen is shown in the workflow in Fig. 12.2.

Phillips et al. (2019) demonstrated point-of-care microfluidic rapid and autonomous analysis device (microRAAD) that automatically detects HIV RNA from whole blood. Treatment of HIV-positive individuals and preventing transmission by the existing laboratory-based testing methods are too complex to perform at the point of care while identifying acute HIV infection. Specifically, molecular techniques can detect HIV RNA within 8–10 days of transmission but require laboratory infrastructure for cold-chain reagent storage and extensive sample preparation performed by trained personnel. They incorporate vitrified amplification reagents, thermally actuated valves for fluidic control, and a temperature control circuit for low-power heating. Reverse transcription loop-mediated isothermal amplification (RT-LAMP) products are visualized using a lateral flow immunoassay (LFIA), resulting in an assay limit of detection of 100 HIV-1 RNA copies when performed as a standard tube reaction. Even after 3 weeks of room-temperature reagent storage, microRAAD automatically isolates the virus from whole blood, amplifies HIV-1 RNA, and transports amplification products to the internal LFIA, detecting as few as 3 × 10⁵ HIV-1 viral particles, or 2.3 × 10⁷ virus copies per mL of whole blood, within 90 min. This integrated microRAAD is a low-cost and portable platform to enable automated detection of HIV and other pathogens at the point of care.

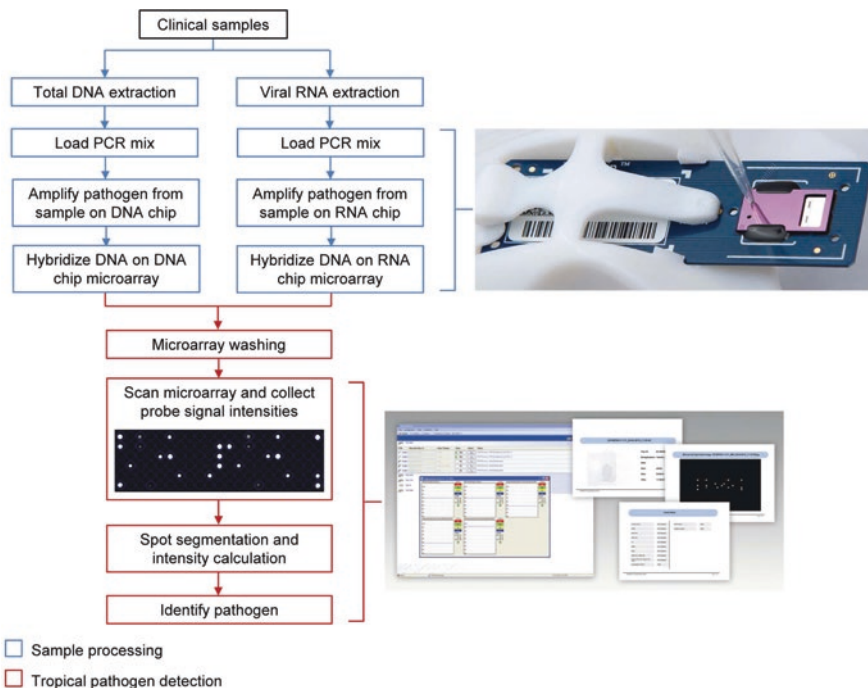


Fig. 12.2 Schematic illustration of tropical pathogen detection workflow. Sample processing steps included the isolation of total DNA and viral RNA from clinical samples, followed by amplification of extracted nuclei acids on the lab-on-a-chip, and hybridization of amplicon to target-specific capture probes (represented in blue). Both the amplification and hybridization processes are performed on the lab-on-a-chip. The steps leading to tropical pathogen identification (as represented in red) comprised of washing and drying of the chip, subsequent reading of the microarray in the optical reader, and software analysis of the microarray image. (Reprinted from Ref. (Tan et al. 2014) with permission from PLOS)

12.4 Conclusion and Future Perspective

In this chapter, we discuss the lab-on-a-chip application to detect the pathogen that can lead to more development of microfluidic system to provide more rapid and accurate early detection system. We include the fabrication and most common technological system used in the devices starting from the sample handling, sample detecting, and signal reading. We also described how the devices can be applied in various fields to detect various sources of pathogen such as bacteria, protozoa, and virus. We foresee that the development of specialized PoC according to the type of the pathogen will become a major breakthrough in the future development of PoC diagnostic tools.

Despite being a potential research area in the last two decades, the realization of an ideal PoC device for pathogen detection is yet to be applied in the society. Development of the devices is a complex multidisciplinary problem and brings

major discrepancy for the integration of both engineering and biochemical technologies. This obstacle must be overcome by choosing an ideal biochemical/bioanalytical technique to facilitate a simple, robust, and portable device with simple functionality. LAMP technology being an isothermal amplification method displaying high speed, high amplification power, and high diagnostic specificity and sensitivity is ideally suited for the development of this next generation of PoC devices. The application of surface-bound nucleic acid amplification techniques could be a direction that has the potential to provide multiplexing capability to the next generation of PoC devices in the near future. Open-source hardware and the possibility of implementing disposable polymer biochips, instead of expensive and cumbersome to fabricate silicon- and silica-based chips, have the potential to overcome the existing design complexities and the engineering hurdles to be successful in developing simple, yet robust, PoC devices. Thus, the new frontiers in the future PoC devices could be fully integrated, simple, compact devices, providing analytical performance superior to that of the current state-of-the-art technologies.

Acknowledgments The Basic Science Research Program supported this work through the National Research Foundation of Korea (NRF) funded by the Ministry of Education (No. 2018R1A6A1A03025582, 2019R1D1A3A03103828, and 2022R1I1A3063302), Republic of Korea.

References

- Afshari A, Schrenzel J, Ieven M, Harbarth S. Bench-to-bedside review: rapid molecular diagnostics for bloodstream infection – a new frontier? *Crit Care*. 2012;16:222.
- Ahn CH, Choi J-W, Beaucage G, Nevin J, Lee J-B, Puntambekar A, Lee RJY. Disposable smart lab on a chip for point-of-care clinical diagnostics. *Proc IEEE*. 2004;92:154–73.
- Amexo M, Tolhurst R, Barnish G, Bates I. Malaria misdiagnosis: effects on the poor and vulnerable. *Lancet*. 2004;364:1896–8.
- Bakajin O, Fountain E, Morton K, Chou SY, Sturm JC, Austin RH. Materials aspects in micro- and nanofluidic systems applied to biology. *MRS Bull*. 2006;31:108–13.
- Breman JG, Alilio MS, Mills A. Conquering the intolerable burden of malaria: what's new, what's needed: a summary. *Am J Trop Med Hyg*. 2004;71:1–15.
- Burke MW. Image acquisition. 1996. <https://doi.org/10.1007/978-94-009-0069-1>
- Castillo-León J. Microfluidics and lab-on-a-chip devices: history and challenges. In: Castillo-León J, Svendsen WE, editors. *Lab-on-a-chip devices and micro-total analysis systems*. Cham: Springer; 2015. p. 1–15.
- Craw P, Balachandran W. Isothermal nucleic acid amplification technologies for point-of-care diagnostics: a critical review. *Lab Chip*. 2012;12:2469.
- Duffy DC, McDonald JC, Schueller OJA, Whitesides GM. Rapid prototyping of microfluidic systems in poly(dimethylsiloxane). *Anal Chem*. 1998;70:4974–84.
- Foudeh AM, Fatanat Didar T, Veres T, Tabrizian M. Microfluidic designs and techniques using lab-on-a-chip devices for pathogen detection for point-of-care diagnostics. *Lab Chip*. 2012;12:3249.
- Giannitsis AT, Min M. Usage of microfluidic lab-on-chips in biomedicine. In: 2010 12th biennial baltic electronics conference. Tallinn: IEEE; 2010. p. 249–52.
- Gupta S, Ramesh K, Ahmed S, Kakkar V. Lab-on-chip technology: a review on design trends and future scope in biomedical applications. *IJBST*. 2016;8:311–22.

- Hopkins H, González IJ, Polley SD, et al. Highly sensitive detection of malaria parasitemia in a malaria-endemic setting: performance of a new loop-mediated isothermal amplification kit in a remote clinic in Uganda. *J Infect Dis.* 2013;208:645–52.
- Izadi D, Nguyen T, Lapidus L. Complete procedure for fabrication of a fused silica ultrarapid microfluidic mixer used in biophysical measurements. *Micromachines.* 2017;8:16.
- Kant K, Shahbazi M-A, Dave VP, Ngo TA, Chidambara VA, Than LQ, Bang DD, Wolff A. Microfluidic devices for sample preparation and rapid detection of foodborne pathogens. *Biotechnol Adv.* 2018;36:1003–24.
- Khanarian G. Optical properties of cyclic olefin copolymers. *Opt Eng.* 2001;40:1024.
- Kovarik ML, Ornoff DM, Melvin AT, Dobes NC, Wang Y, Dickinson AJ, Gach PC, Shah PK, Allbritton NL. Micro total analysis systems: fundamental advances and applications in the laboratory, clinic, and field. *Anal Chem.* 2013;85:451–72.
- Lafleur JP, Jönsson A, Senkbeil S, Kutter JP. Recent advances in lab-on-a-chip for biosensing applications. *Biosens Bioelectron.* 2016;76:213–33.
- Liang C, Chu Y, Cheng S, Wu H, Kajiyama T, Kambara H, Zhou G (2012) Multiplex Loop-Mediated Isothermal Amplification Detection by Sequence-Based Barcodes Coupled with Nicking Endonuclease-Mediated Pyrosequencing. *Anal Chem* 84:3758–3763.
- Ma L, Petersen M, Lu X. Identification and antimicrobial susceptibility testing of *Campylobacter* using a microfluidic lab-on-a-chip device. *Appl Environ Microbiol.* 2020;86:e00096–20.
- Maia Chagas A, Prieto-Godino LL, Arrenberg AB, Baden T. The €100 lab: a 3D-printable open-source platform for fluorescence microscopy, optogenetics, and accurate temperature control during behaviour of zebrafish, *Drosophila*, and *Caenorhabditis elegans*. *PLoS Biol.* 2017;15:e2002702.
- Mandal PK, Biswas AK, Choi K, Pal UK. Methods for rapid detection of foodborne pathogens: an overview. *Am J Food Technol.* 2011;6:87–102.
- Murray CK, Gasser RA, Magill AJ, Miller RS. Update on rapid diagnostic testing for malaria. *Clin Microbiol Rev.* 2008;21:97–110.
- Nasseri B, Soleimani N, Rabiee N, Kalbasi A, Karimi M, Hamblin MR. Point-of-care microfluidic devices for pathogen detection. *Biosens Bioelectron.* 2018;117:112–28.
- Nguyen T, Zoëga Andreasen S, Wolff A, Duong Bang D. From lab on a chip to point of care devices: the role of open source microcontrollers. *Micromachines.* 2018;9:403.
- Nguyen T, Anh Ngo T, Duong Bang D, Wolff A. Optimising the supercritical angle fluorescence structures in polymer microfluidic biochips for highly sensitive pathogen detection: a case study on *Escherichia coli*. *Lab Chip.* 2019;19:3825–33.
- Nguyen T, Chidambara VA, Andreasen SZ, Golabi M, Huynh VN, Linh QT, Bang DD, Wolff A. Point-of-care devices for pathogen detections: the three most important factors to realise towards commercialization. *TrAC Trends Anal Chem.* 2020;131:116004.
- Nikkhoo N, Cumby N, Gulak PG, Maxwell KL. Rapid bacterial detection via an all-electronic CMOS biosensor. *PLoS ONE.* 2016;11:e0162438.
- O’Dempsey TJD, McArdla TF, Laurence BE, Lamont AC, Todd JE, Greenwood BM. Overlap in the clinical features of pneumonia and malaria in African children. *Trans R Soc Trop Med Hyg.* 1993;87:662–5.
- Obahiagbon U, Smith JT, Zhu M, Katchman BA, Arafa H, Anderson KS, Blain Christen JM. A compact, low-cost, quantitative and multiplexed fluorescence detection platform for point-of-care applications. *Biosens Bioelectron.* 2018;117:153–60.
- Oh SJ, Park BH, Jung JH, Choi G, Lee DC, Kim DH, Seo TS. Centrifugal loop-mediated isothermal amplification microdevice for rapid, multiplex and colorimetric foodborne pathogen detection. *Biosens Bioelectron.* 2016;75:293–300.
- Petralia S, Conoci S. PCR technologies for point of care testing: progress and perspectives. *ACS Sens.* 2017;2:876–91.
- Petralia S, Verardo R, Klaric E, Cavallaro S, Alessi E, Schneider C. In-check system: a highly integrated silicon lab-on-chip for sample preparation, PCR amplification and microarray detection of nucleic acids directly from biological samples. *Sensors Actuators B Chem.* 2013;187:99–105.

- Phillips EA, Moehling TJ, Ejendal KFK, et al (2019) Microfluidic rapid and autonomous analytical device (microRAAD) to detect HIV from whole blood samples. *Lab Chip* 19:3375–3386.
- Polley SD, Gonzalez IJ, Mohamed D, et al. Clinical evaluation of a loop-mediated amplification kit for diagnosis of imported malaria. *J Infect Dis.* 2013;208:637–44.
- Reisner W, Larsen NB, Flyvbjerg H, Tegenfeldt JO, Kristensen A. Directed self-organization of single DNA molecules in a nanoslit via embedded nanopit arrays. *Proc Natl Acad Sci U S A.* 2009;106:79–84.
- Sin ML, Gao J, Liao JC, Wong PK. System integration – a major step toward lab on a chip. *J Biol Eng.* 2011;5:6.
- Sun Y, Quyen TL, Hung TQ, Chin WH, Wolff A, Bang DD. A lab-on-a-chip system with integrated sample preparation and loop-mediated isothermal amplification for rapid and quantitative detection of *Salmonella* spp. in food samples. *Lab Chip.* 2015;15:1898–904.
- Tan JLL, Capozzoli M, Sato M, et al. An integrated lab-on-chip for rapid identification and simultaneous differentiation of tropical pathogens. *PLoS Negl Trop Dis.* 2014;8:e3043.
- Taylor BJ, Howell A, Martin KA, et al. A lab-on-chip for malaria diagnosis and surveillance. *Malar J.* 2014;13:179.
- Teo J, Pietro PD, Biagio FS, et al. VereFlu™: an integrated multiplex RT-PCR and microarray assay for rapid detection and identification of human influenza A and B viruses using lab-on-chip technology. *Arch Virol.* 2011;156:1371.
- The malERA Consultative Group on Diagnoses and Diagnostics. A research agenda for malaria eradication: diagnoses and diagnostics. *PLoS Med.* 2011;8:e1000396.
- Thiha A, Ibrahim F, Muniandy S, Dinshaw IJ, Teh SJ, Thong KL, Leo BF, Madou M. All-carbon suspended nanowire sensors as a rapid highly-sensitive label-free chemiresistive biosensing platform. *Biosens Bioelectron.* 2018;107:145–52.
- Tsougeni K, Kastania AS, Kaprou GD, Eck M, Jobst G, Petrou PS, Kakabakos SE, Mastellos D, Gogolides E, Tserepi A. A modular integrated lab-on-a-chip platform for fast and highly efficient sample preparation for foodborne pathogen screening. *Sensors Actuators B Chem.* 2019;288:171–9.
- van den Berg A. Labs on chips for biomedical applications. In: 2013 IEEE 26th international conference on micro electro mechanical systems (MEMS). Taipei: IEEE; 2013, p. 149–152.
- Volpatti LR, Yetisen AK. Commercialization of microfluidic devices. *Trends Biotechnol.* 2014;32:347–50.
- Waldauer SA, Wu L, Yao S, Bakajin O, Lapidus LJ. Microfluidic mixers for studying protein folding. *JoVE.* 2012;3976
- Wang L-J, Sun R, Chang Y-C, Li L. Ultra low-cost, portable smartphone optosensors for mobile point-of-care diagnostics. In: Raghavachari R, Liang R, Pfefer TJ, editors. Design and quality for biomedical technologies XI. San Francisco: SPIE; 2018. p. 32.
- Watanabe R, Buates A, Tsuboi T, Takeo S, Krasaesub S, Suktawonjaroenpon W, Sattabongkot J, Sirichaisinthop J, Han E-T. Evaluation of loop-mediated isothermal amplification (LAMP) for malaria diagnosis in a field setting. *Am J Trop Med Hygiene.* 2011;85:594–6.
- Wittbrodt BT, Glover AG, Laureto J, Anzalone GC, Oppliger D, Irwin JL, Pearce JM. Life-cycle economic analysis of distributed manufacturing with open-source 3-D printers. *Mechatronics.* 2013;23:713–26.
- Yager P, Domingo GJ, Gerdes J. Point-of-care diagnostics for global health. *Annu Rev Biomed Eng.* 2008;10:107–44.
- Zhang X, Lowe SB, Gooding JJ. Brief review of monitoring methods for loop-mediated isothermal amplification (LAMP). *Biosens Bioelectron.* 2014;61:491–9.
- Zhi X, Deng M, Yang H, Gao G, Wang K, Fu H, Zhang Y, Chen D, Cui D. A novel HBV genotypes detecting system combined with microfluidic chip, loop-mediated isothermal amplification and GMR sensors. *Biosens Bioelectron.* 2014;54:372–7.
- Zhu H, Fohlerová Z, Pekárek J, Basova E, Neuzil P. Recent advances in lab-on-a-chip technologies for viral diagnosis. *Biosens Bioelectron.* 2020;153:112041.

Chapter 13

Nanodiagnosics: New Tools for Detection of Animal Pathogens



Atef A. Hassan, Rasha M. H. Sayed-ElAhl, Ahmed M. El Hamaky, Mogda K. Mansour, Noha H. Oraby, and Mahmoud H. Barakat

Abbreviations

| | |
|---------------------|--|
| AFB ₁ | Aflatoxin B ₁ |
| AuNPs | Gold nanoparticles |
| <i>B. anthracis</i> | <i>Bacillus anthracis</i> |
| CNTs | Carbon nanotubes |
| EIS | Electrochemical impedance spectroscopy |
| GQDs | Graphene quantum dots |
| H5N1 | Avian influenza |
| MNPs | Magnetic nanoparticles |
| ND | Newcastle disease |
| NPs | Nanoparticles |
| QCM | Quartz crystal microbalance |
| QDs | Quantum dots |

13.1 Introduction

To date, the urgent worldwide needs for rapid and effective detection of human and animal diseases have shown increasing attentions from all authorities and scientists. The continuous advancement of nanotechnology has helped in the development of novel tools used in disease diagnosis (nanodiagnosics) such as microchips, biosensors, nanorobots, and other tools (Jain et al. 2021; Lastra et al. 2021; Huang et al. 2022). The zoonotic health hazards of human and animal diseases resulted in serious

A. A. Hassan (✉) · R. M. H. Sayed-ElAhl · A. M. El Hamaky · M. K. Mansour · N. H. Oraby
Animal Health Research Institute (AHRI), Agriculture Research Center (ARC), Giza, Egypt
M. H. Barakat
Faculty of Medicine, Cairo University, Cairo, Egypt

adverse effects such as COVID-19 infection (Dong et al. 2020; Rosati et al. 2021). The control of such infections needs rapid and effective detection of causative agents by available methods. To date, conventional diagnostic methods such as molecular biology techniques, which are sensitive and specific in the detection of infective agents in spite of needing expensive instruments and chimerical reagents. Recently, nanotechnology has potentiated the production of nanodiagnostic devices for the successful detection of infectious diseases (Manhas et al. 2021; Kirtane et al. 2021). Several uses of nanomaterial in animal production, disease diagnosis, tumor detection, MRI, and other uses are shown (Alghuthaymi et al. 2021). In these respects, nanosized materials such as gold nanoparticles (AuNPs) have specific characters on the nanodimensional scale (Agasti et al. 2010) that enable successful diagnostic use (Draz and Shafiee 2018). They potentiated imaging, effective diagnosis, and cancer detection. (Xiong et al. 2022). Where diseases result in various health problems for humans and livestock, conventional methods of diagnosis are still not enough (Manhas et al. 2021; Huang et al. 2022). The progressive advancement of microbial infection and their drug resistance potentiated the active search for effective methods of their diagnosis and therapy (Hassan et al. 2016; Qindeel et al. 2021). On the other hand, nanotechnology potentiated the production of novel diagnostic tools in veterinary animals. The nanosized materials have been used in disease treatments and diagnosis of estrus and the fertility hormone (Sagadevan and Periasamy 2014). They have availability for use in maintaining the genital organs and their functions (Saragusty and Arav 2011; Hill and Li 2017). Various combined nanomaterials as nanoshells such as silica NPs, CNTs, AuNPs, AgNPs, and FeONPs have been used in tumor cell detection, coagulation, electrochemical sensors, disease detection, and MRI scanning respectively (Hassan et al. 2020a, 2021a; Jo et al. 2020; Phatruengdet et al. 2022). Moreover, Lastra et al. (2021) and Yoo et al. (2021) reported that single molecule sensors, e.g., **nanopores**, can sense **biomolecules** as patient DNA and protein for accurate disease diagnosis. Hence, the present chapter is aimed at illustrating the possibility of nanotechnology use as nanodiagnostics of human and animal diseases in comparison with old conventional methods. Discussions of different nanodiagnostic types are briefly undertaken.

13.2 Traditional Methods for Detection of Animal Diseases

The conventional methods for diagnosis of animal diseases used several traditional tests such as physical examination (Jain et al. 2021). The detection histopathological changes of organ tissues, biochemical and blood parameters in body secretions were also used for disease diagnosis (El-Nahass et al. 2019; Hassan et al. 2020a, 2021a; Singh et al. 2022). In spite of this, all conventional disease diagnosis tests are time consuming, inaccurate in some cases, and nonspecific. Hence, recent progressive advancement in effective and rapid diagnostics is needed.

13.3 Recent Approaches of Nanomaterial Applications in Detection of Animal Diseases

13.3.1 Types of Nanodiagnostics

Figure 13.1 shows the different types of nanomaterials used in the diagnosis of animal diseases.

13.3.1.1 Nanotubes

Nanotubes are used in the production of electronics that have an electrical structure and excellent conduction of energy. Most nanotubes used are made of carbon nanomaterial conjugated with gold nanomaterial, which can be used in cancer diagnosis (Beishon 2013; Jackson et al. 2017; Habibullah et al. 2021). Similarly, they may be attached with silica nanowires, which have potential in the diagnosis of the constituents of lung breath (Shehada et al. 2015; Sharma et al. 2020a, b).

13.3.1.2 Nanocrystal

Nanocrystals have electrical, thermal, and dynamic characteristics related to the size of the crystals. They are semiconductors measuring 10 nm. By conjugation with silica they can adsorb protein and are used for the treatment of bone afflictions (Kumar and Vijayalakshmi 2006; Roco et al. 2017).

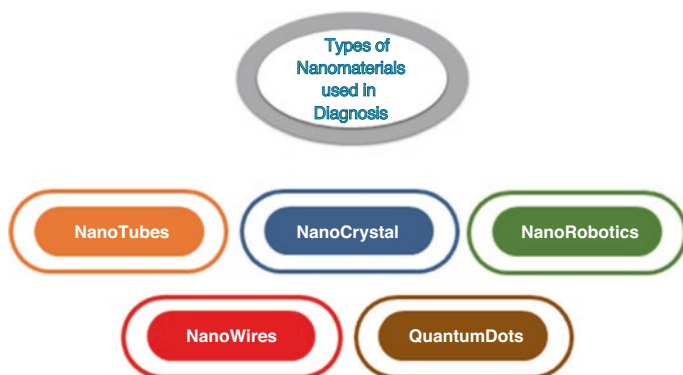


Fig. 13.1 Types of nanomaterials used in diagnosis of animal diseases

13.3.1.3 Nanorobotics

Nanorobots are nanosized robots that are used for diagnosis and as a carrier of drugs in treatment of cancers and diabetes. Also, nanorobotic dentifrices can be used in the identification of bacteria and organic matter in the mouth cavity and thus destroy them (Shetty et al. 2013; Lastra et al. 2021).

13.3.1.4 Nanowires

Nanowires have the ability to transfer electrical currents and may consist carbon nanotubes (CNTs) and metal oxides or silicon. The nanosize of the wires enables them to detect any changes in electrical characteristics conjugated with any biological marker materials such as antibodies. Hence, various nanowires can be conjugated with antibodies and target the diagnosis of cancer such as silicon nanowire (SiNW) used in sensors as field effect transistors (Reimhult and Höök 2015; Jeelani et al. 2020). The silica nanowires have been shown to be used in the diagnosis of prostatic and testicular cancer biomarkers RNA (prostate-specific antigen and testis antigen). Also, they have been functionalized with DNA and enable the diagnosis of breast cancer (Takahashi et al. 2015; Lastra et al. 2021).

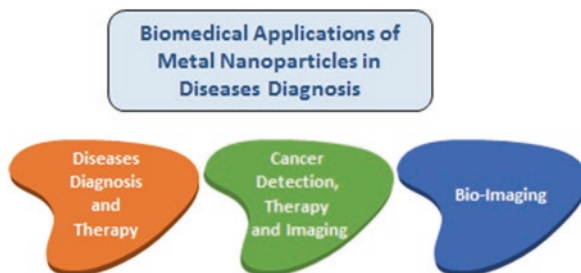
13.3.1.5 Quantum Dots

Quantum dots (QDs) are fluorescent crystalline nanomaterials and the radiation of QDs causes transition of light (dots) according to their size. They can be embedded in a given micro-bead, producing a distinct spectrum of colors once excited. This, when it occurs, has assisted in microbial genotype characterization and diagnosis. In addition, the QDs may be attached to diagnostic tools for effective diagnosis and treatments. They can be conjugated with fluorescence microscopy to perform imaging of cancer cells (Rajasundari and Hamurugu 2011; Campbell et al. 2021; Cao et al. 2022).

13.3.2 *Biomedical Applications of Nanodiagnosics*

Figure 13.2 shows the biomedical applications of metal nanoparticles in disease diagnosis.

Fig. 13.2 Biomedical applications of metal nanoparticles in disease diagnosis



13.3.2.1 Disease Diagnosis and Therapy

Worldwide, the successful detection of infectious diseases is the first step in the efficiency of disease therapy. Nanotechnology initiated the production of novel devices that achieved the detection and treatment of infections. The nanocomposites of AgNPs with oil have been used for detection of skin and mastitis infections in cows (Sanchez et al. 2012; Bansod et al. 2015), whereas the conjugation of biological materials with polymers have enabled their delivery to the targeted tissues (Meena et al. 2018; Kusat and Akgöl 2021). The utilization of chitosan NPs in drug transfer to cancer cells and vaccine delivery was shown (Ghadi et al. 2014 ; Shi et al. 2012), whereas the hybrid of silica NPs with body carbohydrates and proteins help in disease detection and therapy (Burns et al. 2006; Jeelani et al. 2020) and elaboration of drugs to targeted diseased tissues (Shirahata 2011). Moreover, the nanosensors act as nanocarriers and have a significant function in diagnosis and food coating (Neethirajan et al. 2017; Kusat and Akgöl 2021; Derakhshan et al. 2021). They added that their activities depend on conjugated material such as enzymes, antigens, proteins, and others being used for disease detection and delivery of bound materials to target tissues. On the other hand, the conjugation of AuNPs and anti-aflatoxin M_I (AFM_I) enables the immunological detection AFM_I in milk (Wang et al. 2011). Moreover, silica nanoshells and metal nanomaterials searched for and directed at targeted cancer cells (Ajmal et al. 2015), whereas QDs enable scanning of tissues and organ events during infections (Campbell et al. 2021; Hassan et al. 2021a; Zeng et al. 2022).

13.3.2.2 Cancer Detection

Several studies evaluated the efficiency of green synthesized metal nanomaterials and their hybrids in the detection and treatment of cancers. In this respect, AgNPs synthesized by extracts of *Euphorbia nivulia* have cytotoxic effects against human respiratory system tumors (Valodkar et al. 2011), whereas metal nanomaterials and nanocomposites have significant potential to penetrate tumor cells and accumulate inside them, causing their destruction and death. The nanocomposites of sugars and nanomaterials improve the detection and drug delivery in lung cancers (Ajmal et al.

2015). Although ZnNPs cause tumor cell detection and their death and preserve immune cells intact (Abd El Fatah et al. 2017), parental administration of magnetic nanoparticles (MNPs) can adhere them to cancer cells and help in their detection and therapy. The conjugation of QDs with silica NPs and PEGylated lipids are also employed in tumor diagnosis and treatments (Van Schooneveld et al. 2008). In addition, the yolk-shell MNPs, composite of MNPs/QDs, and metallic nanocomposites have significant activities in MRI of tumors and cancer drug delivery (Gao et al. 2008; Xiong et al. 2022). Moreover, NP functionalization with biological materials can help in tumor diagnosis and their treatment in animals (Alexis et al. 2010). In addition to the conjugation of AuNPs with gum arabic potentiated the scanning of tumors and drug delivery (Chanda et al. 2014).

Meanwhile, Osama et al. (2020) demonstrated the ability of liposome nanocomposites to diagnose spleen cancer. However, the functionalization of hybrid NPs with body protein, DNA, and drugs can be improved in cancer detection (Dilbaghi et al. 2013). Moreover, Meena et al. (2018) and Hassan et al. (2020c) illustrated the great benefits of CNTs in the treatment of fungal and tumor infections. Also, Zhu et al. (2016) revealed the efficiency of CNTs in the exploration of thyroid gland tumors. Moreover, the composite of mesoporous silica NPs/folic acid improved drug delivery to targeted cancer tissues in laboratory animals (Lu et al. 2010), whereas, silica NPs and magnetic NPs enabled MRI and treatment of tumors (Kim et al. 2007). Nasar et al. (2019) demonstrated that AgNPs have been inhibiting the activity of hepatic tumor cells in humans at doses of 62.5 $\mu\text{g}/\text{ml}$. Recently, carbon NP suspension injection were shown to be used for the diagnosis of lymphatic mapping and tumors (Li et al. 2016; Zhu et al. 2016; Hassan et al. 2020b) and mammary gland tumors (Wu et al. 2015). They were also used in the detection of thyroid carcinoma (Gu et al. 2015; Zhu et al. 2016), whereas carbon nanomaterials were used in imaging of tissues such as lymph nodes (Wang et al. 2017a, b; Rasheed et al. 2021). He et al. (2009) found that the conjugation of silica NPs with methylene blue dyes potentiated the fluorescent imaging of HeLa cells. Moreover, iron oxide NPs have been applied for the detection of tendon infection in sheep via imaging (Scharf et al. 2015; Phatruengdet et al. 2022).

In a recent study, Campbell et al. (2021) (Xiong et al. 2022) developed novel anti-cancer-nanomaterials based on nitrogen-doped graphene quantum dots (N-GQDs) attached with ferrocene and hyaluronic acid. These materials enable the fluorescence imaging of cancer cells and the therapeutic effect is also obtained. Currently, the strategies of using nanotechnology in cancer detection and therapy are directed at tumor cells without affecting other healthy cells (Figs. 13.3 and 13.4).

13.3.2.3 Bio-imaging

The essential roles in the diagnosis of the correct disease are the detection of internal events and changes in body tissues that relate to the diseased organs. In this respect, some NPs such as MNPs are used in MRI by penetrating the cells and



Fig. 13.3 Nanotechnology improves cancer detection and diagnosis. (Adapted from Zhang et al. 2019)

tissues and hence imaging them (Long et al. 2015; Phatruengdet et al. 2022). Although the $\text{Fe}_3\text{O}_4\text{-Cd-Se}$ nanocomposite passed light signals that caused targeted cells and tissue movements that can be treated and imaged by iron NPs (Gao et al. 2008). The QDs are semiconductor materials and can be applied in the detection of diseases and humeral immune status (Geszke-Moritz and Moritz 2013), although the nanocomposites of cobalt/cadmium/selenium with metals enable signals to be produced in scanning the status of tissues and organs during diseases (Petryayeva et al. 2013). However, the utilization of QDs with natural body components resulted in the formation of significant signals, which enabled them to be used in the effective imaging of diseased tissues (Ruedas-Rama et al. 2012; Petryayeva et al. 2013; Zeng et al. 2022). Various metal nanomaterials such as zinc NPs have been applied in disease diagnosis such as in animal cancers (Raguvaran et al. 2015; Gurunathan et al. 2018). Also, AuNPs can be applied for exploration of chicken influenza virus (Nurulfiza et al. 2011; Yang et al. 2020; Lim et al. 2021), foot and mouth disease virus (Ding et al. 2011), and bluetongue virus (Wang et al. 2013). They were also applied in bacterial and toxin characterization in poultry (Moongkarndi et al. 2011; Meng et al. 2014; Zhu et al. 2014). Similarly, diagnosis of parasitic infection in serum can be achieved using AuNPs (Jahani et al. 2014; Jiang et al. 2015) and *E. coli O157:H7* in cows (Hassan et al. 2020c; Selvarajan et al. 2020). However, carbon nanomaterials are applied in disease diagnosis and treatment (Li et al. 2017; Wang et al. 2017a, b; Kour et al. 2020; Rasheed et al. 2021).

Recently, the development of novel anti-cancer nanomaterials based on N-GQDs attached to ferrocene and hyaluronic acid was undertaken (Campbell et al. 2021; Cao et al. 2022). These materials enabled fluorescence imaging of cancer cells and also therapeutic effects targeting tumors. Therefore, cells/tissue imaging, particularly by MRI, is an effective method in disease diagnosis.

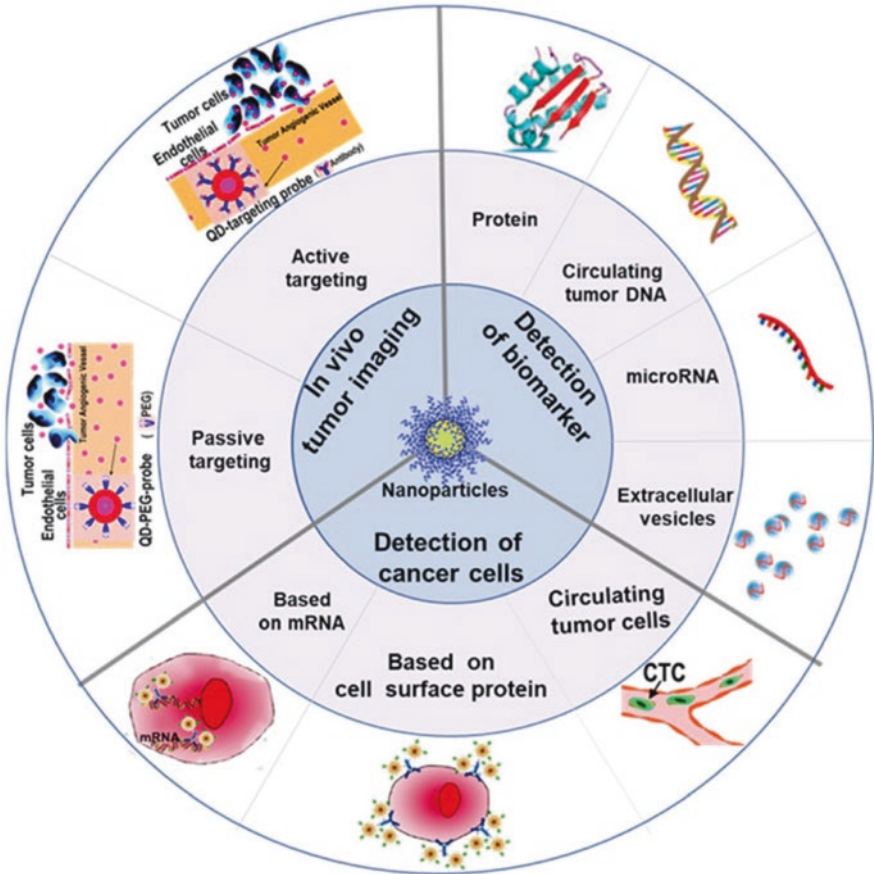


Fig. 13.4 Schematic illustration of nanotechnology applications in cancer diagnosis. (Adapted from: Zhang et al. 2019)

13.4 Methods of Nanoparticle Functionalization for Disease Diagnosis

There is huge popular awareness about the limits of the use of nanomaterials and it needs functionalization to be applied in disease diagnosis (Manhas et al. 2021). The functionalization of NPs can occur via their surface and by their packing in capsule form using biomolecules (Mout et al. 2012; Makvandi et al. 2020) (Fig. 13.5).

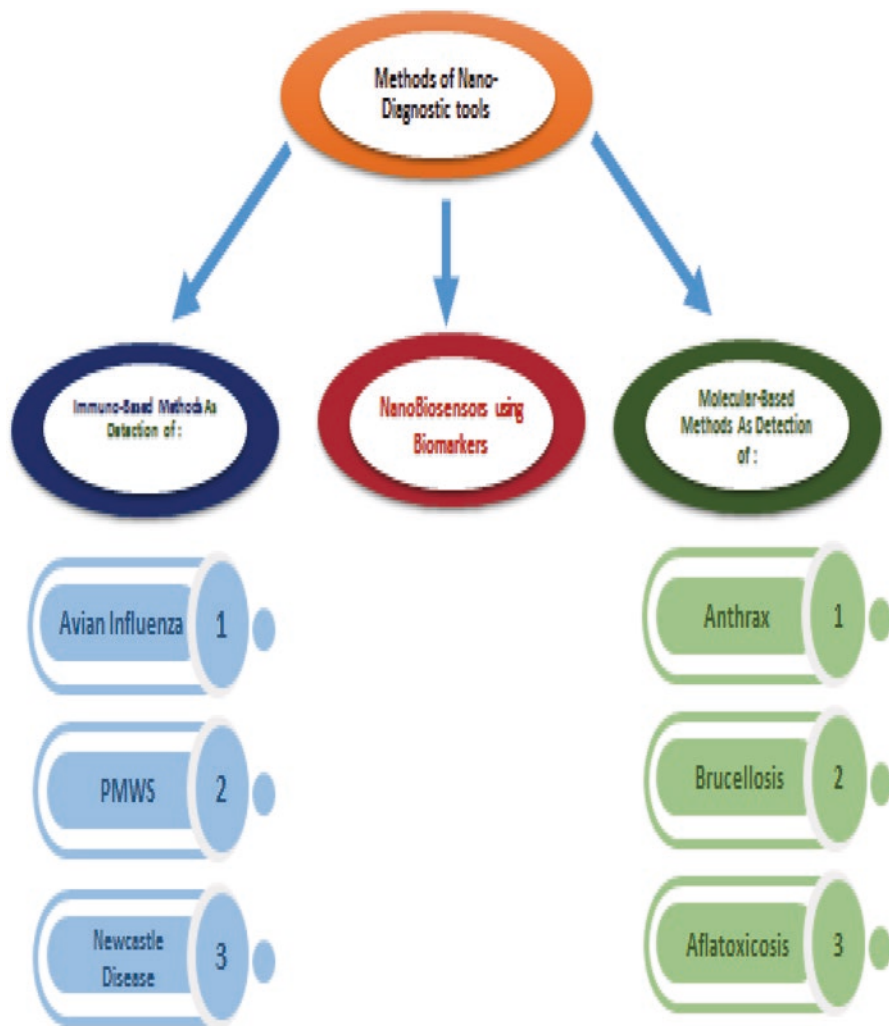


Fig. 13.5 Methods of nanomaterial functionalization

13.4.1 Immuno-Based Methods

Immuno-based methods use biomolecules that are attached to nanomaterials as successful bio-recognition of animal sera antibodies in diagnosis (Vrublevskaya et al. 2017), where they are applied in the detection of various disease pathogens in the secretions of animals (Wu et al. 2016). These nanosized materials are utilized with a pathogen antigen specific to the sera antibodies of infected animals (Sayed et al. 2019). The following diseases can be diagnosed by the detection of antigen or antibody reaction utilizing nanomaterials.

13.4.1.1 Avian Influenza

Avian influenza is a global disease infecting all avians and humans resulted in a health hazard and several economic losses (Allen et al. 2017). The commercial kits used for the diagnosis of avian influenza uses antibodies against this virus conjugated with protein (Matsubara et al. 2020). Nowadays, gold-based immunochromatographic test strips attached to two monoclonal antibodies are used for detection of H7N9 avian influenza viral antigen in tissue culture (Yang et al. 2020) (Fig. 13.6a). They compared this method with molecular detection methods and this immunochromatographic strip test showed higher sensitivity and specificity (Zou et al. 2012; Huang et al. 2016; Jo et al. 2020).

13.4.1.2 Post-weaning Multisystemic Wasting Syndrome

Post-weaning multisystemic wasting syndrome is a non-zoonotic viral disease of pigs that has been shown to cause wasting, respiratory distress, and icterus accompanied by a high mortality rate (Baekbo et al. 2012). This disease is not zoonotic and not transmitted from infected pigs to humans, where it changed in human cells (Liu et al. 2013). The immune-based nanomaterials have been shown to be used in the diagnosis of this infection, whereas PCV2-specific monoclonal antibodies-AuNPs in immunoassay has enabled detection of virus (Zhang et al. 2010; Luo et al. 2013; Liu et al. 2019) (Fig. 13.6b). The detection of viral infections via traditional ELISA has now been improved by nanotechnology to increase its sensitivity in detection, where, in ELISA kits, a recent material of antibody-modified gold-platinum is used instead of horse radish peroxidase, which was present in the old kit (Wu et al. 2020). Hence, the application of nanomaterials in immunological assay resulted in rapid detection of viral infection with low-cost tools.

13.4.1.3 Newcastle Disease

Newcastle disease (ND) is one of the most important viral diseases in poultry, resulting in severe respiratory disorders and decreased production (Hongzhan et al. 2020). ND has been detected in several countries in Asia, Africa, and America. The zoonotic infection of laboratory workers by infected birds may occur in the form of conjunctivitis; hence, a biosafety protocol must be applied (Miller and Koch 2013). The traditional diagnosis of Newcastle disease virus (NDV) depends on isolation and identification of the isolated virus, which takes up to 2 weeks (Senne 2008). Recently, the antigen-based Au-immunochromatographic method conjugated with antigen has enabled identification of ND antibodies (Luo et al. 2018; Yang et al. 2020) (Fig. 13.6c), whereas cadmium QDs can be conjugated with NDV antibodies and iron oxide NPs for detection of the ND antigen (Wang et al. 2010). Therefore, the use of nanotechnology will potentiate the rapid diagnosis of NDVs.

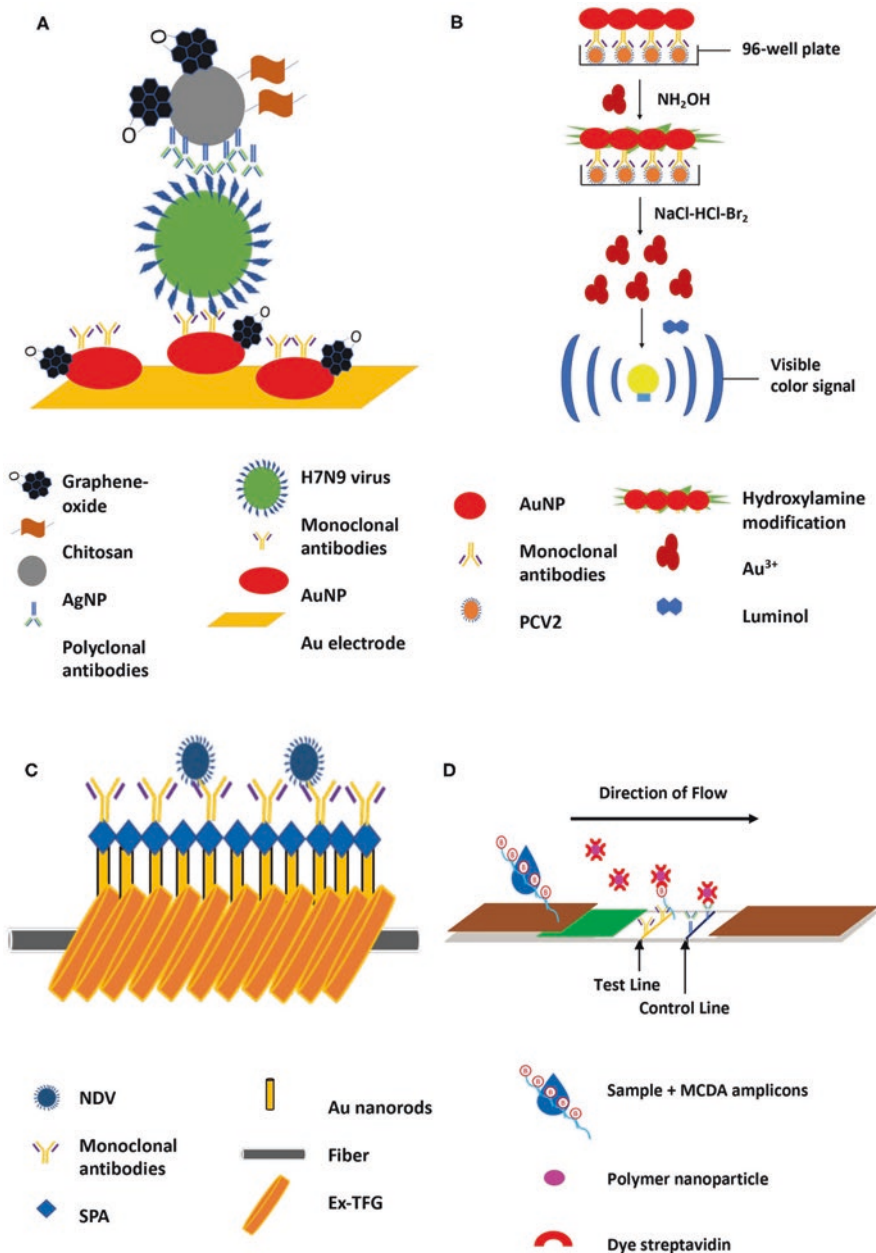


Fig. 13.6 Representative animal disease diagnostic methods incorporated with various nanomaterials (a). Silver nanoparticles in immune-based electrochemical method targeting H7N9 virus (b). Chemiluminescence immunoassay with AuNPs targeting PCV2 (c). Detection of Newcastle disease (ND) by targeting ND antibodies using excessively tilted fiber grating (Ex-TFG) coated with gold nanospheres (d). Polymer nanoparticle-based LFB for detecting brucellosis. (Adapted from Manhas et al. 2021)

13.4.2 *Molecular-Based Methods*

Nowadays, the progressive advancement in nanotechnology potentiated the functionalization of nanomaterials with DNA and RNA to improve diagnosis (aptamers). These methods are more accurate in diagnosis than the immune-based methods. Where the nucleic acids are more stable in human and animal bodies than antibodies, which can be affected by environmental factors as temperature (Frohmeyer et al. 2019). Moreover, the application of molecular-based methods does not require additional methods for final diagnosis, as in the case of antibody-based methods (Song et al. 2012; Lastra et al. 2021). Several infections were diagnosed using a DNA-based technique conjugated with nanosized materials, such as those described in the following sections.

13.4.2.1 **Anthrax**

Anthrax is a worldwide bacterial infection of human and animals caused by *Bacillus anthracis*. Most cases are restricted to human and ruminant animals by consumption of polluted feeds and water (Hugh-Jones and De Vos 2022). Rajput et al. (2017) detected that 30% of sheep and 27.5% of goats were infected with *B. anthracis*. This infection has zoonotic importance and can be transmitted to humans who deal with infected animals (Fasanella et al., 2010). Recently, molecular detection of causative agents has been used for this diagnosis of this disease. In this respect the biosensors were attached with a probe of AuNPs against *B. anthracis* (Deng et al. 2013; Selvarajan et al. 2020). Similarly, Karimi and Dabbagh (2019) detected the viability of CNT aptasensor in the diagnosis of *B. anthracis* infection within 10 min. The current conventional methods of diagnosis are time consuming and of high cost and hence fast diagnostic methods using nanotechnology are of huge importance in this field.

13.4.2.2 **Brucellosis**

Brucellosis is considered the most important disease infecting humans and ruminant animals. The zoonotic role of this disease is due to human consumption of contaminated milk of infected ruminants with brucellosis (Seleem et al. 2010). To date, the diagnosis of such diseases has depended on the isolation and identification of *Brucella* spp. The methods of diagnosis using molecular biology have significant specificity for effective functionalization of nanomaterial probes for the detection of pathogens or their DNA. In this respect, the oligonucleotide can be attached the functionalized AuNP in a cometrix method and enables rapid detection of *Brucella* spp. within 30 min by reacting with the membrane protein layer (Pal et al., 2017) (Fig. 13.6d). Similarly, Sattarahmady et al. (2015), Li et al. (2019a), and Selvarajan et al. (2020) improved the sensitivity of this method with unamplified *Brucella* genomic DNA that has no cross reactivity.

13.4.2.3 Aflatoxicosis

Over the past few decades human and animal mycotoxicosis, particularly aflatoxicosis, has been of significant health importance as it can be detected in animal products (Wang et al. 2018; Hassan et al., 2019a, b, 2020a, 2021a). It is a secondary metabolite of aflatoxigenic *A. flavus* in feeds and food and is present in several forms (B₁, B₂, G₁, and G₂). They have carcinogenic potential against liver cells in humans, animals, and poultry (Nodoushan et al. 2019).

There are different acceptable limits of aflatoxins in food and feeds such as that reported by the European Union (2 ppb AFB₁), whereas the American authority indicated that the permissible limits of aflatoxins are not more than 20 ppb in food, 0.5 ppb in milk, and 100–300 µg/kg in animal feeds (USFDA 2000; Tan et al. 2019).

To date, the traditionally used methods for the detection of mycotoxins included thin-layer and high-performance liquid chromatography, mass spectroscopy, immunoaffinity column methods, and ELISA (AOAC 2000). Currently, the progressive advancement in nanotechnology enables the production of novel tools for effective rapid diagnosis and detection of aflatoxins. In this respect, Nodoushan et al. (2019) developed an aptasensor attached to gold nanowires/graphene for measurement of AFB₁. Also, Tan et al. (2019) detected silica nanomaterial conjugated with amino acids in molecular-based methods and this aptamers can help with sensitivity in the detection of low limits of aflatoxins compared with chromatographic methods.

13.5 Nano Biosensors Using Biomarkers

Early and fast detection is urgently needed for the control of chronic diseases, especially in large populations of animals such as a herd of cattle or poultry. Human and animal diseases cause several economic losses in health and hence their early detection has gained huge attention (Jain et al. 2021). Recently, nanotechnology potentiated the development of novel nanodiagnostic materials such as biosensors that have high efficiency in disease diagnosis depending on their biomarkers of diseases (Jain et al. 2021; Hassan et al. 2021a, b).

13.5.1 Types of Biosensors

Figure 13.7 shows the various types of biosensors

13.5.1.1 Electro-Chemical Biosensors

Electro-chemical biosensors enable the detection of electrical characteristics occurring because of the introduction of electrons in biological materials into infected humans and animals (Mohanty and Kougianos 2006; Al-Mamun et al. 2021). They

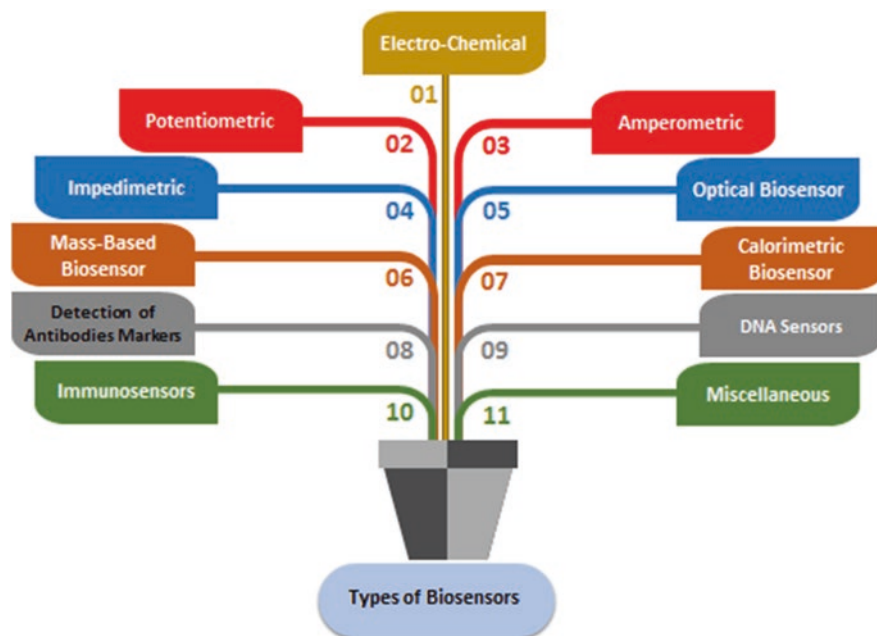


Fig. 13.7 Types of biosensors

interact with investigated materials and elaborated signals that depend on the concentration of target materials. The diagnosis by use of electrochemical biosensors is characterized by significant sensitivity and low costs. Nowadays, the functionalization of nanomaterials in electrochemical methods has resulted in an increase in the quality of lower detection limits as CNT methods have gained huge attention in immunoassay diagnosis, such as electrochemical impedance spectroscopy (EIS), which has high sensitivity and fast detection (Yang et al. 2020). The electrode of this method is functionalized and conjugated with natural biological materials and sometimes includes two or three electrodes in biological material, one is active, the other is the reference electrode, whereas in the case of three electrodes, the third is the counter electrode (Matsubara et al. 2020). The active working electrode must be of a stable and conductive material as gold and silicon nanomaterials which are usually used according to the types of biological materials. These methods of biosensors included potentiometric, amperometric, voltammetric, and impedimetric/conductometric (Velusamy et al. 2010; Al-Mamun et al. 2021).

13.5.1.2 Potentiometric Biosensors

Potentiometric biosensors have been applied by the parallel action of the working electrode and the reference electrode with control (Pohanka and Skladal 2008). They are used in detection by the changes of biomarkers (such as a pathogen) into

significant signals that are measured by a reference electrode (Leonard et al. 2003; Kusat and Akgöl 2021).

13.5.1.3 Amperometric Biosensors

Amperometric biosensors are used for the detection of an enzymatic activity biomarker, which produces electro signals on working electrodes (such as metals) through amperometric biosensors (Leonard et al. 2003). The amperometric biosensors are more suitable for large-scale use than potentiometric biosensors (Pohanka and Skladal 2008).

13.5.1.4 Impedimetric Biosensors

Recently, there have been several inventions for the production of impedimetric biosensors such as EIS. It is considered a significant instrument and has effective sensitivity for the detection of biological events of pathogens in humans and animals (Bahadır and Sezginturk 2016; Hammond et al. 2016). Impedimetric biosensors detected that the antibodies as biomarkers against pathogens are moved onto electrodes, semiconductor chips, or optical fibers.

13.5.2 *Optical Biosensor*

Optical biosensors are the diagnostic tools that are characterized by signal production related to the levels of measured materials. The signals produced resulted from the reaction of sensors with the disease biomarkers, which can be measured using fluorometric methods (Velusamy et al. 2010; Huang et al. 2011; Sharma et al. 2020a, b). These methods, particularly fluorescent biosensors, have significant roles and wide use in disease diagnosis (Girigoswami and Akhtar 2019; Gupta et al. 2020).

13.5.3 *Mass-Based Biosensor*

Mass-based biosensors are also named gravimetric biosensors, which can determine mass by piezoelectric materials producing audible resonance. The conjugation of a quartz crystal microbalance (QCM) tool with antigen–antibody interaction can be used in microbial diagnosis and their toxins (Ozalp et al. 2015; Neethirajan et al. 2018).

13.5.4 Calorimetric Biosensor

Calorimetric biosensors are considered thermal biosensors that determined heat released from the enzymatic reaction of biomarkers (Kopparthy et al. 2015). They are thermistors (to measure the changes in temperatures) or thermopiles (calorimetric biosensors). They are covered by retaining material to insulate the heat that was produced using the reaction of biomarker (enzyme) with analyst. The conventional differential scanning calorimetric methods are complicated, need a large amount of sample, and take a long time to diagnose pathogens (MicroCal 2017). Hence, they are employed to improve the disadvantages of the conventional methods and showed significant efficiency in application (Hohne et al. 2004; Alafeef et al. 2020).

13.5.5 Detection of Antibody Markers

The antibodies are famous biomarkers that have the ability to react with specific pathogen antigens (Connelly and Baeumner 2012). The antibodies that are used in biosensors are monoclonal and polyclonal, and the conjugated ones have been significantly applied in immune-biosensor functionalization (Flajnik et al. 2011; Kusat and Akgöl 2021).

13.5.6 DNA Sensors

To date, the use of molecular DNA-based nanobiosensors are applied in the detection of biomarkers of many diseases. Various infectious diseases are diagnosed as anthrax using a nanopore real-time sensing tool for a DNA probe of toxin (Wang et al. 2014). Infection with *Brucella* disease can be also detected by geno-sensor. Where AuNP ribbon is covered by gold nanoblooms and added to the surface of gold, this can be used with methylene blue to identify redox markers of DNA sequences (Rahi et al. 2015; Sattarahmady et al. 2016; Gupta et al. 2020). Another study detected that gold nanorods utilized and conjugated with DNA probe gene for diagnosis of *Campylobacter* species by PCR (Shams et al. 2019). However, QCM conjugated with a DNA molecular biology technique was reportedly used for effective identification of *Ehrlichia canis*, which is a much simpler and rapid application (Bunroddith et al. 2018).

13.5.7 Aptasensors

Aptasensors are used through several tools for the detection of avian influenza (H5N1) by impedance signals. They were significantly improved by the utilization of AuNPs with H5N1-aptamer. These tools are specific and rapid in laboratory diagnosis for virus at lower limits of detection in agglutination tests (Karash et al. 2016; Al-Mamun et al. 2021).

A nanobiosensor tool that consists of CNTs utilized with aptasensor signals, which are labeled with green dye, is currently used. After the functionalization of *Bacillus anthracis* antigen they produce fluorescent signals and are hence used as rapid and low-cost diagnostic tests for anthrax (Karimi and Dabbagh 2019). On the other hand, the diagnosis of bovine viral diarrhoea disease biomarkers in animals can be made by aptasensors where they functionalized with AuNPs and viral antigen DNA and they were thus able to detect lower limits of DNA (Park et al. 2014).

13.5.8 Immunosensors

For several decades, immune studies via antigen and antibody reaction were successfully used in the rapid detection of human and animal diseases (Jain et al. 2021). These reactions were used in various ways such as colorimetric and fluorescent signals. In this respect, bluetongue virus biomarkers such as surface protein were detected by an AuNP biosensor device that carried monoclonal antibodies and ssDNA of the virus antigen (Yin et al. 2012; Derakhshan et al. 2021). These biosensors enable rapid detection of lower limits of 10^{-2} fg/mL. Similarly, immunobiosensors conjugated with AuNPs were used for the diagnosis of bovine viral diarrhoea virus (Montrose et al. 2015). They conjugated with virus biomarker (antibodies) over AuNP wires for identification of blood antibodies against virus in diseased animals.

Recently, bovine leucosis, a viral disease in cattle, has been detected in the blood of infected animals by immunosensors (Klestova et al. 2019). In another study, optical immunosensors were formed for the detection of the leucosis virus by ZnONPs, which have fluorescent characteristics (Ruban et al. 2017). This tool has significant sensitivity and can detect low levels of antibodies (0.001 mg/mL). Moreover, Longinotti et al. (2010) reported that the detection of foot and mouth disease virus surface protein occurred by electrochemical immunosensor via identification of antibodies in animal blood.

Another animal disease, hydatid infestation in cases of *Echinococcus granulosus* biomarkers can be detected by immunosensor (Lv et al. 2017), where SiNP sensors can be used for the diagnosis of antigen and antibodies in sera of infected animals (protein named protein kinase). Also, Li et al. (2017) used QDs as immunobiosensors; the antigen was carried on silicon pores, which further functionalized with anti-p38-labeled CdSe/ZnSQDs. They help the high sensitive detection limit of 300 fg/mL. Recently, Eissa et al. (2020) formed an immunosensor for the diagnosis

of hydatid disease. In this method, the AuNPs were covered in cysteamine/phenylene isothiocyanate and functionalized with rabbit polyclonal antibody to detect the hydatid antigen. They revealed that the limits of detection for *Echinococcus* antigen and antibody were 0.4 and 0.3 pg/mL respectively and that this tool is sensitive and low cost. Furthermore, the most dangerous disease of poultry worldwide (Newcastle disease) can be diagnosed by electrochemical immunosensor (Thin et al. 2018). Chicken egg yolk antibodies (IgY) were used as a marker of NDV antigen disease and the detection limit was (10^6 – 10^2 EID₅₀/mL⁻¹).

Regarding *Listeriosis* in animals, a similar method used immunosensors functionalized with AuNPs for the detection of conjugating antigen with antibodies against pathogens (Davis et al. 2013). The enteric bacterial diseases have also been detected by immunobiosensors coated with antibodies (Wang et al. 2017a, b).

13.5.9 Miscellaneous

Recently, diagnosis of African swine fever virus was undertaken and the limit of detection was 1 pM in 2 h (He et al. 2020). However, it was shown that the recent application in nanobiosensors explored wearable biosensors for the management of animals, where they can adapt physiological signs and biomarkers in natural body discharge such as saliva and tears (Neethirajan 2017; Singh et al. 2022).

13.6 Conclusions and Future Prospective

Nowadays, the detection and control of diseases in humans and animals are essential for their health management and need accurate diagnostic tools in field. Hence, the applications of nanotechnology in the diagnosis of human and animal diseases diagnosis has attracted huge interest in novel nanodiagnostic tools. The present review discusses the improvement of traditional methods of diagnosis by their functionalization with nanomaterials to provide alternative solutions and recent rapid nanodiagnostics in medical infectious diseases. The essential nanomaterials include AuNPs, AgNPs, SiNPs, FeONPs, QDs, and others, which play significant roles in nanodiagnostic tools of pathogens and toxins of infectious diseases. They have significant sensitivity and high limits of detection. The current conventional methods of infectious disease diagnosis related to microbiological and molecular detection of pathogens, which are high cost, take a long time to apply, and use toxic, hazardous chemicals. Therefore, there is an urgent need for more sensitive, simple, and wide-range practical applications in the field with high specificity. Moreover, the functionalization of biosensors with nanomaterials produces highly specific and significant nanodiagnostic tools for pathogens of infectious diseases. The utilization of nanomaterials helps in the production of effective diagnostic signal amplification labels that potentiate the efficacy of biosensors in pathogen detection in human and animal diseases.

References

- Abd El-Fatah S, Bakry HH, Abo Salem ME, Hassan AA. Comparative study between the use of bulk and nanoparticles of zinc oxide in amelioration the toxic effects of aflatoxins in rats. *Benha Vet Med J.* 2017;33(2):329–42.
- Agasti SS, Rana S, Park M-H, Kim CK, You C-C, Rotello VM. Nanoparticles for detection and diagnosis. *Adv Drug Deliv Rev.* 2010;62:316–28. <https://doi.org/10.1016/j.addr.2009.11.004>.
- Ajmal M, Yunus U, Matin A, Haq NU. Synthesis, characterization and in vitro evaluation of methotrexate conjugated fluorescent carbon nanoparticles as drug delivery system for human lung cancer targeting. *J Photochem Photobiol B.* 2015;153:111–20.
- Alafeef M, Moitra P, Pan D. RNA-extraction-free nano-amplified colorimetric test for point-of-care clinical diagnosis of COVID-19. *Biosens Bioelectron.* 2020;165:112276.
- Alexis F, Pridgen EM, Langer R, Farokhzad OC. Nanoparticle technologies for cancer therapy. *Handb Exp Pharmacol.* 2010;197:55–86.
- Alghuthaymi MA, Hassan AA, Kalia A, Sayed El Ahl RMH, El Hamaky AAM, Oleksak P, Kuca K, Abd-Elsalam KA. Antifungal nano-therapy in veterinary medicine: current status and future prospects. *J Fungi.* 2021;2021(7):494. <https://doi.org/10.3390/jof7070494>.
- Allen T, Murray KA, Zambrana-Torrelío C, Morse SS, Rondinini C, Di Marco M, et al. Global hotspots and correlates of emerging zoonotic diseases. *Nat Commun.* 2017;8:1–10. <https://doi.org/10.1038/s41467-017-00923-8>.
- Al-Mamun M, AbdulWahab Y, Hossain MAM, Hashem A, Johan MR. Electrochemical biosensors with Aptamer recognition layer for the diagnosis of pathogenic bacteria: barriers to commercialization and remediation. *TrAC Trends Anal Chem.* 2021;145:116458. <https://doi.org/10.1016/j.trac.2021.116458>.
- AOAC. Association of Official Analytical Chemists. Official Method 970.45. Aflatoxins in Peanuts and Peanut Products BF method. Official methods of analysis, 17th edn. AOCS – AOAC method; chapter 49; 2000, p. 11.
- Baekbo P, Kristensen CS, Larsen LE. Porcine circovirus diseases: a review of PMWS. *Transbound Emerg Dis.* 2012;59:60–7. <https://doi.org/10.1111/j.1865-1682.2011.01288.x>.
- Bahadir EB, Sezginurk MK. A review on impedimetric biosensors. *Artif Cells Nanomed Biotechnol.* 2016;44(1):248–62.
- Bansod S, Bawskar M, Rai M. In vitro effect of biogenic silver nanoparticles on sterilisation of tobacco leaf explants and for higher yield of protoplasts. *IET Nanobiotechnol.* 2015;9:239–45.
- Beishon M. Exploiting a nano-sized breach in cancer's defences cancer world. 2013, p. 14–21.
- Bunroddith K, Viseshakul N, Chansiri K, Lieberzeit P. QCM-based rapid detection of PCR amplification products of *Ehrlichia canis*. *Anal Chim Acta.* 2018;1001:106–11. <https://doi.org/10.1016/j.aca.2017.10.037>.
- Burns A, Ow H, Wiesner U. Fluorescent core-shell silica nanoparticles: towards “Lab on Particle” architectures for nanobiotechnology. *Chem Soc Rev.* 2006;35:1028–42.
- Campbell E, Hasan T, Gonzalez-Rodriguez R, Truly T, Lee BH, Green KN, Akkaraju G, Naumov AV. Graphene quantum dot formulation for cancer imaging and redox-based drug delivery. *Nanomed Nanotechnol Biol Med.* 2021;37:102408. <https://doi.org/10.1016/j.nano.2021.102408>.
- Cao H, Qi W, Gao X, Wu Q, Tian L, Wu W. Graphene quantum dots prepared by electron beam irradiation for safe fluorescence imaging of tumor. *Nanotheranostics.* 2022;6(2):205–14. <https://doi.org/10.7150/ntno.67070>.
- Chanda N, Upendran A, Boote EJ, Zambre A, Axiak S, Selting K, Katti KV, Leevy WM, Afrasiabi Z, Vimal J. Gold nanoparticle based X-ray contrast agent for tumor imaging in mice and dog: a potential nano-platform for computer tomography theranostics. *J Biomed Nanotechnol.* 2014;10:383–92.
- Connelly J, Baeumner A. Biosensors for the detection of waterborne pathogens. *Anal Bioanal Chem.* 2012;402:117–27.

- Davis D, Guo X, Musavi L, Lin CS, Chen SH, Wu VC. Gold nanoparticle-modified carbon electrode biosensor for the detection of *Listeria monocytogenes*. *Ind Biotechnol*. 2013;9(1):31–6.
- Deng H, Zhang X, Kumar A, Zou G, Zhang X, Liang XJ. Long genomic DNA amplicons adsorption onto unmodified gold nanoparticles for colorimetric detection of *Bacillus anthracis*. *Chem Commun*. 2013;49(1):51–3.
- Derakhshan MA, Amani A, Faridi-Majidi R. State-of-the-Art of nano-diagnostics and nanotherapeutics against SARS-CoV-2. *ACS Appl Mater Interfaces*. 2021;13:14816–43. <https://doi.org/10.1021/acsami.0c22381>.
- Dilbaghi N, Kaur H, Kumar R, Arora P, Kuma S. Nanoscale device for veterinary technology: trends and future prospective. *Adv Mater Lett*. 2013;4(3):175–84.
- Ding YZ, Liu YS, Zhou JH, Chen HT, Zhang J, Ma LN, Wei G. A highly sensitive detection for foot-and-mouth disease virus by gold nanoparticle improved immuno-PCR. *Virology*. 2011;8(148):1–5.
- Dong E, Du H, Gardner L. An interactive web-based dashboard to track COVID-19 in real time. *Lancet Infect Dis*. 2020;20:533–4. [https://doi.org/10.1016/S1473-3099\(20\)30120-1](https://doi.org/10.1016/S1473-3099(20)30120-1).
- Draz MS, Shafiee H. Applications of gold nanoparticles in virus detection. *Theranostics*. 2018;8:1985–2017. <https://doi.org/10.7150/thno.23856>.
- Eissa S, Noordin R, Zourob M. Voltammetric label free-immunosensors for the diagnosis of cystic echinococcosis. *Electroanalysis*. 2020;32(6):1170–7.
- El-Nahass S, Moselhy WA, Hassan NHY, Hassan AA. Evaluation of the protective effects of adsorbent materials and ethanolic herbal extracts against aflatoxins hepatotoxicity in albino rats: histological, morphometric and immunohistochemical study. *Adv Anim Vet Sci*. 2019;7(12):1140–7. <https://doi.org/10.17582/journal.aavs/2019/7.12.1140.1147>.
- Fasanella A, Galante D, Garofolo G, Jones MH. Anthrax undervalued zoonosis. *Vet Microbiol*. 2010;140:318–31. <https://doi.org/10.1016/j.vetmic.2009.08.016>.
- Flajnik MF, Deschacht N, Muyldermans SA. Case of convergence: why did a simple alternative to canonical antibodies arise in sharks and camels? *PLoS Biol*. 2011;9:e1001120.
- Frohnmeyer E, Tuschel N, Sitz T, Hermann C, Dahl GT, Schulz F, et al. Aptamer lateral flow assays for rapid and sensitive detection of cholera toxin. *Analyst*. 2019;144:1840–9. <https://doi.org/10.1039/C8AN01616J>.
- Gao JH, Liang GL, Cheung JS, Pan Y, Kuang Y, Zhao F, Zhang B, Zhang XX, Wu EX, Xu B. Multifunctional yolk-shell nanoparticles: a potential MRI contrast and anticancer agent. *J Am Chem Soc*. 2008;130:11828–33.
- Geszke-Moritz M, Moritz M. Quantum dots as versatile probes in medical sciences: synthesis, modification and properties. *Korean J Couns Psychother*. 2013;33:1008–21.
- Ghadi A, Mahjoub S, Tabandeh F, Talebnia F. Synthesis and optimization of chitosan nanoparticles: potential applications in nanomedicine and biomedical engineering. *Caspian J Intern Med*. 2014;5(3):156–61.
- Girigoswami K, Akhtar N. Nanobiosensors and fluorescence based biosensors: an overview. *Int J Nano Dimens*. 2019;10(1):1–17.
- Gu J, Wang X, Nie W, Wang W, Shang J. Potential role for carbon nanoparticles identification and preservation in situ of parathyroid glands during total thyroidectomy and central compartment node dissection. *Int J Clin Exp Med*. 2015;8:9640–8.
- Gupta A, Garg M, Singh S, Deep A, Sharma AL. Highly sensitive optical detection of *Escherichia coli* using terbium-based metal-organic framework. *ACS Appl Mater Interfaces*. 2020;12:48198–205.
- Gurunathan S, Choi YJ, Kim JH. Antibacterial efficacy of silver nanoparticles on endometritis caused by *Prevotella melaninogenica* and *Arcanobacterium pyogenes* in dairy cattle. *Int J Mol Sci*. 2018;19:1210.
- Habibullah G, Viktorova J, Ruml T. Current Strategies for noble metal nanoparticle synthesis. *Nanoscale Res Lett*. 2021; <https://doi.org/10.1186/s11671-021-03480-8>.
- Hammond JL, Formisano N, Estrela P, Carrara S, Tkac J. Electrochemical biosensors and nanobiosensors. *Essays Biochem*. 2016;60:69–80.

- Hassan AA, Mogda KM, Ibrahim IE, Sayed-ElAhl RH, Al-Kalamawey NM, El Kattan YA, Ali MA. Efficacy of zinc oxide nanoparticles and curcumin in amelioration the toxic effects in aflatoxicated rabbits. *Int J Curr Microbiol App Sci.* 2016;5(12):795–818.
- Hassan AA, Sayed El Ahl RM, Oraby NH, El-Hamaky AMA. Chapter 13: Metal nanoparticles for management of mycotoxigenic fungi and mycotoxicosis diseases of animals and poultry. In: *Nanomycotoxicology*. London: Elsevier Academic Press; 2019a, p. 251–63.
- Hassan AA, Rasha MH, El-Ahl S, Heba ND. Real time quantitative polymerase chain reaction detection of trichothecenes producing fusarium species in animal feed and their control by silver and zinc nanoparticles. *Anim Health Res J.* 2019b;7(4):759–77.
- Hassan AA, Mansour MK, El Hamaky AMA, Sayed El Ahl RMH, Oraby NH. Nanomaterials and nanocomposite application in veterinary medicine. London: Elsevier Academic Press; 2020a.
- Hassan AA, Mogda KM, El Hamaky AM, Sayed-El Ahl RM, Oraby NH. Nanomaterials and nanocomposite application in veterinary medicine. In: *Multifunctional hybrid nanomaterials for sustainable agrifood and ecosystems*. London: Elsevier Academic Press; 2020b, p. 251–63.
- Hassan AA, Mansour MK, Sayed El Ahl RMH, El Hamaky AMA, Oraby NH. Toxic and benefit effects carbon nanomaterial on human and animal health. London: Elsevier Academic Press; 2020c, p. 535–47.
- Hassan AA, Sayed El-Ahl RMH, Oraby NH, El-Hamaky AMA, Mansour MK. Chapter 25: Zinc nanomaterials: Toxicological effects and veterinary applications. In: *Zinc-based nanostructures for environmental and agricultural applications*. London: Elsevier; 2021a, p. 209–52.
- Hassan AA, Yousif MH, Abd-Elkhaliq HMM, Wahba AKA, El-Hamaky AMA. The antimicrobial potential of selenium nanoparticles singly and in combination with cinnamon oil against fungal and bacterial causes of diarrhea in buffaloes. *Adv Anim Vet Sci.* 2021b;9(8):1238–48. <https://doi.org/10.17582/journal.aavs/2021/9.8.1238.1248>. ISSN (Online) | 2307-8316; ISSN (Print) | 2309-3331
- He Y, Kang ZH, Li QS, Tsang CH, Fan CH, Lee ST. Ultra stable, highly fluorescent, and water-dispersed silicon-based nanospheres as cellular probes. *Angew Chem Int Ed Eng.* 2009;48:128–32.
- He Q, Yu D, Bao M, et al. High-throughput and all-solution phase African Swine Fever Virus (ASFV) detection using CRISPR-Cas12a and fluorescence based point-of-care system. *Biosens Bioelectron.* 2020;154:112068. <https://doi.org/10.1016/j.bios.2020.112068>.
- Hill EK, Li J. Current and future prospects for nanotechnology in animal production. *J Anim Sci Biotechnol.* 2017;8(1):26–40.
- Hohne GWH, Hemminger WF, Flammersheim HJ. *Differential scanning calorimetry*. 2nd ed. Berlin: Springer; 2004.
- Hongzhuan Z, Ying T, Xia S, Jinsong G, Zhenhua Z, Beiyu J, et al. Preparation of the inactivated Newcastle disease vaccine by plasma activated water and evaluation of its protection efficacy. *Appl Microbiol Biotechnol.* 2020;104(1):107–17.
- Huang C, Li J, Tang Y, Chen Y, Jin G. Detection of duck hepatitis virus serotype 1 by biosensor based on imaging ellipsometry. *Curr Appl Phys.* 2011;11:353–7.
- Huang J, Xie Z, Xie Z, Luo S, Xie L, Huang L, et al. Silver nanoparticles coated graphene electrochemical sensor for the ultrasensitive analysis of avian influenza virus H7. *Anal Chim Acta.* 2016;913:121–7. <https://doi.org/10.1016/j.aca.2016.01.050>.
- Huang Y, Hsu JC, Koo H, Cormode DP. Repurposing ferumoxytol: diagnostic and therapeutic applications of an FDA-approved nanoparticle. A review. *Theranostics.* 2022;12(2):796–816. <https://doi.org/10.7150/thno.67375>.
- Hugh-Jones M, De Vos V. Anthrax and wildlife. *Rev Sci Tech OIE.* 2022;21:359–84. <https://doi.org/10.20506/rst.21.2.1336>. ISSN (Online) | 2307-8316; ISSN (Print) | 2309-3331
- Jackson TC, Patani BO, Ekpa DE. Nanotechnology in Diagnosis: A Review. *Adv Nanopart.* 2017;6:93–102. <http://www.scirp.org/journal/anp>. ISSN Online: 2169-0529. ISSN Print: 2169-0510

- Jahani Z, Meshgi B, Rajabi-Bzl M, Jalousian F, Hasheminasab S. Improved serodiagnosis of hydrated cyst disease using gold nanoparticle labeled antigen B in naturally infected sheep. *Iran J Parasitol.* 2014;9:218–925.
- Jain U, Shakya S, Saxena K. Chapter 19: Nano-biosensing devices detecting biomarkers of communicable and non-communicable diseases of animals. In: *Concepts and strategies in plant sciences biosensors in agriculture: recent trends and future perspectives.* Cham: Springer Nature; 2021. <https://doi.org/10.1007/978-3-030-66165-6>
- Jeelani PG, Mulay P, Venkat R, Ramalingam C. Multifaceted application of silica nanoparticles. A review. *SILICON.* 2020;12:1337–54.
- Jiang W, Liu Y, Chen Y, Yang Q, Chun P, Yao K, Han X, Wang S, Yu S, Liu Y. A novel dynamic flow immunochromatographic test (DFICT) using gold nanoparticles for the serological detection of *Toxoplasma gondii* infection in dogs and cats. *Biosens Bioelectron.* 2015;72:133–9.
- Jo WK, De Oliveira-Filho EF, Rasche A, Greenwood AD, Osterrieder K, Drexler JF. Potential zoonotic sources of SARS-CoV-2 infections. *Transbound Emerg Dis.* 2020;2020(00):1–11. <https://doi.org/10.1111/tbed.13872>.
- Karash S, Wang R, Kelso L, Lu H, Huang TJ, Li Y. Rapid detection of avian influenza virus H5N1 in chicken tracheal samples using an impedance aptasensor with gold nanoparticles for signal amplification. *J Virol Methods.* 2016;236:147–56.
- Karimi F, Dabbagh S. (2019). Gel green fluorescence ssDNA aptasensor based on carbon nanotubes for detection of anthrax protective antigen. *Int J Biol Macromol.* 2019;140:842–50. <https://doi.org/10.1016/j.ijbiomac.2019.08.219>.
- Kim S, Ohulchansky TY, Pudavar HE, Pandey RK, Prasad PN. Organically modified silica nanoparticles co-encapsulating photosensitizing drug and aggregation-enhanced two-photon absorbing fluorescent dye aggregates for two-photon photodynamic therapy. *J Am Chem Soc.* 2007;129:2669–75.
- Kirtane AR, Verma M, Karandikar P, Furin J, Langer R, Traverso G. Nanotechnology approaches for global infectious diseases. *Nanotechnology.* 2021;16:369.
- Klestova ZS, Yuschenko AY, Dremukh Y, Blotska OF, Venger EF, Dorozinsky GV, et al. Diagnostics of cattle leucosis by using a biosensor based on surface plasmon resonance phenomenon. *Semicond Phys Quantum Electron Optoelectron.* 2019;22(1):111–8.
- Kopparthy VL, Tangutooru SM, Guilbeau EJ. Label free detection of L-glutamate using microfluidic based thermal biosensor. *Bioengineering.* 2015;2(1):2–14.
- Kour R, Arya S, Young S-J, Gupta V, Bandhoria P, Khosla A. Review – recent advances in carbon nanomaterials as electrochemical biosensors. *J Electrochem Soc.* 2020;167:037555.
- Kumar SR, Vijayalakshmi R. Nanotechnology in dentistry. *Indian J Dent Res.* 2006;17:62–9. <https://doi.org/10.4103/0970-9290.29890>.
- Kusat K, Akgöl S. Nanobiosensors: usability of imprinted nanopolymers. In: Denizli A, editor. *Molecular imprinting for nanosensors and other sensing applications.* Amsterdam: Elsevier; 2021. p. 163–202. <https://doi.org/10.1016/B978-0-12-822117-4.00007-1>.
- Lastra LS, Sharma V, Farajpour N, Nguyen M, Freedman KJ. Nano-diagnostics: a review of the medical capabilities of nanopores. *Nanomedicine.* 2021;37:102425. <https://doi.org/10.1016/j.nano.2021.102425>.
- Leonard P, Hearty S, Brennan J, Dunne L, Quinn J, Chakraborty T, O’Kennedy R. Advances in biosensors for detection of pathogens in food and water. *Enzyme Microbiol Tech.* 2003;32:3–13.
- Li Z, Ao S, Bu Z, Wu A, Wu X, Shan F, Ji X, Zhang Y, Xing Z, Ji J. Clinical study of harvesting lymph nodes with carbon nanoparticles in advanced gastric cancer: a prospective randomized trial. *World J Surg Oncol.* 2016;14(1):88–100.
- Li Y, Jia Z, Lv G, et al. Detection of *Echinococcus granulosus* antigen by a quantum dot/porous silicon optical biosensor. *Biomed Opt Express.* 2017;8(7):3458–69. <https://doi.org/10.1364/boe.8.003458>.
- Li S, Liu Y, Wang Y, Wang M, Liu C, Wang Y. Rapid detection of *Brucella* spp. and elimination of carryover using multiple cross displacement amplification coupled with nanoparticles-based lateral flow biosensor. *Front Cell Infect.* 2019a;9(78) <https://doi.org/10.3389/fcimb.2019.00078>.

- Lim J, Cheong Y, Kim Y-S, Chae W, Hwang BJ, Lee J, Roh Y, Seo S-U, Seong BL. RNA-dependent assembly of chimeric antigen nanoparticles as an efficient H5N1 pre-pandemic vaccine platform. *Nanomedicine*. 2021;37:102438.
- Liu J, Bai J, Zhang L, Jiang Z, Wang X, Li Y, Jiang P. Hsp70 positively regulates porcine circovirus type 2 replication in vitro. *Virology*. 2013;447(1-2):52–62.
- Liu X, Ouyang T, Ouyang H, Liu X, Niu G, Huo W, et al. Human cells are permissive for the productive infection of porcine circovirus type 2 in vitro. *Sci Rep*. 2019;9:1–8. <https://doi.org/10.1038/s41598-019-42210-0>.
- Long F, Zhang Z, Yang Z, Zeng J, Jiang Y. Imprinted electrochemical sensor based on magnetic multi-walled carbon nanotube for sensitive determination of kanamycin. *J Electroanal Chem*. 2015;755:7–14. <https://doi.org/10.1016/j.jelechem.2015.07.018>.
- Longinotti G, Ybarra G, Lloret P, et al. Diagnosis of foot-and-mouth disease by electrochemical enzyme-linked immunoassay. *Conf Proc IEEE Eng Med Biol Soc*. 2010;2010:674–6. <https://doi.org/10.1109/IEMBS.2010.5626230>.
- Luo J, Liang M, Li Z, Zink JI, Tamanoi F. Biocompatibility, biodistribution, and drug-delivery efficiency of mesoporous silica nanoparticles for cancer therapy in animals. *Small*. 2010;6:1794–805.
- Luo Z, Li W, Lu D, Chen K, He Q, Han H, et al. A SERS-based immunoassay for porcine circovirus type 2 using multi-branched gold nanoparticles. *Microchim Acta*. 2013;180:1501–7. <https://doi.org/10.1007/s00604-013-1032-5>.
- Luo B, Xu Y, Wu S, Zhao M, Jiang P, Shi S, et al. A novel immunosensor based on excessively tilted fiber grating coated with gold nanospheres improves the detection limit of Newcastle disease virus. *Biosens Bioelectron*. 2018;100:169–75. <https://doi.org/10.1016/j.bios.2017.08.064>.
- Lv X, Xin L, Lv G, Mo J, Gao Z, Jia Z, Wen H. Preparation of a photoluminescent film on a silicon-on-insulator device for the simple, rapid, and quantitative detection of a hydatid disease diagnostic protein marker. *IEEE Photonics J*. 2017;9(4):1–7.
- Makvandi P, Iftekhar S, Pizzetti F, Zarepour A, Zare EN, Ashrafizadeh M, et al. Functionalization of polymers and nanomaterials for water treatment, food packaging, textile and biomedical applications: a review. *Environ Chem Lett*. 2020;19:1–29. <https://doi.org/10.1007/s10311-020-01089-4>.
- Manhas PK, Quintela IA, Wu VCH. Enhanced detection of major pathogens and toxins in poultry and livestock with zoonotic risks using nanomaterials-based diagnostics. *Front Vet Sci*. 2021;8 <https://doi.org/10.3389/fvets.2021.673718>.
- Matsubara T, Michiko U, Takashi Y, Yasuaki E, Tomo D, Takaaki N, et al. Avian influenza virus detection by optimized peptide termination on a boron-doped diamond electrode. *ACS Sens*. 2020;5:431–9. <https://doi.org/10.1021/acssensors.9b02126>.
- Meena N, Sahni Y, Thakur D, Singh R. Applications of nanotechnology in veterinary therapeutics. *J Entomol Zool*. 2018;6(2):167–75.
- Meng K, Sun W, Zhao P, Zhang L, Cai D, Cheng Z, Guo H, Liu J, Yang D, Wang S. Development of colloidal gold-based immunochromatographic assay for rapid detection of *Mycoplasma suis* in porcine plasma. *Biosens Bioelectron*. 2014;55:396–9.
- MicroCal LLC. Use of isothermal titration calorimetry to measure enzyme kinetic constants. 2017. Available [Online]: www.microcalorimetry.com
- Miller PJ, Koch G. Newcastle disease. In: *Diseases of poultry*, Vol. 13. 2013, p. 89–138.
- Mohanty SP, Kougianos E. Biosensors: a tutorial review. *IEEE Potentials*. 2006;25(2):35–40.
- Montrose A, Creedon N, Sayers R, Barry ST, O’Riordan A. Novel single gold nanowire-based electrochemical immunosensor for rapid detection of bovine viral diarrhoea antibodies in serum. *J Biosens Bioelectron*. 2015;2015:1–7.
- Moongkarndi P, Rodpai E, Kanarat S. Evaluation of an immunochromatographic assay for rapid detection of *Salmonella enterica* serovars typhimurium and enteritidis. *J Vet Diagn Investig*. 2011;23:797–801.
- Mout R, Moyano DF, Rana S, Rotello VM. Surface functionalization of nanoparticles for nanomedicine. *Chem Soc Rev*. 2012;41(7):2539–44.

- Nasar MQ, Zohra T, Khalil AT, Saqib S, Ayaz M, Ahmad A, Shinwari ZK. Seripheidium quettense mediated green synthesis of biogenic silver nanoparticles and their theranostic applications. *Green Chem Lett Rev.* 2019;12(3):310–22.
- Neethirajan S. Recent advances in wearable sensors for animal health management. *Sens Bio-Sens Res.* 2017;12:15–29.
- Neethirajan S, Tuteja SK, Huang ST, Kelton D. Recent advancement in biosensors technology for animal and livestock health management. *Biosens Bioelectron.* 2017;98:398–407.
- Neethirajan S, Weng X, Tah A, Cordero JO, Ragavan KV. Nano-biosensor platforms for detecting food allergens—new trends. *Sens Bio-sens Res.* 2018;18:13–30.
- Nodoushan SM, Nasirizadeh N, Kachuei R, Fooladi A. Electrochemical detection of aflatoxin B1: an aptasensor prepared using graphene oxide and gold nanowires. *Anal Methods.* 2019;11:6033–42. <https://doi.org/10.1039/C9AY01673B>.
- Nurulfiza I, Hair-Bejo M, Omar AR, Aini I. Immunochromatographic gold-based test strip for rapid detection of infectious bursal disease virus antibodies. *J Vet Diagn Investig.* 2011;23:320–4.
- Ozalp VC, Bayramoglu G, Erdem Z, Arica MY. Pathogen detection in complex samples by quartz crystal microbalance sensor coupled to aptamer functionalized core-shell type magnetic separation. *Anal Chim Acta.* 2015;853:533–40.
- Pal D, Boby N, Kumar S, Kaur G, Ali SA, Reboud J, et al. Visual detection of Brucella in bovine biological samples using DNA-activated gold nanoparticles. *PLoS ONE.* 2017;12:e0180919. <https://doi.org/10.1371/journal.pone.0180919>.
- Park JW, Jin Lee S, Choi EJ, Kim J, Song JY, Bock GM. An ultra-sensitive detection of a whole virus using dual aptamers developed by immobilization-free screening. *Biosens Bioelectron.* 2014;51:324–9. <https://doi.org/10.1016/j.bios.2013.07.052>.
- Petryayeva E, Algar WR, Medintz IL. Quantum dots in bioanalysis: a review of applications across various platforms for fluorescence spectroscopy and imaging. *Appl Spectrosc.* 2013;67:215–52.
- Phatruengdet T, Khuemjun P, Intakhad J, Krunchanuchat S, Chariyakornkul A, Wongpoomchai R, Pilapong C. Pharmacokinetic/pharmacodynamic determinations of iron-tannic molecular nanoparticles with its implication in MR imaging and enhancement of liver clearance. *Nanotheranostics.* 2022;6(2):195–204. <https://doi.org/10.7150/ntno.63310>.
- Pohanka M, Skladal P. Electrochemical biosensors – principles and applications. *J Appl Biomed.* 2008;6:57–64.
- Qindeel M, Barani M, Rahdar A, Arshad R, Cucchiari M. Nanomaterials for the diagnosis and treatment of urinary tract infections. *Nanomaterials.* 2021;11:546.
- Raguvaran R, Anju M, Balvinder KM. Zinc oxide nanoparticles: opportunities and challenges in veterinary sciences. *Immunol Res.* 2015;11(2):2–8.
- Rahi A, Sattarahmady N, Heli H. Zepto-molar electrochemical detection of Brucella genome based on gold nanoribbons covered by gold nanoblossoms. *Sci Rep.* 2015;5:18060. <https://doi.org/10.1038/srep18060>.
- Rajasundari K, Hamurugu K. Nanotechnology and its application in medical diagnosis. *J Basic Appl Chem.* 2011;1:26–32.
- Rajput M, Kamboh AA, Dewani P, Umrani AP, Rind R. Occurrence of Anthrax spores in small ruminants' hair/wool in district Tharparkar, Sindh. *J Anim Health Prod.* 2017;5:5–9. <https://doi.org/10.14737/journal.jahp/2017/5.1.5.9>.
- Rasheed T, Hassan AA, Kausar F, Sher F, Bilal M, Iqbal HMN. Carbon nanotubes assisted analytical detection – sensing/delivery cues for environmental and biomedical monitoring. *TrAC Trends Anal Chem.* 2021;132:116066.
- Reimhult E, Höök F. Design of surface modifications for nanoscale sensor applications. *Sensors.* 2015;15:Article ID: 163575. <https://doi.org/10.3390/s150101635>.
- Roco MC, Harthorn B, Guston D, Shapira P. Innovative and responsible governance of nanotechnology for societal development. In: *Nanotechnology research directions for societal needs in 2020.* 2017, p. 441–488. <https://www.researchgate.net/publication/226395092>
- Rosati G, Idili A, Parolo C, Fuentes-Chust C, Calucho E, Hu L, Silva CCC, Rivas L, Nguyen EP, Bergua JF, Álvarez-Diduk R, Muñoz J, Junot C, Penon O, Monferrer D, Delamarche E,

- Merkoçi A. Nano-diagnostics to face SARS-CoV-2 and future pandemics: from an idea to the market and beyond. *ACS Nano*. 2021;15(11):17137–49.
- Ruban Y, Shpyrka N, Pareniuk O, Galat M, Taran MS, Ishchenko L, Shavanova K. BLV leucosis biosensor based on ZnO nanorods photoluminescence. In: 2017 IEEE 37th international conference on electronics and nanotechnology (ELNANO). IEEE; 2017, p. 333–7.
- Ruedas-Rama MJ, Walters JD, Orte A, Hall EAH. Fluorescent nanoparticles for intracellular sensing: a review. *Anal Chim Acta*. 2012;751:1–23.
- Sagadevan S, Periasamy M. Recent trends in nanobiosensors and their applications—a review. *Rev Adv Mater Sci*. 2014;36:62–9.
- Sanchez VC, Jachak A, Hurt RH, Kane AB. Biological interactions of graphene- family nanomaterial: an interdisciplinary review. *Chem Res Toxicol*. 2012;25:15–34.
- Saragusty J, Arav A. Current progress in oocyte and embryo cryopreservation by slow freezing and vitrification. *Reproduction*. 2011;141:1–19.
- Sattarahmady N, Tondro GH, Gholchin M, Heli H. Gold nanoparticles biosensor of *Brucella* spp. genomic DNA: visual and spectrophotometric detections. *Biochem Eng J*. 2015;97:1–7.
- Sattarahmady N, Movahedpour A, Heli H, Hatam GR. Gold nanoparticles-based biosensing of *Leishmania major* kDNA genome: visual and spectrophotometric detections. *Sensors Actuators B Chem*. 2016;235:723–31.
- Sayed RH, Abousenna MS, Mohamoud D, Saad MA. Development of a lateral flow kit for detection of IgG and IgM antibodies against rift valley fever virus in sheep. *Indian J Vet Sci Biotechnol*. 2019;15:63–8. <https://doi.org/10.21887/ijvsbt.15.2.17>.
- Scharf A, Holmes S, Thoresen M, Mumaw J, Stumpf A, Peroni J. Superparamagnetic iron oxide nanoparticles as a means to track mesenchymal stem cells in a large animal model of tendon injury. *Contrast Media Mol Imag*. 2015;10:388–97.
- Seleem MN, Boyle SM, Sriranganathan N. Brucellosis: a re-emerging zoonosis. *Vet Microbiol*. 2010;140:392–8. <https://doi.org/10.1016/j.vetmic.2009.06.021>.
- Selvarajan V, Obuobi S, Ee PLR. Silica nanoparticles – a versatile tool for the treatment of bacterial infections. *Front Chem*. 2020;8:602. <https://doi.org/10.3389/fchem.2020.00602>.
- Senne DAD. Newcastle disease. In: Saif YM, Fadly AM, Glisson JR, McDougald LR, Nolanand LK, Swayne DE, editors. *Diseases of poultry*. 12th ed. Ames: Iowa State University Press; 2008. p. 75–100.
- Shams S, Bakhshi B, Tohidi Moghadam T, Behmanesh M. A sensitive gold-nanorods-based nanobiosensor for specific detection of *Campylobacter jejuni* and *Campylobacter coli*. *J Nanobiotechnol*. 2019;17(1):43. <https://doi.org/10.1186/s12951-019-0476-0>.
- Sharma S, Lamichhane N, Parul ST, Roy I. Iron oxide nanoparticles conjugated with organic optical probes for *in vivo* diagnostic and therapeutic applications. *Nanomedicine (London)*. 2020a;16(11):943–62. <https://doi.org/10.2217/nmm-2020-0442>.
- Sharma A, Sharma N, Kumari A, Lee HJ, Kim TY, Tripathi KM. Nano-carbon based sensors for bacterial detection and discrimination in clinical diagnosis: A junction between material science and biology. *Appl Mater Today*. 2020b;18:100467.
- Shehada N, Brönstrup G, Funka K, Christiansen S, Leja M, Haick H. Ultrasensitive Silicon Nanowire for Real-World Gas Sensing: Noninvasive Diagnosis of Cancer from Breath Volatolome. *Nano Lett*. 2015;15:1288–95. <https://doi.org/10.1021/nl504482t>.
- Shetty NJ, Swati P, David K. Nanorobots: future in dentistry. *Saudi Dental J*. 2013:1–4.
- Shi SF, Jia JF, Guo XK, Zhao YP, Chen DS, Guo YY, Cheng T, Zhang XL. Biocompatibility of chitosan-coated iron oxide nanoparticles with osteoblast cells. *Int J Nanomedicine*. 2012;7:5593–602.
- Shirahata N. Silica nanocrystals: a controlled organic-inorganic interface and its implications of color-tuning and chemical design toward sophisticated architectures. *Phys Chem Chem Phys*. 2011;13:7284–94.
- Singh S, Numan A, Cinti S. Point-of-care for evaluating antimicrobial resistance through the adoption of functional materials. *Anal Chem Fundament Appl Rev Anal Chem*. 2022; <https://doi.org/10.1021/acs.analchem.1c03856>.

- Song K-M, Lee S, Ban C. Aptamers and their biological applications. *Sensors*. 2012;12:612–31. <https://doi.org/10.3390/s120100612>.
- Takahashi S, Shiraishi T, Miles N, Trock BJ, Kulkarni P, Getzenberg RH. Nanowire analysis of cancer-testis antigens as biomarkers of aggressive prostate cancer. *Urology*. 2015;85:704.e1–7.
- Tan H, Ma L, Guo T, Zhou H, Chen L, Zhang Y, et al. A novel fluorescence aptasensor based on mesoporous silica nanoparticles for selective and sensitive detection of aflatoxin B1. *Anal Chim Acta*. 2019;1068:87–95. <https://doi.org/10.1016/j.aca.2019.04.014>.
- Thinh TQ, Quan TVV, Thuy TH, Xuan CT, Tuan MA. A label-free electrochemical immunosensor for detection of Newcastle disease virus. In: International conference on the development of biomedical engineering in Vietnam. Singapore: Springer; 2018, p. 699–703.
- USFDA. Guidance for industry: action levels for poisonous or deleterious substances in human food and animal feed. Washington, DC: US FDA; 2000. Available online at: <http://www.fda.gov/Food/GuidanceComplianceRegulatoryInformation/GuidanceDocuments/ChemicalContaminantsandPesticides/ucm077969.htm>. Accessed 26 Feb 2021.
- Valodkar M, Jadeja RN, Thounaojam MC, Devkar RV, Thakore S. Biocompatible synthesis of peptide capped copper nanoparticles and their biological effect on tumor cells. *Mater Chem Phys*. 2011;128(1–2):83–9.
- Van Schooneveld MM, Vucic E, Koole R, Zhou Y, Stocks J, Cormode DP, Mulder WJ. Improved biocompatibility and pharmacokinetics of silica nanoparticles by means of a lipid coating: a multimodality investigation. *Nano Lett*. 2008;8(8):2517–25.
- Velusamy V, Arshak K, Korostynska O, Oliwa K, Adley C. An overview of foodborne pathogen detection: in the perspective of biosensors. *Biotechnol Adv*. 2010;28(2):232–54.
- Vrublevskaya VV, Afanasyev VN, Grinevich AA, Skarga YY, Gladyshev PP, Ibragimova SA, et al. A sensitive and specific lateral flow assay for rapid detection of antibodies against glycoprotein B of Aujeszky's disease virus. *J Virol Methods*. 2017;249:175–80. <https://doi.org/10.1016/j.jviromet.2017.09.012>.
- Wang G, Xie P, Xiao C, Yuan P, Su X. Magnetic fluorescent composite nanoparticles for the fluoroimmunoassays of newcastle disease virus and avian virus arthritis virus. *J Fluoresc*. 2010;20:499–506. <https://doi.org/10.1007/s10895-009-0573-9>.
- Wang JJ, Liu BH, Hsu YT, Yu FY. Sensitive competitive direct enzyme-linked immunosorbent assay and gold nanoparticle immunochromatographic strip for detecting aflatoxin M1 in milk. *Food Control*. 2011;22:964–9.
- Wang X, Dang E, Gao J, Guo S, Li Z. Development of a gold nanoparticle-based oligonucleotide microarray for simultaneous detection of seven swine viruses. *J Virol Methods*. 2013;191:9–15.
- Wang MQ, Wang C, Du YJ, Li H, Tao WJ, Ye SS. Effects of chromium-loaded chitosan nanoparticles on growth, carcass characteristics, pork quality, and lipid metabolism in finishing pigs. *Livest Sci*. 2014;161:123–9.
- Wang W, Liu L, Song S, Xu L, Zhu J, Kuang H. Gold nanoparticle-based paper sensor for multiple detection of 12 *Listeria* spp. by P60-mediated monoclonal antibody. *Food Agric Immunol*. 2017a;28(2):274–87.
- Wang P, Liu J, Gao H, Hu Y, Hou X, Le Croy GE, Bunker CE, Liu Y, Sun YP. Host-guest carbon dots as high-performance fluorescence probes. *J Mater Chem*. 2017b;5:6328–35.
- Wang Y, Zhao G, Li X, Liu L, Cao W, Wei Q. Electrochemiluminescent competitive immunosensor based on polyethyleneimine capped SiO₂ nanoparticles as labels to release Ru (bpy)₃²⁺ fixed in 3D Cu/Ni oxalate for the detection of aflatoxin B1. *Biosens Bioelectron*. 2018;101:290–6. <https://doi.org/10.1016/j.bios.2017.10.042>.
- Wu X, Lin Q, Chen G, Lu J, Zeng Y, Chen X, Yan J. Sentinel lymph node detection using carbon nanoparticles in patients with early breast cancer. *PLoS One*. 2015;10(8):e0135714.
- Wu L, Yin W, Tang K, Shao K, Li Q, Wang P, et al. Highly sensitive enzyme-free immunosorbent assay for porcine circovirus type 2 antibody using Au-Pt/SiO₂ nanocomposites as labels. *Biosens Bioelectron*. 2016;82:177–84. <https://doi.org/10.1016/j.bios.2016.04.001>.
- Wu L, Zhang M, Zhu L, Li J, Li Z, Xie W. Nanozyme-linked immunosorbent assay for porcine circovirus type 2 antibody using HAuCl₄/H₂O₂ coloring system. *Microchem J*. 2020;157:105079. <https://doi.org/10.1016/j.microc.2020.105079>.

- Xiong Y, Wang Z, Wang Q, Deng Q, Chen J, Wei J, Yang X, Yang X, Li Z. Tumor-specific activatable biopolymer nanoparticles stabilized by hydroxyethyl starch prodrug for self-amplified cooperative cancer therapy. *Theranostics*. 2022;12(2):944–62. <https://doi.org/10.7150/thno.67572>.
- Yang F, Xiao Y, Chen B, Wang L, Liu F, Yao H, et al. Development of a colloidal gold-based immunochromatographic strip test using two monoclonal antibodies to detect H7N9 avian influenza virus. *Virus Genes*. 2020;56:1–5. <https://doi.org/10.1007/s11262-020-01742-8>.
- Yin HQ, Jia MX, Yang S, Jing PP, Wang R, Zhang JG. Development of a highly sensitive gold nanoparticle probe-based assay for bluetongue virus detection. *J Virol Methods*. 2012;183(1):45–8. <https://doi.org/10.1016/j.jviromet.2012.03.027>.
- Yoo HJ, Li YG, Cui WY, Chung W, Shin Y-B, Kim Y-S, Baek C, Min J. Discrimination and isolation of the virus from free RNA fragments for the highly sensitive measure ment of SARS-CoV-2 abundance on surfaces using a graphene oxidenanosurface. *NanoConvergence*. 2021;8(1) <https://doi.org/10.1186/s40580-021-00281-8>.
- Zeng Q, Ma X, Song Y, Chen Q, Jiao Q, Zhou L. Review: Targeting regulated cell death in tumor nanomedicines. *Theranostics*. 2022;12(2):817–41. <https://doi.org/10.7150/thno.67932>.
- Zhang H, Li W, Sheng Z, Han H, He Q. Ultrasensitive detection of porcine circovirus type 2 using gold (III) enhanced chemiluminescence immunoassay. *Analyst*. 2010;135:1680–5. <https://doi.org/10.1039/c0an00025f>.
- Zhang Y, Li M, Gao X, Chen Y, Liu T. Nanotechnology in cancer diagnosis: progress, challenges and opportunities. *J Hematol Oncol*. 2019;12:137. <https://doi.org/10.1186/s13045-019-0833-3>.
- Zhu K, Dietrich R, Didier A, Doyscher D, M€artlbauer, E. Recent developments in antibody-based assays for the detection of bacterial toxins. *Toxins*. 2014;6:1325–48.
- Zhu Y, Chen X, Zhang H, Chen L, Zhou S, Wu K, Wang Z, Kong L, Zhuang H. Carbon nanoparticle-guided central lymph node dissection in clinically node- negative patients with papillary thyroid carcinoma. *Head Neck*. 2016;38:840–5.
- Zou X, Huang H, Gao Y, Su X. Detection of avian influenza virus based on magnetic silica nanoparticles resonance light scattering system. *Analyst*. 2012;2012(137):648–53. <https://doi.org/10.1039/C1AN16041A>.

Chapter 14

Nano-Based Robotic Technologies for Plant Disease Diagnosis



Farah K. Ahmed , Mousa A. Alghuthaymi, Kamel A. Abd-Elsalam ,
Mythili Ravichandran, and Anu Kalia

14.1 Introduction

Diagnostic specificity accuracy is a major issue in plant health, and it should be a driving force behind the development of mechatronics and robotic disease management systems. The identification of plant pathogens would allow for quick remedial action to avoid disease spread. Farmer relies on a variety of agricultural strategies and technology to increase yields, including crop rotation to promote soil health, the use of genetically modified seeds, and monitoring plants for infections and pests by growing non-native plants, or sentinel plants (Mansfield et al. 2019). Many diagnostic technologies are also used to identify disease. Current laboratory-based plant diagnostic approaches, on the other hand, are insufficient for point-of-use plant monitoring. In addition to accurate diagnosis of a disease or infection agent, modern diagnostics aspire to provide accurate, quick, and economical identification (Khiyami et al. 2014). Plant disease ecology is inherently interdisciplinary, relying

F. K. Ahmed (✉)

Biotechnology English Program, Faculty of Agriculture, Cairo University, Giza, Egypt

M. A. Alghuthaymi

Biology Department, Science and Humanities College, Shaqra University,
Al Quwaiyah, Saudi Arabia

K. A. Abd-Elsalam

Agricultural Research Center, Plant Pathology Research Institute, Giza, Egypt

M. Ravichandran

Department of Microbiology, Vivekanandha Arts and Science College for Women,
Sankari, India

A. Kalia

Electron Microscopy and Nanoscience Laboratory, Punjab Agricultural University,
Ludhiana, Punjab, India

© The Author(s), under exclusive license to Springer Nature Switzerland AG 2023

K.-T. Lim, K. A. Abd-Elsalam (eds.), *Nanorobotics and Nanodiagnostics*

in *Integrative Biology and Biomedicine*, https://doi.org/10.1007/978-3-031-16084-4_14

327

on various domains, such as ecology, epidemiology, plant physiology, and some genetics factors that play a role in pathogenicity. Plant pathologists have known for over a century that pathogenic microorganisms drive disease dynamics in sensitive plants in presence of specific environmental circumstances (Agrios 2005). Pathogen detection is concerned with identification of a specific target organism in plant tissues, vectors, plant products, or environmental materials, with a focus on symptomless plants.

Nanotechnology has aided in the advancement of numerous diagnostic methodologies by providing modern tools, such as sensors based on bio-techniques, nano-based medical facilities, and bio-photonics, which make it easier to detect pesticides, drug residues, foodborne pathogenic microorganisms, toxin contaminants, and heavy metal ions (Dutta et al. 2021). As it is a prerequisite that the methods used to identify disease and its causal organism should be very sensitive, specific, and deliver quick findings, nanomaterial-based devices or products can be of greater significance. The nano-enabled biosensors are now being employed in a variety of environmental monitoring and medical diagnostic applications. The use of nano-based materials has been proven to improve the accuracy of biosensing devices in terms of detection limit and sensor sensitivity (Razmi et al. 2019). Nanosensors in agriculture have a lot of potential for pathogen management, since they can provide diagnostic tools for early identification of plant diseases. Nanosensor technology may be used to help, guide, and augment conventionally used diagnostic tools in the early identification of plant diseases (Kashyap et al. 2017; Kalia et al., 2020). Isothermal amplification, nanomaterial detection, paper-based approaches, robotics, and lab-on-a-chip analytical devices are among the latest emerging biosensor technologies. These, on the other hand, are the first in early disease detection for achieving the goals of sustainable agricultural research and development (Ali et al. 2021). Sensor-based nanodiagnostic microbial detection systems have yielded some very interesting and promising outcomes (Fig. 14.1). The detection of bimolecular interactions by optical, electrical, and electrochemical biosensors is considerably enhanced by nanomaterials with a high surface to volume ratio.

However, for both abiotic and biotic stress, plant disease detection via artificial intelligence remains an intriguing problem. Robotics-based disease diagnosis techniques are still in the early stages of development, and the availability of standardized applications is unpredictable (Mahlein 2016). Recently, research in automatic disease recognition has expanded, with possible applications in developing robots that can distinguish specific plants, locate and identify diseases, and initiate disease treatment procedures (Ampatzidis et al. 2017). Improved yields can be achieved by monitoring the plant health. Water level, soil quality, and the presence of pathogens and pests may all be monitored in real time using low-cost infield technologies (Roper et al. 2021). There has been fewer research on the use of nanosensors to detect forest tree disease (Kulabhusan et al. 2022). As a result, nano-based and robotic development is critical in several agricultural crops. This chapter focuses on a wide range of plant diseases and the prerequisites for a reliable, rapid, and cost-effective testing procedure, as well as novel nano-based and robotic diagnostic technologies used for the early identification of diseases in field plants and forests. Also,

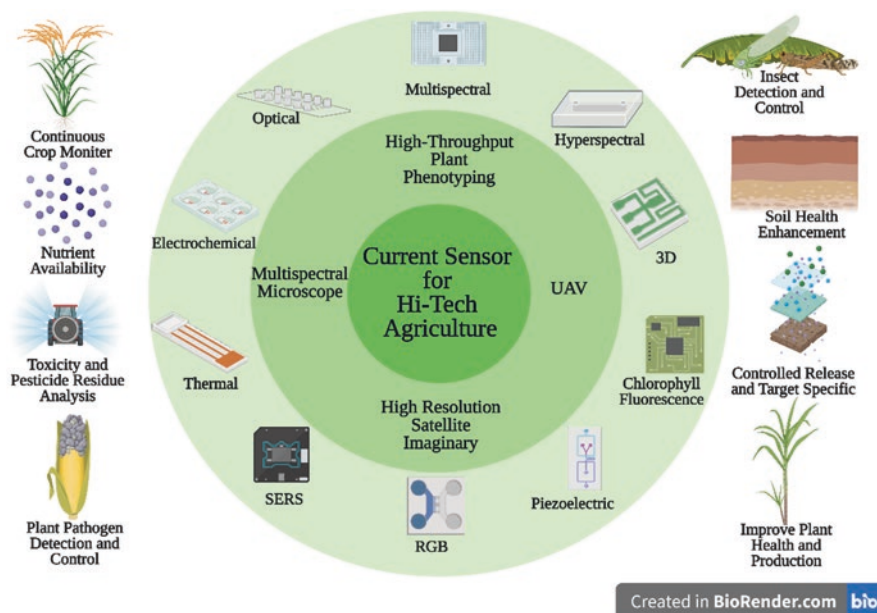


Fig. 14.1 Sensor-based nanodiagnostic applications for smart agriculture

the present chapter examines the advancements and problems of nano-based and robotic diagnostics approaches, which will aid scientists and researchers in developing rapid, accurate, and low-cost detection methods.

14.2 Pathogen Detection Methods

Most disease detection methods rely on either direct or indirect detection methods. Traditional procedures, such as morphological detection of pathogens through cultural detection methods, and molecular approaches, such as polymerase chain reaction, are all direct detection methods that target pathogen molecular, morphological, and serological features. These approaches are successful in detection of causal organisms but have their own set of limits and benefits. The selection of an appropriate approach is influenced by the goal, stage of the diseases, location, simplicity of carrying out the experiment, availability of test samples, and expenses. Rapid diagnosis of plant diseases is helpful in terms of controlling disease spread and reducing yield losses. Many direct and indirect detection methods are difficult to use in on-site settings and take longer to give results. As a result, the development of rapid and cheap sensing systems has been critical to plant disease control research. Pathogen detection, recognition, and evaluation are also critical for scientific research, ecological surveillance, and food security management.

14.2.1 Morphological Tools

Shape, color, and growth are cultural and morphological characteristics that have been utilized for plant disease detection, though these may lead to inaccurate inferences and are more time-consuming. Further, as plant pathogens exhibit morphological similarities, precise identification becomes more challenging (Ghosh et al. 2019). Automatic detection, on the other hand, requires less efforts, takes less time, and can be more accurate. *Ganoderma boninense*, a fungus that causes infection in African oil palms (*Elaeis guineensis*), coconuts (*Cocos nucifera*), and betel nut palms, has unique sporophores. Other pathogens will very certainly require the use of a light microscope or high resolution that a TEM or SEM can provide (Pandey et al. 2015). Brown and yellow spots, early and late scorch, and fungal, viral, and bacterial infections are some of the common diseases affecting plant health (Singh and Misra 2017). Image processing is used to detect the change in color of the affected region besides to estimate the extent of damage caused by pathogenic attack (Ghaiwat and Arora 2014). Visual diagnosis of infections in plants displaying symptoms would need substantial experience for diagnosing plant diseases followed by isolation of the pathogen (Sabah & Navdeep 2012). However, the accuracy of the same does not have to be constant throughout all attempts (Balodi et al. 2017). Traditionally, the most common methods for identifying plant diseases depend on morphological approaches based on axenic culturing of the pathogen. These methods are time-consuming and necessarily require a comprehensive understanding of classical taxonomy (Ghosh et al. 2019). Other limitations include the difficulty of cultivating some species under in vitro conditions and the inability to accurately quantify the pathogens (Ghosh et al. 2015).

14.2.2 Molecular Tools

For accurate plant disease diagnosis, DNA-based approaches have become widespread. New molecular diagnostic tools in the field of fungal detection and differentiation have resulted from recent advancements in standard and different PCR assays. DNA-based detection methods are effective in identifying symptomatic and latent period effected plants by described methods in both single and coinfections. Despite recent advances in molecular diagnostic techniques, there is still much work to be done in the research and application of diagnostic techniques in plant diseases (Hariharan and Prasannath 2020).

14.2.3 Omics Tools

Pathology-relevant omics technologies, such as metabolomics, genomics, metagenomics, volatilomics, and spectranomics exist, and multi-omics approaches have been successfully applied for plant disease ecology studies (Lander et al. 2001;

Weissenbach 2016; Crandall et al. 2020). Every organism's genome is made up of a unique nucleotide sequence, but the degree of conservation of various domains varies. Many distantly related creatures have highly conserved regions, although certain parts, such as microsatellite DNA sequences, which are repetitive and frequently non-transcribed, are quite different. Microbial genomics is a multidisciplinary discipline concerned with the structure, function, evolution, mapping, and editing of genomes in bacteria, fungi, archaea, viruses, and other microscopic species. Ecological concerns, particularly those involving environmental change, can benefit from the integration of genomics questions and technologies (Crandall et al. 2020). Metagenomics uses molecular genomics' methods and ideas to explore DNA directly derived from the environment. Microbial DNA targets can be extracted and amplified different sources, such as from soil, water, air, plants, and animals (Handelsman et al. 1998). To date, metagenomic research on plant health has been focused on two major aspects. The first is for promoting plant growth by acknowledging the role played by endophytic microbes, either within the shoots or roots communities (Fadiji and Babalola 2020). The use of CRISPR approaches to detect plant diseases with great sensitivity and selectivity is another new molecular technology. However, these approaches need the amplification of nucleic acid samples ahead of time in order to acquire many copies of nucleic acids and improve detection performance (Gootenberg et al. 2018; Myhrvold et al. 2018; Zhou et al. 2018).

14.2.4 Nano-Based Diagnostics Tools

Nanotechnology also has the power to enhance agronomic yield through genetic modifications of vegetation, as well as the delivery of genes and pesticides to precise locations at the cellular level. Nano-phytopathology is a cutting-edge discipline that uses nanotechnology to detect, diagnose, and manage plant disease and pathogens at an early stage, hence protecting crops from epidemic diseases (Hussain et al. 2017). Plant defense systems can be strengthened using nanoarray and genomic technologies in disease or stress situations (Younas et al. 2020). The application of nanotechnology in biomedical diagnostics is known as nanodiagnosics. The following sections go over several aspects of the interaction between biomedical nanotechnology and diagnostics. One of the most challenging aspects of plant disease management is detecting the disease at the right phase. For proper disease prevention and management to reduce crop loss, early and accurate disease detection is critical. Gold nanoparticles, magnetic nanoparticles, and quantum dots are the most often employed nanoparticles for molecular detection (Hussain et al. 2017). Because a huge percentage of plant diseases are only discovered at later stages, controlling them becomes a difficult effort. Pesticides and fungicides are often given to plants for protection only after symptoms occur. Instead of providing plant protection, these methods result in severe crop loss (Younas et al. 2020). Nanodiagonastic kit, commonly known as "lab in a box," may be used to measure key parameters in plants in a small space (Khiyami et al. 2014). A smart kit can assist farmers to detect plant pathogens and help in prevention of disease spread (Pimentel 2008; Nezhad

2014). Four myco-sensors have been included in the Nanodiagnostic kit, which can detect different types of mycotoxins on a single strip for cereal crops (Lattanzio et al. 2012). Signaling molecules such as ROS (e.g., H_2O_2), Ca^{2+} , NO, and ABA, which communicate and govern plant responses, are connected to major abiotic and biotic challenges, as well as resource restrictions. The delivery of genetically encoded sensors via nanomaterials enables us to study plant health signaling systems, which in turn can provide information for the design and fabrication of smart plant sensors. Plant chemical signals may be converted into optical, radio, and electric signals that can be monitored by electronic equipment employing optical nanosensors and wearable nanotechnology-based sensors interfaced with plants. Smart nanobiotechnology-based sensors will be able to actuate agricultural equipment for improving plant environment by utilizing machines that can decipher spatiotemporal patterns of plant chemical signals (Fig. 14.2). These nanobiotechnology technologies may be used for a variety of purposes, including laboratory research and development, chemical phenotyping in specialized facilities, and crop monitoring and automation for urban farming and precision agriculture.

14.2.4.1 Nanoparticle-Based Sensors

Quantum Dot

The semiconductor nanocrystals or quantum dots (QDs) emit light of specific wavelength on excitation with high energy radiations. These are three-dimensional nanoparticles (Edmundson et al. 2014) with a wide excitation spectrum that provide

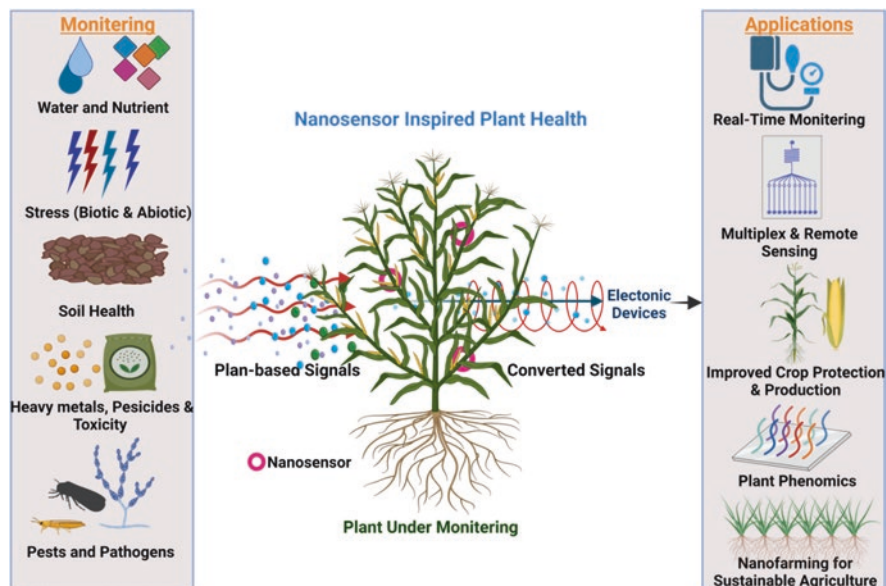


Fig. 14.2 Smart nanosensor modules for conversion of plant-based signals to obtain various information related to plant health and disease prognosis to achieve agricultural sustainability

several advantages. These QDs have a small tunable emission peak and a long fluorescence lifespan, exhibit photo bleach resistance have 10–100 times greater molar extinction coefficient. When compared to typical fluorophores, these can help fluorescent dyes produce brighter probes (Zhao and Zeng 2015). Quantum dots are supposed to be a part of indoor planting owing to its ability to produce light of specific wavelength. The most common applications of QD-FRET-based sensors are in the detection of nucleic acids and enzyme activity (Stanisavljevic et al. 2015).

Metal Nanoparticles

Antimicrobial activity of AgNPs, ZnONPs, and CuONPs have been documented against several foodborne and plant pathogenic bacteria. Some nanoparticles can be employed as antimicrobial, bactericidal or bacteriostatic, but they mostly suppress bacterial growth by inhibiting metabolism or reducing colonization (Younas et al. 2020). To separate and concentrate bound target analytes, the magnetic properties of metal nanoparticles can be used. The advancement of magnetic-based DNA isolation methods significantly increase DNA quality of extractions while decreasing dependence on toxic reagents, powered centrifuges, and heatblocks (Berensmeier 2006). Gold, cadmium sulfide, or silver NPs with refined biological and chemical characteristics have largely been used. These serve as DNA attachment substrates on the sensor surface, increasing the quantity of immobilized DNA while also acting as signal amplifiers, greatly improving diagnostic accuracy, sensitivity, and speed (Dyussebayev et al. 2021).

Gold Nanoparticles for Pathogen Diagnosis

Produced AuNPs with nano-size have appropriate surface-to-volume ratios and energies to enable stable immobilization of a wide variety and number of biomolecules without affecting their bioactivity (Li et al. 2010). AuNPs also have a high electron conductivity. As a result, their usage has had a significant influence on the reliability, sensitivity, and speed of optical and electrical biosensors (Li et al. 2010). AuNPs are also preferable to other forms of NPs, because they can readily be functionalized with thiolated DNA probes and protein molecules (Syed and Bokhari 2011).

Several nano-based assays have been carried out to develop biomolecular detection using DNA or protein functionalized AuNPs as target-specific probes (Fan et al. 2003; Thaxton et al. 2006). Despite this, AuNPs have long been utilized in immunochromatographic strip (ICS) biosensors for sensitivity increase in a variety of nanodiagnostic procedures (Halfpenny and Wright 2010, Syed and Bokhari 2011). Many lateral flow assays based on DNA hybridization to AuNPs were used for the identification of plant pathogens, particularly for *Acidovorax avenae* subsp. *citrulli* (Tarasov et al. 2015) of watermelon (Zhao et al. 2011). AuNPs have been widely used to label antibodies specific to pathogens of interest and have been

developed as a diagnostic tool. The potential of AuNPs to act as fluorescence quenchers was emphasized by Dubertret et al. (2001) and hence might be used to overcome key problems in molecular biology experiments. AuNPs could be the best choice for sensing because of their well-understood mechanism and ease of surface modification with biocompatibility (Kulabhusan et al. 2022). These have been employed for fluorescent tagging of DNA oligonucleotide at its 5' end and conjugation of gold nanoparticles at the 3' end. The effective use of these oligonucleotides in the diagnosis of phytoplasma linked with grapevine *Flavescence dorée* (FD) has been described (Firrao et al. 2005).

Magnetic Nanoparticles

The use of magnetic nanoparticles also allows pathogen isolation, purification, and recognition in difficult conditions. Magnetic nanoparticles (MNPs)-based biosensing techniques have lately gained a lot of interest. Magnetic nanoparticles can also be encased in a silica or gold shell, with the magnetic component acting as the core and the silica or gold acting as the shell. These nanoparticles combine the magnetic and fluorescent properties of materials (Liu 2006). Magnetic fields will most commonly appear transparent to even optically turbid samples. Magnetically marked cells, on the other hand, will have a great contrast against the biological background (Shao et al. 2012). Furthermore, using superparamagnetic nanoparticles (SPMNPs) has advantages, since their magnetic characteristics rise rapidly as the size of the particle decreases (Maalouf et al. 2008).

Diagnostic magnetic resonance (DMR) is a novel magnetic sensing platform (Lee et al. 2008). The amine group gives the magnetic nanoparticles a positive charge, allowing them to easily adhere to negatively charged bacterial cells (Huang et al. 2010). This nonspecific binding might help enrich bacterial cells from water samples. Chen and Zhang (2012) employed gentamicin-conjugated magnetic silica nanoparticles to identify the gram-positive bacterial species *Staphylococcus aureus* in a similar investigation. A faster and less costly method for extracting and quantifying *Meloidogyne hapla* DNA from mineral soils was tested using iron oxide (Fe_3O_4) superparamagnetic NPs. The researchers discovered that addition of 10 mg of NPs to the extraction lysate could increase the yield of DNA while reducing the co-capture of contaminants (Gorny et al. 2018). There are various types of nanoparticles having optical properties, including gold nanoparticles, quantum dots, and magnetic nanoparticles, as well as nanocomposites that combine these qualities, all of which offer specific advantages for monitoring agroecosystems (Fig. 14.3).

Carbon Nanotubes

Carbon in nano-size form is widely synthesized and used in a variety of forms. Carbon nanotubes (CNTs) can aid plant development by improving water and nutrient absorption (Shoala 2019). Because of their sensitivity and selectivity, CNTs

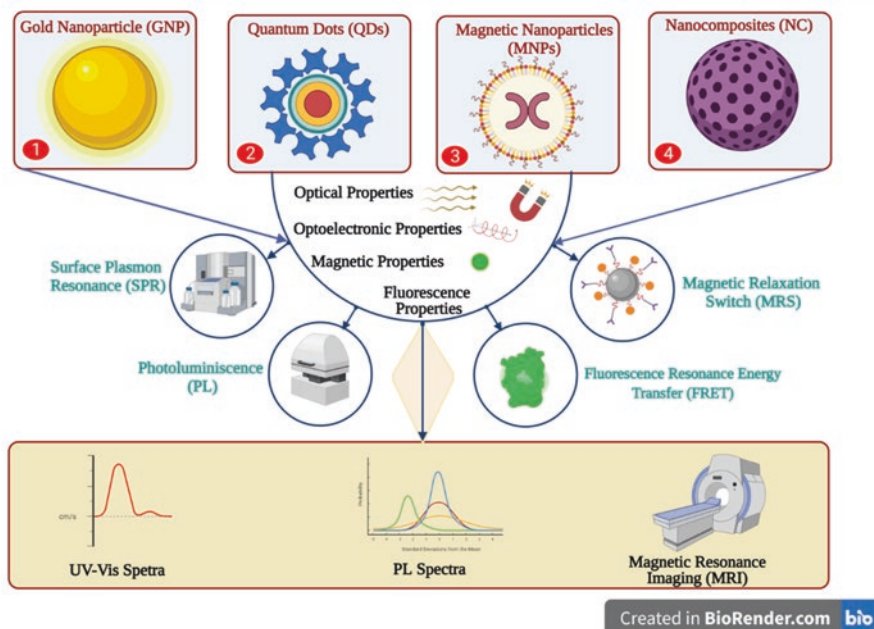


Fig. 14.3 Diagrammatic exposition of nanoparticle-enabled diagnostic systems for pathogen detection in plants vesting prospect edges toward environmental sustainability. 1. Gold nanoparticles, 2. quantum dots, and 3. magnetic nanoparticles, and (4) nanocomposites

have been effectively used as sensors or detectors of phenolic compounds. CNTs can also be used for fabrication of biosensors because to their unique electrochemical features, which include the mediation of rapid electron transfer kinetics, a greater length to diameter ratio, and the ability to connect to any chemical species (Yu 2003; Balasubramanian and Burghard 2006). CNTs are useful as electrodes and transducer components in biosensors due to their unique electrochemical and electrical properties (Shoala 2020). Individual SWCNTs are highly sensitive to their surroundings. Chemiresistors and chemically sensitive field-effect transistors (FETs), using pristine or particularly functionalized CNTs, have been proven to detect biomolecules. FETs have been successfully employed to identify bacterial cells with detection limits of up to 100 cfu/ml of material. (Huang et al. 2011; Villamizar et al. 2008). Bio-nano integrated systems that combine carbon nanotubes with recognition or catalytic biomolecules have shown to be great tools for developing biosensors. (He and Dai 2006, Zhang et al. 2007). For biosensing devices, electrochemical signal readout provides a user-friendly, sensitive, and specific method. Electrodes may be produced from a number of materials, including noble metals, carbon-based materials such as graphene and carbon nanotubes, organic polymers, and can be further modified with NPs to obtain improved signals (Dincer et al. 2019; Fritea et al. 2018).

14.2.5 Nanobiosensors

There is a great deal of interest in creating biosensing devices that can ensure early and accurate identification of the plant pathogens. Emerging and creative biosensor methods are frequently employed as diagnostic procedures for plant, and foodborne pathogens (Khater et al. 2017; Rani et al. 2019). Antibodies, enzymes, DNA probes, and phage-based biosensors are examples of actuators and active receptors that allow particle interactions to detect an analyte in the biosensor device (Singh et al. 2013; Sadani et al. 2019).

For example, detection of *Pseudomonas syringae* with a nanoparticle electrochemical biosensor proved more sensitive than traditional PCR, allowing infected plants to be identified before appearance of any symptoms of the disease (Lau et al. 2017). A phage-based DNA biosensor has been recently reported for sensing and targeting bacterial plant pathogens (Fang and Ramasamy 2015). DNA-based detection methods are more precise, specific, and adequate for detection of a particular pathogen besides multiple targets. The disadvantages of these methods include problems associated with detecting plant pathogens from complex environmental, contaminated, or deteriorated samples, false-negative results, time-intensiveness, the need for technical personnel for handling, low titers in early pathogen detection, and a lack of potential application in on-site phytopathogen detection (Martinelli et al. 2015).

The main advantage of this method is that it detects the nucleic acid of only living bacterial cells, resulting in no false positives (Khater et al. 2019). As detailed in the following sections, the majority of the reported electrochemical immunosensors for plant pathogen detection are based on label-free technologies (impedimetric and quartz crystal microbalance-based ones) and enzymatic label-based voltammetric approaches include the use of mercury, gold, and carbon electrodes (Khater et al. 2019). Most electrochemical DNA biosensors for plant pathogen detection rely on voltammetric detection of DNA hybridization, both labelled and label-free. Emerging techniques based on DNA translocation through nanopores, while not yet described for plant pathogen detection, offer immense potential and have been discussed in detail in the sections that follow.

As a result, techniques for increasing the sensitivity of these biosensors have included the creation of nano-structured materials with superior chemical or electronic properties to enrich the target sequences and amplify the observed signal (Dyussebayev et al. 2021).

There is also a lot of potential for translating new nano-based biosensor techniques developed for human disease diagnostics to early detection of some plant pathogens (Dyussebayev et al. 2021). These biosensors are low-cost, require little expertise, and identify target pathogens quickly with on-field detection advantage. In addition, these biosensors are extremely selective and sensitive.

Functional nanomaterials are commonly used to amplify signals in electrochemical detection. These investigations create electrochemical nucleic acid sensors by altering nanomaterials on electrode surfaces or nanoparticles on report probes,

making effective use of nanomaterials with high electrical conductivity, large specific surface area, and stability (Chen et al. 2020). Khater and his colleagues (2017) examined antibody-based and nucleic acid-based biosensors created in laboratories throughout the world for plant disease detection. DNA-based biosensors have benefits over antibody-based biosensors (Fig. 14.4), mostly due to their higher sensitivity because of the use of nucleic acid amplification methods, which allows for the detection of plant pathogens prior to the appearance of disease symptoms (Khater et al. 2017).

14.2.5.1 CRISPR/Cas-Powered Nanobiosensors

The acceptance and implementation of new technologies in agriculture and plant science has been increased in recent years. CRISPR technology, for example, has already found a wide range of uses in agriculture and the food business. Zhang et al. (2019) have reported creation of CRISPR-based biosensing systems to meet the needs of the animal husbandry, agricultural, and forestry industries. For example, a Cas12a-based lateral flow biosensor paired with PCR amplification was employed to detect the African swine fever virus (ASFV) in swine blood within 2 h, attaining a sensitivity of 2.5×10^{-15} M (Wu et al. 2020). Another Cas12a-based reversible valve-assisted chip was developed for the quick detection of *V. parahaemolyticus* in seafood tests, with a LOD of 30 copies/reaction utilizing 600 μ l of samples (Wu

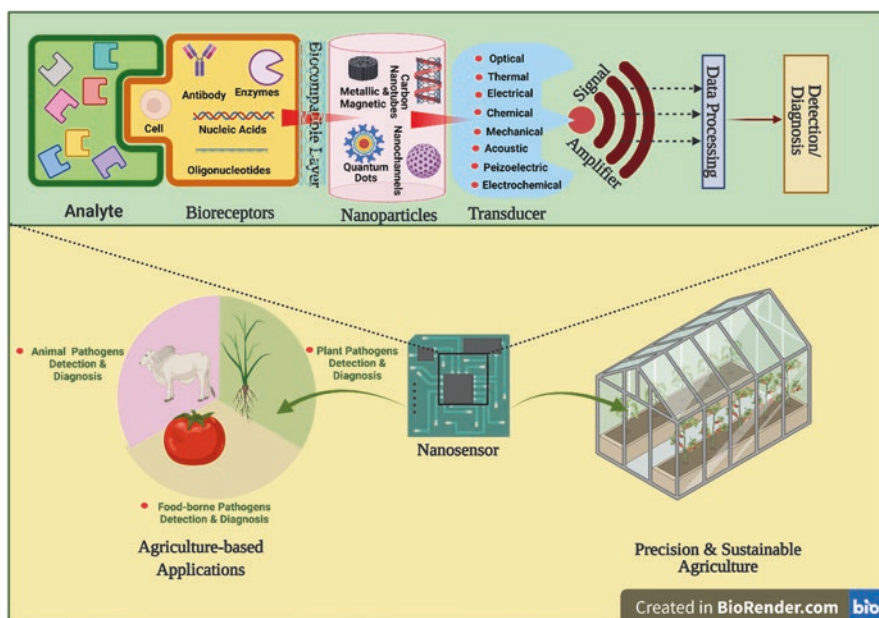


Fig. 14.4 Outline of components and applications of nanosensors for precision agriculture

et al. 2021). The Cas9 system, in conjunction with AuNPs, has been developed in agriculture and forestry to detect plant-associated disease such as detection of *Phytophthora infestans* (Chang et al. 2019). For the diagnosis of citrus scab caused by *Elsinoe fawcettii*, an RPA-CRISPR/associated (Cas) system was created with the integration of a lateral flow assay (LFA) readout device. A crude DNA extract from diseased citrus leaves and fruit might be used as a template for the RPA reaction. This RPA-CRISPR/Cas12a-LFA system offers a sensitive, fast, and cost-effective technique with potential and considerable practical utility for citrus scab diagnosis at the point-of-care level (Shin et al. 2021). A simple, quick, and effective approach that combines RPA and CRISPR/Cas12a for the identification of bacterial spot caused by *Xanthomonas arboricola* pv. *pruni* (Xap). The streamlined RPA/Cas12a assay can identify batch samples immediately in the field. Based on the benefits and advances, we expect that our RPA/Cas12a assay will be used commercially soon (Luo et al. 2021).

The CRISPR-Cas13 technology has recently been used to identify human RNA viruses accurately by visual readout in 90 min or less and by paper-based assay. This technology's multitarget RNA assays have a high potential for use as a quick and accurate diagnostic assay for recognized viroids (Hadidi 2019). To identify plant RNA viruses, an RT-RPA approach was combined with a CRISPR/Cas12a-based one-step detection assay. This diagnostic method can be performed in less than 30 min at a single temperature and integrated with a low-cost commercially available fluorescence visualizer to allow for rapid, infield diagnosis of plant RNA viruses (Aman et al. 2020). The tomato brown rugose fruit virus (ToBRFV), a new and emerging tobamovirus that causes significant damage to the tomato industry globally, was identified using CRISPR/Cas12a. To identify ToBRFV or the similarly related tomato mosaic virus, specific CRISPR RNAs (crRNAs) were created (ToMV). This method allowed for the identification of ToBRFV and ToMV in distinct ways (Alon et al. 2021). Cas12a-based biosensors were created to detect plant DNA viruses (Mahas et al. 2021). A summary of current advances and future prospects on the use of CRISPR/Cas-based genome editing for diagnosing and creating resistance to banana viruses, as well as obstacles in banana genome editing, has already been presented in a review by Tripathi et al. (2020).

Combining CRISPR/Cas detection with lateral flow device-based signal readout will enable very sensitive and accurate pathogen identification in the field. CRISPRdx can be used to detect and diagnose plant pathogens that reduce yield and have a negative impact on crop productivity (Verosloff et al. 2019). A CRISPR/Cas12a diagnostic tool in crops, as well as a paper-based DNA test method based on RPA-Cas12a-LFA, were employed as new method for diagnosis of rice diseases and detection of Bt rice (Zhang et al. 2020). This DNA test method would be a useful tool for crop management and GMO administration due to its simplicity, efficiency, and low cost (Zhang et al. 2020). CRISPR/Cas applications are fast developing to include fundamental plant-pathogen interactions, genome engineering of plant disease resistance, and molecular detection of various infections. Various CRISPR/Cas-enabled technologies have been described to accurately modify the host genome for disease resistance, identify the pathogen promptly for disease management, and

possibly apply gene editing for insect population control using citrus greening disease as an example. As we tackle the difficulties of twenty-first-century agriculture, the CRISPR/Cas toolbox, which is at the bleeding edge of nucleic acid editing and detection, will speed plant breeding and transform crop production and disease control (Wheatley and Yang 2021). These methods will be especially useful for detecting closely related pathogen species or strains.

14.2.6 Nanochips

Nanochips are microarrays comprised of fluorescent oligo-capture probes that can detect specific ligands (RNA, DNA, protein) by using hybridization. The nanochips are well-known for their ability to detect single-nucleotide changes in bacteria and viruses (Lopez et al. 2009). Even though the chips can be fabricated using automatic robotics technology ensuring remarkable precision, the cost per test might be relatively high when compared to alternatives. Scaling this procedure down using nanotechnology to generate lab-on-a-chip assays that use microfluidics is a modern approach of array technology that holds tremendous potential due to reduced reaction volumes (microliters) and a more user-friendly format more suitable for a plant pathology laboratory.

14.2.7 Nanopore-Based Detection

Approaches based on next-generation sequencing (NGS) are particularly promising, since these enable sensitive pathogen detection while also giving the genomic sequence data required for quantitative genotype-specific identification, including new genetic variations (Deurenberg et al. 2017). The use of this innovative technique to identify plant diseases is still in its initial stages. Nanopore appears to be one of the most promising single-molecule detection technologies. A single molecule passes through a nanoscale pore and causes a measurable change in ion current, allowing us to detect the target's important information (Chen et al. 2020). The ability of a portable nanopore-based massively parallel sequencing (MPS) method to detect different plant pathogens in the metatranscriptome of plant and insect tissues infected with *Candidatus Liberibacter asiaticus* or plum pox virus was tested. This method also demonstrated the system's capacity to identify the primary components of the insect vector's microbiome as well as the specific strain of small-genome, high-titer pathogens (Bronzato Badial, et al. 2018). The MinION detects and characterizes several plant viruses that infect a single yam plant. This sequencing platform was successful in finding almost full-length positive-sense single-strand polyadenylated RNA plant viral genomes for three viruses: a badnavirus, a macluravirus, and a potyvirus. The widespread adoption of very portable sequencing systems, such as the MinION, is expected to transform plant disease diagnosis

(Filloux et al. 2018). The possibility of employing Oxford Nanopore's single-molecule sequencing technology as a generic tool for diagnosing plant diseases was investigated. It was evaluated by sequencing DNA or RNA obtained from tissues exhibiting symptoms from plants infected with recognized pathogens from several families. Samples from groups of 200 seeds having one infected seed from each of two or three diseases were analyzed, as were samples with symptoms but unknown pathogens. This method has the following advantages: results are received in real time; sequencing may be conducted in the laboratory or in the field; and interpretation of the data for diagnostic purposes does not require significant understanding of bioinformatics tools. Chalupowicz et al. (2019) and Hu et al. (2019) employed the approach in a nursery to diagnose fungal wheat diseases caused by *Zymoseptoria tritici*, *Puccinia striiformis* f.sp. *tritici*, and *Pyrenophora tritici-repentis*. The nanopore-based technology described here might be a valuable tool for diagnosing Goss's bacterial wilt and blight disease (GBWD) caused by *Clavibacter nebraskensis* by direct processing of corn leaves (Fig. 14.5). Finally, this study provides the first look at *Pseudomonas* population patterns in GBWD necrotic leaf lesions (Xu et al. 2021). Using *Xylella fastidiosa* as a case study, Marcolungo et al. (2022) developed and tested a new all-in-one diagnostic assay based on nanopore sequencing for the detection and simultaneous characterization of quarantine pathogens. The assay was shown to be at least as sensitive as traditional diagnostic assays, and the quantitative results agreed well with qPCR-based analysis.

14.3 Robotics Techniques for Plant Pathogens Detection

Robotics research in agriculture has expanded in recent years, owing to prospective uses and industrial initiatives in development of various types of robots (Bogue 2016). Aside from agronomic techniques, robotic plant protection has been researched, but it may represent the most difficult task for researchers and developers since pathogen identification questions must be considered alongside basic robot-related concerns. Recently, research in automatic disease detection has been quickly expanding, with potential implications for construction of robots capable of recognizing specific plants, locating and identifying disorders, and initiating disease management procedures (Ampatzidis et al. 2017).

Combining colored cameras with multispectral/hyperspectral sensors has been identified to be fruitful to achieve a more accurate and specific identification of the disease and causative pathogen. However, using more complicated structures may not necessarily produce the greatest results. Color cameras can detect powdery mildew in greenhouse-cultivated pepper plants besides the tomato spotted wilt virus (TSWV) with excellent precision (Schor et al. 2016). However, the multispectral cameras detected these two diseases with an accuracy of 80% and 61%, respectively (Schor et al. 2016). Cruz et al. (2017) developed a vision-based, innovative transfer, and deep learning approach for identifying symptoms of leaf scorch on *Olea europaea* leaves infected with *Xylella fastidiosa*, with a true positive rate of 95.8%.

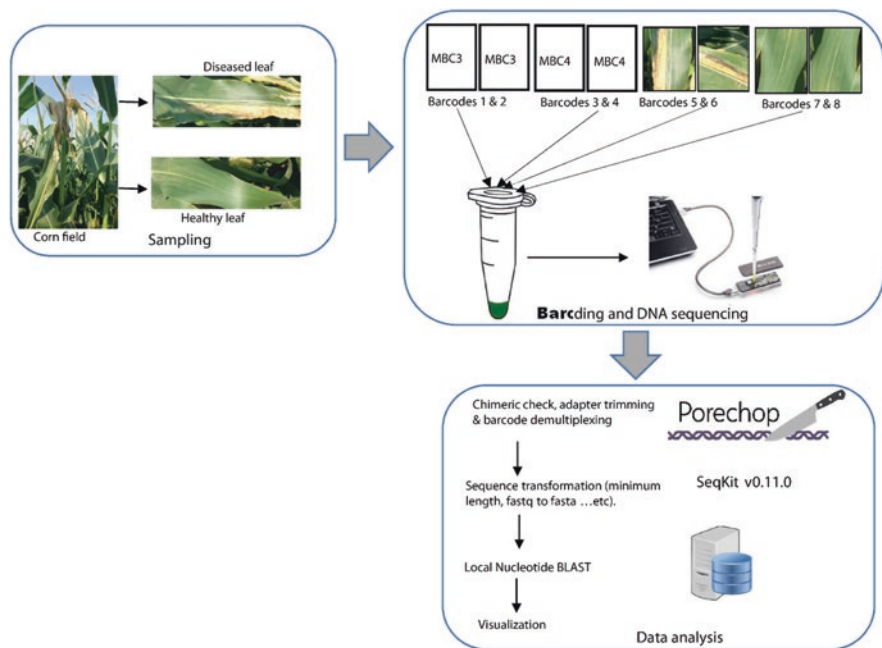


Fig. 14.5 Detection of the purine permease gene in *Clavibacter nebraskensis* utilizing a nanopore sequencing and detection approach with mock bacterial communities (MBC) and sick corn leaf samples. (Reprinted with permission from Xu et al. (2021))

These vision-based devices can be put on mobile vehicles (e.g., autonomous vehicles) to improve disease diagnosis and management procedures. Another approach for detecting *Xylella fastidiosa* in olive trees was introduced (Rey et al. 2019).

Powdery mildew was identified in strawberry plants using a machine vision system centered on artificial cloud lighting requirements, and an accuracy of 72–95% was reached under two distinct lighting circumstances (Mahmud et al. 2019). Furthermore, eAGROBOT has been used to identify a variety of diseases; the accuracy rate for cotton and peanut plants was found to be around 90% (Pilli et al. 2015).

As a preventive measure, early identification of crop disease via agricultural remote sensing is critical. Thermal imaging of normal and diseased leaves was explored in a pot experiment under greenhouse conditions for early detection of powdery mildew in wheat following artificial infection with *Erysiphe graminis*. For early disease identification, temperature differences between infected and healthy wheat leaves, as well as temperature differences between air and leaf-surface temperatures, were measured under greenhouse conditions (Awad et al. 2015). Plant disease detection using image sensors was thoroughly examined by Mahlein (2016). The method for detecting signs of citrus greening diseases (also known as citrus Huanglongbing, HLB, caused by *Candidatus Liberibacter* spp.) on leaves based on visible spectrum image processing has been evaluated. The results of the experiments revealed a high detection accuracy of 91.93% (Deng et al. 2016). The HLB

detection method was assessed in the presymptomatic stage using polarized imaging (Pourreza et al. 2016). Citrus canker produced by *Xanthomonas axonopodis* resulted in foliar symptoms that were studied to determine the efficacy of image analysis (Bock et al. 2008). Aerial (Unmanned Ground Vehicles, UGVs) and ground robots might be used to identify and manage disease in broad areas (rather than only in well-defined locations). UAVs were used in this study to gather spectral pictures and analyze them in order to identify “critical” regions. This data was wirelessly transmitted to the UGV, which travelled to the “important” places to assess and gather leaf samples. The UGV initially evaluated the plant (strawberry) using a spectral camera before collecting leaf samples with a manipulator and Web cameras for leaf localization if it was categorized as “diseased” (Menendez-Aponte et al. 2016).

The use of spectral and textural data to identify yellowness and esca in grapevines was explored, with an overall accuracy of 99% for both diseases (Al-Saddik et al. 2018). Although the preceding research yielded some valuable results, there is almost no evidence supporting the detection of powdery mildew by the fusion of spectral and textural information, particularly in the early stages of disease infection. A robot was conceived and built to offer field-based plant health assessments using visible and near-infrared spectroscopy. It was meant to move through a predetermined path inside an agricultural field and deliver leaf health information as well as position data. Under real field conditions, the technology was tested in a tomato greenhouse. With an accuracy of 83%, the developed approach proved useful in properly categorizing plant health into one of three classes: undeveloped, unhealthy, and healthy. For farmers and agriculturists to monitor plant health across diverse areas, a map containing plant health and locations was created. This system can do early vital health analysis on plants to take timely action and maybe selective pesticide spraying (Rizk and Habib 2018).

14.4 Nanotools for Detection of Plant Pathogens

Alternative effective ways are urgently needed to limit crop disease spread and increase plant pathogen control and early and precise diagnosis. NPs, through more precise and specific plant pathogen probes, promise significant breakthroughs in plant disease diagnosis (Elmer and White 2018). NPs have the potential to be employed in quick diagnostic tools to detect diseases caused by nematodes, bacteria, and fungi (Li et al. 2019; Farooq et al. 2021). Since NPs are faster and more sensitive than standard molecular diagnostics, they can be used as rapid diagnostic tools for nematodes, fungal, bacterial, and viral plant pathogen detection (Khan et al. 2022; Kashyap et al. 2017).

14.4.1 Detection of Bacterial Pathogens

Xanthomonas axonopodis pv. *vesicatoria*, a plant pathogen, causes bacterial spot in tomato and pepper plants, which may be observed by use of fluorescent silica nanoparticles (FSNP) linked with antibodies (Etefagh et al. 2013). *Pseudomonas cannabina* pv. *alisalensis*, which infects cruciferous vegetables, was detected using bioluminescence-phase technology (Schofield et al. 2013). AuNPs' high conductivity and surface area capabilities were employed to magnify the electrochemical signal and conjugate the HRP-labeled anti-PSS detection antibody, which was subsequently used to identify the presence of quarantine bacterial pathogen *Pantoea stewartii* bacterial cells linked to the capture antibody. The new biosensing test had a limit of detection of 7.8×10^3 cfu/mL, which was greater than the standard ELISA, and it also demonstrated nonspecificity to other infections (Zhao et al. 2014). Colorimetric detection of *Pseudomonas syringae* pathovars by DNA molecules was achieved using AuNPs-labeled DNA probes (Li et al. 2010). Specific primers were generated from the conserved N-terminal region of the *hrcV* gene, and probes containing thiol-capping at the 5' or 3' ends of the probes were subsequently created. The colorimetric detection resulted in a color shift from red to purple, allowing the pathogen DNA contained in the sample to be identified Vaseghi et al. (2013). The nanobiosensor was proven to be fast, sensitive, and selective for detecting *R. solanacearum* straight from soil samples without the need for any DNA amplification (Khaledian et al. 2017). Electrochemical impedance spectroscopy (EIS) sensors were recently employed to detect up to seven different strains of *Pseudomonas syringae* pv. *lachrymans* (Psl), which cause diseases in several cucurbit species, resulting in significant production losses (Cebula et al. 2019). A lateral flow immunoassay (LFIA)-based test strip was reported to identify *Ralstonia solanacearum*, a quarantine bacterium that causes potato brown rot, by employing AuNPs (Fig. 14.6) (Razo et al. 2019). When the test strip was dipped in the potato tuber extract, the binding of antibodies linked to AuNPs, migration to the test zone, binding to antibodies, and additional color development after addition of the amplification solution all show an amplified positive signal in the presence of analyte. The presence of AuNPs provides catalytic activity on the amplification solution, resulting in a rise in AuNP size and, as a result, color development (Razo et al. 2019). A novel prospect for nanomaterial-based optical immunoassays with enhanced usage of graphene quantum dots for the early detection of rice bacterial leaf blight disease in agricultural applications was investigated. For the detection of *Xanthomonas oryzae* pv. *oryzae* (Xoo) in rice crops, a turnoff nanosensor system based on graphene quantum dots' (GQDs) fluorescence-based immunoassay was developed. The use of antibody biomolecules and nanoparticle materials (GQDs and AuNPs) in the fluorescent immuno-based detection technique has improved Xoo detection sensitivity (Awaludin et al. 2020). When tested on *P. syringae*-infected *A. thaliana*, the created AuNP-electrochemical biosensor was 10,000 times more sensitive and had the capacity to detect pathogen presence in the very early stages of infection (Ebrahimi et al. 2019). To improve LFIA biosensor-based detection of the potato wilt pathogen *R. solanacearum* by lowering the limit-of-detection value, the AuNPs are

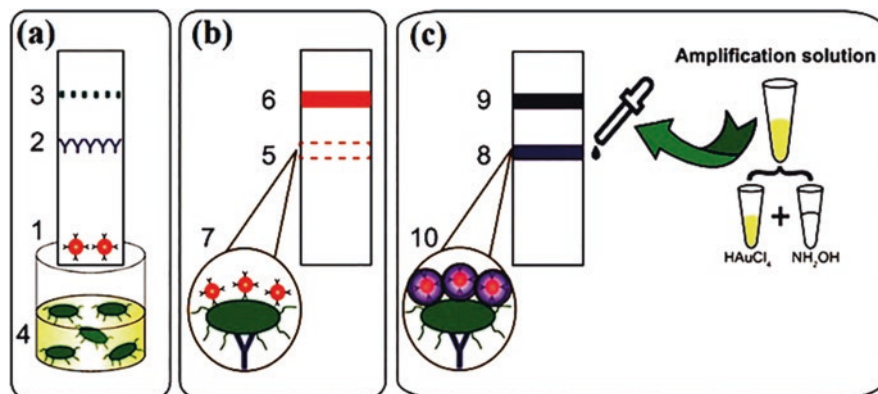


Fig. 14.6 After the amplification of the signal in LFIA: (a) test strip dipped into a sample of potato tuber extract; (b) test strip after conventional LFIA, indicating a negative result because no color band exists in the test zone; (c) addition of amplification solution to the test strip and enlargement of AuNPs. Those numbers indicate (1) AuNP-antibody conjugate on the conjugate pad, (2) an antibody specific for *R. solanacearum* immobilized on the test zone, (3) protein A immobilized on the control zone, (4) potato tuber extract with *R. solanacearum*, (5) no visible color band in the test zone after assay, (6) a clear red color band in the control zone, (7) formed immunity complex (immobilized specific antibodies, *R. solanacearum*, Au conjugate with specific antibody) after conventional LFIA, (8) the test zone after signal amplification, (9) the control zone after signal amplification, and (10) the size of AuNPs increases when amplification solution is added. (Reprinted from Razo et al. 2019)

gold-enhanced (Lau et al. 2017). Magnetic relaxation has also been identified as a new technique for single pot diagnosis of bacterial pathogens (Kaïttanis et al. 2007).

14.4.2 Fungal Pathogens Detection

Rad et al. (2012) devised a strategy for classifying the beet necrotic yellow vein viral vector utilizing QD fluorescence resonance energy, which can also be utilized to identify extremely sensitive *Phytoplasma aurantifolia* on lime. Nanocomposite membranes supplemented with gold electrodes constructed of zinc oxide nanoparticles (ZnO NPs) and chitosan (CHIT) were also employed to create biosensor systems based on the MB redox indicator for voltammetric nucleic acid detection. Techniques using such methodologies and chemicals improve the efficiency, biocompatibility, and electrochemical conductivity of the examined DNA's control of *Trichoderma harzianum* samples was documented (Siddiquee et al. 2014). Recombinase polymerase amplification (RPA) can also be used in conjunction with a surface-enhanced Raman spectrometer to boost signal efficiency (SERS). According to Lau et al. (2016), this spectrometer can detect as little as one copy of plant diseases, such as *Pseudomonas syringae*, *Fusarium oxysporum*, and grapevine spores. *Phytophthora infestans* is a destructive fungus that causes late blight in

potatoes and tomatoes and poses a danger to global agriculture. As a result, detecting *P. infestans* as soon as possible is critical to preventing the disease from spreading further. A combined integrated universal primer-mediated asymmetric PCR with gold nanoparticle-based lateral flow biosensor was used to detect *P. infestans*, the causative agent of late blight in potatoes and tomatoes. DNA was isolated directly from late blight-infected potato field samples and then used in an asymmetric PCR amplification and biosensor test, yielding a low detection limit of 0.1 pg mL^{-1} genomic DNA from *P. infestans* with good specificity within 1.5 h (Zhan et al. 2018). A smartphone-integrated volatile organic compounds (VOCs) sensing device based on AuNP fingerprinting was developed to provide noninvasive diagnosis of late blight caused by *P. infestans* by monitoring distinct volatile emissions from leaf in the field. The sensor platform has been beta-tested in a greenhouse setting for the detection of *P. infestans* in symptomless tomato plants (Li et al. 2019). Lab-on chip (LOC) device may provide rapid microbiological detection with a reduced sample amount. When compared to ELISA tests, the LOC system identified 0.1 pg/L and 10^3 CFU/mL of *Xylella fastidiosa* and *P. infestans*, respectively. Moreover, due to the possible detrimental implications on agricultural and public health, the quick and sensitive detection of fungal spores is of significant interest (Chiriaco et al. 2018; Zhan et al. 2018). The microfluidic device was put to the test on two distinct grape cultivars that were infected with *Botrytis cinerea* and *Erysiphe necator*. In all cases, the microfluidic device successfully identified healthy from infected samples (Brás et al. 2021). Rapid detection of *Aspergillus niger* spores has been performed by using peptides as a recognition probe and AuNPs as a detection label. The peptides allowed for fast binding to the *A. niger* spore, resulting in a discernible shift in the color intensity of the supernatant following spore sedimentation (Lee et al. 2021). When used in conjunction with a smartphone-enabled picture analysis application, this colorimetric test demonstrated a high sensitivity of 50 spores in less than 10 min. In AuNP-enhanced dynamic microcantilever (MCL) and isothermal RPA for the detection of *Leptosphaeria maculans*, a virulent phytopathogen of oilseed rape was developed. It has been discovered that *L. maculans* produces a phytotoxin called sirodesmin PL, which may exist in the environment for an extended time duration. The detection findings demonstrated that the RPA-MCL test had a better sensitivity than the previously investigated fluorescence RPA assay, with a LOD of one copy of *L. maculans* DNA (Lei et al. 2021).

14.4.3 Viral Pathogen Detection

Electrochemical impedance spectroscopy (EIS) sensors (Katz and Willner 2003) are valuable tools for the detection of plant viruses or pathogens of various plant genera (Jócsák et al. 2019). For instance, the $\text{Fe}_3\text{O}_4/\text{SiO}_2$ -based immunosensor revealed the presence of tomato ringspot virus, bean pod mottle virus, and arabis mosaic virus at the concentrations of 10^{-4} mg/mL (Zhang et al. 2013). Using colloidal gold nanoparticles for antibody immobilization, a selective electrochemical immunosensor was

created for the detection of plum pox virus (PPV) in extracts from plum and tobacco leaves (Jarocka et al. 2011). For the detection of two viruses in the orchard (cymbidium mosaic virus (CymMV) and odontoglossum ringspot virus (ORSV), unlabeled SPR immunosensors were constructed utilizing gold nanorods (AuNRs). Lin et al. (2014) adapted orchard virus-specific antibodies using AuNRs as the detecting layer, which demonstrated a larger spectrum range and might help to alleviate color interference difficulties caused by sample matrices. The potential of a multiwalled carbon nanotube-based zinc nanocomposite (MWCNTs-Zn NPs) was investigated for the detection of an agricultural pathogen, i.e., *Chili leaf curl betasatellite* (ChLCB). The specificity of this electrochemical DNA biosensor was found to be three times as compared to noncomplementary DNA (Tahir et al. 2017). An enhanced AuNPs-based dot immunobinding assay (DIBA) was used to detect banana bunchy top virus (BBTV), which is faster and easier than the traditional ELISA. The AuNPs were conjugated to the main antibody in this study, and the DIBA LOD was reported to be 102 at 50% dilution. Similarly, grapevine leafroll-associated virus 3 (GLRaV-3) is a severe infection that reduces grape output significantly (Majumder and Johari 2018). For disease detection in plants, several fluorescence resonance energy transfer (QD-FRET) sensors have been created. In rhizomania disease, for example, *Polymyxa betae* is the sole known vector of BNYVV (beet necrotic yellow vein virus) for viral transfer to beet plants, which has been identified using a QD-FRET-based sensor (Joshi et al. 2019). A DNA hybridization sensor based on screen-printed carbon electrodes modified with AuNPs has been reported for the selective detection of citrus tristeza virus (CTV) even in the presence of other non-specific DNAs, a feature that is especially useful in the case of mixed infections, which is a common occurrence in cultivated plants (Khater et al. 2019). The LSPR of unmodified AuNPs was also tested for detecting the tomato yellow leaf curl virus (TYLCV) genome in infected plants. The complementary DNA probe for the TYLCV coat protein was constructed and hybridized with the extracted total DNA from the infected sample (Razmi et al. 2019). With a sensitivity of 500 g/L of begomoviral DNA, a visual colorimetric signal was created for the detection of *Begomovirus* in chili and tomato plants. A comparison of PCR and AuNPs assays for begomoviral infection in chili plants revealed that the AuNPs test (77.7%) performed better than the routinely used PCR techniques (49.4%). (Lavanya and Arun 2021). Various other types of optical, electrochemical, and immunosensors have also been developed for detecting diverse plant pathogenic microorganisms (Table 14.1).

14.5 Diagnosis of the Plant Varieties and Other Forms

Diagnostics in plant breeding is a comprehensive collection of cutting-edge research on the development and application of molecular approaches for predicting plant performance. However, improvements in plant genomes, particularly in sequencing technologies, have altered the focus of plant sciences from “explanatory” to

Table 14.1 Detection of plant pathogens employs a variety of sensing methods and nanomaterials

| No | Plant disease/ pathogen | Host | NPs | Detection method | LOD | References |
|----|---|--------------------------|--|---|--------------------------------------|-------------------------------------|
| 1 | Tomato yellow leaf curl virus (TYLCV) | Tomato | AuNPs with colorimetric nano- biosensing | Localized surface plasmon resonance | 5 ng | Razmi et al. (2019) |
| 2 | Cucumber mosaic virus (CMV) and papaya ring spot virus (PRSV) | Papaya | Nanowire- based biosensor | Amperometry detection | 0.1 mA/mL | Ariffin et al. (2013) |
| 3 | Witches' broom disease (<i>Candidatus Phytoplasma aurantifolia</i>) | Lime | Quantum dot (QD)-based nanobio sensor | Fluorescence resonance energy transfer (FRET) | 5 ca. P. aurantifolia/ μ L | Rad et al. (2012) |
| 4 | Odontoglossum ringspot virus (ORSV) | Orchid leaves | Anodic aluminum oxide (AAO) with AuNPs | Self-assembled monolayer (SAM) | 0.345 ng/mL | Jian et al. (2018) |
| 5 | Bacterial spot disease by <i>Xanthomonas axonopodis</i> | Solanaceae plant | Fluores- cence silica NPs | Fluorescence- linked immunosorbent assay | NA | Yao et al. (2009) |
| 6 | <i>Ralstonia solanacearum</i> (potato brown rot) | Potato | Enlarging AuNPs | Lateral flow immunoassay | 3×10^4 cells/ mL | Razo et al. (2019) |
| 7 | Karnal bunt disease | Wheat | AuNPs | Surface plasmon resonance (SPR) | NA | Singh et al. (2010) |
| 8 | Powdery mildew | Rose | Colloidal nanosilver (1.5 nm diameter) | Relative fluorescence units | 4.2 μ M ag ions | Choi et al. (2008) |
| 9 | <i>Pseudocercospora fijiensis</i> black Sigatoka (leaf streak disease) | Banana plants | Cell wall protein HF1 of <i>P. Fijiensis</i> immobilized onto gold chip | Surface plasmon resonance- based immunosensor | 11.7 μ g/mL | Luna- Moreno et al. (2019) |
| 10 | Late blight in potatoes and tomatoes (caused by <i>Phytophthora infestans</i>) | Potatoes and tomatoes | AuNPs | PCR with AuNPs-based lateral flow biosensor | 0.1 pg/mL range. | Zhan et al. (2018) |

(continued)

Table 14.1 (continued)

| No | Plant disease/ pathogen | Host | NPs | Detection method | LOD | References |
|-----|---|-----------|---|---|--|-------------------------------|
| 11. | <i>Acidovorax avenae subsp. citrulli</i> | Fruits | AuNPs | Dipstick method | 0.48 nM of DNA | Zhao et al. (2011) |
| 12. | <i>Cymbidium mosaic virus (CymMV)</i> or <i>Odontoglossum ringspot virus (ORSV)</i> | Orchids | Gold nanorods | Optic particle plasmon resonance (FOPPR) immunosensor | 48 and 42 pg/mL for CymMV and ORSV, respectively | Lin et al. (2014) |
| 13. | Tomato ringspot virus (ToRSV), bean pod mottle virus (BPMV), and arabis mosaic virus (ArMV) | Tomato | Fe ₃ O ₄ /SiO ₂ | Nanoparticle- based immunosensor | 10 ⁻⁴ mg/mL | Zhang et al. (2013) |
| 14. | <i>Ganoderma boninense</i> | Oil palms | Multiwalled carbon nanotube | Electro- chemical sensor | 0.0414 mg/L | Isha et al. (2019) |
| 15. | <i>Phytophthora cactorum</i> | Fruits | TiO ₂ or SnO ₂ NPs on screen- printed carbon (SP) electrodes | Electro- chemical nanosensor | 35–62 nM | Fang et al. (2014) |
| 16. | <i>Pseudomonas syringae</i> | Potato | Colloidal AuNPs | Electro- chemical biosensor | 214 pM | Lau et al. (2017) |
| 17. | Aflatoxin B1 | Cereals | AuNPs | SPR nanosensor | 1.04 pg mL ⁻¹ | Akgönüllü et al. (2020) |

“predictive” during the previous decade. The majority of plant genomics research has so far focused on deciphering the genetic aspects of biological processes or phenotypic features. However, in terms of plant breeding, the major focus is on forecasting ideal genotypes based on molecular data for more time and cost-effective breeding schemes. We have included chapters by prominent scholars in their fields on all aspects of the development and implementation of predictive molecular techniques in plant breeding in this book. For example, for event-specific detection of the transgenic maize MIR162, an electrochemical DNA biosensor based on nitrogen-dropped graphene nanosheets and gold nanoparticle nanocomposites was created (Liu et al. 2020). This biosensor has a high level of manufacturing repeatability, selectivity, and stability. Methylene blue differential pulse voltammetry was the response they used to monitor the target DNA hybridization event. The peak current rose linearly with the logarithm of the DNA concentration under ideal circumstances. The biosensor was successfully used to identify MIR162 in actual samples, revealing its potential as a useful and efficient tool for transgenic crop analysis.

14.6 Challenges

The common issues with existing diagnostic methods, such as time requirement, lower accuracy, and cost intensiveness on a wider scale, enable for new low-cost approaches to enhance the precision and speed of plant pathogen identification. The accuracy of detection is influenced by parameters such as sampling technique, sample size, sample length, prevailing weather, background noise, crop stage, and so on, just as it is with any alternative plant pathogen detection approach. Categorizing plants based on their morphological features is a tough problem in machine vision-based diagnostics, especially through eye inspection (Prabha 2021). As a result, distinguishing unhealthy plants from symptomless ones is a difficult undertaking. The inherent difficulty is attributed to the nonspecificity of various symptoms that may be present. Furthermore, the degree of changes caused in various morphological parameters by biotic or abiotic stress may be relatively minimal in comparison to the diversity of appearance in healthy plants, particularly during the early stage of infection.

Nano-based plant diagnostic technologies have few inherent limitations (Konwarh & Sharma 2021). The first problem is the environmental effect and toxicity of manmade nanomaterials. Before any nanosensors can be marketed and used in the field, their safety problems must be addressed, since certain nanoparticles, such as QDs, may be poisonous. More rigorous toxicity testing and regulation are required for nanosensors that will be placed on living plants or consumable agricultural and food items, since dangerous nanomaterial residuals might possibly infiltrate the food chain and be consumed by end users. The second issue is the speed with which data is shared and disease forecasting is done, because the most important aspect of disease diagnosis is the timely reporting and forecasting of infection events on site. The new generation of nanosensors is expected to be connected through wireless system and capable of providing near real-time measurements. Continuous monitoring of plant VOC emissions, for example, is projected to give more time dynamic information than single-point observations, allowing for more accurate plant stress monitoring. In this context, the recent development of field-portable sensor equipment like as smartphone devices or plant wearables opens exciting new possibilities for in-field pathogen research by sharing and transferring data nearly in real-time. Sensor downsizing, wireless data transmission, and integration with computational data processing pipelines such as machine learning and artificial intelligence (AI) will be among the essential topics to be tackled further in order to provide continuous measurement. Third, long-term sensor stability in adverse conditions such as severe cold or heat, prolonged sun exposure, and excessive use must be established. Before any sensors can be deployed in the actual field, more durable and robust sensors that can endure a variety of environmental conditions (e.g., temperature, humidity, air pollution, etc.) are expected. More basic research on innovative sensor materials, such as environmental-resistant substrates and nanoparticles, is required. As an example, for long-term monitoring of field crops and sentinel plants such as wheat or corn, a volatile sensor array made of more

durable materials, such as paper or polymer substrate and photoresistive dyes, will be needed. The sensor signals could be read out wirelessly or scanned by mobile phone readers. Remote and continuous monitoring of biomarkers from symptomless field plants has enormous potential for detecting early infections on a broad scale. Finally, there are some limitations to DNA-based biosensors, including the difficulty of extracting nucleic acids that are prone to deterioration and contamination and are difficult to amplify (Qian et al. 2019). This method has the danger of producing negative or false positive findings and is incapable of distinguishing between dead and live diseases or toxins. Furthermore, enzyme and piezoelectric DNA-based biosensors are extremely sensitive to pH fluctuations in the environment (Batchelor-McAuley et al. 2009). Furthermore, the application of robotic systems for agricultural disease diagnosis is still in its infancy.

According to current understanding, the six primary difficulties with robotic disease detection are as follows:

1. A lack of a database of images for each illness detection/classification model.
2. **Inconsistent field illumination conditions.**
3. Image processing will be sluggish, particularly if a big number of photographs are being processed. B. Hyperspectral imaging can be employed.
4. **the effectiveness of image-based diagnostics is determined by the morphology of the plant architecture, leaf forms, canopy type, and density.**
5. Pathologists' information technology abilities and data engineers' or AI engineers' biological skills are limited. This may be remedied via correct interactions as well as integrated trainings and workshops that benefit both parties by providing them with the fundamental principles of both areas.
6. The most serious difficulty with computer vision technology is that the development of symptoms to the point of detection occurs only after the infection has been established. In such circumstances, delayed identification complicates care.

The paucity of available picture datasets is gradually being addressed as open-access agricultural databases become more accessible and novel techniques of data synthesis have been introduced (Barth et al. 2018). Lighting systems for detecting diseases like as powdery mildew are also being developed at the same time (Mahmud et al. 2019). Future vision systems might detect insects by combining many ultrahigh-definition cameras to detect insects hidden within the leaves, under the plant, or elsewhere on the plant. Even in this scenario, given the large volume and size of photos, an insect identification robot needs to integrate high-performance algorithms in order to function properly (Fountas et al. 2020).

At the broad scale, new surveillance approaches employing monitoring networks (Hartmann et al. 2018) can address all the issues, while at the small scale, new detection and diagnostic technologies enabled by novel sequencing methodologies like nanopores can address the rest. The development of technologies and methodologies that allow the quick identification of disease outbreaks, particularly those associated with new or emerging plant pathogens, as well as the precise diagnosis of the causative agents, will be a major issue in the coming decades. When compared to other fields of production, however, there are still hurdles in making novel techniques accessible on a broad scale.

14.7 Future Trends

Advances in pathogen detection approaches, such as nano-based and robotic methods, depend on a more complicated vision concept. Nanoparticle-based biosensors are being used in a variety of clinical, ecological, and quality-measured applications throughout the globe to improve the quality of life and its components. The use of numerous nanomaterials in the form of nanoparticles, nanotubes, nanorods, and nanowires, such as metal based, carbon allotropes, polymers, composites, and so on, has opened up the possibility of much quicker detection and reproducibility of plant diseases. Nano-based biosensors have previously shown to be critical for diagnosing a variety of health, conservation, and food quality features; nevertheless, plant biosensor data are few. A combination of sensing and robotics technologies could result in new "lab-on-a-drone" analysis platforms, allowing rapid in-flight assays with smartphone connectivity, eliminating sample collection and analysis waste, and enabling emergency response, agricultural bio-surveillance, and veterinary field care scenarios (Buja et al. 2021). Machine learning with sensors, drones, robotics, and intelligent monitoring systems is expected to change the future of farming in plant pathology research and field trials.

14.8 Conclusions

Precision farming is achievable because of the combination of careful monitoring of environmental factors and the use of guided activity. Computers, global satellite positioning systems, nanosensors, and remote sensing tactics are all used in this sort of agricultural system. The use of nanotechnology and artificial intelligence in plant disease diagnosis and management is still in its infancy. Diagnostic molecular methods and technologies that improve the detection speed of plant diseases have become one of the most important approaches considering today's fast-paced lifestyle. This chapter discusses the use of nanomaterials and artificial intelligence (AI) in novel biosensing technologies and plant disease detection, as well as how these technologies have changed the area of plant disease diagnostics utilizing newly designed devices. The potential for translating novel nanoparticle-based biosensor techniques originally developed for human or animal disease diagnostics to early detection of plant disease-causing pathogens is enormous. Nanoscale element devices, such as DNA nanodevices and nanosensors, are designed to recognize a specific chemical, biological component, or environmental condition. These sensors are very specialized, precise tracking, convenient, and cost-effective and detect at a much lower level than their macroscale counterparts. Nanomaterials also provide previously unattainable capabilities like as label-free transduction and highly scalable multiplexing in macroscale systems. Furthermore, the integration of nanomaterials with lab-on-a-chip technologies enables very sensitive detection in more automated and portable forms. Thus, metal nanoparticles are extensively used as a diagnostic tool for plant infections and have largely supplanted the enzyme tagging approach in the

identification of many plant diseases. Furthermore, the integration of nanomaterials with lab-on-a-chip technologies enables very sensitive detection in more automated and portable forms. Thus, metal nanoparticles are extensively used as a diagnostic tool for plant infections and have largely supplanted the enzyme tagging approach in the identification of many plant diseases. The recently created CRISPR-Cas system applications and methodologies encourage the creation of a wide range of diagnostic and detection solutions and have tremendous promise in medical diagnostics, environmental monitoring, and agri-food pathogens. For certain disorders, diagnostic specificity may match traditional diagnostic techniques, but not for all or at all phases of disease progression. Based on the application and plant protection needs, the inherent limits of image processing methods and technologies for plant disease diagnosis must be identified. Phytopathology will be strengthened even more by the integration of digital and computational technology. In plant pathology, AI and machine learning are still in their infancy, but, in the not-too-distant future, artificial intelligence will push plant pathology from a qualitative to a quantitative discipline on all fronts, not only epidemiology. Through the use of diagnostics and management tactics, deep learning and robots will allow automation and high productivity. Through prompt on-field diagnostics and automated metered administration of plant protection chemicals, AI and machine learning may increase accuracy, resulting in precision plant protection. However, the abovementioned new developing technologies for diseases diagnostics are still in their early stages of research, and the availability of standardized applications is unpredictable. Multiplexing will be a focus of future research to improve these nanobiosensors and robots, allowing for simultaneous monitoring and detection of several plant pathogens.

References

- Agrios G. Plant pathology. 5th ed. Burlington: Elsevier Academic Press; 2005.
- Akgönüllü S, Yavuz H, Denizli A. SPR nanosensor based on molecularly imprinted polymer film with gold nanoparticles for sensitive detection of aflatoxin B1. *Talanta*. 2020;219(121219):121219.
- Alon DM, Hak H, Bornstein M, Pines G, Spiegelman Z. Differential detection of the tobamoviruses tomato mosaic virus (ToMV) and tomato brown rugose fruit virus (ToBRFV) using CRISPR-Cas12a. *Plan Theory*. 2021;10(6):1256.
- Al-Saddik H, Laybros A, Billiot B, Cointault F. Using image texture and spectral reflectance analysis to detect yellowness and Esca in grapevines at leaf-level. *Remote Sens*. 2018;10(4):618.
- Ali Q, Ahmar S, Sohail AM, Kamran M, Ali M, Saleem MH, Rizwan M, Ahmed AM, Mora-Poblete F, Amaral Júnior AT, Mubeen M, Ali S. Research advances and applications of biosensing technology for the diagnosis of pathogens in sustainable agriculture. *Environmental Science and Pollution Research*. 2021;28(8):9002-9019. <https://doi.org/10.1007/s11356-021-12419-6>
- Aman R, Mahas A, Marsic T, Hassan N, Mahfouz MM. Efficient, rapid, and sensitive detection of plant RNA viruses with one-pot RT-RPA-CRISPR/Cas12a assay. *Front Microbiol*. 2020;11:610872.
- Ampatzidis, Y., De Bellis, L., & Luvisi, A. (2017). iPathology: Robotic applications and management of plants and plant diseases. *Sustainability*, 9(6), 1010-10.3390/su9061010
- Ariffin SAB, Adam T, Hashim U, Faridah Sfaridah S, Zamri I, Uda MNA. Plant diseases detection using nanowire as biosensor transducer. *Adv Mater Res*. 2013;832:113-7.

- Awad YM, Abdullah AA, Bayoumi TY, Abd-Elsalam K, Hassanien AE. 2015. Early detection of powdery mildew disease in wheat (*Triticum aestivum* L.) using thermal imaging technique. In: Advances in intelligent systems and computing. Cham: Springer 755–765.
- Awaludin N, Abdullah J, Salam F, Ramachandran K, Yusof NA, Wasoh H. Fluorescence-based immunoassay for the detection of *Xanthomonas oryzae* pv. *oryzae* in rice leaf. Anal Biochem. 2020;610(113876):113876.
- Balasubramanian K, Burghard M. Biosensors based on carbon nanotubes. Anal Bioanal Chem. 2006;385(3):452–68.
- Balodi R, Bisht S, Ghatak A, Rao KH. Plant disease diagnosis: technological advancements and challenges. Indian Phytopathol. 2017;70(3):275.
- Barth R, IJsselmuiden J, Hemming J, Van Henten EJ. Data synthesis methods for semantic segmentation in agriculture: a capsicum annum dataset. Comput Electron Agric. 2018;144:284–96.
- Batchelor-McAuley C, Wildgoose GG, Compton RG. The physicochemical aspects of DNA sensing using electrochemical methods. Biosens Bioelectron. 2009;24(11):3183–90.
- Berensmeier S. Magnetic particles for the separation and purification of nucleic acids. Appl Microbiol Biotechnol. 2006;73(3):495–504.
- Bock CH, Parker PE, Cook AZ, Gottwald TR. Visual rating and the use of image analysis for assessing different symptoms of citrus canker on grapefruit leaves. Plant Dis. 2008;92(4):530–41.
- Bogue R. Robots poised to revolutionise agriculture. Ind Rob. 2016;43(5):450–6.
- Brás EJS, Fortes AM, Esteves T, Chu V, Fernandes P, Conde JP. Microfluidic device for multiplexed detection of fungal infection biomarkers in grape cultivars. Analyst. 2021;145(24):7973–84.
- Bronzato Badial A, Sherman A, Stone A, Gopakumar A, Wilson V, Schneider W, King J. Nanopore sequencing as a surveillance tool for plant pathogens in plant and insect tissues. Plant Dis. 2018;102(8):1648–52.
- Buja I, Sabella E, Monteduro AG, Chiriaco MS, De Bellis L, Luvisi A, Maruccio G. Advances in plant disease detection and monitoring: from traditional assays to in-field diagnostics. Sensors (Basel). 2021;21(6):2129.
- Cebula Z, Żołędowska S, Dziąbowska K, Skwarecka M, Malinowska N, Białobrzaska W, Czaczyk E, Siuzdak K, Sawczak M, Bogdanowicz R, et al. Detection of the plant pathogen *Pseudomonas syringae* pv. *lachrymans* on antibody-modified gold electrodes by electrochemical impedance spectroscopy. Sensors (Basel). 2019;19(24):5411.
- Chalupowicz L, Dombrovsky A, Gaba V, Luria N, Reuven M, Beerman A, Lachman O, Dror O, Nissan G, Manulis-Sasson S. Diagnosis of plant diseases using the nanopore sequencing platform. Plant Pathol. 2019;68(2):229–38.
- Chang W, Liu W, Ying L, Zhan F, Chen H, Lei H, Yingju L. Colorimetric detection of nucleic acid sequences in plant pathogens based on CRISPR/Cas9 triggered signal amplification. Mikrochim Acta. 2019;186(4):243.
- Chen L, Zhang J. Biosens Bioelectron. 2012;S11:1–5.
- Chen Y, Qian C, Liu C, Shen H, Wang Z, Ping J, Wu J, Chen H. Nucleic acid amplification free biosensors for pathogen detection. Biosens Bioelectron. 2020;153(112049):112049.
- Chiriaco MS, Luvisi A, Primiceri E, Sabella E, De Bellis L, Maruccio G. Development of a lab-on-a-chip method for rapid assay of *Xylella fastidiosa* subsp *pauca* strain CoDiRO. Sci Rep. 2018;8(1):7376.
- Choi O, Deng KK, Kim N-J, Ross L Jr, Surampalli RY, Hu Z. The inhibitory effects of silver nanoparticles, silver ions, and silver chloride colloids on microbial growth. Water Res. 2008;42(12):3066–74.
- Crandall SG, Gold KM, Jiménez-Gasco MDM, Filgueiras CC, Willett DS. A multi-omics approach to solving problems in plant disease ecology. PLoS One. 2020;15(9):e0237975.
- Cruz AC, Ampatzidis Y, De Bellis L, Luvisi A. Vision-based plant disease detection system using transfer and deep learning. In: Proceedings of the ASABE 2017, Annual International Meeting. Spokane, WA, USA. 2017; p. 16–19.
- Deng X, Lan Y, Hong T, Chen J. Citrus greening detection using visible spectrum imaging and C-SVC. Comput Electron Agric. 2016;130:177–83.

- Deurenberg RH, Bathoorn E, Chlebowicz MA, Couto N, Ferdous M, García-Cobos S, Kooistra-Smid AMD, Raangs EC, Rosema S, Veloo ACM, et al. Application of next generation sequencing in clinical microbiology and infection prevention. *J Biotechnol.* 2017;243:16–24.
- Dincer C, Bruch R, Costa-Rama E, Fernández-Abedul MT, Merkoçi A, Manz A, Urban GA, Güder F. Disposable sensors in diagnostics, food, and environmental monitoring. *Adv Mater.* 2019;31(30):e1806739.
- Dubertret B, Calame M, Libchaber AJ. Single-mismatch detection using gold-quenched fluorescent oligonucleotides. *Nat Biotechnol.* 2001;19(4):365–70.
- Dyussebayev K, Sambasivam P, Bar I, Brownlie JC, Shiddiky MJA, Ford R. Biosensor technologies for early detection and quantification of plant pathogens. *Front Chem.* 2021;9:636245.
- Dutta D, Kaushik A, Kumar D, Bag S. Foodborne Pathogenic Vibrios: Antimicrobial Resistance. *Frontiers in Microbiology.* 2021; 12638331 <https://doi.org/10.3389/fmicb.2021.638331>.
- Ebrahimi M, Norouzi P, Safarnejad MR, Tabaei O, Haji-Hashemi H. Fabrication of a label-free electrochemical immunosensor for direct detection of *Candidatus Phytoplasma Aurantifolia*. *J Electroanal Chem (Lausanne Switz).* 2019;851(113451):113451.
- Edmundson MC, Capeness M, Horsfall L. Exploring the potential of metallic nanoparticles within synthetic biology. *New Biotechnol.* 2014;31(6):572–8.
- Elmer W, White JC. The future of nanotechnology in plant pathology. *Annu Rev Phytopathol.* 2018;56(1):111–33.
- Etefagh R, Azhir E, Shahtahmasebi N. Synthesis of CuO nanoparticles and fabrication of nano-structural layer biosensors for detecting *Aspergillus niger* fungi. *Sci Iran.* 2013;20:1055–8.
- Fadiji AE, Babalola OO. Elucidating mechanisms of endophytes used in plant protection and other bioactivities with multifunctional prospects. *Front Bioeng Biotechnol.* 2020;8:467.
- Fan C, Wang S, Hong JW, Bazan GC, Plaxco KW, Heeger AJ. Beyond superquenching: hyper-efficient energy transfer from conjugated polymers to gold nanoparticles. *Proc Natl Acad Sci U S A.* 2003;100(11):6297–301.
- Fang Y, Ramasamy RP. Current and prospective methods for plant disease detection. *Biosensors (Basel).* 2015;5(3):537–61.
- Fang Y, Umasankar Y, Ramasamy RP. Electrochemical detection of p-ethylguaiacol, a fungi infected fruit volatile using metal oxide nanoparticles. *Analyst.* 2014;139(15):3804–10.
- Farooq T, Adeel M, He Z, Umar M, Shakoor N, da Silva W, Elmer W, White JC, Rui Y. Nanotechnology and plant viruses: an emerging disease management approach for resistant pathogens. *ACS Nano.* 2021;15(4):6030–7.
- Filloux D, Fernandez E, Loire E, Claude L, Galzi S, Candresse T, Winter S, Jeeva ML, Makesh Kumar T, Martin DP, et al. Nanopore-based detection and characterization of yam viruses. *Sci Rep.* 2018;8(1):17879.
- Firrao G, Moretti M, Rosquete MR, Gobbi E, Locci R. Nanobiotransducer for detecting flavescence dorée phytoplasma. *J Plant Pathol.* 2005;87:101–7.
- Fountas S, Mylonas N, Malounas I, Rodias E, Hellmann Santos C, Pekkeriet E. Agricultural robotics for field operations. *Sensors (Basel).* 2020;20(9):2672.
- Fritea L, Tertis M, Sandulescu R, Cristea C. Enzyme-graphene platforms for electrochemical biosensor design with biomedical applications. *Methods Enzymol.* 2018;609:293–333.
- Ghaiwat Savita N, Parul A. Detection and classification of plant leaf diseases using image processing techniques: a review. *Int J Recent Adv Eng Technol.* 2014;2(3):2347–812.
- Ghosh R, Nagavardhini A, Sengupta A, Sharma M. Development of Loop-Mediated Isothermal Amplification (LAMP) assay for rapid detection of *Fusarium oxysporum* f.sp. *ciceris*-wilt pathogen of chickpea. *BMC Res Notes.* 2015;8(1):1–10.
- Ghosh R, Tarafdar A, Chobe DR, Sharath Chandran US, Rani S, Sharma M. Diagnostic techniques of soil borne plant diseases: recent advances and next generation evolutionary trends. *Biol Forum-An Int J.* 2019;11(2):1–13.
- Gootenberg JS, Abudayyeh OO, Kellner MJ, Joung J, Collins JJ, Zhang F. Multiplexed and portable nucleic acid detection platform with Cas13, Cas12a, and Csm6. *Science.* 2018;360(6387):439–44.

- Gorny AM, Hay FS, Wang X, Pethybridge SJ. Isolation of nematode DNA from 100 g of soil using Fe₃O₄ super paramagnetic nanoparticles. *Nematology*. 2018;20(3):271–83.
- Hadidi A. Next-generation sequencing and CRISPR/Cas13 editing in viroid research and molecular diagnostics. *Viruses*. 2019;11(2):120.
- Halfpenny KC, Wright DW. Nanoparticle detection of respiratory infection: nanoparticle detection of respiratory infection. *Wiley Interdiscip Rev Nanomed Nanobiotechnol*. 2010;2(3):277–90.
- Handelsman J, Rondon MR, Brady SF, Clardy J, Goodman RM. Molecular biological access to the chemistry of unknown soil microbes: a new frontier for natural products. *Chem Biol*. 1998;5(10):R245–9.
- Hariharan G, Prasannath K. Recent advances in molecular diagnostics of fungal plant pathogens: a mini review. *Front Cell Infect Microbiol*. 2020;10:600234. <https://doi.org/10.3389/fcimb.2020.600234>.
- Hartmann H, Moura CF, Anderegg WRL, Ruehr NK, Salmon Y, Allen CD, Arndt SK, Breshears DD, Davi H, Galbraith D, et al. Research frontiers for improving our understanding of drought-induced tree and forest mortality. *New Phytol*. 2018;218(1):15–28.
- He P, Dai L. BioMEMS and biomedical nanotechnology; 2006. p. 171–201.
- Hu Y, Green GS, Milgate AW, Stone EA, Rathjen JP, Schwessinger B. Pathogen detection and microbiome analysis of infected wheat using a portable DNA sequencer. *Phytobiomes J*. 2019;3(2):92–101.
- Huang Y-F, Wang Y-F, Yan X-P. Amine-functionalized magnetic nanoparticles for rapid capture and removal of bacterial pathogens. *Environ Sci Technol*. 2010;44(20):7908–13.
- Huang Y, Sudibya HG, Chen P. Detecting metabolic activities of bacteria using a simple carbon nanotube device for high-throughput screening of anti-bacterial drugs. *Biosens Bioelectron*. 2011;26(10):4257–61.
- Hussain T, Isha A, Akanbi FS, Yusof NA, Osman R, Mui-Yun W, Abdullah SNA. An NMR metabolomics approach and detection of ganoderma boninense-infected oil palm leaves using MWCNT-based electrochemical sensor. *J Nanomater*. 2017;6(10):1293–9.
- Isha A, Akanbi FS, Yusof NA, Osman R, Mui-Yun W, Abdullah SNK. *Journal of Nanomaterials* 2019;1–12. <https://doi.org/10.1155/2019/4729706>.
- Jarocka U, Wasowicz M, Radecka H, Malinowski T, Michalczuk L, Radecki J. Impedimetric immunosensor for detection of plum pox virus in plant extracts. *Electroanalysis*. 2011;23(9):2197–204.
- Jian YS, Lee CH, Jan FJ, Wang GJ. Detection of *Odontoglossum* ringspot virus infected *Phalaenopsis* using a nano-structured biosensor. *J Electrochem Soc*. 2018;165(9):H449.
- Jócsák I, Végvári G, Vozáry E. Electrical impedance measurement on plants: a review with some insights to other fields. *Theor Exp Plant Physiol*. 2019;31(3):359–75.
- Joshi SM, De Britto S, Jogaiah S, Ito S-I. Mycogenic selenium nanoparticles as potential new generation broad spectrum antifungal molecules. *Biomol Ther*. 2019;9(9):419.
- Kaittanis C, Naser SA, Perez JM. One-step, nanoparticle-mediated bacterial detection with magnetic relaxation. *Nano Lett*. 2007;7(2):380–3.
- Kalia A, Abd-Elsalam KA, Kuca K. Zinc-based nanomaterials for diagnosis and management of plant diseases: ecological safety and future prospects. *J Fungi (Basel)*. 2020;6(4):222.
- Kashyap PL, Kumar S, Srivastava AK. Nanodiagnostics for plant pathogens. *Environ Chem Lett*. 2017;15(1):7–13.
- Katz E, Willner I. Probing biomolecular interactions at conductive and semiconductive surfaces by impedance spectroscopy: routes to impedimetric immunosensors, DNA-sensors, and enzyme biosensors. *Electroanalysis*. 2003;15(11):913–47.
- Khaledian S, Nikkha M, Hoseinzadeh S. A sensitive biosensor based on gold nanoparticles to detect *Ralstonia solanacearum* in soil Shams-bakhsh. *J Gen Plant Pathol*. 2017;83:231–9.
- Khan MR, Siddiqui ZA, Fang X. Potential of metal and metal oxide nanoparticles in plant disease diagnostics and management: recent advances and challenges. *Chemosphere*. 2022;297(134114):134114.

- Khater M, de la Escosura-Muñiz A, Merkoçi A. Biosensors for plant pathogen detection. *Biosens Bioelectron.* 2017;93:72–86.
- Khater M, de la Escosura-Muñiz A, Quesada-González D, Merkoçi A. Electrochemical detection of plant virus using gold nanoparticle-modified electrodes. *Anal Chim Acta.* 2019;1046:123–31.
- Khiyami MA, Almoammar H, Awad YM, Alghuthaymi MA, Abd-Elsalam KA. Plant pathogen nanodiagnostic techniques: forthcoming changes? *Biotechnol Biotechnol Equip.* 2014;28(5):775–85.
- Konwarh R, Sharma PL. Nanosensor platforms for surveillance of plant pathogens and phytometabolites/analytes vis-à-vis plant health status. In: *Nanomaterials for agriculture and forestry applications.* Elsevier; 2020. p. 357–385.
- Kulabhusan PK, Tripathi A, Kant K. Gold nanoparticles and plant pathogens: an overview and prospective for biosensing in forestry. *Sensors (Basel).* 2022;22(3):1259.
- Lander ES, Linton LM, Birren B, Nusbaum C, Zody MC, Baldwin J, Devon K, Dewar K, Doyle M, FitzHugh W, et al. Initial sequencing and analysis of the human genome. *Nature.* 2001;409(6822):860–921.
- Lattanzio VMT, Nivarlet N, Lippolis V, Della Gatta S, Huet A-C, Delahaut P, Granier B, Visconti A. Multiplex dipstick immunoassay for semi-quantitative determination of *Fusarium mycotoxins* in cereals. *Anal Chim Acta.* 2012;718:99–108.
- Lau HY, Wang Y, Wee EJH, Botella JR, Trau M. Field demonstration of a multiplexed point-of-care diagnostic platform for plant pathogens. *Anal Chem.* 2016;88(16):8074–81.
- Lau HY, Wu H, Wee EJH, Trau M, Wang Y, Botella JR. Specific and sensitive isothermal electrochemical biosensor for plant pathogen DNA detection with colloidal gold nanoparticles as probes. *Sci Rep.* 2017;7:38896.
- Lavanya R, Arun V. Detection of Begomovirus in chilli and tomato plants using functionalized gold nanoparticles. *Sci Rep.* 2021;11(1):14203.
- Lee H, Sun E, Ham D, Weissleder R. Chip-NMR biosensor for detection and molecular analysis of cells. *Nat Med.* 2008;14(8):869–74.
- Lee JI, Jang SC, Chung J, Choi W-K, Hong C, Ahn GR, Kim SH, Lee BY, Chung W-J. Colorimetric allergenic fungal spore detection using peptide-modified gold nanoparticles. *Sens Actuators B Chem.* 2021;327(128894):128894.
- Lei R, Wu P, Li L, Huang Q, Wang J, Zhang D, Li M, Chen N, Wang X. Ultrasensitive isothermal detection of a plant pathogen by using a gold nanoparticle-enhanced microcantilever sensor. *Sens Actuators B Chem.* 2021;338(129874):129874.
- Li Y, Schluesener HJ, Xu S. Gold nanoparticle-based biosensors. *Gold Bull.* 2010;43(1):29–41.
- Li Z, Paul R, Ba Tis T, Saville AC, Hansel JC, Yu T, Ristaino JB, Wei Q. Non-invasive plant disease diagnostics enabled by smartphone-based fingerprinting of leaf volatiles. *Nat Plants.* 2019;5(8):856–66.
- Li Z, Yu T, Paul R, Fan J, Yang Y, Wei Q. Agricultural nanodiagnostics for plant diseases: recent advances and challenges. *Nanoscale Adv.* 2020;2(8):3083–94.
- Lin H-Y, Huang C-H, Lu S-H, Kuo I-T, Chau L-K. Direct detection of orchid viruses using nanorod-based fiber optic particle plasmon resonance immunosensor. *Biosens Bioelectron.* 2014;51:371–8.
- Liu W-T. Nanoparticles and their biological and environmental applications. *J Biosci Bioeng.* 2006;102(1):1–7.
- Liu F, Li K, Zhang Y, Ding J, Wen T, Pei X, Yan Y, Ji W, Liu J, Zhang X, Li L. An electrochemical DNA biosensor based on nitrogen-doped graphene nanosheets decorated with gold nanoparticles for genetically modified maize detection. *Microchimica Acta.* 2020;187:574.
- Luna-Moreno D, Sánchez-Álvarez A, Islas-Flores I, Canto-Canche B, Carrillo-Pech M, Villarreal-Chiu JF, Rodríguez-Delgado M. Early detection of the fungal banana black Sigatoka pathogen *Pseudocercospora fijiensis* by an SPR immunosensor method. *Sensors (Basel).* 2019;19(3):465.
- Luo M, Meng F-Z, Tan Q, Yin W-X, Luo C-X. Recombinase polymerase amplification/Cas12a-based identification of *Xanthomonas arboricola* pv. *pruni* on Peach. *Front Plant Sci.* 2021;12:740177.

- Lopez MM, Llop P, Olmos A, Marco-Noales E, Cambra M, Bertolini E. Are molecular tools solving the challenges posed by detection of plant pathogenic bacteria and viruses? *Curr Issues Mol Biol*. 2009;11:13–46.
- Maalouf R, Hassen WM, Fournier-Wirth C, Coste J, Jaffrezic-Renault N. Comparison of two innovative approaches for bacterial detection: paramagnetic nanoparticles and self-assembled multilayer processes. *Mikrochim Acta*. 2008;163(3–4):157–61.
- Mahas A, Hassan N, Aman R, Marsic T, Wang Q, Ali Z, Mahfouz MM. LAMP-coupled CRISPR-Cas12a module for rapid and sensitive detection of plant DNA viruses. *Viruses*. 2021;13(3):466.
- Mahlein AK. Plant disease detection by imaging sensors—parallels and specific demands for precision agriculture and plant phenotyping. *Plant Dis*. 2016;100:241–54.
- Mahmud MS, Zaman QU, Esau TJ, Price GW, Prithviraj B. Development of an artificial cloud lighting condition system using machine vision for strawberry powdery mildew disease detection. *Comput Electron Agric*. 2019;158:219–25.
- Majumder S, Johari S. Development of a gold-nano particle based novel dot immunobinding assay for rapid and sensitive detection of Banana bunchy top virus. *J Virol Methods*. 2018;255:23–8.
- Mansfield S, McNeill MR, Aalders LT, Bell NL, Kean JM, Barratt BIP, Boyd-Wilson K, Teulon DAJ. The value of sentinel plants for risk assessment and surveillance to support biosecurity. *NeoBiota*. 2019;48:1–24.
- Marcolungo L, Passera A, Maestri S, Segala E, Alfano M, Gaffuri F, Marturano G, Casati P, Bianco PA, Delledonne M. Real-time on-site diagnosis of quarantine pathogens in plant tissues by nanopore-based sequencing. *Pathogens*. 2022;11(2):199.
- Martinelli F, Scalenghe R, Davino S, Panno S, Scuderi G, Ruisi P, Villa P, Stroppiana D, Boschetti M, Goulart LR, et al. Advanced methods of plant disease detection. A review. *Agron Sustain Dev*. 2015;35(1):1–25.
- Menendez-Aponte P, Garcia C, Freese D, Deferli S, Xu Y. Software and hardware architectures in cooperative aerial and ground robots for agricultural disease detection. In: 2016 International conference on collaboration technologies and systems (CTS). IEEE. 2016.
- Myhrvold C, Freije CA, Gootenberg JS, Abudayyeh OO, Metsky HC, Durbin AF, Kellner MJ, Tan AL, Paul LM, Parham LA, et al. Field-deployable viral diagnostics using CRISPR-Cas13. *Science*. 2018;360(6387):444–8.
- Nezhad AS. Future of portable devices for plant pathogen diagnosis. *Lab Chip*. 2014;14(16):2887–904. <https://doi.org/10.1039/c4lc00487f>.
- Pandey P, Pandey NS, Shamim M, Srivastava D, Dwivedi DK, Awasthi LP, Singh KN. Molecular tools and techniques for detection and diagnosis of plant pathogens. In: *Recent advances in the diagnosis and management of plant diseases*. New Delhi: Springer; 2015. p. 253–271.
- Pilli SK, Nallathambi B, George SJ, Diwanji V. eAGROBOT-A robot for early crop disease detection using image processing. In: 2015 2nd International Conference on Electronics and Communication Systems (ICECS). IEEE, 2015; p. 1684–9.
- Pimentel D. Invasive plants: their role in species extinctions and economic losses to agriculture in the USA. In: *Management of invasive weeds*. Dordrecht: Springer; 2008. 1–7.
- Pourreza A, Lee WS, Etxeberria E, Zhang Y. Identification of citrus Huanglongbing disease at the pre-symptomatic stage using polarized imaging technique. *IFAC-PapersOnLine*. 2016;49(16):110–5.
- Prabha K. Disease sniffing robots to apps fixing plant diseases: applications of artificial intelligence in plant pathology—a mini review. *Indian Phytopathol*. 2021;74(1):13–20. <https://doi.org/10.1007/s42360-020-00290-3>.
- Qian C, Wang R, Wu H, Zhang F, Wu J, Wang L. Uracil-mediated new photospacer-adjacent motif of Cas12a to realize visualized DNA detection at the single-copy level free from contamination. *Anal Chem*. 2019;91(17):11362–6.
- Rad F, Mohsenifar A, Tabatabaei M, Safarnejad MR, Shahryari F, Safarpour H, Foroutan A, Mardi M, Davoudi D, Fotokian M. Detection of *Candidatus Phytoplasma aurantifolia* with a quantum dots fret-based biosensor. *J Plant Pathol*. 2012;94:525–534.
- Rani A, Donovan N, Mantri N. Review: the future of plant pathogen diagnostics in a nursery production system. *Biosens Bioelectron*. 2019;111631:111631.

- Razmi A, Golestanipour A, Nikkhah M, Bagheri A, Shamsbakhsh M, Malekzadeh-Shafaroudi S. Localized surface plasmon resonance biosensing of tomato yellow leaf curl virus. *J Virol Methods*. 2019;267:1–7.
- Razo SC, Panferova NA, Panferov VG, Safenkova IV, Drenova NV, Varitsev YA, Zherdev AV, Pakina EN, Dzantiev BB. Enlargement of gold nanoparticles for sensitive immunochromatographic diagnostics of potato brown rot. *Sensors (Basel)*. 2019;19(1):153.
- Rey B, Aleixos N, Cubero S, Blasco J. Xf-rovim. A field robot to detect olive trees infected by *Xylella fastidiosa* using proximal sensing. *Remote Sens (Basel)*. 2019;11(3):221.
- Rizk H, Habib MK. 2018. Robotized early plant health monitoring system. In: *IECON 2018 – 44th annual conference of the IEEE industrial electronics society*. IEEE.
- Roper JM, Garcia JF, Tsutsui H. Emerging technologies for monitoring plant health in vivo. *ACS Omega*. 2021;6(8):5101–7.
- Sabah B, Navdeep S. Remote area plant disease detection using image processing. *IOSR J Electron Commun Eng*. 2012;2(6):31–4.
- Sadani K, Nag P, Mukherji S. LSPR based optical fiber sensor with chitosan capped gold nanoparticles on BSA for trace detection of Hg (II) in water, soil and food samples. *Biosens Bioelectron*. 2019;134:90–6.
- Schofield DA, Bull CT, Rubio I, Wechter WP, Westwater C, Molineux IJ. “Light-tagged” bacteriophage as a diagnostic tool for the detection of phytopathogens. *Bioengineered*. 2013;4(1):50–4.
- Schor N, Bechar A, Ignat T, Dombrovsky A, Elad Y, Berman S. Robotic disease detection in greenhouses: combined detection of powdery mildew and tomato spotted wilt virus. *IEEE Robot Autom Lett*. 2016;1(1):354–60.
- Shao H, Min C, Issadore D, Liang M, Yoon T-J, Weissleder R, Lee H. Magnetic nanoparticles and microNMR for diagnostic applications. *Theranostics*. 2012;2(1):55–65.
- Shin K, Kwon S-H, Lee S-C, Moon Y-E. Sensitive and rapid detection of citrus scab using an RPA-CRISPR/Cas12a system combined with a lateral flow assay. *Plan Theory*. 2021;10(10):2132.
- Shoala T. Nanodiagnostic techniques in plant pathology. In: *Nanotechnology in the life sciences*. Cham: Springer; 2019. p. 209–222.
- Shoala T. Carbon nanostructures: detection, controlling plant diseases and mycotoxins. In: *Carbon nanomaterials for agri-food and environmental applications*. Elsevier; 2020, p. 261–277.
- Siddiquee S, Rovina K, Yusof NA, Rodrigues KF, Suryani S. Nanoparticle-enhanced electrochemical biosensor with DNA immobilization and hybridization of *Trichoderma harzianum* gene. *Sens BioSensing Res*. 2014;2:16–22.
- Singh V, Misra AK. Detection of plant leaf diseases using image segmentation and soft computing techniques. *Inf Process Agric*. 2017;4(1):41–9.
- Singh S, Singh M, Agrawal VV, Kumar A. An attempt to develop surface plasmon resonance based immunosensor for Karnal bunt (*Tilletia indica*) diagnosis based on the experience of nano-gold based lateral flow immuno-dipstick test. *Thin Solid Films*. 2010;519(3):1156–9.
- Singh A, Poshtibtiban S, Evoy S. Recent advances in bacteriophage-based biosensors for food-borne pathogen detection. *Sensors (Basel)*. 2013;13(2):1763–86.
- Stanisavljevic M, Krizkova S, Vaculovicova M, Kizek R, Adam V. Quantum dots-fluorescence resonance energy transfer-based nanosensors and their application. *Biosens Bioelectron*. 2015;74:562–74.
- Syed MA, Bokhari SHA. Gold nanoparticle based microbial detection and identification. *J Biomed Nanotechnol*. 2011;7(2):229–37.
- Tahir MA, Hameed S, Munawar A, Amin I, Mansoor S, Khan WS, Bajwa SZ. Investigating the potential of multiwalled carbon nanotubes-based zinc nanocomposite as a recognition interface towards plant pathogen detection. *J Virol Methods*. 2017;249:130–6.
- Tarasov A, Vilella AJ, Cuppen E, Nijman IJ, Prins P, Sambamba: fast processing of NGS alignment formats. *Bioinformatics*. 2015;31(12):2032–4.
- Thaxton CS, Georganopoulou DG, Mirkin CA. Gold nanoparticle probes for the detection of nucleic acid targets. *Clin Chim Acta*. 2006;363(1–2):120–6.

- Tripathi L, Ntui VO, Tripathi JN, Kumar PL. Application of CRISPR/Cas for diagnosis and management of viral diseases of banana. *Front Microbiol.* 2020;11:609784.
- Vaseghi A, Safaie N, Bakhshinejad B, Mohsenifar A, Sadeghizadeh M. Detection of *Pseudomonas syringae* pathogens by thiol-linked DNA–Gold nanoparticle probes. *Sens Actuators B Chem.* 2013;181:644–51.
- Verosloff M, Chappell J, Perry KL, Thompson JR, Lucks JB. PLANT-dx: a molecular diagnostic for point-of-use detection of plant pathogens. *ACS Synth Biol.* 2019;8(4):902–5.
- Villamizar RA, Maroto A, Rius FX, Inza I, Figueras MJ. Fast detection of *Salmonella Infantis* with carbon nanotube field effect transistors. *Biosens Bioelectron.* 2008;24(2):279–83.
- Weissenbach J. The rise of genomics. *C R Biol.* 2016;339(7–8):231–9.
- Wheatley MS, Yang Y. Versatile applications of the CRISPR/Cas toolkit in plant pathology and disease management. *Phytopathology.* 2021;111(7):1080–90.
- Wu J, Mukama O, Wu W, Li Z, Habimana JDD, Zhang Y, Zeng R, Nie C, Zeng L. A CRISPR/Cas12a based universal lateral flow biosensor for the sensitive and specific detection of African swine-fever viruses in whole blood. *Biosensors (Basel).* 2020;10(12):203.
- Wu H, Chen Y, Yang Q, Peng C, Wang X, Zhang M, Qian S, Xu J, Wu J. A reversible valve-assisted chip coupling with integrated sample treatment and CRISPR/Cas12a for visual detection of *Vibrio parahaemolyticus*. *Biosens Bioelectron.* 2021;188(113352):113352.
- Xu R, Adam L, Chapados J, Soliman A, Daayf F, Tambong JT. MinION Nanopore-based detection of *Clavibacter nebraskensis*, the corn Goss's wilt pathogen, and bacteriomic profiling of necrotic lesions of naturally-infected leaf samples. *PLoS One.* 2021;16(1):e0245333.
- Yao KS, Li SJ, Tzeng KC, Cheng TC, Chang CY, Chiu CY, Liao CY, Hsu JJ, Lin ZP. Fluorescence silica nanoprobe as a biomarker for rapid detection of plant pathogens. *Adv Mater Res.* 2009;79–82:513–6.
- Younas A, Yousaf Z, Rashid M, Riaz N, Fiaz S, Aftab A, Haung S. Nanotechnology and plant disease diagnosis and management. In: *Nanoagronomy.* Cham: Springer; 2020. p. 101–123.
- Yu X. Peroxidase activity of enzymes bound to the ends of single-wall carbon nanotube forest electrodes. *Electrochem Commun.* 2003;5(5):408–11.
- Zhan F, Wang T, Iradukunda L, Zhan J. A gold nanoparticle-based lateral flow biosensor for sensitive visual detection of the potato late blight pathogen, *Phytophthora infestans*. *Anal Chim Acta.* 2018;1036:153–61.
- Zhang Y-B, Kanungo M, Ho AJ, Freimuth P, van der Lelie D, Chen M, Khamis SM, Datta SS, Johnson ATC, Misewich JA, et al. Functionalized carbon nanotubes for detecting viral proteins. *Nano Lett.* 2007;7(10):3086–91.
- Zhang M, Chen W, Chen X, Zhang Y, Lin X, Wu Z, Li M. Multiplex immunoassays of plant viruses based on functionalized upconversion nanoparticles coupled with immunomagnetic separation. *J Nanomater.* 2013;2013:1–8.
- Zhang Y, Malzahn AA, Sretenovic S, Qi Y. The emerging and uncultivated potential of CRISPR technology in plant science. *Nat Plants.* 2019;5(8):778–94.
- Zhang Y-M, Zhang Y, Xie K. Evaluation of CRISPR/Cas12a-based DNA detection for fast pathogen diagnosis and GMO test in rice. *Mol Breed.* 2020;40(1):11.
- Zhao M-X, Zeng E-Z. Application of functional quantum dot nanoparticles as fluorescence probes in cell labeling and tumor diagnostic imaging. *Nanoscale Res Lett.* 2015;10(1):171.
- Zhao W, Lu J, Ma W, Xu C, Kuang H, Zhu S. Rapid on-site detection of *Acidovorax avenae* subsp. *citrulli* by gold-labeled DNA strip sensor. *Biosens Bioelectron.* 2011;26(10):4241–4.
- Zhao Y, Liu L, Kong D, Kuang H, Wang L, Xu C. Dual amplified electrochemical immunosensor for highly sensitive detection of *Pantoea stewartii* subsp. *stewartii*. *ACS Appl Mater Interfaces.* 2014;6(23):21178–83.
- Zhou W, Hu L, Ying L, Zhao Z, Chu PK, Yu X-F. A CRISPR-Cas9-triggered strand displacement amplification method for ultrasensitive DNA detection. *Nat Commun.* 2018;9(1):5012.

Chapter 15

Nanodiagnostic Tools for Mycotoxins Detection



Velaphi C. Thipe, Giovanna de Oliveira Asenjo Mendes, Victoria M. Alves, Thayna Souza, Rachel Fanelwa Ajayi, Ademar B. Lugao, and Kattesh V. Katti

Abbreviations

| | |
|-------|---|
| AFs | aflatoxins |
| AuNPs | gold nanoparticles |
| DON | deoxynivalenol |
| FMs | fumonisin |
| FPIAs | fluorescence polarization immunoassays |
| LFIA | lateral flow immunoassays |
| LOD | limit of detection |
| LSPR | localized surface plasmon resonance |
| mICA | multiplex immunochromatographic assay |
| OTs | ochratoxins |
| POCT | point-of-care testing |
| QB | QD nanobeads |
| QDs | quantum dots |
| SERS | surface-enhanced Raman spectroscopy |
| T-2 | trichothecenes |
| TRFMs | time-resolved fluorescence microspheres |
| ZEA | zearalenone |

V. C. Thipe (✉) · K. V. Katti

Department of Radiology, Institute of Green Nanotechnology, University of Missouri, Columbia, MO, USA

G. de Oliveira Asenjo Mendes · V. M. Alves · T. Souza · A. B. Lugao
Nuclear and Energy Research Institute (IPEN), IPEN-CNEN/SP, São Paulo, Brazil

R. F. Ajayi
SensorLab, Chemistry Department, University of the Western Cape, Cape Town, South Africa

15.1 Introduction

Mycotoxigenic fungi have received special attention due to their threat to food safety and toxicological profiles to human and animal health. Mycotoxins are secondary metabolic products of toxigenic fungi, secreted in food and feed (Rai et al. 2015). They have a great capacity to cause damage to cells, through the activation a cascade of variety of signaling pathways (e.g., MAPK, NRF2, Wnt, P53, and PI3K), known to have detrimental effects to health through causing oxidative stress, cytotoxicity, and genotoxicity to the liver and kidneys (Chen et al. 2022), thus making them extremely dangerous for both humans and animals, even resulting in death, depending on the amount and type of mycotoxin ingested. Fungal growth occurs naturally in food and is more common in grains (e.g., maize, peanuts, etc.), but this growth can be enhanced by humidity and temperature, as well as irregular conditions of production and storage. Fungal poisoning in food and feed through mycotoxin contaminations causes large economic losses; it is estimated that approximately 25% of food worldwide is contaminated by mycotoxins (SILVA et al. 2021).

These mycotoxigenic fungi exist in diverse environments and can contaminate a wide range of agricultural products (Shanakhat et al. 2018). The contamination of agricultural food products by mycotoxins has received a lot of attention in recent decades, due to their high acute or chronic toxicity in humans and animals and due to consumption and exposure time to food or feed contaminated with mycotoxins. This is exacerbated by the impact of the Covid-19 pandemic, civil wars, and conflicts (e.g., Russia-Ukraine conflict, Yemen, Ethiopia, Afghanistan, and other others), further straining food security and nutritional status of the most vulnerable demographic groups, which are anticipated to continue to deteriorate because of health and socioeconomic factors. According to the UN report in 2020, one in three people in the world (~2.37 billion) lack access to adequate safe and nutritional food – an increase of nearly 320 million people from 2019 (FAO, IFAD, UNICEF 2021; Vos et al. 2022). The presence of these mycotoxins in food and feed affects public health and the economy; therefore, it is of great importance to detect and quantify these toxins in agricultural lots. Early detection is essential to maintain food quality and reduce the impact on human and animal health (Li et al. 2021).

Efforts of killing the fungus does not certify nor guarantees that the mycotoxins have been eliminated, because mycotoxins are highly stable (SILVA et al. 2021). There are different types of mycotoxins, mainly categorized into the following groups with the prevalently occurring being: aflatoxins (AFs), AFB₁; ochratoxins (OTs), OTA, fumonisins (FMs), FB₁; deoxynivalenol (DON), patuline, and zearalenone (ZEA), respectively (Rai et al. 2015). The most common mycotoxigenic genera include *Aspergillus*, *Alternaria*, *Fusarium*, *Penicillium*, and *Stachybotrys* (Dobrucka and Długaszewska 2016). A single species of fungus has the capabilities of producing different types of mycotoxins, just as different fungi can produce different types of mycotoxins (SILVA et al. 2021).

It is estimated that more than 300 mycotoxins, which are of concern, have been identified; the growth and proliferation of fungi producing these toxins occur mainly in field cultivation, during the transport and storage of commodities. The main fungi

responsible for mycotoxins are *Aspergillus*, *Penicillium*, and *Fusarium* species. The *Aspergillus* fungal species generally produces mycotoxins that are divided into three different groups. Aflatoxins B (AFB₁ and AFB₂), aflatoxins G (AFG₁ and AFG₂), and aflatoxins M (AFM₁ and AFM₂), where AFB₁ is considered the most dangerous to health due to its high carcinogenic potential. Additionally, the mycotoxin ochratoxin A (OTA) is highly toxic and prevalent; it is produced by *Aspergillus* and *Penicillium* species (Nayaka et al. 2013), exhibiting nephrotoxic and nephrocarcinogenic effects (Ingle et al. 2020), and can be found in several animal products. Another mycotoxin produced by these two species is patulin, which is more common in agricultural commodities such as vegetables, fruits, and cereals. Patulin toxicity is associated with gastrointestinal disorders (Oancea and Stoia 2008).

Fumonisin is mainly produced by *Fusarium proliferatum*, *Fusarium verticillioides*, and *Fusarium nygamai* and are a group of non-fluorescent mycotoxins. The main contaminant is corn and its derivatives; consumption of food contaminated with fumonisins leads to leukoencephalomalacia in horses, hydrothorax, and pulmonary edema in swine (Nayaka et al. 2013). Many other mycotoxins, such as trichothecenes (T-2) and zearalenone (ZEA), are present in agricultural products. The identification of multiple toxins in large batches is of great importance to reduce the negative impact on public health. Effective, sensitive/selective, and low-cost methods are required for the qualitative and quantitative detection of mycotoxigenic fungi that can produce mycotoxin in small quantities.

The main toxicological effects caused by mycotoxins predominantly include carcinogenesis, hepatotoxicity, neurotoxicity, immunosuppression, and mutagenicity (SILVA et al. 2021). A variety of mycotoxins have been classified as carcinogenic, with Aflatoxin B₁ (AFB₁) being the most potent carcinogen and usually the major aflatoxin produced by toxigenic strains (Rai et al. 2015). Mycotoxin exposure is increasingly becoming a global problem, especially with the increase in a significant number of people switching to a vegan diet (Penczynski et al. 2022). Chronic exposure can lead to the development of serious pathologies already mentioned above; therefore, mitigation and elimination of these mycotoxins is essential.

15.2 Conventional Diagnostics for Mycotoxins in Agriculture

All conventional analytical procedures used for mycotoxin detection and quantification include three basic steps: (i) extraction, (ii) purification and cleaning, and (iii) identification and quantification (Shanakhat et al. 2018) as shown in Fig. 15.1 (Li et al. 2021).

(i) Extraction

The detection of mycotoxins is governed by effective sample extraction, assigning the correct methods according to their specificity. In this situation, good sampling guarantees a more accurate result for the overall sample. Generally, the sample is ground, homogenized in extraction solvent and filtered for the purification step.

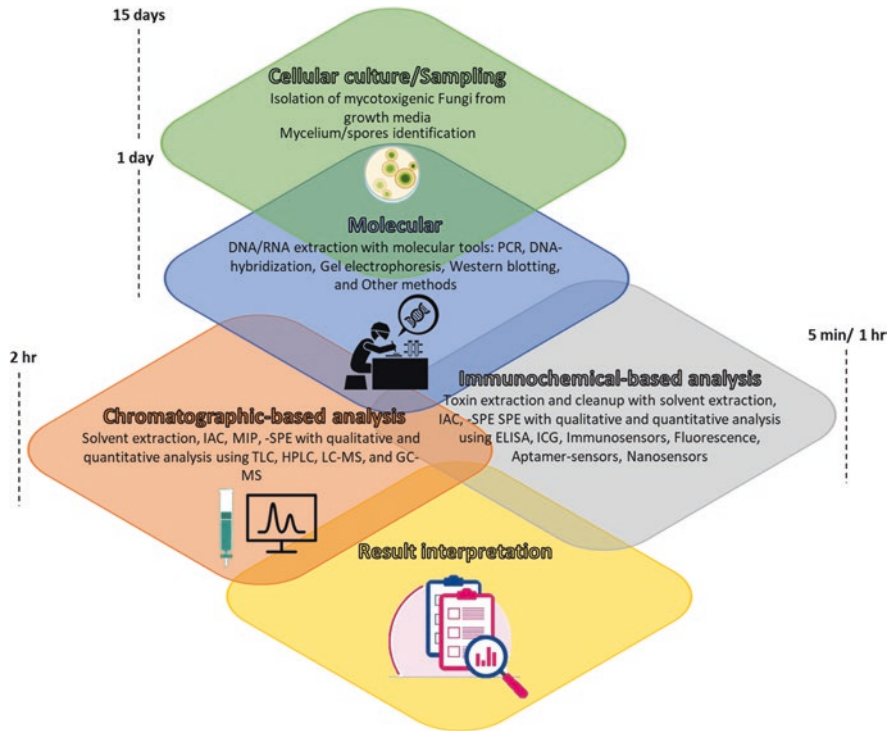


Fig. 15.1 Schematic representation of several methods of mycotoxin detection

In the extraction process, the analyte (mycotoxin) will move in the extraction solvent and thus the desired mycotoxin compound will be removed for analysis (Shanakhat et al. 2018).

(ii) Purification and cleaning

Before identification and quantification of mycotoxins, sample extracts must undergo cleanup to remove co-extracted materials (such as interfering compounds such as proteins, lipids, and carbohydrates). Cleanup is done with an immunoaffinity column (IAC), which has a high selectivity which is achieved by passing the sample through prepackaged cartridges, centrifugation, and extraction techniques in solid phase (Nayaka et al. 2013).

(iii) Identification and quantification

The detection of these mycotoxins in samples can be done through several conventional techniques, such as thin-layer chromatography (TLC), high-performance liquid chromatography (HPLC), gas and/or liquid chromatography often coupled with an ultraviolet detector or with mass spectrometric detectors (GC/GC-MS and LC/LC-MS, respectively), or immunochemical methods such as radioimmunoassay (RIA), enzyme-linked immunosorbent assay (ELISA), column immunity assay (ICA), and lateral flow immunochromatographic strips (ICSTs).

The TLC technique are widely used for their speed, simplicity, and low cost. This technique is very popular, because it can detect more than one mycotoxin in a sample with a detection limit of approximately 0.01 ppm (Oancea and Stoia 2008). TLC is based on the separation of substances by their migration in a specific matrix with a specific solvent (Nayaka et al. 2013). On the other hand, HPLC method has become popular and is often used for analyzing aflatoxins with UV fluorescence detection, with detection limit below ng/g of the product (Oancea and Stoia 2008). Thus, it is a technique that has high sensitivity and a high degree of precision. In agricultural samples, reversed-phase chromatography (RP) is widely used.

Gas chromatography has a limitation, as it requires volatilization. It has a detection of approximately 0.0001 ppm and can be coupled to mass spectrometry (GC-MS), where it combines superior separation in capillary columns with a variety of specific and general detectors. In immunochemical methods, the RIA has a high sensitivity that is due to radiolytic detection, and, therefore, a large amount of sample is not required. The ELISA is the most used immunoassay to identify OTA; the method has simplicity, the ability to immobilize antibodies, and efficiency in analyzing multiple mycotoxins with low molecular weight that would hardly be detected in a single sample with other available methods (Ingle et al. 2020).

15.3 Nanosurveillance to Mitigate Mycotoxins

There is a myriad of conventional techniques for detecting mycotoxins, which include enzyme-linked immunoassay (ELISA), gas chromatography (GC), thin-layer chromatography (TLC), high-performance liquid chromatography (HPLC), etc. The burden of mycotoxin contamination in the global market for testing is at compound annual growth rate (CAGR) 7.9% from 2021 to 2026, which will account for 1052.86 million USD (BCC Research Publishing 2022). Extreme rainfall and drought promote mycotoxin production, and once mycotoxins are released, they are difficult to control and nearly impossible to eradicate. Mycotoxins are the largest toxin that contaminates food and feedstuff, thus causing the largest burden in global food market (Fig. 15.2). Therefore, it is crucial to do mycotoxin testing on every crop produced. Small food processors rely on visual inspection and only test when mycotoxin contamination is identified or suspected. In addition, the risk of mycotoxin contamination in crops and stored food products is anticipated to grow, leading to an increase in the incidence of both human and animal diseases.

The Food and Agriculture Organization (FAO) advocated for improved surveillance and traceability and acknowledged the need to invest in radical new technologies such as nanodiagnostic tools to achieve these goals. Thus, there is a need to develop more advanced, specific, selective, sensitive, and portable methods that require minimal expertise for operation. Microfluidics, lab-on-a-chip, smart nanospectroscopy, and sensor technologies are some of the most important technical interfaces that have been refined from micro- to nano-sizes. The beneficial properties of this size transformation are the result of increased surface-to-volume ratio

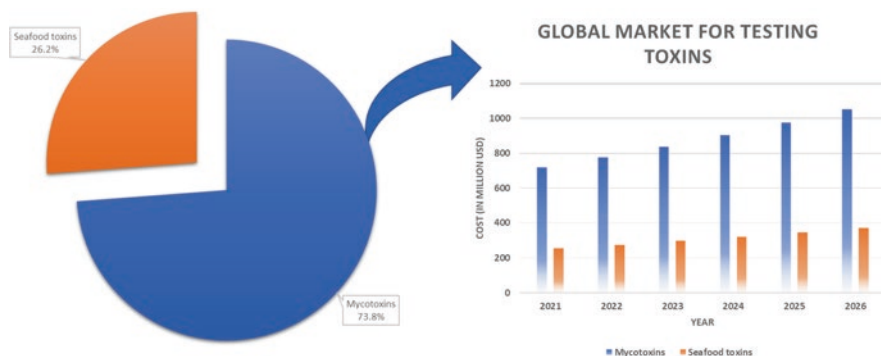


Fig. 15.2 Global market for testing toxins. (Adapted from BCC Research Publishing 2022)

due to the availability of surface atoms, multifunctionality, better catalysis, and reactivity. Moreover, the antimicrobial potential of nanomaterials increases due to the high contact surface-to-volume ratio with fungal surfaces or biomolecules (Kalia et al. 2020b). By interacting with fungal cells, nanomaterials adsorb to oppositely charged functional groups and exhibit the advantage of bypassing intact cell membranes. They can form complexes with biomolecules leading to damage and inactivation of a cascade of pathways involved in maintaining fungal cell homeostasis. These interactions and transformations of biomolecules result in inhibition of fungal growth and mycotoxin production (Kalia et al. 2020a). Microfluidic/optofluidic lab-on-a-chip technologies are a common detection method for mycotoxins. The use of nanotechnology opens up the avenue for the miniaturization and development of nanobiosensors that can be used to detect mycotoxins (Eskola et al. 2020; Thipe et al. 2018).

15.4 Nanodiagnostics for Mycotoxins

15.4.1 *Sensors Based on Nanomaterials for Mycotoxin Surveillance*

Nanomaterial-based sensor technologies provide diversified mitigation methods for quantifying single or multiple analytes, since mycotoxin co-occurrence in a single matrix has become more prevalent. This can aid in early detection with high sensitivity/selectivity of mycotoxigenic fungi and the respective mycotoxin they produce (Kalia et al. 2020a).

15.4.2 *Metallic Nanoparticles*

Many chemical, physical, and biological methods have been used to synthesis of metallic nanoparticles, such as gold (Thipe et al. 2015), silver (Guilger-Casagrande and Lima 2019), copper (Raafat et al. 2021), iron/iron oxide (Devi et al. 2019), zinc (Kalia et al. 2020a), and many others, including their bi- or tri-metallic complexes. Metal and metal oxide nanoparticles demonstrate excellent antimicrobial activities and have bactericidal, fungicidal, viricidal, and algacide action (Kalia et al. 2020a). Kalia and coworkers showed that oxide nanoparticles can control the production of mycotoxins, in addition to neutralizing or adsorbing already secreted mycotoxins. Zinc-derived nanomaterials at substantially low concentrations demonstrate sporidical activity and inhibit vegetative mycelial growth of filamentous fungal plant pathogens (Kalia et al. 2020a; Li et al. 2021).

15.5 Smart Nanosensors

15.5.1 *Nanoparticles with Conductivity-Based Sensors*

Biosensors are the combination of a biological component (in this case, secondary metabolites) with a physicochemical detector or transducer. The transducer transforms the signal received from the interaction between the analyte and the biological component into quantified and easily measurable signals. These signals are then displayed by the signal processor by digital output signals (Rai et al. 2015). Sheini (2020) produced a paper-based sensor array with gold and silver nanoparticles; color changes provide colorimetric signatures attributed by aggregation of nanoparticles from the interaction with mycotoxins (AFB₁, AFG₁, AFM₁, OTA, and ZEN) with a LOD of 2.7, 7.3, 2.1, 3.3, and 7.0 ng/mL, respectively (Sheini 2020).

Liu et al. (2020) designed a smartphone-based multiplexed dual detection mode device integrated AuNPs and time-resolved fluorescence microspheres (TRFMs) LFIA for mycotoxins (AFB₁, ZEN, DON, T-2, and FB₁) in cereals with LODs of 2.5, 0.5, 0.5, 2.5, and 0.5 µg/kg, respectively. Nanoparticles have been incorporated into biosensors to improve analytical parameters, which include limit of detection/quantification, linear range, assay stability/selectivity/sensitivity, and cheap production cost, among other things. In the development of nanosensors, nanoparticles serve as an immobilization support, signal amplifier, mediator, and artificial enzyme label in mycotoxin analysis as shown in Fig. 15.3 (Zhao et al. 2022).

Xiulan and coworkers developed an immunochromatographic method for detecting AFB₁ using a combination of an antibody and a conjugated nanogold probe (Xiulan et al. 2005). Several mycotoxigenic fungi produce diffusible exotoxins, which can be used as markers for the identification and confirmation of phytopathogenic fungi. An indium-tin oxide electrochemical impedance sensor with nano-ZnO film was developed by co-immobilizing antibodies and BSA protein to detect

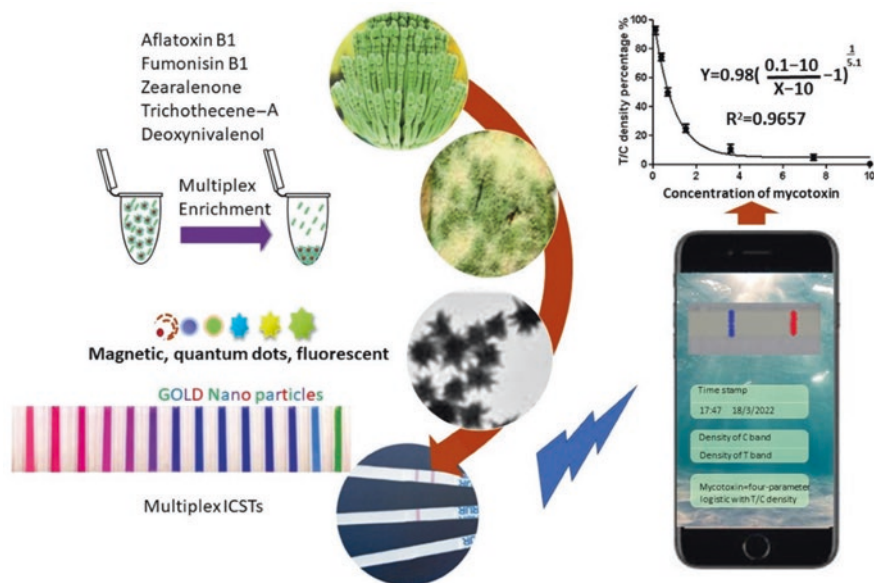


Fig. 15.3 Schematic overview of multiplex detection of mycotoxins employing the enrichment for samples with various nanoparticles based on laminar flow strips and smartphone readouts. This utility functions by (i) using multimodal nanoparticles coated with mycotoxin antibodies to enhance the limit of detection (LOD) of the mycotoxin; (ii) utilizing different labels (e.g., magnetic particles, quantum dots, fluorophores on gold nanoparticles), which may be feasible choices for multiplexed detection; and (iii) developing smartphone apps that can examine the color intensities and be transformed into concentrations. (Adapted with permission from Zhao et al. 2022)

ochratoxin-A in agricultural and other plant-derived products (Ansari et al. 2010). Hernandez et al. (2020) developed a label-free surface-enhanced Raman spectroscopy (SERS) and localized surface plasmon resonance (LSPR) gold nanosensor constructed by immobilizing OTA-, FB₁-, and AFB₁-aptamers on gold nanoprisms (AuNTs) for detecting OTA, FB₁, and AFB₁ in cereals and grains (e.g., green coffee beans, wheat, and amaranth) in complex matrixes, demonstrated by the response of the plasmonic nanosensors with detection at 10–22 ppb (Hernandez et al. 2020). Similarly, Zhang et al. (2020) developed a multiplex SERS-based lateral flow immunosensor for the simultaneous detection of AFB₁, ZEN, OTA, T-2, FB₁, and DON in maize, with LOD of 0.96, 6.2, 15.7, and 8.6 pg/mL, while FB₁ and DON were at 0.26 and 0.11 ng/mL, respectively (Zhang et al. 2020). The work by Zhao et al. (2021) demonstrated the use of novel α -Fe₂O₃ nanocubes as lateral flow immunoassays (LFIA) labels for the simultaneous detection of AFB₁ and DON in corn, mung bean, and millet with the visual LOD of 0.01 and 0.18 ng/mL, respectively (Zhao et al. 2021).

Wu et al. (2020) developed a novel multicolor immunochromatographic test strip nanosensor composed of gold nanoparticles that exhibit different multicolored labels based on the SERS and LSPR of the different morphologies and size of the

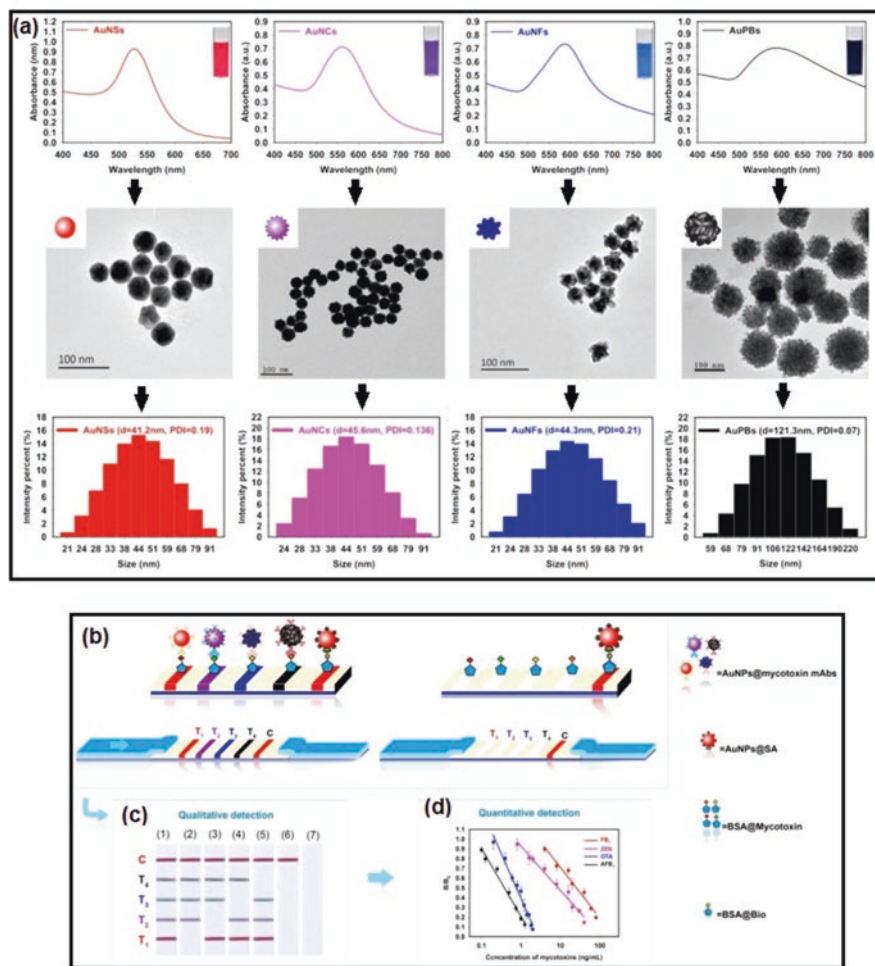


Fig. 15.4 Multicolor immunochromatographic test strip (ICTS) nanosensor: (a) characterization of four different sized or shaped AuNPs (AuNSs, AuNCs, AuNFs, and AuPBs); (b) schematic illustration of multicolor AuNP-based multiplex ICTS nanosensor, where test lines (T₁, T₂, T₃, and T₄) represent the simultaneous detection FB₁, ZEN, OTA, and AFB₁, and one control line indicates the validity of our method; (c) interpretation of qualitative test results; and (d) quantitative test results of multicolor AuNP-based multiplex ICTS nanosensor. (Adapted with permission from Wu et al. 2020)

gold nanoparticles (gold nanospheres (**AuNSs**), gold nanocacti (**AuNCs**), gold nanoflowers (**AuNFs**), and hyperbranched Au plasmonic blackbodies (**AuPBs**)) for simultaneous and accurate detection of AFB₁, FB₁, OTA, and ZEN at 0.06, 3.27, 0.10, and 0.70 ng/mL, respectively, as shown in Fig. 15.4 (Wu et al. 2020).

This can also be achieved utilizing quantum dots (QDs), which are semiconductor nanoparticles with exceptional optical properties (e.g., size-tunable emission,

wide adsorption, narrow photoluminescence spectra, strong photostability, a significant Stokes's shift, and a long fluorescence lifespan). Duan et al. (2019) designed a tricolor QD nanobead (QB)-based multiplex immunochromatographic assay (mICA) for simultaneous qualitative detection of FB₁, OTA, and ZEN in maize that serves as point-of-care testing (POCT) device. The QBs exhibited distinguishable yellow, orange, and red luminescence and conjugated with anti-FB₁, anti-OTA, and anti-ZEN monoclonal antibodies for the detection of FB₁, OTA, and ZEN, respectively. The QB-mICA revealed an LOD of 5, 20, and 10 ng/mL for OTA, FB₁, and ZEN within 10 min, respectively, as shown in Fig. 15.5 (Duan et al. 2019).

15.5.2 Antibody-Coupled Nanomaterials

Antibodies are widely used as molecular recognition receptors for toxin detection due to their specificity and sensitivity (Tothill 2011). Nanomaterials are not only promising adsorbents but are also capable of coupling different molecules. Recently, synthetic receptors, such as aptamers, peptides, proteins, and printed polymers, have been coupled to nanomaterials for the development of nanosensors for the detection of mycotoxins (Thiipe et al. 2018). Direct coupling via adsorption requires specific surface properties that allow interaction with the antibody. Preferably, the covalent binding of the antibody allows interaction with antigen-binding sites (Horky et al. 2018). Table 15.1 presents and compares studies of LFIA's utilized for the detection of mycotoxins in recent years. Additionally, activated carbon has been used as an adsorbent to eliminate mycotoxins for a long time, so the use of carbon nanoforms was thought to be a promising successor to activated carbon. Carbon nanomaterials have high adsorption, stability, inertness, large surface area by weight, and colloidal stability at various pH ranges. Chemically, the carbon-carbon covalent bonds and the crystal structure provide specific properties, such as strength, elasticity, and optimal conductivity. Graphene, graphene oxide, nanodiamonds, fullerenes, fibers, and nanotubes have great potential to become new adsorbents for mycotoxins. Nanocarbon structures are amphoteric, and their surface can be protonated or deprotonated, which results in the binding capacity of polar or nonpolar compounds (Horky et al. 2018).

For the detection of mycotoxins, commercial test kits are often used as an appropriate alternative as a more inexpensive, user-friendly, and quick analysis. These commercial kits often include called the ELISA kits, fluorescence polarization immunoassays (FPIAs), membrane-based immunoassays such as LFIA's, and immunoaffinity column coupled with fluorometric assay. These kits are predominantly based on an immunoassay format that relies on the specific interaction between antigen and antibody. All the commercial kits are designed with nanoparticles to facilitate increase quantification, sensitivity, and selectivity, all attributed to the properties of nanoparticles. Additionally, colorimetric kits are preferred due to its ability to show results for the naked eye. LFIA's are strong competitors in the mycotoxin analysis market due to its acceptable sensitivity, portability, accuracy,

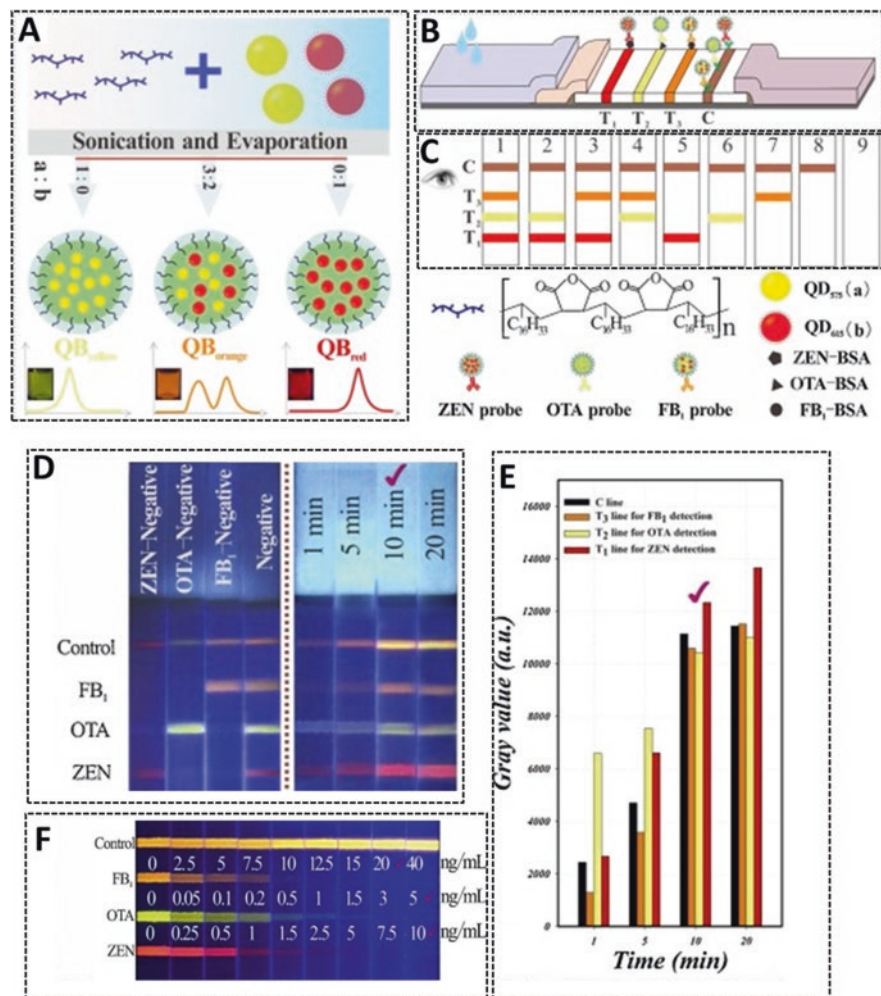


Fig. 15.5 Tricolor QD nanobead (QB)-based multiplex immunochromatographic assay (mICA) for simultaneous qualitative detection of FB₁, OTA, and ZEN: (a) schematic illustration of emulsification evaporation method for the synthesis of tricolor QB; (b) schematic representation of tricolor QB-based mICA, T₁ – ZEN, T₂ – OTA, T₃ – FB₁, and C – control; (c) qualitative result visualization with naked eye; (d) evaluation and optimization of the cross-reaction for each QB-mAbs probe on three T lines, where “✓” represents the optimal interpret time; (e) relationship between reaction time and the gray values on T lines and C line; and (f) sensitivity of QB-based mICA for ZEN, OTA, and FB₁ detection, where “✓” represents LOD for ZEN, OTA, and FB₁

ease of use, short detection time, and no need for specialized personnel (Majdinasab et al. 2020).

The commercially available LFIA test strips commonly use AuNPs or QDs for signal amplification as colored labels. This method can deliver qualitative or semi-quantitative results. For semi-quantitative analysis, portable readers are developed

Table 15.1 Summary of LFIA strips with nanomaterials for detecting mycotoxins

| Mycotoxin | Principle | Nanomaterial | Sample | LOD | References |
|---|--|--|------------------------------|---|--------------------------|
| FB ₁ /ZEN/OTA/AFB ₁ | Competitive LFIA | AuNSs, AuNCs, AuNFs, and AuPBs | Corn | FB ₁ : 3.27 ng/mL ZEN: 0.70 ng/mL OTA: 0.10 ng/mL AFB ₁ : 0.06 ng/mL | Wu et al. (2020) |
| FB ₁ /FB ₂ /DON/ZEN | Immuno-based | QD and AuNPs nanosensor | Corn oats and barley | Maize DON 80 µg/Kg, Wheat DON 400 µg/Kg, | Duan et al. (2019) |
| FB ₁ /DON | Competitive LFIA | AuNFs | Chinese traditional medicine | FB ₁ : 5.0 ng/mL DON: 5.0 ng/mL | Huang et al. (2020a, b) |
| AFs | Surface plasmon resonance-based sensor | Carbon nanomaterial | Peanut and rice | 2.5 ng/mL | Thakur et al. (2022) |
| FB ₁ /DON | Competitive LFIA | AuNSs, AuNFs | Grain | FB ₁ : 20 ng/mL DON: 5 ng/mL | Xi Huang et al. (2020) |
| OTA | Immunochromatographic-based | Chemosynthetic peptide with AuNP probes | Maize, wheat, and rice | 0.19 ng/mL | You et al. (2020) |
| DON/AFB ₁ | Competitive fluorescent LFIA | α-Fe ₂ O ₃ nanocubes | Food | DON: 0.18 ng/mL AFB ₁ : 0.01 ng/mL | Zhao et al. (2021) |
| OTA/ZEN/ Biofilms | FRET-based biofilm and toxin nanobiosensor | DNA aptamers with graphite oxide | Corn | OTA: 1.8 ng/mL ZEN: 1.5 ng/mL | Thakur et al. (2022) |
| CIT/ZEN | Competitive fluorescent LFIA | Europium nanoparticles | Corn | CIT: 0.06 ng/mL ZEN: 0.11 ng/mL | Xu et al. (2021) |
| ZEN/DON | Competitive fluorescent LFIA | Near-infrared dyes | Maize | ZEN: 0.55 µg/kg DON: 3.8 µg/kg | Jin et al. (2021) |
| ZEN/OTA/FB ₁ | Competitive fluorescent LFIA | QDs | Wheat | ZEN: 5 ng/mL OTA: 20 ng/mL FB ₁ : 10 ng/mL | Duan et al. (2019) |
| ZEN/DON | Competitive fluorescent LFIA | Silanized QDs | Maize and wheat | ZEN: 40 µg/kg DON: 400 µg/kg | Goryacheva et al. (2020) |

| Mycotoxin | Principle | Nanomaterial | Sample | LOD | References |
|--|------------------------------------|--|---------------|---|-----------------------|
| AFB ₁ /ZEN/DON/T-2/ FB ₁ | Competitive fluorescent LFIA | TRFMs | Cereals | AFB ₁ : 0.42 µg/kg ZEN: 0.10 µg/kg DON: 0.05 µg/kg T-2: 0.75 µg/kg FB ₁ : 0.04 µg/kg | Liu et al. (2020) |
| AFB ₁ /ZEN | Competitive fluorescent LFIA | TRFMs | Maize | AFB ₁ : 0.05 ng/mL ZEN: 0.07 ng/mL | Tang et al. (2017) |
| AFB ₁ /ZEN/DON | Competitive fluorescent LFIA | QD microbeads | Feedstuff | AFB ₁ : 10 pg/mL ZEN: 80 pg/mL DON: 500 pg/mL | Li et al. (2019) |
| DON/T-2/ZEN | Competitive fluorescent LFIA | Amorphous carbon nanoparticles | Maize | DON: 20 µg/kg T-2: 13 µg/kg ZEN: 1 µg/kg | Zhang et al. (2017) |
| AFB ₁ /FB ₁ /OTA | Competitive fluorescent LFIA | QBs | Cereals | AFB ₁ : 1.65 pg/mL FB ₁ : 1.58 ng/mL OTA: 0.0059 ng/mL | Shao et al. (2019) |
| DON | Competitive fluorescent LFIA | Polydopamine coated zirconium metal-organic frameworks | Meat | 0.18 ng/mL | Li et al. (2020) |
| AFB ₁ | Fluorescence quenching LFIA (IFE) | AuNFs, QDs | Soybean sauce | 0.004 µg/L | Jiang et al. (2018) |
| FB ₁ | Fluorescence quenching LFIA (IFE) | AgNPs, QDs | Maize flour | 62.5 µg/kg | Anfossi et al. (2018) |
| ZEN | Fluorescence quenching LFIA (FRET) | AgNPs, QDs | Cereals | 0.1 µg/L | Li et al. (2018) |
| AFB ₁ /ZEN/FB ₁ /DON/ OTA/T-2 | SERS-based LFIA | DTNB and MBA labelled Au-Ag coreshell nanoparticles | Maize | AFB ₁ : 0.96 pg/mL ZEN: 6.2 pg/mL FB ₁ : 0.26 pg/mL DON: 0.11 pg/mL OTA: 15.7 pg/mL T-2: 8.6 pg/mL | Zhang et al. (2020) |

Adapted from Li et al. (2021)

for on-site detection. Commercially available test kits are developed for the determination of individual or multiple mycotoxins in single sample matrix. The latest trend in LFIA technology is the development of strips with multiple test lines for simultaneous detection of various mycotoxins. ELISA-based kits hold a major portion of the market of mycotoxin detection methods, after the LFIA test strips. Numerous companies offer ELISA kits for the detection of the most commonly occurring mycotoxins. Some of which can detect more than one type of mycotoxins

Table 15.2 Main companies providing commercial colorimetric immuno-kits for mycotoxins analysis

| Company | Kit | Type of Detection |
|---------------------------|----------------|-----------------------|
| Astori Tecnica | ELISA | QTN, semi-QTN for OTA |
| | LFIA | QLT, QNT |
| Charm Sciences Inc. | LFIA | QNT |
| CUSABIO | ELISA | QNT |
| | LFIA | QNT |
| Elabscience | ELISA | QNT |
| | LFIA | QNT |
| EnviroLogix | LFIA | QLT, QNT |
| Eurofins | ELISA | QNT |
| | LFIA | QNT |
| Helica | ELISA | QNT |
| Neogen | ELISA | QNT |
| | LFIA | QLT, QNT |
| R-Biopharm | ELISA | QNT |
| | LFIA | Semi-QNT, QNT |
| Romer Labs | ELISA | QNT |
| | LFIA | QLT, QNT |
| Vicam | LFIA | Semi-QNT, QNT |
| Beacon Analytical Systems | ELISA | QNT |
| Creative Diagnostics | ELISA | QNT |
| | LFIA | QLT, semi-QNT, QNT |
| PerkinElmer | ELISA | QNT |
| | LFIA | QNT |
| Unisensor | LFIA | QNT |
| Pribolab | ELISA | QNT |
| | LFIA | QLT, QNT |
| Randox | ELISA | QNT |
| | Biochip Arrays | QNT |
| Novakits | ELISA | Semi-QNT, QNT |
| | LFIA | QNT |
| Bio-Check | ELISA | QNT |
| | LFIA | QNT |

QNT Quantitative, *Semi-QNT* Semi-quantitative, *QLT* Qualitative

in a single sample matrix. Commercial ELISA kits are selective, sensitive, and high throughput, with minimum sample separation steps. Furthermore, the detection time has been shortened, so that most of them can detect a targeted mycotoxin within 1–2 h. In some kits, cross-reactivity of antibodies can lead to overestimation of results, while matrix effect can play a key role in false-positive results. In order to avoid those effects, most kits define the limited matrices to which ELISA kits can be used (Majdinasab et al. 2020). There are many commercial detection kits available in the current market, as shown in Table 15.2.

While conventional methods are always improving, current research is looking for more innovative solutions. The utilization of nanotechnology is a promising, low-cost, and effective way to minimize the impact of mycotoxins (Horky et al. 2018). There are a number of commercial nanoformulations already in the market used as nanodiagnostic tools for mycotoxins detection (Thipe et al. 2018), as shown in Table 15.3.

Table 15.3 Commercial products with nanoformulations used in agriculture

| Commercial brand | Content | Company |
|---|---|--|
| Nano-pro™ | Nanofertilizer for agriculture and better farming | Aqua-Yield, Utah, United States |
| Biozar Nano-Fertilizer | Combination of organic materials, micronutrients, and macromolecules | Fanavar Nano-Pazhoohesh Marzaki Company, Iran |
| CelluForce NCC™ | Cellulose matrix for heat stability to prevent microbial growth | CelluForce Inc. Montreal, Canada |
| MycofLEX BAT | Multiplex mycotoxin detection device | Randox Food Diagnostics, Crumlin, United Kingdom |
| Nano-Ag Answer® | Microorganism, sea kelp, and mineral electrolyte | Urth Agriculture, CA, United States |
| Nano-Gro™ | Plant growth regulator and immunity enhancer | Agro Nanotechnology Corp., FL, United States |
| Nano Green | Extracts of corn, grain, soybeans, potatoes, coconut, and palms | Nano Green Sciences Inc., India |
| Nanolook™ | Nanodispersed silicates to prolong food shelf life | InMat, Inc., Raritan, United States |
| Nano Max NPK Fertilizer | Multiple organic acids chelated with major nutrients, amino acids, organic carbon, organic micronutrients/trace nutrients, vitamins, and probiotics | JU Agri Sciences Pvt. Ltd. Janakpuri, New Delhi, India |
| Master Nano Chitosan Organic Fertilizer | Water soluble liquid chitosan, organic acid and salicylic acid, phenolic compounds | Pannaraj Intertrade, Thailand |
| TAG NANO (NPK, PhoS, zinc, Cal, etc.) Fertilizers | Proteino-lacto-gluconate chelated with micronutrients, vitamins, probiotics, seaweed extracts, humid acid | Tropical Agrosystem India (P) Ltd., India |

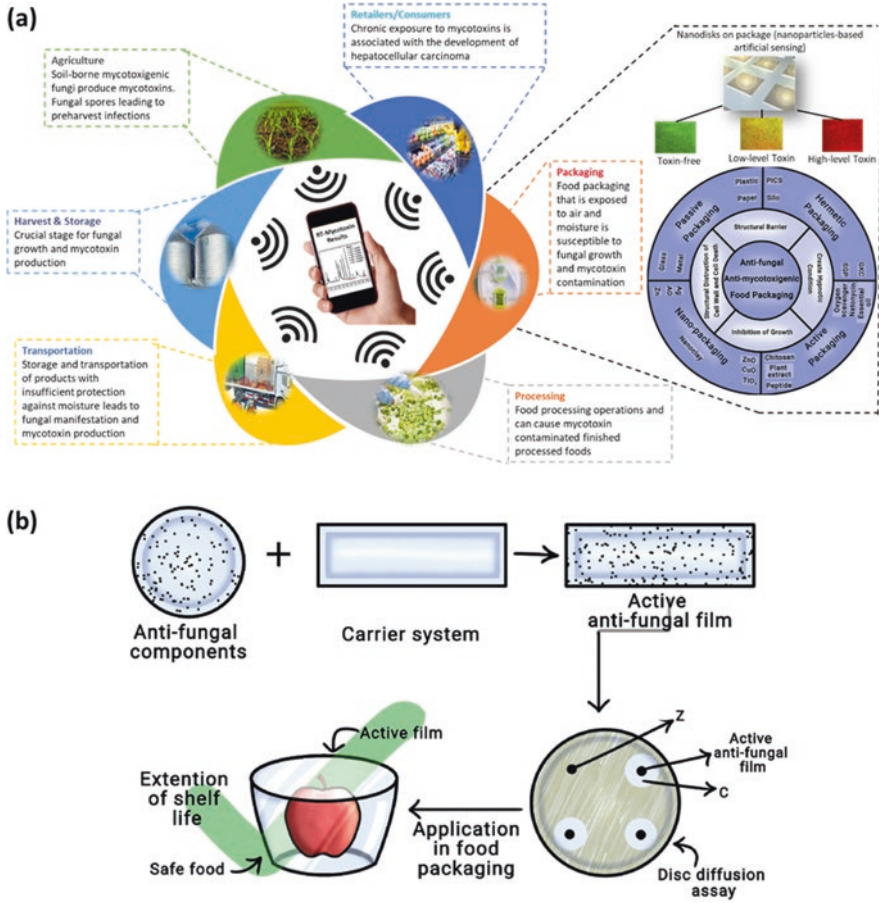


Fig. 15.6 Smart antifungal packaging based on (a) RFID technology and nanodisks (nanoparticles-based artificial sensing) of mycotoxin and (b) nanoparticle-based active antifungal package for improving food quality controls. (Adapted with permission from Caon et al. 2017 and Akhila et al. 2022)

15.6 Smart and Antifungal Packaging Nanosurveillance

Mycotoxin contamination predominately occurs in the field, during pre- and post-harvest, transportation, processing, and improper storage of food and feedstuff. This is evident, since when food is stored properly and exposed to air and moisture, it often deteriorates allowing for the manifestation of fungi with subsequent mycotoxin production. Individual packets of food are not amenable to laboratory-based food deterioration testing. Most recently, technological advances through nanotechnology have utilized nanoparticles-based artificial sensing as nanodisks in spot indicators for sensitive mycotoxin detection on packages (Akhila et al. 2022; Kumar et al. 2017), as shown in Fig. 15.6, while Table 15.4 shows some studies that utilize nanoparticle-based active antifungal packaging.

Table 15.4 Nanoparticle-based active antifungal package

| Active nanoparticle | Matrix/other components in packaging | Microorganism tested | Major findings | References |
|------------------------------------|--|--------------------------------------|---|----------------------------------|
| Zinc oxide (ZnO) | Soy protein isolate (SPI) + cinnamaldehyde (CIN) | <i>A. niger</i> | SPI + CIN + ZnO film showed 1.56- and 1.24-fold stronger inhibition than those of SPI + ZnO and SPI + CIN films | Wu et al. (2019) |
| Titanium oxide (TiO ₂) | Poly (lactic acid) | <i>A. fumigatus</i> | Showed 99.99% effectiveness under the UVA irradiation | Fonseca et al. (2015) |
| Titanium oxide (TiO ₂) | Chitosan | <i>C. albicans</i> , <i>A. niger</i> | Red grapes 22 days before mildew occurred | Xiaodong Zhang et al. (2017a, b) |
| Gold and silver | Chitosan | <i>A. niger</i> | Effectiveness increased with concentration of nanoparticles addition | Youssef et al. (2014) |
| Copper oxide (CuO) | Polyurethane | <i>Penicillium</i> | Film with 2% CuO showed optimal Concentration for inhibition | Ghorbani et al. (2018) |

Adapted from permission from Akhila et al. (2022)

15.7 Concluding Remarks

Due to their unique physiochemical properties, nanomaterials provide a multitude of design options for mycotoxin nanodiagnosis utilizing nanosensor fabrications. The nanomaterials enhanced sensitivity due to surface-atom availability, when functionalized, can exhibit structure-switchable conformational changes upon mycotoxin binding for multiplex detection of mycotoxin. Due to their nanoscale size and reversibility, structure-switchable nano-based assays are widely used for continuous and real-time monitoring of mycotoxins. In this approach, a great number of innovative and new nanomaterials for mycotoxin detection platforms have been investigated. The production of composite/hybrid nanomaterials, quantum structures, and nanomaterials with functionalized surfaces allows for multiplex detection of different mycotoxins within a single sample matrix. In the construction of smart nanosensors, gold and silver nanoparticles are the mostly utilized nanoparticles in the development of nanosensors, particularly due to their plasmon resonance for signal amplification. However, depending on the pH, temperature,

medium, and size of the nanoparticles, their properties can change dramatically under a variety of physiological conditions. In contrast to immunoassays, immunochromatographic assay composed of a variety of nanoparticles or composite/hybrid nanoparticles for the detection of major mycotoxins (AFB₁, FB₁, OTA, and ZEN) are still in the development phase. Future research and investment are required to address the obstacles in the approach for the commercialization of nano-based assays that can be utilized as point-of-care testing (POCT) devices for mycotoxin detection.

Acknowledgments The authors would like to thank the Fundação de Amparo à Pesquisa do Estado de São Paulo (FAPESP) Grant No. 2019/15154-0 for support to Velaphi Clement Thipe.

References

- Akhila PP, Sunooj KV, Navaf M, Aaliya B, Sudheesh C, Sasidharan A, Sabu S, Mir SA, George J, Mousavi Khaneghah A. Application of innovative packaging technologies to manage fungi and mycotoxin contamination in agricultural products: current status, challenges, and perspectives. *Toxicon*. 2022;214:18–29.
- Anfossi L, Di Nardo F, Cavalera S, Giovannoli C, Spano G, Speranskaya ES, Goryacheva IY, Baggiani C. A lateral flow immunoassay for straightforward determination of fumonisin mycotoxins based on the quenching of the fluorescence of CdSe/ZnS quantum dots by gold and silver nanoparticles. *Microchim Acta*. 2018;185:94.
- Ansari AA, Kaushik A, Solanki PR, Malhotra BD. Nanostructured zinc oxide platform for mycotoxin detection. *Bioelectrochemistry*. 2010;77:75–81.
- BCC Research Publishing. (2022). Global markets and technologies for food safety testing.
- Caon T, Martelli SM, Fakhouri FM. In: Grumezescu AMBT-N, editor. *New trends in the food industry: application of nanosensors in food packaging*, vol. 18. Academic Press; 2017. p. 773–804.
- Chen J, Yang S, Li P, Wu A, Nepovimova E, Long M, Wu W, Kuca K. MicroRNA regulates the toxicological mechanism of four mycotoxins in vivo and in vitro. *J Anim Sci Biotechnol*. 2022;13:37.
- da Silva JVB, de Oliveira CAF, Ramalho LNZ. An overview of mycotoxins, their pathogenic effects, foods where they are found and their diagnostic biomarkers. *Food Sci Technol*. 2021;
- Devi HS, Boda MA, Shah MA, Parveen S, Wani AH. Green synthesis of iron oxide nanoparticles using *Platanus orientalis* leaf extract for antifungal activity. *Green Process Synth*. 2019;8:38–45.
- Dobrucka R, Długaszewska J. Biosynthesis and antibacterial activity of ZnO nanoparticles using *Trifolium pratense* flower extract. *Saudi J Biol Sci*. 2016;23:517–23.
- Duan H, Li Y, Shao Y, Huang X, Xiong Y. Multicolor quantum dot nanobeads for simultaneous multiplex immunochromatographic detection of mycotoxins in maize. *Sensors Actuators B Chem*. 2019;291:411–7.
- Eskola M, Kos G, Elliott CT, Hajšlová J, Mayar S, Krska R. Worldwide contamination of food-crops with mycotoxins: validity of the widely cited ‘FAO estimate’ of 25%. *Crit Rev Food Sci Nutr*. 2020;60:2773–89.
- FAO, IFAD, UNICEF, W. and W. Brief to the state of food security and nutrition in the world 2021. In: *Brief to the state of food security and nutrition in the world 2021*. FAO; 2021.
- Fonseca C, Ochoa A, Ulloa MT, Alvarez E, Canales D, Zapata PA. Poly(lactic acid)/TiO₂ nanocomposites as alternative biocidal and antifungal materials. *Mater Sci Eng C*. 2015;57:314–20.

- Ghorbani HR, Alizadeh V, Mehr FP, Jafarpourgolroudbary H, Erfan K, Yeganeh SS. Preparation of polyurethane/CuO coating film and the study of antifungal activity. *Prog Org Coatings*. 2018;123:322–5.
- Goryacheva OA, Guhrenz C, Schneider K, Beloglazova NV, Goryacheva IY, De Saeger S, Gaponik N. Silanized luminescent quantum dots for the simultaneous multicolor lateral flow immunoassay of two mycotoxins. *ACS Appl Mater Interfaces*. 2020;12:24575–84.
- Guilger-Casagrande M, de Lima R. Synthesis of silver nanoparticles mediated by fungi: a review. *Front Bioeng Biotechnol*. 2019;7:1–16.
- Hernandez Y, Lagos L, Galarreta B. Development of a label-free-SERS gold nanoaptasensor for the accessible determination of ochratoxin a. *Sens Bio-Sensing Res*. 2020;28:100331.
- Horky P, Skalickova S, Baholet D, Skladanka J. Nanoparticles as a solution for eliminating the risk of mycotoxins. *Nano*. 2018;8:727.
- Huang X, Huang T, Li X, Huang Z. Flower-like gold nanoparticles-based immunochromatographic test strip for rapid simultaneous detection of fumonisin B1 and deoxynivalenol in Chinese traditional medicine. *J Pharm Biomed Anal*. 2020a;177:112895.
- Huang X, Huang X, Xie J, Li X, Huang Z. Rapid simultaneous detection of fumonisin B1 and deoxynivalenol in grain by immunochromatographic test strip. *Anal Biochem*. 2020b;606:113878.
- Ingle, A., Gupta, I., Jogee, P., Rai, M., 2020. Role of nanotechnology in the detection of mycotoxins. pp. 11–33.
- Jiang H, Zhang W, Li J, Nie L, Wu K, Duan H, Xiong Y. Inner-filter effect based fluorescence-quenching immunochromatographic assay for sensitive detection of aflatoxin B1 in soybean sauce. *Food Control*. 2018;94:71–6.
- Jin Y, Chen Q, Luo S, He L, Fan R, Zhang S, Yang C, Chen Y. Dual near-infrared fluorescence-based lateral flow immunosensor for the detection of zearalenone and deoxynivalenol in maize. *Food Chem*. 2021;336:127718.
- Kalia A, Abd-Elsalam KA, Kuca K. Zinc-based nanomaterials for diagnosis and management of plant diseases: ecological safety and future prospects. *J Fungi*. 2020a;6:1–29.
- Kalia A, Kaur J, Kaur A, Singh N. Antimycotic activity of biogenically synthesised metal and metal oxide nanoparticles against plant pathogenic fungus *Fusarium moniliforme* (F. fujikuroi). *Indian J Exp Biol*. 2020b;58:263–70.
- Kumar V, Guleria P, Mehta SK. Nanosensors for food quality and safety assessment. *Environ Chem Lett*. 2017;15:165–77.
- Li S, Wang J, Sheng W, Wen W, Gu Y, Wang S. Fluorometric lateral flow immunochromatographic zearalenone assay by exploiting a quencher system composed of carbon dots and silver nanoparticles. *Microchim Acta*. 2018;185:388.
- Li R, Meng C, Wen Y, Fu W, He P. Fluorometric lateral flow immunoassay for simultaneous determination of three mycotoxins (aflatoxin B1, zearalenone and deoxynivalenol) using quantum dot microbeads. *Microchim Acta*. 2019;186:748.
- Li R, Bu T, Zhao Y, Sun X, Wang Q, Tian Y, Bai F, Wang L. Polydopamine coated zirconium metal-organic frameworks-based immunochromatographic assay for highly sensitive detection of deoxynivalenol. *Anal Chim Acta*. 2020;1131:109–17.
- Li R, Wen Y, Wang F, He P. Recent advances in immunoassays and biosensors for mycotoxins detection in feedstuffs and foods. *J Anim Sci Biotechnol*. 2021;12:108.
- Liu Z, Hua Q, Wang J, Liang Z, Li J, Wu J, Shen X, Lei H, Li X. A smartphone-based dual detection mode device integrated with two lateral flow immunoassays for multiplex mycotoxins in cereals. *Biosens Bioelectron*. 2020;158:112178.
- Majdinasab M, Aissa SB, Marty JL. Advances in colorimetric strategies for mycotoxins detection: toward rapid industrial monitoring. *Toxins* 2021. 2020;13:13.
- Nayaka SC, Ramana MV, Udayashankar AC, Niranjana SR, Mortensen CN, Prakash HS. Chemical and molecular methods for detection of toxigenic fungi and their mycotoxins from major food crops BT – laboratory protocols in fungal biology: current methods in fungal biology. In: Gupta

- VK, Tuohy MG, Ayyachamy M, Turner KM, O'Donovan A, editors. Laboratory protocol for fungi. New York: Springer; 2013. p. 73–90.
- Oancea S, Stoia M. Mycotoxins: a review of toxicology, analytical methods and health risks. *Acta Univ Cibiniensis Ser E Food Technol.* 2008;XII:19–36.
- Penczynski KJ, Cramer B, Dietrich S, Humpf H-U, Abraham K, Weikert C. Mycotoxins in serum and 24-h urine of vegans and omnivores from the risks and benefits of a vegan diet (RBVD) study. *Mol Nutr Food Res.* 2022;66:2100874.
- Raafat M, El-Sayed ASA, El-Sayed MT. Biosynthesis and anti-mycotoxigenic activity of Zingiber officinale roscoe-derived metal nanoparticles. *Molecules.* 2021;26:2290.
- Rai M, Jogee PS, Ingle AP. Emerging nanotechnology for detection of mycotoxins in food and feed. *Int J Food Sci Nutr.* 2015;66:363–70.
- Shanakhath H, Sorrentino A, Raiola A, Romano A, Masi P, Cavella S. Current methods for mycotoxins analysis and innovative strategies for their reduction in cereals: an overview. *J Sci Food Agric.* 2018;98:4003–13.
- Shao Y, Duan H, Zhou S, Ma T, Guo L, Huang X, Xiong Y. Biotin–streptavidin system-mediated ratiometric multiplex immunochromatographic assay for simultaneous and accurate quantification of three mycotoxins. *J Agric Food Chem.* 2019;67:9022–31.
- Sheini A. Colorimetric aggregation assay based on array of gold and silver nanoparticles for simultaneous analysis of aflatoxins, ochratoxin and zearalenone by using chemometric analysis and paper based analytical devices. *Microchim Acta.* 2020;187:167.
- Tang X, Li P, Zhang Q, Zhang Z, Zhang W, Jiang J. Time-resolved fluorescence immunochromatographic assay developed using two idiotypic nanobodies for rapid, quantitative, and simultaneous detection of aflatoxin and Zearalenone in maize and its products. *Anal Chem.* 2017;89:11520–8.
- Thakur M, Wang B, Verma ML. Development and applications of nanobiosensors for sustainable agricultural and food industries: recent developments, challenges and perspectives. *Environ Technol Innov.* 2022;26:102371.
- Thihe VC, Njobeh PB, Mhlanga SD. Optimization of commercial antibiotic agents using gold nanoparticles against toxigenic aspergillus spp. *Mater Today Proc.* 2015;2:4136–48.
- Thihe V, Keyster M, Katti K. Sustainable nanotechnology: mycotoxin detection and protection; 2018. p. 323–49.
- Tothill I. Biosensors and nanomaterials and their application for mycotoxin determination. *World Mycotoxin J.* 2011;4:361–74.
- Vos R, Food I, Dc W, Programme WF, Dc W, States U, Turn E, Nations U, Change C, Security WF. War in Ukraine and the challenge to global food security. *Nature.* 2022;
- Wu J, Sun Q, Huang H, Duan Y, Xiao G, Le T. Enhanced physico-mechanical, barrier and antifungal properties of soy protein isolate film by incorporating both plant-sourced cinnamaldehyde and facile synthesized zinc oxide nanosheets. *Colloids Surfaces B Biointerfaces.* 2019;180:31–8.
- Wu Y, Zhou Y, Huang H, Chen X, Leng Y, Lai W, Huang X, Xiong Y. Engineered gold nanoparticles as multicolor labels for simultaneous multi-mycotoxin detection on the immunochromatographic test strip nanosensor. *Sensors Actuators B Chem.* 2020;316:128107.
- Xiulan S, Xiaolian Z, Jian T, Zhou J, Chu FS. Preparation of gold-labeled antibody probe and its use in immunochromatography assay for detection of aflatoxin B1. *Int J Food Microbiol.* 2005;99:185–94.
- Xu Y, Ma B, Chen E, Yu X, Ye Z, Sun C, Zhang M. Dual fluorescent immunochromatographic assay for simultaneous quantitative detection of citrinin and zearalenone in corn samples. *Food Chem.* 2021;336:127713.
- You KH, Luo XE, Hu WJ, Xu Y, Guo JB, He QH. Environmental-friendly gold nanoparticle immunochromatographic assay for ochratoxin a based on biosynthetic mimetic mycotoxin-conjugates. *World Mycotoxin J.* 2020;13:267–75.
- Youssef AM, Abdel-Aziz MS, El-Sayed SM. Chitosan nanocomposite films based on Ag-NP and Au-NP biosynthesis by *Bacillus Subtilis* as packaging materials. *Int J Biol Macromol.* 2014;69:185–91.

- Zhang X, Xiao G, Wang Y, Zhao Y, Su H, Tan T. Preparation of chitosan-TiO₂ composite film with efficient antimicrobial activities under visible light for food packaging applications. *Carbohydr Polym.* 2017a;169:101–7.
- Zhang X, Yu X, Wen K, Li C, Mujtaba Mari G, Jiang H, Shi W, Shen J, Wang Z. Multiplex lateral flow immunoassays based on amorphous carbon nanoparticles for detecting three *Fusarium* mycotoxins in maize. *J Agric Food Chem.* 2017b;65:8063–71.
- Zhang W, Tang S, Jin Y, Yang C, He L, Wang J, Chen Y. Multiplex SERS-based lateral flow immunosensor for the detection of major mycotoxins in maize utilizing dual Raman labels and triple test lines. *J Hazard Mater.* 2020;393:122348.
- Zhao S, Bu T, He K, Bai F, Zhang M, Tian Y, Sun X, Wang X, Zhangsun H, Wang L. A novel α -Fe₂O₃ nanocubes-based multiplex immunochromatographic assay for simultaneous detection of deoxynivalenol and aflatoxin B1 in food samples. *Food Control.* 2021;123:107811.
- Zhao X, Byrne HJ, O'Connor CM, Curtin J, Tian F. Limits of detection of mycotoxins by laminar flow strips: a review. *Appl Nano.* 2022;

Chapter 16

CRISPR/Cas Systems: A New Biomedical and Agricultural Diagnostic Devices for Viral Diseases



Aftab Ahmad, Sabin Aslam, Ahmad Munir, Farah K. Ahmed ,
and Kamel A. Abd-Elsalam 

16.1 Introduction

The health of people and the economy are significantly impacted by viruses and current epidemics. Recently, the use of CRISPR in disease diagnostics has increased as a result of our better understanding of CRISPR/Cas system properties. Innovative nucleic acid screening technologies are now possible, thanks to the identification of numerous RNA-directed nucleases and the Cas proteins (Srivastava et al. 2020). Genome editing techniques have brought a new weapon to the arsenal against viruses that affect humans, animals, and plants. Recent developments in the use of CRISPR/Cas technology to recognize and control plant viruses were carefully examined (Kimunye et al. 2021). For example banana RNA viruses may be successfully identified using CRISPR based method, enabling researchers to implement containment strategies. The CRISPR-based diagnostic technique follows the same pattern as reported procedures but at a cheaper cost. Rapid, sensitive, specific, and field-deployable detection is critical for efficient disease management and prevention. CRISPR/Cas system, being a precise genome editing tool, has been explored as a unique and potent diagnostic tool (Abudayyeh and Gootenberg 2021). Several

A. Ahmad · A. Munir

Department of Biochemistry/Center for Advanced Studies in Agriculture and Food Security (CAS-AFS), University of Agriculture Faisalabad, Faisalabad, Pakistan

S. Aslam

National Center for Genome Editing (NCGE), Center for Advanced Studies in Agriculture and Food Security (CAS/AFS), University of Agriculture Faisalabad, Faisalabad, Pakistan

F. K. Ahmed

Biotechnology English Program, Faculty of Agriculture, Cairo University, Giza, Egypt

K. A. Abd-Elsalam (✉)

Agricultural Research Center, Plant Pathology Research Institute, Giza, Egypt

rapid nucleic acid diagnostic kits have been developed and validated using Cas9, Cas12, Cas13, and Cas14 proteins. In this chapter, we offer an overview of current advances and future directions for investigating novel CRISPR/Cas approaches in biomedical and agricultural diagnostic devices for viral infections (Fig. 16.1). We have highlighted the point-of-care (POC) CRISPR sensing and its future research directions. Finally, we have discussed the challenges and future prospects of CRISPR-based diagnostic platforms in biomedicine and agriculture.

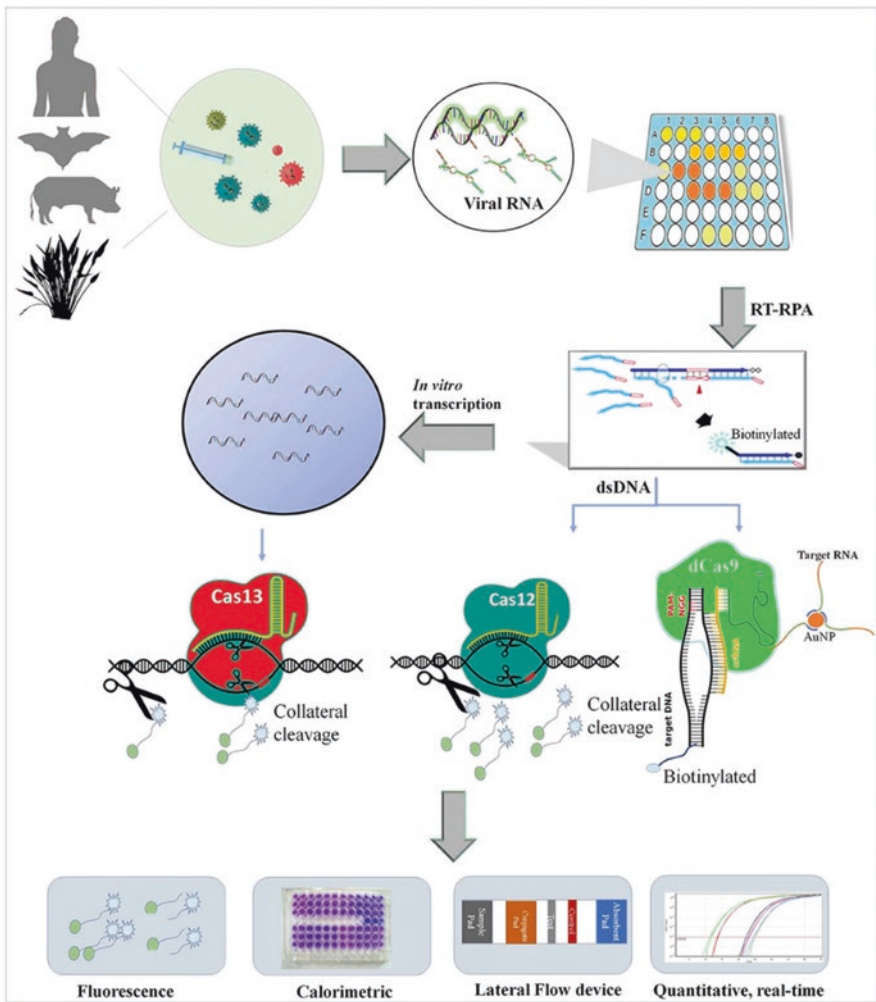


Fig. 16.1 Demonstration of the multiplexing of Cas9, Cas12, and Cas13 to identify viruses from various bio-sources. (Srivastava et al. 2020)

16.2 CRISPR/Cas-Based Diagnostic Tools

16.2.1 CRISPR: An Introduction

CRISPR repeats were discovered initially in *E. coli* in 1987 and were later observed in a variety of prokaryotes. The function of these repeats remained unknown until 2005 when many researchers found potential role of these repeats in adaptive immune system of bacteria (Luo et al. 2021). CRISPR/Cas9 was initially reported for precise eukaryotic genome editing in 2013. At present, CRISPR/Cas is the most widely used genome editing technique with a broad range of applications in agriculture, medicine, and industries. Genome editing of animals and plants has taken many years and millions of dollars before the discovery of CRISPR/Cas in 2012, which has aroused the attention of scientists specially for diagnosis and therapy of diseases because of its effectiveness, less cost, and greater precision compared to previous genome editing methods. CRISPR and CRISPR-associated proteins are important components of the immune system of bacteria, offering protection against invading bacteriophages, plasmids, and other foreign elements of DNA. CRISPR/Cas systems are categorized into two major classes with 6 types and 21 subtypes. The repeat sequence ranges in length from 25 to 40 nucleotides, whereas the spacer sequence ranges from 21 to 71 nucleotides (Liu et al. 2020).

16.2.2 Applications of CRISPR

16.2.2.1 CRISPR Applications in Plant Breeding

CRISPR can be used in diverse fields including agriculture, health metabolic engineering and synthetic biology. It works in almost all organisms and has limitless applications in plant breeding. Improved yield is by far the most investigated characteristic, followed by biofortification and herbicide tolerance, according to an analysis of 52 peer-reviewed studies on the agricultural use of CRISPR.

This is an advanced tool in the toolbox for plant breeders to generate desirable trait in their target plant species, especially when compared to the traditional breeding technique of crossing germplasm, which can take years to produce improved and new varieties.

16.2.2.2 CRISPR Applications in Animal Breeding

As a precise, efficient, and quicker technique of genome editing, the CRISPR system is used in animal breeding and disease modeling. When paired with gene editing technology, there are several methods for creating animal models. By injecting mRNA or RNP (Ribonucleoprotein) into zygotes or using donor cells that have been

genetically modified as embryonic stem (ES) cells, gene-edited animals can be produced. Animal organs can be subjected to genome editing via microcarriers, such as viral vectors and nanoparticles. Various modeling techniques were employed depending on the species. It is possible to create chimeras—gene-edited creatures—by injecting ES cells into rats or other tiny animals with shorter reproductive cycles. From there, homozygous mutant animals can be created by natural mating. However, for large animals, directly injecting the CRISPR system into the zygote and then transferring the embryo is the most efficient method for producing gene-edited animals. As CRISPR's effectiveness and specificity increase, it is being used in large animals, such as monkeys (Barrangou and Doudna 2016).

16.2.2.3 CRISPR Applications in Biotherapy

A lot of laboratories are now working on CRISPR-based medicines. Since there are numerous ongoing preclinical trials to discuss, our goal is to focus on the important clinical research. Gene editing therapies mostly fall into two categories: ex vivo and in vivo. To achieve high efficiency and safety, ex vivo gene editing is preferred for cells that can be removed from patients, altered in the lab, and then grafted back into patients. Hematopoietic genetic disorders may be treated by correcting genetic defects in human hematopoietic stem and progenitor cells (HSPCs). Recently a number of CRISPR treatments have begun clinical trials. More clinical data is required to determine the efficacy and safety of CRISPR-based therapy (Chen et al. 2020).

16.2.3 CRISPR/Cas

The CRISPR/Cas system is a component of the prokaryotic immune system that aids in the resistance to plasmids and phages' genetic elements. This mechanism was found in bacteria, where it collects DNA segments from invading viruses to generate CRISPR arrays. The array aids the bacteria in remembering the viral sequence, allowing them to manufacture these RNA segments from the CRISPR array and target the viral DNA in the event of a reattack. It resembles bacterial immune system (Hille and Charpentier 2016).

16.2.4 CRISPR/Cas Mechanism

CRISPR-based prokaryotic adaptive immunity has two unique molecular mechanisms: (i) immunization/acquisition and (ii) defense/resistance. The alien genetic elements provide a novel spacer sequence known as protospacer. For several CRISPR/Cas systems, the protospacer sequence must be found closer to a short

motif termed the protospacer adjacent motif (PAM). PAM recognition by CRISPR prevents the host CRISPR array from being destroyed by its own Cas machinery. The activity of the Cas1 and Cas2 proteins is critical for the adaptation step. For crRNA biogenesis, CRISPR array elements create precursor crRNAs (pre-crRNA), for processing to mature crRNA (Fig. 16.2).

Cas proteins are responsible for maturation. The crRNA is used by Cas complex to check for sequence complementarity in foreign nucleic acids. The Cas nuclease is triggered, and the foreign genetic material is specifically targeted and destroyed if both complementarity and a PAM site are met. The CRISPR/Cas system has emerged as a breakthrough genetic engineering method due to its great efficiency, specificity, and modular nature. Genome editing, drug discovery, gene expression control, and the diagnosis, prevention, and therapy of a wide range of disorders have all benefited from this technique. The deployment of CRISPR/Cas systems to manage viral diseases and the problems experienced in this field were reviewed in this study (Nussenzweig and Marraffini 2020).

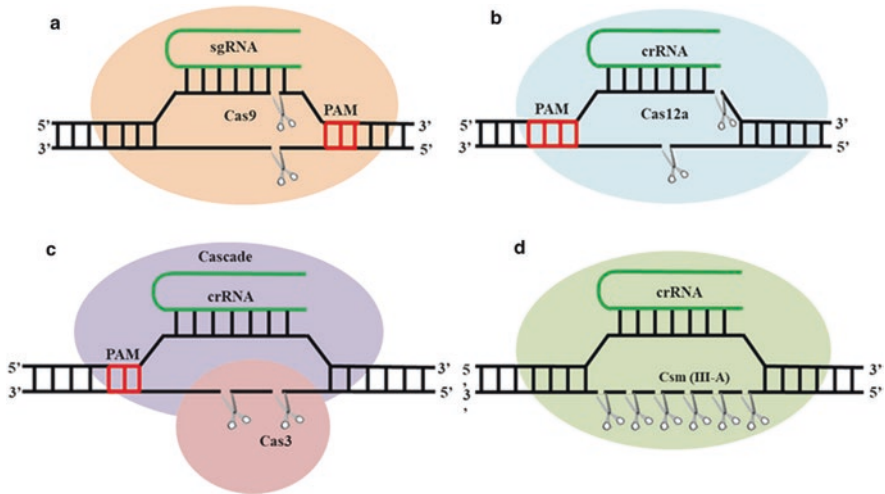


Fig. 16.2 This diagram describes the mechanics of a variety of CRISPR/Cas systems. (a) Type II CRISPR/Cas9. sgRNA guides CRISPR/Cas9 protein to the target region to cleave both strands in the presence of the PAM region, resulting in blunt ends. (b) Type V CRISPR/Cas12a protein. crRNA helps CRISPR/Cas12a protein to recognize target sequence and cleave both strands in the presence of PAM region, resulting in formation of sticky ends. (c) Type I. crRNA, in the presence of the PAM sequence, directs the CRISPR/Cas3 to cleave noncomplementary strand, resulting in a large gap. (d) Type III CRISPR/Cas systems. The sgRNA, in the absence of PAM sequence, instructs the Csm protein to cut the noncomplementary strand, resulting in the formation of short fragments of nucleic acids. The molecular scissors represent the nuclease cleavage site, the green transverse U indicates crRNA or sgRNA, and the PAM region is shown in red nucleotide sequence

16.2.5 CRISPR/Cas System

The number of distinct CRISPR/Cas systems has significantly increased since their discovery. CRISPR/Cas systems are now split into different classes and sub classes based on evolutionary links. The composition of the ribonucleoprotein effector complex defines the class of CRISPR/Cas system. Class 1 system has a complex of several effector proteins, whereas class 2 system has a single crRNA-binding protein. crRNA for the various effector proteins are used in CRISPR diagnostics.

CRISPR/Cas systems are composed of two components, Cas protein for nucleic acid cleavage, whereas second component is gRNA.

16.2.5.1 Cas3

Cas3 endonuclease is recruited by Cascade when it binds to a target to cleave foreign DNA. Type I-E of *Escherichia coli* is the most biochemically defined subtype among the seven subtypes. The type I-E Cascade is made up of five proteins of varying stoichiometry.

16.2.5.2 Cas9

Early CRISPR-based diagnostic approaches often employed variants of Cas9 to recognize dsDNA. The principle of different Cas9 variant-based strategies, which has been reported for detection of DNA, includes destabilization of PAM regions, inactive Cas9-induced guide-directed rearrangements of split proteins, and CRISPR/Cas9-mediated unwinding of non-targeted DNA strand as a target site for isothermal amplification. Nucleic acid sequence-based amplification CRISPR cleavage (NASBACC) is a CRISPR/Cas9-based strategy that includes PAM-dependent identification of target through Cas9 cleavage, isothermal preamplification of target sequence, and toehold sensor to readout. Reverse transcription couples a toehold trigger to RNA fragment amplified through NASBA. If the PAM region is present in amplified region of RNA, CRISPR/Cas9 cleaves this fragment, which results in the formation of shortened RNA fragment that lacks the trigger region. If there is no PAM region, the trigger that is carrying non-cleaved RNA stimulates toehold switch, which is shown by change in color. By identifying PAM sites in specific strains, this technique will allow for separation of virus lineages. The presence of the Zika virus (ZIKV) at low femtomolar levels in infected monkey plasma has been detected by this approach. Another CRISPR/Cas9-based approach called LEOPARD (for leveraging engineered tracrRNAs and on-target DNAs for parallel RNA detection) allows for the detection of multiplex RNA. The strategy is predicated on the observation that tracrRNAs, which are essential for crRNA and crRNA complex formation in type II systems, hybridize with cellular RNAs, resulting in noncanonical

crRNAs. CRISPR/Cas9 may be directed to a DNA target by reconstituting tracrRNA to bind genes of interest and encouraging Cas9-crRNA complex formation through resultant noncanonical crRNAs.

16.2.5.3 Cas12

Cas12 enzymes that cut both dsDNA and ssDNA need a PAM site in the target region for dsDNA cleavage and to cleave ssDNA collaterally. DETECTR is one of the innovative detection algorithms based on Cas12 released in 2018. Cas12a from the *Lachnospiraceae* bacteria (LbCas12a) or Cas12a from another species was guided to dsDNA target by a complementary crRNA, resulting in collateral cleavage of short ssDNA reporters containing a fluorophore and a quencher. Target identification and cleavage of reporter molecules result in the separation of the quencher and fluorophore, generating a fluorescent signal. When DETECTR was used with RPA preamplification, it attained attomolar sensitivity. HOLMES (for 1-hour low-cost multipurpose highly efficient system), which employs PCR as preamplification in conjunction with LbCas12a, and HOLMESv2 uses loop-mediated isothermal amplification (LAMP) in a one-pot reaction with a thermostable Cas12b from *Alicyclobacillus acidoterrestris* (AacCas12b).

HOLMES and HOLMESv2 both have a detection limit of roughly 10 aM. Cas12f targets both dsDNA and ssDNA, although it distinguishes SNPs in ssDNA better than Cas12a.

16.2.5.4 Cas13

CRISPR/Cas13, composed of 900–1300 amino acids, belongs to type VI class 2 recognizes single-stranded RNA in cis and possesses trans-cleavage collateral activity in vitro against single-stranded RNA. In CRISPR/Cas13-based SHERLOCK test (specific high-sensitivity enzymatic reporter unlocking), DNA or RNA is first amplified by a process known as recombinase polymerase amplification, employing a forward primer that recruits a T7 promoter to the target, which causes the synthesis of target RNA that is subsequently recognized and bound by CRISPR/Cas13a. By collateral trans-cleavage activity, the activated CRISPR/Cas13a will cleave both on-target RNA strand and the ssRNA reporter molecules in a target-dependent manner. A short RNA oligomer holds a fluorophore and a quencher together, allowing the fluorophore and quencher to be separated when cleaved, resulting in fluorescence. These methods may detect the presence of bacterial DNA, viral RNA, SNPs, and cancer-related mutations with high attomolar sensitivity ranging from 10 to 18 M. The second version of this assay (SHERLOCKv2) allowed multiplex quantitative detection of nucleic acids at zeptomolar concentrations ranging from 10 to 21 M, as well as a lateral flow readout, which is based on immunochromatographic assay in which cleaved ssRNA reporter molecules have been detected on a paper strip using gold nanoparticles conjugated with antibody.

16.2.5.5 CRISPR/Cas14

The Cas14 gene has 24 variants, which are divided into three subgroups: Cas14a–c. Regardless of sequence variation, all Cas proteins have a conserved RuvC nuclease domain. Cas14, on the other hand, is only found in archaea, but not in bacteria. As a result, this gene may be more primitive than the two Cas protein variants, Cas9 and Cas12. The Cas14 gene's modest size implies that it might function as a stand-alone CRISPR effector. Cas14's ability to target single-stranded DNA implies it may have evolved to protect against single-stranded DNA viruses or mobile genetic elements that can spread via single-stranded intermediary structures (Barrangou and Marraffini 2014).

16.2.6 CRISPR Methods and Techniques

The basic principle of genome editing is based on gene deletion by nonhomologous end joining (NHEJ) and gene knock-in via homologous recombination (HR).

16.2.6.1 CRISPR-Mediated Gene Knockout

When Cas9 induces a DSB, it is repaired by inherent repair pathway (NHEJ). NHEJ is prone to errors and leads to indels at the target site. If indels are present in an exon region, it will result in a frameshift mutation. This phenomenon is termed as gene knockout (KO). Functional genomics, drug development and screening, pathway analysis, and illness modeling are prominent areas of gene knockout applications. Numerous guided RNAs targeting multiple genomic sections can highly increase the efficiency of gene knockouts.

The possibility of disrupting gene function and altering crops in ways that are advantageous from an agronomic standpoint exists because of genome editing. Using an RNA-guided genome editing strategy, the type II CRISPR/Cas9 has recently been employed to successfully produce targeted mutagenesis in a number of plant species including rice, cotton, wheat and tomato. The phytoene desaturase gene (CIPDS), which was chosen for targeted by the CRISPR/Cas9 system due to its albino phenotype, can be altered in watermelons using the CRISPR/Cas9 technology. The CRISPR/Cas9 system was used to edit the genome of watermelon at predetermined locations. What's more, all transgenic watermelon plants possess CIPDS mutations that showed a clear or mildly mosaic albino phenotype, indicating that the CRISPR/Cas9 technique can theoretically completely alter the genome of transgenic watermelon lines. Furthermore, sgRNA-like portions were examined, and it was concluded that there were most likely no off-target modifications. These findings indicated that the CRISPR/Cas9 system is an effective method for genome editing (Yang et al. 2018).

16.2.6.2 CRISPR/Cas Knock-In

When Cas9 introduce DSB in cells, it can be repaired by HDR (Homology directed repair), thereby providing a nick for insertion of a foreign piece of DNA—a technique termed as gene knock-in. To achieve an accurate knock-in, donor template is required. The insert is flanked between the bordering elements that share sequence homology to flanking regions of DSB. Recombinant proteins, viable immortalized cell lines, and gene modeling are the products of gene knock-ins. The phenomenon can be used to fix genetic disorders.

CRISPR knock-ins are difficult to achieve than knockouts as HDR occurs only at a specific stage of cell cycle that markedly lowers the efficiency of CRISPR knock-ins. This problem can be overcome by cell cycle synchronization and therapies that prefer HDR over NHEJ to achieve accurate knock-in (Yang et al. 2018).

16.2.6.3 CRISPRa and CRISPRi

CRISPR system can modulate insertion, deletion, and gene expression. CRISPR activation (CRISPRa) and CRISPR interference (CRISPRi) upregulate and down-regulate gene expression, respectively. Both of these phenomena become activated by combination of a Cas9 variant—catalytically dead Cas9 (dCas9) and transcriptional effectors. Because dCas9 does not cleave DNA, it guides transcriptional effectors toward the gene of interest. Disease prevalence, functional genomics, and screening for gene elements for different therapies are a few of the scientific applications of such gene modulators.

16.2.6.4 CRISPR/Cas System Screens

CRISPR technology has enabled precise, wide range screening of drug discovery trials to better understand the phenotype/genotype linkage. CRISPR/Cas system screens normally implicate generating a large sgRNA library targeting numerous genes, applicable to a range of adaptations to a cell line, and then analyzing its phenotypic effect. Knocking out of various genes in healthy cell lines may lead to determination of pathogen-responsive genes; the same procedure can be followed for identification of therapeutic marks. CRISPR screens offer consistent and precise outcomes with lesser off-target effects than prevailing RNAi screens being utilized in drug discovery. Identification of targets and its validation can be assessed by the latest techniques available. Knockout strategies developed by Synthego for multi-gRNAs proven the marked accuracy for identifying targets and their validation (Yang et al. 2018).

16.2.6.5 Base Editing and Prime Editing

Recent advances in CRISPR system led to the base editing and prime editing that work on smaller scale for modification of single base pair and don't cause double-strand break (DSB). This phenomenon utilizes catalytically deactivated Cas9 (dCas9) or a Cas9 nickase (nCas9). nCas9 produces a nick falsely assumed as single-strand break (SSB) as dCas9 is not capable to cut the DNA. A DNA-modifying enzyme coupled with dCas9 or nCas9 is able to change single nucleotide. Since each conceivable nucleotide can't be changed by base editing, nCas9 can be fused with a customized restriction endonuclease and gRNA to peruse prime editing. Prime editing works in two steps: (1) detection of gene of interest and (2) substitution to repair SSB. Complementary strand auto repairs itself after reading the change made by prime editing. On these basis, prime editing is able to correct nearly 89% of mutations in the human genome (Yang et al. 2018).

16.2.7 CRISPR/Cas Diagnostic Tools

Strong and sensitive isothermal amplification diagnostic tools for bacteria, viruses and different pathogens have been developed using CRISPR/Cas targeting (Chertow 2018; Khambhati et al. 2019). A gRNA aids in the identification of the target DNA sequence and recruits the Cas enzyme to cleave DNA, which is then detected by a chromogenic or fluorometric method. In order to detect numerous infectious viruses and bacterial pathogens using multiple Cas proteins have been discovered (Gootenberg et al. 2017). Cas13 is the best at using RNA guides to find homologous RNA sequences, whereas Cas12 and Cas14 are superior at finding single strand break and double strand break respectively, they direct gRNA to target sites (Fig. 16.3). The "specific high-sensitivity enzymatic reporter unlocking (SHERLOCK)" system was created to identify the target sequence by isothermally amplifying the target molecule using recombinase polymerase amplification (RPA), reverse transcription (RT)-RPA, loop-mediated isothermal amplification (LAMP), or RT-LAMP (Gootenberg et al. 2017). The heating unextracted diagnostic samples to obliterate nucleases (HUDSON) method was also utilized for viral detection in body fluid without a DNA extraction step (Myhrvold et al. 2018). Without the need for nucleic acid extraction, this method has been shown to be sensitive for identifying viral strains and clinically important changes (Myhrvold et al. 2018). CRISPR/Cas diagnostic approaches may preamplify the target molecule using PCR or RT-PCR, or they may use isothermal amplification techniques, such as RPA or RT-RPA and LAMP or RT-LAMP, depending on the kind of target viral genome. Lateral flow device separation techniques, a SYBR Green fluorescence detection system, or signals provided by a reporter RNA molecule based on a fluorophore-quencher are used to identify the target molecules (B. Wang et al. 2020). An enhanced and standardized Exo-RPA isothermal detection method targeting the BBTV (Banana Bunchy Top Virus) DNA segment has been developed for plant

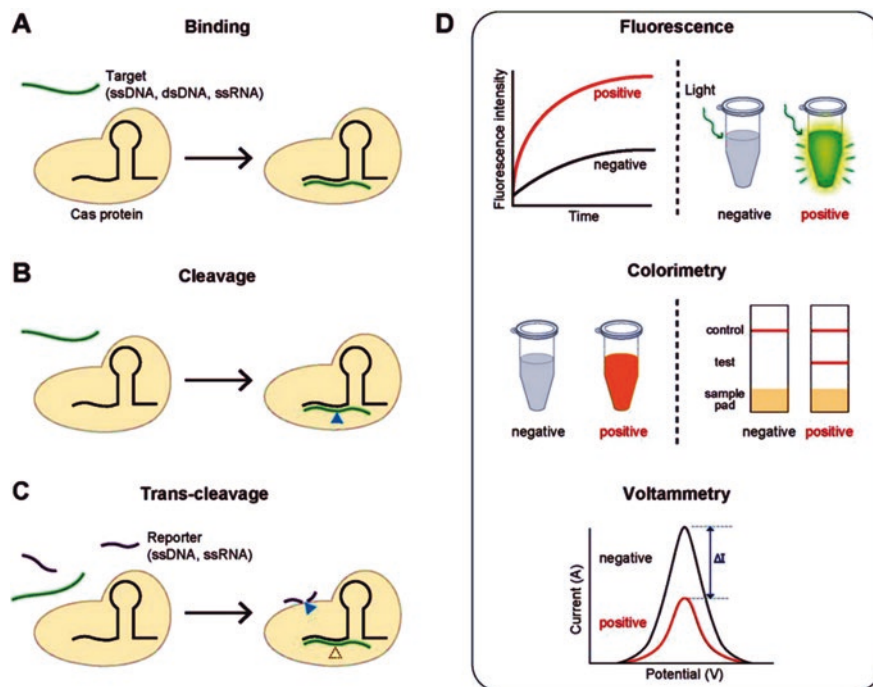


Fig. 16.3 CRISPR/Cas offers three methods for identifying signals that are often picked up by the system. (a–c) The three steps used by the CRISPR/Cas system to identify target genes. (a) Sequence-based target binding. Catalytically inactive Cas proteins bind to the complementary target gene of gRNA. (b) Sequence-based cleavage. Sequence-specific binding occurs after the Cas proteins break the target gene. (c) Trans-cleavage for a particular target. When Cas proteins, such as Cas12a and Cas13a, bind to a target gene, they cleave the ssDNA or ssRNA nearby. (d) Signal detection may be accomplished in one of three ways. The presence of a target gene can be detected by monitoring fluorescence, colorimetric, or electric signals. (Reprinted from Kim, S.; Ji, S.; Koh, H.R. CRISPR as a Diagnostic Tool. *Biomolecules* 2021, 11, 1162)

tissue virus detection (Tripathi et al. 2021). In a fluorometer, the amplified products are recognized using FAM (Fluorescein amidite)-labeled Exo-RPA probes (Khambhati et al. 2019). A HUDSON-SHERLOCK hybrid detection system is being developed using the BBTV Exo-RPA assay to identify viruses both in the lab and in the field is an efficient and cost effective measure. BSV and its variations are being identified using CRISPR-based diagnostics, which are being adapted from the currently used PCR-based BSV detection procedures. CRISPR-based diagnostic approaches have the potential to provide quick and sensitive detection of banana viruses for seed surveillance, health certification, and a variety of other applications because of its robustness for identifying single copies of the target molecules. The focus of this book chapter is on mobile devices for field use and the next generation of CRISPR/Cas-based molecular diagnostic methods.

16.2.7.1 CRISPR/Cas3

CONAN-Cas3

CONAN: Nucleic acid detection using Cas3. The Cas3 endonuclease, in association with Cas5, Cas6, Cas7, Cas8, and Cas11, facilitates targeted DNA cleavage in this CRISPR-based technology. CONAN, when used in conjunction with isothermal amplification protocol, provides a 90 percent reliable method for detecting SARS-CoV-2. This assay not only identifies SARS-CoV-2 in clinical samples but also recognizes single-base-pair mutations in IAV (Influenza A Virus) variants with pinpoint accuracy. In hospitals, this instrument provides for speedy and efficient level testing for patients suspected of having SARS-CoV-2 or drug-resistant IAV infections. When combined with isothermal amplification methods, the CONAN apparatus offers a sensitive, fast, and device-free diagnostic option for SARS-CoV-2 diagnosis. CONAN was constructed in two different formats: fluorescent microplate reader detection or lateral flow analysis. CONAN is appropriate for gene screening, the prevention and control of infectious diseases, and the early detection and treatment of serious disorders. CONAN can be improved by combining existing or new Cas protein variants with a variety of unique characteristics of nucleic acid circuits. Furthermore, combining CONAN can increase the platform's adaptability with microfluidics and nanotechnology.

16.2.7.2 CRISPR/Cas9

CARP-Cas9

CARP (CRISPR/Cas9/sgRNAs-associated reverse PCR) is a new method for detection of DNA fragments based on nuclease activity of Cas9. CARP was created by combination activity of CRISPR/Cas9 with PCR techniques. This approach employs three steps to detect the target DNA: (1) cleavage of detected DNA using CRISPR/Cas9 and sgRNA complex, (2) ligation of cleaved DNA using DNA ligase, and (3) amplification of DNA fragment using PCR (Vatankhah et al. 2021). Cas9 can identify closely similar strain of Zika virus in vitro, and identification of viral RNA was shown by color change from yellow to purple on the paper disc (Pardee et al. 2016). In this process, viral RNA was converted to DNA through RT-PCR, the amplified DNA was verified via CRISPR/Cas9 cleavage, and the results were analysed via colorimetric toehold RNA switch sensors. Another method of improving viral genome detection used CRISPR/Cas9-based isothermal exponential amplification (CAS-EXPAR), which demonstrated attomolar (aM) sensitivity and single-base specificity for differentiating between American and African strains via colorimetric-based detection using SYBR Green fluorescence signals (Huang et al. 2018). For the purpose of detecting the African swine fever virus, the CASLFA (Cas9-assisted lateral flow assay) method was developed. This diagnostic tool kit shows how CRISPR/Cas9 can detect viral nucleic acids with great sensitivity in lateral flow (X. Wang et al. 2020). The proliferation of CRISPR/Cas9 diagnostic kits increases

the demand for dCas9 protein due to the creation of dCas9 or deactivated Cas9, which binds to the target DNA with specificity without inducing cleavage. A method to find COVID-19 virus using dCas9 and FnCas9 was developed to check the viability of a POCT kit for a variety of uses, such as quick detection during pandemic outbreaks, such as COVID-19 (Azhar et al. 2020).

CAS-EXPAR and NASBACC-Cas9

The NASBACC (NASBA-CRISPR cleavage) and CRISPR/Cas9-gRNA complex-isothermal exponential amplification reaction platforms may be employed to distinguish between SNPs and pathogen genotypes. NASBACC is a platform that integrates Cas9, T7 transcriptional promoter, and toehold switch sensors with NASBA (nucleic acid sequence-based amplification), a kind of isothermal amplification of RNA. This approach detects ZIKA virus, differentiates strains with single-nucleotide accuracy, and is suitable for usage in resource-constrained environments. The EXPAR (isothermal exponential amplification reaction) is an oligonucleotide amplification technique, which operates at constant temperature for detection of various molecules, such as DNA or RNA. The EXPAR technique multiplies the nucleic acids 106–109 times in a very short time. But this method has a limitation in molecular detection due to high degree of nonspecific amplification of this method. The CRISPR/Cas9 and guide RNA complex on the platform of CAS-EXPAR offers great specificity and quick DNA/RNA and methylated DNA detection in just 1 hour using specific primers. The remarkable specific activity of this technique is due to nuclease activity of CRISPR/Cas9 and gRNA complex on the target gene and the DNA polymerase enzyme's sequence-dependent amplification (Vatankhah et al. 2021).

FELUDA-Cas9

FnCas9 editor-linked uniform detection assay (FELUDA-Cas9) is a technique used for the diagnosis of genetic disorders and infectious diseases, such as COVID-19. This technique uses FnCas9 in conjugation with RPA or PCR and is very sensitive to detect mismatches in DNA. It was created for rapid and reliable nucleic acid detection and utilizes a very precise readout to identify sequences of nucleic acid. This technique was also tested for SARS-CoV-2 diagnosis because it does not need any other specific tools and may be a cost-effective and time-saving choice to other diagnostic procedures, such as PCR-based technologies. This approach also detected SNVs (single-nucleotide variants) with great precision in Mendelian diseases, such as hemophilia A and sickle cell anemia. The SNV distinction results are analyzed by using gel electrophoresis, suggesting that this technique may be used routinely in molecular labs. Due to the lack of specialist equipment required, FELUDA has been proposed as a substitute for RT-PCR for the detection of SARS-CoV-2 in less than an hour (Vatankhah et al. 2021).

16.2.7.3 CRISPR/Cas12

Despite the fact that it is frequently used to identify many diseases in both humans and animals (Li et al. 2019a) (van Dongen et al. 2020). In order to create CRISPR/Cas diagnostics, the Cas12a and Cas12b enzymes were used. For site-specific cleavage of dsDNA, Cas12a uses the DETECTR method to identify PAM sequences with high T content (DNA endonuclease-targeted CRISPR trans-reporter approach). The target RNA or DNA molecule is amplified using isothermal amplification techniques such as PCR and LAMP/RT-LAMP. The degradation of the ssDNA fluorophore-quencher reporter probe is used to identify amplified dsDNA products. Findings are ascertained using colorimetric or fluorometric detection (Broughton et al. 2020).

The standardization of the HOLMES-based diagnostic test revealed that approximately ten different bacterial Cas12a were suitable for the identification of DNA viruses, such as pseudorabies virus and RNA viruses including Japanese encephalitis virus. As a result of the HOLMES expansion, which makes use of the Cas12b action, the more complex HOLMESv2 was created. In HOLMESv2, Cas12b was standardized for a number of uses, such as single-nucleotide polymorphism (SNP) detection, viral RNA amplification, and detecting and measuring DNA methylation via bisulfite treatment. Human papillomavirus (HPV) detection in the samples was likewise accomplished by DETECTR using RNA-guided Cas12a (Mahas et al. 2021). The generation of CRISPR/Cas12a-based nucleic acid diagnostic methods to differentiate between the two geminiviruses tomato yellow leaf curl virus (TYLCV) and tomato leaf curl New Delhi virus (ToLCNDV). In order to identify TYLCV and ToLCNDV in infected plants, they had good specificity and sensitivity. This novel nucleic acid detection device can finish an experiment in approximately an hour and offers straightforward, cost-effective visual readouts via a straightforward, low-cost fluorescence visualizer, making it a great technology for point-of-use applications. It has been demonstrated in several investigations that LAMP can amplify viral genomes directly from unprocessed samples (loop-mediated isothermal amplification) (Panno et al. 2020). The findings of this study demonstrate the effectiveness of the LAMP-coupled Cas12a method as a fast and accurate diagnostic tool for plant DNA viruses. Because of this, further advancements in the LAMP-coupled Cas12a approach might make it possible to use this assay to construct in-field diagnostic tests. The main advantage of CRISPR-based genome editing is that it can modify crop genomes for antiviral detection of viruses with a minimum amount of off-targeting. The aforementioned research amply demonstrates the adaptability, effectiveness, and precision of CRISPR-based genome editing techniques in the development of potent antiviral immune systems in agricultural plants. Recently, a rapid and efficient RT-RPA-CRISPR/Cas12a system was created as a single-step detection test for plant RNA viruses (Aman et al. 2020). In order to recognize plant RNA viruses, this diagnostic method makes use of a fluorescence visualizer. It might be finished in the field in under 30 minutes at a particular temperature. The DETECTR assay was developed to identify SARS-CoV-2 using novel CRISPR/Cas12-based technologies. It was marketed as a visible and quicker alternative to

the SARS-CoV-2 real-time RT-PCR test (Broughton et al. 2020). The newly released all-in-one dual CRISPR/Cas12a (AIOD-CRISPR) and iSCAN (in vitro specific CRISPR-based assay for nucleic acid detection) Cas12a-based rapid and highly sensitive kits, which successfully identify both SARS-CoV-2 and HIV, are also used to diagnose current SARS-CoV-2 situations (Ali et al. 2020; Ding et al. 2020). These methods likewise rely on the collateral cleavage activity of the ssDNA probes. It has been considered how this protein can help identify shrimp white spot syndrome (Chaijarasphong et al. 2019). Additionally, diagnostic kits for lateral flow devices based on CRISPR/Cas12 and tests using fluorimeters were created. When it comes to diagnostics, Cas12a is the most researched effector. The Cas12a-based approach is more stable in the field since ssDNA probes are used in place of RNA probes. This approach reduces time, expense, and technical errors because it does not require RNA synthesis from amplified target DNA via in vitro transcription, unlike Cas13-based detection. Due to their critical function in the diagnosis of DNA viruses without the need for RNA transcription, Cas12-based diagnostics are helpful for the detection of both DNA and RNA viruses (Table 16.1).

DETECTR-Cas12

DETECTR (DNA endonuclease-targeted CRISPR trans reporter) is a Cas12a-based DNA endonuclease-targeted CRISPR trans-reporter assay for highly sensitive and specific identification of nucleic acids from infected materials. In DETECTR, the target nucleic acid is amplified by RPA or RT-RPA using isothermal amplification, which then binds the Cas12a-sgRNA complex and causes the cleavage of a ssDNA fluorophore-quencher reporter, resulting in a fluorescent signal. DETECTR has attomolar sensitivity and good specificity for detecting DNA sequences. To detect and genotype HPV strains in patient samples, DETECTR was used. DETECTR interacts with Cas12a, which connects to DNA targets using its guide crRNA. When Cas12a binds to dsDNA, it can also cleave unrelated ssDNA, a process known as target-recognizing collateral cleavage. Off-target ssDNA “shredding” was found in numerous species when Cas12 proteins were activated, but not all. In vitro, activation of Cas12a in the DETECTR test results in incredible efficiency. The DETECTR method preamplifies conserved gene regions in the N and E genes of SARS-CoV-2 using reverse transcription-loop-mediated isothermal amplification (RT-LAMP) and then employs Cas12a’s collateral ssDNA cleavage activity to detect the amplicons (Palaz et al. 2021). The DETECTR method’s key benefit is its great sensitivity, as it can identify a single molecule of viral particle inside a microliter of material (Kocak and Gersbach 2018). The DETECTR approach has been utilized to detect this virus, and in the applications reported, it concentrates on recognizing the presence of SARS-CoV-2 N and E gene variants. If both genes are found, a positive result is obtained, and the technique has been refined to eliminate false positives caused by related coronaviruses (Broughton et al. 2020). In concept, the DETECTR (DNA endonuclease-targeted CRISPR trans reporter) technology is similar to SHERLOCK, as depicted in Fig. 16.4.

Table 16.1 Plant virus detection using CRISPR systems

| Plant | Plant pathogens | CRISPR methods | Targeted genomic region | References |
|-------------|---|----------------------|-----------------------------|-------------------------------|
| Tobacco | Tomato leaf curl New Delhi virus and the tomato yellow leaf curl virus (ToLCNDV) | CRISPR/Cas12a | Coat protein (CP) | Mahas et al. (2021) |
| Sugar beet | Necrotic yellow veins in beets (BNYVV) | CRISPR/Cas12a | RNA-1 | V. Ramachandran et al. (2021) |
| Tomato | Tomato mosaic virus (ToMV) | CRISPR/Cas12a | ORF1 | Alon et al. (2021) |
| Tobacco | Cotton leaf curl virus (CLCuV) | CRISPR/Cas9 | Rep, p.C1 | Khan et al. (2020) |
| Tobacco | Tobacco mosaic virus (TMV), potato virus X (PVX), potato virus Y (PVY) | CRISPR/Cas12a | Coat protein (CP) | Aman et al. (2020) |
| Banana | Banana streak virus (BSV) | CRISPR/Cas9 | ORF1, ORF2, and ORF3 of BSV | Kimunye et al. (2021) |
| Apple | Apple necrotic mosaic virus (ApNMV), apple stem pitting virus (ASPV), apple stem grooving virus (ASGV), apple chlorotic leaf spot virus (ACLSV), apple scar skin viroid (ASSVd) | CRISPR/Cas12a | Coat protein (CP) | Jiao et al. (2021) |
| Apple, pear | Fire blight (<i>Erwinia amylovora</i>) | CRISPR (CR1-CR2-CR3) | T3SS, T3E | Mendes et al. (2021) |
| Rice | Rice blast disease (<i>Magnaporthe oryzae</i>) | CRISPR/Cas12a | Cry1 C | Zhang et al. (2020) |

Cited from Sharma et al. (2021)

HOLMES-Cas12a

The HOLMES (1-hour low-cost multipurpose highly efficient system) was the first technique to be developed for nucleic acid detection using collateral activity of CRISPR/Cas12a that amplifies target DNA or RNA with greater efficiency. After recognizing the target sequence, the CRISPR/Cas12a possessing trans-cleavage activity cuts quencher or fluorescence probes of single-stranded DNA. The sensitivity of HOLMES has a range of 1–10 amol/L and is capable of detecting human SNPs and RNA/DNA in less than an hour at an affordable cost. HOLMESv2, an enhanced HOLMES platform, helps to detect mRNA splicing, circular RNA, and RNA viruses in a single step. With the use of AacCas12b and LAMP, RT-LAMP, or Bst 3.0 DNA polymerase, it can also discriminate between single-nucleotide mismatches (SNMs) and quantify the methylation of DNA. LAMP or asymmetric PCR was used to amplify target DNA containing SNPs. To use this biosensing device to recognize RNA, its amplification using Bst 3.0 DNA polymerase is necessary, or

convert it to cDNA through a technology called RT-LAMP. Bst 3.0 DNA polymerase is able to amplify both DNA and RNA templates. The HOLMESv2 system has a limit of detection (LOD) of 10 amol/L for target DNA and 1 pmol/L to 10 amol/L for target RNA in urine samples (Vatankhah et al. 2021).

SENA-Cas12a

SENA (specific enhancer for PCR-amplified nucleic acids) is another CRISPR-based diagnostic technology, which is safe and simple to use and cost-effective. It does not require any extra instrument. SENa has a lower LOD (limit of detection) per reaction than rRT-PCR that is at least of two copies. Significantly, it is capable of effectively overcoming the uncertainty concerns inherent in PCR-based diagnosis, making it relevant to diagnosis of COVID-19 and a variety of other clinical circumstances. Apart from minimizing false positive and negative diagnoses, extremely sensitive approach of this technique can be used to evaluate if the virus has been eliminated from cured patients. Because the qPCR technique is still the most widely used in the detection of molecules and the SENa-Cas12a system is characterized by its operational simplicity, it has potential to overcome the blurriness issues associated with methods of molecular detection, such as qPCR based on nucleic acid amplification.

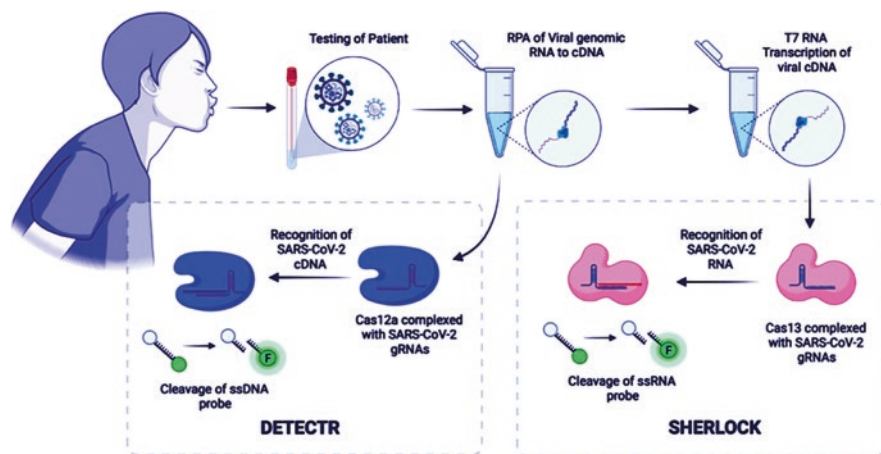


Fig. 16.4 The process involved in using the DETECTR and SHERLOCK CRISPR diagnostics, which use Cas12 and Cas13 collateral cleavage capabilities. (Reprinted from Kirby, E.N.; Shue, B.; Thomas, P.Q.; Beard, M.R. CRISPR Tackles Emerging Viral Pathogens. *Viruses* 2021, 13, 2157)

ITP-CRISPR/Cas12a

This focusing approach enables preconcentration, purifying, mixing, and accelerating reactions between various species of material and reagents. ITP has been used to expedite the extraction of nucleic acids from a variety of biological samples, such as blood (10), cell lysates (11), and urine (9). It has also been used to speed up DNA and RNA hybridization procedures. When choosing between LE and TE for ITP applications involving nucleic acid purification and extraction, the target species (in this case, DNA) is protected. When ITP is used to control homogeneous biological processes, a suitable choice of LE and TE enables responding species to cofocus and preconcentrate in ITP. Concurrent preconcentration of all reagents in ITP speeds up the manufacturing of the final product. ITP was used to show that DNA hybridization assays may be accelerated 14,000-fold. ITP has been used to speed up both homogeneous and heterogeneous biochemical reactions. Two key stages of this investigation are carried out using microfluidics and on-chip electric field control. First, from unprocessed biological materials—in this case, nasopharyngeal (NP) swab samples from COVID-19 patients and healthy controls—researchers employ ITP to retrieve nucleic acids. Second, they employ ITP to control and facilitate quick CRISPR/Cas12 enzymatic activity in response to identification of the target nucleic acid. The latter is achieved by concentrating Cas12-gRNA, reporter ssDNA, and target nucleic acids using a customized on-chip ITP method. This enables mixing in real time and accelerates enzymatic activities (Ramachandran et al. 2020).

AIOD-CRISPR/Cas12a

All-in-one dual CRISPR/Cas12a. This approach employs the Cas12a protein in a quick, specific, and straightforward way for detecting SARS-CoV-2 and HIV viruses with the naked eye. This procedure can also be carried out at a fixed temperature, obviating the necessity for LAMP techniques. Although it has not been tested with clinical samples, it found 1.3 copies of a plasmid containing the nucleocapsid protein of SARS-CoV-2. AIOD-CRISPR assay completely combines all of the components for nucleic acid amplification and CRISPR-based detection in a single, one-pot reaction system and incubates them at a single temperature (for instance, 37 °C), eliminating the need for separate preamplification and amplified product transfer. In addition AIOD-CRISPR assay method targets the nucleoprotein (N) gene of SARS-CoV-2 to identify a small number of nucleic acid copies (DNA or RNA). Using a pair of Cas12a-crRNA complexes made by two distinct crRNAs, the AIOD-CRISPR assay approach binds two distinct places in the target sequence that are close to the recognition sequence of primers. The CRISPR/Cas12a (AIOD-CRISPR) technology was developed to quickly, sensitively, and precisely detect nucleic acids. Dual crRNAs are used in this method to effectively find the target genomic sequence. The AIOD-CRISPR system eliminates the requirement for separate amplification and amplified product transfer by combining all the elements for

target nucleic acid amplification and CRISPR system-based detection into a single analysis. The AIOD-CRISPR system was developed with the goal of detecting SARS-CoV-2 and HIV-1. The AIOD-CRISPR system was examined for its capacity to distinguish each of the nucleic acid states (DNA and RNA) of both viral agents because they are retroviruses, and their nucleic acids were successfully detected (Hillary et al. 2021).

CRISPR-ENHANCE-Cas12a

This method enhanced a detection test using CRISPR technology. This method is based on earlier studies that demonstrated the effectiveness of using chemically modified CRISPR/Cas12a gRNA, adding a hairpin structure of RNA to the sgRNA or expanding the DNA on the crRNA. Using modified crRNA and DNA, authors created the CRISPR-ENHANCE (enhanced analysis of nucleic acids with crRNA extensions) method. As opposed to RNA in a heteroduplex, the conventional only successfully detects RNA when the target strand for crRNA is DNA. This method enhanced a detection test using CRISPR technology. However, according on the findings, crRNA and DNA are superior to wild-type crRNA in terms of enzymatic collateral activity on the DNA/RNA heteroduplex. The N gene's nucleocapsid phosphoprotein is uniquely recognized by SARS-CoV-2 crRNAs. Compared to normal crRNA and DNA, engineered crRNA and 3'DNA7 were proven to have a higher sensitivity for detection within 30 min (Huang et al. 2018).

iSCAN (CRISPR/Cas12a)

The in vitro specific CRISPR-based test for detection of nucleic acids (iSCAN) approach, which utilizes RT-LAMP and CRISPR/Cas12a RT-LAMP, was developed to solve the limitations in detection of SARS-CoV-2. The following are some of the advantages of this technology: (i) fast speed, (ii) accuracy (because the detection is based on CRISPR/Cas12a and involves cleavage of nucleic acid of SARS-CoV-2, (iii) deploy ability of field (because only basic instruments are required), and (iv) simple and user-friendly (providing quick access to test results by combining a colorimetric reaction with lateral immunochromatography flow). The researchers employed RT-LAMP for pathogen identification and multiplication, as well as CRISPR/Cas12 as a particular factor, to build the iSCAN technology for detection of SARS-CoV-2. CRISPR/Cas12's positive signal provides an accurate and precise signal for the identification of the virus. When Cas12a interacts with the target viral gene in the RT-LAMP amplification products, the collateral ssDNA-fluorescently quenched reporter is cleaved. This technique is applicable for identifying and isolating COVID-19 carriers immediately before the virus spreads in the body. (Ali et al. 2020).

16.2.7.4 CRISPR/Cas 13

Cas13

Amplicons are exposed to *in vitro* T7 transcription before RNA is detected using a Cas13-guided reporter assay. When triggered by attaching to a specific RNA region, Cas13, an RNA-guided protein of class 2 type VI, breaks neighboring RNAs (Abudayyeh and Gootenberg 2021). Cas13-based detection methods, such as HOLMES, require isothermal target genome amplification, crRNAs, and fluorescent ssRNA probes. For the purpose of producing *in vitro* RNA, this method calls for an additional step. Cas13 begins cleaving adjacent ssRNA probes after connecting with amplified RNA but before cleaving crRNA. Numerous techniques can be used to measure and quantify fluorescence. The use of CRISPR/Cas13 has improved viral diagnostics, thanks to platform-specific high-sensitivity enzymatic reporter unlocking (SHERLOCK). When fluorescently tagged probes are employed, the outcomes are assessed by chromogenic detection on a lateral flow device or by making use of a fluorometer (Gootenberg et al. 2017). The advent of CRISPR-based genome editing technology might herald the start of a new era in the genomic struggle against harmful plant viruses and viroids. In addition, the recently discovered CRISPR/Cas13 system offers unrivaled potential for plant viroid detection and interference (Mushtaq et al. 2021). Following exposure to *in vitro* T7 transcription on the target amplicons, the Cas13-guided reporter experiment is utilized to determine which RNA molecules were generated. One-of-a-kind class 2 type VI RNA-guided protein Cas13 cleaves adjacent RNAs *in trans* when activated by binding to a target RNA (Abudayyeh and Gootenberg 2021). It is necessary to isothermally amplify the target genome for Cas13-based detection techniques, such as HOLMES. Additionally needed are fluorescent ssRNA probes and crRNAs. This method requires one more step to generate *in vitro* RNA. When crRNA attaches to amplified RNA, Cas13 begins to cut the amplified RNA while also beginning to cut surrounding ssRNA probes. Fluorescence can be found and measured using a variety of methods. Utilizing the platform, CRISPR/Cas13 has helped with viral diagnostics (Mushtaq et al. 2021).

SHERLOCK-Cas13

Cas13a (formerly called C2c2) functions as an effector in SHERLOCK, which binds and cleaves RNA targets through its crRNA. SHERLOCK was first created to identify nucleic acids in order to identify and categorize infections and tumor DNA. SHERLOCKv2 now includes multiplexing, increased sensitivity, quantification, and simple readout. Cas effectors with orthogonal sequence preferences for cleavage of off-targets were identified, allowing the production of mutually distinct reporter probes, each with its distinctive fluorescence property, capable of reporting on up to four distinct target sequences in the same reaction. The quantification procedure involved the search for preamplification and recognition conditions that

were not saturated. Sensitivity was increased independent of target preamplification by constructing a cascade system in which cleavage of a Cas13a reporter acts as an activator for a second CRISPR effector, Csm6, which may result in the catalytic cleavage of reporters when activated (Fig. 16.5). Additionally, the SHERLOCK approach may be improved for the detection of the human immunodeficiency virus (HIV), which continues to be a significant viral disease worldwide (Bhattacharyya et al. 2018). Finally, the SHERLOCK assay improved mobility by the use of two approaches. To begin, it was shown that all of the reagents employed in the original SHERLOCK test may be lyophilized on paper before being reconstituted, allowing for use in field. Secondly, an additional reporter probe was created for SHERLOCKv2 that enables the test to be changed to a lateral flow device with a visual output, which is similar to ELISA (Palaz et al. 2021).

CREST-Cas13a

Researchers developed the Cas13a-based, equitable, robust, and scalable testing (CREST) method to overcome the scaled testing restrictions connected with SARS-CoV-2 diagnosis, including access to resources, such as materials and equipment, as well as highly qualified investors and operators. This CRISPR/Cas13a-based diagnostic method is very sensitive for recognizing SARS-CoV-2 and makes use of readily available tools and reagents. The CREST technology combines the stability and dependability of the PCR method with the accuracy and efficacy of transcriptional identification (Rauch et al. 2021). Without AC power or a sophisticated facility, CREST may transform an RNA sample into a result in less than 2 hours. It might be possible to test for COVID-19 on a wide scale while maintaining sensitivity using a mini-PCR thermocycler and inexpensive chemicals. The nonspecific collateral cleavage activity of the Cas13 effector was used to build the CREST platform. After reverse transcription, the RNA was amplified using the readily available Taq polymerase enzyme. T7 RNA polymerase was used to convert the DNA into RNA substrates for Cas13a. The reporter molecules were cut, and the signal was produced when the Cas13-gRNA combination recognized the target sequence in RNA. A P51 molecular fluorescent visualizer was utilized to detect the data on this platform instead of immunochromatography. While using 30–50 times less reagents and requiring no initial instrument costs than RT-qPCR, CREST is just as sensitive. The SARS-CoV-2 RNA input LOD for the CREST method was 10 copies/mL. CREST was also more accurate and less expensive than Cas13 diagnostic tools that used RT-RPA or RT-PCR for amplifying DNA (Vatankhah et al. 2021).

CARMEN-Cas13a

Multiplexed evaluation of nucleic acids using combinatorial arrayed reactions: This method combines SHERLOCK with microfluidic technology, enabling for the study of a wide spectrum of patient samples. The method was developed to detect

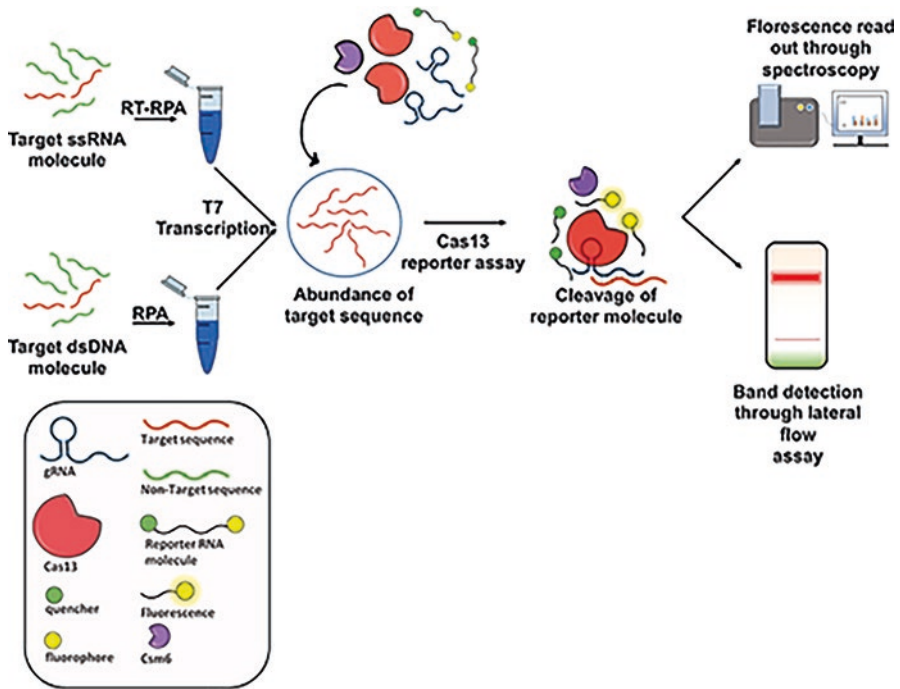


Fig. 16.5 Diagrammatic representation of SHERLOCK; the target sequence is amplified using RT-RPA or isothermal RPA in the presence of appropriate RPA primers. The amplified DNA sequence is then exposed to T7 transcription *in vitro*. The reporter molecule's fluorescence signals may be utilized to detect the synthesized RNA molecule after target recognition by the Cas13 RNase. A lateral flow test may detect the cleaved reporter molecule as bands. The introduction of Csm6 may result in increased amplification of the output signal

169 human-associated viruses, including SARS-CoV-2. It can also detect viruses in a wide range of materials, such as plasma and nose swab samples. SHERLOCKv2, a multiplexed CRISPR/Cas13-based nucleic acid detection technique, was greatly improved by combining high-throughput technologies. As a result, employing microwell array chips, a scalable platform named combinatorial arrayed reactions for multiplexed evaluation of nucleic acids (CARMEN) was devised. More than 4500 crRNA target pairs were detected on a single array using CARMEN and the CRISPR/Cas13 detection method (CARMEN-Cas13). On microwell plates, targeted gRNAs and fluorescent reporter-linked Cas13 complexes are coupled with samples simplified by PCR or RPA. Fluorescence microscopy can thus detect fluorescent signals in numerous wells at the same time. Using this approach, CARMEN-Cas13 was able to concurrently detect 169 human-associated viruses, including the Middle East respiratory syndrome (MERS) virus and the severe acute respiratory syndrome coronavirus 2 (SARS-CoV-2), as well as distinguish between influenza A virus subtypes. CARMEN-Cas13 is more multiplexed, sensitive (attomolar range), and less expensive than SHERLOCKv2 (\$0.61/test). Multiple Cas13-based

diagnostic tools, such as SHERLOCK, SHERLOCKv2, HUDSON, and CARMEN-Cas13, have thus opened up new avenues for detecting viruses with vulnerable RNA genomes (Aquino-Jarquin 2021).

CARVER-Cas13a

The CRISPR/Cas13 enzyme and the CARVER (CRISPR/Cas13-based restriction of viral expression and readout restriction) technology can be used to destroy RNA-based viruses in human cells. In human cultured cells, any CRISPR tool, including Cas13, was used as an antiviral. Recently, Cas13, which usually cuts and modifies viral RNA in bacteria, was repurposed to cut and test for the presence of viruses, bacteria, and other targets. After the enzyme has been thoroughly examined in mammalian cells, it has been shown that it can be made to target specific RNA sequences. It is simple to introduce the protein Cas13 into cells. Cas13, a CRISPR effector that can also cleave programmable RNAs in addition to its crRNA, may work well as an antiviral for ssRNA (Freije et al. 2019).

16.2.8 Challenges

Several aspects, including lab equipment, sequence restrictions, quantitative analysis, standardization, target amplification, DNA imaging, multiplex detection, and so on, are among the hurdles that may affect CRISPR sensing systems (Fig. 16.6). Approaches based on CRISPR collateral cleavage activities that have strong chances for field application, particularly in decreasing epidemic outbreaks in resource-limited regions, stand out for the mobility given by reduced lab equipment needs. It is a typical problem in CRISPR sensing because the range of sequences that can be recognized using CRISPR/Cas effector proteins is constrained. The crRNA that controls CRISPR effector proteins allows them to recognize complementary target sequences on both DNA and RNA. The spacer sequence of the crRNA can be altered to match the target sequence (Deng et al. 2019). Usually, these restrictions can be overcome by altering the target sequence so that any base other than guanine is the first base following the protospacer (Gootenberg et al. 2018). Sequence constraints brought on by the necessity of PAM or PFS for CRISPR-focused recognition have resulted in a limited range of detectable sequences. Another approach to lessening the frequency of off-target modifications is to restrict the amount of time Cas9 expression is active. Successful gene editing with Cas9 mRNA and protein, for instance, causes less off-target effects in the host genome than editing with Cas9 generated from DNA (Naeem et al. 2020).

While single-base analysis at the single-cell level has already been accomplished using CRISPR-mediated in situ imaging technology, genomic DNA imaging, a crucial issue, is still inefficient and falls short of the criteria required for practical applications. Multiplex analysis, which involves measuring multiple samples at once,

enables onboard calibration by allowing known target concentrations to be recorded concurrently under the same circumstances, cancelling out factors that affect sensor performance and alter measurement results. Without on-site calibration, it is challenging to quantify data or standardize it. Established CRISPR-based sensing techniques, such as HOLMES, DETECTR, and SHERLOCK, can only measure the quality of nucleic acids, not their amount.

In addition to calibration, multiplexing—the simultaneous detection of numerous target sequences—is required for precise and conclusive information to be obtained through genomic diagnostics (Dincer et al. 2017). This multiplexed genomic sensing in a single reaction volume is challenging, compromising both sensitivity and specificity, due to limitations in the signal gathering approaches, interference between the numerous detection procedures, and possible cross-reactions. A key issue with single reaction volume multiplexing is the nonspecific cleavage of the same type of nucleotide as observed (Wei et al. 2018). On the other hand, after several Cas-gRNA complexes have been triggered by various targets for multiplex purposes, unspecific cutting is the most challenging barrier for good signal distinction. Differentially labeled signal tags may not be a practical method of understanding the intricacies until other biological activities connected with Cas effectors are uncovered (Li et al. 2019a, b). To enable CRISPR sensing in remote locations without skilled people, several isothermal amplification-based techniques that are simpler to use and can be applied in compact portable devices can be used. Before CRISPR sensing can take the role of traditional biomolecular nucleic acid sensing techniques, such as PCR, there are a number of challenges to be addressed (Kumar et al. 2020).

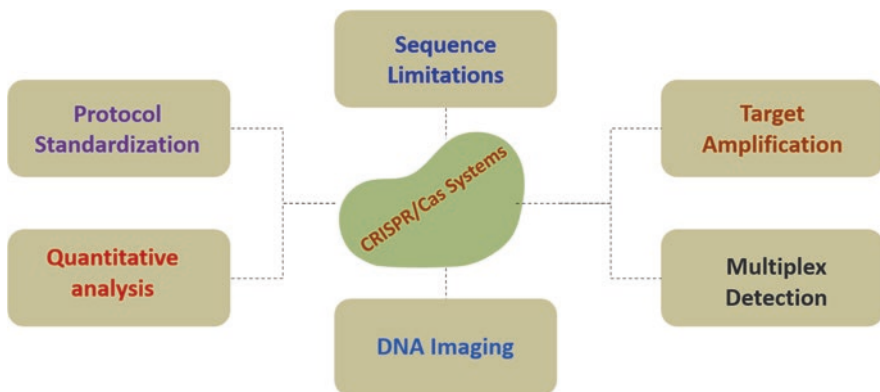


Fig. 16.6 CRISPR sensing systems' challenges in diagnostic devices for viruses and other biomedical and agricultural diseases

16.2.9 Conclusion and Future Outlook

The development of exceptionally precise and sensitive diagnostic tools that integrate signal amplification with fluorescence, potentiometric, colorimetric, and lateral flow assay detection, among other technologies, has made use of a variety of Cas proteins, including Cas3, Cas9, and Cas12. The most recent technologies, including SHERLOCK/v2, DETECTR, CARMEN, and CRISPR-Chip, enable the detection of pathogenic nucleic acids at attomole levels with specificity comparable to PCR but with fewer useful parameters. With a focus on CRISPR/Cas systems previously used for molecular detection of viral infections, we describe CRISPR/Cas classes and types as the foundation for prospective CRISPR-diagnostic platforms in this chapter. We also talk about the technical challenges that need to be taken into account while developing CRISPR/Cas-based diagnostics for disease epidemics. CRISPR/Cas-based diagnostics may be a better choice to develop ultrasensitive, affordable, and quick non-laboratory detection kits for a variety of viruses and diseases. Techniques for CRISPR/Cas detection can help with open fields, portable diagnostics, and pathogen prevention, particularly for newly developing and reemerging viral diseases. But there are certain downsides to CRISPR/Cas multi-functional biosensing, most of which require a lot of research, time, and money. On-site pathogen detection is practical because it can be done anywhere and doesn't need specialized equipment. It has become a common practice to use equipment-free isothermal amplification into CRISPR-based detection methods. More techniques that don't require any equipment, such as lateral flow assay or light-based naked-eye observation, should be used for signal readout. CRISPR/Cas diagnostic testing may be used with artificial intelligence (AI) to offer an early warning system for rapid, precise, and intelligent pathogen identification. In order to detect some pathogenic infections promptly and effectively, communities, hospitals, farms, and even individuals are supplied user-friendly portable CRISPR/Cas-based screening kits. Finally, just a small portion of the developments involve adding nanoparticles to CRISPR-powered biosensors. With innovations, there is no end to the potential changes and improvements.

References

- Abudayyeh O-O, Gootenberg J. CRISPR diagnostics. *Science*. 2021;372(6545):914–5.
- Ali Z, Aman R, Mahas A, Rao G-S, Tehseen M, Marsic T, Salunke R, Subudhi A-K, Hala S-M, Hamdan S-M. iSCAN: an RT-LAMP-coupled CRISPR-Cas12 module for rapid, sensitive detection of SARS-CoV-2. *Virus Res*. 2020;288:198129–32.
- Alon D-M, Hak H, Bornstein M, Pines G, Spiegelman Z. Differential detection of the tobamoviruses tomato mosaic virus (ToMV) and tomato brown rugose fruit virus (ToBRFV) using CRISPR-Cas12a. *Plan Theory*. 2021;10(6):1256.
- Aman R, Mahas A, Marsic T, Hassan N, Mahfouz M-M. Efficient, rapid, and sensitive detection of plant RNA viruses with one-pot RT-RPA–CRISPR/Cas12a assay. *Front Microbiol*. 2020;15:3277.

- Aquino-Jarquín G. Recent progress on rapid SARS-CoV-2/COVID-19 detection by CRISPR-Cas13-based platforms. *Drug Des Discov.* 2021;26(8):2025–35.
- Azhar M, Phutela R, Ansari A-H, Sinha D, Sharma N, Kumar M, Aich M, Sharma S, Rauthan R, Singhal K. Rapid, field-deployable nucleobase detection and identification using FnCas9. *BioRxiv*; 2020.
- Barrangou R, Doudna J-A. Applications of CRISPR technologies in research and beyond. *Nat Biotechnol.* 2016;34(9):933–41.
- Barrangou R, Marraffini L-A. CRISPR-Cas systems: prokaryotes upgrade to adaptive immunity. *Mol Cell.* 2014;54(2):234–44.
- Bhattacharyya R-P, Thakku SG, Hung D-T. Harnessing CRISPR effectors for infectious disease diagnostics. *ACS Infect Dis.* 2018;4(9):1278–82.
- Broughton J-P, Deng X, Yu G, Fasching C-L, Servellita V, Singh J, Miao X, Streithorst J-A, Granados A, Sotomayor-Gonzalez A. CRISPR-Cas12-based detection of SARS-CoV-2. *Nat Biotechnol.* 2020;38(7):870–4.
- Chaijarasphong T, Thammachai T, Itsathitphaisarn O, Sritunyalucksana K, Suebsing R. Potential application of CRISPR-Cas12a fluorescence assay coupled with rapid nucleic acid amplification for detection of white spot syndrome virus in shrimp. *Aquaculture.* 2019;512:734340–5.
- Chen B, Niu Y, Wang H, Wang K, Yang H, Li W. Recent advances in CRISPR research. *Protein & Cell* 2020;11(11): 786–91.
- Chertow DS. Next-generation diagnostics with CRISPR. *Science.* 2018;360(6387):381–2.
- Deng H, Huang W, Zhang Z. Nanotechnology based CRISPR/Cas9 system delivery for genome editing: progress and prospect. *Nano Res.* 2019;12(10):2437–50.
- Dincer C, Bruch R, Kling A, Dittrich P-S, Urban GA. Multiplexed point-of-care testing—xPOCT. *Trends Biotechnol.* 2017;35(8):728–42.
- Ding X, Yin K, Li Z, Liu C. All-in-one dual CRISPR-cas12a (AIOD-CRISPR) assay: a case for rapid, ultrasensitive and visual detection of novel coronavirus SARS-CoV-2 and HIV virus. *BioRxiv*; 2020.
- Freije C-A, Myhrvold C, Boehm C-K, Lin A-E, Welch N-L, Carter A, Metsky H-C, Luo C-Y, Abudayyeh O-O, Gootenberg J-S. Programmable inhibition and detection of RNA viruses using Cas13. *Mol Cell.* 2019;76(5):826–37.
- Gootenberg J-S, Abudayyeh O-O, Lee J-W, Essletzbichler P, Dy A-J, Joung J, Verdine V, Donghia N, Daringer N-M, Freije C-A. Nucleic acid detection with CRISPR-Cas13a/C2c2. *Science.* 2017;356(6336):438–42.
- Gootenberg J-S, Abudayyeh O-O, Kellner M-J, Joung J, Collins J-J, Zhang F. Multiplexed and portable nucleic acid detection platform with Cas13, Cas12a, and Csm6. *Science.* 2018;360(6387):439–44.
- Hillary V-E, Ignacimuthu S, Ceasar S-A. Potential of CRISPR/Cas system in the diagnosis of COVID-19 infection. *Expert Rev Mol Diagn.* 2021;21(11):1179–89.
- Hille F, Charpentier E. CRISPR-Cas: biology, mechanisms and relevance. *Philosophical transactions of the royal society. Biol Sci.* 2016;371(1707):20150496.
- Huang M, Zhou X, Wang H, Xing D. Clustered regularly interspaced short palindromic repeats/Cas9 triggered isothermal amplification for site-specific nucleic acid detection. *Anal Chem.* 2018;90(3):2193–200.
- Jiao J, Kong K, Han J, Song S, Bai T, Song C, Wang M, Yan Z, Zhang H, Zhang R. Field detection of multiple RNA viruses/viroids in apple using a CRISPR/Cas12a-based visual assay. *Plant Biotechnol J.* 2021;19(2):394–405.
- Kellner M-J, Koob J-G, Gootenberg J-S, Abudayyeh O-O, Zhang F. SHERLOCK: nucleic acid detection with CRISPR nucleases. *Nat Protoc.* 2019;14(10):2986–3012.
- Khambhati K, Bhattacharjee G, Singh V. Current progress in CRISPR-based diagnostic platforms. *J Cell Biochem.* 2019;120(3):2721–5.
- Khan S, Mahmood M, Rahman S, Rizvi F, Ahmad A. Evaluation of the CRISPR/Cas9 system for the development of resistance against cotton leaf curl virus in model plants. *Plant Prot Sci.* 2020;56(3):154–62.

- Kimunye J, Jomanga K, Tazuba A-F, Were E, Viljoen A, Swennen R, Mahuku G. Genotype X environment response of 'Matooke' hybrids (Naritas) to *Pseudocercospora fijiensis*, the cause of black Sigatoka in banana. *Agron J.* 2021;11(6):1145.
- Kocak D-D, Gersbach C-A. From CRISPR scissors to virus sensors. *NPG;* 2018.
- Kumar P, Malik YS, Ganesh B, Rahangdale S, Saurabh S, Natesan S, Srivastava A, Sharun K, Yattoo M, Tiwari R. CRISPR-Cas system: an approach with potentials for COVID-19 diagnosis and therapeutics. *Front Cell Infect Microbiol.* 2020;10:639.
- Li Y, Li S, Wang J, Liu G. CRISPR/Cas systems towards next-generation biosensing. *Trends Biotechnol.* 2019a;37(7):730–43.
- Li Y, Liu L, Liu G. CRISPR/Cas multiplexed biosensing: a challenge or an insurmountable obstacle? *Trends Biotechnol.* 2019b;37(8):792–5.
- Liu D, Zhao X, Tang A, Xu X, Liu S, Zha L, Ma W, Zheng J, Shi M. CRISPR screen in mechanism and target discovery for cancer immunotherapy. *Biochimica et Biophysica Acta (BBA). Rev. Cancer.* 2020;1874(1):188378.
- Luo Y, Tan C-W, Xie S-Z, Chen Y, Yao Y-L, Zhao K, Zhu Y, Wang Q, Liu M-Q, Yang X-L. Identification of ZDHHC17 as a potential drug target for swine acute diarrhea syndrome coronavirus infection. *MBio.* 2021;12(5):02342–21.
- Mahas A, Hassan N, Aman R, Marsic T, Wang Q, Ali Z, Mahfouz M-M. LAMP-coupled CRISPR–Cas12a module for rapid and sensitive detection of plant DNA viruses. *Viruses.* 2021;13(3):466.
- Mendes R-J, Luz J-P, Santos C, Tavares F. CRISPR genotyping as complementary tool for epidemiological surveillance of *Erwinia amylovora* outbreaks. *PLoS One.* 2021;16(4):0250280.
- Mushtaq M, Dar A-A, Basu U, Bhat B-A, Mir RA, Vats S, Dar M, Tyagi A, Ali S, Bansal M. Integrating CRISPR-Cas and next generation sequencing in plant virology. *Front Genet.* 2021;12
- Myhrvold C, Freije C-A, Gootenberg J-S, Abudayyeh O-O, Metsky H-C, Durbin A-F, Kellner M-J, Tan A-L, Paul L-M, Parham L-A. Field-deployable viral diagnostics using CRISPR-Cas13. *Science.* 2018;360(6387):444–8.
- Naem M, Majeed S, Hoque M-Z, Ahmad I. Latest developed strategies to minimize the off-target effects in CRISPR-Cas-mediated genome editing. *Cell.* 2020;9(7):1608.
- Nussenzweig P-M, Marraffin LA. Molecular mechanisms of CRISPR-Cas immunity in bacteria. *Annu Rev Genet.* 2020;54:93–120.
- Palaz F, Kalkan A-K, Tozluoyurt A, Ozsoz M. CRISPR-based tools: alternative methods for the diagnosis of COVID-19. *Clin Biochem.* 2021;89:1–13.
- Panno S, Matic S, Tiberini A, Caruso A-G, Bella P, Torta L, Stassi R, Davino S. Loop mediated isothermal amplification, principles and applications in plant virology. *Plan Theory.* 2020;9(4):461.
- Pardee K, Green A-A, Takahashi M-K, Braff D, Lambert G, Lee J-W, Ferrante T, Ma D, Donghia N, Fan M. Rapid, low-cost detection of Zika virus using programmable biomolecular components. *Cell.* 2016;165(5):1255–66.
- Ramachandran A, Huyke D-A, Sharma E, Sahoo M-K, Huang C, Banaei N, Pinsky B-A, Santiago J-G. Electric field-driven microfluidics for rapid CRISPR-based diagnostics and its application to detection of SARS-CoV-2. *PNAS.* 2020;117(47):29518–25.
- Ramachandran V, Weiland J-J, Bolton M-D. CRISPR-based isothermal next-generation diagnostic method for virus detection in sugarbeet. *Front Microbiol.* 2021;10:1760.
- Rauch J-N, Valois E, Solley S-C, Braig F, Lach R-S, Audouard M, Ponce-Rojas J-C, Costello M-S, Baxtex N-J, Kosik K-S. A scalable, easy-to-deploy protocol for Cas13-based detection of SARS-CoV-2 genetic material. *J Clin Microbiol.* 2021;59(4):2402–02420.
- Sharma SK, Gupta OP, Pathaw N, Sharma D, Maibam A, Sharma P, Sanasam J, Karkute SG, Kumar S, Bhattacharjee B. CRISPR-Cas-led revolution in diagnosis and management of emerging plant viruses: new avenues toward food and nutritional security. *Front Nutr.* 2021;8
- Srivastava S, Upadhyay D-J, Srivastava A. Next-generation molecular diagnostics development by CRISPR/Cas tool: rapid detection and surveillance of viral disease outbreaks. *Front Mol Biosci.* 2020;7:378.

- Tripathi L, Ntui VO, Tripathi JN, Kumar PL. Application of CRISPR/Cas for diagnosis and management of viral diseases of banana. *Front Microbiol.* 2021;11:609784–8.
- van Dongen J-E, Berendsen J-T, Steenbergen R-D, Wolthuis R-M, Eijkel J-C, Segerink L-I. Point-of-care CRISPR/Cas nucleic acid detection: recent advances, challenges and opportunities. *Biosens Bioelectron.* 2020;166:112445.
- Vatankhah M, Azizi A, Sanajouyan Langeroudi A, Ataei Azimi S, Khorsand I, Kerachian M-A, Motaie J. CRISPR-based biosensing systems: a way to rapidly diagnose COVID-19. *Crit Rev Clin Lab Sci.* 2021;58(4):225–41.
- Wang X, Xiong E, Tian T, Cheng M, Lin W, Wang H, Zhang G, Sun J, Zhou X. Clustered regularly interspaced short palindromic repeats/Cas9-mediated lateral flow nucleic acid assay. *ACS Nano.* 2020;14(2):2497–508.
- Wei H, Ni S, Cao C, Yang G, Liu G. Graphene oxide signal reporter based multifunctional immunosensing platform for amperometric profiling of multiple cytokines in serum. *ACS Sens.* 2018;3(8):1553–61.
- Yang H, Jaeger M, Walker A, Wei D, Leiker K, Weitao T. Break breast cancer addiction by CRISPR/Cas9 genome editing. *J Cancer.* 2018;9(2):219.
- Zhang F, Abudayyeh O-O, Gootenberg J-S. A protocol for detection of COVID-19 using CRISPR diagnostics. A protocol for detection of COVID-19 using CRISPR. *Diagnosi.* 2020;8(2):226–51.

Chapter 17

DNA-Nanosensors for Environmental Monitoring of Heavy Metal Ions



Heba Elbasiouny, Nahed S. Amer, Sherifa F. M. Dawoud,
Amina M. G. Zedan, and Fathy Elbehiry

Abbreviations

| | |
|------|----------------|
| BSs | Biosensors |
| HMs | Heavy metals |
| NBSs | Nanobiosensors |
| NM | Nanomaterials |
| NPs | Nanoparticles |

17.1 Introduction

Nanotechnology is the creation and utilization of absolutely tiny materials at the nanometer dimensions for many applications in biology, chemistry, physics, materials science, and engineering. Chemical, physical, electrical, and mechanical characteristics of these unique organized nanomaterials (NMs) are varied (Türkoğlu et al. 2013; Das et al. 2018). Thus, nanotechnology advancements have laid the foundations for the production of nanomaterials with unique physiochemical characteristics, application-oriented morphology, faults, bandgaps, and others. Material scientists and researchers have intensively researched these remarkable nanomaterial features to investigate their possible applications in electronics, photonics, catalysis, energy conversion, catalysis, bioimaging, and sensing (Ahmad et al. 2020). Nanoparticles (NPs) serve as a link between bulk material and molecular or atomic structures. Every material's properties change as its size shrinks to nanoscale,

H. Elbasiouny · N. S. Amer · S. F. M. Dawoud · A. M. G. Zedan
Department of Environmental and Biological Sciences, Home Economics Faculty, Al-Azhar
University, Tanta, Egypt

F. Elbehiry (✉)
Department of Basic and Applied Sciences, The Higher Institute for Agricultural
Cooperation, Cairo, Egypt

and one of the major factors is the considerably greater number of surface atoms. Bulk materials with microscale or larger dimensions have a negligible amount of electrons at the surface. The main characteristic of NPs is their high volume-to-surface area ratio (Elbehiry et al. 2022). There is a high need for systems that detect, monitor, and diagnose environmental contaminants in a timely, dependable, and low-cost manner. Traditional analytical methods such as chromatographic and spectroscopic techniques are time-consuming and labor-intensive. Novel biosensors are being created to address these difficulties (Salouti and Khadivi 2020). Thus, at the moment, nanobiotechnology represents an optimistic approach to cleaning up polluted ecosystems. Nanomaterial applications to restore the magnificence of the environment and aid in the identification of contaminated places, as well as prospective cures, have been presented in studies (Boregowda et al. 2021).

Bhushan (2012) defined the sensors as bio-derived membranes that are used to sense element by monitoring an electrical response of the membranes due to an applied stimulus. Jeevanandam et al. (2020) reported that sensor is a broad term for the material used to detect and sense physical parameters and convert them to electrical charge. Sensor is made up of major components: analyte or detectable element, receptor, transducer, and signals unit (Jeevanandam et al. 2020).

Urbanization and fast industrialization have polluted the environment with heavy metals (HMs) in numerous nations during the last few decades (Maric et al. 2019; Eldamaty et al. 2021; Zou et al. 2021). Heavy metal pollution has been found in practically all ecosystems and in every place on the planet, from the air that we breathe to the water that we drink, from land to sea, and from the Arctic to the Antarctic (He et al. 2021). Heavy metals can enter the environment through natural or man-made processes. Unlike organic contamination, the HMs contamination is of particular importance due to its high toxicity, concealment, durability, enriching, nondegradability, and bioaccumulation in higher trophic organisms (Eldamaty et al. 2021; Zhao et al. 2021). Lethal HMs such as cadmium, chromium, copper, lead, mercury, nickel, and zinc are known to trigger long-term and considerable harm to many biotic systems by interfering with biological functions at the cellular level. Numerous risks are brought on by HMs, such as renal tubular dysfunction, cardiovascular, neurological, osteomalacia, kidney, and bone illnesses, as well as nutrient deficiencies, enzyme malfunctions, carcinogenesis, mutagenesis, and teratogenesis. Human activities have significantly disrupted the geochemical cycle and metabolic equilibrium of these elements and increased their concentration in the environment. As a result, one of the greatest issues facing scientists today is developing technologies for recognizing them even at low quantities in environmental samples (Elbehiry et al. 2019; Dey et al. 2021; Sharma et al. 2021). To ensure human health and environmental safety, effective monitoring and risk assessments of HMs pollutants in a range of environmental matrices are crucial, but difficult, area (He et al. 2021). Environmental monitoring of toxic elements is important because of potential adverse impacts on human health (Ullah et al. 2018; Zhu et al. 2018; Elbehiry et al. 2021). In the last few years, the utilization of NMs and advancements in NT have advanced by rapidly increasing. Recent research has focused on nanotechnology's influence on environmental applications, with a special emphasis on pollution

control and the remediation of environmental contaminants from contaminated soils, sediments, solid wastes, air, and water. Novel and possible nanotechnological developments have been employed to overcome many of the prior of traditional techniques bottlenecks with notable gains in biomarkers, illnesses cures, biomedical instrumentations, nanosensors (NSs), displaying systems, agricultural technology, environmental safety, and so on (Das et al. 2018; He et al. 2021; Elbasiouny et al. 2022; Gupta et al. 2022).

Currently, many nanosensors have been utilized to detect several environmental contaminants (Ahmed et al. 2022). Nowadays, a large range of (nanobiosensors) NBSs are accessible to solve diverse diagnostic issues. These highly sensitive NBSs are particularly appealing for detecting analytes at extremely low concentrations. They can be used in clinical diagnostics, environmental monitoring, food analysis, forensic sciences, and medication delivery systems, among other things. Clinical applications include pathogen and biomarker detection, medication analysis in bodily fluids, oxidative stress monitoring, and nucleic acid sensing. This technology will revolutionize individualized diagnostics based on point-of-care systems in the near future. Nanobiosensors are a prominent topic in many domains, and numerous sensors have lately been designed after considering their relevance (Dasgupta et al. 2017). Nanobiosensors can also be used to detect pollutants in food, such as pathogenic bacteria and pesticides. Pollutants, poisons, pesticides, and HMs can all be detected in environmental applications (Kumari et al. 2019). Nanobiosensors have very low detection limit with the range of ppb during 1 month of storage (Rigo et al. 2020). DNA-related probes have the ability to recognize HMs such as Ag, Cd, Cu, Hg, and Pb, allowing for efficient, selective, and accurate detection. One form of aptamer with outstanding HM ion recognition skills is ssDNA, and there are various typical metal ion detection designs (Lian et al. 2020).

This chapter highlights the application of nanosensors, nanobiosensors especially DNA-nanosensors in the environmental monitoring and detection of heavy metals.

17.2 Heavy Metals Pollution and Detection

The growth of many industries raises everyone's living standards; however, it also aggravates the pollution problems and contributes to the global energy crisis (Sabzehmeidani and Kazemzad 2022). Heavy metals (such as Ag, Cu, Pb) contamination in the environment is currently on the rise as a result of increased urbanization and industry. Agricultural runoff, inappropriate use of dangerous chemical fertilizers and pesticides, municipal waste management, mining, electroplating, smelting and transportation are all significant contributors to toxic metals being released into the ecosystem (Zhang et al. 2018; Ali et al. 2022; Wang et al. 2022). As a result, HM content continues to accumulate in nature (Wang et al. 2022). Besides human sources, hazardous metals can also be released into the environment

via geological weathering, atmospheric precipitations, wave's erosion, and bioturbation (Ali et al. 2022).

Due to the previous issues and the properties of long-term accumulation and nondegradability, HMs may reach all organisms, even human, through the food chains and cause irreparable damage. As a result, detecting HMs quickly and accurately has become a critical issue (Zhang et al. 2018; Wang et al. 2022). Thus, to mitigate the hazards presented by harmful metal contaminants in the environment, essential measures are needed (Numan et al. 2021). There is a high demand for HMs detection and analysis in relation to the concentration limitations specified by international standards. Due to their complexity, large-scale application of certain analyzers, such as atomic adsorption spectroscopy and inductively coupled plasma, large-scale implementation of these analytical instruments remains a difficulty. Highly expensive and sophisticated equipment needs time-consuming sample preparation procedures and needs also intensive labor. Further, they are bulky, all of which making them only operational by experts and qualified staffs (Varun and Daniel 2018; Zhang et al. 2018; Sharma et al. 2021; Wang et al. 2022). As a result, much research into analytical methods for HM ion sensing has been undertaken (Zhang et al. 2018). In addition, techniques for detecting and/or determining the degree of pollution that can have an impact on global concerns must be developed. Many scholars have been drawn to the hunt for environmentally friendly and practical solutions to these issues (Sabzehmeidani and Kazemzad 2022). The use of electrochemical detection technologies in combination with engineered nanomaterials (NMs) is a significant promising and creative technique for controlling HM toxicity (Numan et al. 2021). The NMs have lately emerged as one of the most promising approaches for the detection of HMs because of their prospective benefits of simple design and sensitive identification of particular unique metal ions (Zhang et al. 2018). The area of environmental monitoring has been markedly influenced by nanotechnology, and the investigations in nanosensors (NSs) have contributed to the field of HMs detection. Though nanotechnology has the ability to detect HMs quickly and effectively while breaking down obstacles to environmental analysis, it is vital to develop HMs sensors that are both portable and eco-friendly (Varun and Daniel 2018). Furthermore, DNA-based sensors have been intensively investigated among the techniques of HMs detection, owing to their versatility and high programmability. G-quadruplexes (G4) are DNA sequences that include a lot of guanine (G) and may form four-stranded structures via Hoogsteen H bond (Huang et al. 2021).

17.3 Nanobiosensors and Pollution Detection

Nanosensors are mechanical or chemical technique that is performed with nanoscale components that are designed to react to the presence of analytes or environmental conditions (Yang and Duncan. 2021). Biosensors and nanomaterials offer higher benefits in detection and miniaturization (Saravanakumar et al. 2022). Nanomaterials

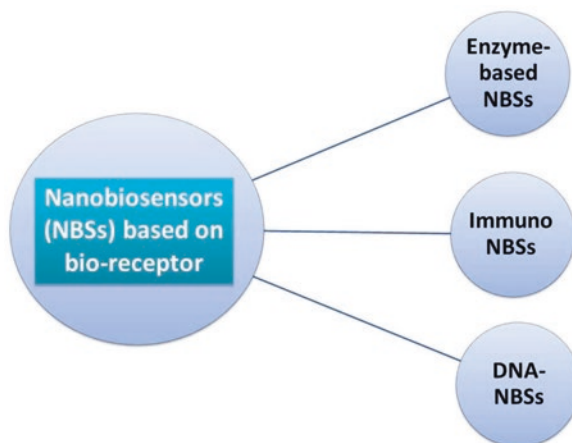
act as key role in either NSs or NBs because of their unique physiochemical properties that differ than the bulk materials (Fouad et al. 2012; Pourtaheri et al. 2019; Mahmoud and Fawzy 2021). The NBSs are microorganisms that are either naturally occurring or designed to produce a detectable signal in response to environmental stimuli. In the most of sensors, a chemical of importance activates the promoters, which causes the synthesis of a reporter gene, leading to an output signals in the forms of colorimetry, luminometry, or fluorimetry (Punetha and Khan 2022). Thus, NBs are the same NSs concept; however, they use a biologically active component to provide a quantifiable signal inversely proportional to the amount of chemicals in any kind of sample. They are founded on biological perception and identification. Consequently, they outperform most traditional sensing devices in terms of biocompatibility, sensitivity, and specificity (Wang and Qu 2013; Touhami 2014; Mahmoud and Fawzy 2021). Therefore, a NBS may detect any biophysical or biochemical signal connected with a specific analyte (molecule). The long-term use of NBS is to analyze the presence and concentration of harmful compounds and pollutants in soil, water, and wastewater. Nanobiosensor applications have also been expanded for environmental monitoring of contaminants, toxicants, microbes, and prevention and detection of bioterrorism in military, net soil contaminants, such as pesticide, herbicide, and HMs. Nanosensors have revolutionized chemical and biological analysis due to their submicron size, allowing for the quick examination of many chemicals in vivo and environmental samples (Salouti and Khadivi 2020). The performance of a NBSs is determined by its parameters, such as resolution, sensitivity, selectivity, response time, drift, repeatability and stability (Khanna 2011; Swierczewska et al. 2012; Mahmoud and Fawzy 2021).

Surface-dependent processes are used by biosensors. As a result, the greater the surface area and the greater the electron transfer proficiency and biocompatibility, the greater the sensing capacity and utility. Piezoelectric or thermal transducers are critical components in converting the concentration and physical qualities of various agents into analog voltage signals, which are then converted into digital signals. The most often used sensing devices are optical and electrochemical sensing. Optical sensing is dependent on the use of spectrophotometers and electrodes, such as pH, whereas electrochemical sensing is dependent on conduction ions. The main limitation of these traditional techniques is the demand for particular biosensor equipment, which results in pricey and unspecified sensing (Sargazi et al. 2022). Integration of nanomaterials with biosensors (BSs) via material identification promotes electron transport between electrodes; without that, they cannot enhance the accuracy of these BSs' identification. Electrochemical nanobiosensor (NBS) has many advantages, including their inexpensive cost, high sensitivity, portability, selectivity, on-site detection ability, enhanced devices performance, and low identifying threshold. Because of their ease of use and measurement, such sensors are commonly utilized in laboratories (García-Aljaro et al. 2010; Ullah et al. 2018). Carbon nanomaterials have many unique properties that make them ideal transducers in the fabrication of NSs for environmental monitoring, health and food safety control, and other applications for the detection of various analytes, such as HM ions, food additives, gas molecules, antibodies, and toxic pesticides (Nehra et al.

2019). In this context, plasmonic NPs have evolved into a well-known technology for sensing purposes, referred to as “NP plasmon sensors”, which can detect the molecules’ presence in the proximity of the NPs by monitoring spectrum shifts, eliminating the requirement for chemical labeling/tagging of the molecules. Single NP plasmon sensors have been satisfactorily used as a label-free analytical technique, for example, to notice the binding of single proteins, to detect the existence of multiple molecules and also their binding affinities concurrently, and to track the spatiotemporal variability of membrane proteins. However, because of the limits of detection and setup disturbance, most biosensing techniques of single NP plasmon sensors have some difficulty detecting tiny analytes, such as heavy metal ions. To address this limitation, gold NP aggregation might be used to improve detection signals. Unfortunately, because the quantity of particles to be aggregated varies, the aggregation detection method will definitely increase the heterogeneity in the detection signal. It was recently demonstrated that using single NP plasmon sensors in conjunction with the spectrum imaging approach is a viable strategy to enhance the detection limit using huge statistics (Ye et al. 2022). Sensors produced using nanoscience and NMs have a variety of uses nowadays. Enzyme-based NSs, for example, are one of the most helpful analytical approaches for identifying toxins in biological samples (Sun et al. 2018). Novel and high-quality BSs, which can be used to detect biomolecules and diagnose illnesses by incorporating biomaterials and converters that function with NMs, can be developed. These BSs can sense elevated levels of environmental pollution high speeds (Mokhtarzadeh et al. 2017). The NSs are gaining popularity as a means of detecting and measuring chemical and physical characteristics in nanoscale biological and industrial systems that are difficult to access (Lim and Ramakrishna 2006).

Nanobiosensors are categorized based on the bio-recognition element utilized for molecular recognition or the kind of detecting transduction used. Nanobiosensors are categorized into three types based on the bio-recognition or bioreceptor used: (a) enzyme-based NBSs, (b) immuno NBSs, and (c) DNA-NBSs (Fig. 17.1).

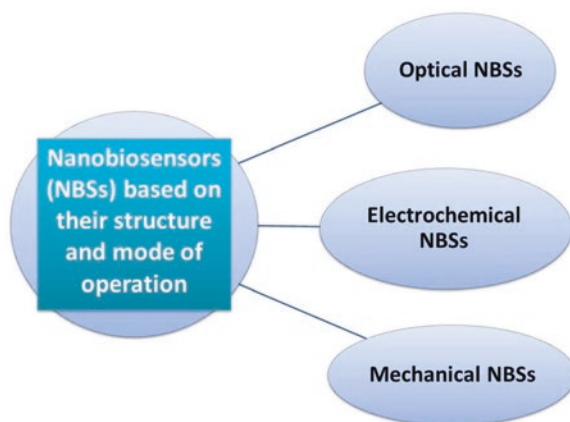
Fig. 17.1 Classification of nanobiosensors based on bioreceptor



Nanobiosensors are categorized into three types based on their structure and mode of operation: (a) optical NBSs, (b) electrochemical NBSs, and (c) mechanical NBSs (Fig. 17.2). Fiber optics utilizing total internal reflection, absorbance, or fluorescence, chemiluminescence, bioluminescence, evanescent wave, or surface plasmon resonance are examples of optical NBSs. Amperometric, potentiometric, impedimetric, and conductometric systems are electrochemical transducers. Mechanical transducers are mass-sensitive piezoelectric materials that take use of the concepts of changing the resonance frequency of wave propagation via piezoelectric material and changing the mass on analyte binding (Kuswandi 2019).

Numerous electrochemical sensing and biosensing methods based on a variety of nanostructures have been devised for use in a variety of biological and biomedical applications (Maduraiveeran et al. 2018). For examples, surface-enhanced Raman spectroscopy and nanojets have been created and used for HMs detection (He et al. 2021). Engineered fluorescent proteins have been produced for a broad range of tiny molecules, including as ions and metabolites, or to detect biophysical activities, such as transmembrane voltage or tension, using genetically encoded sensors (Sadoine et al. 2021). Fluorescent-based bioprobes have been also utilized to produce very sensitive NBSs to detect many biological and chemical agents due to its special qualities, such as high specificity, selectivity, high surface-to-volume ratio, and variable optical and electrical properties. Because they are biodegradable, eco-friendly, cost-effective, more economic, and practical, these sensors outperform other analytical equipment techniques, such as high-performance liquid chromatography, gas chromatography, and capillary electrophoresis (Sargazi et al. 2022). Fluorescent nanosensors are a fascinating family of molecular devices for monitoring HM ions in the environment. Organic dyes (such as cyanine, fluorescein, and rhodamine) were commonly utilized as fluorescent probes in sensors in the past. Photobleaching, poor stability, limited absorption coefficients, low signals, and a narrow excitation spectrum are some of the disadvantages (Singh et al. 2021). Electrochemical-based BSs have been employed in the detection of disease-related biomolecules as well as the screening of a many of toxicants and chemical

Fig. 17.2 Classification of nanobiosensors based on their structure and mode of operation



compounds of interest. With the development of nanoscience, the use of NMs in electrochemical BSs has increased their sensitivity, response time, and conductivity. In accordance with their configuration, substances, particles, and living things interact with recognition receptors to capture the analyte. In contrast to the earlier non-portable forms of detecting systems, NM-based bioelectrochemical sensors offer significant advantages. Since polyaniline improves the mediation of the transfer of electrons in either enzymatic or redox reactions, it has better properties of heightened sensitivity and stability. The integration of polyaniline in an electrochemical BS has boosted the sensitivity of the biosensor (Saravanakumar et al., 2022). In addition, Yun et al. (2017) and Thirumalaisamy et al. (2022) reported that NBS-based Forster resonance energy transfer phenomenon (FRET) are valuable in detecting several metal ions than other traditional sophisticated spectroscopic methods. Table 17.1 show some examples of some nanosensors or nanobiosensors that detected heavy metal.

17.4 DNA Biosensor and DNA Nanobiosensors

Nucleic acids are a type of linear polymer composed of nucleotides. A purine or pyrimidine nucleobase, a pentose sugar, and a phosphate group make up a nucleotide. Adenine (A), guanine (G), cytosine (C), thymine (T), and uracil (U) are the five known bases or nucleotides. In the biopolymer molecule DNA, the base pairing of these nucleotides is A-T and G-C (Fatoyinbo and Hughes 2012). Thus, deoxyribonucleic acid (DNA) is a polymeric chain made up of repeating nucleotide that contains critical genetic information that control biological activity in living cells. DNA is now a key target for ligands in the treatment of many human illnesses, including cancer therapies (Zheng and Tan 2020). Analytical instruments that convert

Table 17.1 Examples of some nanosensors or nanobiosensors that detected heavy metal

| Nanobiosensor | Heavy metal detected | Samples type | Reference |
|--|----------------------|--------------------------|-------------------------|
| DNA sensor enhanced by silver | Hg | Water | Idros et al. (2022) |
| DNAzyme assembled and near-infrared light excited | Pb ²⁺ | Zebrafish (in vivo) | Huang et al. (2021) |
| DNAzyme | Cu ²⁺ | Serum | Zhao et al. (2021) |
| Nanosensor of multifunctionalized cobalt ferrite magnetite nanoparticles (CoFe ₂ O ₄ MNPs) | Cu ²⁺ | Quasi-homogeneous system | Lei et al. (2018) |
| Ligand-capped CdTe QDs (fluorescent nanosensor) | Cu ²⁺ | Water | Elmizadeh et al. (2017) |
| Fluorescence anisotropy by a G-rich thrombin binding aptamer | Pb ²⁺ | Homogeneous solution | Zhang et al. (2018) |

biological reactions into electrical signals are known as BSs (Kaoopae et al. 2020). Turdean (2011) reported that a biosensor is described as a self-contained integrated device capable of supplying particular quantitative or semiquantitative analytical information through the use of a biochemical receptor in direct spatial interaction with a transduction element. Bose et al. (2022) also described the BSs as a scientific instrument that integrates a biological element with a physiological transducer to create an electrical signal that is proportionate to a single analyte. Finally, the generated signal is sent to a detector. Several nanostructural miracles have made revolutionary changes in the area of molecular biology and have offered the chance to increase the performance of a BS in terms of detection limit, sensitivity, and repeatability with far more accuracy because of nanotechnology (Bose et al. 2022). Thus, NMs-based NSs have substantial advantages due to their large reactive surface area and small particle size, which includes improved physical, chemical, and biological features (Maduraiveeran et al. 2018).

DNA-based BSs (genosensors) have recently been extensively developed for environmental pollution detection, food analysis, clinical diagnostics, drug development, and biomedical research. Many kinds of DNA BSs have been improved and launched. These BSs also are applicable biosensors that are used in a variety of fields, including environmental monitoring, food safety, drug development, forensics, and biomedical research (Koopae et al. 2020). DNA-based BSs are both inexpensive and sensitive, and they can be employed as point-of-care diagnostic tools. These sensors offer numerous reading techniques in addition to durability and biocompatibility. A number of output strategies have been described depending on the functioning of DNA-based BSs: fluorescence and FRET-based reading, nanoparticle-based colorimetry, spectroscopy-based approaches, electrochemical signaling, gel electrophoresis, and atomic force microscopy (Chandrasekaran 2017). In the BS structure, nano-synthesized wires from metals (Ag, Cu, Ni, etc.), metal oxides (Fe_2O_3 , and ZnO) and semiconductor gallium silicon (Ca, GaN) spot quantum-based CdSeTe or CdTe, CdSe, carbon nanotubes and metal nanoparticles (NPs) (based on Ag, Cu, Pd, Co, Au, and Pt), and magnetic NPs, NMs have effects on detecting and analyzing sensors and BSs (Dolatabadi et al. 2011; Justino et al. 2017; Qi et al. 2018). Zhu et al. (2018) reported that due to its speedy, easy, on-site, accurate, and low-cost advantages over traditional chemical analysis, BSs based on functional nucleic acids have been created for the specific detection of Pb^{2+} and/or Hg^{2+} ions. In order to achieve a highly selective detection of Pb^{2+} in multiple decades, rationally designed G-quadruplex DNA probes have been intensively researched for lead ion detection. The duplex functional fluorescent probe could determine all genuine lake samples, including those containing Pb^{2+} or Hg^{2+} at 50 nM, with recovery rates of 96% and 104%, respectively. Because this sensor is label-free, simple, time-saving, cost-effective, and easy-to-handle, it might be used to detect Pb^{2+} and Hg^{2+} in a variety of applications (Zhu et al. 2018).

The precise binding of HM ions to bioreceptor DNA molecules alters the characteristics of NMs or DNA, resulting in qualitative and quantitative changes in the signal. Fluorescence intensity, luminescence intensity, visible color change, UV-visible absorption intensity, shift in absorption wavelength, and change in

microcantilever and electrochemical parameters, such as redox/anode/cathode current, impedance, and voltage, can all be caused by a change in signal (Chen et al. 2011 and Kumar and Guleria 2020). Chen et al. (2011) reported that the fluorescence quenching method was used to identify sulfide ions in hot spring and ocean samples. Sulfide ions in the test sample cause a conformational shift in the DNA probe that is present over the Au/Ag nanoclusters, resulting in fluorescence quenching. To eliminate nonspecific interaction with interfering iodide ions, the addition of sodium peroxydisulfate to the sensor is required. Functionalization of a specific DNA template in the presence of iodide ions in the test sample, Au/Ag nanoclusters experience fluorescence emission and color shift from clear to purple red (Li et al. 2017). However, many of these molecules or nanosystems have relatively steady detection limits and are incapable of distinguishing valence state of metal ions and achieving changeable detection ranges based on real demands. Furthermore, these molecules or nanosystems (based on biomolecules, DNA, and small molecules) demonstrated molecular diversity, molecular recognition, and information coding properties that are similar to molecular language employed by organism in nature but have gotten little consideration. Any molecular or nanosystem has specificity and may generate distinct responses to a wide range of chemicals, which are defined by a succession of high and low response signals. This means that these distinct response patterns may be abstracted into binary digital strings that can be encoded, stored, and protected. However, no effort was made to use the selected patterns of a sensing system for information encoding, encrypting, and concealing applications (Yao et al. 2022).

Aptamers are DNA molecules with a single strand. Because of their great affinity for a wide range of binding sites, aptamer-based DNA sensors have shown to be a robust and extremely sensitive platform. When compared to antibodies and other biorecognition components, they are the next most promising class. Because of their resilience and stability even at room temperature, they are superior sensing moieties to antibodies (Cho et al. 2009, Fang and Tan 2010). Aptamers can be tweaked to meet the requirements of the sensors. Aptamer synthesis on a large scale is less expensive than antibody production (Sypabekova et al. 2017). Aptamers are frequently employed in the production of low-cost NS for a wide range of analytes, ranging from biomedical sensors to food adulterant sensors to disease detection, due to their unique binding capabilities and ease of immobilization to the sensor surface (Tombelli et al. 2007 and Dhiman et al. 2017).

The NM-based BSs are the BSs that work at the nanoscale level (Bose et al. 2022). DNA-nanosensor (DNA-NS) is nanobiosensor that uses DNA as a recognition component and NMs as a transducer (Harroun et al. 2018). DNA can also be employed for bio-recognition. All the information in DNA seems encoded as a sequence of amino acids, which serves as the structure's defining basis. As a result, the identification of DNA sequences is critical to the control, decoding, and detecting of these molecules. Thus, the fundamental idea of a DNA-BS is to detect molecular recognition supplied by DNA probes and convert it into signals by a transducer (Kuswandi 2019). A large number of DNA-based NSs have been developed for a variety of human applications, including pollution detection (Harroun et al. 2018).

For example, a DNA-NSs based on Kelvin probe force microscopy has been developed for the detection of Ag⁺ in drinkable water. A conductive cantilever is exposed to AuNPs designed and synthesized with around 100 ssDNA probes. Only in the presence of Ag⁺, complementary target ssDNA with four nucleotide mismatches can bind with AuNPs probe. The binding of target DNA results in changes in surface potential that is proportional to concentration of Ag⁺ (Lee et al. 2018).

Peng et al. (2015) developed a novel fluorescent oligonucleotide-stabilized silver nanoclusters (DNA/AgNCs) probe for specific detection of Cu and Hg ions. The probe is made up of two customized DNA sequences. The first is a signal probe with a cytosine-rich sequence template for AgNCs production and linking sequence across both sides. The other is a guanine-rich sequence for signal amplification and a linking sequence that is complementary to the signal probe's link repeat. Based on the fluorescence-enhancing effect of DNA/AgNCs in the region of guanine-rich DNA sequences, the fluorescence of hybridized double-strain DNA/AgNCs is 200-fold improved after hybridization. The double-strand DNA/AgNCs probe is brighter and more persistent than the single-strain DNA/AgNCs probe, and it may also be employed as a new fluorescent probe to detect Cu and Hg ions. The Cu and Hg ions ranging from 6–240 nM to 6.0–160.0 nM, respectively, can be linearly detected with the limits of detection of 2.1 and 3.4 nM, respectively. The results of Peng et al. (2015) found that the analytical criteria for detecting Cu and Hg ions are greatly better than their corresponding of using single-strain DNA/AgNCs.

17.5 Nanosensors and DNA Nanosensors for Heavy Metals Detection

According to the World Health Organization (WHO), harmful HM ions such as Hg, Cd, Pb, and Cr (VI) have no nutritional value and are a serious public health problem. As a result, regulatory limitations for these components in environmental and food samples have been set. The safe suggested limits for Cd, Cr, Hg, and Pb, and in drinking water, according to the WHO recommendations, are 3.0, 50, 6.0, and 10 $\mu\text{g L}^{-1}$, respectively. Considering the abovementioned aspects of metal cations operating as necessary and hazardous agents in biosystems at small concentrations, BSs can be used to create reliable and sensitive analytical processes with acceptable selectivity (Rocha et al. 2021).

Biosensors, in general, have cheaper acquisition and maintenance costs, lower limit of detection with no need for lengthy sample preparation processes, and acceptable selectivity. Biosensors have been used to accurately determine elements at trace and ultra-trace levels in numerous instances. Despite the low detection limits of electrochemical methods, interference among metal cations has been widely observed, and the use of mask agents, for instance, is often required to overcome limitations. Selectivity is improved in a simple and ecologically friendly approach by altering electrodes with biocomponents. Furthermore, BSs are often readily

downsized, which aids in the creation of in situ and automated techniques that require little sample preparation (Rocha et al. 2021). Because of their capacity to respond to a wide range of HMS, cells are highly preferred biological components in BSs for HM detection. Many types of cells, including bacteria, cyanobacteria, algae, and plant cells, have been identified to be promising for HMs detection. Some of the indicators have been tested to identify the presence of HMs, which include the biological reactions of particular photosynthetic pigments, changes in oxygen content, and changes in the enzyme activity in cells. Chlorophyll as photosynthetic pigment is usually applied as a reporter group in the whole cell BSs. A few BSs using carotenoids as the reporter have also been reported (Wong and Wong 2014).

Nanobiosensors have a high sensitivity and accuracy in recognizing biologically harmful organisms, such as bacteria and viruses. In addition to detecting HMs and environmental toxins, NBSs have replaced time-consuming and expensive approaches. Yeast BSs are one example of this type of BSs (Mohammadi et al. 2018). Nanomaterial-based BSs are being developed to detect the presence of HMs. Nanomaterials, such as NPs, nanowires, nanotubes, and quantum dots, are being employed in BSs for HM detection and have proved to be a viable alternative to traditional approaches (Kuswandi 2019, Bose et al. 2022).

Turdean (2011) reported that A typical BS construct consists of three main components: a recognizing element (DNA, enzyme, antibody, etc.), a signal transducing structure (thermal, optical, or electrical), and an amplification/processing element, with almost the same designs also including a permselective membrane that controls analyte transport to the bioreceptor as in Fig. (17.3). Wong and Wong (2014) briefly reported that a BS is an analytical technique that combines a biological component with an electronic system, allowing the biological component's reaction to be collected and converted into a readable electronic signal. Several accurate enzyme-based BSs, such as urease conductometry BS, chymotrypsin amperometric BS, acetylcholinesterase optical BS, and invertase mutarotase-glucose oxidase-based conductometry BS, have been developed to date for the detection of HMs. Organic compounds and DNA have been used in BSs to identify HMs. Moreover, Salouti and Khadivi (2020) reported that significant range of enzymes was utilized for the inhibitive measurement of trace Hg in an electrochemical biosensor based on enzyme: urease, horseradish peroxidase, glucose oxidase, glycerol 3-phosphate oxidase, alcohol oxidase and invertase. Huang et al. (2021) stated that to detect and visualize Pb^{2+} , a DNAzyme-assembled and near-infrared light stimulated NS was designed. The donor of luminescence resonance energy transfer in this nanosensor was $NaYF_4:Yb, Er$ upconversion NP was inserted as near-infrared-to-Vis transducer, and the energy transfer acceptor was DNAzyme-functionalized black hole quencher 1. With great sensitivity and selectivity, this suggested NS was used to detect Pb^{2+} in solution. In addition, we have effectively established the imaging capacity of this NS in live cells and early-stage zebrafish, with low autofluorescence and strong photostability. The NP-DNAzyme NS upconversion would improve the method of visualizing Pb^{2+} in vivo and might be used to better understand Pb^{2+} metabolism and the process of lead poisoning in biological systems. Zhao et al. (2021) reported that for sensitive measurement of HMs in serum, a triple

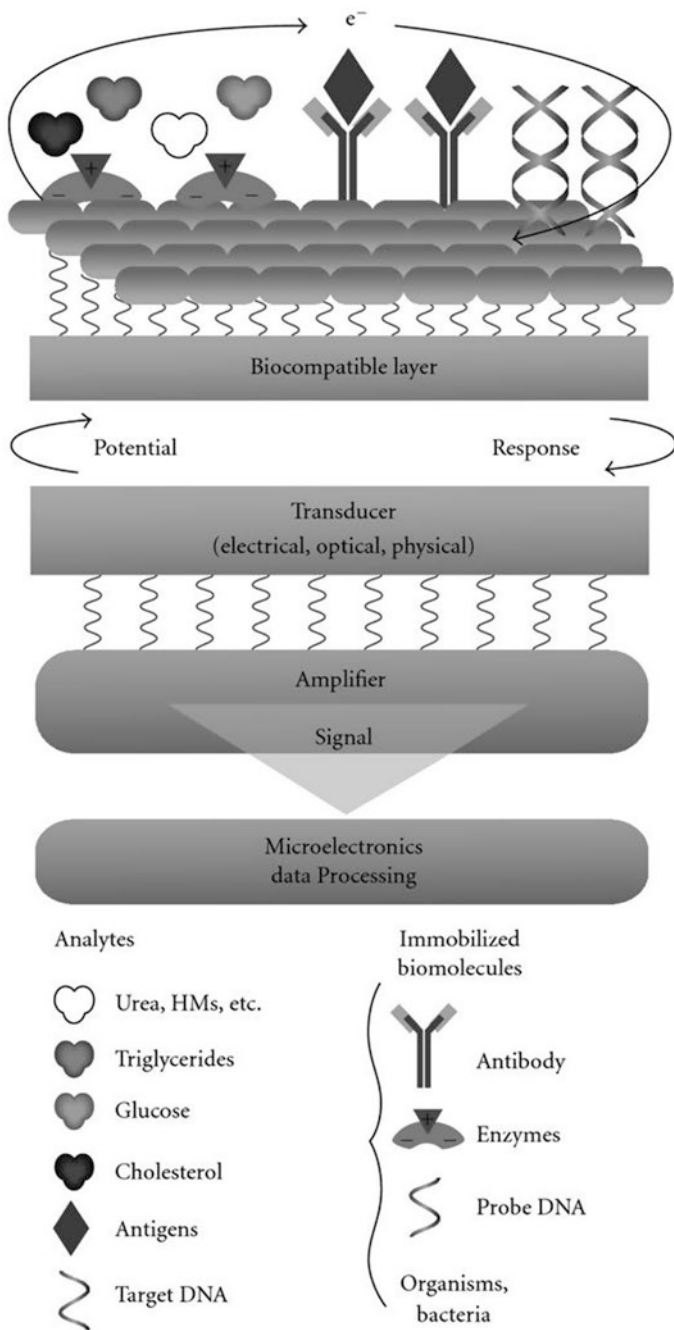


Fig. 17.3 Schematic principle of biosensor operation. (Source: Turdean (2011): <https://www.hindawi.com/journals/ijelc/2011/343125/fig 1/>)

signal-amplified electrochemical sensing platform based on metal-dependent DNAzymes are developed (copper as a model target). The proposed method demonstrated good sensitivity (limit of detection, 0.33 fM for Cu^{2+}) with excellent selectivity and stability under optimized conditions, which is attributed to the following: (1) tetrahedral DNA nanostructures, which were used as a promising scaffold to adjust the selective transformation between heterogeneous and homogeneous reactions, preventing nonspecific binding of electrodes surface and DNA probes, and (2) the magnetic beads, which led to signal a hybridization chain reaction. Unnikrishnan et al. (2021) stated that metal nanozyme-based assay has recently been shown to have the promise to be a viable alternative to traditional techniques because to its mobility, ease of use, and great sensitivity in detecting metal ion concentrations as low as parts per trillion (ppt). Metal nanozyme-based methods for HM ions allow for quick and low-cost screening on the spot using a basic equipment such as an UV-Vis absorption spectrophotometer, making them ideal for use in field operations, particularly in distant locations. A nanozyme-based sensor's detecting process is extremely reliant on its surface characteristics and specific interactions with certain metal ion types. Unlike natural enzyme-based tests, this approach frequently confronts selectivity difficulties.

Zhang et al. (2019) also reported that an HM ions sensor, like other BSs, has three critical components: analyte identification, physical support for probe immobilization, and signal transduction. Sensors of various kinds, such as NPs, field effect transistors, and working electrodes for voltammetry measurement, have been described. There are primarily optical and electrochemical mechanisms for signal transmission. When it comes to analyte detection, specific target identification is always crucial. To identify and interact with HM ions, popular probes include antibodies, peptides/amino acids, and nucleic acids. An antibody as a probe has the highest specificity; however, it has difficulties recognizing HM ions because HM ions are too small to detect directly by an antibody with high sensitivity, and antibody binding reactions may necessitate a fluid environment different from that in which HMIs naturally exist (Zhang et al. 2019). Zhang et al. (2019) reported also that glutathione is well-known for its high affinity with toxic HM ions, as well as its solubility in water, steady activity, and easily availability. As a consequence, glutathione is increasingly being used as a molecular probe in the development of sensors for precise, economical, and accessible HMs detection (Zhang et al. 2019). In recent years, optical approaches based mostly on graphene-derived NMs have improved. Optical chemical sensors operate on the basis of changes in optical properties (emission, absorption, transmission, and lifespan) caused by the binding of the arrested indicator (organic dye) with the analyte. A strategy of appealing graphene-based nanotechnology embarks as an accountable instrument that overcomes such problems and bestows increased performance on the sensing platform. For example, the optical NSs for detecting cadmium that was created utilizing nano-hybrid CdSe quantum dots regained their green photoluminescence (Sharma et al. 2021). Functional deoxynucleic acid has been dedicated to for developing precise and selective techniques for HMs detection, such as single-stranded DNA (ssDNA), DNAzymes, and G-quadruplexes. The sensitivity can be enhanced by using

fluorescent molecules and NMs, such as metal-NPs, QDs, and carbon NMs. Because of the complex system parts, suitable reaction condition requirement, and specific design of DNA molecules, DNA-related technologies have ultrasensitivity and biocompatibility. However, research is limited to certain HMs (Lian et al. 2020). Colorimetry, Raman spectroscopy/scattering, field effect transistors, and surface plasmon resonance are just a few of the DNA-based methods for detecting HMs that have been developed. Furthermore, many researchers have detected HMs using fluorescence resonance energy transfer methods. Fluorescence changes are the most convenient detection technique due to the simplicity of the detection format and low detection limit (Idors et al. 2022).

Yao et al. (2022) built a DNA nanosystem based on CoOOH nanosheets for tunable metal ion detection and polarity distinguishing, as well as molecular crypto-steganography employing molecular variety and identification of DNA, and informational coding functions of selected patterns (Fig. 17.4) fluorescent nanosensing system was built based on the fluorescent cooling ability of CoOOH nanosheets and the distinctive interaction between CoOOH nanosheet, DNA, and metal ion (Fig. 17.4a) to achieve dynamically adjusted detection of metal ions (Fe^{3+} , Hg^{2+} , Cr^{3+}) and distinguish their valence states (such as Fe^{3+} and Fe^{2+} , Fig. 17.4b). CoOOH nanosheets, as excellent nano-quenchers, may induce the fluorescence of carboxyfluorescein (FAM)-labeled DNA to be quenched, as illustrated in Scheme 1B. The fluorescence was further lowered by the interaction of CoOOH nanosheets when particular metal ions were added. Yao et al. (2022) added that the ability of DNA sequences rich in various bases (A, T, C, G) to bind to CoOOH nanosheets differed. The priority order was $\text{G} > \text{C} > \text{A} \approx \text{T}$, and short chains outperformed long chains. Interestingly, various DNA CoOOH nanostructures have distinct response patterns (selectivity) and linear ranges for certain metal ions (such as Fe^{3+} , Hg^{2+} , or Cr^{3+}). These facts suggest that DNA CoOOH sensing systems could be built by utilizing the variations of bases and lengths of DNA sequences to reach interactively attachable detection and valence bias of particular metal ions (Fig. 17.4b) and by

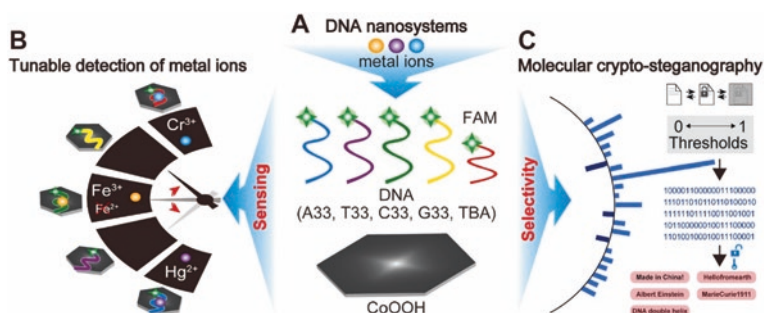


Fig. 17.4 The design of DNA fluorescent nanosystem devices based on CoOOH nanosheets and FAM-labeled DNA (a) and their application in variable detection and valence state separation of metal ions (b), as well as molecular crypto-steganography, is depicted schematically (c)

employing specific structures and binary converting based on specified thresholds to encode, interact, and protect information (Fig. 17.4c).

17.6 Challenges

The discovery of various biologically manufactured NMs and NPs has resulted in their effective use in the remediation of a variety of organic and inorganic contaminants, establishing them as a fresh approach in the area of nanotechnology-based remediation. Biosynthesized NMs have been useful in the replacing of present approaches for on-site remediation of contaminants via different techniques, such as pollutant detection, treatment, and remediation of hazardous waste sites, as technology has advanced (Das et al. 2018). Despite the fact that research into the utilization of nanotechnology is increasing every day, scientific study of naturally occurring nanosystems is still lacking. Standardized test techniques are required to investigate the impact of nanoparticles on living cells to establish the hazard of human exposure to nanoparticles. The toxicity of nanoparticles is poorly understood due to a lack of defined test methodologies and discrepancies in published results. Because of erroneous nanoparticle characterization and interferences generated by nanoparticles in the available test equipment, the presented result is inconclusive (Dasgupta et al. 2017).

Nanomaterials' manufacture, transportation, usage, and dispose may elevate NPs exposure to the environment and humans. Yet, because the physicochemical characteristics of NMs may be changed due to their dynamic interaction with surround environments, we do not have a complete knowledge of their destination and possible influence on the environment and humans (He et al. 2021). Further, there is still a great ambiguity in this area. Even though batch experimental studies have shown a synergistic relationship between NPs and microbes for the remedial work of a few contaminants, there is still a lack of understanding about the synergistic effects between NMs and biotechnology during the nano-bioremediation process, as well as the most efficient NM for HM remediation. Better regulation might result from a better understanding of the interaction between NMs and bio-based techniques during remediation approaches under various environmental conditions. Furthermore, there is a knowledge gap regarding the safety of long-term usage of NPs with microorganisms. When employing such materials, the regulatory system is crucial to consider (Punetha and Khan 2022). On-site application techniques, machine statistical methods, artificial networks, and individuals training are also additional challenges that could be considered in the application of nanobiosensors on the large scale. In addition, creating nanobiosensor that can work in many medias and environments with different circumstance, such as pH, temperature, light, is very crucial from many aspects such as saving a money and stability. Calibration of such sensors is also one of the most important things that should be taken into the consider when working on different scales. Interaction of nanomaterials and

contaminants and their modification, pathways, and effects are challenging also when working in open fields and environments.

17.7 Conclusion and Future Prospective

Heavy metals are known to cause long-term and significant harms to many ecosystems and human health. There is a high demand for new approaches that detect, monitor, and diagnose environmental contaminants in a timely, dependable, and low-cost manner. The traditional method for detection and remediation of pollutants in the environment, especially heavy metals, has many disadvantages, such as time consuming, costs, residues. Novel and eco-friendly approaches are required to avoid such previous disadvantages. Nanotechnology has recently received more attention and focus especially in the field of environmental monitoring. To respond to the presence of analytes or environmental variables, nanosensors use mechanical or chemical techniques with tiny components. Higher advantages in detection and are provided by biosensors and nanomaterials. Nanobiosensors are microorganisms that either develop naturally or are created to respond to environmental stimuli by producing a measurable signal. Thus, integration of nanosensors with bio-based systems to detect and monitor pollutants in the environment can be utilized for the combined benefits of nanobiosensors. The bio-recognition element, used for molecular recognition or the type of detecting used transduction, is employed to categorize nanobiosensors. Based on the bio-recognition or bioreceptor utilized, nanobiosensors are divided into three categories: enzyme-based NBSs, immuno NBSs, and DNA-NBSs. Optical NBSs, electrochemical NBSs, and mechanical NBSs are the three categories of nanobiosensors based on their structure and method of operation. Heavy metals can be detected using DNA-related probes or enzymes in an efficient, selective, and accurate manner. DNA-related technologies offer ultra-sensitivity and biocompatibility due to the complex system components, acceptable reaction conditions, and unique design of DNA molecules. However, study is restricted to a few HMs. A nanozyme-based sensor is one of the most applied sensors, where it is a detecting process which is extremely reliant on its surface properties and specific interaction with certain metal ion types. Many researches have used different types of nanobiosensors to detect heavy metal ions, specially Pb and Hg in many medias. It is proven that nanobiosensors are highly sensitive, selective and accurate, biodegradable, eco-friendly, cost-effective, more economic, and practical. Hence, it outdoes other analytical techniques, such as high-performance liquid chromatography, gas chromatography, and capillary electrophoresis, in detecting heavy metals and environmental toxins. However, most of these researches was practically performed on the lab scale. Therefore, it is recommended to extend the research on this topic specially on the large and field scale to reduce the gap of knowledge especially regarding many heavy other metals.

References

- Ahmad R, Tripathy N, Khosla A, Khan M, Mishra P, Ansari WA, et al. Recent advances in nano-structured graphitic carbon nitride as a sensing material for heavy metal ions. *J Electrochem Soc.* 2020;167(3):037519. <https://doi.org/10.1149/2.0192003JES>.
- Ahmed M, Zhao R, Du J. Nanostructural ZnO-based electrochemical sensor for environmental application. *J Electrochem Soc.* 2022;169:020573. <https://doi.org/10.1149/1945-7111/ac534d>.
- Ali MM, Islam MS, Islam ARMT, Bhuyan MS, Ahmed AS, Rahman MZ, Rahman MM. Toxic metal pollution and ecological risk assessment in water and sediment at ship breaking sites in the Bay of Bengal Coast, Bangladesh. *Mar Pollut Bull.* 2022;175:113274. <https://doi.org/10.1016/j.marpolbul.2021.113274>.
- Bhushan B, editor. *Encyclopedia of nanotechnology*, No. 544.1. Dordrecht: Springer; 2012.
- Boregowda N, Jogigowda SC, Bhavya G, Sunilkumar CR, Geetha N, Udikeri SS, Chowdappa S, Govarthanan M, Jogaiah, S. Recent advances in nanoremediation: Carving sustainable solution to clean-up polluted agriculture soils. *Environ Pollut.* 2021;118728.
- Bose S, Maity S, Sarkar A. Nano-materials as biosensor for heavy metal detection. In: *Food, medical, and environmental applications of nanomaterials*. Amsterdam: Elsevier; 2022. p. 493–526. <https://doi.org/10.1016/B978-0-12-822858-6.00018-2>
- Chandrasekaran AR. DNA nanobiosensors: an outlook on signal readout strategies. *J Nanomater.* 2017;2820619. <https://doi.org/10.1155/2017/2820619>
- Chen WY, Lan GY, Chang HT. Use of fluorescent DNA-templated gold/silver nanoclusters for the detection of sulfide ions. *Anal Chem.* 2011;83(24):9450–5.
- Cho EJ, Lee JW, Ellington AD. Applications of aptamers as sensors. *Annu Rev Anal Chem.* 2009;2:241–64.
- Das S, Chakraborty J, Chatterjee S, Kumar H. Prospects of biosynthesized nanomaterials for the remediation of organic and inorganic environmental contaminants. *Environ Sci Nano.* 2018;5(12):2784–808. <https://doi.org/10.1039/C8EN00799C>.
- Dasgupta N, Ranjan S, Ramalingam C. Applications of nanotechnology in agriculture and water quality management. *Environ Chem Lett.* 2017;15(4):591–605. <https://doi.org/10.1007/s10311-017-0648-9>.
- Dey M, Akter A, Islam S, Dey SC, Choudhury TR, Fatema KJ, Begum BA. Assessment of contamination level, pollution risk and source apportionment of heavy metals in the Halda River water, Bangladesh. *Heliyon.* 2021;7(12):e08625. <https://doi.org/10.1016/j.heliyon.2021.e08625>.
- Dhiman A, Kalra P, Bansal V, Bruno JG, Sharma TK. Aptamer-based point-of-care diagnostic platforms. *Sensors Actuators B Chem.* 2017;246:535–53.
- Dolatabadi JEN, Mashinchian O, Ayoubi B, Jamali AA, Mobed A, Losic D, et al. Optical and electrochemical DNA nanobiosensors. *TrAC Trends Anal Chem.* 2011;30(3):459–72.
- Elbasiouny H, Elbehiry F, El-Ramady H Toxic effects of nanoparticles under combined stress on plants. In *Toxicity of nanoparticles in plants*. Academic Press; 2022 p. 109–129. <https://doi.org/10.1016/B978-0-323-90774-3.00004-0>.
- Elbehiry F, Elbasiouny H, El-Ramady H, Brevik EC. Mobility, distribution, and potential risk assessment of selected trace elements in soils of the Nile Delta, Egypt. *Environ Monit Assess.* 2019;191(12):1–22. <https://doi.org/10.1007/s10661-019-7892-3>.
- Elbehiry F, Elbasiouny H, Cappuyns V, Brevik EC. Available concentrations of some potentially toxic and emerging contaminants in different soil orders in Egypt and assessment of soil pollution. *J Soils Sediments.* 2021;21(11):3645–62.
- Elbehiry F, Elbasiouny H, El-Ramady H. Bioaccumulation and biotransformation of metal-based nanoparticles in plants. In *Toxicity of nanoparticles in plants*. Academic Press; 2022. p. 299–315. <https://doi.org/10.1016/B978-0-323-90774-3.00001-5>.
- Eldamaty HSE, Elbasiouny H, Elmoslemany AM, El-Maoula LMA, El-Desoky OI, Rehan M, Moneim DAE, Zedan A. Protective effect of wheat and barley grass against the acute toxicological effects of the concurrent administration of excessive heavy metals in drinking water on the rats liver and brain. *Appl Sci.* 2021;11:5059. <https://doi.org/10.3390/app11115059>.

- Elmizadeh H, Soleimani M, Faridbod F, et al. Ligand-capped CdTe quantum dots as a fluorescent Nanosensor for detection of copper ions in environmental water sample. *J Fluoresc*. 2017;27:2323–33. <https://doi.org/10.1007/s10895-017-2174-3>.
- Fang X, Tan W. Aptamers generated from cell-SELEX for molecular medicine: a chemical biology approach. *Acc Chem Res*. 2010;43(1):48–57.
- Fatoyinbo HO, Hughes MP. Biosensors. In: Bhushan B, editor. *Encyclopedia of nanotechnology*. Dordrecht: Springer; 2012. https://doi.org/10.1007/978-90-481-9751-4_129.
- Fouad OA, Ali GAM, El-Erian MAI, Makhlof SA. Humidity sensing properties of cobalt oxide/silica nanocomposites prepared via sol-gel and related routes. *Nano*. 2012;7(5):1250038.
- García-Aljaro C, Bangar MA, Baldrich E, Muñoz FJ, Mulchandani A. Conducting polymer nanowire-based chemiresistive biosensor for the detection of bacterial spores. *Biosens Bioelectron*. 2010;25(10):2309–12.
- Gupta A, Kumari A, Kaushal N, Saifi A, Mohanta G, Sachdev A, et al. Recent advances in the applications of carbon nanostructures on optical sensing of emerging aquatic pollutants. *ChemNanoMat*. 2022;8(6):e202200011. <https://doi.org/10.1002/cnma.202200011>.
- Harroun SG, Prévost-Tremblay C, Lauzon D, Desrosiers A, Wang X, Pedro L, et al. Programmable DNA switches and their applications. *Nanoscale*. 2018;10(10):4607–41.
- He X, Deng H, Hwang H. Nanosensors for heavy metal detection in environmental media: recent advances and future trends. In: Kumar V, Guleria P, Ranjan S, Dasgupta N, Lichtfouse E, editors. *Nanosensors for environment, food and agriculture Vol. 1. Environmental chemistry for a sustainable world*, vol. 60. Cham: Springer; 2021. https://doi.org/10.1007/978-3-030-63245-8_2.
- Huang L, Chen F, Zong X, Lu Q, Wu C, Ni Z, et al. Near-infrared light excited UCNPs-DNAzyme nanosensor for selective detection of Pb²⁺ and in vivo imaging. *Talanta*. 2021;227:122156. <https://doi.org/10.1016/j.talanta.2021.122156>.
- Idros N, Stott K, Allen J, Kamboj VS, Corns WT, Newton PJ, et al. Highly sensitive fluorescence-based mercury (II) DNA sensor enhanced by silver (I) activation. *Measurement: Sens*. 2022;20:100368. <https://doi.org/10.1016/j.measen.2022.100368>.
- Jeevanandam J, Kaliyaperumal A, Sundararam M, Danquah MK. Nanomaterials as toxic gas sensors and biosensors. In: Inamuddin AA, editor. *Nanosensor Technologies for environmental monitoring. Nanotechnology in the life sciences*. Cham: Springer; 2020. https://doi.org/10.1007/978-3-030-45116-5_13.
- Justino CI, Gomes AR, Freitas AC, Duarte AC, Rocha-Santos TA. Graphene based sensors and biosensors. *TRAC Trends Anal Chem*. 2017;91:53–66.
- Khanna VK. *Nanosensors: physical, chemical, and biological*. CRC Press; 2011.
- Koopae HK, Rezaei V, Esmailzadeh A. DNA biosensors techniques and their applications in food safety. *Environmental protection and biomedical research: a mini-review. J Cell Dev Biol*. 2020;3(1):28–35.
- Kumar V, Guleria P. Application of DNA-nanosensor for environmental monitoring: recent advances and perspectives. *Curr Pollut Rep*. 2020;1–21. <https://doi.org/10.1007/s40726-020-00165-1>.
- Kumari V, Rastogi S, Sharma V. Emerging trends in nanobiosensor. In: Prasad R, Kumar V, Kumar M, Choudhary D, editors. *Nanobiotechnology in bioformulations. Nanotechnology in the life sciences*. Cham: Springer; 2019. https://doi.org/10.1007/978-3-030-17061-5_18.
- Kuswandi B. Nanobiosensor approaches for pollutant monitoring. *Environ Chem Lett*. 2019;17:975–90. <https://doi.org/10.1007/s10311-018-00853-x>.
- Lee D, Lee H, Lee G, Kim I, Lee SW, Kim W, et al. Extremely sensitive and wide-range silver ion detection via assessing the integrated surface potential of a DNA-capped gold nanoparticle. *Nanotechnology*. 2018;30(8):085501.
- Lei YM, Xiao BQ, Liang WB, Chai YQ, Yuan R, Zhuo Y. A robust, magnetic, and self-accelerated electrochemiluminescent nanosensor for ultrasensitive detection of copper ion. *Biosens Bioelectron*. 2018;109:109–15. <https://doi.org/10.1016/j.bios.2018.03.013>.
- Li Z, Liu R, Xing G, Wang T, Liu S. A novel fluorometric and colorimetric sensor for iodide determination using DNA-templated gold/silver nanoclusters. *Biosens Bioelectron*. 2017;96:44–8.

- Lian J, Xu Q, Wang Y, Meng F. Recent developments in fluorescent materials for heavy metal ions analysis from the perspective of forensic chemistry. *Front Chem.* 2020;8:1016.
- Lim TC, Ramakrishna S. A conceptual review of nanosensors. *Zeitschrift für Naturforschung A.* 2006;61(7–8):402–12.
- Maduraiveeran G, Sasidharan M, Ganesan V. Electrochemical sensor and biosensor platforms based on advanced nanomaterials for biological and biomedical applications. *Biosens Bioelectron.* 2018;103:113–29.
- Mahmoud A, Fawzy M. Nanosensors and nanobiosensors for monitoring the environmental pollutants. In: Makhlof ASH, Ali GAM, editors. *Waste recycling technologies for nanomaterials manufacturing. Topics in mining, metallurgy and materials engineering.* Cham: Springer; 2021. https://doi.org/10.1007/978-3-030-68031-2_9.
- Maric T, Mayorga-Martinez CC, Nasir MZM, Pumera M. Platinum–halloysite nanoclay nanojets as sensitive and selective mobile nanosensors for mercury detection. *Adv Mater Technol.* 2019;4(2):1800502. <https://doi.org/10.1002/admt.201800502>.
- Mohammadi AR, Alae MY, Asadi A, Gholamzadeh S. The role of nanobiosensors in identifying pathogens and environmental hazards. *Anthropog Pollut J.* 2018;2(2):16–25.
- Mokhtarzadeh A, Eivazzadeh-Keihan R, Pashazadeh P, Hejazi M, Gharaatifar N, Hasanzadeh M, et al. Nanomaterial-based biosensors for detection of pathogenic virus. *TrAC Trends Anal Chem.* 2017;97:445–57.
- Nehra M, Dilbaghi N, Hassan A. A, Kumar S. Carbon-based nanomaterials for the development of sensitive nanosensor platforms. In *Advances in nanosensors for biological and environmental analysis.* Elsevier; 2019. p. 1–25. <https://doi.org/10.1016/B978-0-12-817456-2.00001-2>.
- Numan A, Gill AA, Rafique S, Guduri M, Zhan Y, Maddiboyina B, Dang NN. Rationally engineered nanosensors: a novel strategy for the detection of heavy metal ions in the environment. *J Hazard Mater.* 2021;409:124493. <https://doi.org/10.1016/j.jhazmat.2020.124493>.
- Peng J, Ling J, Zhang XQ, Bai HP, Zheng L, Cao QE, Ding ZT. Sensitive detection of mercury and copper ions by fluorescent DNA/Ag nanoclusters in guanine-rich DNA hybridization. *Spectrochim Acta A Mol Biomol Spectrosc.* 2015;137:1250–7.
- Pourtaheri E, Taher MA, Ali GA, Agarwal S, Gupta VK. Electrochemical detection of gliclazide and glibenclamide on ZnIn₂S₄ nanoparticles-modified carbon ionic liquid electrode. *J Mol Liq.* 2019;289:111141.
- Punetha A, Khan A. Application of nanobiotechnology for heavy metal remediation. In: Rai JPN, Saraswat S, editors. *Nano-biotechnology for waste water treatment, Water science and technology library, vol. 111.* Cham: Springer; 2022. https://doi.org/10.1007/978-3-031-00812-2_8.
- Qi H, Yue S, Bi S, Ding C, Song W. Isothermal exponential amplification techniques: from basic principles to applications in electrochemical biosensors. *Biosens Bioelectron.* 2018;110:207–17.
- Rigo AA, Cezaro AMD, Muenchen DK, Martinazzo J, Brezolin AN, Hoehne L, et al. Cantilever nanobiosensor based on the enzyme urease for detection of heavy metals. *Braz J Chem Eng.* 2020;36:1429–37. <https://doi.org/10.1590/0104-6632.20190364s20190035>.
- Rocha DL, Maringolo V, Araújo AN, Amorim CMPG, Montenegro M, d.C.B.S.M. An overview of structured biosensors for metal ions determination. *Chemosensors.* 2021;9:324. <https://doi.org/10.3390/chemosensors9110324>.
- Sabzehmeidani MM, Kazemzad M. Quantum dots based sensitive nanosensors for detection of antibiotics in natural products: a review. *Sci Total Environ.* 2022;810:151997. <https://doi.org/10.1016/j.scitotenv.2021.151997>.
- Sadoine M, Ishikawa Y, Kleist TJ, Wudick MM, Nakamura M, Grossmann G, Frommer WB, Ho CH. Designs, applications, and limitations of genetically encoded fluorescent sensors to explore plant biology. *Plant Physiol.* 2021;187(2):485–503.
- Salouti M, Khadivi DF. Biosensors and Nanobiosensors in environmental applications. In: Ghorbanpour M, Bhargava P, Varma A, Choudhary D, editors. *Biogenic Nanoparticles and their use in agro-ecosystems.* Singapore: Springer; 2020. https://doi.org/10.1007/978-981-15-2985-6_26.

- Saravanakumar K, SivaSantosh S, Sathiyaseelan A, Naveen KV, AfaanAhamed MA, Zhang X, et al. Unraveling the hazardous impact of diverse contaminants in the marine environment: detection and remedial approach through nanomaterials and nano-biosensors. *J Hazard Mater.* 2022;433:128720. <https://doi.org/10.1016/j.jhazmat.2022.128720>.
- Sargazi S, Fatima I, Kiani MH, Mohammadzadeh V, Arshad R, Bilal M, et al. Fluorescent-based nanosensors for selective detection of a wide range of biological macromolecules: a comprehensive review. *Int J Biol Macromol.* 2022;206:115–47. <https://doi.org/10.1016/j.ijbiomac.2022.02.137>.
- Singh H, Bamrah A, Bhardwaj SK, Deep A, Khatri M, Kim K-H, Bhardwaj N. Nanomaterial-based fluorescent sensors for the detection of lead ions. *J Hazard Mater.* 2021;407:124379.
- Sharma P, Pandey V, Sharma M, Patra A, Singh B, Mehta SA. Review on biosensors and nanosensors application in agroecosystems. *Nanoscale Res Lett.* 2021;16:136. <https://doi.org/10.1186/s11671-021-03593-0>.
- Sun Y, Fang L, Wan Y, Gu Z. Pathogenic detection and phenotype using magnetic nanoparticle-urease nanosensor. *Sensors Actuators B Chem.* 2018;259:428–32.
- Swierczewska M, Liu G, Lee S, Chen X. High-sensitivity nanosensors for biomarker detection. *Chem Soc Rev.* 2012;41(7):2641–55.
- Sypabekova M, Bekmurzayeva A, Wang R, Li Y, Nogues C, Kanayeva D. Selection, characterization, and application of DNA aptamers for detection of mycobacterium tuberculosis secreted protein MPT64. *Tuberculosis.* 2017;104:70–8.
- Thirumalaisamy R, Suriyaprabha R, Prabhu M, Thesai AS. Role of nanomaterials in environmental remediation: recent advances—A review. In: Aravind J, Kamaraj M, Karthikeyan S, editors. *Strategies and tools for pollutant mitigation*. Cham: Springer; 2022. https://doi.org/10.1007/978-3-030-98241-6_3.
- Tombelli S, Minunni M, Mascini M. Aptamers-based assays for diagnostics, environmental and food analysis. *Biomol Eng.* 2007;24(2):191–200.
- Touhami AJN. Biosensors and nanobiosensors: design and applications. *Nanomedicine.* 2014;15:374–403.
- Turdean L. Design and development of biosensors for the detection of heavy metal toxicity. *Int J Electrochem.* 2011;15:343125. <https://doi.org/10.4061/2011/343125>.
- Türkoğlu EA, Yavuz H, Uzun L, Akgöl S, Denizli A. The fabrication of nanosensor-based surface plasmon resonance for IgG detection. *Artif cells Nanomed Biotechnology.* 2013;41(3):213–21. <https://doi.org/10.3109/10731199.2012.716066>.
- Ullah N, Mansha M, Khan I, Qurashi A. Nanomaterial-based optical chemical sensors for the detection of heavy metals in water: recent advances and challenges. *TrAC Trends Anal Chem.* 2018;100:155–66. <https://doi.org/10.1016/j.trac.2018.01.002>.
- Unnikrishnan B, Lien CW, Chu HW, Huang CC. A review on metal nanozyme-based sensing of heavy metal ions: challenges and future perspectives. *J Hazard Mater.* 2021;401:123397. <https://doi.org/10.1016/j.jhazmat.2020.123397>.
- Varun S, Daniel SCGK. Emerging nanosensing strategies for heavy metal detection. *Nanotechnol Sustain Water Resour.* 2018;5:199–225. <https://doi.org/10.1002/9781119323655.ch7>.
- Wang J, Qu X. Recent progress in nanosensors for sensitive detection of biomolecules. *Nanoscale.* 2013;5(9):3589–600.
- Wang X, Kong L, Zhou S, Ma C, Lin W, Sun X, et al. Development of QDs-based nanosensors for heavy metal detection: a review on transducer principles and in-situ detection. *Talanta.* 2022;239:122903. <https://doi.org/10.1016/j.talanta.2021.122903>.
- Wong LS, Wong CS. A new method for heavy metals and aluminium detection using biopolymer-based optical biosensor. *IEEE Sensors J.* 2014;15(1):471–5.
- Yang T, Duncan TV. Challenges and potential solutions for nanosensors intended for use with foods. *Nat Nanotechnol.* 2021;16:251–65. <https://doi.org/10.1038/s41565-021-00867-7>.
- Yao QF, Zhu QY, Bu ZQ, Liu QY, Quan MX, Huang WT. DNA nanosensing systems for tunable detection of metal ions and molecular crypto-steganography. *Biosens Bioelectron.* 2022;195:113645. <https://doi.org/10.1016/j.bios.2021.113645>.

- Ye W, Yu M, Wang F, Li Y, Wang C. Multiplexed detection of heavy metal ions by single plasmonic nanosensors. *Biosens Bioelectron.* 2022;196:113688. <https://doi.org/10.1016/j.bios.2021.113688>.
- Yun W, Wu H, Liu X, Fu M, Jiang J, Du Y, Yang L, Huang Y. Simultaneous fluorescent detection of multiple metal ions based on the DNAzymes and graphene oxide. *Anal Chim Acta.* 2017;986:115–21. <https://doi.org/10.1016/j.aca.2017.07.015>.
- Zhang L, Peng D, Liang RP, Qiu JD. Graphene-based optical nanosensors for detection of heavy metal ions. *TrAC Trends Anal Chem.* 2018;102:280–9. <https://doi.org/10.1016/j.trac.2018.02.010>.
- Zhang J, Sun X, Wu J. Heavy metal ion detection platforms based on a glutathione probe: a mini review. *Appl Sci.* 2019;9(3):489. <https://doi.org/10.3390/app9030489>.
- Zhao S, Xiao J, Wang H, Li L, Wang K, Lv J, Zhang Z. Rapid heavy metal sensing platform: a case of triple signal amplification strategy for the sensitive detection of serum copper. *Anal Chim Acta.* 2021;1181:338908. <https://doi.org/10.1016/j.aca.2021.338908>.
- Zheng XT, Tan YN. Recent development of nucleic acid nanosensors to detect sequence-specific binding interactions: from metal ions, small molecules to proteins and pathogens. *Sensors International.* 2020;1:100034. <https://doi.org/10.1016/j.sintl.2020.100034>
- Zhu Q, Liu L, Xing Y, Zhou X. Duplex functional G-quadruplex/NMM fluorescent probe for label-free detection of lead (II) and mercury (II) ions. *J Hazard Mater.* 2018;355:50–5. <https://doi.org/10.1016/j.jhazmat.2018.04.082>.
- Zou W, Tang Y, Zeng H, Wang C, Wu Y. Porous Co₃O₄ nanodisks as robust peroxidase mimetics in an ultrasensitive colorimetric sensor for the rapid detection of multiple heavy metal residues in environmental water samples. *J Hazard Mater.* 2021;417:125994. <https://doi.org/10.1016/j.jhazmat.2021.125994>.

Chapter 18

Smart Nanosensors for Pesticides and Heavy Metals Detection



Nilesh Satpute, Kamlesh Shrivastava, and Khemchand Dewangan

18.1 Introduction

Agriculture is the main occupation worldwide and is considered an essential aspect of everyone's life. It is not only a source of livelihood, but it is a way of life too. It is regarded as the main foundation of the economic development of a nation. Therefore, to keep healthy crops and agricultural products, many pesticides or plant protection products are being used to prevent them from disease and infections. According to the market estimates of the United States (US) Environmental Protection Agency (EPA), nearly 56 billion dollars of pesticides were used annually at the producer level globally in 2012 (Atwood and Paisley-Jones 2017). According to the directorate Plant Protection, Quarantine, and Storage (PPQS) from India, about 62 metric tons of chemical pesticides were consumed in 2020–2021 (PPQS 2021). Pesticides generally include herbicides, fungicides, insecticides, acaricides, insect repellants, and nematocides. These are mostly synthetic chemicals that typically include organochlorides, organophosphates, carbamates, pyrethrin, pyrethroids, diazinon, and dichlorodiphenyltrichloroethane (DDT) (Sharma et al. 2019). Also, sometimes these pesticides are used for public health protection programs to protect humans from malaria, dengue, schistosomiasis, etc. Pesticides can be an essential part of integrated pest management systems; however, these products can create further alternative pest problems as these establish resistance toward pesticides or harm people and wildlife. When these pesticides are applied on crops by any agricultural means (like spray, granulate, or seed treatment) to target pests, the

N. Satpute · K. Dewangan (✉)

Department of Chemistry, Indira Gandhi National Tribal University, Amarkantak, MP, India
e-mail: khemchand.dewangan@igntu.ac.in

K. Shrivastava (✉)

School of Studies in Chemistry, Pt. Ravishankar Shukla University, Raipur, CG, India

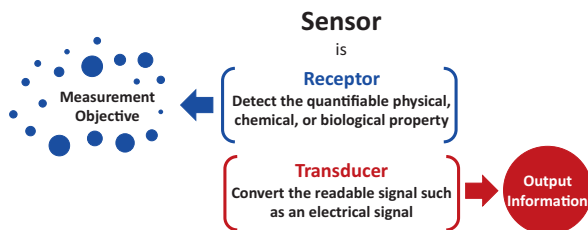
whole site gets affected, including crop plants, soil, and organisms. It causes oxidative stress that retard growth and photosynthetic efficiency in plants. Also, these pesticides get transmitted through air, water, and soil medium to humans and animals directly or indirectly. Considering the toxicity of pesticides in agriculture, the World Health Organization (WHO) had grouped pesticides into four different classes: extremely toxic, highly toxic, moderately toxic, and slightly toxic (WHO 2020).

In addition, systematic reviews of the impact of pesticides on human health and the ecosystem were extensively studied, and it was concluded that all classes of chemical pesticides are associated with human and environmental issues (Nicolopoulou-Stamati et al. 2016; Rani et al. 2021). For example, Calvert et al. studied 3271 cases of acute pesticide poisoning in the United States from 1998 to 2005 and reported that 71% were employed as farm workers (Calvert et al. 2008). A recent survey from US Geological Survey (USGS) monitored ground and surface water and found multiple pesticides and their degrades in water sources even though 90% of streams and 50% of wells are tested positive for being affected by at least one pesticide (Bexfield et al. 2021; Stackpoole et al. 2021).

On the other hand, toxic heavy metals are also a worldwide concern (Crisponi and Nurchi 2015; Martin 2006). They are nonbiodegradable in the environment and can quickly accumulate in air, soil, and surface water and pollute the environment. Heavy metals, including arsenic (As), cadmium (Cd), lead (Pb), and mercury (Hg), are used in several industries, including electronics, automobiles, machinery, and the paint industry. Thus, they are being released into nearby soil (lands) and water sources, and they get transported by runoff water and contaminate other water sources, like rivers, ponds, and lakes. Apart from that, mining activities are also responsible for the various contaminations, as it is also a source of these heavy metals. Also, rampant industrialization, urbanization, and modern synthetic activities have enormously increased heavy metals usage. Therefore, their concentration is increased in different habitats compared to natural background levels. Heavy metals have already been proven to have severe toxic effects in biological systems via enzyme inhibition, oxidative stress, and impaired antioxidant metabolism. However, high-level exposure can cause acute diseases, like schizophrenia, neurological disorders, liver disease, cancer, and kidney failure.

At present, many researchers are working on detection and removal mechanisms of heavy metals to reduce their toxic effectivity on nature and human beings. In this context, compared to bulk counterparts, brand new properties of nanomaterials enhanced the sensitivity and selectivity to evaluate contaminants present in environments and territory. In addition, the recent advancement of nanotechnology enables us to design portable and smart nanosensors/nanobiosensors for rapid and real-time analysis.

Fig. 18.1 Schematic representation of receptor and transducer in a sensor



18.2 Overview of Sensing Techniques

A sensor means a system that precisely measures something input using physical, chemical, or biological interactions. Basically, a sensor contains two central functional units: first a receptor and second a transducer (Fig. 18.1). The receptor in a sensor is one of the essential components concerning selectivity and sensitivity to a specific kind of material and therefore allows one to obtain reliable results with no or little interference from other substances. When it interacts with a specific and selective analyte, the information of the investigative material is converted into a form of energy that is further processed by the transducer for a sensible signal. The transducer is a machine part of a sensor that does not show any selectivity but can convert energy carrying the information relating to the sample into a useful analytical signal (Dewangan et al. 2020).

18.2.1 The Need for Smart and Intelligent Nanosensors

Various traditional methods such as chromatography and spectroscopy have been used to detect and monitor toxicants present in different samples in the environment. These conventional methods may take more time to obtain results and require maximum investment in the capital and time for sample preparation and detection process. Also, the limit of detection (LOD) and reproducibility are very challenging in conventional technologies. Therefore, in the last few decades, a combination of several sophisticated analytical techniques, such as gas chromatography-mass spectrometry (GC-MS), high-performance liquid chromatography (HPLC), HPLC-MS, and inductively coupled plasma-mass spectroscopy (ICP-MS), has been employed to evaluate pesticides, toxic metals, and other pollutants in trace amounts with high reliability and reproducibility, though these instrumental techniques apply a massive amount of solvents for purification, extraction, and derivatization. Also, these techniques require a skilled person to operate instruments and analysis. Further, these techniques cannot be appropriate at the sample sources to determine target analytes present in the air, water, soil, food, etc.

18.2.2 Smart Nanosensors and Nanobiosensors

Nanosensor is a sensing device, where the receptor component is made of nanomaterials/nanocomposites. Similarly, a nanobiosensor is a nanosensor, where the nano-component of the receptor comprises a pure/hybrid biomolecule (antibody, enzyme, protein, DNA, etc.) that serves as a template for the material to be detected. Generally, nanosensors/nanobiosensors are very tiny sensors in the size of a few nanometers of about 10–100 nm. They are very particular and sensitive toward physical or chemical(biochemical) changes that can detect an extremely low concentration of the substance as well as a single virus. The potentiality, importance, and smartness of these nanoscience-based sensors are depicted in Fig. 18.2.

At present, smart and intelligent nanosensors/nanobiosensors are beneficial tools in our everyday life, being used to detect allergens in food, toxicants in water, in chronic diseases control, pregnancy tests, and other diagnostic applications.

18.2.3 Operation Modes of Nanosensors

A nanosensor (or bionanosensor) is made of a sensitive layer of receptor, viz., nanomaterials (or nano biomolecules), which is covalently attached to the transducer. Interactions between target analyte and receptor generate a physiochemical change, which is converted into useful electrical signals by a transducer. According to the mode of operation of the transducer, smart nanosensors are tabulated in Table 18.1.

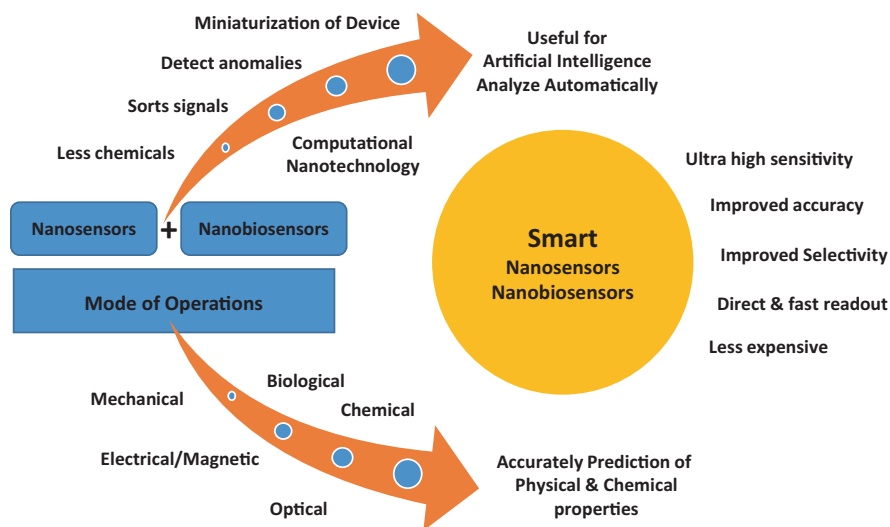


Fig. 18.2 Potentiality and importance of nanosensors/nanobiosensors

Table 18.1 Operating modes of smart nanosensors/nanobiosensors

| Optical | Electrical/magnetic | Mechanical | Chemical | Biological |
|--------------------|-------------------------|-------------|------------------------|---------------|
| Absorbance | Electrical permittivity | Density | Molecule concentration | Aptamers |
| Diffraction | Conductivity | Force | Oxidation-reduction | Antibodies |
| Fluorescence | Current | Mass | pH level | Enzymes |
| Luminescence | Magnetic | Pressure | | Nucleic acids |
| Optothermal Effect | Semiconductor | Temperature | | Whole cells |
| Phosphorescence | | Vibration | | |
| Reflection | | | | |
| Scattering | | | | |

The sensitivity, detection limit, response time, linearity, stability, hysteresis, life cycle, accuracy, and precision are the most crucial parameters for validating newly developed static and dynamic nanosensors. Various research groups have well reorganized and clarified these parameters toward chemical sensors in their book chapters/review articles (Correa et al. 2017; Li et al. 2019b; Munonde and Nomgongo 2021).

18.3 Nanomaterials and their Types

18.3.1 General Aspect of Nanomaterials

Nanomaterials are commonly defined as materials with an average grain size of less than 100 nm. It is extremely small, with at least one external dimension measuring 1–100 nm (where 1 billion nm = 1 m). Our human eyes cannot detect these materials. It is shocking to know that the average width of human hair is on the order of 100,000 nm. On October 18, 2011, the European Commission adopted the following definition of a nanomaterial “a natural, incidental, or manufactured material containing particles, in an unbound state or as an aggregate and for 50 % or more of particles in number size distribution, one or more external dimensions is in size range 1–100 nm” (European Union 2011). Nevertheless, 100 nm as an upper limit for a nanomaterial is not always accepted. Worldwide, many organizations used different thresholds for the nanoscale, although 100 nm still remains the most common shared limit (Klaessig et al. 2011).

The first, informal, and applicable criterion to define nanomaterials is based on the dimensions. Conventionally, nanomaterials are defined as materials having at least a dimension between 1 and 100 nm. Consequently, nanoparticles (NPs) have all three dimensions (3D) in the nanometer range and allow electron movement inside the shape. However, confined electron movement in 3D NPs is known as

Table 18.2 Common definitions of terms with the “nano” suffix

| Type | Dimensional | Description |
|---------------|-------------|---|
| Nanoscale | Definition | Size range 1–100 nm |
| Nano-object | 3D | Material with one, two, or three external dimensions in the nanoscale |
| NPs | 3D | Nano-object with all three external dimensions in the nanoscale, but electron movement is allowed in all the directions – For example, nano-powder, nanodiamond |
| NPs | 0D | Nano-object with all three external dimensions in the nanoscale, but electron movement is restricted in all three directions: QDs, nanodots, and fullerenes |
| Nanotemplate | 2D | Nano-object with one external dimension in the nanoscale and the other two external dimensions significantly larger – For example, nanofilms, nanocoatings, graphenes |
| Nanofiber | 1D | Nano-object (flexible or rigid) with two external dimensions in the nanoscale and the third dimension significantly larger |
| Nanotube | 1D | Hollow nanofiber |
| Nanorod | 1D | Solid nanofiber |
| Nanowire | 1D | Electrically conducting or semiconducting nanofiber |
| Nanocomposite | – | Integration of more than one material at a nano level |

zero-dimensional (0D) nanomaterials, for example, quantum dots (QDs). Nanoplates represent only one dimension (1D) below 100 nm, whereas nanofibers have two dimensions (2D) in the range of nano, being the remaining remarkably longer. Some common terminologies of the nanorange world are listed in Table 18.2. In addition, a hierarchical classification of nanomaterials has been proposed based on the particular feature falling in the nanometer size domain, for example, nanocomposite, nanoporous, nanofoam, and nanolayers.

18.3.2 Type of Nanomaterials

In the past few years, nanomaterials and nanotechnology have been attracted in all fields of researchers because of their relatively more effective characteristics than the bulk materials. Some of them are carbon-based nanomaterials, metal-based nanomaterials, dendrimers, nanocomposites, biomolecule-based nanomaterials, etc. Among these, carbon nanomaterials, also known as nanocarbons, are composed mainly of carbon and are most commonly available in the hollow sphere, ellipsoids, and tubes. Spherical and ellipsoid carbon nanomaterials are called fullerenes, while cylindrical are called nanotubes. These are more potent and lighter materials and have many applications in various fields of science and technology (Li et al. 2015). Metal-based nanomaterials generally include QDs, nanogold, nanosilver, metal oxides, metal nitrides, and metal sulfide. QDs are closely packed semiconductor crystals comprised of 100–1000 atoms, whose size is on the order of a few nm to

100 nm. The change in size of QDs leads to changes in their optical properties (Bera et al. 2010; Farzin and Abdoos 2021). Dendrimers nanomaterials are nanosized polymers that have been made from branched units. Its surface has numerous chain ends, which can be functionalized with a specific group to perform specific chemical reactions. It can also be utilized as a catalyst for the process and drug delivery. Composites are heterogeneous/hybrid materials produced by mixing at least two materials at a nanometric scale. For example, nanosized clay is being used for products from autoparts to packaging materials to improve its mechanical, thermal, barrier, and flame resistance properties (Ates et al. 2020).

On the other hand, naturally occurring biomolecules having size and shape at nano regime have also been directly or indirectly employed for various applications, especially in sensing technology. Some examples of biomolecules are enzymes, DNA, RNA, and antibodies. Generally, these biomolecules are naturally extracted and used as a receptor to fabricate nanobiosensor. Sometimes they are functionalized with other suitable nanomaterials also.

18.4 Nanomaterial-Based Nanosensors/Nanobiosensors and Their Applications

A nanosensor is generally a chemical or mechanical sensor that can be used to sense the presence of any chemical species or monitor physical parameters, like temperature and pressure. Nowadays, they are being used in the progression of a number of fields, like medical, agriculture, technology, plant nano bionics, prognostics, diagnostics, and many industrial applications. Some critical applications of nanomaterial-based sensors being used are:

- To detect various chemicals in gases toward pollution control.
- For medical diagnostics purposes, either as blood-borne sensors or in lab-on-a-chip type devices.
- To monitor physical parameters like displacement, temperature, and pressure.
- To monitor plant signaling and metabolism to understand plant biology.
- As accelerometers in microelectromechanical system (MEMS) devices like air-bag sensors.
- To study neurotransmitters in the brain for understanding neurophysiology.
- To detect pesticides, synthetic materials, and fertilizers used in agro-fields.

Likewise, a nanobiosensor is a biosensor, where measurement for the detection of an analyte is mainly due to the biological component present in the receptor. In other words, a nanobiosensor is defined as a biosensor in which the nanosize receptor matrix contains at least one biomolecule. Some specific areas of nanobiosensors are:

(i) Biological applications.

- DNA sensors: Genetic monitoring and disease monitoring.
- Immunosensors: HIV, hepatitis, drug testing.
- Cell-based sensors: Functional sensors.
- Bacteria sensors: Detection of bacteria, like *E. coli* and streptococcus, is generally used in medical, environmental safety, and food industries.
- Enzyme sensors: Drug testing, biomolecule monitoring.

(ii) Environmental applications.

- Recognition of environmental pollution and toxicity.
- Agricultural products monitoring.
- Groundwater screening.
- Ocean monitoring.

(iii) Future applications: (Cancer diagnosis and monitoring).

- Nanobiosensors could play a significant role in the early stage of cancer diagnosis in body fluids. In this monitoring method, a nanosensor is designed with a cancer-specific antibody or other biorecognition elements. The interaction of a cancer cell or a target protein generates the optical, electrical, or mechanical signal for recognition.

There are several ways to make nanosensors/nanobiosensors like top-down, bottom-up, or their combination. They have been proven of several benefits in terms of sensitivity and specificity over other traditional sensors, due to the unique and unusual features of nanomaterials. Nanosensors/nanobiosensors have increased selectivity, because they operate at a smaller scale along with natural biological processes. In addition, they offer noteworthy advantages in cost and response time that make them suitable for high-throughput applications. Moreover, they provide real-time monitoring as compared to conventional techniques, such as chromatography and spectroscopy. For illustration, ZnO nanowire is a type of 1D receptor matrix that was used for gas sensing applications. They exhibit high sensitivity toward low gas concentrations under ambient conditions and can be fabricated easily at a low cost (Tiwale 2015).

18.4.1 Nanosensors for Pesticides and Heavy Metal Detection

Technologies have been developed over the last two decades in nanomaterial-enabled sensors, which give precise and sensitive detection of elements present in any specimen. This book's chapter theme is smart nanosensors for detecting pesticides and toxic elements, so the following headline will only focus on this aspect.

18.4.1.1 Noble Metal-Based Nanosensors

Nanostructured Au, Ag, and Cu like noble metals have been extensively applied for visual detection of pesticides and toxic metals in the environment and its territory due to their specific stable localized surface plasmon resonance (LSPR) in the region of UV-vis and surface-enhanced Raman scattering (SERS). When these plasmonic nanomaterials interact with the electromagnetic wave, they exhibit enhanced absorption/scattering band due to the free oscillation of electrons present on the surface of nanomaterials. Hence, the LSPR/SERS signal of corresponding nanomaterials is applied as a sensing probe for the quantitative/qualitative evaluation of different kinds of chemical ingredients. For example, Lee et al. developed a cast effect paper-based SERS sensor to detect thiram and ferbam pesticides at a sub-nanomolar level. Aqueous Ag nanoparticle dispersion was incorporated into alkyl ketene dimer modified filter paper to fabricate the sensor (Lee et al. 2018). Au nanoislands were fabricated on a paper substrate by the ion sputtering method to prepare a SERS-based sensitive platform to detect the mixture of pesticides malachite green, crystal violet, and methylene blue in pond water with limits of detection (LODs) of 10 nM. Also, heavy metal ions Cd^{2+} , Cu^{2+} , and Ni^{2+} in grounded rice were successfully evaluated with LOD down to 1 μM (Song et al. 2020). Our research group recently demonstrated the theoretically and experimentally colorimetric recognition of histidine and arginine in fruit and vegetable samples using Ag nanoparticles (NPs) (Shrivastava et al. 2021). In another report, water dispersed citrate-capped CuNPs were found that Hg^{2+} could enhance the peroxidase-like activity and cause the color to turn bright blue, which is dependent linearly on the Hg^{2+} ion concentration. Thus, a colorimetric process for Hg^{2+} ion recognition was established with a linear range from 0.050 to 10.000 μM and a LOD of 0.185 μM (Li et al. 2019a). The peroxidase-like activity of Cu nanocluster was also used to detect cholesterol based on the chemiluminescence principle (Xu et al. 2016). Also, Das et al. explored luminescence of Cu nanoclusters can be utilized for cell-imagine probes and as a selective Fe^{3+} sensor (Das et al. 2015).

18.4.1.2 Semiconductor-Based Nanosensors

A variety of nanostructured semiconductors, such as quantum dots (CdTe, ZnSe), oxide (ZnO , TiO_2 , Cu_2O , V_2O_5), and sulfides (ZnS , CdS), have been designed for the fabrication of sensing devices. Working mechanisms of nanostructured semiconductors are mainly based on the changes in their optical (absorbance, fluorescence, phosphorescence) or electrical properties (Lian et al. 2020). For example, in ZnO nanowires, when any target molecule bonds with ZnO nanowires, the conductance of the wire changes. The amount of conductance changes directly depends on the concentration of the analyte (Rackauskas et al. 2017). Similarly, V_2O_5 nanowires decorated with SnO_2 were used to sense ethanol at room temperature, where sensitivity is defined as the ratio between resistance in air and testing gas (Wang et al. 2015). In another report, thioglycerol-capped fluorescent CdS quantum dots (QDs)

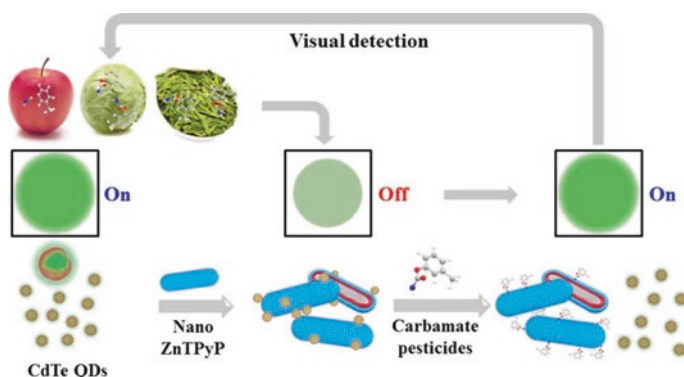


Fig. 18.3 A turn ON/OFF fluorescence paper-based sensor of carbamate pesticides in food-based samples. (Reproduced with permission from (Chen et al. 2020). Copyright © 2020, Elsevier)

were investigated to interact with 14 metal ions in water and observed that the fluorescence intensity of capped QDs was quenched only in the presence of Al^{3+} ions in the range 0.2–10 μM (Ben Brahim et al. 2018). MoS_2 QDs functionalized with boronic acid were used for the fast and selective determination of Hg^{2+} ions in environmental water samples (Guo et al. 2020). Liu and coworkers prepared Mn-doped ZnS QDs for a selective phosphorescence probe to detect thiram pesticide by an affinity reaction with Ag^+ ions (Zhang et al. 2017). CdTe QDs functionalized with ZnTPyP (ZnTPyP: zinc 5, 10, 15, 20-tetra(4-pyridyl)-21H-23H-porphine) were employed as a turn *on/off* fluorescence paper-based sensor for visual detection of carbamate pesticides in food-based samples, as displayed in Fig. 18.3 (Chen et al. 2020).

18.4.1.3 Nanocarbon-Based Nanosensors

Nanocarbons, including carbon QDs (CQDs), carbon nanotubes (CNTs), graphene, graphene dots, have been extensively studied all the time due to their superior instincts electronic, magnetic, and optical properties. Besides that, their nontoxicity, chemical stability, availability, excellent catalytic activity, and easy surface functionalization properties make them a potential candidate as sensing materials. For example, ultrasensitive fluorogenic CQDs were synthesized using a simple hydrothermal carbonization approach by pesticide-free cauliflower juice as a carbon source. The fluorescence quenching property of CQDs was demonstrated to identify detection limits of 0.25, 0.5, and 2 ng ml^{-1} for pesticides of diazinon, semicarbazone, and glyphosate, respectively (Ashrafi Tafreshi et al. 2020). Reduced graphene oxide (rGO)-based nanoelectronic sensor was developed for the detection of Hg^{2+} using field-effect transistor-based micropattern. As compared to frequently used fluorescence-based detection methods, such a nanoelectronic sensor provides high sensitivity, fast, real-time, easy, and label-free detection (Sudibya et al. 2011).

Recently, the excitation of surface plasmon resonance property of multiwalled CNTs (MWCNTs) is used to design a sensing device for 2,4-dichlorophenoxyacetic and chlorpyrifos pesticide solution with the lowest detection limit of 10 ng and the sensitivities of 1.38×10^{-2} /ppm and 2.0×10^{-3} /ppm, respectively (Wang et al. 2020).

18.4.1.4 Nanocomposite-Based Nanosensors

Nanocomposites are prepared by mixing a minimum of two nanosystems at the nano level in a matrix by physical, chemical, or their combined strategies. They are generally classified according to the mixing components, like inorganic-inorganic, inorganic-organic, or organic-organic nanocomposites. Nanocomposites exhibit improved properties compared to mixing parents nanosystems, and sometimes they display novel and unusual properties, which are absent in their parents' counterparts. For example, MWCNTs embedded in ZnO nanofiber-based electrode were demonstrated as an electrochemical sensor for the detection of atrazine pesticide. Researchers have achieved the sensitivity and LOD of the sensor as $21.61 (K\Omega \mu\text{g}^{-1} \text{mL}^{-1}) \text{cm}^{-2}$ and 5.368 zM for a wide detection range of 10 zM–1 μM due to high conductivity, surface area, and low bandgap of MWCNT-ZnO nanofibers (Supraja et al. 2020). A smartphone-assisted electrochemical sensor was developed using MoS_2/rGO nanocomposite to evaluate the toxicity of Cd^{2+} , Pb^{2+} , and Hg^{2+} in rice (Jiang et al. 2021). Shrivas and coworkers were reported a smartphone-assisted paper-based sensor using Cu-Ag core-shell nanostructure for selective evolution of phenthoate pesticides in water and food samples (Shrivas et al. 2020). The mechanism for the detection of pesticides is based on the high affinity of phenthoate to interact with Ag nanoparticles present on the surface of the Cu core, which results in aggregation and a change in the color of the paper device. The quenching of room temperature phosphorescence intensity of PbO/SiO_2 nanocomposite by addition of sulfide was explored to sense sulfide. This response behavior depends on the pH of solution LOD which was estimated to be 0.138 μM (Zhou et al. 2010).

18.4.2 *Nanobiosensors for Pesticides and Heavy Metal Detection*

A nanobiosensor probe measures a biochemical or biological occurrence by sensing any electronic, optical, or magnetic changes via a compact nanosize biosensor. Recent advancements of nanotechnology and advanced fabrication technology in electronics meet toward creating a new set of nanobiosensors in a new age of bionanotechnology for many sensing technologies. Mainly, these nanobiosensors offer numerous advantages in terms of evolution and detection of pesticides and heavy metal ions over nanosensors, as they are very specific in response and may work very effectively even if the environment is not clean. A wide range of biomolecular

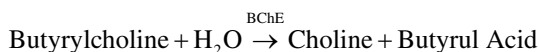
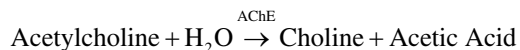
recognition elements (Table 18.1) have been used to fabric nanobiosensors with potential environmental applications. Some of these biomolecules-based nanosensors are discussed in the following subheading toward these applications.

18.4.2.1 Enzyme-Derived Nanobiosensors

Many enzyme-based innovative immobilized nanobiosensors have been developed to detect pesticides and other compounds. Also, the use of enzymes as recognition elements in nanobiosensors has increased due to the easy and compatible combination of enzymes with nanomaterials. They are sensitive, stable, and have an excellent shelf life for the improved electrochemical interface. In an enzymatic nanobiosensor, the enzyme (receptor element) selectively interacts with a substrate (target analyte). These sensors measure the catalysis or the inhibition of enzymes process by the target analyte in either of two ways as given below:

- The enzyme can metabolize the target analyte; hence, the analyte concentration is determined by measuring the catalytic transformation of the analyte by the enzyme.
- The analyte can inhibit the enzyme so that the concentration of the analyte is associated with a decreased enzymatic product formation.

Organophosphate (OP), a synthetic compound developed during World War II, was used as a pesticide and nerve agent, which exhibited severe toxicity on the human nervous system. As it is well-known, pesticides like OP and carbamates are the main cholinesterase (ChE) inhibitors. Thus, these are detected by ChE-based biosensors. Two types of natural ChE enzymes are known – acetylcholinesterase (AChE) and butyrylcholinesterase (BChE). These two have been widely used from many years for the detection of neurotoxic compounds. These enzymes have different substrates: AChE hydrolyses acetyl esters, such as acetylcholine, whereas BChE hydrolyses butyrylcholine:



AChE enzyme can be isolated from various sources like human blood, horse serum, bovine, or human erythrocytes. AChE enzyme is commonly used in biosensors to detect OP pesticides, as trace amounts of such compounds inhibit its catalytic activity. Such inhibitions are monitored by the change of oxidation current in amperometric biosensors. Table 18.3 recaps some of the common enzyme-derived nanobiosensors.

Table 18.3 Enzyme-derived nanobiosensors for pesticides detection

| S no. | Enzyme-based nanobiosensor | Mode of sensing | Pesticides | References |
|-------|-------------------------------|---------------------|--|---|
| 1 | AChE | Electrochemical | Review article | Pundir and Chauhan (2012) and Liu et al. (2013) |
| 2 | AChE + CdTe QDs + rGO | Electroluminescence | OP | Chen et al. (2017) |
| 3 | AChE + Si QDs | Photoluminescence | Carbaryl, parathion, diazinon, phorate | Yi et al. (2013) |
| 4 | AChE + UCNPs-Cu ²⁺ | Fluorescence | Diazinon | Wang et al. (2019) |
| 5 | AChE + MWCNTs + chitosan | Amperometric | Acetylthiocholine | Du et al. (2007) |
| 6 | BChE | Fluorescence | Tacrine | Zhang et al. (2021) |
| 7 | BChE + magnetic nanoparticle | Electrochemical | OP | Du et al. (2011) |

18.4.2.2 Immuno-Derived Nanobiosensors

Polyclonal, monoclonal, and recombinant antibodies have frequently been selected for various applications, including food safety, environmental monitoring, clinical analysis, and medical diagnosis. Antibodies production involves the exploitation of the immune system of murine, leporine, ovine, or avian hosts. Many immunosensors have been designed for pesticides detection that utilizes transducers on electrochemical, optical, piezoelectric, and mechanical methods. For example, Pérez-Fernández and groups demonstrated a screen-printed electrode using a monoclonal antibody-based electrochemical immunosensor for the detection of imidacloprid pesticide (Pérez-Fernández et al. 2019). Also, piezoelectric immunosensors were reported for the detection of various pesticides, like chlorpyrifos and triclopyr (March et al. 2009; Marrazza 2014). Moreover, a disposable electrochemical immunosensor was developed using human serum albumin (HSA) and anti-HAS antibody to trace Bi³⁺ with LOD of 0.2 µg/mL (Wang et al. 1998).

Also, antibodies combined with nanomaterials are used to fabricate nanobiosensors. In this context, there was a method designed to detect atrazine pesticides in red wines by Valera et al., which mainly involves immobilization of pesticides on interdigitated µ-electrodes. In this method, an antibody was added to the solution, and free atrazine was detected through a competitive reaction with immobilized pesticide (Valera et al. 2010a, b). It was demonstrated that AuNPs amplify the conductive signal and permit assay of atrazine with the help of direct current measurements. The detection was based on the fact that AuNPs were labeled with antibodies, and their presence gave the conductivity signals. Similarly, electrochemical immunosensors are used to determine phenyl urea herbicide-diuron by electrode containing Prussian blue-Au nanoparticles and using rabbit anti-IgG antibody (Sharma et al. 2011). T2 antibody-based immunosensor was prepared for ultrasensitive detection of chlorpyrifos pesticide residue via click and triggered coordination chemistry (Dong et al. 2019).

18.4.2.3 Nucleic Acid-Derived Nanobiosensors

Aptamers are considered single-stranded nucleic acids that can be a part of DNA, RNA, and XNA. They can be developed with high binding affinity and specificity to interact with a broad range of desired target molecules. They have been extensively employed in facilitating discoveries in basic research, including food safety and monitoring the environment (Lake et al. 2019; McConnell et al. 2020; Zhang et al. 2019). These aptamers have numerous advantages compared to antibodies, such as reproducibility, accurate chemical composition, stability, and no requirement of host for production. Also, they can be easily modified with a suitable functional group without any effect on their activity and can perform in extreme conditions. Due to their many merits, aptamer-based nanobiosensors have been developed to detect pesticides and heavy metals ions in the environment and related territories (McConnell et al. 2020; Sekhon et al. 2018; Xie et al. 2022). Wu et al. designed a fluorescent DNAzyme-AuNP-based nanoprobe as a general platform to detect uranyl ion (UO_2^{2+}) within a cellular environment. The probe was made with 13 nm Au nanoparticles core functionalized with a shell of UO_2^{2+} -specific 39E DNAzyme, as depicted in Fig. 18.4 (Wu et al. 2013). The label-free modified RNA aptasensor was developed for the determination of small molecules in the biological sample like neomycin B, tetramethylrhodamine (de-los-Santos-Álvarez et al. 2007; Wu et al. 2020).

Moreover, DNA aptamers linked with photoluminescent graphene oxide QDs (GDQDs) were used as a nanosensor for detection of trace amount of Pb^{2+} ion. The DNA aptamer on the surface of GOQDs explicitly caught the target Pb^{2+} , which can prompt electron transfer from GOQDs to Pb^{2+} upon UV-irradiation, thus causing the fluorescence quenching of the GOQDs (Park et al. 2015). In concern of pesticide detection, a colorimetric nanobiosensor based on Au nanoparticles–aptamer was developed to detect organophosphorus pesticide phorate. The red color of the well-dispersed AuNPs changes to blue upon aggregation, resulting in the shifting of the surface plasmon band to a longer wavelength (Bala et al. 2016). On the other hand, Wang and the research groups demonstrated that double-stranded DNA could be used as a template to develop Cu nanoparticles based on fluorescent nanobiosensors. They have shown that this approach can effectively be applied to detect Hg^{2+} , S^{2-} , and Pb^{2+} . Recently, Zheng et al. reviewed the detection of metal ions, pathogens, and small molecules to protein by using DNA-based nanosensors. Herein,

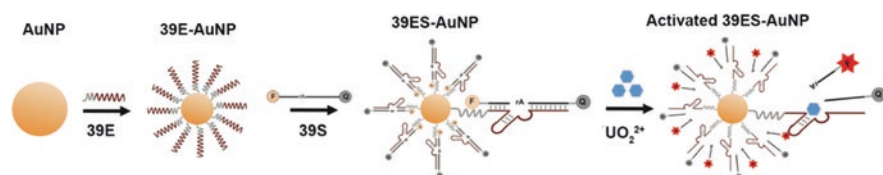


Fig. 18.4 Design of a fluorescent DNAzyme immobilized onto AuNPs as selective probe of uranyl inside live cells. (Reproduced with permission from (Wu et al. 2013) Copyright © 2013, Americal Chemical Society)

they have summarized the biological function of DNA and its interaction with target analytes (Zheng and Tan 2020).

18.4.2.4 Whole-Cell Biosensors

These nanobiosensors use living organisms such as bacteria, fungi, yeast, algae, and tissue culture cells (from animals or plants) as recognition elements. They sense analytical signals by measuring the general metabolic status of these living organisms, like its growth inhibition, cell viability, cell respiration, or bacterial bioluminescence (Gui et al. 2017). Compared to other nanobiosensors, this nanobiosensor can detect a broad spectrum of analytes and provide rapid analysis, cost-effectiveness, and sensitivity to the change in the electrochemical state of a sample, environment, or any other cells. For example, Ag nanowires with genetically engineered M13 bacteriophages expressed a tryptophan-histidine-tryptophan peptide sequence-based sensor was fabricated to detect various pesticides via a surface-enhanced Raman scattering mechanism (Koh et al. 2018). Rodrigue and coworkers have shown that the TD2158 wild-type *E. coli* gave rise to a ten times more active and sensitive nanobiosensor than its W3110 *E. coli* K12 equivalent. This biosensor could confidently detect Ni concentrations as little as $4.7 \mu\text{g L}^{-1}$ (Cayron et al. 2017). In another report, a label-free optical whole-cell *E. coli* bacteria was used as a biomarker for the detection of pyrethroid insecticide. The biosensor uses a whole surface displaying anti-3-PBA (3-phenoxybenzoic acid) as the detection element (Riangrunroj et al. 2019). Table 18.4 summarizes different whole-cell-based nanobiosensor used for heavy metal ion detection.

18.5 Conclusion and Future Prospective

This chapter highlights the necessity of nanosensors in this modern agricultural and urbanization era. The harmful effects of pesticides and the availability of heavy metals in nature were also discussed. This chapter also mentioned that pesticides and

Table 18.4 Whole-cell-based nanobiosensors for heavy metal ion detection

| S. No. | Heavy metals | Cellular organism | Type of transducer | References |
|--------|---|----------------------------------|--------------------|------------------------|
| 1 | Cu^{2+} | <i>Ralstonia Metallidurans</i> | Bioluminescence | Leth et al. (2002) |
| 2 | Zn^{2+} , Hg^{2+} , Cd^{2+} , Cr^{3+} | <i>E. coli</i> | Bioluminescence | Ivask et al. (2002) |
| 3 | Cd^{2+} , Pb^{2+} , Sb^{2+} | <i>E. coli</i> | Fluorescence | Liao et al. (2006) |
| 4 | Hg^{2+} | <i>Vibrio anguillarum</i> | Bioluminescence | Golding et al. (2002) |
| 5 | Cu^{2+} , Ni^{2+} | <i>Chlamydomonas reinhardtii</i> | Amperometric | Shitanda et al. (2005) |

heavy metal residue cause direct and indirect damage to flora, fauna, physiochemical, and biological properties of soil, including human beings. Heavy metals coming out from industries and mining activities create a huge problem for our motherland. Like, Cd affects the essential microorganisms and absorbs nutrients (organic matter) present in the soil. The accumulation of Pb affects the pH and sorption capacity of the soil. Similarly, many others also inhibit beneficial microbe activity, mineral transportation, seed germination, crop yielding process, biosynthesis of chlorophyll, etc. When these substances reach the human body directly or indirectly, it causes harmful health problems, such as lung cancer, asthma, neurodegenerative disorder, ovarian cancer, reproductive hormonal imbalance, genetic damage, and many more. As future perspective and recommendations, the occurrence of pesticides and heavy metals residue, its interaction with nature, and its toxicity need to be investigated in detail. Several new methods and approaches should be adopted to reduce their toxicity.

References

- Ashrafi Tafreshi F, Fatahi Z, Ghasemi SF, Taherian A, Esfandiari N. Ultrasensitive fluorescent detection of pesticides in real sample by using green carbon dots. *PLoS One*. 2020;15:e0230646.
- Ates B, Koytepe S, Ulu A, Gurses C, Thakur VK. Chemistry, structures, and advanced applications of nanocomposites from biorenewable resources. *Chem Rev*. 2020;120:9304–62.
- Atwood D, Paisley-Jones C. Pesticides industry sales and usage 2008–2012 market estimates. Washington, DC: United States Environmental Protection Agency; 2017.
- Bala R, Sharma RK, Wangoo N. Development of gold nanoparticles-based aptasensor for the colorimetric detection of organophosphorus pesticide phorate. *Anal Bioanal Chem*. 2016;408:333–8.
- Ben Brahim N, Poggi M, Lambry J-C, Bel Haj Mohamed N, Ben Chaâbane R, Negrerie M. Density of grafted chains in thioglycerol-capped CdS quantum dots determines their interaction with aluminum(III) in water. *Inorg Chem*. 2018;57:4979–88.
- Bera D, Qian L, Tseng T-K, Holloway PH. Quantum dots and their multimodal applications: a review. *Materials (Basel)*. 2010;3:2260–345.
- Bexfield LM, Belitz K, Lindsey BD, Toccalino PL, Nowell LH. Pesticides and pesticide degradates in groundwater used for public supply across the United States: occurrence and human-health context. *Environ Sci Technol*. 2021;55:362–72.
- Calvert GM, Karnik J, Mehler L, Beckman J, Morrissey B, Sievert J, Barrett R, Lackovic M, Mabee L, Schwartz A, Mitchell Y, Moraga-McHaley S. Acute pesticide poisoning among agricultural workers in the United States, 1998–2005. *Am J Ind Med*. 2008;51:883–98.
- Cayron J, Prudent E, Escoffier C, Gueguen E, Mandrand-Berthelot M-A, Pignol D, Garcia D, Rodrigue A. Pushing the limits of nickel detection to nanomolar range using a set of engineered bioluminescent *Escherichia coli*. *Environ Sci Pollut Res*. 2017;24:4–14.
- Chen H, Hu O, Fan Y, Xu L, Zhang L, Lan W, Hu Y, Xie X, Ma L, She Y, Fu H. Fluorescence paper-based sensor for visual detection of carbamate pesticides in food based on CdTe quantum dot and nano ZnTPyP. *Food Chem*. 2020;327:127075.
- Chen H, Zhang H, Yuan R, Chen S. Novel double-potential electrochemiluminescence ratiometric strategy in enzyme-based inhibition biosensing for sensitive detection of organophosphorus pesticides. *Anal Chem*. 2017;89:2823–9.
- Correa DS, Pavinatto A, Mercante LA, Mattoso LHC, Oliveira JE, Riul A. 6 – chemical sensors based on hybrid nanomaterials for food analysis. In: Grumezescu AM, editor. *Nanobiosensors*. Academic Press; 2017. p. 205–44.

- Crisponi G, Nurchi VM. Metal ion toxicity. In: Scott RA, editor. Encyclopedia of inorganic and bioinorganic chemistry. Wiley; 2015. p. 1–14.
- Das NK, Ghosh S, Priya A, Datta S, Mukherjee S. Luminescent copper nanoclusters as a specific cell-imaging probe and a selective metal ion sensor. *J Phys Chem C*. 2015;119:24657–64.
- de-los-Santos-Álvarez N, Lobo-Castañón MJ, Miranda-Ordieres AJ, Tuñón-Blanco P. Modified-RNA aptamer-based sensor for competitive impedimetric assay of neomycin B. *J Am Chem Soc*. 2007;129:3808–9.
- Dewangan K, Shrivastava K, Kurrey R. Chapter 9 - hybrid nanomaterials as chemical sensors. In: Abd-El Salam KA, editor. Multifunctional hybrid nanomaterials for sustainable agri-food and ecosystems. Elsevier; 2020. p. 213–39.
- Dong Y, Zheng W, Chen D, Li X, Wang J, Wang Z, Chen Y. Click reaction-mediated T2 immunosensor for ultrasensitive detection of pesticide residues via brush-like nanostructure-triggered coordination chemistry. *J Agri Food Chem*. 2019;67:9942–9.
- Du D, Huang X, Cai J, Zhang A, Ding J, Chen S. An amperometric acetylthiocholine sensor based on immobilization of acetylcholinesterase on a multiwall carbon nanotube–cross-linked chitosan composite. *Anal Bioanal Chem*. 2007;387:1059–65.
- Du D, Wang J, Wang L, Lu D, Smith JN, Timchalk C, Lin Y. Magnetic electrochemical sensing platform for biomonitoring of exposure to organophosphorus pesticides and nerve agents based on simultaneous measurement of total enzyme amount and enzyme activity. *Anal Chem*. 2011;83:3770–7.
- European Union. The European Commission recommendations of 18 October 2011 on the definition of nanomaterial. *Off J Europ Uni*. 2011;L275:38–40.
- Farzin MA, Abdoos H. A critical review on quantum dots: from synthesis toward applications in electrochemical biosensors for determination of disease-related biomolecules. *Talanta*. 2021;224:121828.
- Golding GR, Kelly CA, Sparling R, Loewen PC, Rudd JWM, Barkay T. Evidence for facilitated uptake of hg(II) by vibrio anguillarum and Escherichia coli under anaerobic and aerobic conditions. *Limnol Oceanogr*. 2002;47:967–75.
- Gui Q, Lawson T, Shan S, Yan L, Liu Y. The application of whole cell-based biosensors for use in environmental analysis and in medical diagnostics. *Sensors*. 2017;17:1623.
- Guo X, Huang J, Wei Y, Zeng Q, Wang L. Fast and selective detection of mercury ions in environmental water by paper-based fluorescent sensor using boronic acid functionalized MoS₂ quantum dots. *J Hazard Mater*. 2020;381:120969.
- Ivask A, Virta M, Kahru A. Construction and use of specific luminescent recombinant bacterial sensors for the assessment of bioavailable fraction of cadmium, zinc, mercury and chromium in the soil. *Soil Biol Biochem*. 2002;34:1439–47.
- Jiang D, Sheng K, Gui G, Jiang H, Liu X, Wang L. A novel smartphone-based electrochemical cell sensor for evaluating the toxicity of heavy metal ions Cd²⁺, Hg²⁺, and Pb²⁺ in rice. *Anal Bioanal Chem*. 2021;413:4277–87.
- Klaessig F, Marrapese M, Abe S. Current perspectives in nanotechnology terminology and nomenclature. In: Murashov V, Howard J, editors. Nanotechnology standards. nanostructure science and technology. New York: Springer; 2011. p. 21–52.
- Koh EH, Mun C, Kim C, Park S-G, Choi EJ, Kim SH, Dang J, Choo J, Oh J-W, Kim D-H, Jung HS. M13 bacteriophage/silver nanowire surface-enhanced raman scattering sensor for sensitive and selective pesticide detection. *ACS Appl Mater Interfaces*. 2018;10:10388–97.
- Lake RJ, Yang Z, Zhang J, Lu Y. DNAzymes as activity-based sensors for metal ions: recent applications, demonstrated advantages, current challenges, and future directions. *Acc Chem Res*. 2019;52:3275–86.
- Lee M, Oh K, Choi H-K, Lee SG, Youn HJ, Lee HL, Jeong DH. Subnanomolar sensitivity of filter paper-based SERS sensor for pesticide detection by hydrophobicity change of paper surface. *ACS Sensors*. 2018;3:151–9.

- Leth S, Maltoni S, Simkus R, Mattiasson B, Corbisier P, Klimant I, Wolfbeis OS, Csöregi E. Engineered bacteria based biosensors for monitoring bioavailable heavy metals. *Electroanalysis*. 2002;14:35–42.
- Li Q, Wu F, Mao M, Ji X, Wei L, Li J, Ma L. A dual-mode colorimetric sensor based on copper nanoparticles for the detection of mercury-(II) ions. *Anal Methods*. 2019a;11:4014–21.
- Li Z, Askim JR, Suslick KS. The optoelectronic nose: colorimetric and fluorometric sensor arrays. *Chem Rev*. 2019b;119:231–92.
- Li Z, Liu Z, Sun H, Gao C. Superstructured assembly of nanocarbons: fullerenes, nanotubes, and graphene. *Chem Rev*. 2015;115:7046–117.
- Lian J, Xu Q, Wang Y, Meng F. Recent developments in fluorescent materials for heavy metal ions analysis from the perspective of forensic chemistry. *Front Chem*. 2020;8:593291.
- Liao VH-C, Chien M-T, Tseng Y-Y, Ou K-L. Assessment of heavy metal bioavailability in contaminated sediments and soils using green fluorescent protein-based bacterial biosensors. *Environ Pollut*. 2006;142:17–23.
- Liu S, Zheng Z, Li X. Advances in pesticide biosensors: current status, challenges, and future perspectives. *Anal Bioanal Chem*. 2013;405:63–90.
- March C, Manclús JJ, Jiménez Y, Arnau A, Montoya A. A piezoelectric immunosensor for the determination of pesticide residues and metabolites in fruit juices. *Talanta*. 2009;78:827–33.
- Marrazza G. Piezoelectric biosensors for organophosphate and carbamate pesticides: a review. *Biosensors*. 2014;4:301–17.
- Martin BR. Metal ion toxicity. *Encyclopedia of inorganic chemistry*; 2006. <https://doi.org/10.1002/0470862106.ia136>.
- McConnell EM, Nguyen J, Li Y. Aptamer-based biosensors for environmental monitoring. *Front Chem*. 2020;8:434.
- Munonde TS, Nomngongo PN. Nanocomposites for electrochemical sensors and their applications on the detection of trace metals in environmental water samples. *Sensors*. 2021;21:131.
- Nicolopoulou-Stamati P, Maipas S, Kotampasi C, Stamatis P, Hens L. Chemical pesticides and human health: the urgent need for a new concept in agriculture. *Front Pub Health*. 2016;4:148.
- Park M, Ha HD, Kim YT, Jung JH, Kim S-H, Kim DH, Seo TS. Combination of a sample pretreatment microfluidic device with a photoluminescent graphene oxide quantum dot sensor for trace lead detection. *Anal Chem*. 2015;87:10969–75.
- Pérez-Fernández B, Mercader JV, Checa-Orrego BI, de la Escosura-Muñiz A, Costa-García A. A monoclonal antibody-based immunosensor for the electrochemical detection of imidacloprid pesticide. *Analyst*. 2019;144:2936–41.
- PPQS. *Government of India*; 2021. <http://ppqs.gov.in/statistical-database>.
- Pundir CS, Chauhan N. Acetylcholinesterase inhibition-based biosensors for pesticide determination: a review. *Anal Biochem*. 2012;429:19–31.
- Rackauskas S, Barbero N, Barolo C, Viscardi G. ZnO nanowire application in chemoresistive sensing: a review. *Nanomaterials (Basel)*. 2017;7:381.
- Rani L, Thapa K, Kanojia N, Sharma N, Singh S, Grewal AS, Srivastav AL, Kaushal J. An extensive review on the consequences of chemical pesticides on human health and environment. *J Clean Prod*. 2021;283:124657.
- Riangrunroj P, Bever CS, Hammock BD, Polizzi KM. A label-free optical whole-cell *Escherichia coli* biosensor for the detection of pyrethroid insecticide exposure. *Sci Rep*. 2019;9:12466.
- Sekhon SS, Park G-Y, Park D-Y, Kim SY, Wee J-H, Ahn J-Y, Kim Y-H. Aptasensors for pesticide detection. *Toxicol Environ Health Sci*. 2018;10:229–36.
- Sharma A, Kumar V, Shahzad B, Tanveer M, Sidhu GPS, Handa N, Kohli SK, Yadav P, Bali AS, Parihar RD, Dar OI, Singh K, Jasrotia S, Bakshi P, Ramakrishnan M, Kumar S, Bhardwaj R, Thukral AK. Worldwide pesticide usage and its impacts on ecosystem. *SN Appl Sci*. 2019;1:1446.
- Sharma P, Sablok K, Bhalla V, Suri CR. A novel disposable electrochemical immunosensor for phenyl urea herbicide diuron. *Biosens Bioelectron*. 2011;26:4209–12.

- Shitanda I, Takada K, Sakai Y, Tatsuma T. Amperometric biosensing systems based on motility and gravitaxis of flagellate algae for aquatic risk assessment. *Anal Chem.* 2005;77:6715–8.
- Shrivas K, Monisha PS, Thakur SS, Shankar R. Food safety monitoring of the pesticide phenthoate using a smartphone-assisted paper-based sensor with bimetallic Cu@Ag core–shell nanoparticles. *Lab Chip.* 2020;20:3996–4006.
- Shrivas K, Naik W, Kumar D, Singh D, Dewangan K, Kant T, Yadav S, Tikeshwari KN. Experimental and theoretical investigations for selective colorimetric recognition and determination of arginine and histidine in vegetable and fruit samples using bare-AgNPs. *Microchem J.* 2021;160:105597.
- Song Y, Ma Z, Fang H, Zhang Q, Zhou Q, Chen Z, Yang H, Wang F. Au sputtered paper chromatography tandem raman platform for sensitive detection of heavy metal ions. *ACS Sensors.* 2020;5:1455–64.
- Stackpoole SM, Shoda ME, Medalie L, Stone WW. Pesticides in US rivers: regional differences in use, occurrence, and environmental toxicity, 2013 to 2017. *Sci Total Environ.* 2021;787:147147.
- Sudibya HG, He Q, Zhang H, Chen P. Electrical detection of metal ions using field-effect transistors based on micropatterned reduced graphene oxide films. *ACS Nano.* 2011;5:1990–4.
- Supraja P, Singh V, Vanjari SRK, Govind Singh S. Electrospun CNT embedded ZnO nanofiber based biosensor for electrochemical detection of atrazine: a step closure to single molecule detection. *Microsys Nanoeng.* 2020;6:3.
- Tiwale N. Zinc oxide nanowire gas sensors: fabrication, functionalisation and devices. *Mater Sci Technol.* 2015;31:1681–97.
- Valera E, Muñiz D, Rodríguez Á. Fabrication of flexible interdigitated μ -electrodes (FID μ Es) for the development of a conductimetric immunosensor for atrazine detection based on antibodies labelled with gold nanoparticles. *Microelect Eng.* 2010a;87:167–73.
- Valera E, Ramón-Azcón J, Barranco A, Alfaro B, Sánchez-Baeza F, Marco MP, Rodríguez Á. Determination of atrazine residues in red wine samples. A conductimetric solution. *Food Chem.* 2010b;122:888–94.
- Wang J, Tian B, Rogers KR. Thick-film electrochemical immunosensor based on stripping potentiometric detection of a metal ion label. *Anal Chem.* 1998;70:1682–5.
- Wang P, Li H, Hassan MM, Guo Z, Zhang Z-Z, Chen Q. Fabricating an acetylcholinesterase modulated UCNPs-Cu²⁺ fluorescence biosensor for ultrasensitive detection of organophosphorus pesticides-diazinon in food. *J Agri Food Chem.* 2019;67:4071–9.
- Wang R, Yang S, Deng R, Chen W, Liu Y, Zhang H, Zakharova GS. Enhanced gas sensing properties of V₂O₅ nanowires decorated with SnO₂ nanoparticles to ethanol at room temperature. *RSC Adv.* 2015;5:41050–8.
- Wang Y, Cui Z, Zhang X, Zhang X, Zhu Y, Chen S, Hu H. Excitation of surface plasmon resonance on multiwalled carbon nanotube metasurfaces for pesticide sensors. *ACS Appl Mater Interfaces.* 2020;12:52082–8.
- WHO. The WHO recommended classification of pesticides by hazard and guidelines to classification, 2019 edition. Geneva: World Health Organization; 2020.
- Wu P, Hwang K, Lan T, Lu Y. A DNAzyme-gold nanoparticle probe for uranyl ion in living cells. *J Am Chem Soc.* 2013;135:5254–7.
- Wu R, Karunanayake Mudiyanelage APKK, Ren K, Sun Z, Tian Q, Zhao B, Bagheri Y, Lutati D, Keshri P, You M. Ratiometric fluorogenic RNA-based sensors for imaging live-cell dynamics of small molecules. *ACS Appl Bio Mater.* 2020;3:2633–42.
- Xie M, Zhao F, Zhang Y, Xiong Y, Han S. Recent advances in aptamer-based optical and electrochemical biosensors for detection of pesticides and veterinary drugs. *Food Cont.* 2022;131:108399.
- Xu S, Wang Y, Zhou D, Kuang M, Fang D, Yang W, Wei S, Ma L. A novel chemiluminescence sensor for sensitive detection of cholesterol based on the peroxidase-like activity of copper nanoclusters. *Sci Rep.* 2016;6:39157.

- Yi Y, Zhu G, Liu C, Huang Y, Zhang Y, Li H, Zhao J, Yao S. A label-free silicon quantum dots-based photoluminescence sensor for ultrasensitive detection of pesticides. *Anal Chem.* 2013;85:11464–70.
- Zhang C, Zhang K, Zhao T, Liu B, Wang Z, Zhang Z. Selective phosphorescence sensing of pesticide based on the inhibition of silver(I) quenched ZnS:Mn²⁺ quantum dots. *Sens Actuators B Chem.* 2017;252:1083–8.
- Zhang Q, Fu C, Guo X, Gao J, Zhang P, Ding C. Fluorescent determination of butyrylcholinesterase activity and its application in biological imaging and pesticide residue detection. *ACS Sensors.* 2021;6:1138–46.
- Zhang Y, Lai BS, Juhas M. Recent advances in aptamer discovery and applications. *Molecules.* 2019;24:941.
- Zheng XT, Tan YN. Recent development of nucleic acid nanosensors to detect sequence-specific binding interactions: from metal ions, small molecules to proteins and pathogens. *Sens Inter.* 2020;1:100034.
- Zhou T, Wang N, Li C, Yuan H, Xiao D. Sulfide sensor based on room-temperature phosphorescence of PbO/SiO₂ nanocomposite. *Anal Chem.* 2010;82:1705–11.

Index

A

Ablation agents, 140, 141, 154–157, 159–163
Animal diseases, 299–305, 315, 316, 351, 365
Artificial intelligence (AI), 2, 5, 19, 229, 252, 328, 349–352, 407
Avian influenza, 308, 315

B

Biological imaging, 109–134
Biomedical, 1, 2, 5, 10, 17, 36, 53, 81, 82, 84, 87, 96, 101, 114, 190, 201, 221, 265, 266, 285, 286, 331, 384, 387, 406, 413, 419, 420
Biomedical applications, 2–4, 7, 18, 54, 55, 61, 64, 81, 90, 111, 124, 159, 173, 184, 190, 204, 205, 208, 213, 216, 253, 263–279, 286, 302–305, 417
Biomedicine, v, 1–10, 18, 150, 174, 178, 384
Biosensing, v, 2, 4–6, 8, 16, 25–27, 53, 71, 265, 328, 334–337, 343, 351, 398, 407, 416, 417
Biosensors, 95, 160, 231, 286, 290, 291, 299, 310–316, 328, 333, 335–338, 343–348, 350, 351, 367, 407, 412, 414, 415, 418, 419, 421–423, 427, 439, 443, 444, 447

C

Cancer biomedicine, 139–163
Cancers, 6, 16–20, 23, 26, 35, 39, 40, 42, 45–47, 61, 62, 70, 71, 73, 79, 80, 87, 90–94, 98–100, 115, 139–163, 184,

201, 202, 212, 214–216, 218, 222, 272, 300–305, 418, 434, 440, 448

Cas proteins, 383, 387, 388, 390, 392–394, 407

Controlled release, 95, 172, 186, 205, 208, 209

COVID-19, 300, 395, 399–401, 403

CRISPR, v, 331, 337–339, 383–407

CRISPR-associated nucleases, 394, 395

CRISPR diagnostics, 383–407

D

Diagnoses, 3–5, 8, 16, 26, 53, 69, 79, 80, 91–94, 98–100, 109, 142, 202, 207, 243, 245, 246, 265, 287, 293, 294, 299–316, 327–352, 385, 387, 394, 395, 397, 399, 403, 440

Diagnostic nanotechnology, v, 1, 2, 5, 26, 328

DNA bionanosensors, 418–421

Drug delivery, v, 2–6, 8, 9, 16–21, 27, 28, 36–39, 43–45, 53, 54, 56, 61–64, 66, 68, 69, 71, 73, 80, 88, 91, 93–95, 99, 100, 110, 112, 115, 116, 121, 172, 173, 177, 179, 181, 183–185, 201–204, 206–208, 211–213, 215, 218, 220, 221, 273, 275, 276, 304, 439

E

Environmental, 37, 61, 134, 190, 266, 272, 274, 287, 288, 292, 310, 328, 331, 335, 336, 347, 349, 351, 352, 411–427, 433, 434, 440, 442, 444, 445

F

Fabrication methods, 267
 Flexible sensors, 4, 8, 230–233, 235, 236, 239, 241, 252, 253
 Functional proteins, 7

G

Gene detection, 287–289

H

Heavy metals pollutions, 413–414

I

Insects, 84, 86, 339, 350, 433
 Integrative biology, 1–10
 Isothermal amplification, 291–294, 328, 388, 389, 392, 394–397, 407

L

Lab-on-a-chip, v, 8, 263–279, 285–296, 328, 339, 351, 352, 366, 439
 Layer-by-layer assembly, 218

M

Magneto-responsive materials, 110, 111
 Medical diagnosis, 26, 230, 233, 243, 279, 285–296, 445
 Medical diagnostics, 5, 8, 230, 253, 328, 352, 439
 Microfluidics, 4, 5, 7, 16, 81, 82, 85, 111, 241, 263–279, 286, 289, 291, 292, 294, 295, 339, 345, 365, 366, 394, 400, 404
 Microswimmers, 57, 59–61, 63–67
 Microsystems, 5, 25, 62, 275
 Multiplex, 293, 294, 368–370, 375, 377, 388, 389, 405, 406
 Mycotoxins, 8, 332, 362–378

N

Nanobots, v, 2–9, 28, 36–42, 46–48, 67, 69, 72, 73
 Nano-diagnostics, v, 1–10, 300, 311, 316, 329, 331, 333, 366–367, 375
 Nanohybrids, 8, 79, 99, 101, 111–134, 144, 173, 177–179, 185, 424
 Nanomaterials, 2, 4–8, 15, 26, 36, 80, 98–100, 110–112, 140–154, 162, 163, 173, 174,

177, 178, 192, 201–222, 265, 270, 273, 300–308, 310–312, 316, 328, 332, 336, 337, 347–349, 351, 352, 366, 367, 371–373, 377, 411, 412, 414, 415, 422, 426, 427, 434, 436–441, 444, 445

Nanorobotics, v, 1–10, 71, 190, 201, 302
 Nanorobots, v, 2–4, 6, 15–28, 35–48, 53–73, 79, 80, 82, 91, 93, 94, 97, 99–101, 299, 302
 Nanosensors, 5, 8, 25–27, 303, 328, 332, 337, 343, 347, 349, 351, 368, 369, 371, 372, 377, 413–415, 417, 418, 421–427, 433–448
 Nanotechnologies, v, 1, 2, 5, 10, 15, 17, 23, 26, 27, 37, 109, 172, 174, 201, 203, 299, 300, 303–305, 308, 310, 311, 316, 328, 331, 339, 351, 366, 375, 376, 394, 411, 412, 414, 419, 424, 426, 427, 434, 438, 443
 Nanotherapeutics, 5, 8, 114, 201–203, 208, 210, 216, 222

P

Pathogen detections, 285–296, 316, 328, 329, 335, 336, 339, 342, 347, 351, 407
 Pathogens, v, 5, 6, 8, 141, 142, 285, 287–289, 291–295, 307, 310, 312–314, 316, 327–352, 367, 392, 395, 399, 401, 407, 413, 446
 Pesticides, 5, 8, 328, 331, 342, 413, 415, 433–435, 439–448
 Photodynamic therapy, 80, 98, 143–144, 163
 Photothermal therapy, 4, 45, 98, 100, 141–143, 163
 Physical stimuli, 5, 110, 203, 221, 222
 Pollutants, 274, 412, 413, 415, 426, 427, 435
 Pollution detection sensors, 414–418
 Polymer nanohybrids, 4, 179, 192, 193
 Polymers, 4, 6, 9, 22, 37, 54, 58, 60, 62, 65, 66, 69, 71, 80–91, 95–97, 99–101, 111, 114–117, 123, 142–144, 149, 151, 154, 155, 159, 161, 171–194, 204–208, 210, 213, 216, 219, 221, 232, 253, 267–269, 286, 287, 292, 296, 303, 313, 335, 350, 351, 371, 418, 439
 Pressure sensors, 5, 229–231, 233–235, 237–255
 Programmability, 37, 203, 414

S
 Smart materials, 172, 209, 212

- Smart-nanosensor, 332
- Stimuli, 4, 5, 62–64, 99, 110, 152, 173, 181, 184, 185, 193, 203, 208, 212, 213, 216, 218–222, 231, 238, 240, 253, 412, 415, 427
- Stimuli-responsive, v, 5, 8, 37, 61, 63, 94, 109, 110, 201, 203, 205, 218, 221, 222, 268
- Stimuli-responsiveness, 37, 172, 173
- 202–204, 207, 208, 211, 213, 215, 221, 222, 265, 305, 336, 390–392, 402
- Theranostics, 4, 6, 8, 45, 61, 79–101
- 3d printing, 2, 17, 54–65, 69, 71, 73, 81, 172, 279
- Toxic metal ions, 435
- Toxins, v, 17, 100, 305, 313, 314, 316, 328, 350, 362, 363, 365, 371, 416, 422, 427
- T**
- Targeted therapy, 62, 71
- Targeting, 9, 19–22, 36, 38, 61, 91–95, 98, 99, 118, 119, 121, 123, 134, 172, 190,
- W**
- Wearable sensors, 230, 232, 241, 253, 255
- Wound healing, 3, 9, 42, 95, 142–154, 161–163, 171–173, 177, 179, 186–193